THE UNIVERSITY OF QUEENSLAND

AUSTRALIA

Uncovering New Candidate Genes for Involvement in Disorders of Sex Development using RNA-seq and Morpholinos

Kathryn S McClelland

BSc. Hons I

A thesis submitted for the degree of Doctor of Philosophy at

The University of Queensland in 2015

Institute for Molecular Bioscience

Abstract

Male development depends on the successful development of testes in the embryo, a process beginning with the differentiation of Sertoli cells, directed by the Y-linked gene *SRY*. The virilisation of the XY embryo is then directed by steroid hormones, which are produced by fetal Leydig cells (FLCs) that reside in the embryonic testis. As only around 20% of XY disorders of sex development (DSDs) are able to be explained at the molecular genetic level, I reasoned that genes involved in the development and function of FLCs may represent an unappreciated source of candidate XY DSD genes. To pinpoint these genes, and to develop a more detailed understanding of the regulatory networks supporting the formation of the somatic cell populations of the developing testes, I developed methods for isolating Sertoli cell, FLC and non-steroidogenic interstitial cell-enriched subpopulations using the *Sf1*-eGFP transgenic mouse line. RNA-sequencing of the subpopulations at 12.5 dpc, followed by rigorous bioinformatic filtering, identified genes upregulated in Sertoli cells, FLCs and non-steroidogenic interstitial cells. The bioinformatic analysis revealed that expression of components of neuroactive ligand signaling pathways were prevalent in FLCs and Sertoli cells. In addition, I identified 61 genes expressed preferentially in early FLCs with no previous association with FLC specification or differentiation that may be functionally significant. I also sought to identify factors that are possibly involved in signaling between the Sertoli cells, FLCs and non-steroidogenic interstitial cell populations. This study also identified fetal expression of a number of known DSD causing genes in the early somatic cell populations of the gonad, providing further evidence for the fetal origins of gonadal phenotypes in some DSDs. This dataset offers a platform for investigating the biology of FLCs and understanding their role in testicular development. In addition, this dataset provide a foundation for targeted studies aimed at identifying the causes of idiopathic XY DSDs.

Conducting a transcriptomic project identified dozens of highly promising gonadogenesis candidate genes and highlighted the challenge of determining gene function when overwhelmed with potential candidate genes. In addition, many candidate genes for human developmental disorders are being identified in rare disease cohorts thanks to whole exome and whole genome sequencing. It is clear that traditional gene targeting methods in mice are too complex and time consuming to clear this backlog, especially when conditional deletion methods are required. To address the need for first pass functional screening methods, I developed a novel technique for assessing gene function, in a knockdown context, by injection of modified antisense morpholino oligonucleotides (MOs) into the

heart of mid-gestation mouse embryos. Circulation of the MOs through the embryonic vasculature allowed targeting of multiple organs. Tissues of interest were explanted, cultured and analysed for expression of key markers. As a proof-of-principle, I used MO injection to partially phenocopy known gene knockout phenotypes in the fetal gonads (*Stra8, Sox9*) and pancreas (*Sox9*). In addition, I created a novel double knockdown of *Gli1* and *Gli2,* which revealed defects in FLC differentiation. I also investigated the role of *Adamts19* and *Ctrb1*, genes of unknown function in sex determination and gonadal development. This proof-of-principle study demonstrated the utility of this method as a means of first-pass analysis of gene function during organogenesis before undertaking a detailed genetic analysis.

In addition, I used MO knockdown to validate a candidate gene for 46,XY DSD. Using whole exome sequencing *SART3* was identified as a potential candidate for DSD in 46,XY DSD patients. By performing MO knockdown of SART3 in the fetal mouse gonad I modelled the haploinsufficiency that results from heterozygous deletion of *SART3* and provided evidence supporting *SART3* as the disease-causing gene in the DSD patients in this study. In addition, this work provided data on the function of SART3 in the developing gonad.

Overall, this thesis describes the generation of the most comprehensive somatic cell transcriptome of developing testicular somatic cell populations to date and develops a method for screening the genes of interest that come out of such a study. These resources will be able to be used for the identification and characterisation of genes in gonad development. In addition this work will hopefully provide a platform for identifying new candidates for the fetal origins of DSDs originating from defects in the FLC population.

Declaration by author

This thesis is composed of my original work, and contains no material previously published or written by another person except where due reference has been made in the text. I have clearly stated the contribution by others to jointly-authored works that I have included in my thesis.

I have clearly stated the contribution of others to my thesis as a whole, including statistical assistance, survey design, data analysis, significant technical procedures, professional editorial advice, and any other original research work used or reported in my thesis. The content of my thesis is the result of work I have carried out since the commencement of my research higher degree candidature and does not include a substantial part of work that has been submitted to qualify for the award of any other degree or diploma in any university or other tertiary institution. I have clearly stated which parts of my thesis, if any, have been submitted to qualify for another award.

I acknowledge that an electronic copy of my thesis must be lodged with the University Library and, subject to the policy and procedures of The University of Queensland, the thesis be made available for research and study in accordance with the Copyright Act 1968 unless a period of embargo has been approved by the Dean of the Graduate School.

I acknowledge that copyright of all material contained in my thesis resides with the copyright holder(s) of that material. Where appropriate I have obtained copyright permission from the copyright holder to reproduce material in this thesis.

Publications during candidature

Peer-reviewed papers.

McClelland KS, Wainwright EN, Bowles J and Koopman P. (2014) Rapid screening of gene function by systemic delivery of morpholino oligonucleotides to live mouse embryos. *PLOS ONE* 10(1): e0114932. doi:10.1371/journal.pone.0114932

Wainwright EN, Jorgensen JS, Kim Y, Truong V, Bagheri-Fam S, Davidson T, Svingen T, Fernandez-Valverde SL, **McClelland KS,** Taft RJ, Harley VR, Koopman P, Wilhelm D. (2013) SOX9 regulates microRNA miR-202-5p/3p expression during mouse testis differentiation. *Biology of Reproduction*, 89: 34, 1-12

McClelland KS, Bell K, Larney C, Harley VR, Sinclair A, Oshlack A, Koopman P and Bowles J (2015) Purification and transcriptomic analysis of mouse fetal Leydig cells reveals candidate genes for disorders of sex development. *Biology of Reproduction,* doi:10.1095/biolreprod.115.128918

Review papers

McClelland K, Bowles J and Koopman P. (2012) "Male sex determination: insights into molecular mechanisms." *Asian Journal of Andrology*, 14(1):164-71

Publications included in this thesis

McClelland K, Bowles J and Koopman P. (2012) "Male sex determination: insights into molecular mechanisms." *Asian Journal of Andrology*, 14(1): 164-71

– incorporated as parts of Chapter 1 (including Figures).

Contributor	Statement of contribution
McClelland KS (Candidate)	Wrote and edited paper (50%) Figures (100%)
Bowles J	Wrote and edited paper (25%)
Koopman P	Wrote and edited paper (25%)

McClelland KS, Wainwright EN, Bowles J and Koopman P. (2014) Rapid screening of gene function by systemic delivery of morpholino oligonucleotides to live mouse embryos. *PLOS ONE ONE* 10(1): e0114932. doi:10.1371/journal.pone.0114932

– incorporated as Chapter 2.

Contributor	Statement of contribution
McClelland KS (Candidate)	Designed experiments (70%) Performed experiments – excluding injections (95%) Experimental injections (80%) Wrote and edited paper (60%)
Wainwright EN	Staining and Imaging in Fig. 2.4J (100%) Performed experiments – excluding injections (5%) Wrote and edited paper (5%)
Bowles J	Designed experiments (15%) Experimental Injections – assisted (20%) Wrote and edited paper (15%)
Koopman P	Designed experiments (15%) Wrote and edited paper (20%)

McClelland KS, Bell K, Larney C, Harley VR, Sinclair A, Oshlack A, Koopman P and Bowles J (2015) Purification and transcriptomic analysis of mouse fetal Leydig cells reveals candidate genes for disorders of sex development. *Biology of Reproduction,* doi:10.1095/biolreprod.115.128918

– incorporated as Chapter 3.

Contributor	Statement of contribution
McClelland KS (Candidate)	Designed experiments (70%) Performed experiments – excluding Bioinformatics and GO analysis (100%) Performed Bioinformatics and GO analysis (20%) Wrote paper (65%) Edited paper (25%) Paper development (20%)
Bell K	Performed Bioinformatics and GO analysis (65%) Edited paper (5%) Paper development (10%)
Larney C	Performed Bioinformatics and GO analysis (15%) Edited paper (5%)
Harley VR	Paper development (10%) Edited paper (5%)
Sinclair A	Paper development (10%) Edited paper (5%)
Oshlack A	Paper development (10%) Edited paper (5%)
Bowles J	Designed experiments (15%) Wrote paper (15%) Edited paper (25%) Paper development (20%)
Koopman P	Designed experiments (15%) Wrote paper (20%) Edited paper (25%) Paper development (20%)

Contributions by others to the thesis

Prof Peter Koopman contributed to the concept and design of the research projects. Prof Koopman contributed to the interpretation of the research data and provided critical proofing and revision of the papers included in this thesis and the thesis itself.

Dr Josephine Bowles contributed to the concept and design of the research projects. Dr Bowles contributed to some technical aspects of the work, including assistance with conducting the MO heart injections (Chapter 2). In addition she contributed to the interpretation of the research data and provided critical proofing and revision of the papers included in this thesis and the thesis itself.

Ms Tara-Lynne Davidson contributed technical advice for the mouse work in this thesis. Ms Davidson set up the majority of the mouse crosses required to complete this work and helped to develop a robust MO heart injection experimental protocol.

Ms Kim Miles contributed to a technical aspect of the work in Chapter 2, namely assistance with conducting the MO heart injections.

Dr Elanor Wainwright performed the whole-mount mesonephros staining and imaging in Fig. 2.4J, and provided critical proofing and revision of the paper in Chapter 2 (PLOS ONE) that is included in this thesis.

Dr Stefanie Eggers performed the whole exome sequencing and the down-stream analysis that lead to the identification of *SART3* and *NR0B2* as DSD candidate genes as part of her PhD. The MO knockdown of *SART3* and *NR0B2* (Chapter 2) was completed as part of a collaboration with Dr Eggers and Prof. Sinclair. Figures 2.12 and 2.14 are reproduced from Dr Eggers' PhD thesis with permission. Dr Eggers also assisted in the interpretation of the MO knockdown data from the genes *Sart3* and *Nr0b2* and allowed the publication of unpublished results (personal communications) relevant to this project.

Prof Andrew H Sinclair provided critical proofing and revision of the paper in Chapter 3 of this thesis. The MO knockdown of *SART3* and *NR0B2* (Chapter 2) was completed as part of a collaboration with Prof. Sinclair and Dr Eggers. Prof. Sinclair also assisted in the interpretation of the MO knockdown data from the genes *Sart3* and *Nr0b2* and allowed the publication of unpublished results relevant to this project.

Dr Katrina Bell contributed to the concept and design of the differentially expressed gene analysis for the RNA-seq data in Chapter 3. Dr Bell contributed to some technical aspects of the work by mapping the RNA-seq reads to the genome and then worked with the candidate to design a strategy

to create the differentially expressed gene lists (Supplemental Data 1 and 2). She also provided training in the use of the gene ontology DAVID database. Dr Bell also provided proofing and revision of the paper included in Chapter 3 of this thesis.

Mr Christian Larney performed the reanalysis of published microarray data used in this work. Mr Larney contributed to technical implementation of experiments designed by the candidate including mapping the reprocessed microarray data back to the RNA-seq data (Fig. 3.9) and extracting gene information from OMIM (Supplemental Table 8). Mr Larney also provided proofing and revision of the paper included in Chapter 3 of this thesis.

Dr Alicia Oshlack contributed to the concept and design of the differentially expressed gene analysis for the RNA-seq data in Chapter 3 and provided critical proofing and revision of the paper in Chapter 3 of this thesis.

Prof Vincent R Harley provided critical proofing and revision of the paper in Chapter 3 of this thesis.

Ms Kathryn McClelland was responsible for the remainder of the work

Statement of parts of the thesis submitted to qualify for the award of another degree

None.

Acknowledgements

There are many people whom I wish to thank for supporting me throughout the PhD journey. Firstly, this journey would not have been possible without the support of my supervisors Peter Koopman and Josephine Bowles. I would like to thank Koops for his time, advice, patience and support through my time in the Koopman Lab starting in undergrad, throughout Honours and finally throughout my PhD. Under his guidance I have developed as a scientist and a writer. Koops has always demanded the best and I have tried my upmost to achieve that. Thank you very much for shepherding me through this journey. I would like to thank Jo for her commitment to endless meetings and her valuable input throughout my PhD. She has kept me on the straight and narrow and supported me through all the rough patches. Her commitment, accuracy and can-do attitude are something I hope I will take away with me. Thank you to both of you for helping me to reach my full potential.

I am also grateful to Amanda Carozzi for her constant support and advice throughout my PhD. Thank you to my committee members Ben Hogan and Annemiek Beverdam for your support, advice and mentorship throughout each milestone. Thank you to Andrew Sinclair and Vincent Harley for your feedback, support and advice throughout my time with the Program. Thank you to Vincent Harley and Janelle Ryan for facilitating the sequencing undertaken at the Monash Medical Genomics Facility. Thank you also to my collaborators Elanor Wainwright, Stefanie Eggers, Andrew Sinclair, Katrina Bell and Alicia Oshlack for bringing our work to fruition.

Thank you to the members of the Koopman Lab both past and present for your passion, friendship and help. Thank you to Cassy, Liang and Alex for all your advice. I would like to particularly thank Terje Svingen who started off as my supervisor in the Koopman Lab all those year ago. Thank you for training me up and instilling in me a passion for science. Thanks to those in the morning crew; Ee Ting, Jess, Kim and Elanor for all the before 8am laughs and cups of tea. This experience would not have been the same without the other PhD students on Level 4 North and the SIMBA crew. I would also like to thank all members of the GDD division and members of the NHMRC Program Grant in DSD for their support, friendship and constructive feedback. In particular, I would like to thank Claudio Cortes, Tam Duong, Darya Vanichkina and Joelle Kartopawiro for their magnificent friendship throughout this time. Also a special thank you to Ashley Cooper and Joanna Rakoczy. We started our journey together in Honours and having you by my side throughout my PhD has been wonderful. Many thanks must also go to Elanor Wainwright who has supported me

intellectually and as a friend throughout this journey.

This PhD would not have been the same without a journey to Woods Hole for the 120th Embryology course. This course and the people on it have transformed my PhD journey. A special thank you to Richard Behringer and Alejandro Sánchez Alvarado for their mentorship during the course and beyond, and to Lori Sussel for her guidance in all things pancreatic. Thank you to friends scattered far and wide, especially Tetstuto, Nathan and Sophie M. Thank you for all your smiles. Additionally, thank you to the *John & Madeleine Trinkaus Endowed Scholarship,* which covered my tuition fees for the 2013 Embryology Course at the Marine Biological Laboratories, Woods Hole.

Thank you to the people behind the fantastic facilities at UQ and at the IMB used in this project. Special mention to Virginia Nink from the QBI Flow Cytometry Facility who can get something out of almost nothing – this thesis would not have been possible without all our hours of FACS sorting. Also thank you to John Griffith at the IMB ACRF Microscopy Facility. I would also like to thank Tara Davidson for her management of all things mouse and Kim Miles for all her fabulous conversation during injections. I also appreciate the financial support I was fortunate to receive in the form of an APA scholarship, an UQ scholarship and support from Peter Koopman, for attending conferences and meetings. Thank you also to *Developmental Dynamics* for the travel award to attend the Sixth International Symposium on Vertebrate Sex Determination in 2012.

On a personal note, I could not have completed this PhD without the support and encouragement of my friends and family over the last four years. Special thanks to my mother Carolyn, my sister Allison, my godmother Laurie and my father Randall. I also thank my friends and extended family for their support and encouragement. Thank you to Mason and Alice for keeping me smiling and always knowing the right thing to say. I would like to thank Greta for keeping me level and saving me from Word. Words cannot describe how much you need something zany in your life at times like these so thank you to my friends for keeping me smiling and happy through the various snafus in this journey. Particular thanks go to Cariad, Ryan, Madeleine, Jason, Nick, Tahlee, Thom, Amelia, Christie, Laura, Mafumi, and all the Priestesses of the Skull – you know who you are. Thank you for your patience, perspective and the fun you've brought with you. Finally, I would like to dedicate this thesis to Joyce and Fred Bylett who taught me the value of education. I am forever grateful to you.

Keywords

sex-determination, gonadogenesis, knockdown, testis, leydig, masculinisation, rna-seq, morpholino, transcriptomics, neuroendocrine

Australian and New Zealand Standard Research Classifications (ANZSRC)

ANZSRC code: 060403 Developmental Genetics (incl. Sex Determination), 70%

ANZSRC code: 060102, Bioinformatics, 20%

ANZSRC code: 060199, Biochemistry and Cell Biology not elsewhere classified, 10%

Fields of Research (FoR) Classification

FoR code: 0604, Genetics, 70%

FoR code: 0601, Biochemistry and Cell Biology, 30%

Table of Contents

List of Figures

List of Tables

List of Supplemental Files

Refer to accompanying video, .xls and .pdf files associated with the thesis.

Supplemental Video 1. Demonstration of heart injection of constructs in 11.5 dpc embryo.

Supplemental Data 1: RNA-seq expression data.

Supplemental Data 2: Genes upregulated in enriched cell populations at 12.5 dpc.

Supplemental Data 3: GO of genes upregulated in enriched cell populations at 12.5 dpc.

Supplemental Data 4: Genes "on" at 11.5dpc in gonadal microarray screens that are detected as upregulated in the FLC enriched population by RNA-seq at 12.5 dpc.

List of Abbreviations

The following abbreviations are used in this thesis. Only gene names directly refered to in the text or in a figure are featured in this table.

γ-H2ax/γ-H2AX	H2A histone family, member X
*Adamts19/16/*ADAMTS19/16	a disintegrin-like and metallopeptidase [reprolysin type] with thrombospondin type 1 motif, 19/16
Adcy7/ADCY7	adenylate cyclase 7
*Adcyap1/*ADCYAP1	adenylate cyclase activating polypeptide 1
*Adhfe1/*ADHFE1	alcohol dehydrogenase, iron containing, 1
ALC/s	adult Leydig cells
*Aldh1a1/a2/a3/*ALDH1A1/A2/A3	aldehyde dehydrogenase family 1, subfamily A1/A2/A3
*Alk3/*ALK3	Bmpr1a, bone morphogenetic protein receptor, type 1A
*Amh/*AMH	anti-Müllerian hormone
*Ar/*AR	androgen receptor
*Arhgdig/*ARHGDIG	Rho GDP dissociation inhibitor (GDI) gamma
*Arx/*ARX	aristaless related homeobox
BAC/YAC	bacterial/yeast artifiical chromosome
BMP	bone morphogenetic protein
*Bmp2/*BMP2	bone morphogenetic protein 2
BPES	Blepharophimosis, epicanthus inversus, and ptosis
*Car2/*CAR2	carbonic anhydrase 2
*Cdh1/*CDH1	Cadherin 1/E-cadherin
cDNA	complementary DNA
ChIP-seq	Chromatin Immunoprecipitation sequncing
*Clca1/*CLCA1	chloride channel calcium activated 1
*Clcn2/*CLCN2	chloride channel 2
CRHR1/GRH	corticotropin releasing hormone receptor 1/gonadotropin releasing hormone 1
CRISPR/Cas9 system	clustered, regularly interspaced, short palindromic repeat (CRISPR) technology with Cas-9 RNA-guided nucleases
*Ctnnb1/*CTNNB1	catenin (cadherin associated protein), beta 1
*Ctrb1/*CTRB1	chymotrypsinogen B1
*Cyp11a1/*CYP11A1	cytochrome P450, family 11, subfamily a, polypeptide *1*
*Cyp17a1/*CYP17A1	cytochrome P450, family 17, subfamily a, polypeptide 1
*Cyp26b1/*CYP26B1	cytochrome P450, family 26, subfamily b, polypeptide 1
DAPT	γ-secretase inhibitor and indirectly an inhibitor of Notch
DBP	Dibutyl phthalate
*Ddx4/*DDX4	Deadbox polypeptide 4/MVH
DES	Diethylstilbestrol
*Dhh/*DHH	desert hedgehog
*Dmc1/*DMC1	DMC1 dosage suppressor of mck1 homolog, meiosis-specific homologous recombination
DNA	Deoxyribonucleic acid
dpc	days post coitum

dpn	days postnatal
DSD	disorders of sex development
*Dusp6/*DUSP6	dual specificity phosphatase 6
*Ermap/*ERMAP	erythroblast membrane-associated protein
ES cells	embryonic stem cells
F-MO	carboxyfluorescein-labelled MO
faDE	fetal adrenal enhancer
FGF	fibroblast growth factor
*Fgf9/13/16/18/*FGF9/13/16/18	fibroblast growth factor 9/13/16/18
*Fgfr1/2/3/4/*FGFR1/2/3/4	fibroblast growth factor receptor 1/2/3/4
FLC/s	fetal Leydig cell/s
FLE	fetal Leydig enhancer
*Flrt3/*FLRT3	fibronectin leucine rich transmembrane protein
*FoxL2/*FOXL2	Forkhead box L2
*Fras1/*FRAS1	Fraser syndrome 1 homolog
*Frem2/*FREM2	Fras1 related extracellular matrix protein 2
FSH	follicle-stimulating hormone
*Fst/*FST	follistatin
*Gata4/*GATA4	GATA binding protein 4
GC	germ cell
GFP	green fluorescent protein
*Ghrh/*GHRH	growth hormone releasing hormone
*Ghrl/*GHRL	Ghrelin
*Gli1/2/3/*GLI1/2/3	GLI-Kruppel family member 1/2/3
*Glug/*GLUG	glucagon
GnRH	gonadotropin releasing hormone
GO	gene ontology
*Grip/*GRIP	glutamate receptor interacting protein 1
*Gsta4/*GSTA4	glutathione S-transferase, alpha 4
*Gstm1/7/*GSTM1/7	glutathione S-transferase, mu 1/7
h	hours
*H-Pgds/*H-PGDS	hematopoietic prostaglandin D synthase
*Hcrtr1/*HCRTR1	hypocretin (orexin) receptor 1
*Hes1/5/*HES1/5	hairy and enhancer of split 1/5
Hh	Hedgehog
HMG	high hobility group
HPG	hypothalamus-pituitary-gonadal
*Hs6st1/*HS6ST1	heparan sulfate 6-O-sulfotransferase 1
*Hsd17b/*HSD17B	hydroxysteroid (17-beta) dehydrogenase 1
Hsd3β/HSD3β	hydroxy-delta-5-steroid dehydrogenase, 3 beta- and steroid delta-isomerase 1
*Igf1/*IGF1	insulin-like growth factor 1
IHH	idiopathic hypogonadotropic hypogonadism
*Il17rd/*IL17RD	interleukin 17 receptor D
ILC/s	infantile Leydig cells
InGE	indifferent gonad enhancer
*Inhba/*INHBA	inhibin beta-A
INS	Insulin

Ins1/2	insulin 1
Insl3/INSL3	insulin-like 3
Irx3/IRX3	Iroquois related homeobox 3
Itga9/ITGA9	integrin alpha 9
Jag1/JAG1	jagged 1
Kal1/KAL1	anosmin 1/ Kallmann syndrome interval gene 1
Kctd14/KCTD14	potassium channel tetramerisation domain containing 14
Kiss1/KISS1	KiSS-1 metastasis-suppressor
Kissr1/KISSR1	KISS1 receptor
KS	Kallmann syndrome
LAM	Laminin
L-Pgds/L-PGDS	prostaglandin D2 synthase
Lgr5/LGR5	leucine rich repeat containing G protein coupled receptor 5
LH	luteinizing hormone
Lhx9/LHX9	LIM homeobox protein 9
Mafb/MAFB	v-maf musculoaponeurotic fibrosarcoma oncogene family, protein B
MAPK	Mitogen-activated protein kinases
Mc2r/4r/MC2R/4r	melanocortin 2/4 receptor
min	minutes
MO/MOs	antisense morpholino oligonucleotides
mRNA	messenger RNA
nIHH	normosmic idiopathic hypogonadotropic hypogonadism
Npr1/NPR1	natriuretic peptide receptor 1
Nr0b1/NR0B1	nuclear receptor subfamily 0, group B, member 1/Dax1
Nr0b2/NR0B2	nuclear receptor subfamily 0, group B, member 2/SHP
Nr2f2/NR2F2	nuclear receptor subfamily 2, group F, member 2/COUP-TFII
Nr5a1/NR5A1	nuclear receptor subfamily 5, group A, member 1/SF1
Nrg1/NRG1	neuregulin 1
Nrp1/NRP1	neuropillin1
NSIC/s	non-steroidogenic interstitial cells
Nts/NTS	neurotensin
OMIM	Online Mendelian Inheritance in Man
Pak3/PAK3	p21 protein (Cdc42/Rac)-activated kinase 3
Pax6/PAX6	paired box 6
PDGF	platelet derived growth factor
PDGF-BB	platelet derived growth factor- BB isoform
Pdgfa/b/c/	platelet derived growth factor, alpha/B polypeptide/C polypeptide
Pdgfra/b/PDGFRa/b	platelet derived growth factor receptor, alpha/beta polypeptide
Pdx1/PDX1	pancreatic and duodenal homeobox 1
PE	pituitary enhancer
Pecam1/PECAM1	platelet/endothelial cell adhesion molecule 1
PGD2	prostaglandin D2

Plekha1/PLEKHA1	pleckstrin homology domain containing, family A (phosphoinositide binding specific) member 1
POF	premature ovarian failure
POMC	Pro-opiomelanocortin polypeptide
Pou5f1/POU5F1	POU domain, class 5, transcription factor 1/OCT4
Ppt1/Ppt1	palmitoyl-protein thioesterase 1
Ppy/PPY	Pancreatic polypeptide
PRLR/PRL	prolactin receptor/prolactin
Prok2/PROK2	prokineticin 2
Prokr2/PROKR2	prokineticin receptor 2
Prox1/PROX1	prospero homeobox 1
Ptch1/PTCH1	Patched homolog 1
Ptgds/PTGDS	prostaglandin D2 synthase
RA	retinoic acid
Rec8/REC8	REC8 meiotic recombination protein
Rgs11/RGS11	regulator of G-protein signaling 11
RNA	Ribonucleic acid
Robo2/ROBO2	roundabout homolog 2
Rspo1/RSPO1	R-spondin homolog
s	seconds
Sart3/SART3	squamous cell carcinoma antigen recognized by T cells 3
Scp3/SCP3	synaptonemal complex protein 3
Sgpl1/SGPL1	sphingosine phosphate lyase 1
Shh/SHH	sonic hedgehog
shRNA	short-hairpin RNA
Slc6a18/SLC6A18	solute carrier family 6 (neurotransmitter transporter), member 18
SLIT2/3	slit homolog 2/3
Smo/SMO	smoothened homolog
Smoc1/SMOC1	SPARC related modular calcium binding 1
SNV	single nucleotide variation
SOX	SRY (sex determining region Y)-box
Sox9/18/SOX9/18	SRY (sex determining region Y)-box 9/18
Sp5/SP5	trans-acting transcription factor 5
Spg11/SGP11	spastic paraplegia 11
Spry1/4/SPRY1/4	sprouty homolog 1/4
Srpx2/SRPX2	sushi-repeat-containing protein, X-linked 2
Sry/ SRY	sex determining region of Chr Y
Sst/SST	Somatostatin
Sstr4/SSTR4	somatostatin receptor 4
Star/STAR	steroidogenic acute regulatory protein
Stc2/STC2	stanniocalcin 2
Stra8/STRA8	stimulated by retinoic acid gene 8
Tac2/4/TAC2/4	tachykinin 2/4
Tacr3/TACR3	tachykinin receptor 3
Tbp/TBP	TATA binding protein
Tbx4/TBX4	T-box 4

Tcf21/TCF21	transcription factor 21/POD1
TESCO	testis-specific enhancer element
Tgfbr3/TGFBR3	transforming growth factor, beta receptor III
Tle6/TLE6	transducin-like enhancer of split 6, homolog of Drosophila E(spl)
TSS	transcription start site
Trank1/TRANK1	tetratricopeptide repeat and ankyrin repeat containing 1
ts	tail somites
Tyro3/TYRO3	TYRO3 protein tyrosine kinase 3
UGR	urogenital ridge
Vcam1/VCAM1	vascular cell adhesion molecule 1
VEGF/VEGFR	vascular endothelial growth factor/vascular endothelial growth factor receptor
Vegfr2/VEGFR2	KDR, kinase insert domain protein recptor; vascular endothelial growth factor receptor 2
Vipr1/VIPR1	vasoactive intestinal peptide receptor 1
VMH/VE	ventromedial hypothalamus enhancer
WES/WGS	whole exome sequencing/ whole genome sequencing
Wnt4/WNT4	wingless-related MMTV integration site 4
Wt1/WT1	Wilms tumor 1 homolog
XLAG/LISX2	Lissencephaly, X-linked 2

Chapter 1: Review of the Literature

1.1 Sex Determination and Human DSD

All mammals inherit an X or a Y sex chromosome from their father and an X chromosome from their mother during fertilisation. The resulting chromosomal sex, XX or XY, leads to the transformation of the embryo into a female or a male. Before gonadal sex determination, in both XX and XY human embryos, the bipotential gonadal primordium exists that has the potential to differentiate into either testes or ovaries. Activation of the Y-linked gene *Sry* (*sex determining region Y*) initiates testicular development in XY individuals and, when *Sry* is expressed ectopically in XX mice, the testis pathway is initiated (Koopman et al., 1991). When *Sry* is not present, as in XX individuals, or non-functional, as can occur in some XY individuals, the bipotential gonads do not follow the testicular pathway and instead develop into ovaries ((Gubbay et al., 1990; Lovell-Badge and Robertson, 1990); Fig. 1.1).

In males, differentiation of the supporting cell lineage into Sertoli cells results in organisation of the developing testis into two main compartments. The first compartment is the testis cords, which comprise aggregates of germ cells surrounded by a layer of Sertoli cells, which are in turn encased by peritubular myoid cells. Surrounding the cords is the testis interstitium, which includes the steroidogenic fetal Leydig cells (FLCs), non-steroidogenic interstitial cells, macrophages and the testis vasculature (Fig. 1.1).

In females, the supporting cell lineage differentiates into at least three different fetal ovarian somatic cell populations: LGR5-positive cells (leucine rich repeat containing G protein coupled receptor 5); FOXL2-positive cells (forkhead box L2) and NR2F2-positive cells (COUP-TFII; nuclear receptor subfamily 2, group F, member 2; (Rastetter et al., 2014)). In addition, a dense microvasculature network forms along with ovarian cysts, which are clusters of germ cells that form at around 13.5 dpc (days post coitum; (Bullejos et al., 2002; Pepling and Spradling, 1998)). Dramatic reorganisation of the ovary and the emergence of steroidogenic cells occur at about 1-3 dpn (days postnatal) when the primordial follicles form (for review see (Richards and Pangas, 2010); Fig. 1.1).

It could be said that the morphogenesis of the bipotential gonads into testes or ovaries dictates the phenotypic sex of the male or female individual, as it is the gonads that produce the masculinising or feminising hormones that shape the formation of secondary sex characteristics such as the development of the external genitalia. Early in gestation the gonad regulates the production of hormones independently. However, later in gestation and post partum cues are sent from the hypothalamus to the pituitary that prompt the gonads to scale-up hormone production. Upregulation of hormones by the hypothalamus-pituitary-gonadal (HPG) axis is essential for full sexual maturation. The activation of the HPG axis completes a complex process of sexual development that begins with chromosomal sex and then the development of the gonad. This process typically resolves into in a male or female phenotypic sex but this system can be disrupted at a number of stages (Fig. 1.1; 1.2).

Disorders of sex development (DSDs) are congenital conditions in which chromosomal, gonadal or anatomical sex of the individual is atypical. Clinical presentation can range from complete sex reversal to conditions such as hypospadias, the incorrect placement of the penile urethral opening. The most rare DSDs often are bundled with other clinical features that impact on quality of life. While the term DSD includes a wide spectrum of conditions, loss or compromised function of genes directing gonadal development is a common cause (for review see Ono and Harley, 2013). Mutations are commonly found in genes regulating Sertoli cell development and/or function (e.g. SRY, SOX9, SF1/NR5A1) or androgen synthesis by adult Leydig cells and/or adrenal steroidogenic cells (e.g. HSD17B, STAR) and genes regulating response to androgen hormones (e.g. AR; (Ostrer, 2014)). In other cases, mutated genes may encode ligand-receptor pairs that are central to the functionality of the HPG axis such as PROK2/PROKR2 and KISS1/KISS1R ((Valdes-Socin et al., 2014); Fig. 1.2). However, the underlying genetic cause of DSD in many patients is still unknown (Ono and Harley, 2013). As a result, many groups are working to identify the genetic changes that result in unclassified DSDs by sequencing large cohorts of patients and their families and by profiling the transcriptome of embryonic murine gonads. Without a molecular diagnosis it is difficult for medical specialists to provide clinical management, if it is required. Additionally, a molecular diagnosis provides the possibilty of assessing long-term outcomes for the patient, including the likelihood of fertility later in life. A role for the HPG axis and adult Leydig cells (ALCs) in DSDs and infertility is well established (for review see The Leydig Cell in Health and Disease, 2007), but the role of FLCs in DSDs is less clear cut. In this thesis I postulate that defects in FLC specification and function during gestation, or defects in the precursor cells to ALCs, also present during fetal life, may underlie some syndromic features of human DSDs.

1.2 Identifying genes involved in gonadogenesis

Investigation into the transcriptome of the gonad has identified numerous genes that are integral to the process of gonadogenesis, many of these genes, when mutated can cause DSDs. The gonadal transcriptome has been investigated using a number of approaches. Initially cDNA subtraction screens were performed to identify enriched transcripts (Bowles et al., 2000; McClive et al., 2003; Menke and Page, 2002; Nordqvist and Töhönen, 1997). These approaches profiled gonads at different timepoints and compared transcripts between multiple libraries made from whole gonads. However, in these cases a complex mix of cell types was profiled. Subsequent screens have tried to limit the noise created by multiple cell populations and lineages by comparing sorted cell populations. Initially, pre-Sertoli cells were isolated and profiled by subtraction screen using a *porcine Sry*-GFP mouse line which only allowed isolation of XY cell populations (Boyer et al., 2004; Daneau et al., 2002). Microarrays were used to profile whole gonad transcriptomes over developmental timecourses (Grimmond et al., 2000; Small et al., 2005), but also to profile enriched populations of somatic cells. Initial screens for genes important in gonadogenesis and sex determination used cells that were isolated from XX and XY gonads with an *Nr5a1* (*nuclear receptor subfamily 5, group A, member 1/Sf1*) promoter driving a GFP-transgene in order to isolate pre-Sertoli/granulosa and pre-fetal Leydig cells (Beverdam and Koopman, 2006; Nef et al., 2005). Subsequently, a murine *Sry* promoter driving GFP transgenic line was produced and used to isolate XX and XY somatic supporting cells, Sertoli cells and granulosa cells, at 13.5 dpc for profiling (days post coitum; (Bouma et al., 2007)). An additional study profiled XX and XY somatic support cells using sorted cells from an *Sry*-GFP line at 11.5-12.5 dpc (Bouma et al., 2010). Efforts have also been made to profile the germ cell population during early gonadogenesis using an *Oct3/4*-GFP line, using which the germ cells can be isolated by FACS, and by comparing genes expressed in the W^v/W^v XX and XY gonads, which lack germ cells, to those expressed in wild-type gonads (Mise et al., 2008; Rolland et al., 2011).

More recently, microarrays have been performed comparing cell lineages isolated from XX and XY gonads from five transgenic reporter lines. This has allowed the isolation and characterisation of highly pure enriched populations supporting cells (Sertoli) and germ cells (Jameson et al., 2012b). Also profiled were a heterogeneous population of mixed interstitial/endothelial cells (Jameson et al., 2012b). The currently available data sets have provided a detailed characterisation of the Sertoli

cell lineage at the resolution allowed by the microarray platform – although caveats must be noted about the reliability of microarrays, which lack the resolution of more recent RNAseq approaches. Isolation of other cell populations, including the FLC population, has been more challenging due to a dearth of suitable reported lines. FLC-specific genes were poorly represented in screens using NR5A1-positive Sertoli cell and FLC populations isolated using *Sf1*-eGFP lines (Beverdam and Koopman, 2006; Nef et al., 2005). The poor characterisation of the FLC lineage and other lineages of the testis interstitium has hampered our understanding of the dynamics and development of the interstitial space. Additionally, the interstitial/somatic populations profiled in the literature so far have been comprised of a heterogeneous mix of FLC and non-steroidogenic interstitial cells (NSICs). This heterogeneity has made answering questions about how FLCs, NSICs and other interstitial populations are specified difficult.

Importantly, almost all screens to date have discovered genes of interest by comparing the transcriptomes of XX and XY cells to identify genes that are differentially expressed in a sexually dimorphic pattern. The assumption that sexually dimorphic expression of a gene during gonadogenesis will allow identification of the most essential genes required for testicular or ovarian development has resulted in the identification of many key players. Nonetheless, it is inevitable that this targeted approach has resulted in the exclusion of many important genes. This criteria for defining genes of interest will have meant that many genes been missed in previous research. It must be considered that sexually dimorphic expression of a gene does not necessarily mean the gene has a function in gonadogeneis, just as equal expression in both XX and XY gonads does not mean that a gene does not play a potentially critical role in gonad development. By comparing genes between groups (cell types) within the XX or XY gonads instead of comparing XX and XY groups (sexes), I propose that we will be able to identify important gonadogenesis genes that have been missed in previous studies.

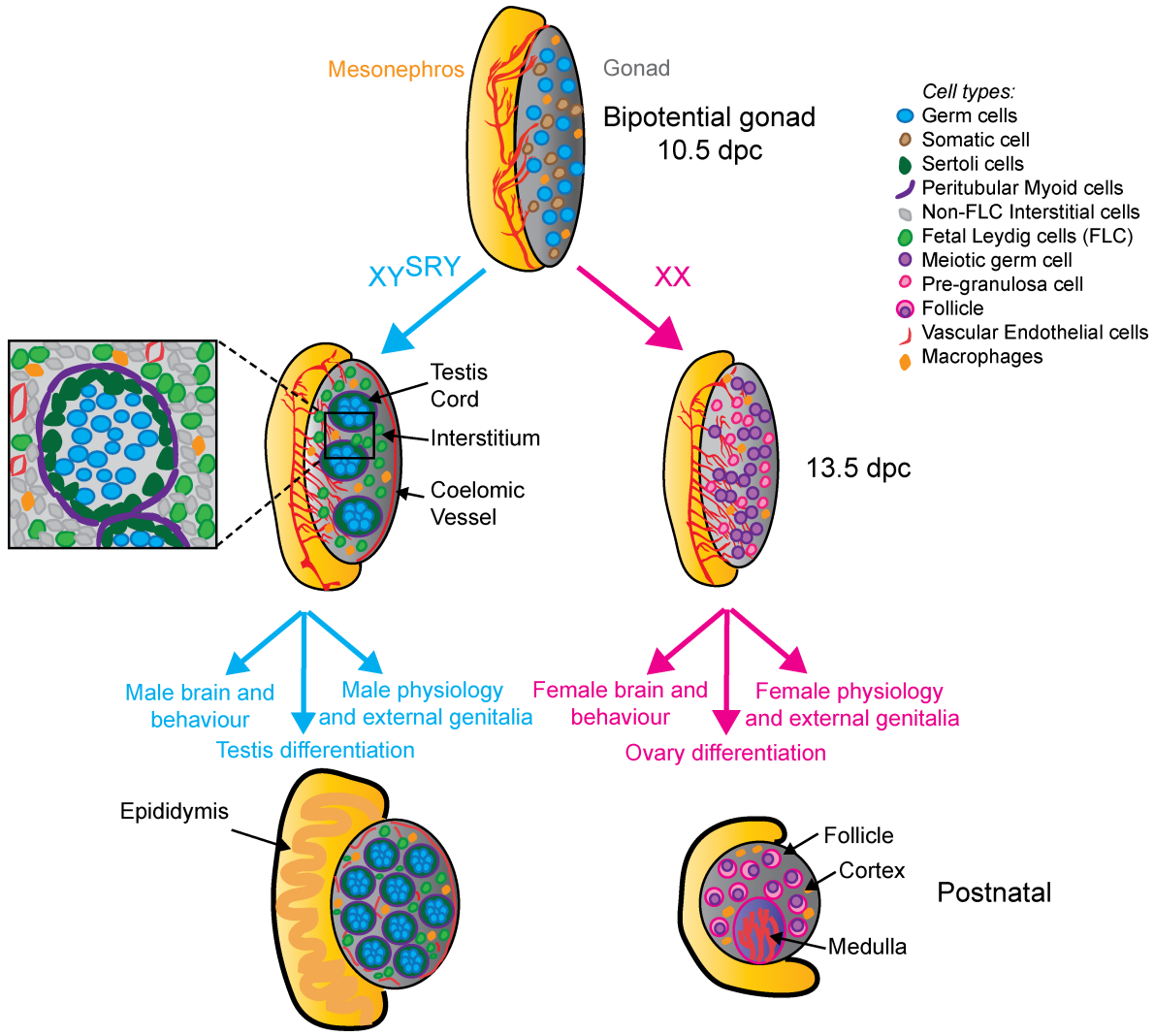

Figure 1.1. Overview of mouse gonadogenesis.

The expression of *Sry* and *r5a* at 10.5–11.5 dpc in the bipotential gonad initiates testis differentiation. By 13.5 dpc basic testis morphology is established: the formation of testis cords, the coelomic blood vessel, and differentiation and activation of steroidogenesis in Leydig cells has occurred, and androgens are then produced by the testes. In the ovary further differentiation is delayed. In the XX gonad, around 13.5 dpc germ cells have entered meiosis. At this point vascularisation and remodelling of the ovary occurs to form germ cell cysts. Later, the cortical and medullar domains begin to be established and folliculogenesis takes place. Secondary sexual characteristics include the establishment of the male and female genital tract and duct system, sex-specific brain dimorphisms and behaviours and external genitalia. The establishment of secondary sexual characteristics involves organ-specific, regulatory gene networks. (Modified from (McClelland et al., 2012))

1.3 Testis differentiation

SRY is a SOX-family transcription factor with a DNA–binding high-mobility group-box (HMG) domain (Kashimada and Koopman, 2010; for review of SRY molecular dynamics and properties see Polanco and Koopman, 2007). In mice, expression of *Sry* in the developing XY gonad is both brief and carefully regulated (for review of *SRY* transcriptional regulation see Larney et al., 2014). In addition to sufficiently early onset of expression of *Sry*, a threshold level of expression must be achieved for complete testis differentiation to occur. In mice, expression of *Sry* is initiated at 10.5 dpc, peaks at 11.5 dpc and is extinguished by 12.5 dpc (Hacker et al., 1995; Jeske et al., 1995; Koopman et al., 1990). *Sry* expression occurs in a wave-like pattern beginning in the central region of the gonad and expanding out towards the poles (Albrecht and Eicher, 2001; Bullejos and Koopman, 2001; Swain et al., 1998; Wilhelm et al., 2009). In humans *SRY* has a broader spatiotemporal expression profile, occurring in multiple tissues such as the adrenal gland and heart, and is maintained for longer in the testis, apparently through to adulthood (Clepet et al., 1993). *Sry/SRY* is also expressed in the brain of both mice and humans (Clepet et al., 1993; Lahr et al., 1995; Mayer et al., 1998).

SRY plays a role in a number of DSDs: loss of function of SRY results in complete male to female sex reversal (Jager et al., 1990; Maier et al., 2003), whereas ectopic expression of SRY in XX individuals, due to chromosomal translocation of SRY, may result in female to male sex reversal. It is estimated that SRY translocation is responsible for 10% of all 46,XX female to male sex reversal cases (Nieto et al., 2004). Formation of ovotestes, where ovarian and testicular tissue coexist in the same gonad, can also occur in cases of ectopic SRY activity (Margarit et al., 2000; Sharp et al., 2005).

The supporting cells of the XY gonad cell-autonomously differentiate into Sertoli cells under the influence of SRY and its direct target SOX9 (Sry-box containing gene 9; (Sekido and Lovell-Badge, 2008)). SOX9 appears to directly or indirectly control testis development (Bishop et al., 2000; Vidal et al., 2001). However, before hallmarks of testis development emerge, differences exist between XX and XY gonad. After expression of *Sry* and the upregulation of *Sox9,* male-specific proliferation of the epithelium at the coelomic surface of the genital ridges occurs (Karl and Capel, 1998; Schmahl et al., 2000). This sex-specific proliferation is thought to amplify the population of cells expressing the transcription factor NR5A1 at high levels. Following proliferation

between 8-18 ts (tail somites; 8 ts is approximately 10.5 dpc, 18 ts is approximately 11.5 dpc; (Hacker et al., 1995)), the cells expressing NR5A1 at high levels migrate into the gonad proper (Schmahl and Capel, 2003; Schmahl et al., 2000). These cells are later capable of differentiating into Sertoli cells, the first testicular cell type to arise, which are required for formation of the testis cords (Karl and Capel, 1998; Magre and Jost, 1980; Schmahl and Capel, 2003; Schmahl et al., 2000). A subset of FLC precursors may also exist in this early wave of migration (DeFalco et al., 2011). Following the migration of NR5A1-high cells into the gonad the coelomic epithelium continues to proliferate and cells that express low levels of NR5A1 migrate into the gonad proper between 19-25 ts (25 ts is approximately 12.0 dpc; (Hacker et al., 1995)). These cells are believed to contribute to non-Sertoli lineages (Schmahl et al., 2000). The molecular mechanism that induces coelomic epithelial proliferation is unknown. As testes develop normally in transgenic XX mice overexpressing the SRY target *Sox9*, it appears that male-specific proliferation of the coelomic epithelium, and all other aspects of fetal testis development, are under the control, directly or indirectly, of SOX9 (Bishop et al., 2000; Vidal et al., 2001).

1.3.1 Sertoli cells

Like SRY, SOX9 is necessary for testis differentiation: mice lacking *Sox9* undergo complete XY sex reversal (Barrionuevo et al., 2006; Chaboissier et al., 2004). Additionally, 75% of human patients with a heterozygous mutation in *SOX9* manifest with complete or partial XY sex reversal (Foster et al., 1994; Wagner et al., 1994). In mouse, *Sox9* is upregulated in pre-Sertoli/supporting cells when a protein complex of SRY and NR5A1 (Steroidogenic factor 1; NR5A1, nuclear receptor subfamily 5, group A, member 1) binds to a *Sox9* enhancer element known as TESCO (testis-specific enhancer of *Sox9* core element) (Sekido and Lovell-Badge, 2008). Bipotential supporting cells can cell-autonomously differentiate into Sertoli cells under the influence of SRY and SOX9. In XX-XY chimera studies almost all Sertoli cells were XY whilst other cell types did not exhibit a chromosomal bias (Palmer and Burgoyne, 1991; Patek et al., 1991). However, some Sertoli cells were always found to be XX (Palmer and Burgoyne, 1991). This indicated that there are paracrine pathways by which SRY-positive/SOX9-positive/NR5A1-positive cells can recruit additional cells to the Sertoli fate. This mechanism could recruit cells such as XX cells in the chimera experiments, or cells that express unusually low levels of *Sry* in normal XY gonads, to the Sertoli fate.

Two independent mechanisms of Sertoli cell recruitment have been identified: FGF9 (fibroblast growth factor 9) and PGD_2 (prostaglandin D2) mediated recruitment. *Fgf9* expression occurs in a

wave emanating from the central zone of the XY gonad similar to *Sry* and *Sox9* (Hiramatsu et al., 2010). *Fgf9*-/- mice exhibit XY sex reversal (Colvin et al., 2001; Kim et al., 2006). Conditional deletion of *Fgfr2* (FGF-receptor 2) in pre-Sertoli cells showed that FGFR2 is required in pre-Sertoli cell differentiation, indicating that FGFR2 is the major receptor for FGF9 in the XY gonad (Bagheri-Fam et al., 2008; Kim et al., 2007). *Sox9-/-* XY gonads do not express *Fgf9* indicating there is a positive feedback loop in place between FGF9 and SOX9 (Kim et al., 2006). The expression of the ovarian gene *Wnt4* (*wingless-related MMTV integration site 4*) is increased in *Fgf9-/-* XY gonads (Kim et al., 2006) and it has been shown that WNT4 and β-CATENIN, are able to repress the expression of *Sox9* in the XY gonad (Chang et al., 2008; Kim et al., 2006; Maatouk et al., 2008). Jameson et al. (2012a) then showed that in *Wnt4-/-/Fgfr2*-/- or *Wnt4-/-/Fgf9*-/- XY gonads sex reversal was rescued. These data indicate that FGF9/FGFR2 signaling in Sertoli cells represses the expression of *Wnt4* so that when WNT4 is expressed in the *Fgf9-/-* or *Fgfr2-/-* situation it can disrupt testicular development (Jameson et al., 2012a). Therefore, testicular development relies on the expression of genes such as *Sox9* as much as the repression of expression of genes, such as *Wnt4*.

In an independent pathway, PGD_2 is also able to induce Sertoli cell differentiation *in vivo* by amplifying the number of cells expressing SOX9 and thereby canalising the male pathway. Treatment of XX gonads with PGD_2 resulted in upregulation in *Sox9* and its direct downstream target *Amh* (the gene encoding anti-Müllerian hormone) which masculinises the XX gonad (Adams and McLaren, 2002; Moniot et al., 2009; Wilhelm et al., 2005). Notably, two receptors for PGD_2 are expressed in somatic cells of the 13.5 dpc XY gonad (Moniot et al., 2014). There are two prostaglandin D synthase enzymes, L-PGDS (lipocalin-prostaglandin D2 synthase) and H-PGDS (hematopoietic-prostaglandin D2 synthase), which regulate synthesis of PGD_2. *L-Pdgs* is expressed in the Sertoli cells from 11.5 dpc in the XY mouse gonad, with SOX9 initiating and maintaining the expression *L-Pgds* (Adams and McLaren, 2002; Moniot et al., 2009; Wilhelm et al., 2005). *H-Pgds/*H-PDGS is also expressed in somatic cells in the XY gonad from 11.5 dpc, but the expression of *H-Pdgs* precedes that of *L-Pdgs* by a few hours (Moniot et al., 2014; Moniot et al., 2011). It has been suggested that H-PDGS may mediate the earliest PGD_2 signaling in the XY gonad. This early signalling may be important for initiating nuclear translocation of SOX9 in pre-Sertoli cells. At 11.5 dpc SOX9 is restricted to the cytoplasm of the pre-Sertoli cells in the in *H-Pdgs-/-* XY gonads, but at 12.5 dpc SOX9 has localised to the nucleus and testicular development proceeds (Moniot et al., 2011; Moniot et al., 2014). This recovery indicates that H-PDGS is not essential for SOX9 nuclear translocation or differentiation of the testis. Similarly there is a subtle delay in Sertoli cell

differentiation and SOX9 nuclear localisation in *L-Pgds-/-* XY gonads (Moniot et al., 2009). Notably the initiation of the expression of *L-Pgds* is unperturbed in *Fgf9-/-* XY gonads, therefore FGF9 is not necessary for transcriptional activation of the *L-Pgds* gene (Moniot et al., 2009). Successful differentiation of Sertoli cells is required for the differentiation of the FLC population, which is directed in part by Sertoli-secreted signaling molecules (Barsoum and Yao, 2010; Yao et al., 2002).

1.3.2 Fetal Leydig cells

Leydig cells reside in the testis interstitium and are the primary source of virilsing hormones such as androgens, which are responsible for the differentiation of secondary male sexual characteristics. The steroid hormones produced by Leydig cells are also important for fertility later in life, as well as the reinforcement of male specific characteristics of the testis and individual (for review see Wu et al., 2007). The characteristics of the FLC population in human and in mouse are similar during fetal life (Svechnikov et al., 2010; Tapanainen et al., 1981). In mammals the ALC population takes over the role of hormone production postnatally and is important for the progression of puberty. In the primates there also exists a transient population of infantile Leydig cells (ILCs) that become active a few months after birth. As ILCs are not present in the mouse, they will not be discussed further here.

In mice, the FLC population arises during testis differentiation at around 12.5 dpc. FLCs are most abundant just before birth, after which numbers of FLCs decline and the ALC population emerges (Hazra et al., 2013). The increase in FLC numbers throughout development is thought to be the result of continued differentiation from the interstitium, as the FLC population is largely mitotically inactive (Orth, 1982). Hormones produced by the FLCs direct the very early masculinisation of the embryo because the production of testosterone and its conversion to the metabolite, dihydrotestosterone is independent of cues from the pituitary during gestation (for review see Huhtaniemi and Pelliniemi, 1992). This early period of FLC differentiation and activity is critical for the masculinisation of the embryo.

The ALC population is gonadotropin-dependent and maintains androgen production throughout life. In the mouse the ALC population begins to emerge at about 7 dpn concomitant with proliferation of Sertoli cells (Nef et al., 2000; O'Shaughnessy et al., 2012; Vergouwen et al., 1993). The number of

ALCs and the steroidogenic capacity of the cells increase dramatically around 25 dpn as a result of the pubertal rise in LH (luteinising hormone; (Baker and O'Shaughnessy, 2001; Ma et al., 2004; O'Shaughnessy et al., 1998; O'Shaughnessy et al., 2002; Vergouwen et al., 1993; Zhang et al., 2001)). The production of androgens is required for spermatogenesis and maintenance of masculine secondary sexual characteristics and as such, a role for ALC in DSDs and infertility is well established (The Leydig Cell in Health and Disease, 2007).

The primary role of Leydig cells is to convert cholesterol into testosterone in a dynamic process involving multiple substrates (Habert and Picon, 1984; Warren et al., 1972). Testosterone may be synthesised *de novo* from the primary substrate, cholesterol, or from intermediate products of the estrogen-androgen synthesis pathway. The series of reactions, of which there are many intermediate state equilibria, is mediated by steroidogenic P450 enzymes (synthesis reviewed in Chapter 10 in The Leydig Cell in Health and Disease, 2007). Some of the steroidogenic P450 enzymes are able to catalyze multiple steps in the pathway, and facilitate both forward and reverse reactions (Fig. 1.3). Different steroidogenic enzymes are often used as a measure of FLC maturity and as a functional read-out of differentiation and capacity to produce testosterone. At a basic level the most common markers, in order from least to most differentiated, are: *Star* (*steroidogenic acute regulatory protein; cytochrome P450, family 11, subfamily a, polypeptide 1* (*Scc*)), *Cyp11a1, Hsd3β* (*hydroxy-delta-5-steroid dehydrogenase, 3 beta- and steroid delta-isomerase 1*) and *Hsd17β3 (hydroxysteroid (17-beta) dehydrogenase 3*; (see Chapter 10 in The Leydig Cell in Health and Disease, 2007)). *Insl3* (*insulin-like 3*), a product of FLCs later in gestation, is often used as a late FLC marker but it is not directly involved in steroid biosynthesis (Ivell et al., 2013). Notably, it has recently been demonstrated that during gestation the FLC population does not express *Hsd17β3,* the gene encoding the enzyme that mediates the final conversion of androstenedione to testosterone (Shima et al., 2013). As a result FLCs can only synthesise androstenedione, but *Hsd17β3* has been shown to be active in fetal Sertoli cells indicating that it is the Sertoli cells that convert androstenedione to testosterone during fetal life (Shima et al., 2013). HSD17β3 is expressed in ALCs, therefore they can synthesise testosterone without the aid of the Sertoli cell population (for review see The Leydig Cell in Health and Disease, 2007).

In late gestation the production of testosterone by FLCs is greatly increased possibly in response to signals from the newly established HPG axis ((Japon et al., 1994; O'Shaughnessy et al., 1998; Pakarinen et al., 2002; Zhang et al., 2001); Fig. 1.2). Formation of the HPG axis initiates from 10.0 dpc but all the components are not in place until around 16.5 dpc. A key element of the HPG axis is

GnRH (gonadotropin-releasing hormone) neurons which migrate from the olfactory placode to the hypothalamus during embryonic development, and control the release of LH and FSH (follicle stimulating hormone) from the anterior pituitary (Schally et al., 1971), thereby facilitating reproductive function. The GnRH neurons arise at 10.0-11.0 dpc in the mouse and are derived from progenitor cells in the olfactory placodes (Wray et al., 1989b). Between 12.5-15.5 dpc the GnRH neurons migrate, via the vomeronasal complex, through the nasal septum into the forebrain ultimately achieving an adult-like distribution in the olfactory bulb and hypothalamus by 16.5 dpc (Wray et al., 1989b; Wray et al., 1989a). From 16.5 dpc the components of the hypothalamic-pituitary-gonadal axis are assembled.

The GnRH-neural circuitry is a key component of the HPG axis; the formation and activation of the GnRH-neural circuitry involves a series of neuroactive ligand/receptor pairs. GnRH secretion from the mature neurons results in pulsatile release of LH and FSH from the anterior pituitary. LH and FSH are present in the pituitary from around 17.5 dpc, but, GnRH is required for the release of LH and FSH into the circulatory system ((Aubert et al., 1985; Warren et al., 1984); Fig. 1.2). It is predicted that circulatory levels of LH do not reach stimulatory levels until days later, nevertheless, around 15.5-16.5 dpc, the LH receptor is expressed on FLCs. It is unclear if these low levels of pituitary-secreted LH result in the increased biosynthesis of testicular androgen compounds. Therefore the point at which the testis becomes gonadotropin-dependent is controversial (El-Gehani et al., 1998; Japon et al., 1994; O'Shaughnessy et al., 1998). Notably, XY rat embryos can undergo normal testicular development in the absence of circulating gonadotropes later in gestation, indicating that for the most part fetal testicular steroidogenesis in the early FLCs is independent of GnRH-stimulated release of LH (O'Shaughnessy et al., 1998).

Mutation of genes involved in the set-up and maintenance of the neuroendocrine circuitry often results in DSDs, and it has been assumed that this is primarily associated with HPG axis dysfunction (Bianco and Kaiser, 2009; Hardelin and Dode, 2008; Mastorakos et al., 2006). For example, in Kallmann syndrome, a form of idiopathic hypogonadotrophic hypogonadism (IHH), GnRH neurons fail to migrate normally to the olfactory bulb and the hypothalamus, resulting in anosmia (the loss of the sense of smell), and a failure of GnRH secretion which leads to limited secretion of LH and FSH (Schwanzel-Fukuda and Pfaff, 1989; Schwanzel-Fukuda et al., 1989). As a result the adult Leydig cells of testes in these individuals are not stimulated to produce androgens and individuals do not synthesise normal levels of testosterone (Dode and Hardelin, 2009; Sykiotis et al., 2010).

I hypothesise that the interstitium plays a larger role in human DSDs and infertility than is currently appreciated. I propose that differentiation of FLCs and their ability to produce steroid hormones during early gestation is likely to contribute to aspects of syndromic features of human DSDs and infertility. Recently it has emerged that NR2F2-positive non-steroidogenic interstitial cells (NSICs) in the embryonic testis give rise to a proportion of ALCs later in life (Kilcoyne et al., 2014). Therefore evidence is accumulating that perturbed differentiation or function of FLCs and NSICs during fetal life may have both immediate effects on embryonic masculinisation (FLCs) and long term effects on post-birth masculinisation (NSICs to ALCs). As a result there are several key questions remaining surrounding the biology of FLCs: the origin/s of the FLC population; how the FLC population is induced to differentiate from the interstitium; why FLCs respond to Sertoli derived cues when NSICs do not; how the FLC function and communicate with the surrounding NSICs and the role of the FLC population and fetal androgen production in DSDs.

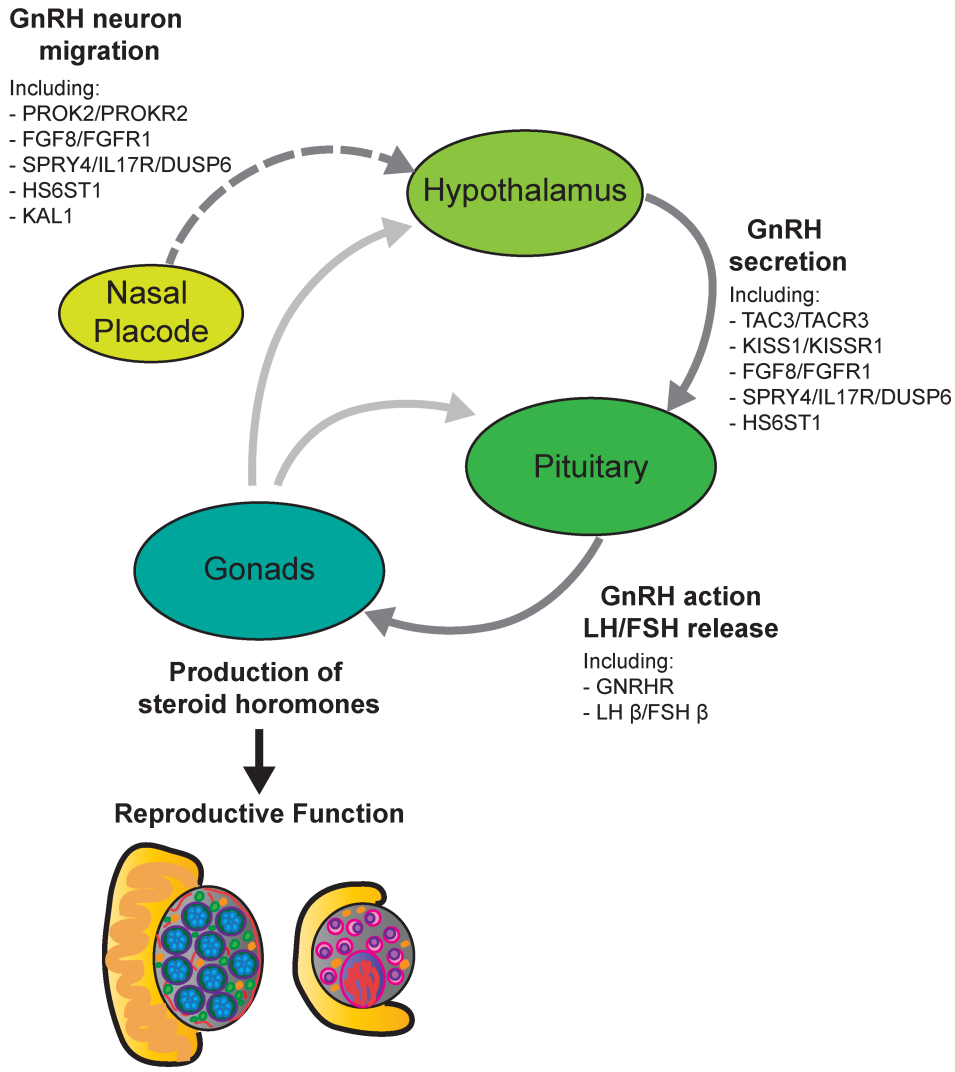

Figure 1.2. HPG axis and idiopathic hypogonadotropic hypogonadism.

GnRH neurons migrate from the nasal/olfactory placode to the hypothalamus during embryonic development. The secretion of GnRH controls the anterior pituitary mediated release of LH and FSH, which stimulates the production of steroid hormones in the gonads, forming a feedback loop. A functional HPG axis is required for proper reproductive function. The genetic basis of idiopathic hypogonadotropic hypogonadism (IHH) often involves mutations in genes that encode proteins that regulate GnRH neuronal migration, GnRH secretion or GnRH action. Modified from (Bianco and Kaiser, 2009).

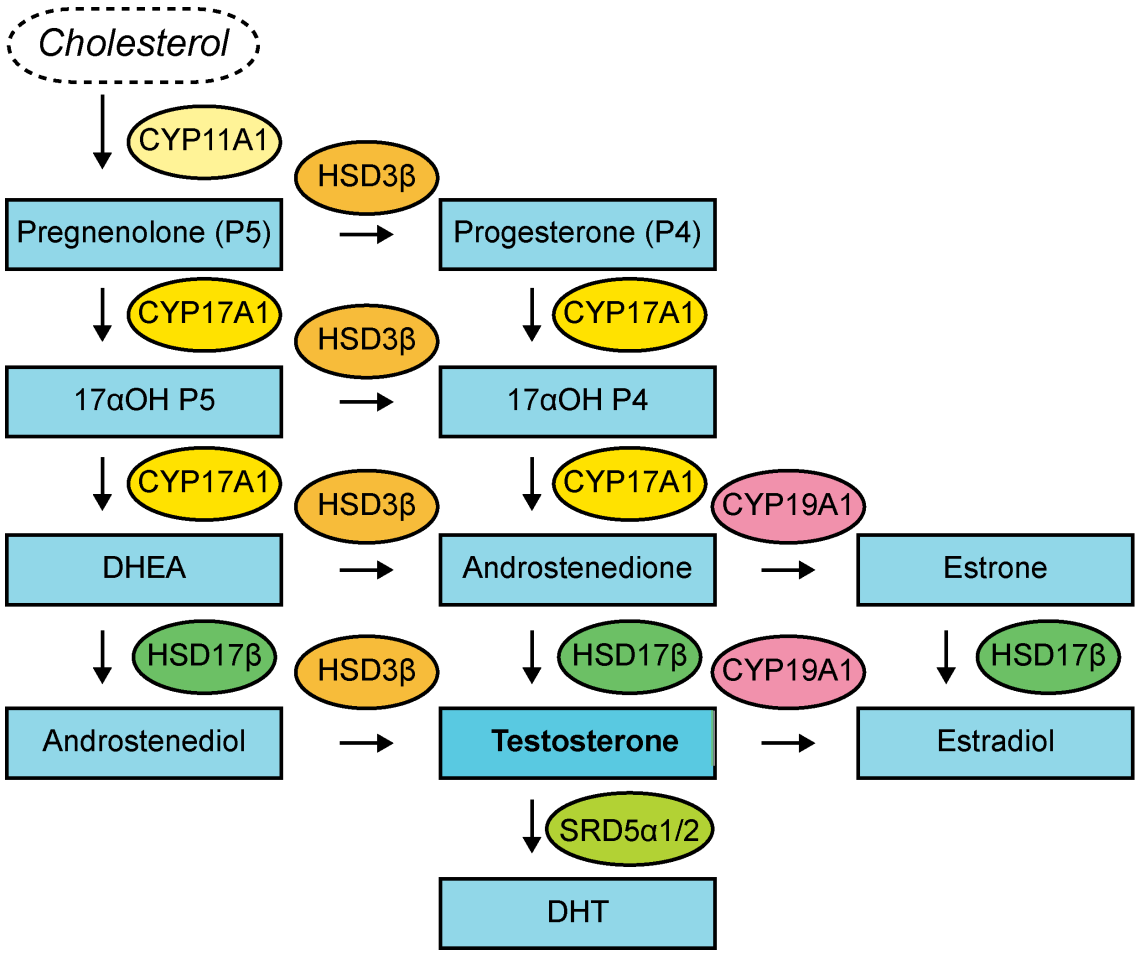

Figure 1.3. The steroidogenic pathway and androgen synthesis.

Androgen synthesis is the primary function of Leydig cells. Androgens are synthesised de novo from cholesterol, in a process that involves multiple enzymes and intermediate products. CYP11A1 mediates conversion of cholesterol to pregnenolone (P5), which begins the synthesis process. The synthesis of testosterone is mediated by cytochrome P450 enzymes and hydroxysteroid dehydrogenases. The P450 enzymes and hydroxysteroid dehydrogenases can be used as markers of the steroidogenic cell population and different enzymes can mark the "maturity" or stage of functional differentiation of the cell. It should be noted that some enzymes catalyze multiple steps in the steroidogenesis pathway. Additionally, some enzymes are capable of mediating both forward and reverse reactions. Note that HSD17β is not expressed in FLCs. Modified from (Griswold and Behringer, 2009).

1.3.2.1 The origins of FLCs

The origin of the FLC population remains disputed. Cell lineage tracing and live imaging studies suggest that FLCs may arise from multiple origins including the gonad/mesonephros border and the coelomic epithelium (DeFalco et al., 2011; Di Giovanni et al., 2011; Karl and Capel, 1998; Schmahl et al., 2000). As discussed previously, in the 11.0-12.0 dpc XY gonad there are two "waves" of coelomic epithelium proliferation. Some "first wave" cells differentiate into interstitial cells, but cells contributing to the interstitium mostly derive from the "second wave" of cells which does not contribute to the Sertoli cell population (DeFalco et al., 2011; Schmahl et al., 2000). It was proposed that FLC defects in the *Pdgfr-α -/-* (*platelet derived growth factor receptor, alpha*) XY gonad may result from defects in the "second wave" of coloemic epithelium proliferation, but, it was noted that most of these proliferating "second wave" cells are "NR5A1-negative" (Brennan et al., 2003). The end fate of these "second wave" cells remained uncertain until a suitable early interstitial marker could be identified. Expression of the gene *Mafb* (*v-maf musculoaponeurotic fibrosarcoma oncogene family, protein B*) marks a subset of the interstitial FLC and NSIC populations. Some of the "second wave" of proliferating cells that arise after 18 ts are *Mafb*-positive interstitial cells (DeFalco et al., 2011). These *Mafb*-positive cells presumably represent the previously reported NR5A1-low/NR5A1-negative cell population (Brennan et al., 2003; Schmahl et al., 2000). Although some of the *Mafb*-positive cells did differentiate into HSD3β-positive cells, the majority although interstitial, were not HSD3β-positive (DeFalco et al., 2011). Therefore it appears that these "NR5A1-negative, second wave" cells primarily contribute to the NR5A1-negative NSIC population that goes on to form the ALCs after birth (Karl and Capel, 1998; Kilcoyne et al., 2014; Schmahl et al., 2000).

There is also evidence that FLCs and ALCs may be derived from the intermediate mesoderm. Conditional deletion of the BMP signalling receptor *Alk3* (*bone morphogenetic protein receptor, type 1A; Bmpr1a*) in the intermediate mesoderm using *Rarb2-Cre* (*retinoic acid receptor β-Cre*) resulted in a decrease in the number of *Cypa11a1/Insl3*-positive cells in 18.5 dpc XY gonads (Di Giovanni et al., 2011). In addition, at 30 dpn the number of *Cyp11a1*-positive immature ALCs was reduced, which corresponded to lower testosterone levels and infertility (Di Giovanni et al., 2011). As loss of *Alk3* resulted in a decrease in FLCs and a pertubation of the NSIC population that goes on to form the ALC population postnatally, these data indicate that a proportion of FLCs and NSICs (pre-ALCs) may be derived from *Alk3*-positive intermediate mesoderm. More strikingly, this work indicated that early mesodermal defects resulting in pertubation of the FLC and NSIC populations could translate into defects in masculinisation and ALC dysfunction in postnatal life.

Therefore, cell lineage tracing and conditional deletion suggests that FLCs and NSICs can share a regional origin and can arise from the gonad/mesonephros border, the coelomic epithelium and the intermediate mesoderm. Further dissection of the contribution of each of these regions to the NSIC and FLC populations has been hampered by a dearth of suitable early FLC markers and markers that differentiate between NSICs and pre-FLCs early in gonadogeneis. NR5A1 remains the earliest marker of somatic cells, but it marks pre-Sertoli and pre-steroidogenic cells in the developing genital ridge and is therefore ill-suited to FLC/NSIC lineage tracing (Hatano et al., 1994; Luo et al., 1994).

1.3.2.2 NR5A1 in development and DSDs

NR5A1 is part of the orphan nuclear receptor NR5A family of transcription factors and is required for the development and function of the adrenal cortex, gonads, pituitary gonadotrope, ventromedial hypothalamus and spleen (Ikeda et al., 1993; Ikeda et al., 1995; Ingraham et al., 1994; Luo et al., 1994; Morohashi et al., 1999; Sadovsky et al., 1995; Shinoda et al., 1995). Studies in mice and humans show that *Nr5a1* mutant phenotypes are sensitive to dosage and genetic background (Luo et al., 1994). *Nr5a1-/-* mice initiate early gonadal and adrenal development, but the organs begin to regress by 11.5 dpc (Luo et al., 1994; Sadovsky et al., 1995). Transgenic expression of NR5A1 in *Nr5a1-/-* mice has been shown to rescue gonad development and induce ectopic adrenal glands (Fatchiyah et al., 2006; Zubair et al., 2009). In *Nr5a1*-haploinsufficient mice, adrenal and testis development was disrupted, but hypoplastic testes did form (Bland et al., 2004; Park et al., 2005). These data indicate that mouse adrenal development requires both copies of *Nra51* to be active, whereas the gonad can partially develop if a single copy is present.

The requirement for a threshold level of *Nr5a1* expression in the adrenal region and gonad is supported by phenotype of the *Cited-2-/-* mouse where the adrenal cortical primordium is seriously disrupted but abnormal testis differentiation can proceed. In *Cited2-/-* embryos, *Nr5a1* levels are approximately one third of wild-type levels. As a result, the *Cited2-/-* embryo is often used as a proxy for attenuated *Nr5a1* expression and function. In the *Cited2-/-* XY gonad, expression of the genes encoding *Sox9*, *Cyp11a1* and *Nr5a1* is decreased at 11.5 dpc, but expression rebounds to around *wild-type* levels by 13.5 dpc (Val et al., 2007). Closer investigation of the gonadal phenotype by Combes et al., (2010) revealed that normal testis morphology was perturbed in XY *Cited2-/-* gonads and did not recover by 14.5 dpc, although the transcriptional program apparently recovered by 13.5 dpc (Val *et al.*, 2007). As *Wt1* (*Wilms tumor 1*) is involved in *Nr5a1* regulation

(Wilhelm and Englert, 2002) it was expected that *Cited2+/-/Wt1+/-* embryos would show defects in adrenal and gonadal development. Initial reports showed that the adrenal gland of *Cited2+/-/Wt1+/-* embryos was small and mis-localised (Val et al., 2007). Complete loss of *Cited2* was required to achieve partial sex reversal in XY *Cited2-/-/Wt1+/-* and *Cited2-/-/Nr5a11+/-* gonads (Val et al., 2007). Introduction of a weakened *Sry* by using a Y^{POS} strain was required to induce full sex reversal (Buaas et al., 2009). However, the loss of an *Nr5a1* allele resulted in a more severe phenotype than loss of a *Wt1* allele in the *Cited2-/-* XY gonad (Buaas et al., 2009; Val et al., 2007). These findings further indicated that achieving a threshold level of *Nr5a1* is essential for obtaining normal testis morphology and adrenal development in mouse.

In humans, *NR5A1* mutations are a common underlying feature of 46,XY DSDs. Data from patients indicate that inheritance can be dominant or recessive and that NR5A1 mutation can result in a wide spectrum of phenotypes including gonadal dysgenesis, hypospadias, adrenal insufficiency, androgen synthesis defects and infertility (for review see Ferraz-de-Souza et al., 2011). In humans, *NR5A1* mutations are predominately heterozygous with rare homozygous exceptions (Achermann et al., 1999; Achermann et al., 2002). Usually, heterozygous NR5A1 mutations give rise to 46,XY DSD with normal adrenal function, indicating that the testis is more susceptible to NR5A1 dosage. Ambiguous genitalia and impaired androgen synthesis are commonly described in 46,XY DSD but information on gonadal pathology is limited (Correa et al., 2004; Coutant et al., 2007; Hasegawa et al., 2004; Köhler et al., 2008; Lin et al., 2007; Lourenco et al., 2009; Mallet et al., 2004; Reuter et al., 2007; Warman et al., 2011). Interestingly, missense mutations in the gene encoding *NR5A1* are also associated with male infertility (Bashamboo et al., 2010; Lourenco et al., 2009). Overall, mutation in *NR5A1* appears to be a relatively rare cause of adrenal failure but a common cause of 46,XY DSD in human, seemingly opposite to the reported phenotypes in mice (Bland et al., 2004; Lin et al., 2006).

NR5A1 also plays an important role in postnatal ovarian function and as such mutations in the gene encoding *NR5A1* have been associated with primary ovarian insufficiency and primary ovarian failure in 46,XX women (Bashamboo et al., 2010; Lourenco et al., 2009). However, adrenal insufficiency with normal prepubertal ovarian development in an 46,XX individual has also been reported (Biason-Lauber and Schoenle, 2000). There has been a case where a heterozygous mutation in *NR5A1* that was associated with primary ovarian failure in a mother was inherited where it resulted in 46,XY DSD in the child (Lourenco et al., 2009). These data indicate that NR5A1/*NR5A1* plays a complex role in adrenal and sexual development in mice and humans.

1.3.2.3 The tissue specific enhancers of the Nr5a1 *promoter*

Due to its essential role in the development of many tissues, the promoter of the *Nr5a1* gene has been studied in detail. The expression of *Nr5a1* is regulated by a number of tissue-specific enhancers that have been identified using reporter mouse lines. Initially, BAC and YAC clones of the NR5A1 gene locus reproduced endogenous NR5A1 expression (Karpova et al., 2005; Stallings et al., 2002). However, these lines maintained expression of the GFP reporter in the XX gonad after 11.5 dpc when endogenous NR5A1 protein is no longer expressed (Hatano et al., 1994; Ikeda et al., 1994; Morohashi et al., 1995; Stallings et al., 2002). Subsequently identification of tissue-specific enhancers using transgenic mice was performed using the reductionist approach of testing regions of the proximal upstream region in transgenic reporter mice. Wilhelm and Englert (2002) demonstrated that a small region of approximately 500 bp could drive transgene expression in the bipotential gonad and that WTI/LHX9 (Lim homeobox protein 9) binding sites in this 500 bp region were required for *Nr5a1* transcription. An *Sf1-LacZ* reporter mouse was generated using a 674 bp fragment of the promoter that included the 500 bp region (Wilhelm and Englert, 2002). Beverdam et al., (2006) subsequently used the 674 bp fragment to recapitulate the expression of NR5A1 in the *Sf1*-eGFP line (this line is extensively used in this thesis; Fig. 1.4). The *Sf1*-eGFP line showed expression in the 10.5-11.5 dpc gonad and GFP expression persisted until at least 14.5 dpc in a variety of XY somatic cells (this line is profiled in detail in Chapter 3). More recently, the fetal Leydig enhancer (FLE) was identified by Shima et al., (2012). This enhancer is responsible for FLC expression of NR5A1; it lies 3.1 kb upstream of the transcription start site, outside the 674 bp region included in the *Sf1*-eGFP line. In addition, a ventromedial hypothalamus enhancer was identified in intron 6, a pituitary gonadotrope enhancer also in intron 6 and a fetal adrenal enhancer was identified in intron 4 ((Shima et al., 2005; Shima et al., 2008; Zubair et al., 2009; Zubair et al., 2006); Fig. 1.4).

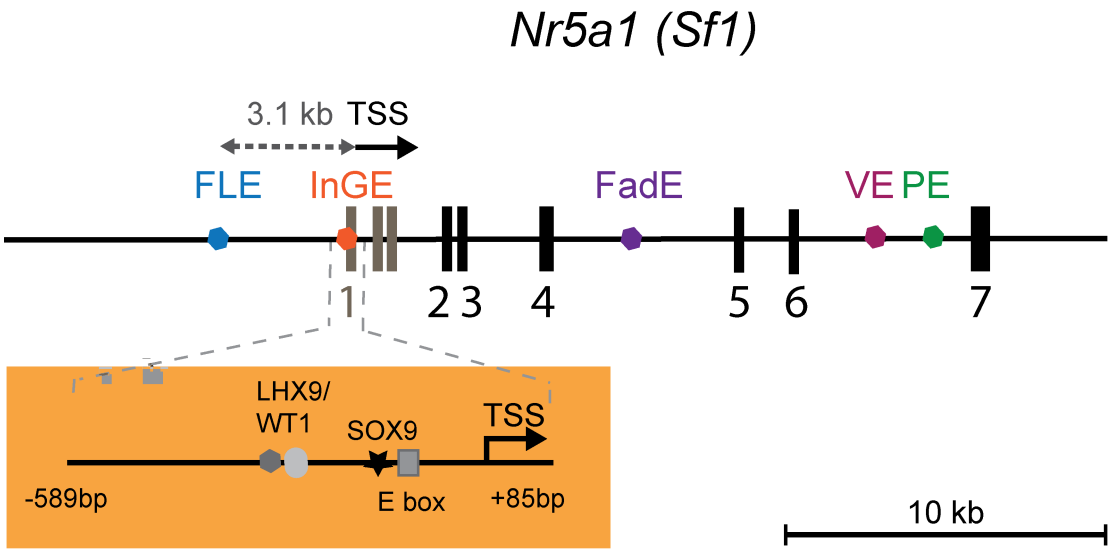

Figure 1.4. Tissue-specific enhancers in the Nr5a1 (Sf1) promoter and gene.

Numerous enhancer regions have been identified within *Nr5a1* and its promoter. Regions controlling expression in the gonad only (InGE), an enhancer specific for fetal adrenal expression (FadE), an enhancer for VMH neuronal expression (VE), a pituitary–specific enhancer (PE) and fetal Leydig cell lineage enhancer (FLE) have been identified. The 674bp promoter fragment driving GFP in the *Sf1*-eGFP mouse used in this thesis (orange region including the InGE enhancer) is gonad specific and excludes the fetal Leydig enhancer (FLE) element, which lies 3.1 kb upstream of the transcription start site (TSS). This region contains LHX9/WT1/SOX9 binding sites and an E-box element that has been shown to be important for gonadal expression of *Nr5a1*.

1.3.2.4 Pathways involved in FLC differentiation

Several signalling pathways and transcription factors have been implicated in FLC differentiation and maintenance. In contrast to Sertoli cells there are no reliable early FLC markers - other than the steroidogenic pathway members, most "markers" of the FLC population mark the entire interstitium that includes both FLCs and NSICs. Indeed, known positive regulators of FLC differentiation are apparently active in the entire interstitium. Therefore, it is unclear what gives the pre-FLC population competency to differentiate into steroid-producing cells and it is difficult to separate these two distinct cell types early in development. The mechanism that determines the differentiation of steroid-producing cells from the cells of the interstitium or the predestination of a cell population to become FLCs is poorly understood.

1.3.2.4.1 Positive regulators of FLC differentiation

For the purposes of categorising FLC knock-out phenotypes, "positive regulators" of FLC function are considered those genes that when knocked out result in restriction of the FLC population. Positive regulators of FLC differentiation include members of the Hedgehog (Hh) and PDGF (platelet derived growth factor) pathways and ARX (Aristaless related homeobox).

In the testis the Hh signalling pathway uses the ligand DHH (desert hedgehog), which is secreted by Sertoli cells, to promote FLC differentiation. The signaling centre of the Hh pathway, the primary cilium, is observed predominately on the interstitial cells of the fetal testis (Wainwright et al., 2014). At 13.5 dpc a primary cilium is present on HSD3β-positive FLCs, NSICs, and in peritubular myoid cells (Wainwright et al., 2014). Unfortunately, the presence of a cilium does not necessarily indicate that these populations are undergoing active Hh signaling (Rohatgi et al., 2009). Nonetheless, the expression of components of the Hh signalling pathway, such as the receptor *Ptch1* (patched homolog-1; (Yao et al., 2002)) and downstream targets of hedgehog signalling, *Gli1* (*glioma-associated oncogene family zinc finger 1*) and *Gli2* (*glioma-associated oncogene family zinc finger 2*), throughout the entire interstitium indicates that Hh signalling is not restricted to the FLC population (Barsoum and Yao, 2011). *Dhh*-/- mice have a FLC differentiation defect, with fewer *Cyp11a1/Hsd3β*-positive and strongly NR5A1-positive interstitial cells present in the *Dhh*-/- XY gonads (Bitgood and McMahon, 1995; Bitgood et al., 1996; Yao et al., 2002). Human patients

with mutations in DHH can present with mixed, partial or pure gonadal dysgenesis or as seemingly unaffected carriers (Canto et al., 2004; Canto et al., 2005; Umehara et al., 2000).

Treatment of 11.5 dpc gonads with cyclopamine, a small molecular antagonist of *Smo* (*Smoothened homolog*), that works by blocking GLI-mediated Hh pathway activation in the absence of Hh ligand, also resulted in a marked reduction in *Cyp11a1*-positive cells. However, *Gli1* and *Gli2* null mice display normal FLC differentiation, indicating functional redundancy between the GLI factors in FLCs (Barsoum and Yao, 2011). In the complementary experiment, ectopic activation of the Hedgehog signalling pathway was achieved by constitutive expression of *Smo* using the *Sf1-Cre* line ("Hh-activated line"), which is active in cells throughout the ovary (Bingham et al., 2006). Ectopic activation of the pathway was sufficient to induce the differentiation of steroidogenic cells within an ovarian environment (Barsoum et al., 2009). These ectopic cells upregulated expression of NR5A1, and its target *Cyp17a1* (cytochrome P450, family 17, subfamily a, polypeptide 1; (Barsoum et al., 2009)), but the identity of the cells marked by the *Sf1-Cre* that differentiated into NR5A1/CYP17A1-positive cells in the XX Hh activated gonads is not clearly established. In the XY Hh activated animals the effect of constitutive Hh activation on the NR5A1-positive cell population has been studied in detail.

Constitutive activation of the Hh pathway activation in NR5A1-positive cells alters the population distribution of NR5A1-positive and HSD3β-positive FLCs during fetal development. FLCs typically transition from being interstitial pre-steroidogenic FLCs which are NR5A1-positive/HSD3β-negative, into FLCs that are NR5A1-positive/HSD3β-positive and, finally, some steroidogenic cells become NR5A1-negative/HSD3β-positive. In the Hh activated model, of the total population of FLCs, approximately 28% more NR5A1-positive FLCs had acquired HSD3β expression than in the control at 13.5 dpc, a pattern that was also observed at 16.5 dpc (18% more) and 18.5 dpc (23% more) (Barsoum et al., 2013). These data indicated that constitutive Hh signaling could prompt precocious maturation of NR5A1-positive pre-steroidogenic FLCs. At 35 dpn there was a decrease in the number of ALCs in the testis, the weight of testis and epididymis and the number of sperm in Hh activated testis but levels of FSH, LH and testosterone were equivalent to the controls (Barsoum et al., 2013). It is unclear how Hh activation in NR5A1-positive cells and precocious development of steroidogenic capacity in FLCs could impact the differentiation of ALCs from NR2F2-positive NSICs.

Another important signalling pathway involved in FLC and ALC development is the PDGF pathway. PDGF receptors, *Pdgfr*α (platelet derived growth factor receptor, alpha polypeptide) and *Pdgfr*β (platelet derived growth factor receptor, beta polypeptide) are expressed in Leydig and theca cells, while PDGF ligands (*Pdgfa*, *Pdgfb*, and *Pdgfc* (platelet derived growth factor a/b/c)) are expressed in the Sertoli cells of the testis cords and the ovarian follicles (Basciani et al., 2002; Gnessi et al., 1995; Loveland et al., 1995; Sleer and Taylor, 2007; Yoon et al., 2006). In rat Leydig cell primary culture systems PDGF ligands can stimulate testosterone production in an LH-dependent context (Loveland et al., 1993; Risbridger, 1993). *In vivo* it was observed that in the *Pdgfrα*-/- testes FLC number is severely diminished. This phenotype was recapitulated by using the an *Sf1-Cre* to achieve a conditional loss of *Pdgfr*α in FLCs and Sertoli cells (Brennan et al., 2003; Schmahl et al., 2008). However, it must be kept in mind that as *Pdgfrα*-/- testes also have defects in proliferation of Sertoli cells and mesonephric cell migration (Brennan et al., 2003), the Leydig cell phenotype may be influenced by Sertoli cell dysfunction. It has also been suggested that the decrease in FLCs may result from a decrease in FLC progenitor proliferation of *Pdgfrα*/*Nr5a1*-positive cells at 11.5 dpc (Griswold and Behringer, 2009). Such a mechanism has yet to be proven but it has been shown that perturbations to the earliest FLC progenitors and NSICs can result in decreased FLC and ALC number later in development (Di Giovanni et al., 2011; Kilcoyne et al., 2014).

In 42 dpn testes conditional loss of *Pdgfr*α using the *Sf1-Cre* resulted in a reduced number of ALCs, indicating that PDGF signaling through *Pdgfr*α is also required for a fully functional ALC population (Schmahl et al., 2008). *Sgpl1* (sphingosine phosphate lyase 1) and *Plekha1* (pleckstrin homology domain containing, family A member 1) are targets of PDGF signaling and are expressed in the testis interstitium (Schmahl et al., 2008). Postnatal *Sgpl1-/-* and *Plekha1-/-* testes had a reduced number of CYP11A1-positive cells at 42 dpn and greatly reduced production of testosterone at 6 weeks and 10 weeks (Schmahl et al., 2008). The authors noted that the *Sgpl1-/-* and *Plekha1-/-* testes looked grossly normal before 20 dpn indicating that FLC were most likely functional, but reduced numbers of CYP11A1-positive FLCs were detected at 7 dpn (Schmahl et al., 2008). Based on these data it was suggested that PDGF signaling may manipulate differentiation of steroidogenic cells or the ability of a cell to acquire steroidogenic capacity (Schmahl et al., 2008).

Arx is an X-linked homeobox gene that is expressed in the forebrain, floor plate and developing gonads (Kitamura et al., 2002; Miura et al., 1997; Miyabayashi et al., 2013). Its loss is associated with X-linked lissencephaly with abnormal genitalia (XLAG or X-linked lissencephaly 2, LISX2; OMIM:300215; (Kitamura et al., 2002)) which is one of a spectrum of developmental lissencephaly disorders. Affected males have hypothalamic dysfunction and ambiguous genitalia characterised by small testes and penis (Bonneau et al., 2002; Dobyns et al., 1999; Kitamura et al., 2002; Ogata et al., 2000). *Arx* is strongly expressed in the interstitium of the testis, in peritubular myoid cells, vascular endothelial cells, and interstitial fibroblast-like cells (presumptive NSICs), but has not been detected in Sertoli, Leydig and germ cells (Kitamura et al., 2002; Miyabayashi et al., 2013). Some ARX-positive cells are also detected within the XX gonad (Miyabayashi et al., 2013). *Arx-/-* XY gonads were characterised by a dysplastic interstitium, where the number of HSD3β-positive cells was severely diminished (Kitamura et al., 2002) despite the fact that *Arx* is expressed HSD3β-negative interstitial cells. It was noted that the number of HSD3β-positive cells was variable between individuals (Kitamura et al., 2002). Together these data suggest that ARX may have an indirect role in restricting/bestowing FLC progenitor competency (Miyabayashi et al., 2013). Interestingly, a detailed expression analysis by Miyabayashi et al. (2013) demonstrated that although ARX-positive cells were predominately NR5A1-negative, a small number of NR5A1-positive cells were also ARX-positive and could transition into HSD3β-positive FLCs. As HSD3β-positive cells have been shown to have a very low rate of proliferation compared to other testicular cells types (Miyabayashi et al., 2013; Orth, 1982). It was posited that the *Arx-/-* gonadal phenotype was due to either an early pre-steroidogenic pre-FLC pool proliferation defect or some sort of restriction of FLC fate attainment in the early FLC progenitor pool which is presumably mediated by NSICs.

In some cases early steroidogenic capacity and associated gene expression can be attenuated without a change to, or with recovery of, the FLC population number relative to testis size. *Tgfbr3 (transforming growth factor, beta receptor III/betaglycan)* is a co-receptor for the TGFβ-superfamily of ligands which includes TGFβ, inhibins and BMPs. TGFBR3 is expressed in CYP11A1-positive FLCs cells and peritubular myoid cells of XY gonad at 14.5 dpc (Sarraj et al., 2007). In *Tgfbr3-/-* XY gonads the testis cord architecture is disrupted; the basal lamina surrounding the cords is discontinuous, the arrangement of the Sertoli cells in the cords was not uniform and expression of Sertoli cell marker genes such as *Amh* is greatly decreased from 13.5 dpc (Sarraj et al., 2010). Notably expression of the genes encoding *Dhh* and *Nr5a1* is decreased at 14.5

dpc but not at 12.5 dpc in the *Tgfbr3-/-* XY gonads (Sarraj et al., 2010). Expression of the genes encoding markers of the steroidogenic pathway, such as *Cyp11a1* and *Star,* are decreased from 12.5 dpc when there is an apparent decrease in the CYP11A1-positive cell population. However, although FLC function remains apparently compromised, at 14.5 dpc the number of FLCs per gonad or interstitial area unit in the *Tgfbr3-/-* XY gonads had recovered and was equivalent to that of the wild-type (Sarraj et al., 2010). Whether the attenuation of steroidogenesis in this model has an effect on later testis development, or whether the recovery of the phenotype is due to other TGFβ signaling pathway members being able to rescue FLC differentiation, is unknown.

1.3.2.4.2 Negative regulators of FLC function

For the purposes of categorising FLC knock-out phenotypes, "negative regulators" of FLC function are considered those genes that when knocked out result in an expansion of the FLC population. Negative regulators of FLC differentiation include the transcription factor TCF21 (POD-1, transcription factor 21) and members of the Notch pathway.

Tcf21 is a basic helix-loop-helix transcription factor with multiple roles in embryonic development (Quaggin et al., 1998). The *Tcf21-/-* XY embryo has multiple urogenital defects including feminised external genitalia. This phenotype is likely the result of the *Tcf21-/-* XY embryo having small, poorly organised, undescended testis (Cui et al., 2004; Quaggin et al., 1998; Quaggin et al., 1999). Embryonically *Tcf21* is expressed throughout the testis interstitium, particularly around the coelomic epithelium from 10.5 dpc (Cui et al., 2004; Tamura et al., 2001). Fetal *Tcf21-/-* XY gonads have an increased number of FLCs, indicating that *Tcf21* may be involved in restriction of FLC differentiation (Cui et al., 2004). *In vitro* studies have demonstrated that TCF21 can suppress expression of the gene encoding *Nr5a1,* indicating that the mechanism by which it restricts FLC differentiation may be in restricting expression of *Nr5a1* (França et al., 2013). From 11.5 dpc in XY *Tcf21-/-* UGRs there is an expansion of NR5A1-positive cells in the coloemic and gonad-mesonephric border regions (Cui et al., 2004). With the expansion of NR5A1-positive cells, the population of *Cyp11a1*-postive cells differentiates precociously at 11.5 dpc and is expanded later. It was proposed that the ectopic expression of NR5A1 forced a larger population of NSICs to aberrantly commit to becoming FLCs (Cui et al., 2004). Whether this expanded population of cells is directly derived from the precocious *Nr5a1*-positive cells or whether they can produce later FLC products such as HSD3β and INSL3 is unknown. Notably at 13.5 dpc, nuclear NR5A1 and

cytoplasmic *Tcf21-LacZ* do not appear to colocalise in the same cells in the testis interstitium (Cui et al., 2004).

The NOTCH pathway also apparently acts to restrict differentiation of FLC progenitors. The four Notch receptors bind *delta-like* or *jagged* (e.g. *Jag1* (*jagged 1*)) ligands to activate the pathway. The most well defined targets of the NOTCH signaling pathway are the genes encoding the basic helix-loop-helix transcription factors *Hes1* and *Hes5* (*hairy and enhancer of split 1/5*). *Notch1* is expressed in the vasculature of the XY gonads, whereas expression of *Jag1, Notch2* and *Notch3* are restricted to the interstitium at 13.5 dpc (*Notch 2* is expressed in the Sertoli cells at 12.5 dpc; (Brennan et al., 2002; Tang et al., 2008)). *Hes1* expression is restricted to the interstitium, while *Hes5* is expressed in the Sertoli cells at 13.5 dpc (Tang et al., 2008), indicating NOTCH signalling is activated in the Sertoli and interstitial cell populations. The activation of the NOTCH pathway using the *Sf1-Cre* does not affect the differentiation of the Sertoli cell population, but cord formation is stunted (Tang et al., 2008). Deletion of the NOTCH pathway target *Hes1* in XY gonads was used to model inhibition of the NOTCH pathway. Notably, germ cells and cord structure is adversely affected even though *Hes1* is not expressed in these populations (Tang et al., 2008). In the interstitium, both *in vitro* (DAPT compound treatment) and *in vivo* (*Hes1-/-*) inhibition of the NOTCH pathway resulted in an increased number of FLCs in the testis but no change to Sertoli cell number (Tang et al., 2008). Likewise, conditional deletion of the ligand *Jag1* in interstitial and perivascular cells resulted in a decrease in the number of VCAM1-positive (vascular cell adhesion molecule 1) NSICs and a dramatic increase in HSD3β-positive cells at 14.5 dpc (Defalco et al., 2013), mirroring the phenotype of the *Hes1-/-* testis. Conversely, constitutive activation of the NOTCH pathway in *Nr5a1*-positive FLC and Sertoli cell precursors from 11.5 dpc resulted in maintenance of interstitial undifferentiated LHX9-positive progenitor cells (presumptive NSICs) and a decrease in HSD3β-positive FLCs. These data indicate that the NOTCH pathway somehow mediates transitions between NSIC, pre-FLC and steroidogenic FLC fate.

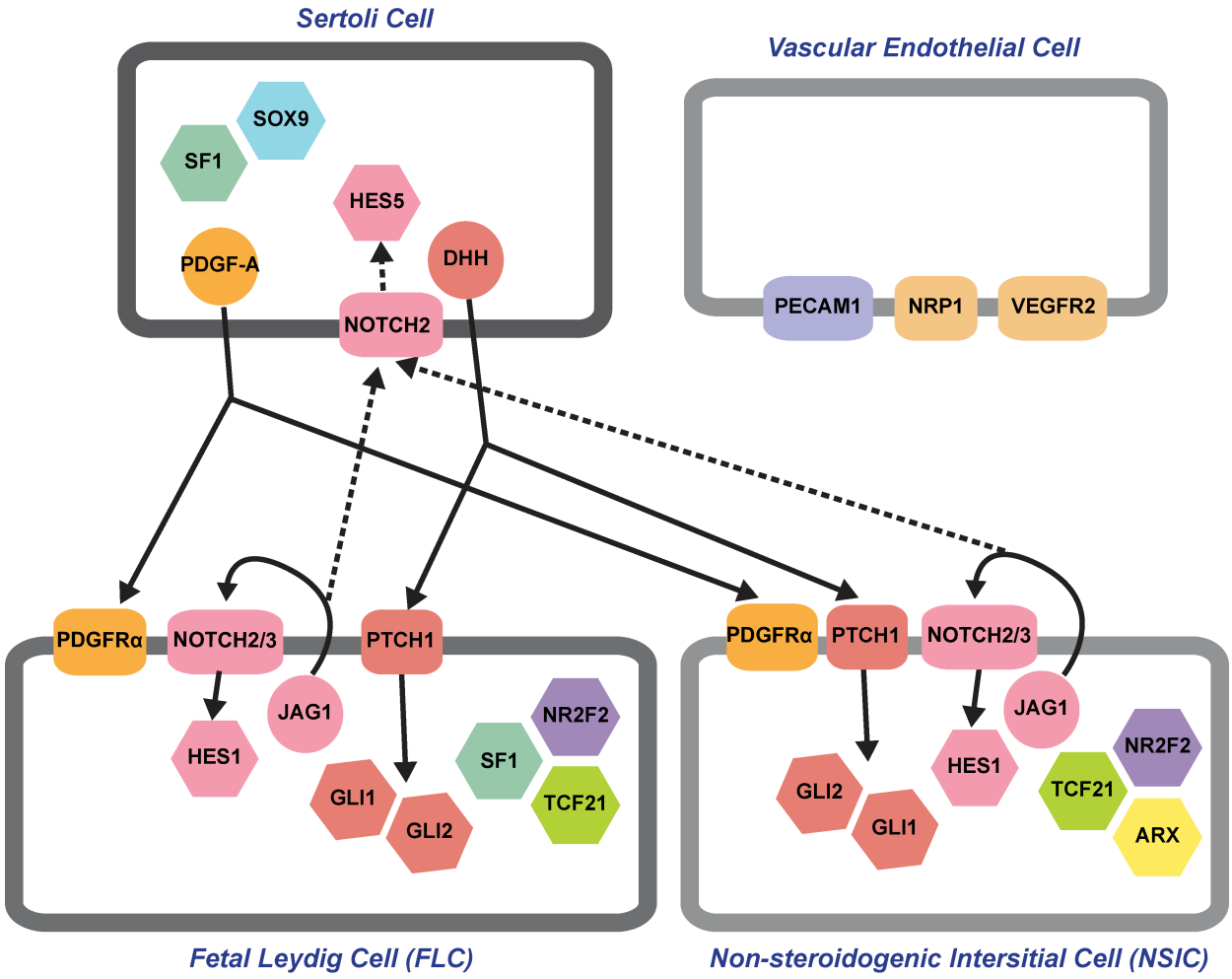

Figure 1.5. The characteristics of FLCs and NSICs at 12.5 dpc as currently published.

To date we know of few differences between FLCs and NSICs. The major difference defined between FLCs and NSICs is the expression of the transcription factors (hexagon) ARX in NSICs and NR5A1 in FLCs (NR5A1 is also expressed in SOX9-positive Sertoli cells). NR2F2 and TCF21 are apparently expressed in FLCs and NSICs. Sertoli cells produce the secreted factors (circles) PDGFA and DHH that promote FLC differentiation. However, the receptors PDGFRα and PTCH1 (rounded rectangles) are expressed on NSICs and FLCs (as are downstream products of Hh signaling GLI1 and GLI2). The Notch pathway is active in the fetal testis with NOTCH2/3 expressed on NSICs and FLCs (NOTCH2 is also observed in Sertoli cells). The Notch pathway ligand JAG1 is expressed by NSICs and FLCs, as is the downstream target HES1 (HES5 is expressed in Sertoli cells). The characteristics of vascular endothelial cells are not well defined; markers include PECAM1, NRP1 and VEGFR2 (KDR).

1.3.3 The rest of the interstitium

The interstitium of the testis is comprised of the cells excluded from the testis cords. The most well-defined cell lineage of the testis interstitium is the FLC population. However, the interstitium also includes non-steroidogenic interstitial cells (NSICs), vascular endothelial cells, macrophages and other cell types and lineages that have yet to be defined, as discussed below.

1.3.3.1 ARX-positive and NR2F2-positive NSICs

ARX and NR2F2 are emerging as important transcription factors that affect Leydig cell differentiation. As discussed above, the role of ARX is unusual among previously identified regulators of steroidogenic fate. Nuclear expression of ARX is observed in the peritubular myoid cells lining the testis cords and the NR5A1-negative interstitial cells of the testis. In *Arx-/-* testis, the testis cords formed appropriately and SOX9-positive cell number was maintained but there was decreased numbers of NR5A1/HSD3β-positive interstitial cells (Miyabayashi et al., 2013). The result of this FLC loss at 18.5 dpc in *Arx-/-* testis is undescended testes, likely due to a decrease in *Insl3* expression, a decrease in intratesticular testosterone levels and a dysmorphic coelomic vessel (Miyabayashi et al., 2013). Expression of testicular pathway genes such as *Dhh, Ptch1* and *Pdfrα* was unaffected in the XY *Arx-/-* gonad, indicating that these pathways were not perturbed by loss of ARX. Conversely, in masculinised XX *Wnt4-/-*gonads, WT1-positive interstitial cells were maintained later in development and *Arx* expression was expanded (Miyabayashi et al., 2013). What makes the effect on FLCs unusual is the fact that ARX is expressed in NSICs. It has been speculated that loss of ARX in NSICs must somehow affect the early FLC progenitor pool presumably by preventing attainment of steroidogenic capacity.

A similar expression pattern to ARX can be observed for NR2F2 at 18.5 dpc (Kilcoyne et al., 2014; Miyabayashi et al., 2013). Recently it has emerged that NR2F2-positive non-FLC interstitial cells in the embryonic testis give rise to ALCs later in life (Kilcoyne et al., 2014). Expression of *Nr2f2* in the interstitium of the testis was noted from 13.5 dpc (Pereira et al., 1995; Pereira et al., 1999) but loss of *Nr2f2* is embryonic lethal at 10 dpc due to cardiovascular defects (Pereira et al., 1999) precluding the study of gonadogenesis without a suitable conditional/inducible system. Interestingly, SHH (Sonic hedgehog) was found to regulate expression of *Nr2f2* in neurons (Krishnan et al., 1997a; Krishnan et al., 1997b). Considering that all Hh ligands act through

PTCH1, which is expressed on the surface of FLCs and NSICs, it is plausible that DHH, which is required for differentiation of the FLC population, may also have an effect on the NSIC population, conceivably by upregulating *Nr2f2* expression (Martin and Tremblay, 2010).

Prepubertal ablation of NR2F2 at 14 dpn in XY mice results in infertility, hypogonadism and spermatogenic arrest as a result of reduced testosterone biosynthesis (Qin et al., 2008). NR2F2 was found to be essential for progenitor ALC formation and maturation into functional ALCs. Leydig cell function and reproduction were unaffected by ablation of NR2F2 mature ALCs indicating that NR2F2 is not required for the maintenance of ALCs but is required for their formation from progenitor cells (Qin and Bishop, 2005). Subsequently it was demonstrated that cells that are NR2F2-positive in the 18.5 dpc testis are the cells that give rise to the ALCs (Kilcoyne et al., 2014). NR2F2 is the first identified transcription factor intrinsic to ALC function that also plays an essential role in the maturation of progenitor ALCs during fetal life. The presence of NR2F2-positive cells in the developing testis provides the first evidence that levels of testosterone during fetal gonadogenesis and masculinisation can "program" the final adult testosterone levels by effecting the NR2F2-positive "ALC progenitor cells", which are the source of testosterone after puberty.

Treatment of rat embryos with dibutyl phthalate (DBP) or dexamethasone diethylstilbestrol (DES) induces masculinisation defects such as hypospadias and cryptorchidism in a dose-dependent manner. Van den Driesche et al. (2012) showed that treatment of rat embryos with DBP or DES results in defects in the production of testosterone by the FLC population but that FLC number remains unchanged. This phenotype is possibly due to a decrease in transcription of steroidogenic genes that are regulated by the transcription factor NR5A1. However, while expression of the genes encoding *Cyp11a1*, *Star* and *Cyp17a1* was reduced in DBP treated testis the expression of the gene encoding *Hsd3β* was unaltered (van den Driesche et al., 2012). The genes *Cyp11a1*, *Star* and *Cyp17a1* all have dual NR5A1/NR2F2 binding sites in their promoter regions while *Hsd3β* has only an NR5A1 binding site (van den Driesche et al., 2012). Therefore it has been proposed binding of NR2F2 and NR5A1 may be disrupted by DBP treatment (van den Driesche et al., 2012). In the rat testis, at 15.5 dpc 85% of NR2F2-positive interstitial cells are also HSD3β-positive, by 19.5 dpc only approximately 20% of cells are HSD3β/NR2F2-positive. At 21.5 dpc in rat testis NR2F2 is not expressed in FLCs in the wild type testis, but exposure to DBP resulted in ectopic expression of NR2F2 in the FLCs in a dose dependent manner. Unlike in the rat, in mice exposure to DBP does

not result in a decrease of steroidogenic gene expression (van den Driesche et al., 2012). Additionally, exposure to DBP does not result in an increase in NR2F2/HSD3β-positive cells at 18.5 dpc (equivalent to 21.5 dpc in rats). On the other hand exposure to DES results in a 28% increase in the number of HSD3β/NR2F2-positive cells at 18.5 dpc. However, in mice the expression of NR2F2 in the testis has not been characterised in detail throughout gonadogenesis. Therefore, whether NR5A1 and NR2F2 could act together to transcriptionally activate steroidogenic genes in murine FLCs has not been substantiated.

1.3.3.2 Vasculature: blood vasculature and lymphatic vasculature

A functional vasculature network is important for the delivery of oxygen, hormone and nutrients, and for the removal of waste. The role of the gonads as endocrine organs also requires a functional vasculature network to facilitate the delivery and circulation of hormones to the rest of the embryo. In the process of gonadogenesis, the formation of the vasculature is important for the overall architecture and development of the testis. On the other hand, lymphangiogenesis, the formation of the lymphatic network, occurs much later in gonadal development after the architecture of the testis is mostly established.

Vascular patterning in the gonad is a sex-specific process (Brennan et al., 2002). Testis vasculature is formed by migration of endothelial cells into the developing testes (Combes et al., 2009b; Cool et al., 2008). At 10.5-11.5 dpc microvessels extend from the mesonephric vasculature plexus into the gonadal tissue in both the XX and XY gonad (Coveney et al., 2008a). Unlike the ovary, in the testis the early vasculature network develops by a non-angiogenic process whereby the endothelial cells migrating from the mesonephric vascular plexus are rearranged into the new network (Brennan et al., 2002; Bullejos et al., 2002; Coveney et al., 2008a). By 12.5 dpc a prominent artery known as the coelomic vessel can be seen along the anterior–posterior length of the testis, in addition to extensive microvasculature network in the testis interstitum. Ectopic masculinised vascular networks reminiscent of the coelomic vessel are observed in gonads of XX mice mutant for *Rspo1* (R-spondin homologue 1), *Wnt4*, *Fst* (follistatin) and *Ctnnb1* (catenin beta 1; (Chassot et al., 2008; Jeays-Ward et al., 2003; Liu et al., 2009; Tomizuka et al., 2008; Yao et al., 2004)). *Rspo1* is a regulator of WNT4 signalling that involves *Ctnnb1*, while *Fst* (*follistatin*) is downstream of WNT4 (Tevosian and Manuylov, 2008), implicating the WNT signalling pathway in vessel formation and patterning (Coveney et al., 2008b). Additionally, overexpression of *Wnt4* disrupts normal testis

vasculature, indicating that WNT4 inhibits formation of gonad vasculature (Jordan et al., 2003). Notably, where testis vasculature is disrupted, as in the WNT4 overexpressing mice, Sertoli and FLCs still differentiate (Jeays-Ward et al., 2003; Jordan et al., 2003), but several models have disruptions in both testis cord formation and vascular network development (Brennan et al., 2003; DeFalco et al., 2014; Yao et al., 2006), indicating that the two processes are interdependent.

Vascularisation of the testis has been shown to play an important instructive role in testis cord formation (Combes et al., 2009b; Cool et al., 2008; Cool et al., 2011). The vascular endothelial cells of the early testis express markers such as PECAM1 (which is also expressed in germ cells), NRP1 (neuropillin 1) and VEGFR2 (KDR, kinase insert domain protein recptor; vascular endothelial growth factor receptor 2; (Cool et al., 2011)). When endothelial migration was suppressed in testes by blocking vascular endothelial growth factors with VEGF-Trap or by using an antibody against vascular endothelial cadherin, testis cord morphogenesis was impaired (Combes et al., 2009b; Cool et al., 2011). Antagonising vessel maturation also reduced proliferation of interstitial mesenchymal cells that appear to segregate the precursor territories for testis cords; this proliferation could be rescued by the addition of platelet derived growth factor isoform BB (PDGF-BB; (Combes et al., 2009a; Cool et al., 2008; Cool et al., 2011)). However, the mechanisms governing testis vascularisation and cord segregation are still unclear. Likewise the mechanisms governing the invasion of the venous vasculature network into the testis are not well studied. Some evidence suggests that the venous vasculature network also is derived from the mesonephros, perhaps following the establishment of the arterial vascular network (Brennan et al., 2002; Coveney et al., 2008a).

Alongside the blood vascular network exists the lymphatic vascular network, which acts to maintain tissue fluid homeostasis. PROX1 (prospero homebox 1) is a marker of lymphatic vessels. Using a *Prox1-LacZ* reporter lymphatic vessels have been detected along the gonad–mesonephric border from 13.5 dpc, but the lymphatic vessels only invaded the testis proper at around 18.5 dpc (Brennan et al., 2002; Wigle and Oliver, 1999). A more recent study using a *Prox1*-eGFP reporter mouse found that lymphangiogenesis in the testis begins at 17 dpc (Svingen et al., 2012). The invading vessels originated from the pre-existing lymphatic network residing along the mesonephric region (Svingen et al., 2012). Notably the lymphatic vessels did not penetrate deep into the testis: vessels only penetrated immediately inferior to the tunica albuginea (Svingen et al., 2012). This observation

was consistent with previous data describing the invasion of the lymphatic vasculature network into murine testes (Hirai et al., 2012).

1.3.3.3 Macrophages

In the postnatal and adult testis macrophages may compose approximately 25% of the interstitial cells population and are important for Leydig cell functionality, but the role of macrophages in the fetal testis has remained unexplored until recently (for review see Svingen and Koopman, 2013). Postnatally, interstitially residing testicular macrophages form close associations with Leydig cells (Christensen and Gillim, 1969; Hutson, 1990; Miller et al., 1983). Indeed macrophages can even influence the steroidogenic capacity of ALCs by secreting cholesterol compounds that the ALCs can use to synthesise testosterone (Lukyanenko et al., 2000; Lukyanenko et al., 2001; Nes et al., 2000).

Recently the role of macrophages in fetal testicular development has been explored. De Falco et al. (2014) found that from 10.5 dpc macrophages cluster along the gonad–mesonephros vasculature plexus. Macrophages later clustered along the expanded vascular plexus, around the coelomic vessel and alongside the vascular branches invading and enwrapping the testis. In the fetal testis a regular and ordered series of testis cords are formed by 13.5 dpc and migration of endothelial cells into the testis is required for the formation of the cords (Combes et al., 2009a; Combes et al., 2009b). As discussed previously, this was demonstrated by using a VE-cadherin antibody to block endothelial cell migration and vascular organisation which in turn disrupted the formation of the testis cords (Combes et al., 2009b). DeFalco et al. (2014) found that macrophages were found to be often directly associated with the gonadal endothelial cells and expressed endothelial markers such as VEGF (vascular endothelial growth factor). Indeed, localisation and migration of macrophages into the XY gonad was shown to be dependent on the process of VEGF-mediated vascularisation by blocking VEGF signaling using a VEGFR (VEGF receptor) small molecule inhibitor (a cord phenotype was not reported). In 13.5 dpc testes specifically depleted of macrophages there were also fewer resident endothelial cells, a poorly organised coelomic vessel and an enlarged mesonephric vascular plexus (DeFalco et al., 2014). In macrophage-depleted testis (approximately 95% depletion), while basic partitioning of the cord elements from the interstitial space occurred, the cords that formed were irregular (DeFalco et al., 2014). Together these data indicate that the combined invasion of endothelial cells with associated macrophages is important for testicular vascularisation, cord formation and partitioning of the testis.

1.4 Ovarian Differentiation

1.4.1 Three patterns and three populations of somatic cells in ovarian development

In contrast to the cord-level structural organisation seen in the testis at 12.5 dpc, the ovary is a mixture of both somatic and clustered germ cells during fetal life. The characterisation of different somatic lineages in the ovary is limited. During postnatal life the ovary regionalises and follicular granulosa cells surround the matured germ cells, the oocytes. However, the regionalisation of the fetal ovary and the specification of the different cell lineages are poorly understood.

There is a suite of genes that are important for ovarian development including *Wnt4* (Vainio et al., 1999), *Rspo1* (Chassot et al., 2008; Parma et al., 2006) and *FoxL2* (Ottolenghi et al., 2005; Schmidt et al., 2004). All these genes can be used as markers of pre-granulosa cells and as readouts of the ovarian pathway. Recently it has been demonstrated that the ovary can be regionally classified by expression of granulosa cell marker genes showing that the population of somatic cells at or adjacent to the coelomic epithelium are distinct from the cells adjacent to the mesonephros (Chen et al., 2012). Chen et al. (2012) identified three spatial expression patterns displayed by somatically-expressed ovarian genes: (1) expression across the gonad from the mesonephros, which goes on to form the ovarian medulla, up to a few cell layers from the coelomic epithelium, which goes on to form the ovarian cortex (genes include *Fst, FoxL2* and *Wnt4*); (2) genes expressed throughout the developing ovary, including the coelomic epithelium (genes include *Rspo1* and *Irx3* (iroquois related homebox 3)) and (3) a gradient of expression across the gonad with higher expression at the side of the coelomic epithelium and weaker expression towards the mesonephros (genes include *Bmp2* (bone morphogenetic protein 2); Fig. 1.6A). Based on gene expression, another study has classified the somatic cell lineages of the ovary into four somatic lineages: vasculature; vascular-associated; somatic coelomic epithelial and pre-granulosa cell populations ((Maatouk et al., 2012); Fig. 1.6B). More recently, a study identified three distinct somatic cell lineages in the ovary marked by mutually exclusive expression of LGR5, FOXL2 or NR2F2 ((Rastetter et al., 2014); Fig. 1.6C).

It is clear that there are two classes of pre-granulosa cells in the fetal mouse ovary (Mork et al., 2011; Rastetter et al., 2014; Zheng et al., 2014). One class of pre-granulosa cell is characterised by the expression of FOXL2 early in development; these cells are destined to become the granulosa cells of medullary follicles (Mork et al., 2011) which mature before puberty. These follicles are

important for the onset of puberty and early fertility (Zheng et al., 2014). A different class of pre-granulosa cells do not express FOXL2 and contribute to the cortical follicles. These cortical granulosa cell precursors are characterised by expression of LGR5, an RSPO1 receptor (Mork et al., 2011; Rastetter et al., 2014). In the developing ovary, WNT4 and RSPO1 signaling upregulates expression of the gene encoding *Lgr5*, which is required for germ cell differentiation (Rastetter et al., 2014). The cortical follicles progressively mature and constitute the reproductive pool of primordial follicles for the individual throughout their reproductive life (for review see Monget et al., 2012). Granulosa cells surrounding follicles residing in the medulla and cortex all express FOXL2 postnatally (for review see Pisarska et al., 2011).

In the fetal ovary, vasculature-associated somatic cells are marked by MAFB expression (Maatouk et al., 2012). In the testis MAFB marks the interstitial and FLC population (DeFalco et al., 2011). Presumably, MAFB also marks some somatic cells in the ovary (Jameson et al., 2012b; Maatouk et al., 2012). As NR2F2 is also expressed by the testis interstitium and is important for ALC differentiation (Kilcoyne et al., 2014; Qin et al., 2008), it is possible that NR2F2 marks the counterparts to the Leydig cells in the developing ovary, the steroidogenic theca cells. The theca cells first produce steroids after birth in the preantral follicle (Palermo, 2007). Currently it is hypothesised that the follicular granulosa cells, the Sertoli cell counterparts, produce signals that stimulate the differentiation of theca cells from the interstitium, similar to how molecules such as DHH promote FLC differentiation in the testis (Yao and Capel, 2002; Young and McNeilly, 2010). No markers of the embryonic theca progenitor cell population have yet been identified.

Therefore, the fetal mouse ovary contains at least three different somatic cell types that can be identified early in ovarian development: precursors for medullary granulosa cells, FOXL2-positve cells; precursors for cortical granulosa cells, LGR5-positive cells and presumptive pre-theca cells, NR2F2-positive cells. Whether there is overlap between expression of WT1 or MAFB and expression of markers such as NR2F2 and LGR5 is unknown. Identifying additional cell-lineage specific markers will provide new tools investigate the development and maturation of the ovary.

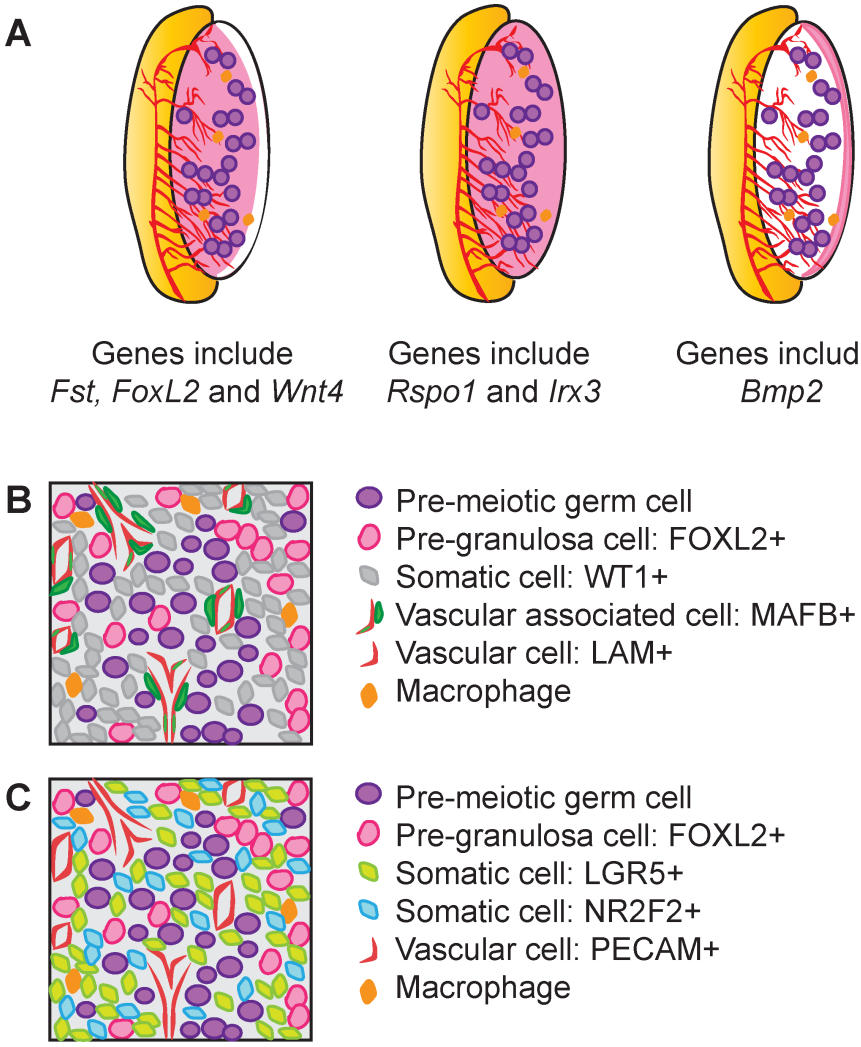

Figure 1.6. The cell lineages of the fetal ovary.

(A) An *in-situ* hybridization screen of 13.5 dpc XX embryos for somatic cell marker genes identified three different expression domains: (1) genes expressed across the gonad up to a few cell layers from the coelomic epithelium; (2) genes expressed through the developing ovary and (3) genes expressed in a graded expression across the gonad with weaker expression near the mesonephros (Chen et al., 2012). A series of somatic subpopulations have been defined using different marker genes. Three studies have shown that FOXL2-positive and vascular endothelial cells form only a subpopulation of the somatic cells of the developing ovary (Maatouk et al., 2012; Mork et al., 2011; Rastetter et al., 2014). The remaining somatic cell population was classed as (B) WT1-positive with vascular associated MAFB-positive cells (Maatouk et al., 2012) or (C) LGR5-positive and NR2F2-positive (Rastetter et al., 2014). Whether any WT1- and MAFB-positive cells are also LGR5- or NR2F2-positive is unknown. (LAM, laminin; PECAM1, platelet/endothelial cell adhesion molecule 1)

1.4.2 Pathways that influence ovarian development

In the absence of SRY and SOX9 expression or in XX individuals, the transcriptional networks responsible for ovarian development are triggered. Several genes have been identified as key players in ovarian development but no ovarian-determining factor has yet been identified. β-catenin signaling is a key player in ovarian determination/differentiation and WNT4, FST and RSPO1 are secreted positive effectors of β-catenin signaling and expression. In each of the XX *Wnt4 -/-, Fst-/-* and *Rspo1-/-* models there are gross functional defects in ovarian development (Chassot et al., 2008; Vainio et al., 1999; Yao et al., 2004)).

In humans, duplication of a section of chromosome 1p, which includes the *WNT4* gene, leads to 46,XY male-to-female sex reversal (Jordan et al., 2001). In mouse, the *Wnt4-/-* ovary is masculinised but not sex reversed. *Wnt4* is expressed in the 11.5 dpc gonad in both sexes but expression of *Wnt4* is only maintained in the ovary (Vainio et al., 1999). Notably, *Wnt4* expression is maintained in the mesonephros of both sexes. The expression of NR5A1 in XX and XY *Wnt4-/-* gonads during early gonadogenesis is abnormal (Jeays-Ward et al., 2003). This may contribute to phenotypes later in development where ectopic CYP11A1-positive cells and masculinised vascular structures form in *Wnt4-/-* ovaries (Heikkila et al., 2005; Vainio et al., 1999). Postnatally, testosterone production can be detected in *Wnt4-/-* XX animals (Heikkila et al., 2005), but classic hallmarks of ovotesticular development such as the differentiation of Sertoli cells do not occur. Jameson et al. (2012a) demonstrated that in *Wnt4-/-/Fgf9-/-* XX gonads masculinised vasculature and steroidogenic cells were present at 16.5 dpc; these masculinised features were observed in *Wnt4-/-* but not *Fgf9-/-* XX control gonads. These data indicate that FGF9 is not an essential player in the ectopic masculinisation of the *Wnt4-/-* XX gonad. This conclusion was supported by the observation that conditional loss of the FGF9 receptor *Fgfr2* in endothelial cells did not impact the formation of the masculine vasculature network in the XY gonad. In *Wnt4-/-* XY gonads Sertoli cell differentiation and testis cord structure is compromised (Jeays-Ward et al., 2003; Jeays-Ward et al., 2004; Vainio et al., 1999). In one mouse model of *Wnt4* overexpression in the XY gonad, masculine vasculature networks are disrupted and testosterone synthesis is repressed possibly through action of WNT4 on *Nr5a1* and β-catenin mediated signaling pathways (Jordan et al., 2003).

Rspo1 is expressed in the FOXL2-positive XX somatic cells of the gonad (Chen et al., 2012; Parma et al., 2006; Rastetter et al., 2014) while the putative RSPO1 receptor, LGR5 is expressed in the

FOXL2-negatitve somatic pre-granulosa cells (Rastetter et al., 2014). In *Rspo1-/-* ovaries differentiation of Sertoli cells does not occur, but there is a failure to upregulate the expression of the gene encoding *Wnt4* and subsequent WNT4 target gene expression (Tomizuka et al., 2008). Additionally, in the *Rspo1-/-* ovary, the male Wolffian duct fails to regress, ectopic steroidogenic cells differentiate and a masculinised vasculature forms, features reminiscent of the *Wnt4-/-* ovary (Tomizuka et al., 2008). In germ cells RSPO1 regulates WNT/β-catenin signaling such that in the *Rspo1-/-* ovary there is also an impediment that prevents germ cells from entering meiosis at 14.5 dpc as they would in the wild-type (Chassot et al., 2008; Tomizuka et al., 2008).

The β-catenin-associated WNT4/RSPO1 pathway can influence the expression of TGFB pathway components such as *Fst*, which encodes a secreted TGFβ pathway inhibitor. The *Fst*-/- ovary shares many similarities with the *Rspo-/-* and *Wnt4*-/- ovary. In *Wnt4*-/- XX gonads, expression of the gene encoding *Fst* is lost, explaining the similarities between loss-of-function models in this pathway (Yao et al., 2004). Like *Wnt4-/-* XX gonads, the *Fst-/-* XX gonads also develop a masculinised vessel network around 12.5 dpc, but unlike in *Wnt4-/-* and *Rspo1-/-* ovaries no *Cyp11a1*-positive ectopic cells are observed (Tomizuka et al., 2008; Vainio et al., 1999; Yao et al., 2004). At birth there is widespread germ cell loss in *Wnt4-/-* XX gonads; in *Fst-/-* XX gonads, germ cells begin apoptosing at around 16.5 dpc, which results in widespread loss of germ cells by birth (Vainio et al., 1999; Yao et al., 2004).

Due to the importance of the WNT/β-catenin pathway in ovarian development, a knock out of *Ctnnb1,* the gene that encodes β-catenin, in NR5A1-positive cells has been generated by Liu et al. (2009) using *Sf1-Cre,* which is active throughout the ovary (Bingham et al., 2006). The effect of removing functional β-catenin in the somatic ovarian cells was a downregulation of the expression of the genes encoding *Wnt4* and *Fst,* but not *Rspo1* (Liu et al., 2009). Therefore, functionally β-catenin appears to act upstream of *Wnt4* and *Fst*, but downstream of *Rspo1,* in agreement with the observation that in *Rspo1-/-* XX gonads *Wnt4* and *Fst* expression is downregulated. No expression of testicular pathway genes such as *Sox9* was detected, but similar to the *Rspo1-/-, Wnt4-/-* and *Fst-/-* knockouts*,* β-catenin ablation in the XX gonad resulted in the formation of a masculinised vascular network and loss of germ cells (Liu et al., 2009). These data implicate β-catenin in the process of vascular remodeling and germ cell survival in all these scenarios. As in the *Wnt4-/-* and *Rspo-/-* XX gonads, clusters of *Cyp17a1*-positive steroidogenic cells were also observed in the β-catenin ablated XX gonads, indicating that this phenotype may also be mediated by β-catenin.

Notably, the β-catenin ablated XX gonads did not express *Insl3* and although there was retention of the Wolffian duct and its derivatives, the external genitalia presented similar to the wild-type XX individual.

FOXL2 is the earliest granulosa cell marker to appear in the developing ovary and seems to act independently of the WNT/β-catenin signaling pathway. It is expressed from 12.5 dpc in a subpopulation of somatic cells during development before being expressed in cortical and medullary granulosa cells in adulthood (Loffler et al., 2003; Ottolenghi et al., 2005; Rastetter et al., 2014; Schmidt et al., 2004). In humans, mutations in *FOXL2* cause BPES and premature ovarian failure (OMIM:110100/608996; (Crisponi et al., 2001; De Baere et al., 2003)). BPES is characterised by dysplasia of the eyelids and can also be associated with premature ovarian failure. Notably, there is clinical variation in the presentation of premature ovarian failure associated with FOXL2 mutations (De Baere et al., 2003; De Baere et al., 2001). Eyelid and craniofacial development is affected in the *FoxL2-/-* mouse and in XX animals ovarian development and fertility are perturbed, recapitulating the phenotypes seen in humans (Ottolenghi et al., 2005; Schmidt et al., 2004; Uda et al., 2004). In *FoxL2-/-* XX gonads defects in granulosa cell differentiation leads to premature depletion of the pool of primordial follicles which results in oocyte atresia and infertility (Schmidt et al., 2004; Uda et al., 2004).

Using a tamoxifen-inducible Cre/loxP system it has been demonstrated by Uhlenhaut et al. (2009) that the expression of FOXL2 in the postnatal ovary is required to prevent transdifferentiation of ovarian cells into testicular-like cell types. In the ovary of the XX *FoxL2-/-*, and in the induced deletion of *FoxL2* (where at 56 dpn/8 weeks *FoxL2* was deleted in the ovarian follicles), robust upregulation of a series of testis-specific genes, including the genes encoding *Sox9* and *Dhh,* was observed (Ottolenghi et al., 2005; Uhlenhaut et al., 2009). In the induced deletion model, the expression of SOX9 in the granulosa cell lineage resulted in a downregulation of ovarian-specific genes and the granulosa and theca cell lineages differentiated into Sertoli-like and Leydig-like cells (Uhlenhaut et al., 2009). Additionally, the transdifferentiated steroidogenic theca cell population began synthesising HSD17β3 and were subsequently able to synthesise testosterone at levels comparable to XY males (Uhlenhaut et al., 2009). These data show that expression of FOXL2 is required for folliculogenesis but also for the suppression of the male pathway in somatic cells and maintenance of the postnatal ovary (Ottolenghi et al., 2005; Uhlenhaut et al., 2009).

1.5 Germ cell development

Germ cells are the precursors of oocytes and spermatozoa in the fetal gonad. The sexual fate of the germ cell is determined by signalling factors that the germ cells are exposed to upon entry to the gonad, rather than by their chromosomal constitution (Adams and McLaren, 2002; Bowles et al., 2010; Bowles et al., 2006; Koubova et al., 2006; McLaren and Southee, 1997). Much of what is known about the origin and regulation of germ cell identity is derived from studies in mice, as discussed below. As germ cells are not the focus of the work presented in this thesis the following provides only a brief overview of germ cell development.

In an ovary, germ cells must enter meiosis during fetal life if they are to initiate oogenesis correctly; conversely, meiosis must be avoided in male germ cells in the fetus if they are to embark on the spermatogenic pathway. The interplay between FGF9 and retinoic acid (RA) appears to be key to the correct specification of the germ cells in the mouse: meiosis is induced by RA in the fetal ovary and inhibited by FGF9, which is secreted by Sertoli cells, in the fetal testes (Bowles et al., 2006; Bowles et al., 2010; Colvin et al., 1999; Koubova et al., 2006). In the developing testis, meiosis is avoided because RA is degraded by the P450 enzyme CYP26B1 (cytochrome P450, family 26, subfamily b, polypeptide 1; (MacLean et al., 2007)). Thus, CYP26B1 acts to suppress meiosis indirectly by the removal of RA, while FGF9 directly suppresses meiosis and acts to maintain pluripotency (Bowles et al., 2006; Bowles et al., 2010; Koubova et al., 2006). This mechanism is supported by *in vivo* evidence from *Cyp26b1*-/- mice where degradation of RA does not occur in XY gonads, resulting in upregulation of RA-responsive *Stra8* (*stimulated by retinoic acid gene 8*) and germ cell entry into meiosis (Bowles et al., 2006; MacLean et al., 2007).

A double-knockout of *Aldh1a2/Aldh1a3* (*aldehyde dehydrogenase family 1, subfamily A2/A3*), genes encoding key synthesisers of RA in the mesonephros, demonstrated that some meiosis still occurred in the fetal ovary (Kumar et al., 2011). These data indicate that either RA does not drive meiosis or, more likely, that there is an additional source of RA that remains in these mice. More in-depth analysis of this model will be required to clarify this point. Regardless, a strong antagonism exists between meiosis-promoting (female) factors and meiosis-suppressing (male) factors that push the resident germ cells into their respective fates.

Relatively little is known about whether these mechanisms are used in humans. Culture experiments demonstrate that RA initiates meiosis in the human ovary and can upregulate *STRA8* (Childs et al., 2011; Le Bouffant et al., 2010). However, it appears that the human gonad has the capacity to produce RA, evidenced by the strong expression of *ALDH1A1* (aldehyde dehydrogenase family 1, subfamily A1) in the ovary around the time of meiosis initiation (Childs et al., 2011; Le Bouffant et al., 2010). Most striking is the apparent lack of *CYP26B1* expression in the fetal human testes and the expression of RA receptors, indicating that the testes may be exposed to, and may be able to respond to, RA, unlike the situation in the mouse (Childs et al., 2011; Cupp et al., 1999).

Expression of STRA8 is essential for germ cells entry into meiosis (Anderson et al., 2008; Baltus et al., 2006; Mark et al., 2008). In the ovary, entry into meiosis occurs around 13.5-14.5 dpc whereas in the testis germ cells enter meiosis postnatally. *Stra8-/-* mice are infertile, with meiosis defects evident in the fetal ovary (Baltus et al., 2006) and postnatal testis (Anderson et al., 2008; Mark et al., 2008). In the *Stra8-/-* fetal XX gonads and the postnatal XY gonads, meiosis does not proceed past entry into prophase I demonstrating that the expression of *Stra8* is necessary for germ cell entry into meiosis in the XX and XY gonad (Anderson et al., 2008; Baltus et al., 2006; Mark et al., 2008). In germ cells of *Stra8-/-* gonads, expression of *Sycp3* (*synaptonemal complex protein 3*) and *Rec8* (*REC8 meiotic recombination protein*) is mislocalised (Anderson et al., 2008; Baltus et al., 2006), up-regulation of *Spo11* (*SPO11 meiotic protein covalently bound to DSB homolog*) and *Dmc1* (*DMC1 dosage suppressor of mck1 homolog, meiosis-specific homologous recombination*) does not occur (Anderson et al., 2008) and γ-H2AX-positive (H2A histone family, member X) double stranded breaks are not observed. These data indicates that *Stra8* plays a role in pre-meiotic DNA replication, which is essential for meiotic progression. A comprehensive understanding of the mechanisms surrounding germ cell entry into meiosis in the fetal ovary and postnatal testis will be important as incorrect meiotic progression can result in infertility and germ cell tumours.

1.6 Functional validation of candidate genes in mice

The microarray screens described in section 1.2 have identified large numbers of genes that are potentially involved in gonadogenesis. In addition to this data, research groups are embarking on RNA-seq projects, and genes underlying human developmental disorders are being identified in rare disease cohorts due to the widespread adoption of whole exome sequencing (WES) and whole genome sequencing (WGS). Together these data provide many opportunities, but also create many challenges. One of the primary challenges facing the community is the functional validation of all the candidate genes being identified. Classic ('knock-out'/'knock-in') or newer (CRISPR/Cas9) mouse genetic manipulation measures remain costly, time-consuming and high-risk. As a result there have been numerous attempts to develop a methodology to assess gene function during development of embryos and organs to enable pre-screening candidate genes.

In the field of gonadal development knockdown protocols have been based on modification of established *ex vivo* organ culture methods. The two major considerations have been the type of construct delivered and the construct delivery method. Delivery methods have included injection, electroporation or liposome-based introduction of the construct into the tissue. These constructs have been mostly plasmid-based or shRNA-based (Nakamura et al., 2002; Ryan et al., 2011; Svingen et al., 2009b). Nakamura et al. (2002) microinjected a plasmid construct and then electroporated the plasmid construct into the gonad, but it was estimated that only 2% of cells took up and expressed the construct. Svingen et al. (2009b) also introduced the plasmid construct/shRNA into the gonad by microinjection, the plasmid was coated in magnetic nanoparticles which facilitated magnetically mediated gene transfection ("magnetofection") to induce the construct to move into the cell. This approach achieved a variable rate of delivery, the construct was expressed in approximately 20% of cells, but these cells were mainly localised around the injection site (Svingen et al., 2009b). A major concern with these methodologies was that the delivery of the construct was predominately restricted to near the injection site where the damage to the tissue by the blunt force of the injection made interpreting phenotype difficult. To get around this problem, Ryan et al. (2011) delivered a plasmid by electroporation into the gonad using a "nucleofection" protocol, which does not rely on microinjection of the construct into the tissue, but only approximately 11% of cells successfully expressed the delivered plasmid.

Passive uptake of morpholino oligonucleotides (MOs) has been used by others to knock down gene function in the lung and the kidney (Dean et al., 2005; Gross et al., 2003; Hartwig et al., 2010; Quaggin et al., 1998; Quaggin et al., 1997; Yates et al., 2010). MOs provide a means of knocking down protein expression; they are synthetic oligonucleotides of approximately 25 nucleotides in length that hybridise to complementary sequences in mRNAs. There are two main classes of MO; translation blocking MOs and splice site MOs. Translation blocking MOs target and block the translation start site of mRNA. An immediate decrease in protein may not be observed, as pre-existing protein must be degraded before protein signal decreases. Splice site MOs hybridise across an intron-exon junction sequence in the pre-spliced mRNA, so that an exon is skipped and a misspliced protein product is produced (Morcos, 2007). Splice site MOs should lead to the production of mRNA that is abnormal and hence susceptible to nonsense mediated decay (Morcos, 2007). However, it is possible that an abnormal protein retaining some activity will be produced. More recently vivo-MOs have been developed, these MOs have been covalently linked to a dendrimeric octaguanidine delivery moiety which enables them to be more efficiently delivered from the circulation into the cytosol and the nuclei of the cell (Morcos et al., 2008; Moulton and Jiang, 2009; Wu et al., 2009). Improved systemic delivery efficiency has been reported for vivo-MO over standard MOs (Morcos et al., 2008; Moulton and Jiang, 2009).

In the lung, MOs could penetrate the epithelium and mesenchyme of murine lung and lacrimal gland explants by passive diffusion from the surrounding culture media (Dean et al., 2005). MOs were added to the media that the explant cultures were bathed in at a concentration of 10 μM or 15 μM and cultured as appropriate (Dean et al., 2005; Yates et al., 2010). Delivery to the lung and lacrimal gland in the explanted tissue could be visualised by addition of a fluorescein-tagged MO which could be detected with an antibody post-culture (Dean et al., 2005). Using this approach branching morphogenesis defects were detected in targeted explants (Dean et al., 2005; Yates et al., 2010). Passive uptake of MOs from supplemented media has also been used in the kidney, where a concentration of 5μM MO with added Lipofectamine or 20 μM MO only was used to supplement the media (Gross et al., 2003; Quaggin et al., 1997; Quaggin et al., 1998). Using this system a change in glomeruli number was observed after treatment with a MO against *Spry1* (Sprouty homolog 1; (Gross et al., 2003)). Subsequent work in the kidney used media supplemented with 10 μM vivo-morpholino, but others have failed to reliably replicate this work ((Hartwig et al., 2010); M. Little, personal communication). Therefore, *ex vivo* knockdown of gene function in organ culture remains a key challenge for the field in functionally validating the roles of genes of interest.

1.7 Concluding remarks

The bipotenial nature of the gonad and its somatic cell lineages makes it an ideal model to study processes such as cell differentiation and organ morphogenesis. In turn, the study of gonadogenesis in mouse increases our understanding of how and why DSDs arise in human patients, helps to provide molecular diagnosis and informs clinical best practice.

The critical importance of endocrine function in reproduction and general health has meant that Leydig cells, in the postnatal and adult context, have been studied extensively. On the other hand, our understanding of the origins, impact and characteristics of FLCs is far less developed. Extrapolation of our knowledge of ALCs to FLCs can take us only so far. It is clear that FLCs are important during development, but the impact that perturbation of FLC function or differentiation has on masculinisation is still unclear. Characterisation of the early FLC population will likely reveal key players in early differentiation and pre-steroidogenic function of the population. In addition, identification of early FLC markers that are exclusive to the FLC population (in particular exclusive of the NSIC and Sertoli cell populations) will be important for characterisation of early FLC function.

In looking at the consequences of endocrine function in fetal development it is becoming clear that the NSIC population will also likely play a key role. As we are now aware that precursor ALCs are present in the fetal testis this indicates that the origin of some ALC defects may be perturbations during fetal life. The NSIC population is poorly characterised. New markers of NSIC sub-populations and markers that can be used for lineage tracing will be essential to uncovering the role that this population plays in fetal and postnatal life.

Considering the central role of these two cell lineages I propose that it is likely that novel DSD genes may be uncovered by studying these populations. In the past characterisation of the gonadal transcriptome has proved informative in uncovering likely DSD candidate genes. Conversely, the undertaking of WGS and WES of patient cohorts will also uncover DSD candidate genes that will then require validation. This volume of genes needing functional validation will require more efficient screening methods to be developed.

Chapter 2: Morpholino-based screen for gene function in mouse embryo

2.1 Publications

McClelland KS, Wainwright EN, Bowles J, Koopman P (2015) *Rapid Screening of Gene Function by Systemic Delivery of Morpholino Oligonucleotides to Live Mouse Embryos.* PLoS ONE 10(1): e0114932. doi:10.1371/journal.pone.0114932

2.2 Project Summary:

There is a need for a medium throughput technique to knockdown gene function during organogenesis in the mouse embryo as a pre-screening tool in order to prioritise candidate genes for more detailed analysis. In this project I developed a novel technique for assessing gene function. Modified antisense morpholino oligonucleotides (MOs) were injected into the beating heart of mid-gestation mouse embryos allowing delivery of the MO around the embryo to knockdown the gene/s of interest. This work resulted in the publication contained within entitled "*Rapid screening of gene function by systemic delivery of morpholino oligonucleotides to live mouse embryos"* in PLoS ONE. In this work, we knocked down *Stra8, Sox9, Gli1/2, Ctrb1* and *Adamts19* in the fetal gonad and *Sox9* in the fetal pancreas. We also used this technique in work in collaboration with Allen Feng (Koopman Lab, IMB) by knocking down *Cdx2* in the fetal gonad at 11.5 dpc and extended the technique by successfully performing heart injection and gonad culture one day earlier at 10.5 dpc (data not shown). In addition we targeted two genes with roles in early gonadogenesis, *Wnt4* and *Nr0b1,* and *Gli3,* a hedgehog pathway member.

Furthermore, I used this technique to investigate the role of putative disease causing genes during gonad development. Two genes, identified by our collaborators as putative causative genes on the basis of results from whole exome sequencing of DSD patients, namely *NR0B2* and *SART3*, were tested. This work was part of an ongoing collaboration with Stefanie Eggers and Andrew Sinclair (Murdoch Childrens Research Institute, Australia).

2.3 Chapter Introduction

Data from RNA-seq and microarray screens has identified many candidate gonadal development genes which now require functional evaluation in model systems. On top of these data, whole exome and whole genome sequencing of rare disease cohorts has identified a plethora of possible causative genes for human developmental disorders, and these too require validation. Modelling genetic mutations in human development, physiology and disease in the mouse model has provided invaluable insights. However, the generation of multiple complete or conditional loss-of-function mutations in the mouse is technically complex and time-consuming, even with recent advances in genome editing technologies such as the CRISPR/Cas-9 system (for review see Hsu et al., 2014). Considering that there is a significant risk that a knockout of a gene may result in embryonic lethality or little to no phenotype, the generation of a loss-of-function mouse model for every interesting candidate remains impractical. In order to prioritise candidates for further characterisation we need to develop a technique to assess the probable effects that the loss-of-function of a gene-of-interest may have on organogenesis.

To address this need I developed a method to knock down gene function in the mid-gestation mouse embryo, and then culture the organs *ex vivo*. There were two main hurdles to overcome in developing this strategy for mouse tissues: delivery of the compound and the nature of the compound itself. These challenges are discussed in detail in the paper within this chapter.

I chose to optimise and assess the success of the knockdown protocol by attempting to phenocopy established genetic knockout models in the developing gonad and pancreas. The gonad and pancreas are suited to vascular delivery of compounds, are easily explanted and cultured, and their development is well characterised. In order to assess specificity and off-target effects of the MO I assessed the expression of multiple markers in targeted and non-targeted cell types. Developing a knockdown system in the gonad provides the additional advantage that sexually dimorphic gene expression can be used as a further control for general toxicity and/or off-target effects of the construct; the expression of genes with sexually dimorphic patterns can be used as a broad read-out of the male or female pathway.

2.4 Published manuscript

Rapid screening of gene function by systemic delivery of morpholino oligonucleotides to live mouse embryos

Kathryn S. McClelland, Elanor N. Wainwright, Josephine Bowles* and Peter Koopman

Institute for Molecular Bioscience, The University of Queensland, Brisbane, QLD, Australia

* Author for correspondence:
Email: j.bowles@imb.uq.edu.au (JB)

Running title: Morpholino-based screen for gene function in mouse embryos

Key words: Functional genomics, gene knockdown, sex determination, testis development, germ cells, pancreas, antisense

Abstract

Traditional gene targeting methods in mice are complex and time consuming, especially when conditional deletion methods are required. Here, we describe a novel technique for assessing gene function by injection of modified antisense morpholino oligonucleotides (MOs) into the heart of mid-gestation mouse embryos. After allowing MOs to circulate through the embryonic vasculature, target tissues were explanted, cultured and analysed for expression of key markers. We established proof-of-principle by partially phenocopying known gene knockout phenotypes in the fetal gonads (*Stra8, Sox9*) and pancreas (*Sox9*). We also generated a novel double knockdown of *Gli1* and *Gli2,* revealing defects in Leydig cell differentiation in the fetal testis. Finally, we gained insight into the roles of *Adamts19* and *Ctrb1*, genes of unknown function in sex determination and gonadal development. These studies reveal the utility of this method as a means of first-pass analysis of gene function during organogenesis before committing to detailed genetic analysis.

Introduction

One of the central challenges in the era of functional genomics is to understand gene function and unravel the complex networks in which proteins operate to determine phenotype. With RNA-seq data amassing on top of an already large list of genes gleaned from microarray screens, many candidate genes now require functional assessment. In addition, possible causative genes for human developmental diseases are being identified rapidly in rare disease cohorts as a result of whole exome and whole genome sequencing.

Much of the functional genomics effort focuses on the mouse model because of its relevance to human development, physiology and disease. Investigation of gene function in mouse has traditionally involved the generation and breeding of complete or conditional loss-of-function alleles via homologous recombination, involving a complex and time-consuming experimental pipeline. Even with advances in genome editing technologies such as the CRISPR/Cas-9 system (for review see (Hsu et al., 2014)), the generation of knockout animals for every promising gene candidate is impractical. Moreover, it is often the case that, after investing the time and resources required to generate a conventional or conditional gene knockout, little or no phenotype results. Therefore, there is a pressing need to develop methods that provide insight into developmental gene function either as a pre-screen before committing to genome manipulation approaches *in vivo*, or as a means of prioritising candidates for further analysis.

With this goal in mind, a variety of methods for accelerated *ex vivo* functional analysis have been reported. In the field of gonadal development, these methods have included injection, electroporation or liposome-based delivery of viral-based or siRNA-based constructs into explanted tissue (Nakamura et al., 2002; Ryan et al., 2011; Svingen et al., 2009b), followed by organ culture and histological or molecular analysis. Typically, these approaches have caused damage to the target tissue as well as being limited in delivery area. For other developing organs, such as mouse lung and kidney, morpholino antisense oligonucleotides (MOs) have been added to the culture media, but these experiments show high variability due to limited passive uptake of the MO (Dean et al., 2005; Gross et al., 2003; Hartwig et al., 2010; Quaggin et al., 1998; Yates et al., 2010).

We aimed to develop a method whereby gene function could be perturbed *ex vivo*, rapidly and without injury to the target organ. Here we show that injection of commercially available MOs into

the beating heart of a 11.5 dpc (days *post coitum*) mouse embryo results in delivery via the vasculature to the gonads and pancreas. We demonstrate knockdown of protein expression for a number of target genes, leading to predicted downstream effects for known genes and novel functional insights for other genes or combinations of genes. This method offers a rapid, reproducible, efficient means of rapidly pre-screening gene candidates for likely function, as a prelude to more rigorous functional studies in mice.

Materials and Methods

Morpholino design

Splice site MOs were designed to target exon/intron boundaries of target genes (for sequences see Supplemental Table 1). All MOs were vivo-MOs which incorporate a dendrimeric octaguanidine delivery moiety end modification, with the exception shown in Fig. 2.1H, I, where a carboxyfluorescein-labelled standard control MO (F-MO) was used.

Heart injections

For ease of sexing embryos, we used the X-linked GFP line (Hadjantonakis et al., 1998), maintained on an outbred Swiss albino background (Quackenbush strain). Noon on the day on which the mating plug was detected was designated as 0.5 days *post coitum* (dpc). All animal work was conducted according to protocols approved by the University of Queensland Animal Ethics Committee. This study was approved by the University of Queensland Animal Ethics Committee (Permit Number: IMB/176/13/NHMRC/ARC).

Embryos were explanted at 11.5 dpc and placed into PBS (phosphate buffered saline) at 37°C with the amniotic sac intact and the placenta attached. If required, embryos were sexed by GFP expression. The amniotic sac was opened, taking care not to damage any major blood vessels. The left ventricle of the beating heart of the embryo was injected with a MO-cocktail (20 ng/μL (single target) or 15 ng/μL (per MO, two targets) and 6% commercial food dye (Queen Fine Foods Pty. Ltd.)). For each embryo either control or MO targeted against gene of interest (Gene Tools, LLC) was delivered using a Sutter-pulled glass capillary needle. Injection was continued until the marker dye was observed in the head vein (approx. 6-8 heart beats, equivalent to ~20-27 ng MO/embryo (single MO) or ~30-40 ng MO/embryo (combination of two MOs); see Supplemental Video 1 and Fig. 2.1). Embryos with non-beating or weakly beating hearts, or where injection was unsuccessful as judged by lack of circulation of the dye (about 1 in 15 embryos), were excluded from further study. Embryos were left to recover for 30 min in pre-warmed PBS in an incubator at 37°C, 5% CO_2; hearts were still beating at the end of this period. Video of the above procedure was captured on an Olympus SZX-12 Stereomicroscope (see Supplemental Video 1).

For assessing delivery area using a F-MO: 20 µg/mL F-MO (20-27 ng/embryo) and 2% India ink was delivered by heart injection as described above (*n*=3). After 5 and 30 min recovery the genital ridge was imaged on an Olympus BX-51 Upright Fluorescence/Brightfield microscope.

For gonad culture, UGR (urogenital ridge: gonad plus mesonephros) was dissected out and hanging drops were prepared by pipetting 40 µL of media (BJGB media (Gibco) with 4% Serum Supreme (Lonza), 1% penicillin/streptomycin (Gibco) and 200 mg/mL ascorbic acid (Sigma Aldrich)) containing a single UGR onto the inner face of the lid of a 24 well tissue culture plate. PBS (500 µL) was added to each well and the lid was then inverted to close the plate. After 48 h, cultured gonads were washed in PBS for 5 min and processed for qRT-PCR, Western blot or immunohistochemistry.

For pancreas culture, the foregut endoderm was isolated and any non-affiliated organs removed. The foregut was placed on a Millipore (5 µM TPMT) filter floating on 600 µl of culture medium (M199 media (Gibco) with 10% Serum Supreme (Lonza) and 2% penicillin/streptomycin (Gibco)) and cultured for 4-6 days at 37°C, 5% CO_2 with the media changed every other day. After culture, tissues were washed in PBS for 5 min and processed for qRT-PCR or immunohistochemistry.

Quantitative RT-PCR analysis

Total RNA was extracted and cDNA generated from cultured gonad or pancreas as previously described (Bowles et al., 2010). Duplicate assays were carried out on an ABI Prism 7500 Sequence Detector System. *Tbp* (TATA box binding protein) was used as an endogenous control to normalise gene expression levels (Svingen et al., 2009a). Taqman gene expression sets were as listed in Supplemental Table 2.

Relative transcript abundance was calculated using the $2^{-\Delta CT}$ method. Error bars represent S.E.M. calculated from independent biological replicates; statistical significance was assessed using unpaired (two-tailed) Student's *t*-test.

Immunofluorescence

Analyses were carried out on fixed, paraffin-embedded 7 μm sections using standard methods. Briefly, gonad plus mesonephros complexes or foreguts were fixed in 4% paraformaldehyde in phosphate buffered saline overnight at 4°C. Tissues were embedded in 1.5% low melt agarose, ethanol dehydrated, paraffin-embedded and 7 μm sections were cut using a Leica Microtome. Slides were dewaxed by 2 x 10 min washes in xylene, re-hydrated and boiled for 5 min in Antigen Unmasking Solution (Vector Laboratories), then incubated at room temperature for 60 min. The slides were washed for 3 x 10 min in 0.1% Triton-X in PBS (PBTX). The sections were incubated with primary antibodies, which were diluted in blocking buffer at 4°C overnight (for primary antibodies see Supplemental Table 3). Antibodies were removed with three washes in PBTX, and the slides re-blocked for 30 min at room temperature. Secondary antibodies were incubated at room temperature for 2 h. The secondary antibodies were removed with three PBS washes before DAPI staining and mounting with a 60% glycerol/PBS solution. Secondary antibodies were all from Invitrogen Molecular Probes (see Supplemental Table 4). Sections were examined by confocal microscopy using a Zeiss LSM-510 META or LSM-710 META confocal microscope.

Whole-mount immunofluorescence

Whole mount immunofluorescence was performed as detailed in (Combes et al., 2009a).

Cell quantification

For quantification of the number of INS- and PAX6-positive cells in the pancreas, and HSD3β, NR5A1, SOX9-positive cells in the XY gonad, de-identified gonads or foreguts were serially sectioned at 7 μm and processed as per the immunofluorescence protocol. Quantification was performed on all sections per sample using the ImageJ64 “Cell Counter” plugin. Error bars depict S.E.M. calculated from independent biological replicates; statistical significance was determined using unpaired (two-tailed) Student's *t*-test. Asterisks indicate level of statistical significance in pertinent comparisons.

Western blot

Western blots were carried out as described previously (Zhao et al., 2008), with slight modifications. Briefly, gonad pairs were dissociated with a 13-gauge needle and lysed in 1× SDS sample buffer (62.5 mM Tris–HCl (pH 6.8), 2% SDS, 10% glycerol, 50 mM dithiothreitol, and

0.01% w/v bromophenol blue), separated on SDS-PAGE and transferred to a PVDF membrane (Millipore). SOX9 primary antibody was incubated for 2 h at room temperature and then overnight at 4°C with 13.5 dpc testis as a positive control and 13.5 dpc ovary as a negative control. For primary antibodies see Supplemental Table 3, for secondary antibodies see Supplemental Table 4. Proteins were visualised using Clarity Western ECL Substrate (Bio-Rad) on a ChemiDoc machine (Bio-Rad). Raw intensity of bands was determined using Image Lab Software (version 4.0). SOX9 intensity units were calculated relative to α-TUB or β-ACT loading control and relative downregulation calculated with cMO sample set to 1 for individual cMO vs. Sox9MO-treated samples on each of 3 blots. Error bars represent S.E.M. calculated from independent biological replicates; statistical significance was assessed using unpaired (two-tailed) Student's *t*-test.

Flow cytometry and cell sorting

Flow cytometry and cell sorting was carried out as described previously (Wainwright et al., 2013). Briefly, 12.5 dpc *Sf1*-eGFP (Beverdam and Koopman, 2006) litters were dissected, gonads sexed by eye and separated from the mesonephros before being dissociated. Cells were incubated with SSEA1-PE antibody (BD Biosciences) to tag germ cells. FACS was performed using a BD FACS Aria cell sorter. Pools of germ (SSEA1-positive) and eGFP-positive cells were collected separately and total RNA was extracted and cDNA prepared as described (Bowles et al., 2010). Cells from three or four independent litters and sorting experiments were used for qRT-PCR analysis.

All Supplementary Tables for reagents are listed in the Appendix.

Results

Method development: Delivering morpholinos to fetal organs

Initially, we trialled the inclusion of standard 'naked' MOs or vivo-MOs (in which the MO is linked to a dendrimeric octaguanidine delivery moiety) in the media for *ex vivo* organ culture from 11.5 dpc for 48h (data not shown), using a protocol similar to those previously published for lungs and kidneys (Hartwig et al., 2010; Yates et al., 2010), but were unable to achieve widespread tissue uptake and hence efficacy. Therefore, we developed a novel protocol that relied on a combination of two approaches.

First, in order to deliver the compounds uniformly through the organs of interest in the mid-gestation embryo, we looked to classic experiments in mouse and chick, where India ink was used to visualise the early vasculature (for review see (Nagy, 2010)). This approach has also been utilised to deliver siRNA and viral constructs to the embryo (Sanes et al., 1986), and to deliver lectin to the 11.5 dpc gonad via the vasculature (Cool et al., 2011). These studies relied on injection of compounds into the beating embryonic heart, and so we reasoned that this approach might offer a way to successfully deliver MOs to vascularised tissues in the mouse embryo.

Second, Vivo-Morpholinos (Gene Tools, LLC) were chosen for injection as they reportedly show improved systemic delivery efficacy compared to standard MOs (Morcos et al., 2008; Moulton and Jiang, 2009; Wu et al., 2009). Oligonucleotides were designed to span intron/exon boundaries within the pre-mRNA to produce non-functional, mis-spliced gene products. A standard commercial 25-mer MO (see Materials and Methods) was used as a control for the specificity of MO effects.

We trialled our knockdown procedure using the developing ovaries, testes and pancreas as a test-bed. These organs are well suited to vascular delivery of compounds, are readily explanted, develop normally in organ culture, and are well characterised in terms of morphological and molecular markers of differentiation and morphogenesis. Examination of organogenesis allows specificity and off-target effects of the MO to be assessed by testing for markers of differentiation of the targeted cell type and multiple non-targeted other cell types. Inclusion of developing gonads in these studies

offers the additional advantage that known differences in sexually dimorphic gene expression can be used as a further control for general toxicity and/or off-target effects.

A summary of the workflow is shown in Fig. 2.1A, and the detailed protocol is described in Materials and Methods. Conceptuses were explanted at 11.5 dpc and the amniotic sac of individual embryos opened, taking care not to disrupt major amniotic blood vessels. A MO/food dye cocktail was injected into the left ventricle of the beating heart (Fig. 2.1B,F) until the dye was observed to travel around the embryo and into the vessels in the head, typically after 6-10 heart beats (Fig. 2.1C-E; Supplemental Video 1). After injection, embryos were allowed to recover for ~30 min to enable delivery of MO throughout the vasculature. Subsequently, tissues of interest were explanted, and cultured *ex vivo*, before detailed analysis of gene and protein marker expression. In preliminary experiments, we used carboxyfluorescein-labelled MO (F-MO) to assess the extent of delivery to tissues (n= 3). In the case of the developing gonads, F-MO and India ink were observed in the nascent mesonephric vasculature at 5 min post-injection (Fig. 2.1G,H) and were clearly visible in the gonadal tissue after 30 min (Fig. 2.1I), suggesting that the dye and MO had accessed the target tissue.

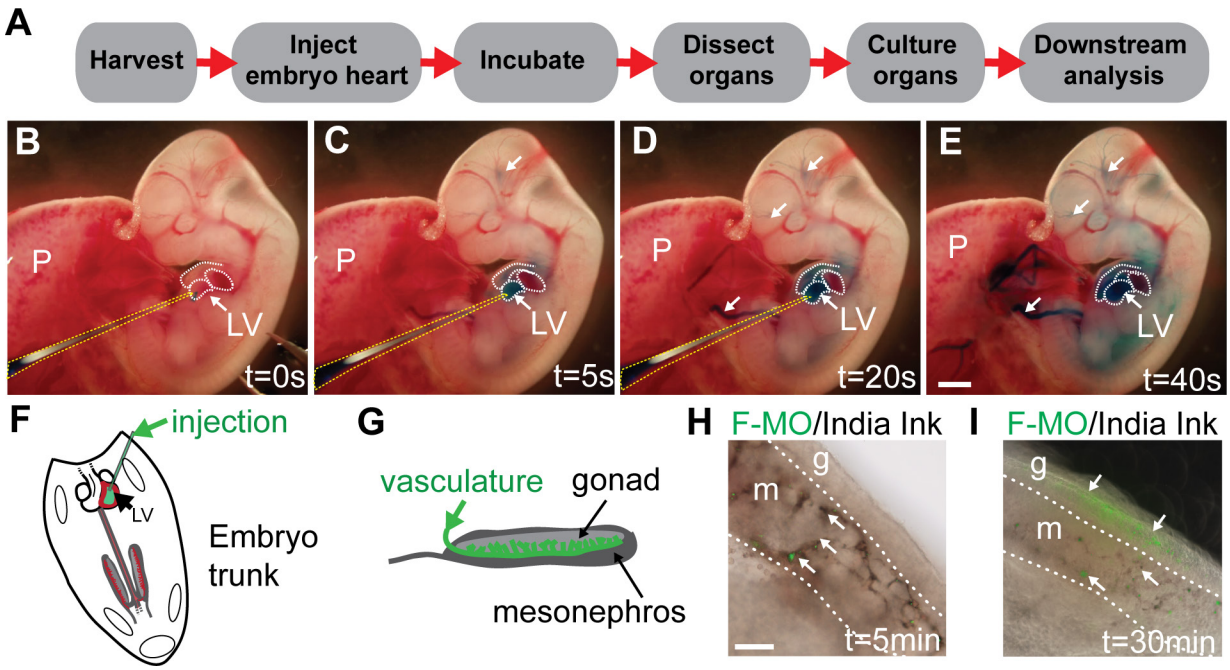

Figure 2.1. Overview of method: MO delivery by heart injection.

(A) Experimental pipeline from harvest of embryos through to injection, culture and downstream analyses. Visualisation of heart injection protocol can be seen in Supplemental Video 1 and images B-E. The cocktail of dye and MO in PBS is delivered via injection into the left ventricle of the beating heart at 11.5 dpc (B). Dye can be visualised going around the embryonic vasculature (indicated by white arrows) (C,D) and into the head vasculature (D) before the whole embryo is coloured (E). Schematic of ventricle injection (F) and the embryonic gonad which is highly vascularised (G). Delivery of India ink and F-MO (indicated by white arrows) shows the compounds reaching the mesonephric plexus at 5 min post-injection (H; n= 3); after 30 min F-MO positive cells were observed in the gonad proper (I; n= 3). s = seconds; min = minutes; g = gonad; m = mesonephros; F-MO = carboxyfluorescein-labelled standard control morpholino oligonucleotide. Scale bars: E = 1 mm, H = 0.5 mm.

Proof of principle: STRA8 in the developing ovary

The germ cells of the gonad are the precursors of sperm (XY) or oocytes (XX): whether they adopt the male or female developmental pathway is determined by their somatic environment (for review see (McLaren, 2003)). Upregulation of the gatekeeping gene *Stra8* (*stimulated by retinoic acid gene 8*) at 12.5 dpc is essential for germ cell entry into meiosis in the developing ovary, as demonstrated by the blockade of meiosis in XX *Stra8*$^{-/-}$ gonads (Baltus et al., 2006; for review see (Feng et al., 2014)). Since *Stra8*$^{-/-}$ gonads have a well-defined phenotype, we tested MO knockdown of *Stra8* as a proof-of-principle experiment.

Although *Stra8* transcript could still be detected after MO treatment (Fig. 2.3A), expression of STRA8 protein was greatly decreased as measured by immunofluorescence in Stra8MO-treated XX gonads, indicating successful knockdown (Fig. 2.2A). Strikingly, meiotic markers γ-H2AX (H2A histone family, member X; Fig. 2.2A) and SCP3 (synaptonemal complex protein 3; Fig. 2.2B) were not localised to the nucleus in XX Stra8MO samples, in contrast to control ovaries, where germ cells began to show these hallmark signs of entry into meiosis. Stra8MO knockdown did not have a direct effect on qRT-PCR expression of other meiosis markers (Fig. 2.3C-E). However, functional aspects of meiosis, such as SCP3 nuclear localisation, were clearly affected by Stra8MO treatment (Fig. 2.2A,B).

We tested for possible effects of generalised toxicity in MO-treated gonads by examining expression of a range of cell lineage markers. Immunofluorescence and qRT-PCR for markers of germ cells—OCT4/POU5F1 (POU domain, class 5, transcription factor 1; Figs 2.2B, 2.3G), *Mvh/Ddx4* (Deadbox polypeptide 4; Fig. 2.3F) and CDH1 (Cadherin 1; Fig. 2.3H,I) indicated that the number of germ cells was unaffected in Stra8MO treated gonads, suggesting no qualitative or quantitative detrimental effect on germ cells. Furthermore, expression of the somatic marker FOXL2 (Forkhead box L2; Fig. 2.3B,I) was unchanged in Stra8MO XX gonads, indicating that gonadogenesis in general was not impaired by MO-treatment. Combined, these data show that the reduced meiotic marker expression was likely a specific consequence of MO antagonism of STRA8 expression, rather than generalised toxicity.

In summary, the suppression of markers associated with meiotic entry suggests that germ cells failed to successfully enter meiosis in Stra8MO knockdown XX gonads. Thus, the Stra8MO knockdown partially phenocopied the *Stra8*$^{-/-}$ gonad phenotype.

Proof of principle: SOX9 in the developing testis

To test whether MO treatment can influence phenotype when the protein of interest is already abundant at the time of treatment, we performed MO knockdown of SOX9 (SRY (sex determining region Y)-box 9) at 11.5 dpc. SOX9 expression stimulates the male pathway by promoting Sertoli cell differentiation (Wainwright and Wilhelm, 2010). In *Sox9*$^{-/-}$ XY embryos, gonadal sex reversal occurs as SOX9 is both necessary and sufficient for male sex determination (Barrionuevo et al., 2006; Bishop et al., 2000). However, in heterozygous *Sox9*-mutant XY embryos, Sertoli cells are able to differentiate and the SOX9 downstream target anti-Müllerian hormone (AMH) is still produced (Bi et al., 2001; Chaboissier et al., 2004). Since SOX9 protein is already abundant in the XY genital ridge at 11.5 dpc, the time of MO treatment, we asked whether MO treatment might result in no effect, full gonadal sex reversal, or an intermediate phenotype.

We found that SOX9 protein abundance was significantly decreased in the Sox9MO treated gonads, as assessed by Western blot (Fig. 2.2C, for blots see Fig. 2.5) and immunofluorescence (Fig. 2.4H), although the expression of *Sox9* transcript was unchanged (Fig. 2.4A). Moreover, the expression of *bona fide* direct SOX9 target genes *Amh* (Arango et al., 1999) and *Ptgds* (*prostaglandin D2 synthase*; (Wilhelm et al., 2007)) were significantly reduced (Fig. 2.2D; Fig. 2.4B) in Sox9MO treated XY gonads compared to XY controls, and AMH protein expression levels were also reduced compared to the control XY gonad (Fig. 2.2E).

In Sox9MO-treated gonads, residual SOX9 and therefore AMH expression was sufficient to initiate Müllerian duct regression by 13.5 dpc (Fig. 2.4J). Consistent with this finding, we showed that SOX9 levels were not sufficiently suppressed as to allow upregulation of the female somatic pathway; FOXL2-positive cells were not observed (Fig. 2.4H) and expression of *Fst* (*follistatin*), a female somatic marker, was not upregulated in XY Sox9MO samples compared to XY cMO samples as assessed by qRT-PCR (Fig. 2.4F).

The expression of another Sertoli expressed gene, *Dhh* (*desert hedgehog*; (Bitgood et al., 1996)) was not significantly downregulated (Fig. 2.4C). Accordingly, fetal Leydig cell (FLC) differentiation occurred in the knockdown of SOX9 in XY gonads, as assessed by expression of FLC markers *Cyp11a1* (*cytochrome P450, family 11, subfamily a, polypeptide 1*; Fig. 2.4E *Nr5a1/*NR5A1 (nuclear receptor subfamily 5, group A, member 1; Fig. 2.4D,I) and HSD3β (hydroxy-delta-5-steroid dehydrogenase, 3 beta- and steroid delta-isomerase 1; Fig. 2.3E). As expected, germ cells were unaffected by Sox9MO treatment in both XX and XY gonads, as assessed by the expression of *Ddx4* (Fig. 2.4G) and CDH1 (cadherin 1; Fig. 2.4I).

In summary, treatment with Sox9MO at 11.5 dpc resulted in a phenotype similar to that of the heterozygous *Sox9* genetic knockout, with reduced target gene expression but no gonadal sex reversal. There was no effect of Sox9MO treatment on germ cells, suggesting the phenotype observed was not due to off-target or toxic effects of the MO.

Proof of principle: SOX9 in the developing pancreas

To demonstrate the utility of MO heart injections for functional assay in other developing organs, we knocked down SOX9 in the developing pancreas. In addition to its roles in gonadogenesis, SOX9 also plays a role in endocrine cell differentiation in the pancreas (Seymour et al., 2008; Seymour et al., 2007). Heterozygous *Sox9*-mutant mice (most closely phenocopied by the Sox9MO effects on gonadal development described above) form fewer endocrine islets, but insulin- and glucagon-positive daughter cells still differentiate (Seymour et al., 2008). Additionally, heterozygous *Sox9*-mutant mice have decreased expression of *Pdx1* (*pancreatic and duodenal homeobox 1*; expressed in SOX9-positive multipotent progenitor cells) and *Ngn3* (*neurogenin 3;* endocrine progenitor cells) (Dubois et al., 2011). We therefore investigated whether treatment with Sox9MO at 11.5 dpc would cause a decrease in expression of *Pdx1/Ngn3* and genes associated with insulin production and/or a decrease in the number of endocrine insulin-positive cells.

We conducted our analyses at 4 days and 6 days post-treatment, the equivalent of 15.5 dpc and 17.5 dpc, respectively. These timepoints were chosen as at 15.5 dpc the endocrine cell population of the pancreas expresses INS in a subset of PAX6-positive cells, whereas at 17.5 dpc, the endocrine cell population is more established and has matured. By immunofluorescence we saw a decrease in SOX9 expression (Fig. 2.6K,L) in Sox9MO treated pancreata at 15.5 dpc. Importantly, PAX6-

positive (Fig. 2.6I,J; Fig. 2.2H) and INS-positive (Fig. 2.2I) endocrine cells were present in Sox9MO treated pancreata, indicating that the residual SOX9 expression after MO treatment at 11.5 dpc is sufficient to allow endocrine cell types to differentiate. We observed a significant decrease in the expression of *Ins1* (*insulin 1*) and *Ins2* (*insulin 2*) in Sox9MO treated pancreata at 17.5 dpc (Figs 2.2F; Fig. 2.6D), however the number of INS-positive (Insulin I/II) cells was unperturbed (Fig. 2.2I). We also investigated the expression of *Pax6* (*paired box 6*), which marks endocrine cells, and found no change in *Pax6* expression (Fig. 2.2G) or the number of PAX6-positive cells (Fig. 2.2H) in response to Sox9MO treatment in the cultured pancreata. We found by qRT-PCR that expression of putative direct SOX9 target *Pdx1* (Fig. 2.6C; (Dubois et al., 2011)) was unaltered but *Ngn3* (Fig. 2.6B; (Dubois et al., 2011)) expression was significantly decreased at 17.5 dpc.

SOX9 knockdown partially mimicked the heterozygous *Sox9*-mutant mouse phenotype as the effect we saw on endocrine cells was restricted to expression of *Ins1, Ins2* and *Ngn3*. Expression of *Sox9* was unaltered (Fig. 2.6A), as was expression of non-β cell sub-type markers including *Glug* (*glucagon*; α-cells, Fig. 2.6E), *Ghrl* (*Ghrelin*; ε-cells, Fig. 2.6F), *Ppy* (*Pancreatic polypeptide*; PP-cells, Fig. 2.6G) and *Sst* (*Somatostatin*; δ-cells, Fig. 2.6H) at both timepoints.

Together, these results suggest that *Ins1, Ins2* and *Ngn3* transcription in the pancreas was specifically suppressed by Sox9MO treatment which, therefore, partially phenocopied the heterozygous *Sox9*-mutant mice (Dubois et al., 2011; Seymour et al., 2008). The specificity of these effects suggests that MO treatment did not result in off-target effects or generalised toxicity in the pancreas. Moreover, the effects of MO knockdown were detectable for at least 6 days post treatment.

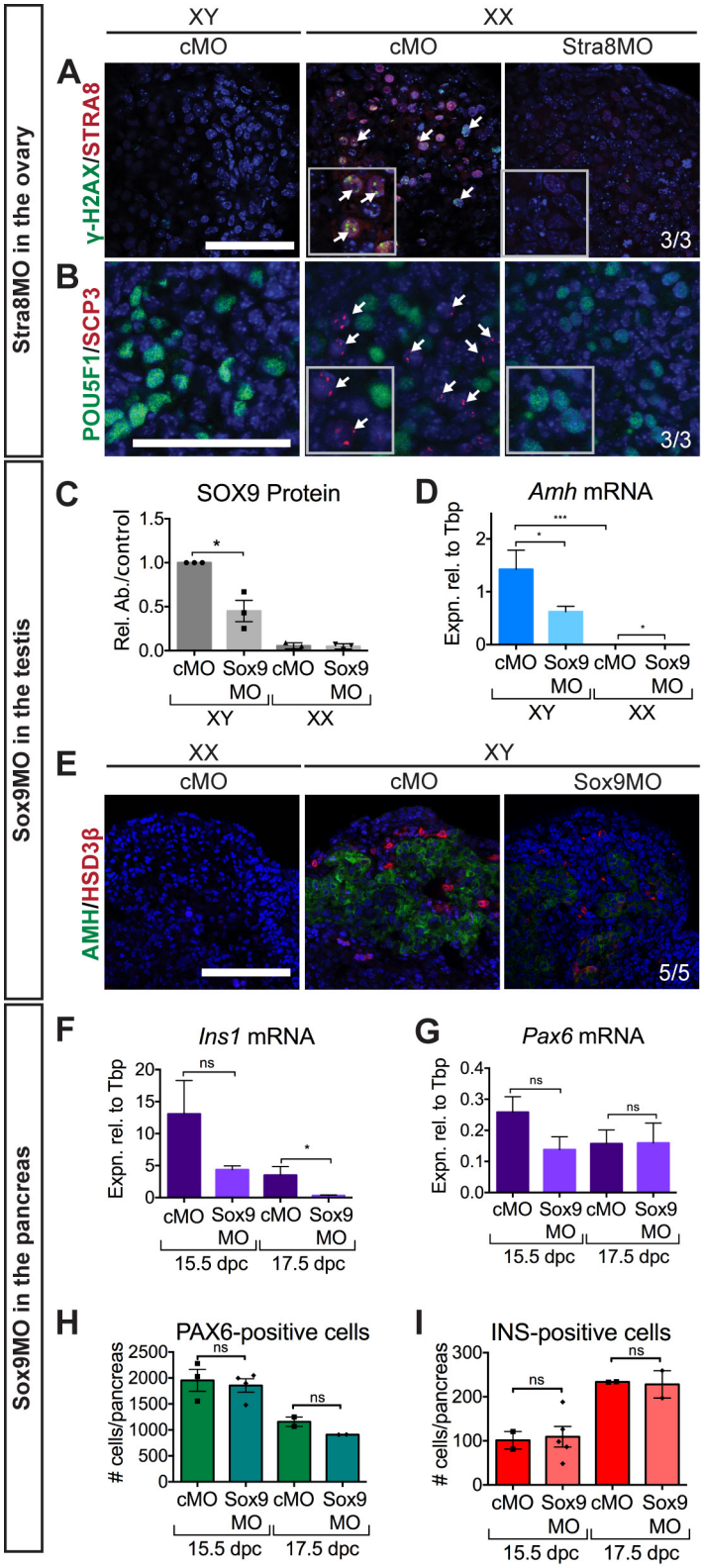
Stra8MO in the ovary
Sox9MO in the testis
Sox9MO in the pancreas
XY
XX
cMO
Stra8MO
A
γ-H2AX/STRA8
3/3
B
POU5F1/SCP3
3/3
C
SOX9 Protein
Rel. Ab./control
cMO Sox9 MO cMO Sox9 MO
XY XX
D
Amh mRNA
Expn. rel. to Tbp
E
XX
XY
cMO
cMO
Sox9MO
AMH/HSD3β
5/5
F
Ins1 mRNA
Expn. rel. to Tbp
ns
15.5 dpc
17.5 dpc
G
Pax6 mRNA
H
PAX6-positive cells
cells/pancreas
I
INS-positive cells

Figure 2.2. Partial phenocopy of known gene knockouts in gonad and pancreas.

(A,B) STRA8 knockdown: IF showed knockdown of STRA8 (A) in Stra8MO-treated XX gonads. Nuclear localisation of meiosis markers (γH2AX (A) and SCP3 (B); indicated by white arrows; see inserts) was absent but germ cells were present (POU5F1 (B); see inserts) in XX Stra8MO-treated gonads. (C-E) Knockdown of SOX9 in the gonad: Western blot for SOX9 (relative to α-TUBULIN or β-ACTIN) showed a downregulation of SOX9 (C) after Sox9MO treatment in XY gonads (*n*= 3). Downregulation of expression of SOX9 target gene *Amh* (D) expression was observed by qRT-PCR (*n*= 8, 15, 11, 4). IF for AMH and HSD3β (E) showed that AMH staining was weaker in XY Sox9MO samples compared to XY controls and that HSD3β-positive FLCs were present but staining was weaker in XY Sox9MO-treated gonads. (F-I) Knockdown of SOX9 in the pancreas: qRT-PCR of Sox9Mo treated pancreata showed *Ins1* (F) was downregulated but *Pax6* (G) was unchanged (*n*= 5, 5, 5, 5). Quantification of PAX6/INS-positive cells revealed that PAX6-positive (H) and INS-positive (I) cell number was unaltered by Sox9MO treatment (*n*= 3, 4, 2, 2). Scale bars = 100 μM; cMO = control morpholino; xMO = morpholino targeting gene x. For Western blots SOX9 levels were normalised to α-TUBULIN or β-ACTIN loading controls and Sox9MO-treated XY gonads measured relative to cMO treated XY gonads with expression for each blot set to 1. Rel. Ab./control = Relative Abundance of SOX9 to α-TUBULIN or β-ACTIN. For all qRT-PCR levels are shown relative to *Tbp,* error = S.E.M. For cell quantification error = S.E.M. with individual counts plotted. * = p = 0.05, ** = p = 0.001, *** = p = 0.0001, ns = not statistically significant.

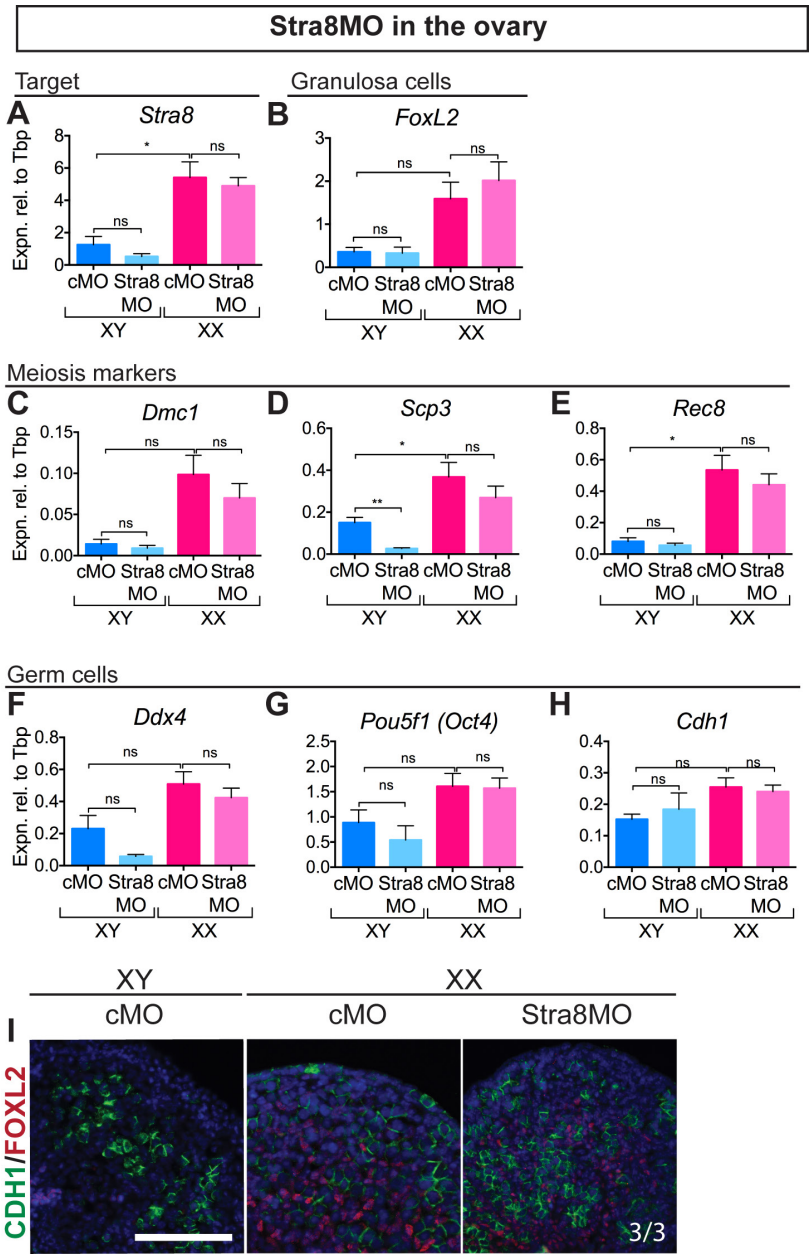

Figure 2.3. Knockdown of STRA8 does not affect general markers of gonadal or germ cell development.

Gene expression profiled by qRT-PCR in cMO-treated (XX and XY) versus Stra8MO- treated XX gonads (*n*= 4, 4, 10, 14) showed that target gene *Stra8* (A) and female marker gene *FoxL2* (B) were unchanged. Similarly, meiosis marker genes *Dmc1* (DMC1 dosage suppressor of mck1 homolog, meiosis-specific homologous recombination; C) *Scp3,* (D) and *Rec8* (REC8 meiotic recombination protein; E) and germ cell marker genes *Ddx4* (F), *Pou5f1* (G) and *Cdh1* (H) were unperturbed. IF for CDH1 and FOXL2 indicated that germ cells and somatic cells are present in Stra8MO-treated XX gonads (I; *n*= 3). Scale bars = 100 µM; cMO= control morpholino; xMO = morpholino targeting gene x. For all qRT-PCR levels are shown relative to *Tbp,* error = S.E.M., * = p = 0.05, ** = p = 0.001, ns = not statistically significant.

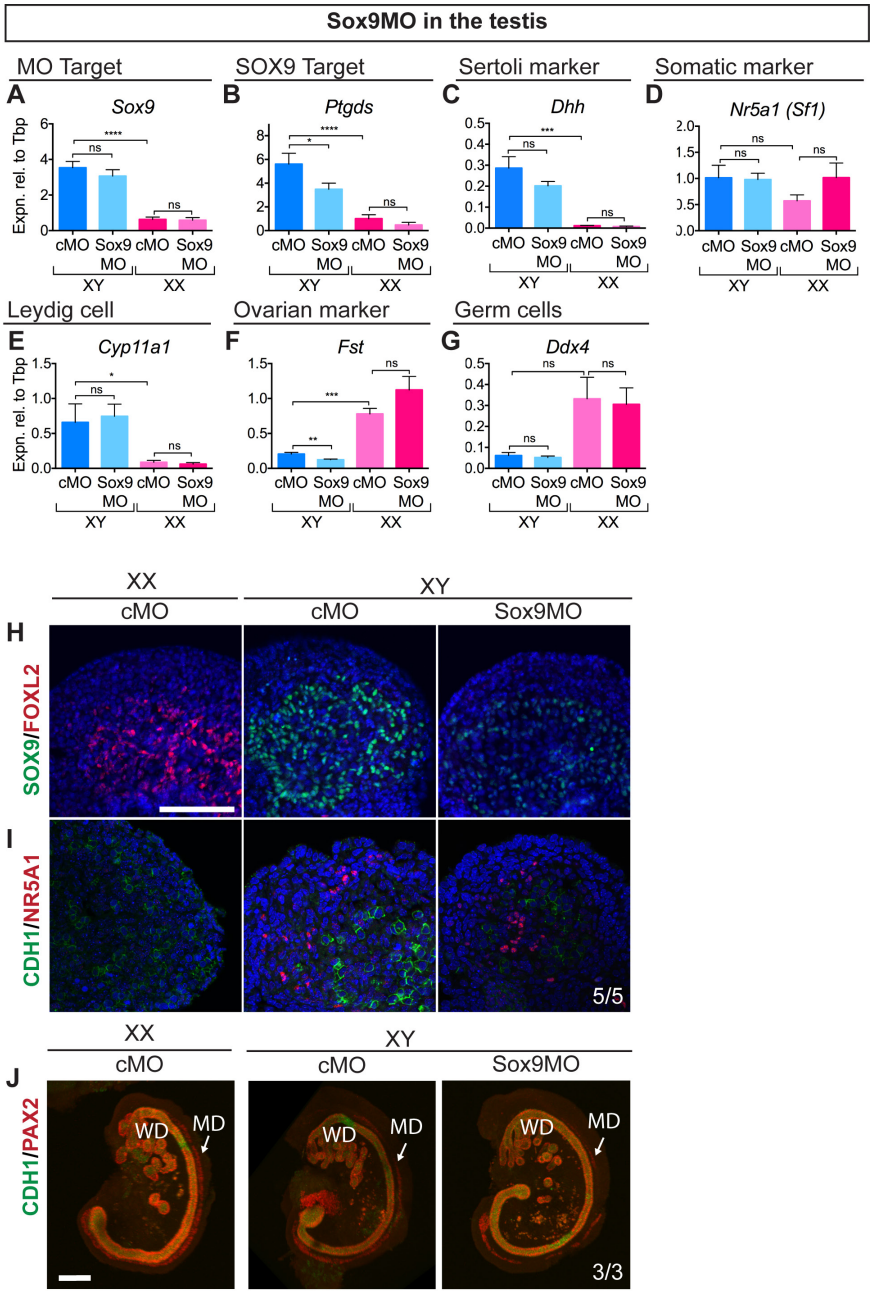

Figure 2.4. Knockdown of SOX9 using Sox9MO in gonad is specific to Sertoli cells but does not cause sex reversal.

qRT-PCR showed that knockdown of SOX9 in the gonad (A,B: *n*= 8, 15, 11, 4; C-G: *n*= 5, 9, 6, 4) had no apparent effect on target gene *Sox9* (A), however, downregulation of expression of SOX9 target gene *Ptgds* (B) was observed. Levels of Sertoli gene *Dhh* (C), somatic gene *Nr5a1* (D), FLC marker *Cyp11a1* (E) were unperturbed in Sox9MO-treated gonads. While expressed at very low levels in XY gonads, ovarian marker *Fst* (F) was significantly decreased in XY Sox9MO-treated gonads. Expression of germ cell marker *Ddx4* (G) was unperturbed. IF of XY Sox9MO treated gonads showed a decrease in SOX9 expression with no evidence of sex reversal (FOXL2-positive cells) (H; *n*= 5). Germ cells (CDH1) and FLCs (NR5A1) could be observed in XY Sox9MO treated gonads by IF (I). Whole-mount IF of gonad mesonephroi staining (J; *n*= 3): PAX2 (paired box 2), marks the Müllerian duct (MD), Wolffian duct (WD) and mesonephric tubules, and CDH1, marks the Wolffian duct and mesonephric tubules. The Müllerian duct is not retained in XY Sox9MO-treated mesonephroi indicating that the low level of AMH present can regress the duct as normal. Scale bars = 100 µM; cMO = control morpholino; xMO = morpholino targeting gene x. For all qRT-PCR: levels are shown relative to *Tbp,* error = S.E.M., * = p = 0.05, ** = p = 0.001, *** = p = 0.0001, **** = p = 0.00001, ns = not statistically significant.

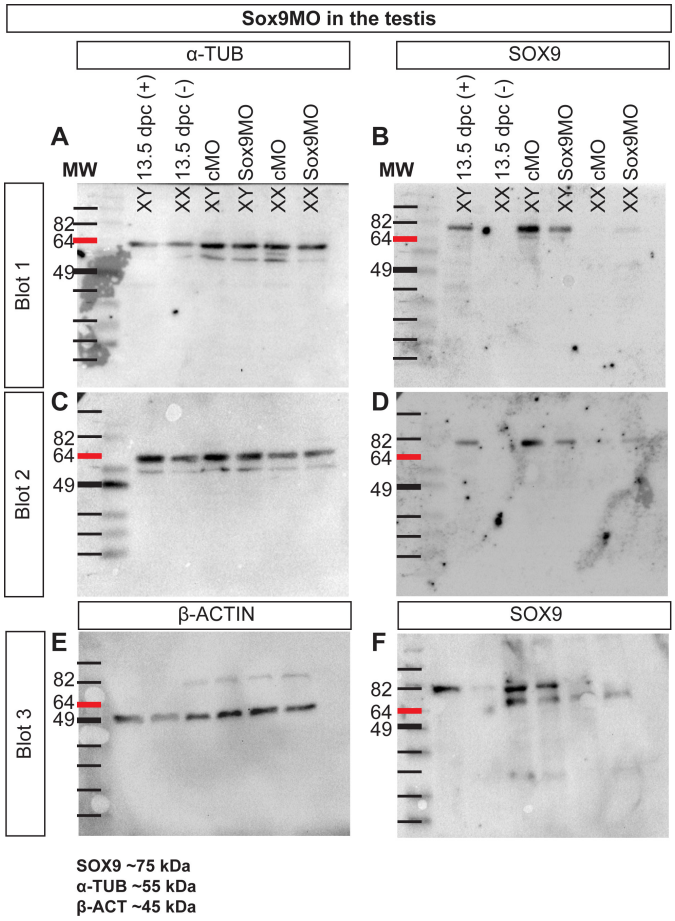

Figure 2.5. Raw Western blots showing knockdown of SOX9 in the Sox9MO treated XY gonad.

(A-F) Western blot for SOX9 (relative to α-TUBULIN or β-ACTIN) showed a downregulation of SOX9 upon Sox9MO treatment in XY gonads (*n*= 3) quantified in Fig. 2C. For Western blots SOX9 levels (B,D,F) were normalised to α-TUBULIN or β-ACTIN loading controls for each blot (A,C,E) and Sox9MO-treated XY gonads measured relative to cMO treated XY gonads with expression for each blot set to 1. 13.5 dpc XY gonads were used as a positive control and 13.5 dpc XX gonads were used as a negative control for SOX9 antibody specificity. cMO = control morpholino; xMO = morpholino targeting gene x.

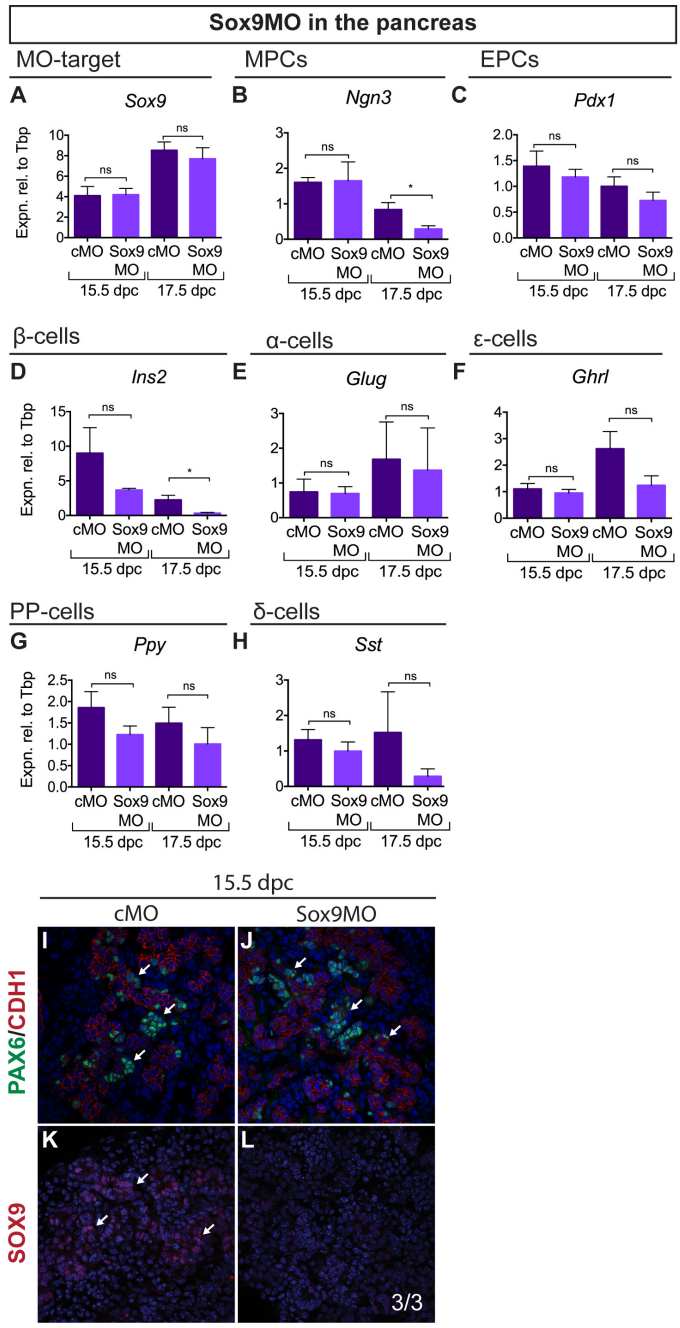

Figure 2.6. Knockdown controls for in Sox9MO treated pancreata.

qRT-PCR (*n*=5, 5, 5 ,5) showed that *Sox9* (A) expression was unperturbed by Sox9MO-treatment. Expression of *Ngn3* (B; marker of multipotent progenitor cells (MPCs)) was significantly decreased at 17.5 dpc. Expression of *Pdx1* (C; marker of endocrine progenitor cells (EPCs)) was unaltered, but *Ins2* (D) expression was significantly decreased in the Sox9MO-treated pancreata at 17.5 dpc. Expression of non-β-cell sub-type markers: α-cells *Glug* (E), ε-cells *Ghrl* (F), PP-cells *Ppy* (G) and δ-cells *Sst* (H) were all unaltered by treatment with Sox9MO. IF at 15.5 dpc showed that as in the cMO-treated pancreata (I), PAX6-positive cells (indicated by white arrows) differentiate when treated with Sox9MO (J), however, SOX9 expression (K,L; indicated by white arrows) is diminished when treated with Sox9MO. cMO = control morpholino; xMO = morpholino targeting gene x. For all qRT-PCR: levels are shown relative to *Tbp,* error = S.E.M., * = p = 0.05, ** = p = 0.001, ns = not statistically significant.

MO-mediated double knockdown of GLI transcription factors

We next investigated whether this approach could be used to knock down multiple genes simultaneously, as is commonplace in zebrafish and *Xenopus* studies. To this end we created a double knockdown of the downstream Hedgehog pathway activators GLI1 (GLI-Kruppel family member 1) and GLI2 (GLI-Kruppel family member 2). The Hedgehog signaling pathway promotes the differentiation of the steroidogenic FLC population during testis development. During this process, the ligand DHH (Desert hedgehog) is secreted by Sertoli cells. Hedgehog receptor, PTCH1 (Patched homolog 1), which is induced by Hedgehog signaling, as well as Hedgehog targets GLI1 and GLI2, are expressed by cells of the entire interstitial space that surrounds the testis cords (Barsoum and Yao, 2011; Bitgood et al., 1996; Yao et al., 2002). In *Dhh*-knockout XY gonads, there are greatly reduced numbers of steroidogenic FLCs (Bitgood et al., 1996; Yao et al., 2002). However, the differentiation of the FLC population is unaffected in XY gonads of either of *Gli1* or *Gli2* single-knockout embryos, suggesting that GLI factors act redundantly in the testis (Barsoum and Yao, 2011).

To address this potential redundancy, we generated a double knockdown of *Gli1/Gli2* using MO heart injection at 11.5 dpc and examined the effects 48h post-injection equivalent to 13.5 dpc. As a result, we detected by qRT-PCR a decrease in expression of steroidogenic pathway genes *Nr5a1, Star* (*steroidogenic acute regulatory protein*)*, Cyp11a1* and *Hsd3β* (Fig. 2.7A-D), indicating a reduction in steroidogenic cell number or capacity. The decrease in *Nr5a1* expression was consistent but not statistically significant. Notably, no change in the expression of these genes was detected in single Gli1MO (Fig. 2.7E-H) or Gli2MO (Fig. 2.7I-L) knockdowns. Thus, the attenuation of steroidogenic gene expression was specific to the Gli1/2MO double knockdown. No difference was observed in levels of the Hedgehog receptor gene *Ptch1* by qRT-PCR in the double or single knockdowns relative to controls (Fig. 2.8C,F,I), indicating that the extent of GLI knockdown was not sufficient to perturb expression of at least one known GLI target.

We quantified the number of steroidogenic cells to determine whether the decrease in steroidogenic gene expression was due to a decrease in cell number or to an impediment to cell maturation. There was no significant difference in the number of NR5A1-positive/SOX9-negative (immature FLC) or HSD3β-positive (FLC) cells between Gli1/2MO treated XY gonads and controls (Fig. 2.7M,N,O), suggesting that the observed phenotype is due to a decrease in steroidogenic capacity of the Leydig

cell population. Testis cords formed properly and expression of Sertoli cell marker *Amh*/AMH (Fig. 2.8A,D,G) and germ cell markers *Ddx4*/POU5F1 (Fig. 2.7M; Fig. 2.8B,E,H) appeared unaffected by the Gli1/2MO treatment (Fig. 2.7C,D), consistent with a lack of off-target or broadly toxic effects. Our results support functional redundancy between *Gli1* and *Gli2* in FLCs, and demonstrate proof-of-principle that heart injection of MO can be used to target multiple genes simultaneously to assess possible genetic interactions.

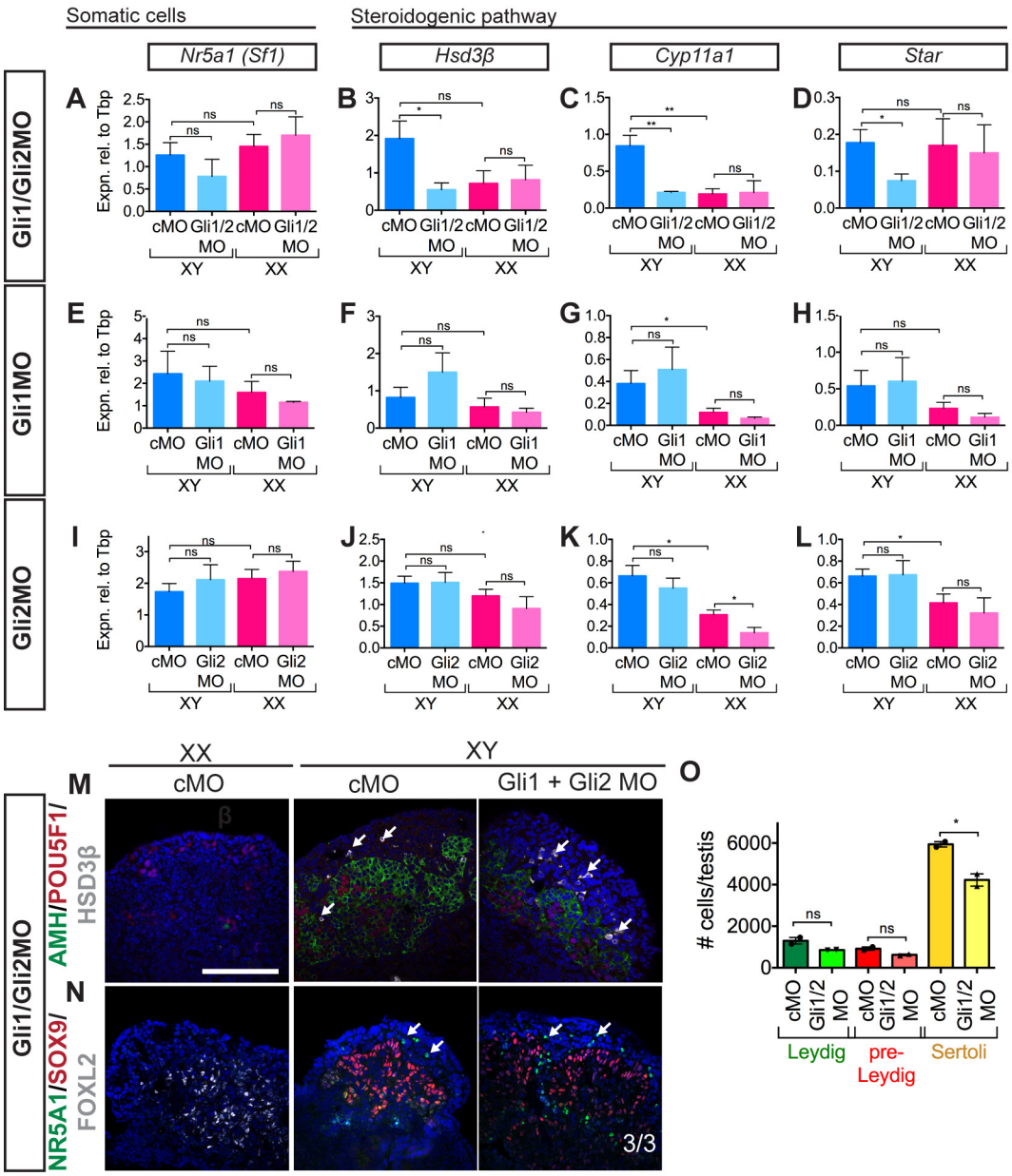

Figure 2.7. Double knockdown of Gli1/Gli2 in XY gonads.

(A-D) Knockdown of GLI1/GLI2 in the gonad: qRT-PCR showed that treatment with Gli1/Gli2MO (*n*= 6, 5, 5, 8) resulted in no significant downregulation in steroidogenic regulator *Sf1/Nr5a1* (A) but a significant downregulation in expression of steroidogenic pathway enzymes *Hsd3β* (B), *Cyp11a1* (C) and *Star* (D). No change was observed in *Nr5a1* expression in Gli1MO or Gli2MO knockdown (E,I). Similarly, there were no changes in expression of steroidogenic pathway enzymes *Hsd3β* (F,J), *Cyp11a1* (G,K) and *Star* (H,L) in Gli1MO (E-H; *n*= 6, 6, 7, 5) or Gli2MO (I-L; *n*= 8, 7, 4, 3) single knockdowns. IF showed Sertoli cells (AMH (M) and SOX9 (N)) and germ cells (POU5F1 (M)) were present in XY Gli1/Gli2MO treated gonads and no FOXL2-positive cells were observed (N). Steroidogenic *Hsd3β*-positive (M) and *Nr5a1*-positive (N) cells were still present in Gli1/Gli2MO treated XY gonads. Quantification (*n*= 2) of steroidogenic cells revealed no change in the number of HSD3β-positive Leydig cells (O; green) or NR5A1-positive/SOX9-negative pre-Leydig cells (O; red). There was a decrease in the number of SOX9-positve Sertoli cells in the Gli1/2MO treated XY gonads (O; yellow). Scale bars = 100 μM; cMO = control morpholino; xMO = morpholino targeting gene x. For all qRT-PCR levels are shown relative to *Tbp,* error = S.E.M. For cell quantification error = S.E.M. with individual counts plotted. * = p = 0.05, ** = p = 0.001, ns = not statistically significant.

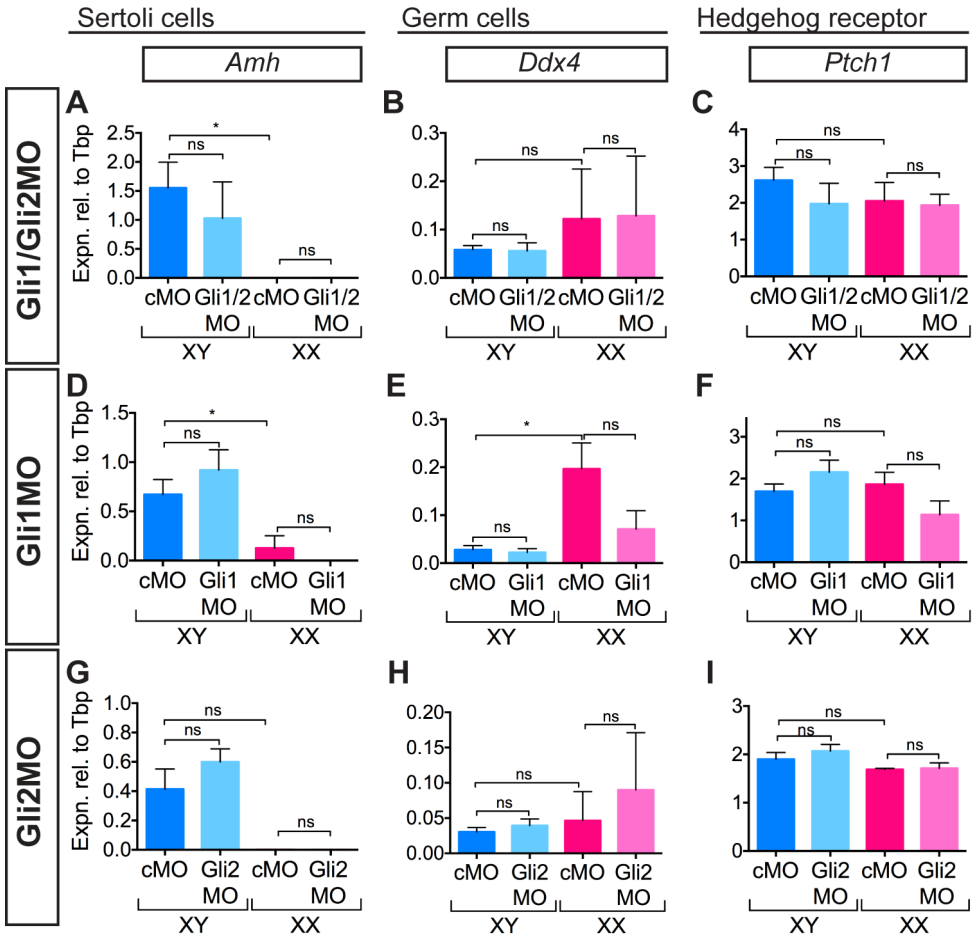

Figure 2.8. Gli1/2MO treatment has no effect of Sertoli or germ cells.

(A-C) Knockdown of GLI1/GLI2 in the gonad (*n*= 6, 5, 5, 8): qRT-PCR for Sertoli cells marked by *Amh* (A), germ cells marked by *Ddx4* (B) and hedgehog receptor *Ptch1* (C) showed no change after Gli1/Gli2MO treatment. The same trend was observed in the Gli1MO knockdown (*n*= 6, 6, 7, 5; *Amh* (D); *Mvh* (E); *Ptch1* (F)) and the Gli2MO knockdown (*n*= 8, 7, 4, 3; *Amh* (G); *Mvh* (H); *Ptch1* (I)). cMO = control morpholino; xMO = morpholino targeting gene x. For all qRT-PCR levels are shown relative to *Tbp,* error = S.E.M., * = p = 0.05, ns = not statistically significant.

Addressing novel gene function: Adamts19 and Ctrb1

Finally, we characterised the knockdown of two genes to which functions have not previously been ascribed, so as to test the utility of the system for first-pass functional characterisation of novel genes. We focused first on the ovarian gene *Adamts19* (*a disintegrin-like and metallopeptidase [reprolysin type] with thrombospondin type 1 motif, 19*), identified in a PCR-based cDNA subtraction screen, and in which polymorphisms have since been associated with premature ovarian failure (POF; (Knauff et al., 2009; Menke and Page, 2002; Pyun et al., 2013). The function of this gene remains unknown at the molecular, cellular or whole organism levels.

We performed qRT-PCR on FACS-sorted somatic cells at 12.5 dpc and confirmed that *Adamts19* was expressed in FOXL2-positive somatic cells, and not in the XX germ cells (Fig. 2.9A). MO knockdown of *Adamts19* resulted in no change in XX granulosa somatic markers *Fst* or *Irx3* (*Iroquois related homeobox 3;* Fig. 2.9B,C) and slight but not statistically significant decrease in expression of the germ cell marker *Ddx4* (Fig. 2.9D). However, there were no observed gross changes in the ratio of the number of FOXL2-positive (somatic) to MVH-positive (germ) cells by immunofluorescence (Fig. 2.9H). qRT-PCR expression of male markers *Amh* (Fig. 2.9E) and *Cyp11a1* (Fig. 2.9G) and somatic marker *Nr5a1* (Fig. 2.9F) were unperturbed by Adamts19MO treatment indicating there were no broad off-target effects of MO treatment. These results do not indicate a clear role for *Adamts19* in the developing ovary. Importantly, these data illustrate that treatment with a MO does not always perturb gonadogenesis, pointing to a lack of generalised non-specific artefacts.

We also examined the Sertoli-expressed gene *Ctrb1* (*chymotrypsinogen B1*), which has been implicated in gonadal development. In a screen of XX *Wnt4*-knockout (*wingless-related MMTV integration site 4*) mice, which exhibit partial sex reversal, expression of *Ctrb1* was increased, suggesting an association with the testis development pathway (Coveney et al., 2008b). Differential expression data sets indicate that *Ctrb1* is testis-specific from 12.5 dpc and that it is expressed in the Sertoli cell lineage (Jameson et al., 2012b).

Knockdown of *Ctrb1* resulted in no change to Sertoli cell markers *Sox9* and *Amh,* but a statistically significant increase in the expression of *Ptgds* in the testis by qRT-PCR (Fig. 2.9I, J, K). In the XX Ctrb1MO treated gonad, *Ptgds* expression was decreased compared to the XX control. No changes

were observed in the expression of the steroidogenic gene *Cyp11a1,* granulosa cell marker *Fst* or germ cell marker *Ddx4* (Fig. 2.9L, M, N) in the XY Ctrb1MO treated gonad, suggesting that the other testis cell lineages are unperturbed. The increase in *Ptgds* expression resulting from knockdown of *Ctrb1* implicates *Ctrb1* in processes downstream of SOX9, such as *Ptgds* regulation and as such provides a basis for the instigation of further genetic studies.

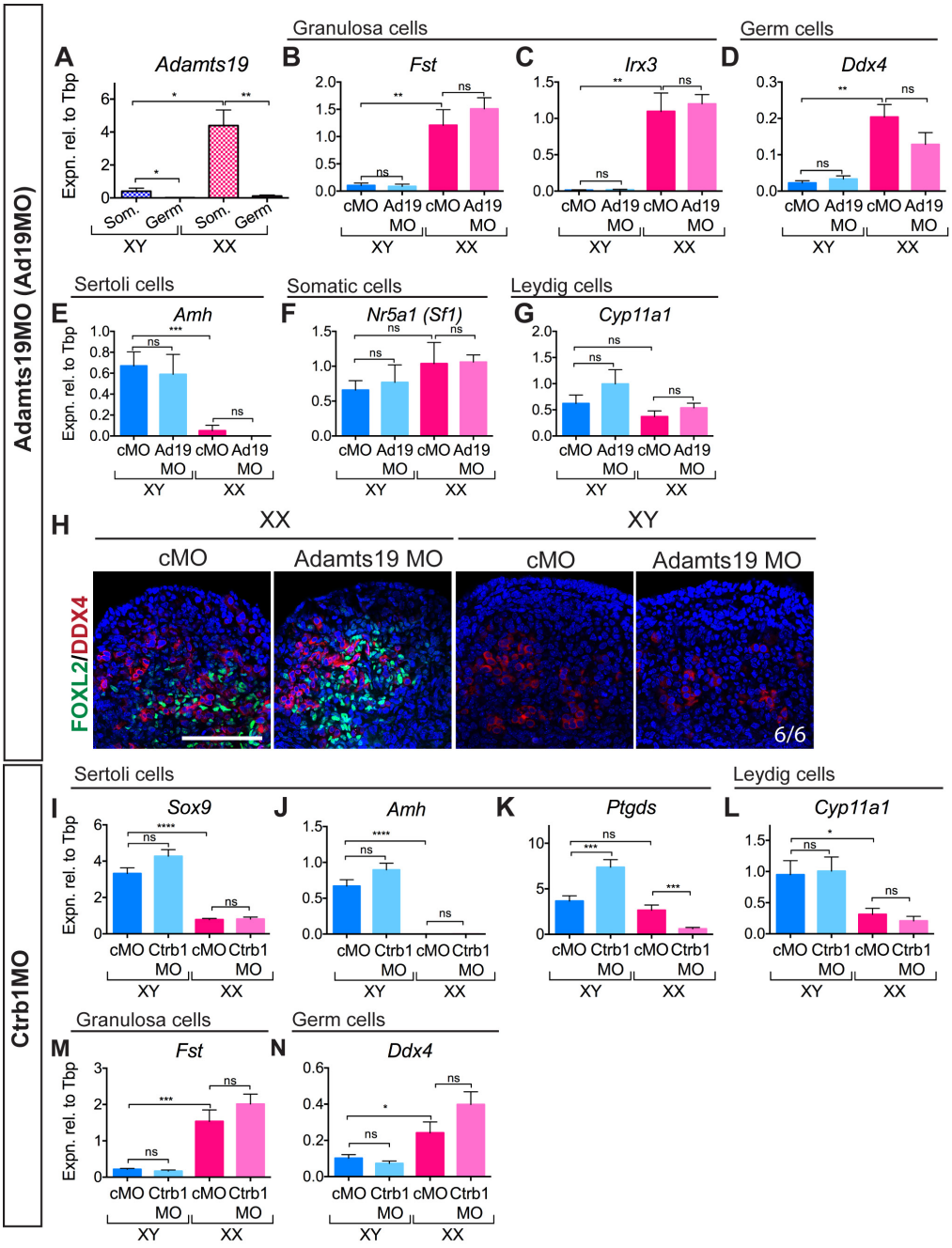

Figure 2.9. Knockdown of Adamts19 in XX gonads and Ctrb1 in XY gonads.

(A) qRT-PCR on FACS-sorted somatic and germ cells (*n*= 3, 4, 3, 4) shows that *Adamts19* is expressed in the somatic cells of the ovary at 12.5 dpc and at much lower levels in somatic cells of the testis. Knockdown of ADAMTS19 in the XX gonad (n= 7, 8, 5, 5) showed no change in female somatic markers *Fst* (B) and *Irx3* (C) and a slight decrease in expression of germ cell marker *Ddx4* (D). Male markers, *Amh* (Sertoli cells; E), *Nr5a1* (Somatic cells; F) and *Cyp11a1* (Leydig cells; G) were unperturbed. IF showed no discernable difference in the ratios of FOXL2-positive/DDX4-positive cells in the Adamts19MO-treated XX gonad compared to the control (H). Knockdown of CTRB1 in the XY gonad (*n*= 19, 16, 14, 14) resulted in no change to male somatic markers *Sox9* (I) or *Amh* (J) but an increase in *Ptgds* (K) was observed in the Ctrb1MO-treated XY gonad. Expression of Leydig cell marker *Cyp11a1* (L), female somatic marker *Fst* (M) and germ cell marker *Ddx4* (N) was unchanged. Germ = germ cells, Som. = somatic cells. Scale bars = 100 µM; cMO = control morpholino; xMO = morpholino targeting gene x. For all qRT-PCR: levels are shown relative to *Tbp,* error = S.E.M., * = p = 0.05, ** = p = 0.001, *** = p = 0.0001, **** = p = 0.00001, ns = not statistically significant.

Discussion

We describe here a novel first-pass screening method that can provide insights into the function of candidate organogenesis genes, singly or in combination, either to assist with the design of in-depth genetic and biochemical investigations, or to prioritise lists of candidate genes for these investigations. By injection of MOs into the heart of mouse embryos, we exploited the embryonic vasculature to deliver the MO to the target tissues, which were then explanted, cultured and analysed. Using this technique we partially reproduced known gene knockout phenotypes in the fetal gonads and pancreas, created a novel double knockdown of GLI1 and GLI2, and screened *Adamts19* and *Ctrb1* for potential function in early gonadal development. These studies reveal the utility of this method to obtain insights into gene function during organogenesis rapidly and relatively simply.

The method described here provides a significant improvement on previous injection- and electroporation-based delivery strategies, which suffered from limited delivery area and/or uptake, tendency for tissue damage and lack of reproducibility. Published methods of gain-of-function (cDNA) or loss-of-function (shRNA) construct delivery by magnetofection, nucleofection or liposome-mediated methods in cultured gonads have shown delivery of the effector construct to 2-20% of cells in the target tissue (Gao et al., 2011; Nakamura et al., 2002; Ryan et al., 2011; Svingen et al., 2009b). In contrast, we visualised delivery of fluorescent MO throughout the tissue of interest, saw consistent knockdown of downstream target genes throughout the cultured organ, and showed in the XY gonad that the MO could target genes in multiple cell lineages. Secondly, injection of the MO into the heart avoids compromising the integrity of the target tissue by direct contact with needles and/or electrodes. Finally, relying on systemic delivery rather than direct injection of the effector construct avoids experimental error and instead produced consistent gene knockdown for the target gene in multiple experiments performed over a two-year period.

Encouragingly, in our proof-of-principle and double-knockdown experiments, it was the capacity of a cell population to express downstream target genes and proteins, rather than the number of expressing cells, that was altered by MO treatment. The knockdown of the target protein was incomplete in all cases; this allowed differentiation of the target cells but their functionality was reduced. For example, FLCs still differentiated in normal numbers in the *Gli1/Gli2* MO treated XY gonads, but they did not produced steroid enzymes at the same capacity as the controls. This

indicates that the processes controlled by GLI factors were being perturbed by MO treatment, similarly to the Sox9MO treated XY gonads and pancreata. Importantly, the subtle outcomes of MO treatment were highly reproducible, as shown by our qRT-PCR analyses, suggesting that the information generated provides a robust basis on which to base mechanistic hypotheses and further experiments.

In addition to partially reproducing several established null mouse models, using MO injection we strengthened the case for creating a complex genetic conditional double knockout of GLI1 and GLI2 in FLCs (Barsoum and Yao, 2011). Our findings suggest that there is functional redundancy between GLI1 and GLI2 in the developing testis and that further genetic analysis is likely to be fruitful.

With any experiments involving MOs, careful attention to controls is required (Eisen and Smith, 2008). By careful examination of untargeted cell populations in the organ of interest, we were able to identify and exclude off-target effects and toxicity. Nonetheless, concerns have been raised regarding the difference between MO knockdown phenotypes and other functional analysis methods (Schulte-Merker and Stainier, 2014). This difference is at least partly explained by the fact that MO knockdown only partially reduces overall activity of the target protein; certainly, in our Sox9MO experiments, the phenotypes obtained more closely resembled heterozygous than homozygous knockouts. All things considered, it is clear that genetic targeting by homologous recombination or CRISPR/Cas9 approaches will remain the gold standard for functional analysis. Therefore, we suggest that, once a likely effect is revealed by MO studies, it would be more useful to advance to definitive functional experiments, rather than to devote additional resources to definitively excluding off-target effects (for example by assaying multiple MOs for each gene of interest).

End of published paper

Additional work using MO heart injection outlined below:

For the work herein:

All reagents are described in Supplemental Tables 1-4. All additional work was performed as described in the manuscript (above). Additionally the cell sorting and statistical analysis for Fig. 2.13A-C and Fig. 2.15I-J was performed as described in Chapter 3 (statistical significance was determined using one-way ANOVA with Bonferroni's multiple comparisons test)

2.5 Hedgehog signalling pathway: GLI3 in the developing gonad

In the publication in this chapter I created a double knockdown of the downstream Hedgehog pathway activators GLI1 and GLI2. The Hedgehog signaling pathway promotes the differentiation of the FLC population during testis development. The ligand DHH is secreted by Sertoli cells, whilst the receptor (PTCH1) and targets (GLI1 and GLI2) are expressed by cells of the entire interstitial space that surrounds the testis cords (Barsoum and Yao, 2011; Bitgood et al., 1996; Yao et al., 2002). In *Dhh*-knockout XY gonads, there are greatly reduced numbers of steroidogenic FLCs (Bitgood et al., 1996; Yao et al., 2002). However, in either the *Gli1* or *Gli2* knockout testis the differentiation of the FLC population is unaffected, suggesting that GLI factors act redundantly (Barsoum and Yao, 2011). We demonstrated that, as in the genetic knockout, knockdown of either GLI1 or GLI2 had no effect on steroidogenesis, but double knockdown of GLI1 and GLI2 resulted in reduced expression of steroidogenic pathway genes. Overall, the same number of FLCs differentiated in control and Gli1/Gli2MO treated XY gonads, but in Gli1/Gli2MO-treated XY gonads transcription of genes encoding steroidogenic enzymes was attenuated.

The role of GLI3 has not been investigated in testicular development previously. It is thought that GLI1 and GLI2 act primarily as transcriptional activators, while GLI3 is a transcriptional repressor (Pan et al., 2006). A testicular *Gli3* -/- phenotype has not been described, so I used a Gli3MO to knock down *Gli3* from 11.5 dpc in the gonad. Knockdown of GLI3 alone did not perturb gonadogenesis. Expression of the genes encoding markers of the male pathway such as somatic cell marker *Nr5a1* (Fig. 2.10A), Sertoli cell marker *Amh* (Fig. 2.10B) and interstitial cell marker *Notch2* (Fig. 2.10D) were unperturbed by Gli3MO treatment. In response to a hedgehog ligand such as DHH, transcription of *Ptch1* is up-regulated (Ingham and McMahon, 2001) and, therefore, expression of *Ptch1* can be used as a read-out of HH pathway activity. In Gli3MO-treated XY gonads, expression of *Ptch1* (Fig. 2.10C) was unchanged, as was the expression of steroidogenic cell markers, *Star, Cyp11a1* and *Hsd3β* (Fig. 2.10E-G), indicating that Hh signaling and FLC

development were unperturbed by GLI3 knockdown. As expected, expression of the genes encoding ovarian marker *FoxL2* (Fig. 2.10H) and germ cell marker *Ddx4* (Fig. 2.10I) was unaltered by Gli3MO treatment. These data indicate that single knockdown of GLI3 does not perturb FLC development and function in XY gonads. It is possible, however, that GLI3 loss is compensated for by the presence of GLI1 and/or GLI2.

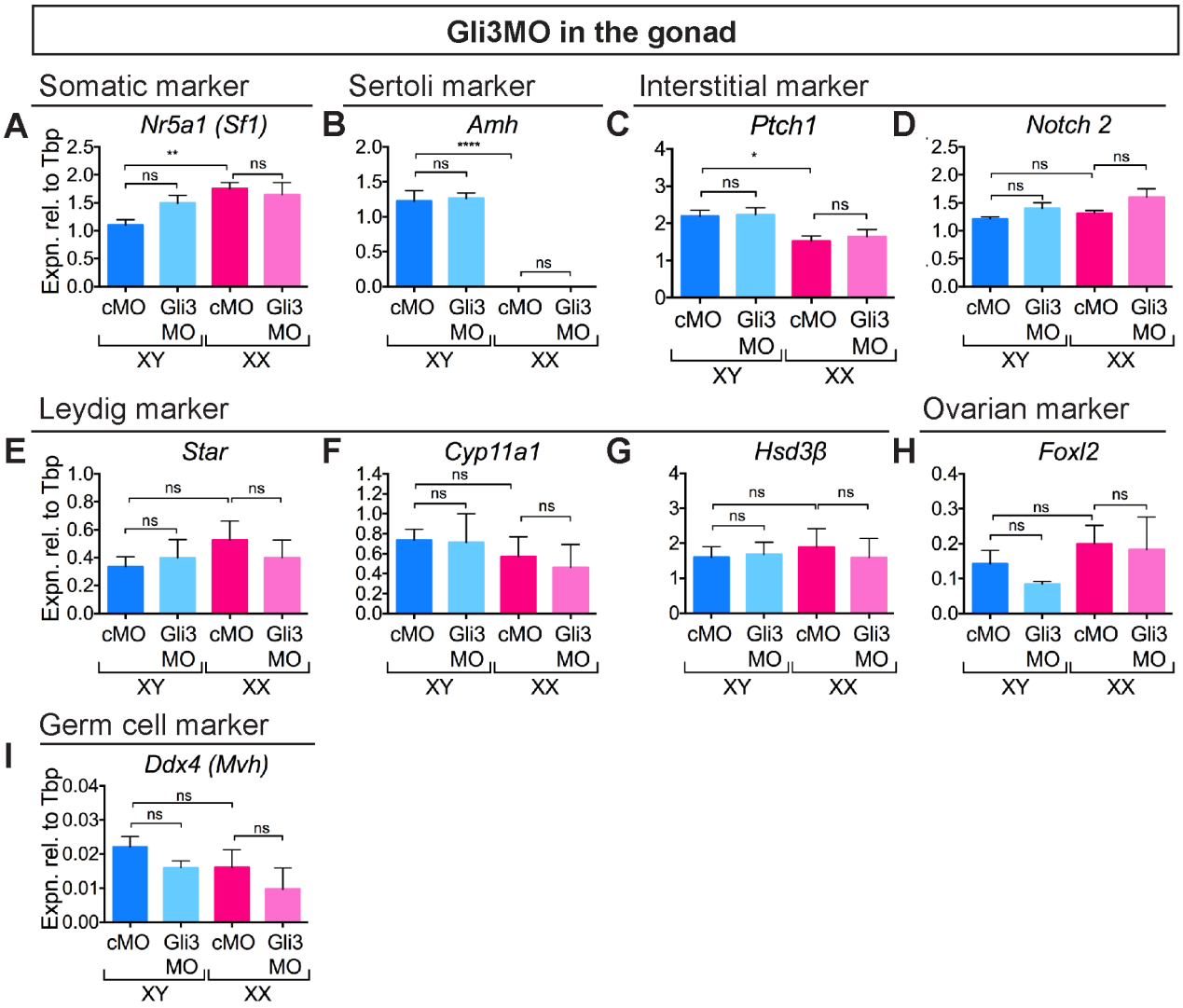

Figure 2.10. Knockdown of Gli3 in the gonad.

(A-I) Knockdown of GLI3 in the gonad: qRT-PCR showed that treatment with Gli3MO (*n*= 5, 5, 4, 3; *n*= 1 = pool of 3 single gonads from 3 embryos) resulted in no significant downregulation in steroidogenic regulator *Nr5a1* (A) or Sertoli cell marker gene *Amh* (B). Expression of DHH target and receptor *Ptch1* (C) was unaltered and was interstitial marker *Notch2* (D). Expression of steroidogenic pathway members *Star* (E), *Cyp11a1* (F) and *Hsd3β* (G) was unaltered in Gli3MO gonads. No change was observed in expression of ovarian marker *FoxL2* (H) or germ cell marker *Ddx4* (I) in the Gli3MO knockdown. cMO = control morpholino; xMO = morpholino targeting gene x. For all qRT-PCR levels are shown relative to *Tbp,* error = S.E.M. * = p = 0.05, ** = p = 0.001, *** = p = 0.0001, ns = not statistically significant.

2.6 Wnt4: targeting genes that act early in gonadogenesis

In the publication in this chapter I used MOs against *Stra8* and *Sox9* as controls for the development of the heart injection protocol. In addition we also trialled using a MO to knockdown WNT4, with injection of the MO at 11.5 dpc followed by 48 h culture. WNT4 is important for ovarian development and it expressed robustly from 11.5 dpc. Like SOX9, WNT4 was chosen as a candidate for MO knockdown to assess if knockdown of candidate genes could phenocopy aspects of the knockout when target transcript is already abundant at the time of injection.

Wnt4 is expressed in the 11.5 dpc XX and XY gonad and is later maintained in the ovary and in the mesonephros of both sexes (Vainio et al., 1999). The early expression of NR5A1 in XX and XY *Wnt4-/-* gonads is abnormal (Jeays-Ward et al., 2003). In XX *Wnt4-/-* mice, ovaries are masculinised: ectopic steroidogenic cells are present and the ovaries form a vascular network reminiscent of the coelomic vessel. On the other hand, in *Wnt4-/-* XY gonads Sertoli cell differentiation and testis cord structure are compromised (Jeays-Ward et al., 2003; Jeays-Ward et al., 2004; Vainio et al., 1999).

A published screen of *Wnt4-/-* XX gonads aimed to detect genes downstream of WNT4 signaling in the differentiating ovary (Coveney et al., 2008b). This screen identified *Sp5* (trans-acting transcription factor 5), a known target of Wnt/β-catenin signaling in zebrafish, as a putative WNT4 target in the mouse gonad (Coveney et al., 2008b; Weidinger et al., 2005). Additionally, expression of *Ctrb1*, an XY-enriched gene in wild-type gonads, was increased in XX *Wnt4-/-* gonads compared to XX wild-type gonads, indicating it may be a WNT4 target (Coveney et al., 2008b).

WNT4 is robustly expressed at the stage of injection (11.5 dpc) and likely exerts its influence early in gonadogenesis, and so it was expected that knockdown of WNT4 would result in only a mild gonadal phenotype or no phenotype. As anticipated, gonadogenesis was apparently unperturbed by Wnt4MO treatment at 11.5 dpc. qRT-PCR on single gonad samples demonstrated that expression of the target gene *Wnt4,* and ovarian marker genes *Fst* and *FoxL2,* was unperturbed by Wnt4MO injection (Fig. 2.11A-C). Additionally, expression of WNT4-responsive genes *Sp5* and *Ctrb1* was not altered by Wnt4MO treatment (Fig. 2.11E,F). Expression of the genes encoding Sertoli cell marker *Sox9,* Leydig cell marker *Cyp11a1* and germ cell marker *Ddx4* was equivalent between Wnt4MO-treated and control gonads (Fig. 2.11D,G,H). Therefore, Wnt4MO did not result in any

changes in the expression of WNT4-responsive genes or the differentiation of ectopic steroidogenic cells in the XX Wnt4MO treated gonad (Fig. 2.11D,G,H). It is likely that the MO treatment was insufficient to perturb the primary function of WNT4. These data highlight the limitations of the technique. As a result, I have also extended the utility of the heart injection technique by successfully performing heart injection and gonad culture one day earlier at 10.5 dpc, followed by 3 day hanging drop culture (data not shown; collaboration with Allen Feng, Koopman Lab, IMB, UQ).

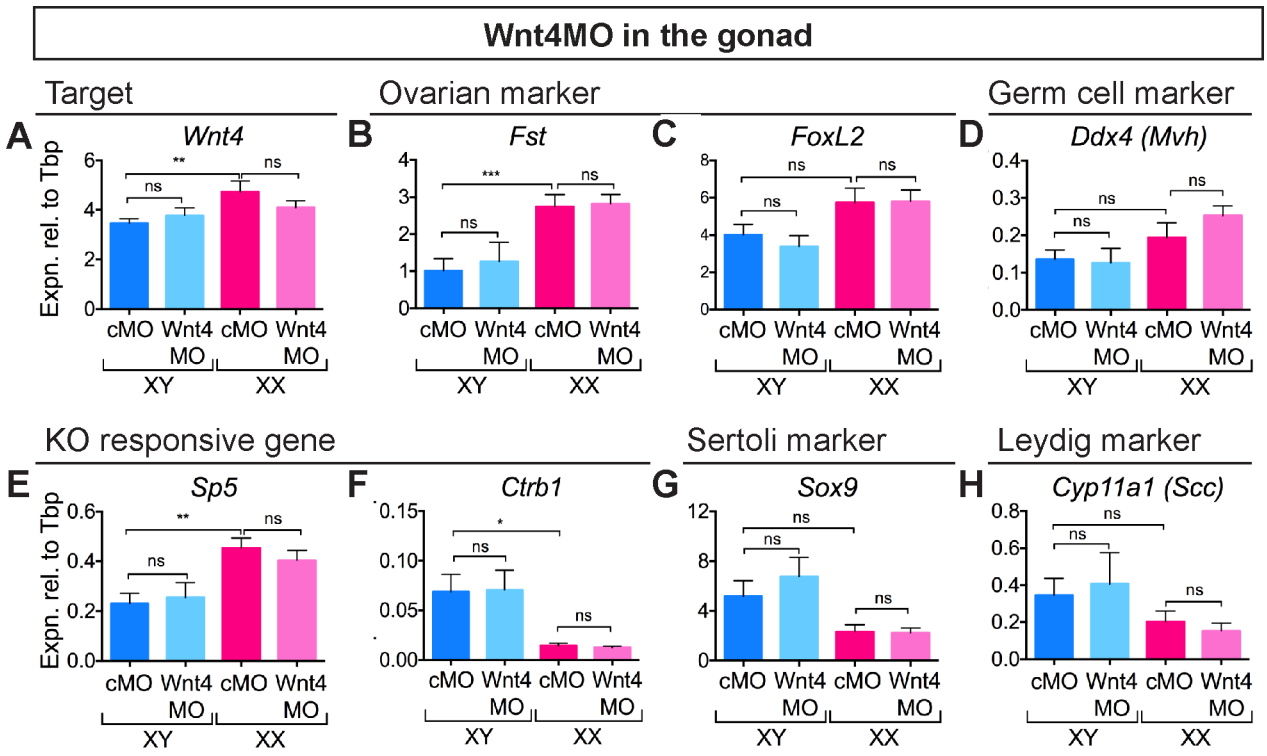

Figure 2.11. Knockdown of Wnt4 in the gonad.

(A-H) Knockdown of WNT4 in the gonad: qRT-PCR showed that treatment with Wnt4MO (*n*= 16, 8, 13, 22) resulted in no perturbation of *Wnt4* (A), ovarian marker genes *Fst* (B) and *FoxL2* (C) or germ cell marker gene *Ddx4* (D). Expression of *Wnt4*-/- responsive genes *Sp5* (E) and *Ctrb1* (F) was unaltered by treatment with Wnt4MO, as was Sertoli marker *Sox9* (G) and Leydig cell marker *Cyp11a1* (H). cMO = control morpholino; xMO = morpholino targeting gene x. For all qRT-PCR levels are shown relative to *Tbp,* error = S.E.M. For cell quantification error = S.E.M. with individual counts plotted. * = p = 0.05, ** = p = 0.001, *** = p = 0.0001, ns = not statistically significant.

2.7 Novel DSD candidate genes

The following studies are part of a collaborative project with Stefanie Eggers and Andrew Sinclair (MCRI, Melbourne) as part of the *NHMRC Program in Human Disorders of Sexual Development*. The data pertaining to initial DSD candidate gene identification from whole exome sequencing of patients and families (Fig. 2.12, 2.14) were generated by Stefanie Eggers as part of her PhD. Initial expression analysis of the candidate gene and MO injections were performed by me (Fig 2.13; see declaration for more details).

2.7.1 SART3: candidate for 46,XX and 46,XY DSD

SART3 was identified as a potential DSD candidate gene in two Morroccan/Libyan Jewish families from Israel using whole exome sequencing. The two families each had an individual with 46,XY DSD and intellectual disability, a 46,XX individual with intellectual disability only, and unaffected parents (Fig. 2.12A). Relatedness and inbreeding calculations suggested that the two Israeli families were likely to be related and therefore were likely to share haplotypes. Linkage analysis identified a linkage peak on chromosome 12, where all four affected children were identical by descent, as the critical region. Of the 89 genes contained in this region the gene *SART3* was the only gene containing a variant that followed the proposed autosomal recessive inheritance pattern in both families (parents all het, affected children all homozygous). In both families, *SART3* contained a single nucleotide variant, which was predicted to be deleterious, in exon 17 (Fig.2.12B,C). Additionally, a heterozygous mutation in *SART3* was identified in an unrelated individual with 46,XY DSD who had hearing impairment but no reported intellectual disability. A previously published patient with a deletion of the region including *SART3* was also identified; this patient had 46,XX DSD with intellectual disability and hearing impairment (Petek et al., 2003). These data from two unrelated families and a published case suggest that *SART3* is the causative DSD gene.

In support of a role for *SART3* in testicular development and 46,XY DSD, *SART3* is expressed in the adult human testes (Liu et al., 2002; Nagase et al., 1995; Yang et al., 1999). The function of *SART3* in sexual development has not been established, but there is some *in vitro* evidence from AR transactivation luciferase assays that *SART3* can bind the androgen receptor (AR) and suppress AR transcriptional activation of downstream genes through its nuclear-receptor box (LXXLL-motif) (Liu et al., 2004). Dual-luciferase reporter trans-activation assays performed by Stefanie Eggers demonstrated that, *in vitro,* at a low androgen concentration that mimics endogenous female levels,

wild-type SART3 abolishes transcriptional activation of AR target genes. On the other hand, at higher testosterone concentrations, that mimic endogenous male levels, SART3 allowed the activation of downstream targets of AR. However, mutant-*SART3* with the exon 17 SNV exhibited a concentration-independent repression of AR; this mechanism would indicate that expression of mutant-*SART3* in the testis might create a pseudo-female state despite the high androgen concentration (S. Eggers, personal communication). Additionally, these data indicate that the SNV identified in exon 17 is a gain-of-function mutation that acts as a dominant negative, resulting in constitutive suppression of the ability of AR to activate downstream targets. This model would explain why a gonadal/DSD phenotype is observed in the 46,XY children, but not in the 46,XX children who carry the same mutation. Under this model, in XX individuals with the exon 17 SNV *SART3* mutation, the androgen response would be further suppressed, reinforcing the *status quo* in XX individuals and resulting in normal ovarian development.

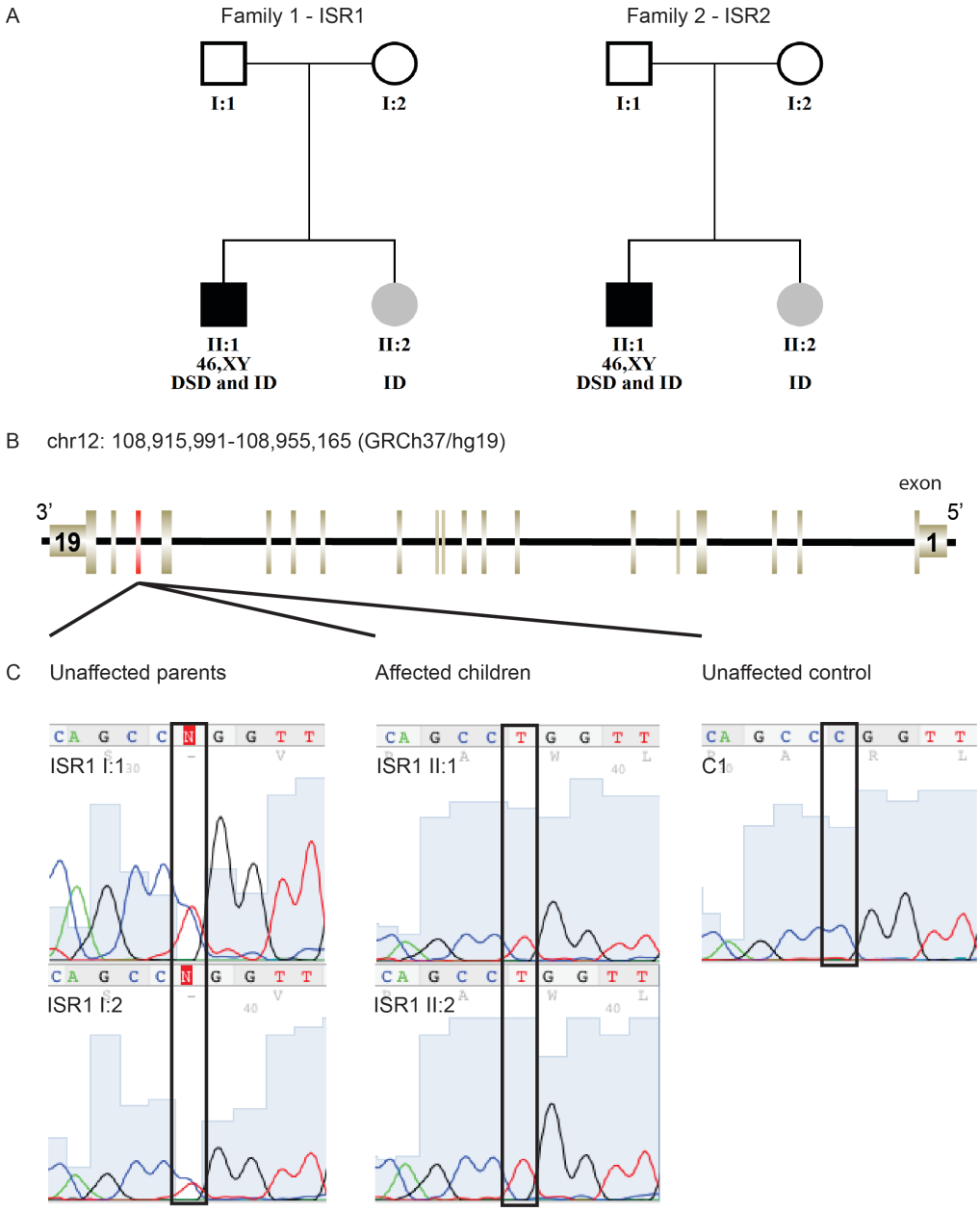

Figure 2.12. A novel single nucleotide variant (SNV) in exon 17 of SART3 was identified in both families to be associated with 46,XY DSD and ID.

(A) Pedigrees of the two families, showing all eight individuals that were available for this study. Squares and circles represent males and females, respectively. Open symbols indicate unaffected individuals, filled squares and circles highlight affected individuals. 46,XY DSD/ID patients are shown as black squares, and the two girls affected by isolated ID are indicated by light grey circles. (B) Schematic view of the *SART3* genomic region on chr12: 108,915,991-108,955,165 (GRCh37/hg19) including the exon-intron structure (*SART3* is located on the reverse strand and shown here in its 3'-5' orientation from left to right). Exon 17 is highlighted in red. (C) Electropherograms (forward strand) of both unaffected parents of family ISR1 (father ISR1 I:1 and mother ISR1 I:2) showing the heterozygous SNV (c.2507G>A (reverse strand) or C>T (forward strand), both affected children of ISR1 (46,XYDSD/ID ISR1 II:1 and 46,XX ID ISR1 II:2) showing the homozygous SNV, and one control sample (C1) showing the wild-type *SART3* exon 17 sequence (*data, figure and legend produced by Stefanie Eggers, reproduced with permission*).

Sart3 Expression and Knockdown

To validate the function of *SART3* in gonadogenesis the expression and function of *Sart3* were examined in the mouse. Published microarray expression data indicated that *Sart3* was expressed in all major cell lineages in XX and XY gonads (Jameson et al., 2012b). We used FACS-sorted *Sf1*-eGFP XY cells to confirm by qRT-PCR that *Sart3* is expressed at similar levels in the Sertoli cells, FLCs, NSICs and germ cells of the XY gonad from 12.5-14.5 dpc (Fig. 2.13A-C). Similarly, *Sart3* was expressed in the somatic and germ cells of the XX gonad from 12.5-14.5 dpc (Fig. 2.13A-C). These data indicated that expression of *Sart3* was not sexually dimorphic or restricted to a single cell lineage in XX or XY gonads. Immunofluorescence and *in situ* hybridization in mouse tissues during embryonic development and into adulthood showed expression of *Sart3*/SART3 throughout the testis and ovary, and in regions of the hippocampus (CA1-CA3 regions; S. Eggers, personal communication).

To determine the function of SART3 during gonad development I used a Sart3MO to examine the effect of SART3 knockdown on gonadogenesis. The Sart3MO knockdown modelled haploinsufficiency, or heterozygous deletion, of *SART3,* as described in the 46,XX DSD patient (Petek et al., 2003). Therefore, it was expected that knockdown of SART3 would result in an XX gonadal phenotype. qRT-PCR demonstrated that expression of the genes encoding *Nr5a1* and Sertoli cell markers *Sox9, Amh, Ptgds*, *Dhh* and *Gata4* was unaffected by Sart3MO injection in XX and XY gonads (Fig. 2.13D-I). Moreover, by immunofluorescence expression of AMH and testis cord structure appeared normal and similar between XY Sart3- and control-MO treated gonads (Fig. 2.13U), indicating that Sertoli cells were unaffected by SART3 knockdown. Additionally, expression of the genes encoding *Nr0b1* and female somatic markers *Wnt4, FoxL2* and *Fst* was equivalent between the control and Sart3MO injected samples, indicating that female somatic cells were unperturbed by SART3 knockdown (Fig. 2.13O-R). qRT-PCR showed that expression of the gene encoding germ cell marker *Ddx4*/DDX4 was unaffected, as was DDX4 protein expression, indicating that germ cells were unperturbed by SART3 knockdown (Fig. 2.13S,T).

Interestingly, the SART3 protein has an LXXLL-motif and so has the ability to interact with transcription factors such as NR5A1, and therefore, could potentially regulate steroid biosynthesis/response pathways (Liu et al., 2004). Hence, I investigated if the expression of *Nr5a1* and steroidogenic pathway genes was altered by knockdown of SART3. By qRT-PCR there was no

change in expression of *Nr5a1* between Sart3MO and control treated gonads (Fig. 2.13D). However, expression of the gene encoding the early steroidogenic pathway component *Star,* which mediates the transfer of cholesterol across the mitochondrial membrane, was elevated in XX/XY Sart3MO treated samples compared to controls (Fig. 2.13J). Additionally, in XX Sart3MO treated gonads, expression of the gene encoding the early steroidogenic pathway enzyme *Cyp11a1,* which catalyses the second step of the steroid biosynthesis pathway, was significantly increased, to levels equivalent to those observed in XY control gonads (Fig. 2.13K). Expression of the gene encoding later steroidogenic pathway enzyme *Hsd3β* was also elevated to levels similar to the XY control in XX Sart3MO treated gonads (Fig. 2.13L). Expression of *Insl3,* a marker of FLC maturation that is not associated with steroidogenesis, was not expressed at biologically meaningful levels in XX Sart3MO treated gonads, and *Igf1* expression was unchanged (Fig. 2.13M-N). These data indicated that the steroidogenic pathway was being ectopically activated as a result of SART3 knockdown in XX gonads.

Ectopic activation of the steroidogenic pathway in the ovary has been achieved by constitutive expression of *Smo:* ectopic SMO expression in the ovary allows Hh ligand-independent derepression the Hh pathway (Barsoum et al., 2009). Additionally, ES cells can be directed to differentiate into a gonadal-like steroidogenic lineage by forced expression of NR5A1 (Jadhav and Jameson, 2011). Although there was no change in expression of *Nr5a1* by qRT-PCR, NR5A1 protein appeared to be ectopically expressed in the XX Sart3MO treated gonads (Fig. 2.13D,T). Additionally, although there was no change in *Dhh* expression, numerous HSD3β-positive cells were detected in XX Sart3MO treated gonads (Fig. 2.13H,U). These data indicate that knocking down SART3 allows DHH-independent ectopic activation of the steroidogenic pathway in the XX gonad, probably mediated through ectopic expression of NR5A1. The ectopic activation of steroidogenesis in early ovarian development may lead to the subsequent masculinisation of the ovary.

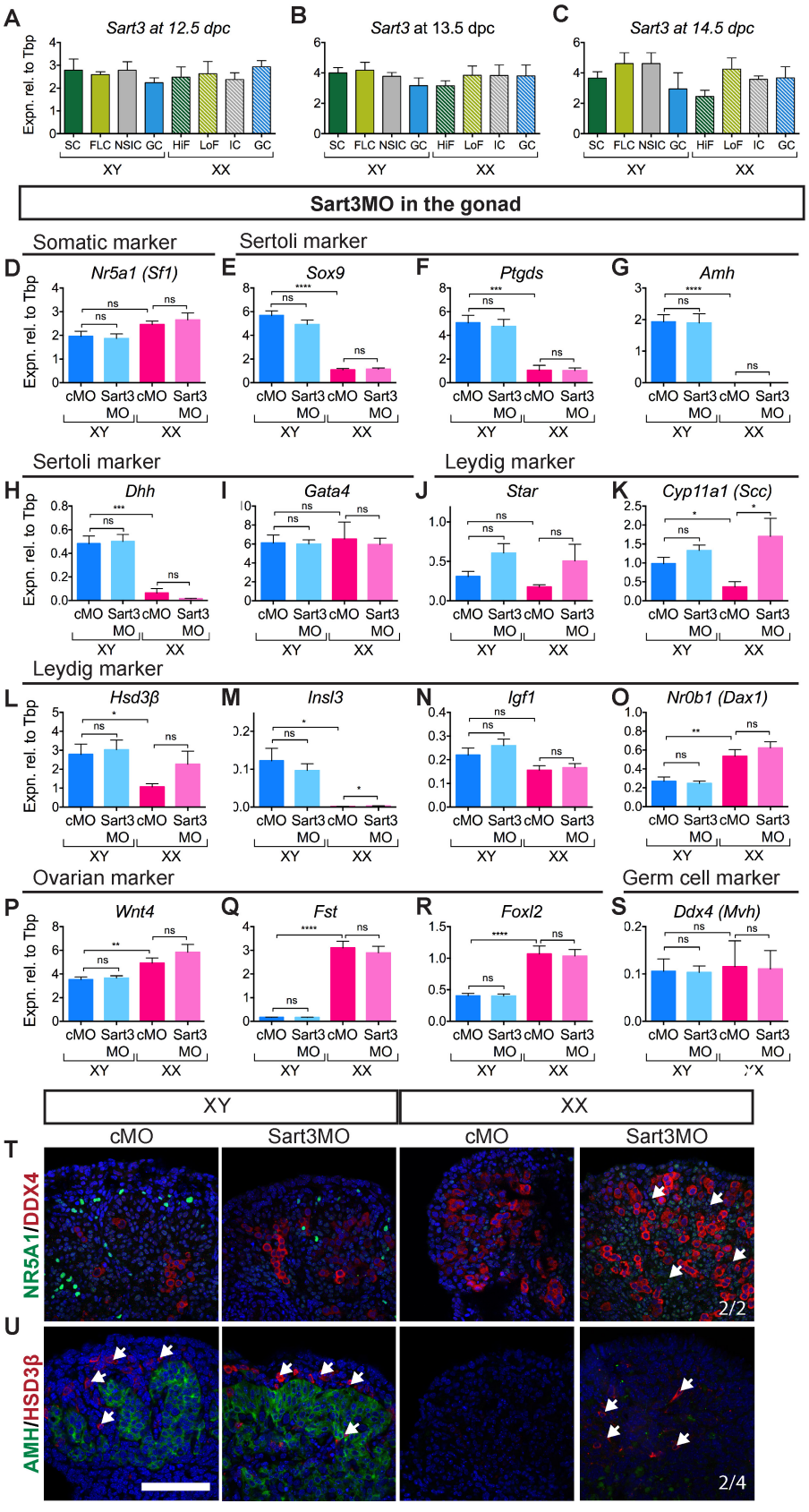
A
Sart3 at 12.5 dpc
B
Sart3 at 13.5 dpc
C
Sart3 at 14.5 dpc
Expn. rel. to Tbp
SC FLC NSIC GC HiF LoF IC GC
XY XX
Sart3MO in the gonad
Somatic marker
Sertoli marker
D Nr5a1 (Sf1)
E Sox9
F Ptgds
G Amh
Sertoli marker
Leydig marker
H Dhh
I Gata4
J Star
K Cyp11a1 (Scc)
Leydig marker
L Hsd3β
M Insl3
N Igf1
O Nr0b1 (Dax1)
Ovarian marker
Germ cell marker
P Wnt4
Q Fst
R Foxl2
S Ddx4 (Mvh)
cMO Sart3 MO
XY
XX
T
cMO
Sart3MO
NR5A1/DDX4
2/2
U
AMH/HSD3β
2/4

Figure 2.13. Knockdown of Sart3 in the gonad.

(A-C) Expression of *Sart3* in the XY and XX gonad at 12.5 dpc (A), 13.5 dpc (B) and 14.5 dpc (C) in sorted cell lineages shows ubiquitous expression throughout XX and XY gonads (*n* = 4 (A,C), 3 (B); ns for all comparisons at each timepoint). (D-S) Knockdown of SART3 in the gonad: qRT-PCR showed that treatment with Sart3MO (B-E,I,N-Q *n*= 14, 19, 8, 10; F-H,J-M *n*= 14, 19, 8, 8) resulted in no significant downregulation in steroidogenic regulator *Nr5a1* (D) or Sertoli cell marker genes *Sox9* (E), *Ptgds* (F), *Amh* (G)*, Dhh* (H) and *Gata4* (I). Expression of steroidogenic pathway members *Star* (J) and *Hsd3β* (L) was elevated in Sart3MO XX gonads, whilst expression of *Cyp11a1* (K) was significantly upregulated. Expression of *Insl3* (M) was unappreciable and expression of *Igf1* (N) was unchanged in Sart3MO XX gonads. No change was observed in expression of *Nr0b1* (O), ovarian markers *Wnt4* (P), *Fst* (Q) and *FoxL2* (R) or germ cell marker *Ddx4* (S) in the Sart3MO knockdown. IF showed germ cells (DDX4 (T)) and Sertoli cells (AMH (U)) were present in XY Sart3MO treated gonads. Ectopic steroidogenic NR5A1-positive (T) and HSD3β-positive (U) cells were present in Sart3MO treated XX gonads. Scale bars = 100 μM; cMO = control morpholino; xMO = morpholino targeting gene x. For all qRT-PCR levels are shown relative to *Tbp,* error = S.E.M. For cell quantification error = S.E.M. with individual counts plotted. * = p = 0.05, ** = p = 0.001, ns = not statistically significant.

Conclusions

I found that Sart3MO knock-down modelled the *SART3* heterozygous deletion of *SART3* described in one 46,XX DSD patient (Petek et al., 2003). However, the exon 17 SNV in *SART3* identified in the two related families in this study is a putative gain-of-function mutation resulting in 46,XY DSD. Therefore, it was anticipated that SART3 knockdown in the murine XX gonad could result in ovarian masculinisation. Indeed, XX Sart3MO-treated gonads ectopically expressed NR5A1 protein, a key regulator of the transcription of steroidogenic pathway components such as *Cyp11a1*, the expression of which was indeed elevated. Therefore, SART3 knockdown in the XX gonad results in ectopic NR5A1 expression, which promotes ectopic expression of the genes encoding steroidogenic pathway members *Star*, *Cyp11a1* and *Hsd3β,* in a DHH-independent manner. Increased steroidogenic gene expression in Sart3MO treated gonads was sufficient for some XX cells to differentiate into HSD3β protein expressing cells. These data support the possibility that a loss-of-function mutation in SART3 could result in ectopic expression of steroidogenic pathway proteins such as HSD3β in the embryonic ovary. Ectopic expression of steroidogenic enzymes during gonadogenesis could result in low-level production of testosterone that would allow for masculinisation of the ovary and the embryo as seen in 46,XX DSD patients (Fig. 1.3). Although the mechanics of the conversion of cholesterol to testosterone have been extensively studied, the transcriptional regulation of many enzymes involved in steroid hormone production is poorly understood. The effect of mutant SART3 on AR-regulated gene expression, combined with the ectopic steroidogenic cell differentiation in the of SART3 knock-down, indicates that SART3 may be involved in the regulation of steroidogenesis.

In addition to its expression in the gonads, SART3 expression was also detected in the hippocampal regions of the embryonic and adult mouse brain (data not show; S. Eggers, personal communication), which raises the possibility that the SART3 mutation may be responsible for the intellectual disability seen in 46,XX and 46,XY patients. As *SART3* seems to be the likely causative gene for both the 46,XY and 46,XX DSD in the four affected children. Others in the lab are currently making mouse models of the human mutations using the CRISPR/Cas-9 strategy. That project is ongoing.

2.7.2 NR0B1 and NR0B2: nuclear receptors with links to DSD

Nuclear receptors are a family of transcription factors that control cellular functions such as steroidogenesis, puberty and cell cycle. NR5A1 (SF1) and NR5A2 (LRH1) are both transcriptional regulators of steroidogenesis. NR0B2 (SHP, small heterodimer partner) and NR0B1 (DAX1, nuclear receptor subfamily 0, group B, member 1) are nuclear receptors that have been shown to be able to repress the transcriptional activity of other nuclear receptors: NR0B1 can repress transcriptional activation by NR5A1 (Crawford et al., 1998) and NR0B2 can transcriptionally repress NR5A2 (LU, 2000). While mutations in NR0B1 in humans result in 46,XY sex reversal (OMIM:300018; (Bardoni et al., 1994)) or adrenal hypoplasia with hypogonadotrophic hypogonadism (OMIM:300200), currently no mutations in NR0B2 have been shown to result in DSD.

Nr0b1 expression in the mouse indicates a role in early sex determination, as *Nr0b1* is expressed in both sexes initially before being down-regulated in the testes. Indeed, NR0B1 has been implicated in both ovarian and testicular development. In the testis, *Nr0b1* is expressed in the Sertoli cells and somatic cells underlying the coelomic epithelium (Swain et al., 1998; Swain et al., 1996). Deletion of *Nr0b1* results in normal gonadal development in XX mice, but in XY mice testis cord formation was found to be abnormal due to a failure to properly up-regulate *Sox9* expression, although expression of *Sry* appeared normal (Meeks et al., 2003a) (Ludbrook and Harley, 2004). Complete male-to-female sex reversal could be achieved when the *Nr0b* deletion was crossed onto the Y^{POS} background, which is characterised by a weakened *Sry* (Meeks et al., 2003b). Subsequently, it was determined that overexpression of *Sry* in the XY *Nr0b1-/-/*Y^{POS} mouse seemed to facilitate up-regulation of *Sox9*, which corrected testis development (Ludbrook and Harley, 2004). This was confirmed by Bouma et al. (2005) who found that although expression of *Sry* was normal, upregulation of *Sox9* did not occur in *Nr0b1-/-/*Y^{POS} XY gonads, however forced overexpression of *Sry* could initiate upregulation of *Sox9* allowing testis development to proceed.

Nr0b2 is expressed in the Sertoli cells during early postnatal development but becomes highly expressed in the interstitial and Leydig cells in the adult testis (Volle et al., 2007). In the patient BEL-S3 (from the patient cohort of S. Eggers and A.H. Sinclair, MCRI) no mutations were found in known DSD genes after whole exome sequencing. When looking for predicted protein-protein

interactions between known DSD candidate genes and the proteins for which variants were found in a patient, a heterozygous 1-bp c.227del deletion in *NR0B2* was identified and confirmed by Sanger sequencing (Fig. 2.14A,B). The variant is predicted to cause a frameshift and premature stop-codon. The KGGseq tool, which prioritises putative disease causing variants using protein-protein interaction and pathway data, reported protein-protein interactions between NR0B2 and the proteins products of four DSD genes in the STRING database (a database of known and predicted protein-protein interactions): *SOX3*, *ESR1*, *ESR2*, and *NR5A1* (S. Eggers, personal communication).

A role for NR0B2 has been identified in the postnatal testis. The XY *Nr0b2 -/-* mouse has increased testosterone output, presumably due to an increase in testicular expression of the genes encoding *Star* and *Cyp11a1* (Volle et al., 2007). It has been proposed that NR0B2 is able to suppress testicular steroid production by inducing expression of *Nr5a1* and *Nr5a2*. These two family members recognise many of the same binding sites and are known to modulate the expression of several steroidogenic genes (Volle et al., 2007). Postnatally, NR0B2 expression is regulated by pulsatile release of LH by the pituitary. The expression of *Nr0b2* in Leydig cells of the postnatal testis is then mediated by the cAMP/PKA/AMPK pathway (Vega et al., 2014). Therefore, in the postnatal and adult state expression of NR0B2 is gonadotropin-dependent.

I first performed MO knockdown of NR0B1. Nr0b1MO was injected at 11.5 dpc, when *Nr0b1* is already expressed in the XX and XY genital ridge and, therefore, it was expected that there would be a weak attenuation of the male pathway. For qRT-PCR analysis, three gonads were pooled for analysis after being cultured individually for 48 h. Expression of the target gene *Nr0b1* and the gene encoding the nuclear receptor *Nr5a1* was unperturbed by Nr0b1MO treatment (Fig. 2.15A,B). Similarly, expression of the SRY target *Sox9* and its downstream target, *Amh,* were unaffected by Nr0b1MO treatment (Fig. 2.15C,D). Expression of Leydig cell marker genes *Cyp11a1* and *Hsd3β,* ovarian marker gene *FoxL2* and germ cell marker gene *Ddx4* was also unchanged by Nr0b1MO treatment (Fig. 2.15E-H). Therefore, treatment with Nr0b1MO did not result in changes in expression of key male pathway genes. Lack of phenotype in the Nr0b1MO knock down is likely due to the incomplete knockdown of NR0B1 and/or the presence of NR0B1 at the time of injection, such that NR0B1 may be able to exert its primary role even in the knockdown.

Subsequently I investigated the expression and the role of the DSD candidate gene NR0B2 in the murine gonad (this work was conducted as part of the collaboration with S. Eggers and A. Sinclair). Expression of *Nr0b2* has not been reported in the fetal gonad. qRT-PCR was performed on FACS-isolated *Sf1*-eGFP cells from 12.5-14.5 dpc XX and XY gonads. These populations corresponded to enriched populations of Sertoli cells, FLCs, NSICs and germ cells in the XY gonad. We demonstrated that *Nr0b2* was expressed in Sertoli cells and FLCs of the XY gonad from 12.5-14.5 dpc (Fig. 2.15I). Notably expression of *Nr0b2* in the XY gonad was restricted to NR5A1-positive cell populations. In the XX gonad, *Nr0b2* was only weakly expressed in somatic cells from 12.5-14.5 dpc (Fig. 2.15J).

To establish if NR0B2 has a role in early gonad development, a NR0B2 knockdown was generated. An Nr0b2MO was injected at 11.5 dpc and the gonads were cultured for 48h. Expression of the genes encoding close family member *Nr0b1* and nuclear receptor *Nr5a1* was unchanged by treatment with the Nr0b2MO (Fig. 2.15K,L). Expression of Sertoli cell marker genes such as *Sox9, Amh, Ptgds, Dhh* and *Cyp26b1,* was similarly unperturbed by Nr0b2MO treatment (Fig. 2.15M-Q). The gonadotropin-independent expression of steroidogenic genes *Star* or *Cyp11a1* was unchanged by Nr0b2MO treatment (Fig. 2.15R,S). Expression of the *Hsd3β* gene appeared elevated in the NR0B2 knockdown XY gonad but this change was not statistically significant (Fig. 2.15T). Expression of the gene encoding the ovarian marker *FoxL2* was unchanged by Nr0b2MO treatment, indicating that NR0B2 knockdown did not affect the somatic cells of the ovary. Expression of germ cell marker gene *Ddx4* in the XX Nr0b2MO treated gonads was not significantly different from the control (Fig. 2.15U,V). More detailed characterisation of the NR0B2 knockdown will be required to substantiate any gonadotropin-independent steroidogenic phenotype.

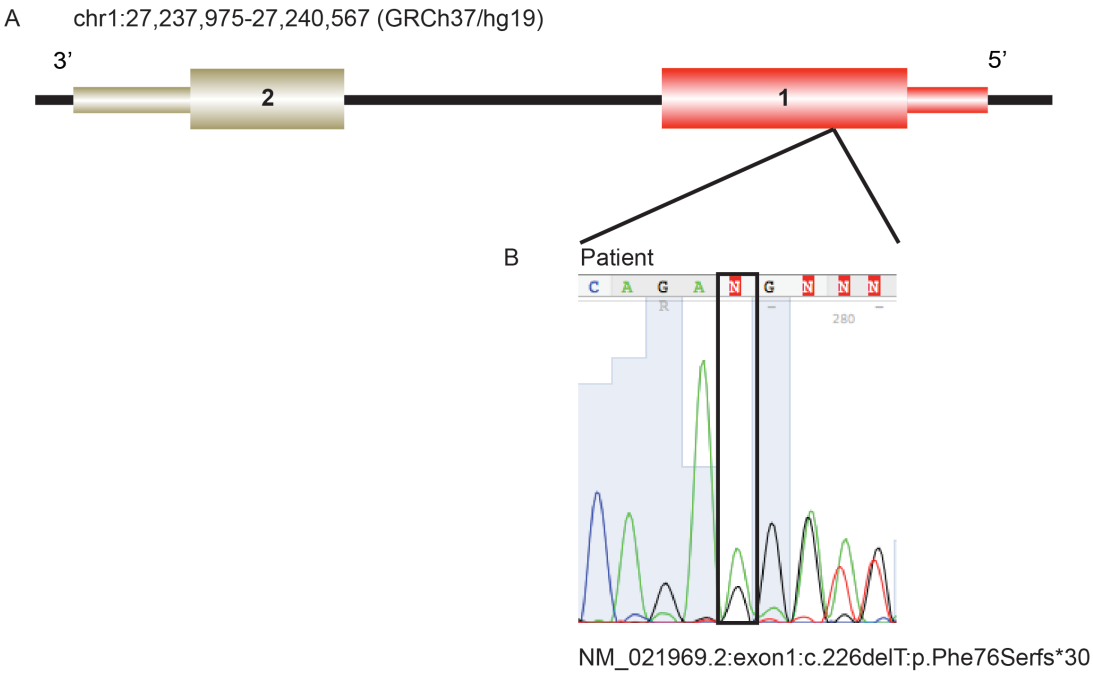

Fig. 2.14. Rare functional 1-bp deletion in exon 1 of NR0B2 found in sample BEL-S3.

(A) Location of *NR0B2* (hg19) and exon/intron structure of the gene. Non-coding exons are shown as thin blocks, coding exons as thick blocks. Both exons are numbered. The exon habouring the mutation is highlighted in red. (B) Electropherogram of part of the *NR0B2* exon 1 sequence confirming heterozygous 1-bp deletion in the patient. The black squares highlights c.227. (*data, figure and legend produced by Stefanie Eggers, reproduced with permission*).

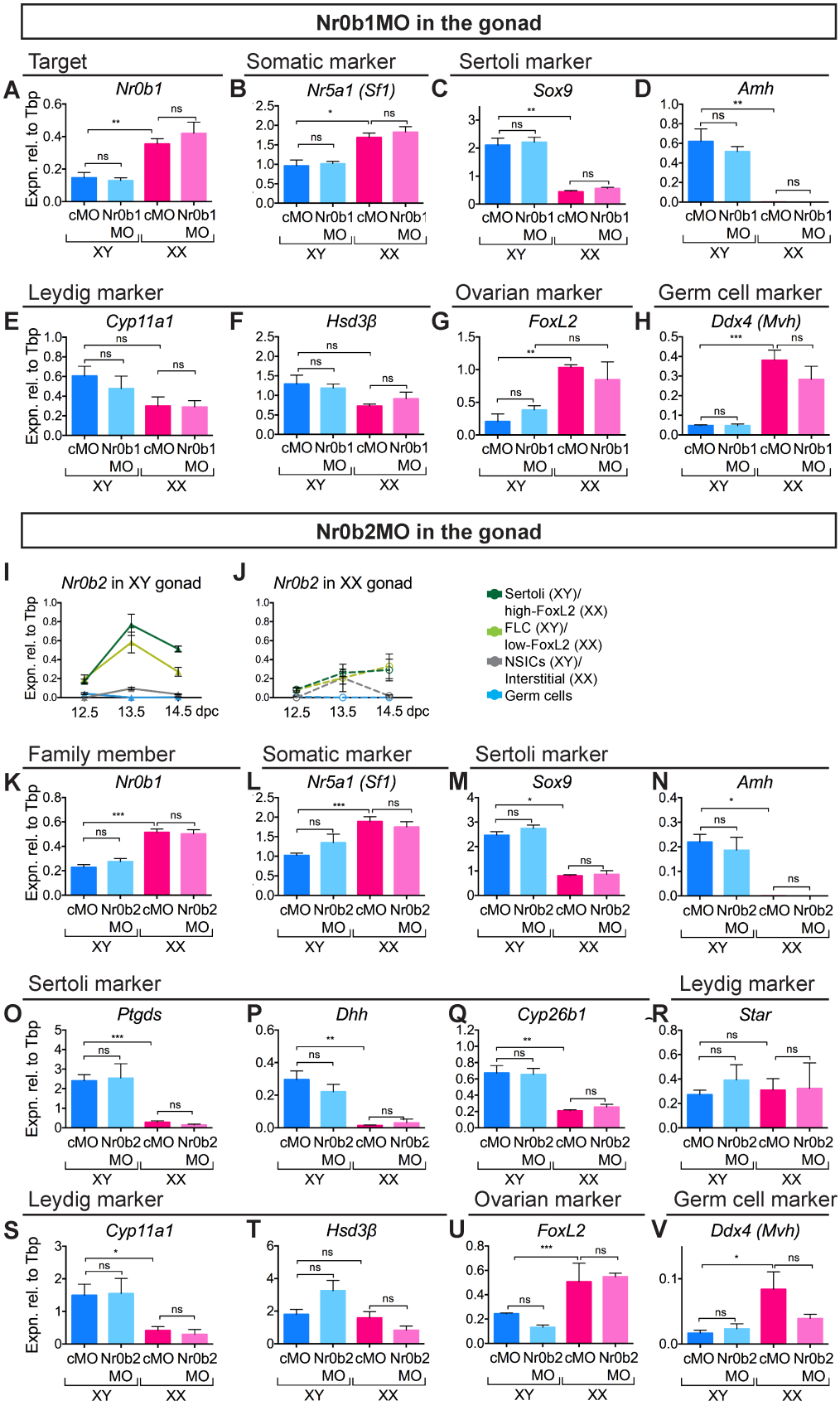
Nr0b1MO in the gonad
Target
Somatic marker
Sertoli marker
A
Nr0b1
B
Nr5a1 (Sf1)
C
Sox9
D
Amh
Expn. rel. to Tbp
cMO Nr0b1 cMO Nr0b1
MO MO
XY XX
Leydig marker
Ovarian marker
Germ cell marker
E
Cyp11a1
F
Hsd3β
G
FoxL2
H
Ddx4 (Mvh)
Nr0b2MO in the gonad
I
Nr0b2 in XY gonad
J
Nr0b2 in XX gonad
12.5 13.5 14.5 dpc
Sertoli (XY)/
high-FoxL2 (XX)
FLC (XY)/
low-FoxL2 (XX)
NSICs (XY)/
Interstitial (XX)
Germ cells
Family member
Somatic marker
Sertoli marker
K
Nr0b1
L
Nr5a1 (Sf1)
M
Sox9
N
Amh
cMO Nr0b2 cMO Nr0b2
Sertoli marker
Leydig marker
O
Ptgds
P
Dhh
Q
Cyp26b1
R
Star
Leydig marker
Ovarian marker
Germ cell marker
S
Cyp11a1
T
Hsd3β
U
FoxL2
V
Ddx4 (Mvh)

Figure 2.15. Knockdown of Nr0b1 and Nr0b2 in the gonad.

(A-H) Knockdown of NR0B1 in the gonad: qRT-PCR of cultured gonads showed that treatment with Nr0b1MO (*n*= 4, 5, 3, 4; *n*= 1 = 3 gonads from separate embryos pooled after culture) resulted in no changes in expression of *Nr0b1* (A), somatic marker *Nr5a1* (B) or Sertoli cell markers *Sox9* (C) and *Amh* (D). Expression of Leydig cell markers *Cyp11a1* (E) and *Hsd3β* (F), ovarian marker *FoxL2* (G) and germ cell marker *Ddx4* (H) was unperturbed by treatment with Nr0b1MO. (I-J) Expression of *Nr0b2* in sorted *Sf1*-eGFP cells of the XX (I) and XY (J) gonad from 12.5-14.5 dpc. (K-V) Knockdown of NR0B2 in the gonad: qRT-PCR of cultured gonads showed that treatment with Nr0b2MO (*n*= 4, 3, 4, 4; *n*= 1 = 2 gonads from separate embryos pooled after culture) resulted in no changes in expression of close family member *Nr0b1* (K), somatic marker *Nr5a1* (L) or Sertoli cell markers *Sox9* (M), *Amh* (N), *Ptgds* (O), *Dhh* (P) or *Cyp26b1* (Q). Expression of Leydig cell markers *Star* (R) and *Cyp11a1* (S) were unperturbed whereas *Hsd3β* (T) expression was elevated in the Nr0b2MO XY gonad. Ovarian marker *FoxL2* (U) was unperturbed while germ cell marker *Ddx4* (V) was somewhat decreased in XX gonads by treatment with Nr0b2MO. cMO = control morpholino; xMO = morpholino targeting gene x. For all qRT-PCR levels are shown relative to *Tbp,* error = S.E.M. For cell quantification error = S.E.M. with individual counts plotted. * = p = 0.05, ** = p = 0.001, *** = p = 0.0001, ns = not statistically significant.

2.8 Chapter Discussion

This chapter demonstrates that gene knockdown using MO injected into the heart followed by *ex vivo* organ culture can be successfully used for first-pass functional analysis. Initial proof-of-principle work demonstrated that this technique could partially recapitulate knockout phenotypes in the testis and pancreas. This work also demonstrated that this approach could be used to look at more complicated knockdowns of multiple genes. This work showed that the caveat to using this technique is that, ideally, the MO should be delivered around the time that expression of the transcript begins if one is to have the highest chance of successfully knocking down the resultant protein.

Additionally, I demonstrated that MO knockdown could be used to uncover the developmental origins of DSD phenotypes. qRT-PCR showed that *Sart3* is expressed ubiquitously in mouse XX and XY gonads. Knockdown of SART3 in the developing gonad provided insight into the possible mechanism behind the role of SART3 in the patient phenotype. This analysis informed us about what the pathways that were likely to be disrupted in the genetic patient-mutation-model A similar analysis was performed for the DSD candidate gene *NR0B2*. *Nr0b2* was primarily expressed in FLCs and Sertoli cells in the developing mouse testis. Knockdown of NR0B2 indicated that it might have a gonadotropin-independent role in steroidogenesis in the early testis.

For further discussion see Chapter 4.

Chapter 3: Transcriptomic analysis of the somatic cells of the developing testis

3.1 Publications:

McClelland KS, Bell K, Larney C, Harley VR, Sinclair A, Oshlack A, Koopman P and Bowles J (2015) Purification and transcriptomic analysis of mouse fetal Leydig cells reveals candidate genes for disorders of sex development. *Biology of Reproduction,* doi:10.1095/biolreprod.115.128918

3.2 Project Summary:

This project used the *Sf1*-eGFP transgenic mouse line as the basis for the separation of mouse fetal somatic cells into distinct subpopulations using a FACS-based protocol (Beverdam and Koopman, 2006). This enabled the isolation of three XY gonad somatic cell populations: Sertoli cells; fetal Leydig cells (FLCs) and non-steroidogenic interstitial cells (NSICs). Following the validation of this novel protocol I performed RNA-seq on the three major somatic populations of the 12.5 dpc XY gonad. Bioinformatic analysis identified genes upregulated in each population and I then validated a selection of genes of interest. The body of this work resulted in the published manuscript contained within entitled "*Purification and transcriptomic analysis of mouse fetal Leydig cells reveals candidate genes for specification of gonadal steroidogenic cells*". In this manuscript I constructed a molecular portrait of FLCs at the onset of steroidogenesis. This manuscript looked most closely at cues produced by the Sertoli cells and received by the FLCs and NSICs. I also examined the fetal expression of known DSD genes as fetal expression may underlie the origins of DSD phenotyes. In the second part of this chapter I looked more closely at the Sertoli cell population and the potential role of IHH genes in gonadal development. In addition to the thorough analysis of the XY somatic cell populations a preliminary characterisation of different XX somatic cell populations was performed. Lastly, I looked in more detail at the expression of NR2F2 in the XY gonad as a novel marker of the NSIC population.

3.3 Collaborators:

Bioinformatic analysis (differentially expressed gene list generation and read mapping) for this project was completed by Katrina Bell and Alicia Oshlack (MCRI, Australia). Christian Larney (Koopman Lab, IMB) assisted in generation of various lists used in this project.

3.4 Chapter Introduction:

There are three principal somatic cell types in the developing testis: Sertoli cells, the master regulators; FLCs, the producers of masculinising hormones and NSICs, some of which go on to differentiate into adult Leydig cells. To date, FLC-expressed genes have been underrepresented in microarray screens of somatic gonadal cells. Moreover, in existing screens and expression reports, no distinction has been made between candidates expressed throughout the interstitial space, in FLCs and NSICs, and those restricted to the early FLCs.

I hypothesise that defects in FLC or interstitial cell specification and differentiation may underlie some classes of human DSDs. Currently, few genes and encoded factors are known to direct FLC fate determination and differentiation, and even less is known regarding how ALC progenitors are specified from interstitial cells during fetal life (Kilcoyne et al., 2014). We separated FLCs and NSICs to investigate the features that distinguish the early FLCs from their neighbours. To profile these cell populations at 12.5 dpc we used next-generation sequencing (RNA-seq), which offers improved detection and sensitivity compared to microarrays (Sultan et al., 2008).

In addition to addressing questions regarding cell fate and differentiation, this study aimed to identify genes that may underlie fetal origins of DSD. Most XY DSDs remain unexplained at the molecular level and, while the term DSD includes a wide spectrum of conditions, DSDs often occur as the result of loss or compromised function of genes involved in gonadal development (for review see Ono and Harley, 2013). However, mutations in genes involved in neuroendocrine system are also an important cause of certain classes of DSDs such as IHH (idiopathic hypogonadotropic hypogonadism). The development of a functional reproductive program and associated sexual characteristics relies on a functional hypothalamic–pituitary–gonadal (HPG) axis. The HPG axis is controlled by neurons located in the hypothalamus that secrete GnRH (gonadotropin releasing hormone). These neurons originate in the nasal placode and migrate into the forebrain along the olfactory-vomeronasal nerves (for review see Wray, 2002). This complex migration is mediated by a series of neuroactive-ligand-receptor pairs: failures in the migration or function of the GnRH neurons result in the heterogeneous group genetic disorders including IHH (for review of IHH causative genes see Valdes-Socin et al., 2014). Due to the important role played by GnRH neurons in postnatal life, any impact that dysfunction of neuroendocrine genes may have on fetal testicular function has been largely overlooked. I demonstrate in this chapter that a number of genes encoding

neuroactive-ligands and receptors involved in HPG axis formation and neural development are also expressed in the developing testis. I hypothesise that mutations in these genes may alter testis development before GnRH-mediated phenotypes impact sexual maturation later in development.

3.5 Published manuscript

Purification and transcriptomic analysis of mouse fetal Leydig cells reveals candidate genes for specification of gonadal steroidogenic cells

Kathryn S McClelland[3], Katrina Bell[4], Christian Larney[3], Vincent R Harley[5], Andrew H Sinclair[4], Alicia Oshlack[4], Peter Koopman[2,3] and Josephine Bowles[3]

1. Supported by the Australian Research Council (ARC; grant DP140104059) and the National Health and Medical Research Council (NHMRC) of Australia (grant 546517). P.K. is a Senior Principal Research Fellow of the NHMRC (APP1059006). Data GEO accession GSE65498

2. Correspondence: Peter Koopman, Tel: +61 7 3346 2059, Fax: +61 7 3346 2101, Email: p.koopman@imb.uq.edu.au

3. Institute for Molecular Bioscience, The University of Queensland, Brisbane, QLD 4072, Australia

4. Murdoch Childrens Research Institute, Royal Children's Hospital, Melbourne, VIC 3052, Australia

5. Monash Institute of Medical Research-Prince Henry's Institute (MIMR-PHI) Institute of Medical Research, Melbourne, VIC 3168, Australia

Running title: Characterising the fetal Leydig cell transcriptome

Summary Sentence: RNA-seq analysis of enriched fetal Leydig, non-steroidogenic and Sertoli cell populations in the fetal XY gonad: neuroactive genes identified as candidates for fetal Leydig cell specification.

Keywords: RNA-seq, sex determination, gonadogenesis, Sertoli cell, neuroactive, transcriptome, differentiation, steroidogenesis, Leydig cell

Abstract

Male sex determination hinges on the development of testes in the embryo, beginning with the differentiation of Sertoli cells under the influence of the Y-linked gene *SRY*. Sertoli cells then orchestrate fetal testis formation including the specification of fetal Leydig cells (FLCs) that produce steroid hormones to direct virilisation of the XY embryo. As the majority of XY disorders of sex development (DSDs) remain unexplained at the molecular genetic level, we reasoned that genes involved in FLC development might represent an unappreciated source of candidate XY DSD genes. To identify these genes, and to gain a more detailed understanding of the regulatory networks underpinning the specification and differentiation of the FLC population, we developed methods for isolating fetal Sertoli, Leydig and interstitial cell-enriched subpopulations using an *Sf1*-eGFP transgenic mouse line. RNA-sequencing followed by rigorous bioinformatic filtering identified 84 genes upregulated in FLCs, 704 genes upregulated in non-steroidogenic interstitial cells and 1217 genes upregulated in the Sertoli cells at 12.5 dpc. The analysis revealed a trend for expression of components of neuroactive ligand interactions in FLCs and Sertoli cells and identified factors potentially involved in signaling between the Sertoli cells, FLCs and interstitial cells. We identified 61 genes that were not known previously to be involved in specification or differentiation of FLCs. This dataset provides a platform for exploring the biology of FLCs and understanding the role of these cells in testicular development. In addition, they provide a basis for targeted studies designed to identify causes of idiopathic XY DSD.

Introduction

The morphogenesis of the testes involves the co-ordinated differentiation of a number of bipotential cell lineages in the gonadal primordium into testis-specific cell types (for review, see (Svingen and Koopman, 2013)). This process begins with the expression of the Y-linked gene *Sry* (sex determining region of Chr Y), which directs differentiation of Sertoli cells that assemble into cords encapsulating the germ cells. Sertoli cells then influence the differentiation of other cell types within the testes, including the fetal Leydig cells (FLCs), which arise in the interstitium and act as factories for the production of steroid hormones (androgens) that play a major role in masculinisation of the XY individual. Other cell types also arise in the testicular interstitium, the nature and function(s) of which are mostly unclear. Some interstitial cells that do not differentiate as FLCs are thought to give rise to adult Leydig cells (ALCs), which maintain androgen production throughout life (Kilcoyne et al., 2014). The differentiation, function and interaction of the various cellular sub-compartments of the developing testis need to be carefully orchestrated, in a spatio-temporal manner, but how this regulation is achieved remains poorly understood.

Disorders of sex development (DSDs) are congenital birth defects characterised by development of atypical chromosomal, gonadal, or anatomical sex. While the term DSD includes a wide spectrum of conditions, loss or compromised function of genes directing gonadal development during fetal life is a common cause (for review see Ono and Harley, 2013). As many of the known genes at fault in XY DSD are those regulating gonadogenesis, we hypothesised that defects in specification and differentiation of FLCs or non-steroidogenic interstitial cells may underlie some classes of human DSD. Currently, few genes and encoded factors are known to direct FLC fate determination and differentiation (Griswold and Behringer, 2009), and even less is known regarding how ALC progenitors are specified from interstitial cells during fetal life (Kilcoyne et al., 2014). Hedgehog signalling is evidently a positive regulator of FLC differentiation, given that *Dhh*$^{-/-}$ (Desert hedgehog) XY gonads have reduced FLC numbers (Bitgood et al., 1996; Clark et al., 2000; Yao et al., 2002), and that constitutively active hedgehog signaling in the ovary is sufficient to induce some interstitial cells to differentiate along the steroidogenic pathway (Barsoum et al., 2009). Similarly, *Pdgfrα*-/- (platelet derived growth factor receptor, α-polypeptide) XY gonads show abnormal FLC differentiation (Brennan et al., 2003). Additionally, the aristaless-related homeobox gene (ARX) plays some role in fetal Leydig cell specification based on the fact that *Arx*$^{-/-}$ XY mouse gonads have reduced FLC numbers. Interestingly, *Arx* is not expressed in FLCs, although it may be expressed in their progenitors (Kitamura et al., 2002; Miyabayashi et al., 2013).

Previous transcriptomic studies aimed at identifying genes important for development of the fetal gonads in mice, or for establishing the molecular signatures of the component cell lineages, have been performed using microarrays (Beverdam and Koopman, 2006; Bouma et al., 2007; Bouma et al., 2010; Jameson et al., 2012b; Nef et al., 2005). While this method reveals the expression dynamics of thousands of genes simultaneously, it is limited by the incomplete representation of genes on the array and also by the relatively low sensitivity and dynamic range offered (Marioni et al., 2008). Additionally, the non-Sertoli gonadal somatic populations studied in previous microarray screens have included a mixture of FLCc and non-steroidogenic interstitial cells due to an inability to separate these two populations. Hence, using available microarray datasets, it has been difficult to address the specific question of how FLCs arise and to determine the molecular characteristics of these cells at 12.5 dpc, prior to the expression of steroidogenic pathway genes.

In this study, we designed and implemented a strategy to separate mouse fetal gonadal cells into four distinct subpopulations—Sertoli cells, germ cells, FLCs and heterogeneous non-steroidogenic interstitial cells (NSICs)—using a FACS-based protocol in combination with a *Sf1*- enhanced green fluorescent protein (eGFP) transgenic mouse line (Beverdam and Koopman, 2006). We used massively parallel sequencing (RNA-seq) to carry out differential gene expression analysis and construct a molecular portrait of FLCs at 12.5 dpc, just at the onset of steroidogenesis. The aim of this study was to identify early lineage markers of the FLC and NSIC populations in order to provide insight into the signaling interactions in the early gonad. The output generated by our approach reveals potential markers for pre-steroidogenic FLCs, suggests likely signaling relationships among Sertoli cells, FLCs and NSICs and reveals new candidate genes that may underlie the fetal origins of DSDs.

Materials and Methods

Mouse strains

Embryos were collected from timed matings of *Sf1*-eGFP (*Nr5a1*) strain mice (Beverdam and Koopman, 2006), with noon of the day on which the mating plug was observed designated 0.5 days *post coitum* (dpc). All animal protocols were approved by the University of Queensland Animal Ethics Committee.

Immunofluorescence

Section:

Embryos were fixed in 4% paraformaldehyde in PBS (phosphate buffered saline) overnight at 4°C, dehydrated, and embedded in paraffin; 7 μm sections were cut using a Leica Microtome. Slides were dewaxed by 2 x 10 min washes in xylene, re-hydrated and boiled for 5 min in Antigen Unmasking Solution (Vector Laboratories), and incubated in the unmasking solution at room temperature for 60 min. The slides were washed for 3 x 10 min in 0.1% Triton-X in PBS (PBTx) and incubated with primary antibodies diluted in blocking buffer (10% heat-inactivate serum supreme in PBTX) at 4° C overnight followed by washing, and re-blocking for 30 min at room temperature. Slides were incubated with secondary antibodies in blocking buffer at room temperature for 2 h, washed and mounted in 60% glycerol/PBS. Sections were imaged by confocal microscopy using a Zeiss LSM-510 META or a LSM-710 META confocal microscope. For details of primary antibodies and secondary antibodies see Supplemental Tables 3 and 4.

FACS cells:

Protocol modified from online methods for (Hajkova et al., 2008). Briefly, cells were sorted as described below from 12.5 dpc gonad-only samples into ice-cold PBS and kept on ice. A volume of PBS containing between 3000-10000 "events" (~200 μL) was plated into an area demarcated on a Tissue Tack slide (Polysciences Inc., 24216) and allowed to adhere for 15 min before being fixed in 4% paraformaldehyde for 15 min at room temperature and washed with PBS. Slides were blocked in permeablisation/blocking buffer (P/B buffer, 1% BSA in PBTx) for 30 min at RT and incubated at 4° C overnight with the primary antibody diluted in P/B buffer. The slides were washed for 1 x 5 min P/B buffer and then 3 x 10 min in PBTx and incubated with secondary antibodies diluted in P/B buffer for 1 h at room temperature. Slides were DAPI stained, washed and mounted in 60%

glycerol/PBS. Fields of cells were imaged by fluorescent microscopy using a Olympus BX-51 microscope and counted in ImageJ using the CellCounter plug in. For details of primary antibodies and secondary antibodies see Supplemental Tables 3 and 4.

FACS sorting of cell populations

Sf1-eGFP litters (11.5-14.5 dpc) were dissected in cold PBS and gonads sexed by eye, based on the presence of testis cords (12.5-14.5 dpc) or by presence of Barr Bodies (11.5 dpc; (Burgoyne et al., 1983)). For 11.5 dpc samples the mesonephros was left attached, but it was removed for 12.5-14.5 dpc samples. It should be noted that GFP-transgene expression is restricted to the somatic cells of gonad, exclusive of the mesonephros ((Beverdam and Koopman, 2006); this study). As only GFP-positive cells were profiled at 11.5 dpc there was no mesonephric contamination. Stage-matched CD1 gonads, with mesonephros removed, were used as a negative control to determine GFP-positive populations.

Gonads were enzymatically dissociated using 0.25% Trypsin EDTA (Gibco) or TryplE Express (12604-013, Gibco) with 5 U/ml DNase1 (Sigma) for 20 min at 37 °C and then mechanically dissociated using 18- and 23-gauge syringes. PBS (1 mL) was added to the cells that were then pelleted by centrifugation (900*g* at 4 °C for 10 min); after supernatant was removed the cells were resuspended in 400 µL of ice-cold PBS and stored on ice. Cells were then incubated with anti-SSEA1-PE (#FAB2155P, R&D Systems; specific for germ cells, FUT4, fucosyltransferase 4) or anti-CD31-APC (#551262, Becton Dickinson; specific for germ and endothelial cells, PECAM1, platelet/endothelial cell adhesion molecule 1) antibody for 20 min and washed with ice-cold PBS. Cells were resuspended in 400 µL PBS for sorting. Anti-SSEA1-PE was used in characterization of cell population studies whilst anti-CD31-APC was used to remove germ and endothelial cells prior to RNA-seq. Cells were fractionated using a BD FACSAria Cell Sorter; Fig. 3.1 shows FACS plots illustrating how gating parameters were derived. Specifically, GFP-negative CD1 stage-matched controls (Fig. 3.1A,B) and GFP-positive but antibody-negative controls (Fig. 3.1C) were used to place gates for sorting GFP-high, GFP-low, GFP-neg and antibody sorted (SSEA1-PE or CD31-APC) populations (Fig. 3.1D). These populations were collected in PBS and kept on ice before further processing.

Quantitative RT-PCR analysis

Total RNA was extracted (Micro RNeasy kit with carrier RNA, Qiagen) and cDNA generated (High Capacity cDNA Reverse Transcription Kit, Invitrogen) from isolated populations of FACS-sorted cells as previously described (Bowles et al., 2010). Duplicate assays were conducted on an ABI Prism 7500 Sequence Detector System. The cycle conditions for quantitiative RT-PCR (qRT-PCR) were 2 min at 50 °C, then 10 min at 95 °C followed by 40 cycles of 92 °C for 15 s then 60°C for 60 s.

Expression levels of mRNA were normalised to *Tbp* (*TATA box binding protein*; (Svingen et al., 2009a)) and relative transcript abundance was determined using the $2^{-\Delta CT}$ method. *Tbp* was used as a normalising gene on the assumption that there were equal amounts of *Tbp* in each cell population, as in the whole gonad (Svingen et al., 2009a). For Taqman Gene Expression Assay reference numbers, see Supplemental Table 2. S.E.M. was calculated from independent biological replicates ($n \geq 3$) and statistical significance was determined using one-way ANOVA with Bonferroni's multiple comparisons test to compare the four sample groups with the exception of populations sorted at 11.5 dpc where only two groups were compared and so statistical significance was determined using unpaired (two-tailed) Student's *t*-test.

RNA extraction and library preparation for deep sequencing

Total RNA was extracted (Micro RNeasy kit without carrier RNA, Qiagen) from CD31-treated FACS-sorted cells. Each sample represented approximately 10 sorting experiments conducted on different days with 4-10 litters of *Sf1*-eGFP embryos in each experiment. We prepared for each of 3 cell types (high-GFP, low-GFP, GFP-negative with GC/EC removed), replicate A, replicate B and replicate C (C was an equal mix of samples A and B) resulting in 9 samples for sequencing. A cDNA library was prepared from each sample using TruSeq Stranded Total RNA Libraries (RS-122-2201, Truseq stranded Total RNA LT (with Ribo-Zero Human/Mouse/Rat), Set A; Illumina protocol 15031048 Rev C, Sep 2012). The 9 samples were run on 4 lanes of an Illumina HiSeq 1500, with all samples run over all lanes, generating 100bp paired end reads after ribosomal depletion. Sequencing and library preparation was completed by the Monash Health Translation Precinct (MHTP) Medical Genomics Facility, Australia. Data has been submitted to GEO, accession GSE65498.

RNA-seq analysis

An average of 65 million raw reads were generated per sample. The quality of the sequencing files was examined using the FastQC program (FastQC; www.bioinformatics.babraham.ac.uk/projects/). Tophat2 (Kim et al., 2013) was used to map reads to the mouse genome (mm10), with mouse gene model annotations (mm10, downloaded from Ensembl (http://www.ensembl.org/info/data/ftp/index.html)) supplied via the -G option. On average over 85% of the reads mapped to the mouse genome. Read counts were then summarised across genes using HTSeq-count (Anders et al., 2014), with Ensembl mm10 gene annotation. No lane-specific technical effects were observed; therefore all lane files per sample were merged into one file per sample for differential gene expression analysis.

Differential gene expression analysis

The count data was analysed within the R statistical computing environment. Only genes with at least 1 count per million in three or more samples were retained for further analysis. This reduced the number of features to 14,307 for the differential gene expression analysis (complete data in Supplemental Data 1). The count data of reads per gene features were analysed using TMM (Robinson and Oshlack, 2010) and Voom (Law et al., 2014) for normalisation and limma (Smyth, 2004) for differential expression analysis, which applies empirical Bayes methods to compute moderated t-tests and p-values adjusted for multiple testing using the Benjamini-Hochberg method (Benjamini and Hochberg, 1995). Lists of the differentially expressed genes between each pair (contrast) of the three cell types were generated and annotated based on Ensembl mm10 annotation. Genes that were upregulated in one cell type compared to the other two cell types (adjusted *p* value <0.05 and log fold change of at least 1 or 0.6 for each contrast), formed the upregulated gene lists for each of the cells types. The adjusted *p* value of the moderated F-statistic (F), which combines the t-statistics for all the contrasts into an overall test of significance for each gene, was used to rank the cell specific gene lists for discussion. The full gene lists for all comparisons are listed in Supplemental Data 2.

To validate the RNA-seq data, we used the normalised sequence counts per million (cpm) to indicate of expression of various marker genes (Supplemental Data 1). S.E.M. was calculated from the 3 sequencing replicates and statistical significance was determined using one-way ANOVA with Bonferroni's multiple comparisons test.

Previously reported genes

Genes that have testicular expression previously reported as having expression in the testis in articles on PubMed are listed in Supplemental Table 5.

Eurexpress database ISH mining

We searched the 14.5 dpc data set from *Eurexpress Transcriptome Atlas Database for Mouse Embryo* (http://www.eurexpress.org) for in situ hybridization (ISH) data that might verify testicular expression for genes of interest identified in our RNA-seq analysis. Representative section images were downloaded and the testis region selected in Photoshop. Gene IDs and Eurexpress IDs are listed in Supplemental Table 7.

Gene ontology analysis

Gene ontology analysis was performed using the DAVID Bioinformatics Package (v6.7) (http://david.abcc.ncifcrf.gov; (Huang et al., 2009a; Huang et al., 2009b)). The following three GO terms were used to categorise each population:

Transmembrane factor: SP_PIR_KEYWORDS transmembrane (GO:0016021; TM)

Secreted factor: SP_PIR_KEYWORDS secreted (GO:0005576; SF)

Transcription Factor: GOTERM_MF_FAT transcription factor activity (GO:0003700; TF)

For details of additional GO terms used see Supplemental Data 3 and Tables 3.2; 3.5 and 3.7. The genes identified in each GO term category were then mapped back to the differentially expressed gene lists and ranked by F-statistic.

Genes putatively regulated by NR5A1

List of genes putatively regulated by NR5A1 is from Baba et al. (2014). Full list of overlapping genes in Supplemental Table 6 and Table 3.8.

11.5 dpc expression of FLC genes

From our list of genes preferentially expressed in Leydig cells at 12.5 dpc, we sought to determine if any might potentially also mark Leydig cells at 11.5 dpc. To do this, we considered the data available for these genes at 11.5 dpc (Jameson et al., 2012b). Genes found to be enriched in Leydig cells at 12.5 dpc that also show differing expression between the interstitial and supporting cell compartments of 11.5 dpc testes are putative pre-FLC marker genes. Data was obtained from GEO (GSE27715) and analysed with R and Bioconductor. Raw data were normalised using oligo (Carvalho and Irizarry, 2010) and differential expression analysis was carried out with limma (Smyth, 2004). Int. Exp (interstitial) and Sup. Exp (supporting) show median normalised expression of the gene in each of these two cell types, while Int. Rank (interstitial) and Sup. Rank (supporting) indicate the position of the gene in a list ranked by expression in that cell type (0=lowest expression, 100=highest expression; Supplemental Data 4). For our final list of genes of interest we noted those genes with expression in interstitial cells more than four times that in supporting cells (log fold change ≥ 2). Of particular interest in predicting putative markers for FLCs are the 10 genes with low expression in supporting cells (Sup Exp ≤ 6; marked in grey in Table 3.4).

Genes identified in OMIM

A full list of genes associated with human disease from the OMIM database (accessed 12 November, 2014, http://omim.org/) is listed in Supplemental Table 8.

All Supplementary Tables for reagents are listed in the Appendix.

Results

Evaluation of GFP as a proxy for NR5A1/SF1 expression in Sf1-eGFP mouse fetal testes

We have previously used a 674 bp-fragment of the *Sf1/Nr5a1* (steroidogenic factor 1/nuclear receptor subfamily 5, group A, member 1) promoter to drive GFP expression in a subpopulation of somatic cells of the developing gonad in *Sf1*-eGFP transgenic mice (throughout this study we will refer to the this mouse line using the common name SF1/*Sf1*-eGFP). (Beverdam and Koopman, 2006). In that study, we profiled gene expression in the GFP-positive cell population at 10.5 and 11.5 dpc with the aim of identifying genes expressed in the Sertoli/granulosa cell lineage that may play a role in male or female sex determination. In the present study, we exploited a published observation that the NR5A1-positive cell population of the early male gonad can be subdivided into a high-NR5A1 expressing population that differentiates into pre-Sertoli cells, and a low-NR5A1 expressing population that differentiates into a subset of the interstitial cells (presumptive FLCs) between 11.25 and 11.75 dpc (Schmahl et al., 2000). Specifically, we sought to determine whether FLCs could be isolated from fetal testes based on GFP expression level in *Sf1*-eGFP transgenic mice. We reasoned that this strategy might allow molecular characterisation of the FLC lineage at 12.5 dpc, a time point that would allow identification of genes involved in FLC specification prior to large-scale upregulation of steroidogenesis genes.

In our previous study we established colocalisation of NR5A1 and GFP at 11.5 dpc and we confirmed this here (Fig. 3.3A,B,G; (Beverdam and Koopman, 2006)). We showed that NR5A1/GFP-positive cells were SOX9-positive and ARX/DDX4-negative at 11.5 dpc (DEAD box polypeptide 4; MVH; Fig. 3.3A,B,G). We then demonstrated that endogenous expression profile of NR5A1 was mirrored by GFP expression in XY gonads at 12.5 dpc. Immunofluorescence analysis showed that cells with nuclear NR5A1 expression showed cytoplasmic expression of the GFP transgene (Fig. 3.2, first column). As this analysis was performed using single confocal slices on sectioned embryos not all cells in an image would be expected to have both nuclear and cytoplasmic staining. We then used lineage-specific marker antibodies to determine which cell types express GFP/NR5A1 in our transgenic line. GFP/NR5A1-positive cells lined the testis cords and NR5A1-positive nuclei in "strongly" GFP-positive cells co-localised with nuclear SOX9 at 12.5 dpc and later, indicating that the transgene was expressed in Sertoli cells (Fig. 3.2A; Fig. 3.3B,D,F). We deduced that interstitial "weakly" GFP-positive cells were pre-steroidogenic FLCs by virtue of their nuclear expression of NR5A1 (Fig. 3.2A-C, first column; (Hatano et al., 1994; Morohashi et al., 1995)). This was confirmed by immunofluorescence for ARX, a nuclear marker of non-FLC

interstitial cells at 12.5 dpc: ARX did not colocalise with the NR5A1-positive nuclei of GFP-positive interstitial cells (Fig. 3.2B). Additional analysis at 13.5-14.5 dpc showed that GFP/ NR5A1-positive cells in the interstitium that were exclusive of ARX-positive nuclei expressed cytoplasmic HSD3β, confirming that FLCs expressed the GFP transgene (Fig. 3.3C,E,H,J). We also confirmed that the transgene was not expressed in germ cells: GFP/ NR5A1-positive cells were negative for germ cell marker DDX4 (Fig. 3.2C; Fig. 3.3G,I,K). These results demonstrate that GFP, like endogenous NR5A1, is expressed in the Sertoli cell and FLC populations in *Sf1*-eGFP transgenic testes at 12.5 dpc and beyond.

Isolation and characterisation of fetal testis cell populations

The above observations suggested that it might be possible to separate three populations of somatic cells from 12.5 dpc *Sf1*-eGFP transgenic testes based on GFP fluorescence: strongly GFP-positive ("high-GFP") Sertoli cells, weakly GFP-positive ("low-GFP") FLCs, and a GFP-negative population of NSICs (non-steroidogenic interstitial cells). In addition, a fourth cell population, the germ cells, could be isolated using well-characterised antibodies to cell surface markers. To this end, we explanted and dissociated *Sf1*-eGFP testes, incubated the cells with antibodies to either SSEA-1 (recognizing germ cells only) or CD31 (recognizing germ and endothelial cells), and used fluorescence-activated cell sorting (FACS) to separate the four cell populations (Fig. 3.4A).

We profiled expression of key marker genes by qRT-PCR in the four populations of cells, to investigate their composition. As expected, the high-GFP population (Fig. 3.4, dark green) robustly expressed Sertoli cell hallmarks including *Nr5a1*, *Sox9*, *Amh* (anti-Müllerian hormone) and *Ptgds* (prostaglandin D2 synthase; Fig. 3.4B-E). These cells expressed low levels of Leydig cell markers *Star* (steroidogenic acute regulatory protein) and *Cyp11a1* (cytochrome P450, family 11, subfamily a, polypeptide 1; Fig. 3.4F,G). This pattern of marker expression was established at 11.5 dpc (Fig. 3.5A,B) and retained until at least 14.5 dpc (Fig. 3.4J-L; Fig. 3.5C-E,H-M). Therefore, we conclude that the high-GFP expressing population is enriched for Sertoli cells. Surprisingly, *Ptch1* was expressed at similar levels in the high-GFP (putative Sertoli) and low-GFP (putative FLC) populations (Fig. 3.4H): despite reports that *Ptch1* expression is characteristic of FLCs (McDowell et al., 2012; Yao et al., 2002), high quality expression data agree with our findings and indicate that *Ptch1* is expressed at similar levels in Sertoli and testicular interstitial cell populations at 12.5 dpc ((Jameson et al., 2012b); this study).

The low-GFP expressing population (Fig. 3.4, light green) was characterised by reduced expression of *Nr5a1* at 12.5 dpc and weak expression of *Sox9*, *Amh* and *Ptgds* (Fig. 3.4B-E). At this stage of testis development, expression of steroidogenic genes begins at a low level in the FLCs. Accordingly, expression of early FLC marker *Star* was similar between GFP-positive populations, however, elevated levels of early steroidogenic pathway member *Cyp11a1* were detected in the low-GFP population (Fig. 3.4F,G). These and other steroidogenic markers became more highly expressed in the low-GFP population at 13.5 and 14.5 dpc (Fig. 3.4L; Fig. 3.5D,E,K-M). Therefore, we conclude that the low-GFP expressing population is enriched for FLCs at 12.5 dpc.

The germ cell-depleted, GFP-negative, putative non-steroidogenic interstitial cell population (Fig. 3.4, grey) showed minimal expression of *Nr5a1*, Sertoli cell markers *Amh*, *Ptgds* and *Dhh*, and FLC markers *Star*, *Cyp11a1* and *Hsd3β* (hydroxy-delta-5-steroid dehydrogenase, 3 beta- and steroid delta-isomerase 1) indicating that it was devoid of Sertoli and FLCs (Fig. 3.4B-G,J-L; Fig. 3.5C-E,H-M). Amongst the genes we examined, only the DHH receptor *Ptch1* (patched homolog 1) and *Arx* were expressed in the GFP-negative population (Fig. 3.4H,I; Fig. 3.5F,G,H,N,O). These data indicated that the germ cell-depleted, GFP-negative population was enriched for NSICs that did not express NR5A1/*Nr5a1* or any other Sertoli or FLC markers.

While germ cells were not the focus of this analysis, we also examined the expression of *Ddx4* to examine the efficiency of germ cell depletion from the GFP-negative fraction. As expected, expression of *Ddx4* was robust in this cell population from 12.5-14.5 dpc (Fig. 3.5P-R), but some expression was also in the GFP-negative fraction at 12.5 dpc (Fig. 3.5P), indicating a low level of germ cell contamination.

To validate the purity of the high-GFP and low-GFP cell populations using the high-GFP/low-GFP FACS separation strategy described above, we performed immunofluorescence on FACS-sorted cell populations for NR5A1, Sertoli cell marker SOX9, germ cell marker DDX4 and vascular endothelial cell marker iB4 (isolectin B4; Fig. 3.1E-G). We found that virtually all cells in both the high-GFP and low-GFP populations were NR5A1-positive, as expected, while the GFP-negative population was devoid of NR5A1-positive cells (Fig. 3.1E). Results of this analysis were consistent with those obtained by qRT-PCR and indicate that virtually all cells in the high-GFP population

(putative Sertoli cells) were SOX9-positive, therefore, this population was a relatively pure population of Sertoli cells (Fig. 3.4C; Fig. 3.1F). On the other hand, about 7.6% of cells isolated in the low-GFP population (putative FLCs) were SOX9-positive, indicating that a low level of Sertoli cell contamination was present in the FLC population (Fig. 3.4G; Fig. 3.1F). Although our strategy attempted to remove the majority of germ and endothelial cells using a CD31 antibody, we found that about 22% of cells in the GFP-negative fraction were DDX4-positive germ cells and that approximately 6.4% of the GFP-negative population of cells were iB4-positive endothelial cells (Fig. 3.4A; Fig. 3.1G). We also tested for staining of Leydig cell markers CYP11A1 and HSD3β, but, as in section immunofluorescence, these markers proved uninformative at 12.5 dpc. These data indicated that the population purity of the three FACS isolated somatic cell populations was sufficient to represent the different enriched fetal testis cell populations.

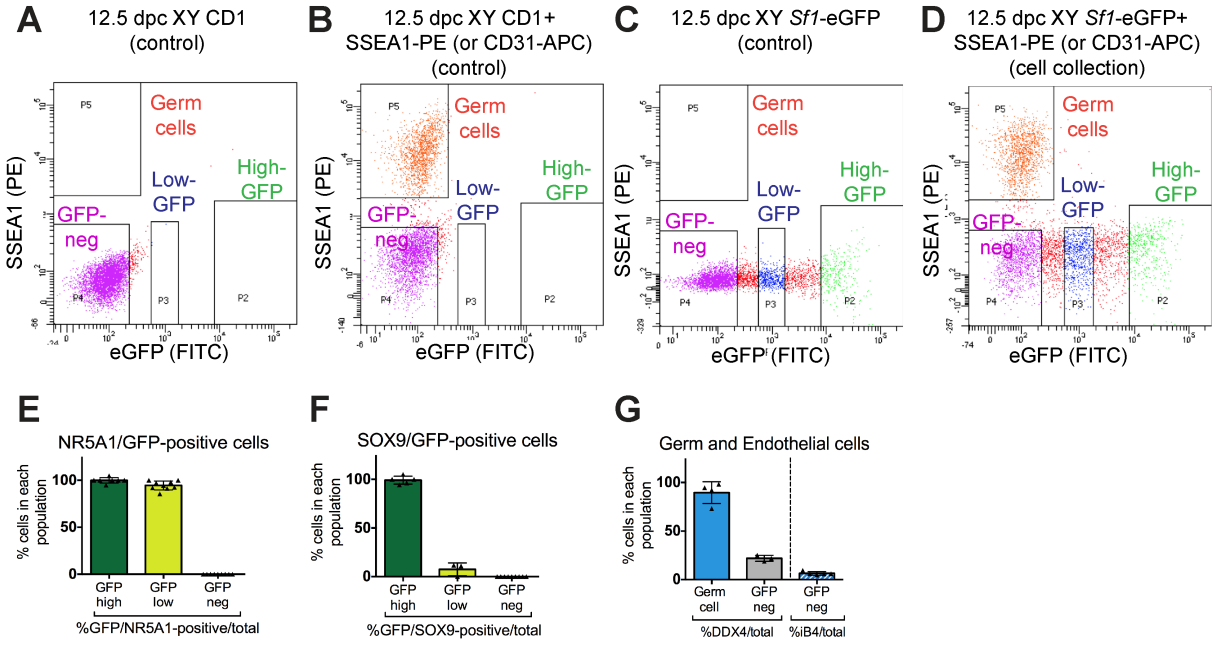

Figure 3.1: Isolation of populations and assessment of population purity.

(A-D) Representative FACS plots of dissociated CD1 and *Sf1*-eGFP gonadal cells labeled with/without a PE-tagged antibody to SSEA-1, a marker of germ cells. Four distinct populations can be isolated: P2, high-GFP (green); P3, low-GFP (blue); P4, GFP-negative (purple); P5, SSEA1-positive germ cells (orange). (A) 12.5 dpc XY gonad CD1 (GFP-negative), PE-negative (antibody-negative) control. (B) 12.5 dpc XY gonad CD1 (GFP-negative), PE-positive (antibody-positive) control. (C) 12.5 dpc XY gonad *Sf1*-eGFP (GFP-positive), PE-negative (antibody-negative) control. (D) 12.5 dpc XY gonad *Sf1*-eGFP (GFP-positive), PE-negative (antibody-positive) sample used for cell collection. (E-G) The purity of sorted cell populations was estimated using immunofluorescence. Double staining with anti-NR5A1 and anti-GFP antibodies showed that NR5A1-positive cells were captured in both GFP-positive populations (E; n= 7, 9, 9). Anti-SOX9/GFP double staining demonstrated that the high-GFP population was almost completely SOX9-positive with little contamination from other cell types. There was a low level of contamination in the low-GFP population; approximately 7.6% of low-GFP population cells were SOX9/GFP-positive (F; n= 5, 3, 9)). After depletion of germ cells and endothelial cells from the GFP-negative population, using an antibody to CD31, approximately 22% of the cells in the GFP-negative cell population were DDX4-positive escaped germ cells (G; n=4,3). Additionally, 6.4% of the GFP-negative population was identified as iB4-positive endothelial cells (G; n= 5).

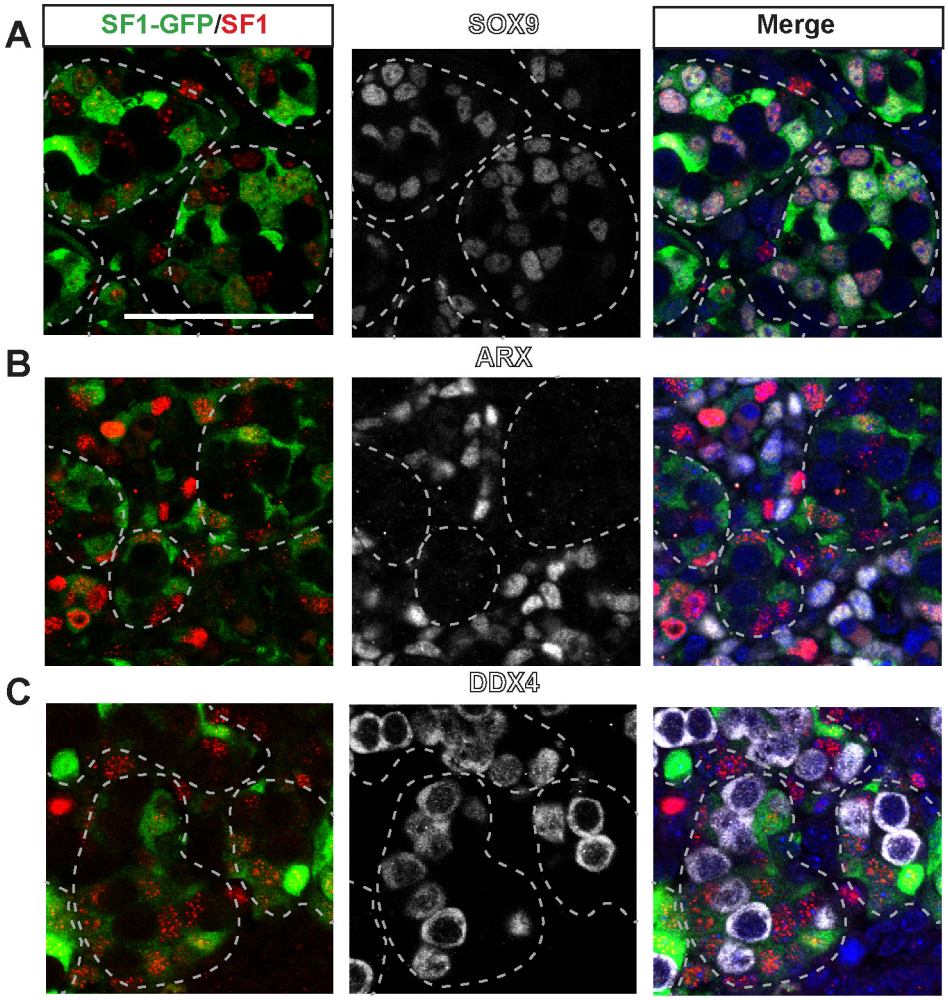

Figure 3.2. GFP-positive cells mark FLCs and SCs in Sf1-eGFP 12.5 dpc XY gonads.

(A-C) Immunofluorescence of *Sf1*-eGFP gonads demonstrates that nuclear NR5A1 is expressed in the same cells that express cytoplasmic GFP in the 12.5 dpc XY gonad. (A) GFP/NR5A1-positive cells line the cords; nuclear SOX9 and NR5A1 colocalise in GFP-positive cells, indicating that GFP marks Sertoli cells. (B) Some GFP/NR5A1 cells reside interstitially, these NR5A1-positive cells do not co-stain with ARX, a marker of non-FLCs, indicating that interstitial GFP/ NR5A1-positive cells are pre-steroidogenic FLCs. (C) DDX4-positive germ cells are GFP/ NR5A1-negative. Scale bar = 100 μM.

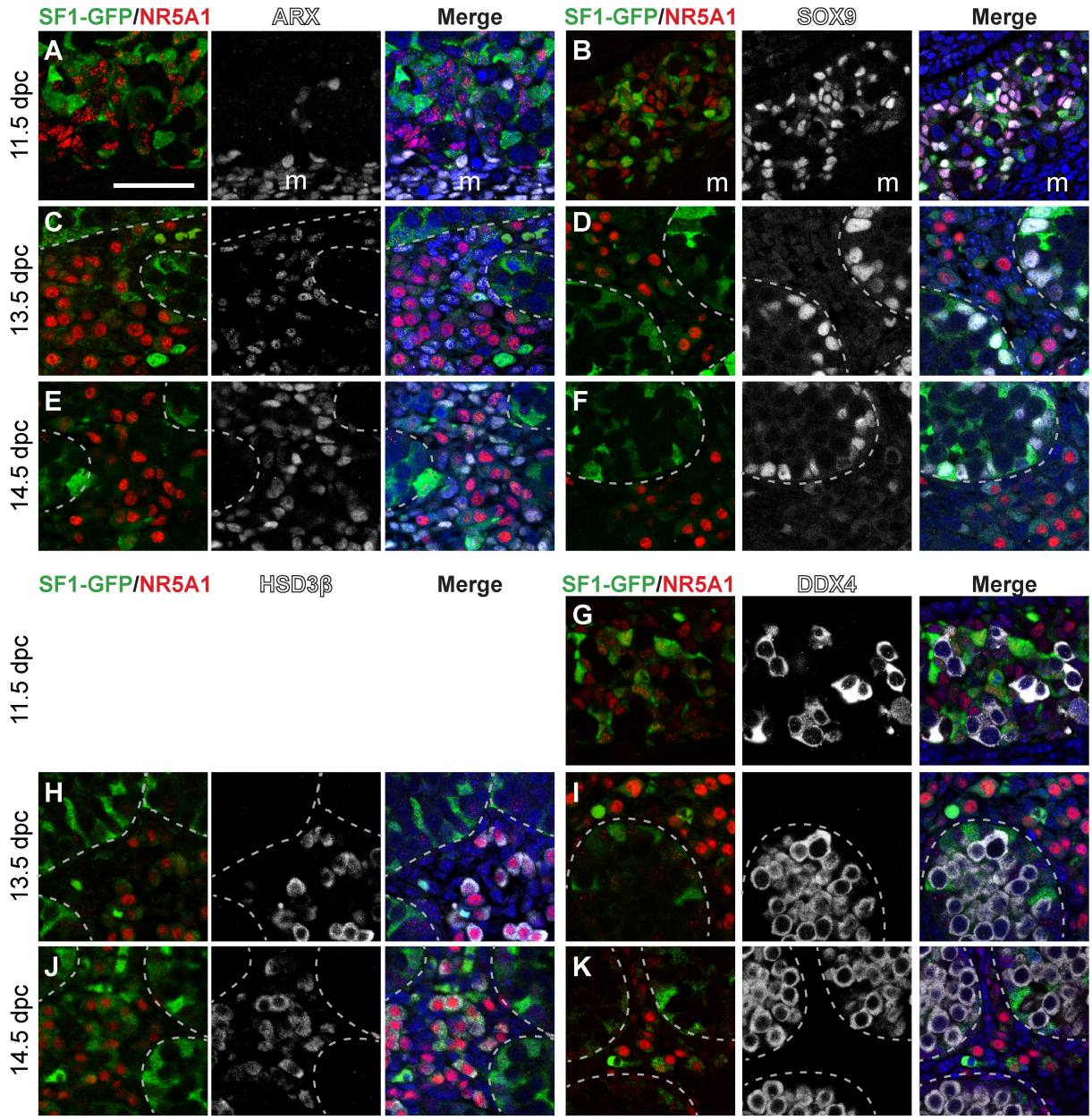

Figure 3.3. GFP-positive cells mark FLC and Sertoli cell populations in Sf1-eGFP XY gonads.

IF of *Sf1*-eGFP XY gonads at 18ts (~11.5dpc) shows that NR5A1 and GFP colocalise. At 11.5 dpc ARX-positive cells were NR5A1/GFP-negative cells in the gonad (A) whereas SOX9 colocalises with numerous NR5A1/GFP-positive cells (B). NR5A1/GFP-positive cells are exclusive of ARX-positive cells at 13.5 dpc (C) and 14.5 dpc (E). SOX9-positive cells are GFP-positive and line the cords at 13.5 dpc (D) and 14.5 dpc (F). Interstitial NR5A1/GFP-positive cells colocalise with HSD3β at 13.5 dpc (H) and 14.5 dpc (J). NR5A1/GFP-positive cells are exclusive of DDX4-positive cells at 11.5 dpc (G), 13.5 dpc (I) and 14.5 dpc (K). m = mesonephros; scale bar = 100 μM.

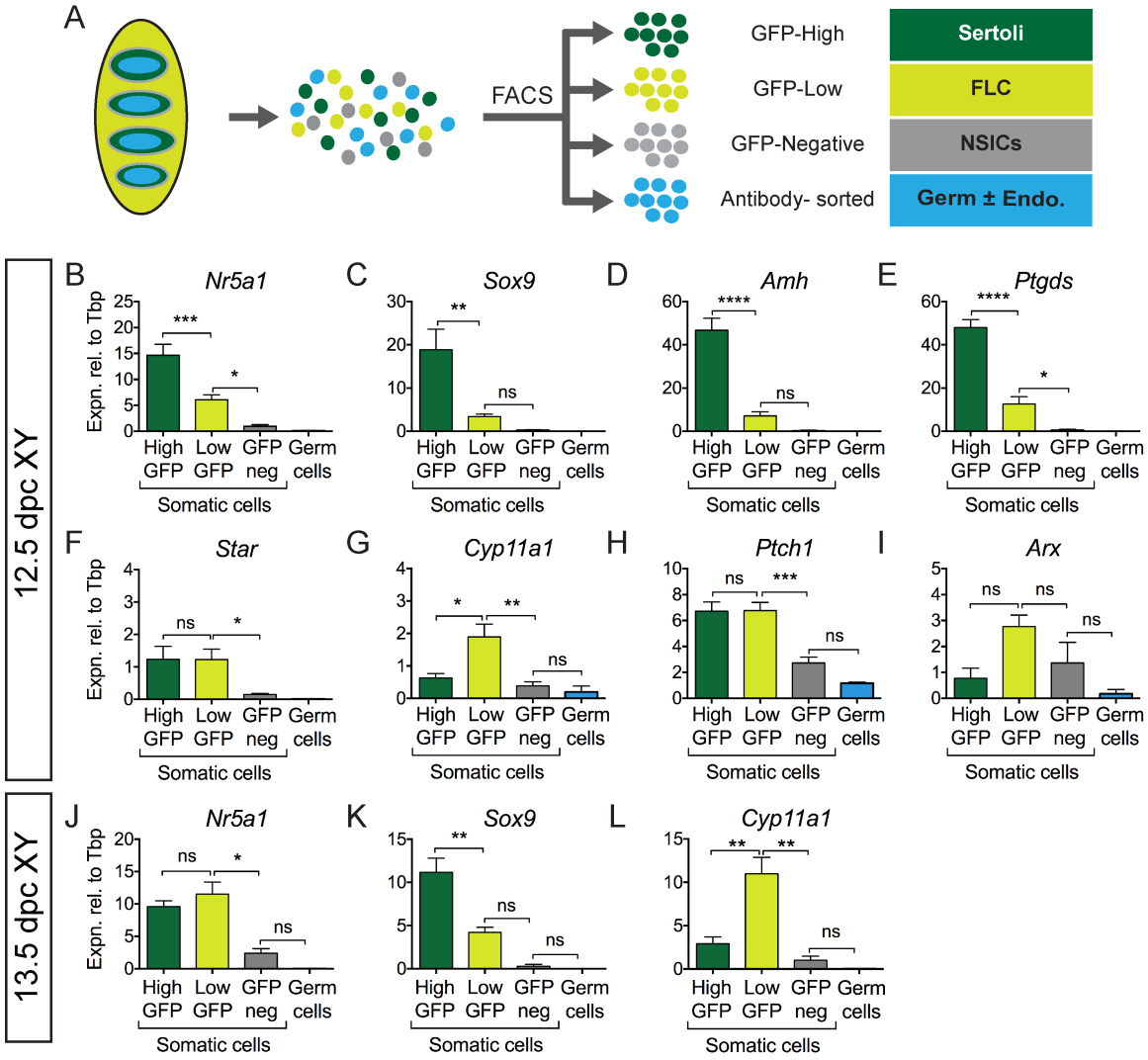

Figure 3.4. High-GFP population represents Sertoli cells and the low-GFP population represents FLCs in 12.5 dpc XY Sf1-eGFP gonads.

(A) Schematic of FACS protocol for the XY *Sf1*-eGFP gonads; four cell populations were isolated by FACS using a germ (GC) or germ cell/endothelial cell (GC/EC) depleted sorting method. (B-I) At 12.5 dpc, qRT-PCR for somatic marker *Nr5a1* (B) and Sertoli cell markers, *Sox9* (C), *Amh* (D) and *Ptgds* (E) showed that the high-GFP expressing cell population was enriched for Sertoli cells. The low-GFP expressing cell population expressed low levels of Sertoli cell markers. Early FLC marker *Star* (F) was similar in the two GFP-positive populations, however, *Cyp11a1* (G) was elevated in the low-GFP population. Interstitial markers *Ptch1* (H) and *Arx* (I) are the only markers expressed in the GFP-negative population. The same trend was observed at 13.5 dpc: high-GFP expressing cells expressed *Nr5a1* (J) and high levels of *Sox9* (K), whereas, low-GFP expressing cells were confirmed to be enriched for FLCs, as they express high levels of *Cyp11a1* (L). For all qRT-PCR: levels are shown relative to *Tbp,* error = S.E.M., * = p = 0.05, ** = p = 0.001, *** = p = 0.0001, **** = p = 0.00001, ns = not statistically significant. For 12.5 dpc, *n* values for (*Nr5a1, Sox9 n*= 4, 5, 4, 4 (GC/EC); *Star n*= 4, 5, 5, 5 (GC/EC); *Cyp11a1 n*= 3, 4, 4, 4 (GC); *Amh, Ptgds, Arx n*= 4, 4, 4, 4; *Ptch1 n*= 3, 5, 5, 5 (GC/EC)). For 13.5 dpc, *n* values for (*Nr5a1 n*= 8, 8, 5, 5; *Sox9 n*= 7, 7, 4, 4; *Cyp11a1 n*= 8, 8, 4, 4 (GC)).

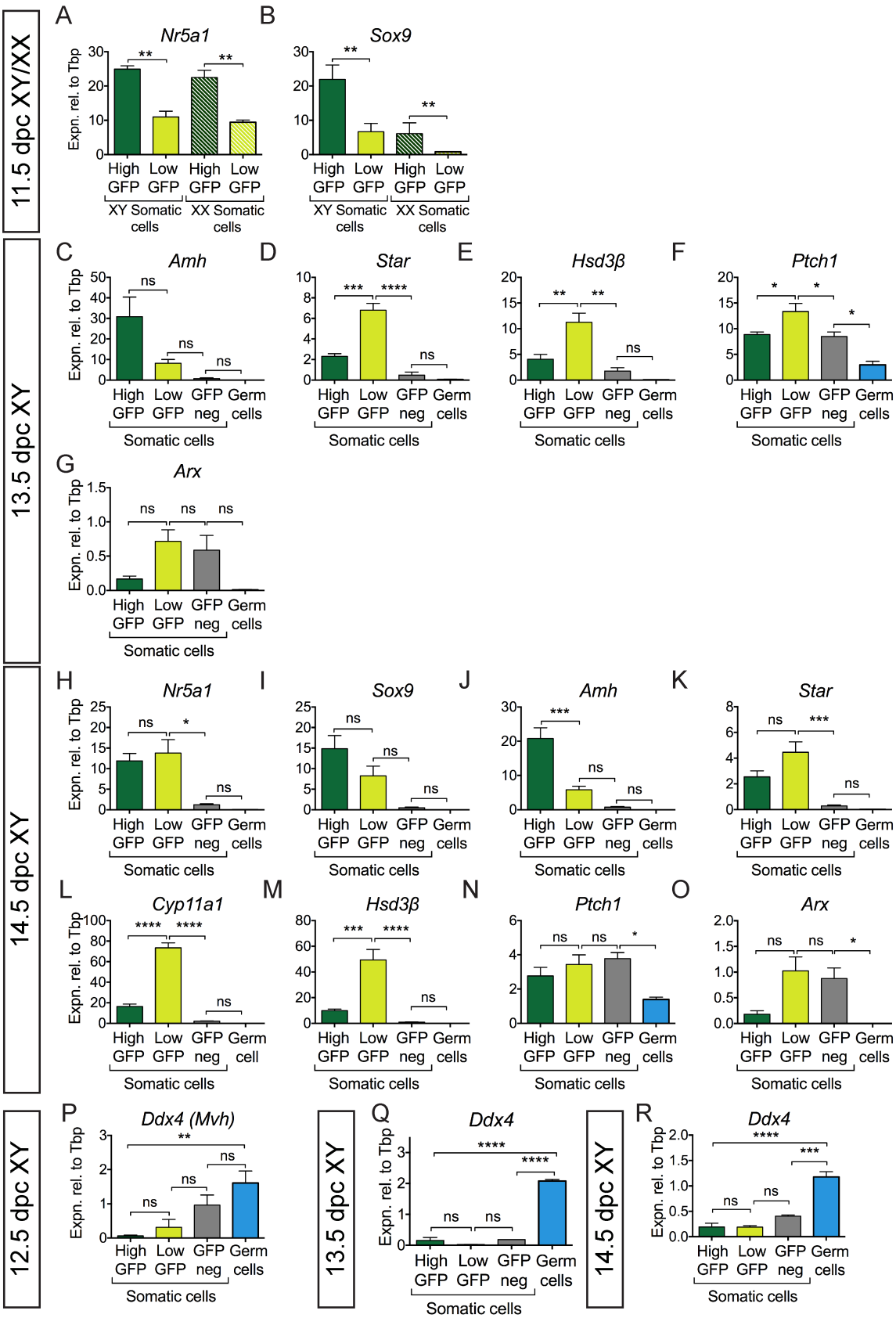
11.5 dpc XY/XX
13.5 dpc XY
14.5 dpc XY
12.5 dpc XY
13.5 dpc XY
14.5 dpc XY
A
Nr5a1
B
Sox9
C
Amh
D
Star
E
Hsd3β
F
Ptch1
G
Arx
H
Nr5a1
I
Sox9
J
Amh
K
Star
L
Cyp11a1
M
Hsd3β
N
Ptch1
O
Arx
P
Ddx4 (Mvh)
Q
Ddx4
R
Ddx4
Expn. rel. to Tbp
High GFP
Low GFP
GFP neg
Germ cells
Germ cell
XY Somatic cells
XX Somatic cells
Somatic cells

Figure 3.5. High-GFP cell population represents Sertoli cells and the low-GFP population represents FLCs in XY Sf1-eGFP gonads.

qRT-PCR identifies the low-GFP expressing population as enriched for FLCs and the high-GFP expressing population as enriched for Sertoli cells. At 11.5 dpc, in XX and XY *Sf1*-eGFP gonads, two populations of GFP-expressing cells were isolated by FACS using a germ cell depleted sorting method (*n*= 4, 4, 4, 4): qRT-PCR for somatic marker *Nr5a1* (A) and Sertoli cell marker *Sox9* (B), showed that the high GFP expressing cell population was enriched for Sertoli cell markers and the low GFP-expressing population expressed low levels of *Nr5a1*. qRT-PCR on sorted cells from XY *Sf1*-eGFP gonads at 13.5 dpc showed that Sertoli cell marker *Amh* (C) were enriched in the high-GFP population, whilst FLC markers *Star* (D) and *Hsd3β* (E) were enriched in the low-GFP population. Interstitial marker *Ptch1* (F) was expressed in all somatic cells whereas *Arx* (G) was expressed in the low-GFP and GFP-negative populations. At 14.5 dpc these patterns were maintained. qRT-PCR showed that: *Nr5a1* (H) was expressed in both GFP-positive populations; *Sox9* (I) and *Amh* (J) were enriched in the high-GFP population and FLC markers *Star* (K), *Cyp11a1* (L) and *Hsd3β* (M) were enriched in the low-GFP population. Interstitial marker *Ptch1* (N) was expressed most highly in somatic cell populations while *Arx* (O) was expressed in the low-GFP and GFP-negative populations. *Ddx4* was used as a marker of germ cells to examine the efficacy of antibody selection in GC/EC depletion at 12.5 dpc (P) and GC-depletion at 13.5 (Q) and 14.5 dpc (R); some germ cell contamination was detected in the GFP-negative population. *n* values for C,E: *n*= 8, 8, 3, 3; D,G: *n*= 3, 3, 3, 3; F,Q,P: *n*= 4, 4, 4, 4; H,I: *n*= 8, 8, 4, 3; J,K,L,M,N,O,R: *n*= 4, 4, 4, 3. For all qRT-PCR: levels are shown relative to *Tbp,* error = S.E.M., * = p = 0.05, ** = p = 0.001, *** = p = 0.0001, **** = p = 0.00001, ns = not statistically significant.

Generation and quality of RNA-seq data

We next analysed the transcriptomes of the sorted testicular cell populations by RNA-seq. Cells were collected from 12.5 dpc *Sf1*-eGFP XY gonads, depleted of germ and endothelial cells using a CD31 antibody, and fractionated into three populations using the methods described above (Fig. 3.4A). Triplicate samples of each somatic cell population were generated, RNA was isolated and reverse-transcribed, and the resulting cDNA deep-sequenced using a paired end 100bp stranded sequencing format on Illumina HiSeq 1500. An average of 65 million raw reads were generated per sample. Supplemental Data 1 provides a spreadsheet of cpm RNA-seq data for all Ensembl gene IDs detected at >1cpm in 3 or more samples (data can be accessed from GEO; GSE65498).

To validate the RNA-seq data, we examined the normalised sequence counts per million (cpm) as an indicator of expression of various marker genes (Fig. 3.6A-I; Supplemental Data 1). The results of this analysis were consistent with results obtained by qRT-PCR, with the exception of *Star,* where transcripts were detected in the NSIC population at low levels in the RNA-seq data (Fig. 3.4B-I; Fig. 3.6A-I). These data indicated that the RNA-seq output accurately represented the transcriptomes of the different enriched fetal testis cell populations.

Differentially expressed gene analysis

Genes were identified as being up-regulated in a cell population if they showed >1 log fold change and adjusted *p*-value < 0.05 in the differential expression (DE) analysis compared to either of the other cell types. As expected, the GFP-negative fraction isolated by FACS was negative for Sertoli and FLC markers. However, each of the GFP-positive populations contained some transcripts characteristic of other populations, consistent with results obtained qRT-PCR (Fig. 3.4B-L; Fig. 3.5; Fig. 3.6). That is, some FLCs were likely to have contaminated the Sertoli cell-enriched fraction (Fig. 3.4G, low level expression of *Cyp11a1*) and some Sertoli cells were likely to have been present in the FLC-enriched fraction (Fig. 3.4C, low level expression of *Sox9*). For this reason, the log fold cutoff off was lowered to >0.6 for these samples, to reduce the potential of obtaining false negatives when compiling lists of cell type-specific genes. In this way, we identified a group of genes upregulated in each enriched cell population: 84 FLC-enriched genes, 704 NSIC-enriched genes and 1217 Sertoli cell-enriched genes (Supplemental Data 2). Validation of a subset of the genes from the lists of upregulated transcripts demonstrates that a gene in these lists is likely to be expressed in a single testicular cell population at 12.5 dpc.

Validation of the FLC-enriched gene dataset

As a first step in validating the 84 candidate FLC genes, we compared them to results of published studies. Of these genes, 72% (61 genes) were previously unreported in the two published microarray datasets that have provided lists of candidate FLC genes at 12.5 dpc ((Jameson et al., 2012b; McDowell et al., 2012); Fig. 3.7A; Table 3.1). A number of genes had been identified as being expressed in whole adult testis, although for most no further gonadal or fetal gonadal characterisation has been performed (Supplemental Table 5). Four of the 84 genes (*Htra3*, *Vcam1, Bmp2* and *Kcnk3*) overlapped with a list of 567 genes identified as putatively regulated by NR5A1 by performing RNA-seq on Y-1 cells treated with *Nr5a1*-siRNA (2014) consistent with *Nr5a1's* pivotal role in FLC specification and differentiation.

We next analysed temporal and cell-specific gene expression of candidate FLC genes by qRT-PCR on sorted *Sf1*-eGFP cell populations at 12.5-14.5 dpc. These analyses confirmed FLC-enriched expression of *Tacr3*, *Tac2, Prlr, Sox18*, *Mc2r* and *Adcy7* compared to NSICs (Fig. 3.7B,C,E-G,I). *Prlr* was expressed in the FLC-population with expression increasing from 12.5 dpc (Fig. 3.7E). *Robo2* and *Clca1* appeared to be expressed equally in FLCs and NSICs by qRT-PCR (Fig. 3.7D,H). Expression of *Tacr3* was elevated in the FLC-enriched population at 12.5 dpc and was subsequently expressed in the FLC and NSIC populations (Fig. 3.7B). Interestingly, *Tac2*, *Sox18* and *Adcy7* were expressed more highly in the FLC than in the NSIC population at 12.5 dpc only before becoming either expressed in multiple populations or downregulated (Fig. 3.7C,F,I).

Lastly, we examined the in situ hybridization (ISH) staining patterns of the FLC genes identified by RNA-seq, at 14.5 dpc when FLCs have upregulated steroid production, using the Eurexpress whole embryo section *in situ* hybridization (ISH) database (Diez-Roux et al., 2011). Of the 8 expression profiles analysed in this way (*Adcy7, Clca1, Itga9, Nrg1, Nts, Prlr, Srpx2* and *Tacr3*), all showed the expected expression in the interstitial space, similar to the known FLC marker *Cyp11a1* (Fig. 3.8A,D-K), and distinct from the cord-associated expression of the Sertoli cell marker *Amh* (Fig. 3.8C). Taken together, these validation steps confirmed that the putative FLC gene dataset generated in this study represents an accurate subset of the FLC transcriptome.

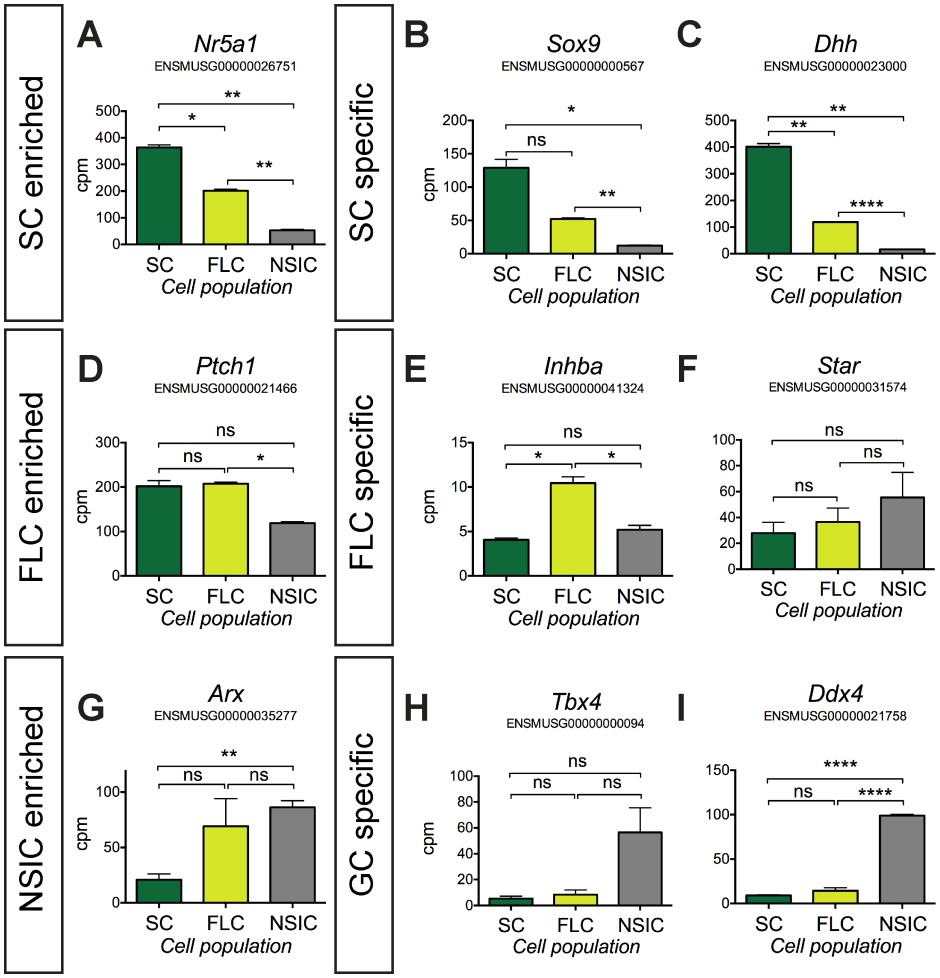

Figure 3.6. RNA-seq counts for specific genes recapitulate qRT-PCR results.

Counts per million reads (cpm) from RNA-seq data recapitulate qRT-PCR results for the Sertoli cell, NSIC and FLC populations. *Nr5a1* (A) was enriched in Sertoli cell as were Sertoli marker genes *Sox9* (B) and *Dhh* (C). *Ptch1* (D) was enriched in somatic cells whilst FLC marker *Inhba* (E; *inhibin beta-A*), was upregulated in FLCs, although *Star* (F) was not robustly upregulated at this timepoint. *Arx* (G) was enriched in NSIC and FLCs similar to qRT-PCR results. Germ cell markers *Tbx4* (H; *T-box 4*) and *Ddx4* (I) were present in the NSICs indicating some GC contamination.

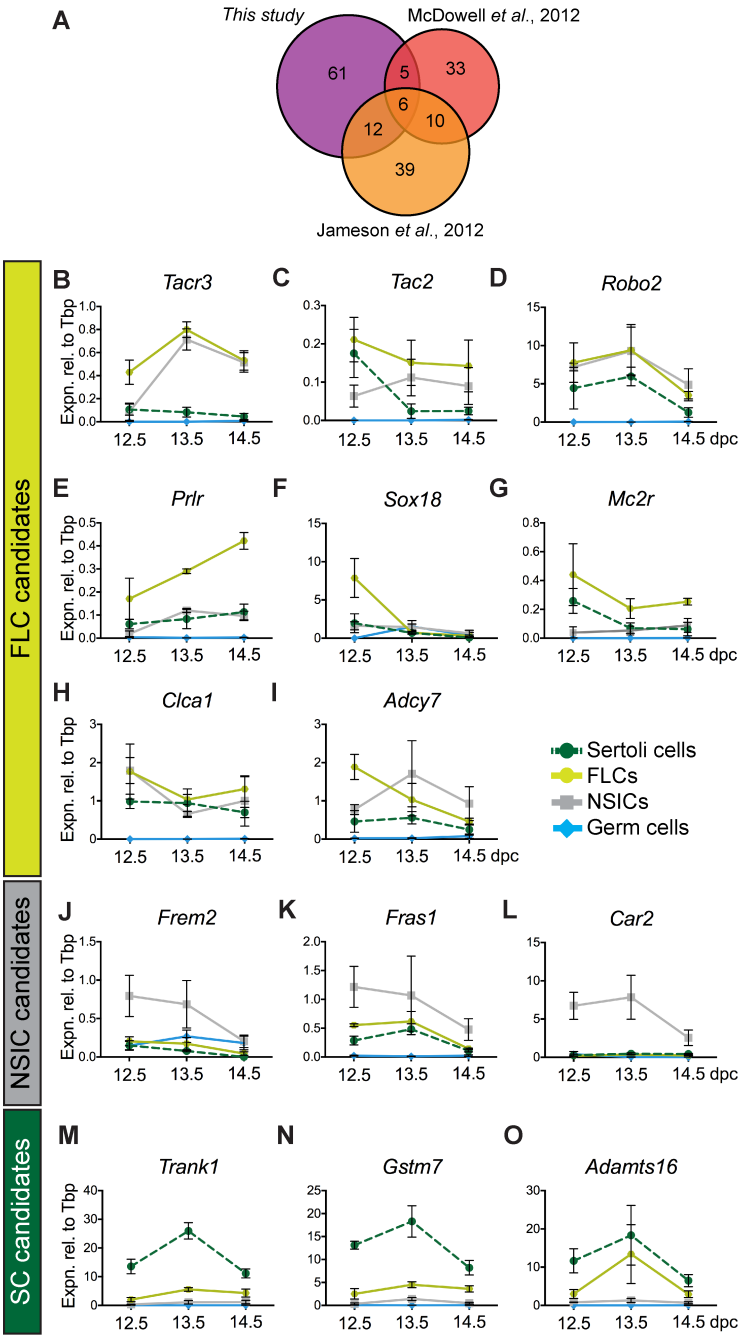

Figure 3.7. qRT-PCR validation of cell lineage expression of novel candidate genes from 12.5-14.5 dpc.

(A) Comparison between our dataset of genes upregulated in the FLC enriched population and the McDowell et al., (2012) and Jameson et al., (2012b) datasets is represented, only 6 genes are present in all three datasets. See Table 1 for lists of genes in each category. (B-O) qRT-PCR for candidate genes identified as being differentially expressed between cell types on sorted cell populations from the 12.5-14.5 dpc *Sf1*-eGFP XY gonad. Novel genes identified as being highly expressed in enriched FLC: (B) *Tacr3,* (C) *Tac2*, (D) *Robo2,* (E) *Prlr,* (F) *Sox18*, (G) *Mc2r,* (H) *Clca1* and (I) *Adcy7*. Novel genes highly expressed in enriched NSICs: (J) *Frem2,* (K) *Fras1* and (L) *Car2*. Novel genes identified as being highly expressed in enriched Sertoli cells: (M) *Trank1,* (N) *Gstm7* and (O) *Adamt16*. (B,C,E,G,L,M,N: 12.5/13.5 dpc, n= 3, 3, 3, 3, 14.5 dpc, n= 4, 4, 4, 3; D,F,H,I,J,K,O: 12.5/13.5 dpc, n= 3, 3, 3, 3, 14.5 dpc, n= 3, 4, 4, 3) For all qRT-PCR: levels are shown relative to *Tbp,* error = S.E.M.

Table 3.1. Genes represented in three different characterisations of the FLC population

FLC genes is found in:	Gene lists:
This study, Jameson (Jameson et al., 2012b) and McDowell (McDowell et al., 2012)	*Inhba, Ppp1r14a, Prlr, Prokr2, Robo2, Vsnl1*
This study and Jameson (Jameson et al., 2012b)	*C7, Casq2, Cbln1, Grin2a, Hhip, Hspa12a, Itga9, Kcnj3, Mc2r, Nts, Stc1, Vcam1*
This study and McDowell (McDowell et al., 2012)	*Crhr1, Htra3, Itih5, Srpx2, Vgll3*
Jameson (Jameson et al., 2012b) and McDowell (McDowell et al., 2012)	*Aebp1, AI427809, Cyp11a1, Cyp17a1, Fads1, Gramd1b, Hsd3b1, Lhcgr, Npy, Star*
This study only	*Adamts5, Adcy7, Arhgap6, Armcx6, Art3, Bmp2, Btnl9, Chst1, Chst2, Clca1, Clec1b, Col23a1, Cyp1b1, Ffar2, Gja5, Gm11549, Gm13659, Gm14396, Gm5067, Gpr153, Gpr174, Gpr20, Grrp1, Hoxd10, Hoxd11, Hsd11b2, Irf8, Itga4, Kcnk3, Kcns2, Lars2, Lrrtm3, Mc4r, Mme, Mmp28, Myh11, Myh7, Myl4, Myoc, Ngfr, Nrg1, Oit3, Otof, Pcp4l1, Pdyn, Plcxd3, Pnmal1, Ptpro, Rad51ap2, Serpina3g, Sertm1, Slitrk2, Sox18, Speer7-ps1, Sstr4, Syt15, Tac2, Tacr3, Tg, Trac, Vipr1*
Jameson only (Jameson et al., 2012b)	*A430107O13Rik, Ace2, Adam12, Alas1, Armcx2, Atp1a3, Clca2, Col6a1, Copz2, Cxcr7, Cyp51, Enpep, Ephx1, Fat3, Fdps, Fdx1, Gpc3, Gpm6a, Grk5, Hsd17b7, Jag1, Mobkl3, Osr2, Pltp, Prkar2b, Pros1, Rbp4, Ren1, Sc4mol, Scarb1, Sct, Slc6a15, Smoc2, Ssfa2, Tgfbr3, Tnc, Tpm2, Trib2, Zeb2*
McDowell only (McDowell et al., 2012)	*1200009O22Rik, 4930474M22Rik, 5031410I06Rik, Abcc9, Adamts7, Alcam, Arx, B3galt1, Cd36, Cdkn2c, Dlc1, Fbn1, Glipr2, Gpx3, Gria4, Gsta2, Gucy1b3, Inha, Insl3, Itgb8, Itm2a, Lrrk2, Ltbp4, Ng23, Nuak1, Pi15, Ptrf, Scd1, Sec24d, Slc29a1, Speer4d, Thbd, Tm7sf2*

Table 3.1: Genes represented in three different characterisations of the FLC population (see Fig. 3.7A).

List of FLC genes identified in this study, the McDowell data set (McDowell et al., 2012) and the Jameson dataset (Jameson et al., 2012b) at 12.5 dpc indicating unique and overlapping genes between data sets. This data is displayed in a Venn diagram in Fig. 3.7A.

Mining of the FLC-enriched gene dataset

We sought to generate a transcriptional portrait of the FLCs based on the RNA-sequencing dataset. We performed gene ontology (GO) analysis, using the DAVID Bioinformatics Package, for each of the three outputs of the differentially expressed gene analysis. Ten of the identified genes for each of three ontologies (transmembrane factors, secreted factors and transcription factors) for each sorted cell population are listed in Fig. 3.9. Among the 84 candidate FLC genes, we identified 35 genes encoding transmembrane components (p= 2.33E-03), of these there was an overrepresentation of genes involved in neurogenesis/neurotransmission (Table 3.2), with 8 encoding receptors, or receptor components, for neuroactive ligands (*Tacr3, Mc4r, Prlr, Crhr1, Mc2r, Sstr4, Grin2a* and *Vipr1; p*= 2.96E-03). Additionally, five receptors were identified as being involved in cell adhesion (*Robo2, Itga4, Itga9, Vcam1, Arhgap6; p*= 9.86E+01). Secreted factors were also overrepresented, with 14 secreted factors upregulated in the enriched FLC population including *Tac2, Hhip, Pdyn* and *Inhba* (p= 9.98E-02). Finally we identified four genes encoding transcription factors in the FLC enriched population: *Hoxd10, Hoxd11, Irf8* and *Sox18* (p= 1.00E+02).

We queried the Online Mendelian Inheritance in Man (OMIM) Database and found that 30 of the candidate FLC genes are associated with human disease phenotypes (26 where the molecular basis is known; eight listed in Table 3.3; full list Supplemental Data 8). Analysis of published literature revealed that genetic deletion of some of the genes upregulated in the FLC-enriched population results in embryonic lethality (Table 3.3) from a variety of causes including cardiac (*Nrg1;* (Meyer and Birchmeier, 1995)), respiratory (*Hhip;* (Chuang et al., 2003)) and vascular defects (*Ngfr;* (Schack et al., 2001)). Among these, gene knockout of *Robo2, Prokr2* and *Tacr3* in mice resulted in defects in postnatal urogenital and reproductive system development (Grieshammer et al., 2004; Matsumoto et al., 2006; Yang et al., 2012). Interestingly, these three genes encode transmembrane receptors important for neuroactive-ligand signalling.

Finally, we sought to determine if any FLC genes at 12.5 dpc might also mark pre-FLCs at 11.5 dpc and might therefore be useful in clarifying the developmental origin of FLCs. We re-analysed a previously-published microarray dataset (Jameson et al., 2012b) and considered whether genes we found to be enriched in FLCs at 12.5 dpc were also robustly upregulated in the "interstitial" population (which includes pre-FLCs) compared with the "supporting" (pre-Sertoli) population at

11.5 dpc: we reasoned that such genes may mark FLCs even before they attain sterodogenic capacity. This analysis resulted in the identification of 10 genes of interest: *Prokr2; Itga9; Ptpro; Ngfr; Clca1; Adamts5; Nrg1; Arhgap6; Myl4* and *Hsd11b2* (Table 3.4; Supplemental Data 4). These genes, characterising non-Sertoli NR5A1-positive cells prior to FLC maturation (which occurs between 12.5 and 13.5 dpc), may act as early markers for the FLC lineage and, therefore, may aid our understanding of FLC specification and differentiation.

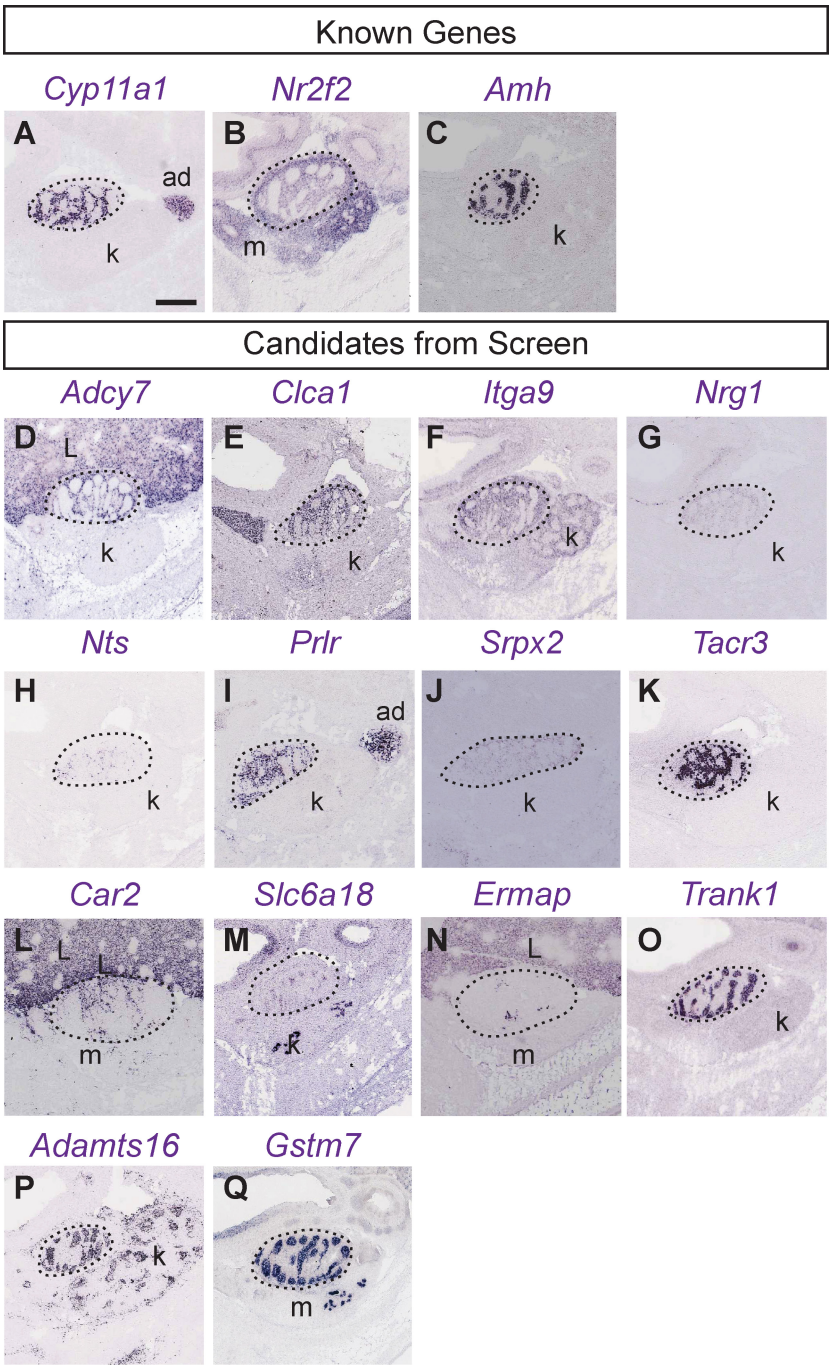

Figure 3.8: In situ hybridisation for genes identified by RNA-seq to be over-expressed in FLCs, NSICs and Sertoli cells.

ISHs for newly identified candidate genes at 14.5 dpc from *Eurexpress Transcriptome Atlas Database for Mouse Embryo* (http://www.eurexpress.org). Marker genes *Cyp11a1* (A) shows FLC expression pattern, *Nr2f2* (B; nuclear receptor subfamily 2, group F, member 2) shows an interstitial pattern and *Amh* (C) shows a Sertoli cell expression pattern. Novel FLC genes, *Adcy7* (D), *Clca1* (E), *Itga9* (F), *Nrg1* (G), *Nts* (H), *Prlr* (I), *Srpx2* (J) and *Tacr3* (K; also shows adrenal expression (data not shown)) show expression in cells distributed outside the testis cords indicating that FLC-expressed genes are being detected. Novel NSIC genes, *Car2* (L), *Slc6a18* (M) and *Ermap* (N) show expression in cells distributed outside the testis cords indicating the NSIC expressed genes are being detected. Novel Sertoli cell genes, *Trank1* (O), *Adamts16* (P) and *Gstm7* (Q) show expression in cells distributed around the border of the testis cords indicating Sertoli cell expression. The testis region is demarcated by a dotted line. Scale = 0.5 mm. k= kidney; ad= adrenal; L= liver; m= mesonephros; *Eurexpress* probe IDs can be found in Supplemental Table 7.

Table 3.2. Subset of clusters of from DAVID GO Analysis on enriched FLCs (Enrichment > 3).

Annotation	GO clusters	Benjamani P-value
Neuro	*Enrichment: 5.72*	
	G-protein coupled receptor	7.02E-08
	Transducer	6.72E-08
	Receptor	1.19E-07
	GO:0007186 G-protein coupled receptor protein signaling pathway	6.01E-06
	GO:0007166 Cell surface receptor linked signal transduction	2.06E-05
	PIRSF800006 Rhodopsin-like G protein-coupled receptors	1.82E-05
	Cell membrane	2.95E-05
	mmu04080 Neuroactive ligand-receptor interaction	1.49E-04
	GO:0042923 Neuropeptide binding	7.19E-04
	GO:0008188 Neuropeptide receptor activity	7.19E-04
	GO:0001653 Peptide receptor activity	1.77E-03
	GO:0008528 Peptide receptor activity, G-protein coupled	1.77E-03
	GO:0042165 Neurotransmitter binding	1.10E-02
	GO:0030594 Neurotransmitter receptor activity	1.10E-02
	GO:0042277 Peptide binding	1.64E-02
	Palmitate	4.69E-02
	Lipoprotein	5.73E-02
Cell membrane	*Enrichment: 4.88*	
	Cell membrane	2.95E-05
	Transmembrane	3.59E-05
	GO:0005886 Plasma membrane	6.09E-04
	Membrane	7.03E-04
	GO:0016021 Integral to membrane	3.95E-03
	GO:0031224 Intrinsic to membrane	2.84E-03
Secreted	*Enrichment: 4.64*	
	Signal	1.22E-07
	Secreted	1.12E-03
	Cleavage on pair of basic residues	6.84E-03
	GO:0005576 Extracellular region	3.78E-02

Table 3.2. Subset of clusters of from DAVID GO Analysis on enriched FLCs (Enrichment > 3).

Clusters identified by DAVID analysis in the FLC enriched gene list with an "Enrichment Value" of ≥3

Table 3.3. Subset of genes upregulated in 12.5 dpc FLCs ($p < 0.05$).

ID	Gene Name		Chr	Phenotype	OMIM assoc.	Reference
ENSMUSG00000052516	Robo2	Roundabout homolog 2	16	urogenital and organ patterning defects	610878	(Grieshammer et al., 2004)
ENSMUSG00000056025	Clca1	Chloride channel calcium activated 1	3	-	-	-
ENSMUSG00000028172	Tacr3	Tachykinin receptor 3/neuromedin K receptor (Nk3r)	3	postnatal defects; males have small testes and low FSH	614840*	(Topaloglu et al., 2009; Yang et al., 2012)
ENSMUSG00000062991	Nrg1	Neuregulin 1	8	embryonic lethal at 10.5 dpc; cardiac defect	603013	(Meyer and Birchmeier, 1995)
ENSMUSG00000024087	Cyp1b1	Cytochrome P450, family 1, subfamily b, polypeptide 1	17	no lethal developmental defects	231300	(Buters et al., 1999)
ENSMUSG00000027820	Mme	Membrane metallo endopeptidase/NEP	3	no lethal developmental defects	-	(Lu et al., 1997)
ENSMUSG00000026824	Kcnj3	Potassium inwardly-rectifying channel, subfamily J, member 3	2	no lethal developmental defects	-	(Bettahi et al., 2002)
ENSMUSG00000064325	Hhip	Hedgehog-interacting protein	8	lethal at P0; respiratory defects	-	(Chuang et al., 2003)
ENSMUSG00000050963	Kcns2	K+ voltage-gated channel, subfamily S, 2	15	-	-	-
ENSMUSG00000031654	Cbln1	Cerebellin 1 precursor protein	8	no lethal developmental defects : postnatal cerebellum defects	-	(Hirai et al., 2005)
ENSMUSG00000050558	Prokr2	Prokineticin receptor 2	2	no gross FLC phenotype; postnatal atrophy of the reproductive system and olfactory bulb defects	244200*	(Dode et al., 2006; Matsumoto et al., 2006; Svingen et al., 2011)
ENSMUSG00000027009	Itga4	Integrin alpha 4	2	embryonic lethal; placentation defect and cardiac haemorrhage	-	(Yang et al., 1995)
ENSMUSG00000020682	Mmp28	Matrix metallopeptidase 28 (Epilysin)	11	no lethal developmental defects	-	(Manicone et al., 2009)
ENSMUSG00000039115	Itga9	Integrin alpha 9	9	no lethal developmental defects ; postnatal thorax and lymphatic valve defects	-	(Bazigou et al., 2009; Huang et al., 2000)
ENSMUSG00000030223	Ptpro	Protein tyrosine phosphatase, receptor type, O	6	no lethal developmental defects ; sensory and glomerular defects postnatally	614196	(Gonzalez-Brito and Bixby, 2009; Wharram et al., 2000)
ENSMUSG00000050368	Hoxd10	Homeobox D10	2	nervous system, hind-limb and musculoskeletal defects	192950	(Carpenter et al., 1997)
ENSMUSG00000047259	Mc4r	Melanocortin 4 receptor	18	no lethal developmental defects ; obesity	601665	(Huszar et al., 1997)
ENSMUSG00000022894	Adamts5	A disintegrin-like and metallopeptidase with thrombospondin type 1 motif, 5	16	no lethal developmental defects ; postnatal cartilage aggrecanase	-	(Glasson et al., 2005; Stanton et al., 2005)
ENSMUSG00000027962	Vcam1	Vascular cell adhesion molecule 1	3	embryonic lethal at 12.5 dpc; required for chorioallantoic fusion and placentation	-	(Gurtner et al., 1995)
ENSMUSG00000025092	Hspa12a	Heat shock protein 12A	19	-	-	-
ENSMUSG00000040283	Btnl9	Butyrophilin-like 9	11	-	-	-
ENSMUSG00000014813	Stc1	Stanniocalcin 1	14	no lethal developmental defects	-	(Chang et al., 2005)
ENSMUSG00000031659	Adcy7	Adenylate cyclase 7	8	embryonic lethal; -/+ survive	-	(Hines et al., 2006)

ENSMUSG00000000120	Ngfr	P75 NTR/ nerve growth factor receptor	11	40% perinatal loss of -/- between 15.5dpc-birth due to vascular defects	-	(Schack et al., 2001)
ENSMUSG00000031355	Arhgap6	Rho gtpase activating protein 6	X	no lethal developmental defects	-	(Prakash et al., 2000)

Table 3.3. Subset of genes upregulated in 12.5 dpc FLCs ($p < 0.05$).

Phenotype indicates the embryonic or postnatal phenotype of the null animal. Information from published reports where there was postnatal survival mutations were classified as: "*no lethal developmental defects*" (indicates that the null offspring were obtained as adults at the expected Mendelian ratios) or "*fertile*" (indicates that the mice were able to reproduce normally). References are the primary report of the null or mutant mouse and any subsequent clarifying reports. (Chr., chromosome; OMIM assoc. = OMIM reference number if the gene is associated with any type of human disorder (* indicates a genitourinary, endocrine or DSD phenotype); FSH, follicle stimulating hormone).

Table 3.4. Genes identified at 12.5 dpc in FLCs that are putative marker genes of pre-FLCs at 11.5 dpc

Genes	logFC	P.Value	adj.P.Val	Int. Exp	Sup Exp	Int. Rank	Sup. Rank
Cyp1b1	5.03	2.83E-15	9.22E-12	11.77	6.87	98	35
Prokr2	4.54	2.23E-11	1.30E-08	10.34	4.90	88	6
Itga9	4.49	6.39E-09	1.40E-06	8.42	3.92	61	0
Ptpro	4.38	3.10E-06	2.21E-04	9.27	4.99	75	7
Hoxd10	4.02	9.18E-14	1.48E-10	10.58	6.71	90	32
Ngfr	3.71	4.10E-12	3.11E-09	9.73	5.81	82	17
Robo2	3.58	4.34E-07	4.55E-05	10.38	6.08	89	21
Clca1	3.46	6.34E-10	2.09E-07	8.48	5.11	62	9
Adamts5	3.28	3.75E-13	4.49E-10	8.35	5.11	60	9
Nrg1	3.11	2.74E-08	4.67E-06	8.23	4.95	58	7
Hoxd11	3.02	6.18E-11	3.06E-08	8.86	6.11	69	22
Arhgap6	2.88	1.96E-03	2.89E-02	8.68	4.84	66	6
Cbln1	2.75	4.93E-16	2.29E-12	11.07	7.97	94	56
Mc2r	2.72	1.54E-07	1.96E-05	9.61	6.55	80	29
Myl4	2.52	8.50E-05	2.98E-03	8.12	5.72	56	16
Hsd11b2	2.52	1.51E-05	7.82E-04	8.91	5.19	70	10
Mme	2.08	2.46E-04	6.60E-03	9.56	7.66	79	50
Vcam1	2.04	1.18E-06	1.03E-04	7.99	6.03	54	21

Table 3.4. Genes identified at 12.5 dpc in FLCs that are putative marker genes of pre-FLCs at 11.5 dpc.

Genes found to be enriched in Leydig cells at 12.5 dpc that also show differing expression between the interstitial and supporting cell compartments of 11.5 dpc testes are putative pre-FLC marker genes. This table summarises top results from the full dataset, noting those genes with expression in interstitial cells more than four times that in supporting cells (logFC $\geq$ 2). Of particular interest in predicting putative markers for FLCs are the 10 genes with low expression in supporting cells (Sup Exp $\leq$ 6; marked in grey). The logFC, P.Value, and adj.P.Val columns indicate results from differential expression analysis. Int. Exp (interstitial) and Sup. Exp (supporting) show median normalised expression of the gene in each of these two cell types, while Int. Rank (interstitial) and Sup. Rank (supporting) indicate the position of the gene in a list ranked by expression in that cell type (0=lowest expression, 100=highest expression).

NSICs vs FLC transcriptomes: Clues to the origin of FLCs

It is clear that signaling from Sertoli cells to interstitial cells plays a critical role in the specification of FLCs (Griswold and Behringer, 2009). Early expression of NR5A1 in pre-FLCs precedes steroidogenesis and is likely important for their future steroidogenic capacity. However, it is not clear why only some interstitial cells respond to signals such as DHH by initiating steroidogenesis; this is especially puzzling because non-FLCs of the interstitium are apparently capable of responding to DHH as they express the receptor PTCH1 (Yao et al., 2002). Here we confirm that NSICs express PTCH1 (Fig. 3.3H, Fig. 3.5F,N): previous studies have demonstrated that PTCH1, along with receptors for other Sertoli-produced factors such as PDGFα, are expressed in a pan-interstitial manner (Brennan et al., 2003). We reasoned that knowledge of early markers that do discriminate NSICs from FLCs may help explain why only FLCs differentiate in response to Sertoli–derived cues.

NSICs that express NR2F2 at 18.5 dpc are considered progenitor cells for the ALC population (Kilcoyne et al., 2014) but it is not known whether these cells also express NR5A1 (Barsoum and Yao, 2010). To help clarify this issue, we examined whether NR2F2-positive cells in the fetal testis were also positive for NR5A1. At 11.5 dpc most NR2F2-positive cells also expressed ARX, a smaller proportion expressed NR5A1 and some triple-positive cells were seen (Fig. 3.10A). From 12.5 to 14.5 dpc, NR2F2 cells were ARX-positive but negative for NR5A1 (Fig. 3.10B-D) with few exceptions (grey arrow, Fig. 3.10B-D). Unless NR2F2 cells begin to express NR5A1 at later timepoints, these data would suggest that ALC progenitors do not express NR5A1 during fetal life.

We looked at the heterogeneity of the isolated NSIC population by performing DAVID analysis on the upregulated genes 704 genes. We established that the NSIC population contained both blood cells and macrophages, which have been shown to be important for testis morphogenesis and vascularisation (DeFalco et al., 2014). We identified a subset of genes involved in haematopoiesis (29 genes; p= 1.26E-04), leukocyte activation (24; p= 3.02E-04) and immune response (32; p= 1.99E-05) in the gene list (Supplemental Data 3).

Subsequently, we performed qRT-PCR on sorted *Sf1*-eGFP cell populations to verify the NSIC-enriched expression of genes upregulated in the NSIC list. We detected expression of *Car2* in

NSICs but not FLCs by qRT-PCR (Fig. 3.7L) while expression of *Car2*, *Slc6a18* and *Ermap* by ISH was consistent with the predicted interstitial expression pattern for the candidate genes (Fig. 3.8B,L-N) and distinct from the cord-associated expression of the Sertoli cell marker *Amh* (Fig. 3.8C). Therefore, at least *Car2* appears to be a novel marker for NSICs that warrants further investigation.

Next we looked to identify additional factors that set NSICs apart from FLCs. We observed an overrepresentation of genes associated with developmental processes (Table 3.5) in the NSIC-enriched population. Interestingly, the NSIC population was marked by expression of transcription factors, including *Hoxd3; Hoxb2; Olig1* and *Gata5* (57 genes; p = 1.49E-05; Table 3.5), suggesting that this population is involved in active developmental processes at this critical stage of gonadal development; we found very few transcription factors characteristic of the FLC population. In addition, GO analysis identified numerous transmembrane component genes not expressed in the FLC population that may be involved in Sertoli-NSIC cell signalling (including *Frem2, Prokr1, Ntrk2, Cdh16* and *Adam22*; 177 genes; p= 2.22E-04; Table 3.5; Fig. 3.9). 203 of the genes identified as being upregulated in the NSIC-enriched population have been associated with a phenotype in OMIM and for 162 of these the molecular basis is known (eight listed in Table 3.6; full list Supplemental Table 7).

One of the transmembrane components identified in NSICs but not FLCs was *Frem2/FREM2* (Fras1 related extracellular matrix protein 2), a cell surface receptor that is a known DSD gene causing Fraser Syndrome (OMIM:219000; Table 3.6; (Jadeja et al., 2005)). Expression of *Frem2* has not been reported previously in the fetal gonad. By qRT-PCR we established that *Frem2,* and its close family member *Fras1* (Fraser syndrome 1 homolog), which is also involved in Fraser syndrome, are expressed in the NSIC-enriched population of the testis at 12.5-13.5 dpc (Fig. 3.7J,K). These data established that there is a large group of factors, some of which are known to be relevant to human DSD, which set NSICs apart from FLCs during early development. These genes may be relevant to the fate decisions made by NSICs at the time of FLC specification.

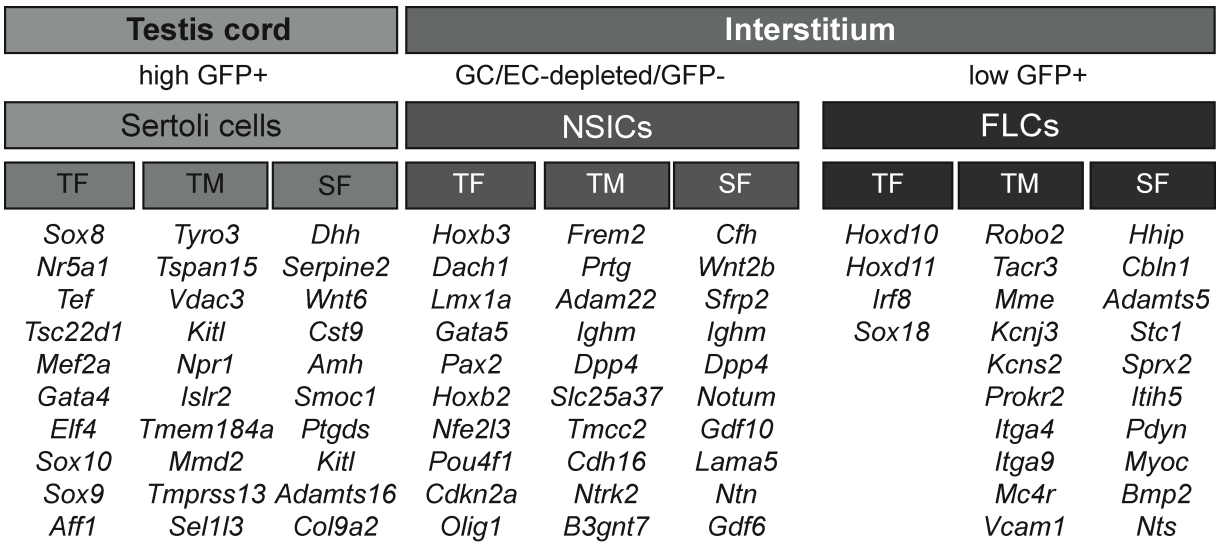

Figure 3.9. Subset of transcription factors, transmembrane factors and secreted factors identified by gene ontology analysis in each cell population.

Using DAVID pathway analysis the transcription factors (TF), transmembrane factors (TM) and secreted factors (SF) present in each cell enriched population were identified. A subset of genes identified in each category are listed (for full listing of GO terms and data see Supplemental Data 3; for overrepresentation analysis for FLCs and NSICs see Tables 3.2 and 3.5).

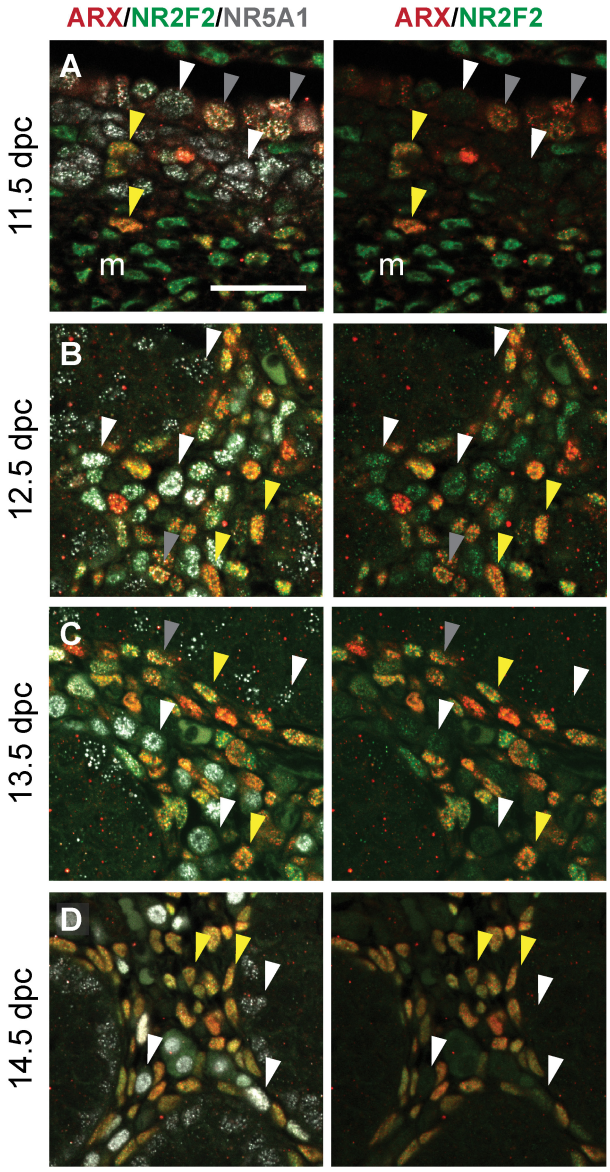

Figure 3.10. NR2F2-positive cells are predominately ARX-positive, NR5A1/GFP/HSD3β-negative interstitial cells.

(A,B) Immunofluorescence for NF2R2 at 11.5 dpc shows that mesonephric cells are NR2F2-positive and that a few NR2F2-positive cells can be observed in the XY gonad. (B-D) From 12.5-14.5 dpc NR2F2 is expressed in predominately ARX-positive/NR5A1-negative cells of the interstitium. White arrow indicates NR5A1-positive nuclei; yellow arrow indicates ARX/NR2F2-positive nuclei; grey arrow indicates ARX/NR5A1/NR2F2-positive nuclei. m = mesonephros; scale bar = 100 μM.

Table 3.5. Subset of clusters of from DAVID GO Analysis on enriched NSICs (Enrichment > 3)

Annotation	GO clusters	Benjamani P-value
Signal Peptide	*Enrichment: 19.48*	
	Disulfide bond	1.84E-20
	Glycoprotein	2.35E-17
	Signal	6.89E-16
Transmembrane	*Enrichment: 6.94*	
	Glycoprotein	2.35E-17
	Transmembrane	2.22E-04
	Membrane	4.71E-04
	GO:0031224 Intrinsic to membrane	2.43E-02
	GO:0016021 Integral to membrane	6.00E-02
Development	*Enrichment: 5.83*	
	Homeobox	3.81E-11
	GO:0043565 Sequence-specific DNA binding	6.61E-06
	GO:0048706 Embryonic skeletal system development	2.53E-05
	GO:0048704 Embryonic skeletal system morphogenesis	3.58E-05
	GO:0009952 Anterior/posterior pattern formation	2.93E-04
	GO:0048568 Embryonic organ development	3.11E-04
	GO:0003002 Regionalization	3.85E-04
	GO:0048705 Skeletal system morphogenesis	5.84E-04
	DNA binding	2.18E-04
	GO:0007389 Pattern specification process	1.47E-03
	GO:0048562 Embryonic organ morphogenesis	2.63E-03
	GO:0043009 Chordate embryonic development	4.79E-03
	GO:0048598 Embryonic morphogenesis	5.20E-03
	GO:0009792 Embryonic development ending in birth or egg hatching	5.38E-03
	GO:0001501 Skeletal system development	1.32E-02
Immune system	*Enrichment: 5.14*	
	GO:0030097 Hemopoiesis	1.26E-04
	GO:0048534 Hemopoietic or lymphoid organ development	2.03E-04
	GO:0002520 Immune system development	3.19E-04
	GO:0030099 Myeloid cell differentiation	1.25E-01
Cell Adhesion	*Enrichment: 4.56*	
	GO:0022610 Biological adhesion	6.60E-04
	GO:0007155 Cell adhesion	6.60E-04
	GO:0016337 Cell-cell adhesion	3.91E-03
	Cell adhesion	5.42E-03
Blood	*Enrichment: 3.93*	
	Erythrocyte	2.44E-07
	GO:0015669 Gas transport	3.31E-04
	GO:0005833 Hemoglobin complex	2.45E-04
	Oxygen transport	1.71E-04
	GO:0015671 Oxygen transport	7.31E-04
	GO:0005344 Oxygen transporter activity	1.02E-03

	GO:001982 Oxygen binding	2.09E-03
	Blood	6.13E-04
	Oxygen carrier	6.13E-04
	Embryo	1.09E-03
	PIRSF500045 Hemoglobin, vertebrate type	1.88E-02
	Chromoprotein	1.30E-03
	PIRSF036518 Globin	2.67E-02
	GO:0046906 Tetrapyrrole binding	7.07E-02
	Heme	1.79E-02
	GO:0020037 Heme binding	9.62E-02
	Metalloprotein	4.50E-02
	Heterotetramer	1.41E-01
	GO:0044445 Cytosolic part	4.26E-01
	Iron	2.96E-01
	GO:0005506 Iron ion binding	6.94E-01
Transcription	*Enrichment: 3.68*	
	Homeobox	3.81E-11
	GO:0043565 Sequence-specific DNA binding	6.61E-06
	GO:0003700 Transcription factor activity	1.49E-05
	DNA-binding	1.20E-04
	GO:0030528 Transcription regulator activity	5.52E-02
	GO:0051252 Regulation of RNA metabolic process	9.63E-02
	GO:0006355 Regulation of transcription, DNA-dependent	1.19E-01
	GO:0003677 DNA binding	2.52E-01
	GO:0045449 Regulation of transcription	3.86E-01
	Transcription regulation	2.93E-01
	Transcription	3.98E-01
	GO:0006350 Transcription	8.41E-01
	Nucleus	1.00E+00
Homodimerisation	*Enrichment: 3.34*	
	GO:0042802 Identical protein binding	1.29E-03
	GO:0046983 Protein dimerization activity	1.30E-01
	GO:0042803 Protein homodimerization activity	1.43E-01
Cell motility	*Enrichment: 3.35*	
	GO:0016477Cell migration	7.01E-03
	GO:0051674 Localization of cell	3.19E-02
	GO:0048870 Cell motility	3.15E-02
Immunity	*Enrichment: 3.11*	
	GO:0002252 Immune effector process	1.60E-05
	GO:0009611 Response to wounding	2.63E-05
	GO:0006955 Immune response	1.99E-05
	GO:0006952 Defense response	3.11E-04
	GO:0002443 Leukocyte mediated immunity	3.28E-04
	GO:000695 Inflammatory response	1.52E-03
	GO:0050778 Positive regulation of immune response	1.57E-03

	GO:0002253 Activation of immune response	1.72E-03
	GO:0006959 Humoral immune response	6.98E-03
	mmu04610 Complement and coagulation cascades	5.55E-03
	GO:0002449 Lymphocyte mediated immunity	9.02E-03
	GO:0048584 Positive regulation of response to stimulus	1.84E-02
	GO:0002460 Adaptive immune response based on somatic recombination of immune receptors built from immunoglobulin superfamily domains	2.32E-02
	GO:0002250 Adaptive immune response	2.32E-02
	GO:0016064 Immunoglobulin mediated immune response	3.12E-02
	GO:0019724 B cell mediated immunity	3.41E-02
	GO:0002541 Activation of plasma proteins involved in acute inflammatory response	1.20E-01
	GO:0002455 Humoral immune response mediated by circulating immunoglobulin	1.20E-01
	GO:0006956 Complement activation	1.20E-01
	GO:0045087 Innate immune response	1.81E-01
	mmu05322 Systemic lupus erythematosus	2.01E-01
	Immune response	1.21E-01
	Complement pathway	1.41E-01
	GO:0002526 Acute inflammatory response	2.64E-01
	GO:0006958 Complement activation, classical pathway	2.78E-01
	PIRSF002477 Complement subcomponent C1q chain A	5.89E-01
	GO:0051605 Protein maturation by peptide bond cleavage	4.34E-01
	Innate immunity	3.15E-01
	GO:0016485 Protein processing	7.83E-01
	GO:0051604 Protein maturation	8.40E-01
	Hydroxylation	6.43E-01
	mmu05020 Prion diseases	8.08E-01
	Collagen	8.05E-01

Table 3.5. Subset of clusters of from DAVID GO Analysis on enriched NSICs (Enrichment > 3).

Clusters identified by DAVID analysis in the NSIC enriched gene list with an "Enrichment Value" of ≥3.

Table 3.6. Subset of genes upregulated in 12.5 dpc NSICs ($p < 0.05$).

ID	Gene Name		Chr	Phenotype	OMIM assoc.	Reference
ENSMUSG00000025105	Bnc1	Basonuclin 1	7	subferiltle; postnatal spermatid expression	-	(Zhang et al., 2012)
ENSMUSG00000037016	Frem2	Fras1 related extracellular matrix protein 2	3	syndactyly, cryptophthalmos and urogential defects, ambiguous genitalia	219000*	(Jadeja et al., 2005)
ENSMUSG00000026365	Cfh	Complement component factor h	1	no lethal developmental defects; fertile	126700/609814/235400/610698	(Coffey et al., 2007; Pickering et al., 2002)
ENSMUSG00000073530	Pappa2	Pappalysin 2	1	post natal growth retardation; fertile, with compromised fecundity	N/A	(Conover et al., 2011)
ENSMUSG00000027840	Wnt2b	Wingless-type MMTV integration site family, member 2B	3	no lethal developmental defects; fertile; olfactory bulb defect	-	(Tsukiyama and Yamaguchi, 2012)
ENSMUSG00000038587	Akap12	A kinase anchor protein12	10	delayed fertility; urogenital hyperplasia	-	(Akakura et al., 2008)
ENSMUSG00000023039	Krt7	Keratin 7	15	no lethal developmental defects; fertile	-	(Sandilands et al., 2013)
ENSMUSG00000027996	Sfrp2	Secreted frizzled-related protein 2	3	$Sfrp2^{-/-}$ viable and fertile; $Sfrp2^{-/-}$ /$Sfrp1^{-/-}$ gonadal defects, embryonic lethal at 16.5 dpc,	-	(Cox et al., 2006; Satoh et al., 2006; Warr et al., 2009)
ENSMUSG00000030774	Pak1	p21 protein (Cdc42/Rac)-activated kinase 1	7	no lethal developmental defects; fertile	-	(Asrar et al., 2009)
ENSMUSG00000018659	Pnpo	Protogenin homolog	11	-	610090	-
ENSMUSG00000036030	Prtg	Pyridoxine 5'-phosphate oxidase	9	-	-	-
ENSMUSG00000029223	Uchl1	Ubiquitin carboxy-terminal hydrolase L1	5	no lethal developmental defects; fertile; develops ataxia	615491/613643	(Saigoh et al., 1999)
ENSMUSG00000040537	Adam22	α disintegrin and metallopeptidase domain 22	5	no lethal developmental defects; fertile	-	(Sagane et al., 2005)
ENSMUSG00000035000	Dpp4	Dipeptidylpeptidase 4 (CD26)	2	no lethal developmental defects	-	(Marguet et al., 2000)
ENSMUSG00000025889	Snca	Synuclein, alpha	6	no lethal developmental defects	127750/168601/605543	(Abeliovich et al., 2000)
ENSMUSG00000021182	Ccdc88c	Coiled-coil domain containing 88C	12	-	236600	-
ENSMUSG00000009628	Tex15 6	Testis expressed gene 15	8	germ cell expression; males infertile	-	(Yang et al., 2008)
ENSMUSG00000041605	5730559C18Rik	RIKEN cDNA 5730559C18 gene	1	-	-	-
ENSMUSG00000034248	Slc25a37	Solute carrier family 25, member 37	14	-	-	-
ENSMUSG00000005360	Slc1a3	Solute carrier family 1, member 3	15		612656	
ENSMUSG00000042066	Tmcc2	Transmembrane and coiled-coil domains 2	1	no lethal developmental defects	N/A	(Watase et al., 1998)
ENSMUSG00000031881	Cdh16 ^	Cadherin 16	8	-	-	(Wertz and Herrmann, 1999)
ENSMUSG00000038193	Hand2	Heart and neural crest derivatives expressed transcript 2	8	embryonic lethal at 10.5 dpc; cardiac defects	-	(Srivastava et al., 1997)
ENSMUSG00000050244	Heatr1	HEAT repeat containing 1	13	-	N/A	-

ENSMUSG00000024151	Msh2 ^	MutS homolog 2 (E. coli)	17	no lethal developmental defects; fertile	120435/ 276300/158320	(Paul et al., 2007)
ENSMUSG00000063506	Arhgap22	Rho GTPase activating protein 22	14	-	-	-
ENSMUSG00000032186	Tmod2	Tropomodulin 2	9	no lethal developmental defects; fertile	-	(Cox et al., 2003)

Table 3.6. Subset of genes upregulated in 12.5 dpc NSICs ($p < 0.05$).

Classification used the same criteria as Table 3.3. We manually removed high-ranking known haematopoiesis-related genes to display 25 genes (8 genes removed; see Supplemental Data 2). References are the primary report of the null or mutant mouse and any subsequent clarifying reports. (Chr., chromosome; ^ indicates reported expression in germ cells; OMIM assoc. = OMIM reference number if the gene is associated with any type of human disorder (* indicates a genitourinary, endocrine or DSD phenotype)).

Sertoli cells: Signalling to the FLCs and NSICs

Understanding of the process of interstitial cell specification requires knowledge of all potential paracrine factors produced by newly-specified Sertoli cells. In addition to published microarray data from enriched Sertoli cells we used RNA-seq to survey the Sertoli cells in greater detail (Jameson et al., 2012b). Our RNA-seq analysis identified 1217 genes upregulated in the Sertoli cell-enriched population (Supplemental Data 2) and these included a number of previously described fetal Sertoli cell genes (*Aard, Dhh, Mro, Ptk2b, Cst9, Col9a3, Aldh1a1, Amh*) thereby validating our approach. We identified *Trank1*, *Gstm7* and *Adamts16* as novel genes expressed in the Sertoli cell population by qRT-PCR and ISH (Fig. 3M-O; Fig. 4C,O-Q). DAVID analysis identified genes that encoded transmembrane factors (330 genes; p= 3.19E-10) and 44 genes with transcription factor activity (p= 6.7E-1) were up-regulated in the Sertoli cell-enriched population (Fig. 3.9).

Interestingly, as in the FLC-enriched population list, we found a number of GnRH (gonadotropin-releasing hormone) signalling pathway components (11; including *Ptk2b, Src, Adcy9* and *Plcb2*; p= 3.50E-01) and neurogenesis related genes (20; including *Islr2, Robo1, Hes5, Sema6c* and *Serpine2*; p= 2.30E-02). This abundance of neuroactive signalling related genes further hints at a potential role for neuroactive ligand/receptor pairs in gonadogenesis.

Signals, such as DHH, from the Sertoli cells to the interstitium are essential for FLC development. In our group of Sertoli-enriched genes we identified an overrepresentation of 128 secreted factors (p = 2.24E-17; Fig. 3.8) including *Dhh*. We looked for known ligand pairs for the 35 FLC receptors identified in our RNA-seq data and the reprocessed Jameson et al (2012b) data. We identified expression of the genes encoding known ligands to the neuroactive receptors (*Mc2r, Mc4r, Crhr, Vipr1, Prlr, Sstr4, Tacr3*), a related receptor (*Adcy7*) and two neurogenesis related receptors (*Prokr2/Robo2*) in our RNA-seq data and/or the re-analysed Jameson data set (Fig. 3.11).

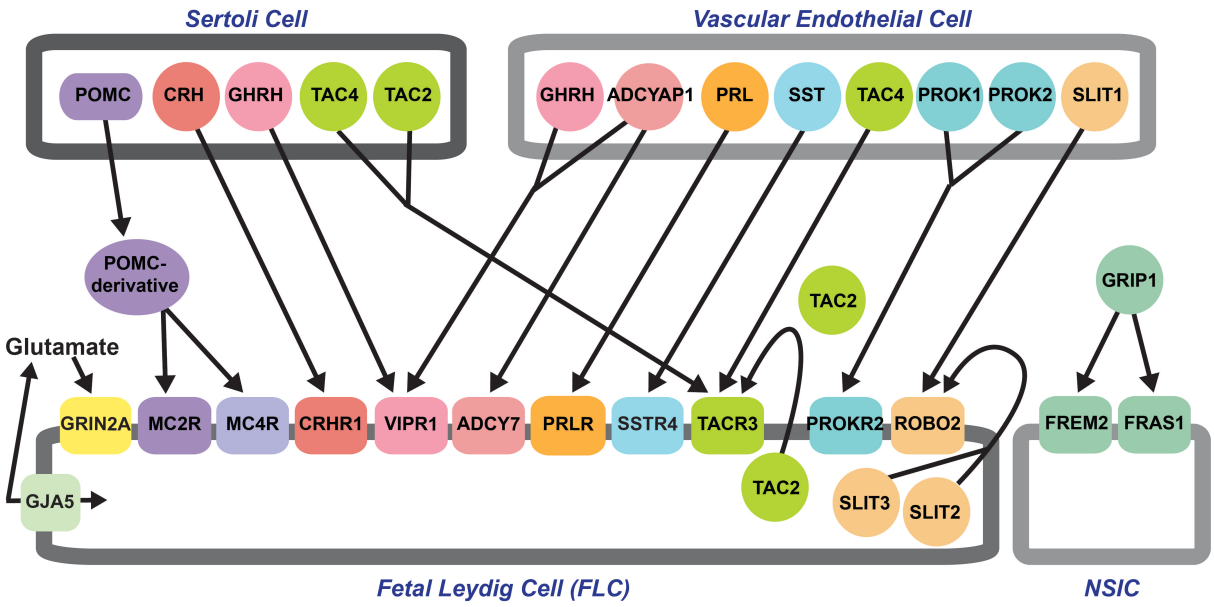

Figure 3.11. Schematic of putative receptor-ligand interactions focusing on the receptors overexpressed on FLCs and NSICs.

Receptors associated with neuroactive ligand signaling and/or DSD are represented. Ligands were identified from the literature and expression of ligands in cell types of the testis at 12.5 dpc was determined using data from this study and reprocessed Jameson et al. (Jameson et al., 2012b) data. The resulting schematic details proposed receptor-ligand interactions inferred from data at 12.5 dpc in the XY gonad. GJA5 shuttles glutamate which is a for ligand for the NMDA receptor of which GRIN2A is a subunit. The POMC-complex is produced by Sertoli cells and its derivatives activate MC2R and MC4R. CRH is a ligand for CRHR1 while GHRH and ADCYAP1 (or PACAP) are ligands for VIPR1. ADCYAP1 can also activate ADCY7. PRL and SST are the ligands for PRLR and SSTR4 respectively and are expressed by VECs (vascular endothelial cells). TAC2 is predominately expressed by FLCs but also be Sertoli cells, whilst VECs and Sertoli cells express TAC4. Both TAC2 and TAC4 can activate TACR3. PROK1 and PROK2 can activate PROKR2. SLIT1/2/3 can activate ROBO2 and are expressed in the testis. The ligand GRIP1 is responsible for activating FREM2 and its close family member FRAS1.

Discussion

We used RNA-seq to define the transcriptome of FLCs, and compare it to those of NSICs and Sertoli cells in mice at 12.5 dpc, in order to identify novel early markers of individual cell types in the developing testis, with particular focus on the FLC population. We anticipated that a detailed portrait of the genes expressed in FLC just prior to the onset of steroidogenesis, in comparison to a similar picture of the Sertoli and NSIC transcriptomes, would prove informative in terms of understanding how FLCs come to be specified and how they differentiate to become functional hormone-producing cells. Although previous studies have profiled somatic cells early in gonadogenesis (Jameson et al., 2012b; McDowell et al., 2012), the present study provides the first RNA-seq analysis of enriched FLC, NSICs and Sertoli cell populations in the XY gonad.

The method we developed for separating cell types has yielded the purest and most validated population of pre-FLCs yet reported. Determining which cell types a given gene is expressed in has hitherto been typically a labour intensive task (Svingen et al., 2011; Wainwright et al., 2013). Aside from providing the basis for our transcriptomic analysis, the system we developed will be useful in future studies designed to assign expression of any novel gene to a particular cell lineage using qRT-PCR.

We found that 61 of the overexpressed genes in the FLC-enriched population were previously unreported in the fetal gonad and therefore represent novel candidates for involvement in FLC specification. By checking previously published 11.5 dpc microarray data for genes we identified as FLC-upregulated at 12.5 dpc, we identified 10 robustly-expressed putative pre-steroidogenic FLC marker genes. One of these is *Prokr2* which we have previously shown to be expressed in the XY 11.5 dpc genital ridge (Svingen et al., 2011) thereby validating this approach. Some of these 10 genes may prove useful in identifying pre-FLCs before they begin to express characteristic steroidogenic enzyme genes.

Hormones produced by the FLCs direct the masculinisation of the embryo. Even though key components of the hypothalamic-pituitary-gonadal (HPG) axis are in place from around 16.5 dpc, the production of hormones by FLCs is thought to be independent of the HPG axis (Baker and

O'Shaughnessy, 2001; Japon et al., 1994; O'Shaughnessy et al., 1998; Pakarinen et al., 2002; Zhang et al., 2001). The GnRH-neural circuitry is a key component of the HPG; the formation and activation of the GnRH-neural circuitry involves a series of neuroactive ligand/receptor pairs; mutation of genes involved in this circuitry often results in DSD, which it has been assumed, is primarily associated with HPG axis dysfunction (Bianco and Kaiser, 2009; Hardelin and Dode, 2008; Mastorakos et al., 2006). Oddly, we found that a number of genes associated with these processes, which occur after the differentiation of FLCs, are expressed in the Sertoli cells and FLCs at 12.5 dpc. Of the 35 genes that encode receptors, in the FLC upregulated list, DAVID analysis identified eight factors associated with neuroactive-ligand signaling (*Mc2r*, *Mc4r*, *Grin2a*, *Crhr1*, *Vipr1*, *Prlr*, *Sstr4*, *Tacr3*, Fig. 6). In addition, we identified *Adcy7,* which encodes a receptor that is a regulator of intracellular cAMP concentration and that shares the ligand PACAP, encoded by the gene *Adcyap1*, with VIPR1 (Acquaah-Mensah et al., 2012; Halvorson, 2014). Also of interest was the expression of the *Gja5,* which encodes a gap junction protein CX40 involved in shuttling glutamate, an activator of the N-methyl-D-aspartate (NMDA) glutamate receptor, of which GRIN2A is a subunit (Fig. 3.6; (Bai, 2014; Monyer et al., 1994; Monyer et al., 1992)). Furthermore, *Robo2* and *Prokr2* were of interest as both are implicated in neuronal processes and GnRH signaling (Cole et al., 2008; Kidd et al., 1998; Lu et al., 2007; Matsumoto et al., 2006). Assessment of the known ligands for the 11 receptors of interest indicated that putative ligand pairs were expressed in the FLCs, Sertoli cells or vascular endothelial cells (Fig. 3.6; this study; (Jameson et al., 2012b)). Whether the testicular expression of these genes plays a role in gonadogenesis is yet to be determined, but the observation that they dominate the subgroup of FLC-upregulated genes that are not associated with steroidogenesis may be significant.

These findings also have implications for identifying the causes of DSD. Of the neuro-active genes identified, some that are upregulated in FLCs have previously been associated with DSDs that have urogenital phenotypes, for example *PROKR2* and *TACR3*. Mutations in *PROKR2* (OMIM: 244200; (Dode et al., 2006)) and *TACR3* (OMIM: 614840; (Gianetti et al., 2010; Topaloglu et al., 2009)) are associated with hypogonadotrophic hypogonadism in humans and mice. As many of the factors associated with neuroactive-ligand receptor activation and other neuronal processes are expressed robustly in the FLCs or the Sertoli cells of the developing testis (this study; (Svingen et al., 2009a)) it is tempting to speculate that gonadal production of these factors may precede HPG-driven production and explain male bias in individuals affected by hypogonadotrophic hypogonadism (Dode et al., 2006; Dodé et al., 2003; Hardelin and Dode, 2008; Svingen et al., 2011).

Prokr2-/- mice have reproductive defects and we have previously shown that there was no change in expression of FLC marker HSD3β/*Hsd3β* in *Prokr2*$^{-/-}$ embryos compared to *wild-type* littermates (Matsumoto et al., 2006; Svingen et al., 2011). However, embryonic *Prokr2*$^{-/-}$ testes display vasculature dysmorphology, a phenotype often associated with FLC impairment (Miyabayashi et al., 2013; Svingen et al., 2011). *Tacr3-/-* mice have a variety of reproductive and fertility defects and a postnatal hormone profile similar to several other GnRH-deficient mouse models (Lapatto et al., 2007; Matsumoto et al., 2006; Yang et al., 2012). Our results suggest that more detailed analysis of the postnatal and embryonic gonadal phenotype of the *Tacr3-/-* mouse to assess the effect of TACR3 loss before HPG axis activation occurs.

We identified that *Frem2* and *Fras1*, known DSD genes, are overexpressed in the NSIC population of the XY gonad from 12.5-13.5 dpc. Mutations in *Frem2* and *Fras1* result in Fraser Syndrome (OMIM:219000; (Jadeja et al., 2005; Shafeghati et al., 2008)) a multisystem disorder with ambiguous genitalia in 20% of patients (for review see Smyth and Scambler, 2005). *Frem2* knockout mice also have multiple developmental defects, however the ambiguous genitalia phenotype seen in patients has not been characterised in mouse (Jadeja et al., 2005). We postulate that a requirement for expression of *Frem2* and *Fras1* in NSICs early in gonadogenesis may contribute to the ambiguous genitalia phenotype seen in this model. This finding supports the idea that NSICs, not just Sertoli and FLCs, may play an important role in masculisation during fetal life.

It has recently been shown that some non-FLC of the interstitium differentiate into ALCs postnatally (Kilcoyne et al., 2014), establishing that a functional fetal NSIC population is important for postnatal masculinsation of the individual. We find that early in gonadogenesis the NSIC population is characterised by expression of NR2F2 and a set of transcription factors and transmembrane receptors that are distinct from the FLC population. The differences we have identified between transcriptomic profiles in FLC and NSIC enriched populations may provide leads as to how pre-FLCs are selected or how NSICs resist selection from within the total interstitial population.

Functional investigation into individual genes shown to be upregulated in the various cell types, and processes highlighted as likely to be active within and between cells, will be needed if we are to

gain a clearer understanding of gonadogenesis and postnatal sexual development, particularly as they relate to steroid production. We envisage that this dataset will be a resource to identify genes involved in normal gonadogenesis, in mouse and human, and to pinpoint genes likely to underlie some cases of human DSD.

End of published manuscript

The following files are appended to the preceding manuscript submission:

Supplemental Data 1: RNA-seq expression data

(see Supplemental Data 1 in Appendices).

Somatic cells isolated from the *Sf1*-eGFP testis (Sertoli, FLC and NSICs) at 12.5 dpc. This workbook contains the cpm data from this gonad cell lineage RNA-seq paper. Only genes with at least 1 count per million in three or more samples were retained (features= 14,307). This data can be accessed on GEO (GSE65498) as an editable workbook which provides results for all retained ENSMUSG transcripts. The counts for a transcript can be graphed using this editable file in the "graph cpm" sheet.

Supplemental Data 2: Genes upregulated in enriched cell populations at 12.5 dpc

(see Supplemental Data 2 in Appendices).

This workbook contains the genes that were upregulated in each enriched cell population:

1) Genes upregulated in a Sertoli specific manner ("Sertoli_Specific_UP")

2) Genes upregulated in a FLC specific manner ("FLC_Specific_UP")

3) Genes upregulated in a NSIC manner ("NSIC_Specific_UP_incl_gc")

4) Genes upregulated in a NSIC manner with any gene that is annotated as a germ cell genes in the Jameson et al. (2012) dataset removed ("NSIC_Specific_UP_no_gc")

This workbook also contains the results of the direct comparisons between "Leydig vs Sertoli" (5), "Leydig vs NSIC" (6) and "Sertoli vs NSIC"(7).

Supplemental Data 3: List of previously published data on testis expression for 84 FLC-enriched genes

(listed as Supplemental Table 5 in Appendices).

List of genes that have been previously reported to be expressed in the adult or fetal mouse testis or in human testis/DSD in PubMed as of Nov 12, 2014.

Supplemental Data 4: GO of genes upregulated in enriched cell populations at 12.5 dpc.

(see Supplemental Data 3 in Appendices)

Gene ontology analysis was performed using the DAVID Bioinformatics Package (v6.7) (http://david.abcc.ncifcrf.gov; (Huang et al., 2009a; Huang et al., 2009b)) The genes identified for each TF, TM and SF GO term category were then mapped back to the respective file in Supplemental Data 2 and ranked by the moderated F-statistic. The top 10 genes are listed in Fig. 4. The cluster and chart results for each population are also listed in their entirety in this file.

Supplemental Data 5: Genes putatively regulated by NR5A1

(listed as Supplemental Table 6 in Appendices and Table 3.8 in this Chapter).

We identified overlap between the upregulated and downregulated gene lists produced by Baba et al., (2014) and our three lists of genes upregulated in FLCs, NSICs and Sertoli cells (Supplemental Data 2). Genes that overlap in the data sets are putatively regulated by NR5A1 and are listed under each cell type as either being putatively up- or down-regulated by NR5A1 in this file.

Supplemental Data 6: Genes "on" at 11.5dpc in gonadal microarray screens that are detected as upregulated in the FLC enriched population by RNA-seq at 12.5 dpc.

(see Supplemental Data 4 in Appendices)

Leydig cell enriched genes at 12.5 dpc that also show differential expression between interstitial and supporting cell of 11.5 dpc XY gonad are putative pre-FLC marker genes. Supplemental Table 7 summarises top results. The logFC, P.Value, and adj.P.Val columns indicate results from differential expression analysis. Int. Exp (interstitial) and Sup. Exp (supporting) show median normalised expression of the gene in each of these two cell types, while Int. Rank (interstitial) and

Sup. Rank (supporting) indicate the position of the gene in a list ranked by expression in that cell type (0=lowest expression, 100=highest expression).

Supplemental Data 7: Genes detected as upregulated in each population that have an annotation in OMIM.

(see Supplemental Table 8 in Appendices)

The following information is drawn from the Online Mendelian Inheritance in Man, OMIM® data base currated by McKusick-Nathans Institute of Genetic Medicine, Johns Hopkins University (Baltimore, MD), accessed on 12 November 2014. URL: http://omim.org/. This workbook shows whether there is any known association between upregulated genes in each population and an OMIM phenotype. The nomenclature and symbols used in the list are indicated on the first page of the workbook.

Additional work:

For the work herein:

All reagents are described in Supplemental Tables 1-4. All additional work was performed as described in the manuscript (above). Statistical significance was determined using one-way ANOVA with Bonferroni's multiple comparisons test with the exception of Fig. 3.14G-Q" where only two groups were compared therefore statistical significance was assessed as described in Chapter 2 with an unpaired (two-tailed) Student's t-test.

3.6 Sertoli cells: The master regulators of testis morphogenesis

The analysis of the FLC, Sertoli cell and NSIC transcriptomes presented in the manuscript provides insight into the signalling dynamics within the testis, in particular, signalling to and within the interstitium. The analysis in the manuscript aims to provide insight into how signalling molecules are able to target pre-FLCs and to characterise the early FLC population. In addition to the analysis in the manuscript I also examined the Sertoli cell transcriptome in more detail. The following analysis looks more broadly at the characteristics of the early Sertoli cell population and FGF signalling.

The Sertoli cell population coordinates much of testicular development. The earliest Sertoli cells express SRY which directly upregulates SOX9 (Sekido et al., 2004). The transcription factor SOX9 directly or indirectly coordinates testis development as a whole (Bishop et al., 2000; Vidal et al., 2001). Additional cells can be recruited to the SOX9-positive, Sertoli cell fate by mechanisms involving FGF9 and PGD_2 (Adams and McLaren, 2002; Colvin et al., 2001; Kim et al., 2006; Moniot et al., 2009; Schmahl et al., 2004; Wilhelm et al., 2005).

Shortly after SOX9 expression and Sertoli cell recruitment, at around 12.0 dpc, the Sertoli cells aggregate into primitive tubules encasing the germ cells. These tubes form *de novo* and are insulated from the interstitial environment by a layer of peritubular myoid cells. Once organised into testis cords the Sertoli cells start producing masculinising factors, such as AMH and DHH, which direct the development of the testis and the reproductive tract. This analysis characterises the Sertoli cell population shortly after testis cords have been formed, when AMH and DHH are being produced.

IHH is a genetic condition that can be associated with either normal sense of smell, normosmic IHH (nIHH), or anosmia, the loss of the sense of smell, which is termed Kallmann syndrome (KS). Most of the known genes that are mutated in individuals with IHH encode ligand-receptor pairs that are central to the functionality of the HPG axis such as PROK2/PROKR2 and TAC3/TACR3, which the manuscript presented herein has shown to be expressed in early FLCs. IHH can have a polygenic inheritance pattern and can occur in association with other distinct clinical features. As discussed in the manuscript presented above, IHH occurs much more frequently in XY individuals. In this section I find that key factors associated with FGF signalling in IHH are also expressed in the Sertoli cells of the embryonic testis. This observation suggests the possibility that some testicular IHH phenotypes may precede compromised GnRH-driven HPG axis activity.

Mining of the Sertoli cell-enriched gene dataset

Within the manuscript in this chapter I demonstrated that the high-GFP population of cells sorted from the *Sf1*-eGFP XY gonad was SOX9-positive (Fig. 3.1F) and was enriched for expression of genes encoding Sertoli cells markers such as *Sox9, Amh* and *Ptgds* by qRT-PCR (Fig. 3.4; Fig. 3.5; Fig. 3.6A-C). The RNA-seq analysis described in the manuscript identified 1217 genes upregulated in the Sertoli cell-enriched population (SData 2), including a many previously described fetal Sertoli cell genes (including *Aard, Dhh, Mro, Ptk2b, Cst9, Col9a3, Aldh1a1* and *Amh*). In addition, I identified *Trank1*, *Gstm7* and *Adamts16* as novel genes expressed in the Sertoli cell population, by qRT-PCR and ISH (Fig. 3.7M-O; Fig. 3.8C,O-Q).

In this additional analysis I used the Eurexpress database to confirm that a further 16 genes of interest, identified in the RNA-seq analysis, were expressed in the testis cords at 14.5 dpc. *Ptgds* and *Col9a3* are Sertoli cell marker genes and were used as controls (Fig. 3.11A,B). Robust expression in the Sertoli cells was detected for the following genes: *Tle6*, *Gstm1*, *Ppt1*, *Kctd14*, *Tyro3*, *Adhfe1*, *Arhgdig*, *Pak3*, *Hs6st1*, *Gsta4*, *Smoc1*, *Hctr1*, *Clcn2*, *Npr1*, *Rgs11* and *Stc2* (Fig. 3.11C-R).

Initial DAVID analysis presented in the manuscript herein identified the genes that encoded transmembrane factors, secreted factors and transcription factors that were up-regulated in the Sertoli cell-enriched population (Fig. 3.9; Supplemental Data 2). Further gene ontology analysis of upregulated genes revealed that many genes overexpressed in the Sertoli cells were also identified

as being expressed in neuronal synapses (39; GO:0045202; p = 1.25E-02; Table 3.7), in line with finding that neurogenesis related genes were overrepresented (20; p= 2.30E-02). 60 of the transmembrane protein-encoding genes identified were also found to be involved in cell adhesion (GO:0007155; p = 2.09E-02). Of note was an overrepresentation of factors identified with glutathione S-transferase activity (10; *Gstm1/2/6/7, Gsta3/4, Gstt2/3* and *Clic5*; GO:000436; p = 4.76E-03). Additionally, an overrepresentation of genes encoding factors involved in enzyme and peptidase inhibition was observed (23; GO:0004857; p = 3.56E-02; 19; GO:0030414; p = 3.07E-03; Table 3.7).

SF1/NR5A1 plays an important role for both Sertoli cell and FLC function. Accordingly, I identified that 6.24% (76 genes) of the 1217 genes identified as upregulated in the Sertoli cell-enriched population were putative NR5A1 targets ((Baba et al., 2014); Table 3.8). The ChIP-seq performed by Baba et al. (2014) on Y-1 cells treated with an *Nr5a1* siRNA aimed to identify NR5A1-regulated genes. However, genes such as *Amh*, which are known to be regulated by NR5A1 but are specific to Sertoli-like cell lines, were not identified as NR5A1 targets in the Y-1 cell analysis. The published screen identified 243 genes with decreased expression and 324 genes with increased expression that were "putatively regulated by NR5A1". Therefore, in total, 13.4% of the genes found to be "putatively regulated by NR5A1" in the Baba et al. study were present in our Sertoli cell-enriched data set.

For some of the Sertoli cell upregulated genes, previously published knock-out mouse models were found to have defects in fertility or fecundity (*Dhh, Gatm, Serpine2, Wnt6, Tyro3*; see Table 3.9). 233 genes upregulated in the Sertoli-enriched population are listed as disease-causing in OMIM (194 where the molecular basis is known; eight listed in Table 3.9; full list Supplemental Table 8), including known DSD genes that are expressed during testicular development such as *DHH* (OMIM:233420; (Canto et al., 2004), OMIM:607080; (Umehara et al., 2000)), *AMH* (OMIM:261550; (Knebelmann et al., 1991)), *SOX9* (OMIM:114290; (Foster et al., 1994)), *NR0B1* (OMIM:300018; (Muscatelli et al., 1994)) and *HSD17B3* (OMIM:2643000; (Geissler et al., 1994)).

I identified two additional genes that were overexpressed in Sertoli cells at 12.5 dpc and that, when mutated in humans, result in hypogonadotropic hypogonadism with or without anosmia: *SPRY4* (sprouty homolog 4; OMIM:615266; (Miraoui et al., 2013)) and *HS6ST1* (heparan sulfate 6-O-

sulfotransferase 1; OMIM:614880; (Tornberg et al., 2011)). Both *Spry4* and *Hs6st1* are associated with FGF signalling (Fig. 3.11. A). RNA-seq counts data confirmed that *Hs6st1* is expressed predominately in the Sertoli cell population (Fig. 3.12B). Additionally, ISH confirmed that *Hs6st1* was expressed in Sertoli cells at 14.5 dpc (Fig. 3.12K; 3.13B; (Sedita et al., 2004)). *Hs6st1* encodes a heparan sulfotransferase enzyme. Heparan 6-O-sulfation by HS6ST1 has been shown to be essential for FGF receptor dimerisation and subsequent signalling (Loo and Salmivirta, 2002; Tornberg et al., 2011). In IHH patients, mutation in the gene encoding *HS6ST1* are found in combination with mutations in genes such as FGFR1 (FGF-receptor 1; (Miraoui et al., 2013)).

A fully functional FGF8-FGFR1 (fibroblast growth factor 8) signalling pathway is essential for correct development and activity of the GnRH-neurons of the HPG axis. Mutations in FGF8 (OMIM:612702; (Falardeau et al., 2008)) and FGFR1 (OMIM:147950; (Dodé et al., 2003)) are associated with IHH and GnRH deficiency. Mutations in IHH patients have been identified in FGF17 (fibroblast growth factor 17), an FGF8 family member, and the "FGF8-synexpression group", which includes, IL17RD (interleukin 17 receptor D), DUSP6 (dual specificity phosphatase 6), SPRY4 and FLRT3 ((Miraoui et al., 2013); Fig. 3.13A). IL17RD, DUSP6 and SPRY4 all act to inhibit the MAPK signalling pathway activation downstream of FGF signalling ((for review see Miraoui et al., 2013); fibronectin leucine rich transmembrane protein 3; Fig. 3.13A). I identified that *Spry4* was upregulated in the Sertoli cell population (Fig. 3.13 C). In addition, the genes encoding *Dusp6* and *Il17rd* were also expressed in the 12.5 dpc testis (Fig. 3.13D-E). *Flrt3*, encodes an enhancer of FGF signalling but was not found to be expressed in the 12.5 dpc testis (data not shown).

FGFR1 to -4 are expressed in XY gonad and can be activated by FGF9 *in vitro* (Ornitz et al., 1996; Schmahl et al., 2004). In the early Sertoli cells the primary mode of FGF-signalling is FGF9 through FGFR2. XY *Fgfr2-/-* mice are partially sex reversed and conditional deletion of *Fgfr2* results in a phenocopy of the *Fgf9-/-* which sex reverses (Bagheri-Fam et al., 2008; Kim et al., 2007). On the other hand, *Fgfr3-/-* and *Fgfr4-/-* males that survive to reproductive age are fertile and *Fgfr1* chimeras have normal testis development and fertility (Colvin et al., 1996; Deng et al., 1997; Deng et al., 1996; Weinstein et al., 1998). The RNA-seq data show that *Fgfr1* is expressed at similar levels to *Fgfr2* in the 12.5 dpc testis, while *Fgfr3* and *Fgfr4* are minimally expressed (Fig. 3.13F-I). The RNA-seq data also demonstrate that in addition to *Fgf9,* there are three other FGF ligands expressed preferentially in the Sertoli cell population at 12.5 dpc: *Fgf13* (fibroblast growth

factor 13), *Fgf16* (fibroblast growth factor 16) and *Fgf18* (fibroblast growth factor 18; Fig. 3.13J-M). A role for signalling through FGFR1 or by FGF13/16/18 has not yet been demonstrated in the fetal testis. As most of the components of FGF signalling that are associated with IHH are expressed in the early testis, this suggests that disruption of global FGF signalling in the embryo may impact early testis development before HPG axis-mediated phenotypes arise later in development.

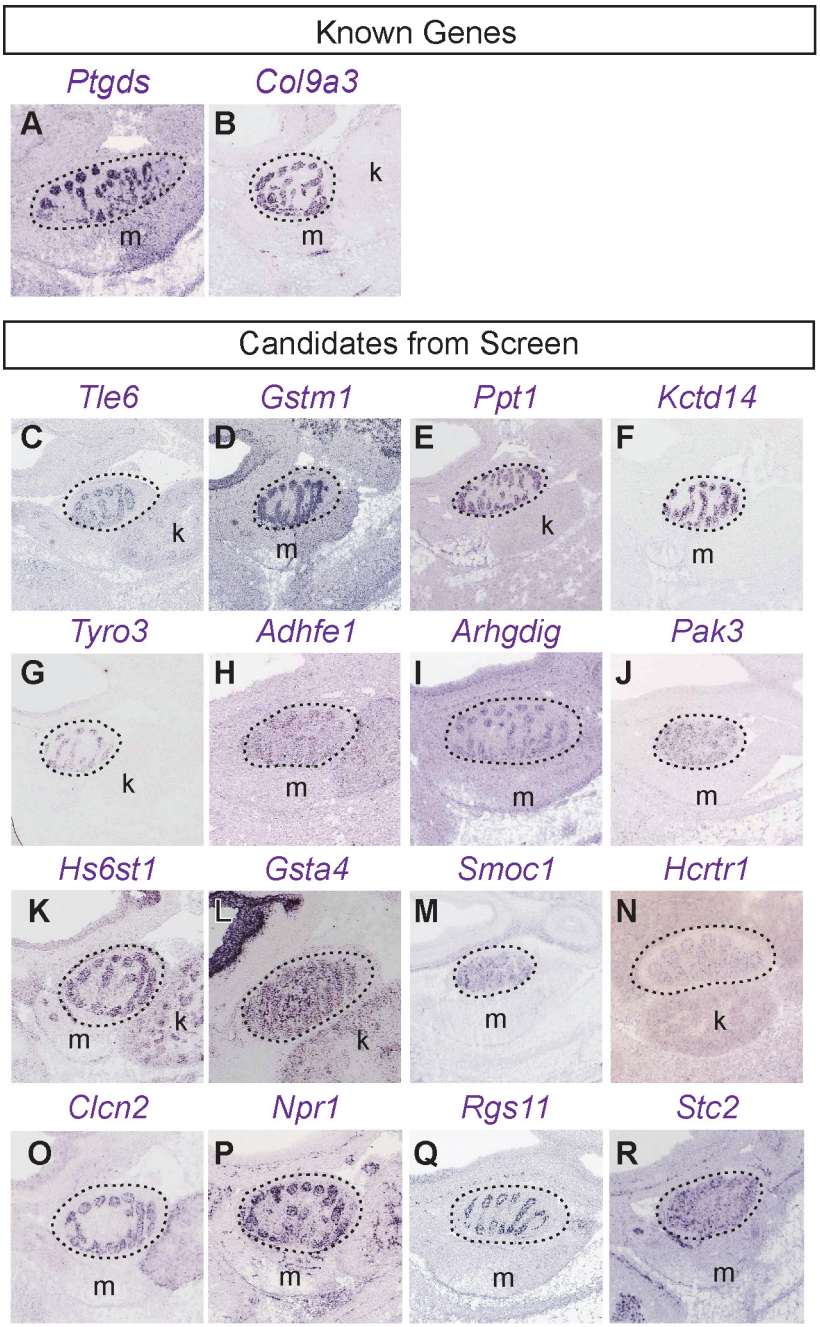

Figure 3.12. In situ hybridisation for genes identified by RNA-seq to be over- expressed in Sertoli cells.

ISHs for newly identified candidate genes at 14.5 dpc from *Eurexpress Transcriptome Atlas Database for Mouse Embryo* (http://www.eurexpress.org). Marker genes *Ptgds* (A) and *Col9a3* (B) shows a Sertoli cell expression pattern. NovelSertoli cell genes, *Tle6* (C), *Gstm1* (D), *Ppt1* (E), *Kctd14* (F), *Tyro3* (G), *Adhfe1* (H), *Arhgdig* (I), *Pak3* (J), *Hs6st1* (K), *Gsta4* (L), *Smoc1* (M), *Hctr1* (N), *Clcn2* (O), *Npr1* (P), *Rgs11* (Q) and *Stc2* (R) show expression in cells distributed within and around the border of the testis cords indicating that Sertoli cell-expressed genes are being detected. (k= kidneym= mesonephros; *Eurexpress* probe IDs can be found in Supplemental Table 7).

Table 3.7. Subset of clusters from DAVID GO Analysis on enriched Setroli cells (Enrichment >3)

Annotation	GO clusters	Benjamani P-value
Signal Peptide	*Enrichment: 17.86*	
	Glycoprotein	5.44E-25
	Signal	1.82E-20
	Disulfide bond	2.29E-17
	Secreted	2.24E-17
	GO:0005576 Extracellular region	4.20E-14
	GO:0044421 Extracellular region part	2.70E-03
Membrane	*Enrichment: 9.55*	
	Transmembrane	2.09E-02
	Membrane	2.09E-02
	GO:0031224 Intrinsic to membrane	1.42E-02
	GO:0016021 integral to membrane	4.78E-01
Cell adhesion	*Enrichment: 3.88*	
	GO:0022610 Biological adhesion	2.09E-02
	GO:0007155Cell adhesion	2.09E-02
	Cell adhesion	1.42E-02
	GO:0016337 Cell-cell adhesion	4.78E-01
Enzyme inhibitor	*Enrichment: 3.57*	
	Protease inhibitor	2.43E-04
	GO:0030414 Peptidase inhibitor activity	3.70E-03
	GO:0004866 Endopeptidase inhibitor activity	2.95E-03
	GO:0004869 Cysteine-type endopeptidase inhibitor activity	1.95E-02
	GO:0004857 Enzyme inhibitor activity	3.56E-02
	Thiol protease inhibitor	1.98E-02
	Serine protease inhibitor	8.28E-02
	GO:0004867 Serine-type endopeptidase inhibitor activity	3.12E-01
	PIRSF001630 Serpin	9.95E-01
Glutathione metabolism	*Enrichment: 3.37*	
	GO:0004364 Glutathione transferase activity	4.76E-03
	mmu00980 Metabolism of xenobiotics by cytochrome P450	4.66E-03
	mmu00982 Drug metabolism	4.95E-03
	PIRSF000503 Glutathione transferase	5.19E-02
	mmu00480 Glutathione metabolism	1.25E-01
	Dimer	1.54E-01
	GO:0016765 Transferase activity, transferring alkyl or aryl (other than methyl) groups	4.74E-01

Table 3.7. Subset of clusters from DAVID GO Analysis on "upregulated" enriched Sertoli cell genes (Enrichment > 3).

Clusters identified by DAVID analysis in the Sertoli cell enriched "upregulated" gene list with an "Enrichment Value" of ≥3.

Table 3.8. Genes putatively regulated by NR5A1 in Sertoli cells

Genes putatively upregulated by NR5A1		Genes putatively downregulated by NR5A1	
Abca2	*Man2b2*	*2200002J24Rik*	*Nr0b2*
Adam10	*Mapk4*	*5330417C22Rik*	*Nr5a1*
Adamts9	*Masp1*	*Ablim2*	*Pik3ap1*
Adh1	*Mgst1*	*Aldh1a1*	*Plod2*
Akr1c14	*Mxd4*	*Aldh1a7*	*Ppp1r16b*
Ank	*Olfml3*	*Arhgdig*	*Pqlc1*
Aplp2	*P2rx4*	*Cst8*	*Prss35*
Aqp5	*Pink1*	*Ctsh*	*Pvrl1*
Ctsf	*Secisbp2l*	*Dok7*	*Rab20*
Cx3cl1	*Sema3b*	*Eno1*	*Rgs10*
Dbp	*Serpini1*	*Fam195a*	*Sema4a*
Enpp5	*Slc27a6*	*Fam63a*	*Slc27a3*
Epdr1	*Smpdl3a*	*Fdxr*	*Tle6*
Fam189a2	*St3gal4*	*Foxa3*	*Trim62*
Fkbp9	*Stim1*	*G6pdx*	*Ttyh3*
Fuca1	*Tapbp*	*Gjb2*	
Gpr37	*Tcn2*	*Hspb1*	
Gsta4	*Thra*	*Inhbb*	
Gstt3	*Ube2e2*	*Me1*	
Man2b1	*Ucp2*	*Nfil3*	
	Vamp5		

Table 3.8. List of genes that are putatively regulated by NR5A1 in the "upregulated" Sertoli cell enriched list.

76 genes were identified that overlapped between the upregulated and downregulated gene lists produced by Baba et al., (2014) and our list of 1217 genes upregulated in Sertoli cells. Genes that overlap in the data sets are listed as either being putatively up- or down-regulated by NR5A1.

Table 3.9. Subset of genes upregulated in 12.5 dpc Sertoli cells ($p < 0.05$).

ID	Gene Name		Chr	Phenotype	OMIM assoc.	Reference
ENSMUSG00000068522	**Aard**	**Alanine and arginine rich domain containing protein**	**16**	**-**	**N/A**	**-**
ENSMUSG00000058135	Gstm1	Glutathione S-transferase, mu 1	2	no apparent developmental defects; fertile	-	(Yochum et al., 2010)
ENSMUSG00000028657	Ppt1	Palmitoyl-protein thioesterase 1	3	viable and fertile; after birth developed neuronal ceroid lipofuscinosis	256730	(Gupta et al., 2001)
ENSMUSG00000040562	Gstm2	Glutathione S-transferase, mu 2	4	-	-	-
ENSMUSG00000060147	Serpinb6a	Serine (or cysteine) peptidase inhibitor, clade B, member 6a	3	viable and fertile; normal fecundity	613453	(Scarff et al., 2004)
ENSMUSG00000023000	**Dhh**	**Desert hedgehog**	**13**	**viable but infertile; reduced germ cells and FLCs**	**607080*; 233420***	(Bitgood et al., 1996; Yao et al., 2002)
ENSMUSG00000027199	Gatm	Glycine amidinotransferase	15	viable; impaired spermatogenesis	612718	(Choe et al., 2013)
ENSMUSG00000064036	**Mro**	**Maestro**	**2**	**no apparent developmental defects; fertile**	**-**	(Smith et al., 2008)
ENSMUSG00000004035	Gstm7	Glutathione S-transferase, mu 7	18	-	N/A	-
ENSMUSG00000026249	Serpine2	Serine (or cysteine) peptidase inhibitor, clade E, member 2	3	viable; males are infertile and reduced fecundity	-	(Murer et al., 2001)
ENSMUSG00000033227	Wnt6	Wingless-type MMTV integration site family, member 6	1	XX have compromised pregnancy and reduced fecundity	-	(Wang et al., 2013)
ENSMUSG00000059456	**Ptk2b**	**PTK2 protein tyrosine kinase 2 beta**	**1**	viable and fertile	-	(Okigaki et al., 2003)
ENSMUSG00000027445	**Cst9**	**Cystatin 9**	**14**	**normal sex ratio, sex-differentiation, gamete production and fertility**	**N/A**	(Hasegawa et al., 2006)
ENSMUSG00000027570	**Col9a3**	**Collagen, type IX, alpha 3**	**2**	**-**	**600969; 603932**	**-**
ENSMUSG00000042155	Klhl23	Kelch-like 23	2	-	N/A	-
ENSMUSG00000001313	Rnd2	Rho family GTPase 2	2	-	-	-
ENSMUSG00000025955	Akr1cl	Aldo-keto reductase family 1, member C-like (4921521F21Rik)	11	-	N/A	-
ENSMUSG00000031284	Pak3	p21 protein (Cdc42/Rac)-activated kinase 3	1	viable and fertile	300558	(Asrar et al., 2009)
ENSMUSG00000032418	Me1	Malic enzyme 1 (Mod-1)	X	viable and fertile	-	(Lee et al., 1980)
ENSMUSG00000027298	Tyro3	TYRO3 protein tyrosine kinase 3	9	sKO: viable and fertile; Tyro 3/Axl/Mer KO viable and infertile with multiple major organ defects	-	(Lu et al., 1999; Sun et al., 2010)
ENSMUSG00000053279	**Aldh1a1**	**Aldehyde dehydrogenase family 1, subfamily A1**	**2**	viable and fertile (redundant with Aldh1a2/3)	**-**	(Fan et al., 2003)
ENSMUSG00000062296	Trank1	Tetratricopeptide repeat and ankyrin repeat containing 1	19	-	N/A	-
ENSMUSG00000035262	**Amh**	**Anti-Mullerian hormone**	**9**	**failure of Mullerian duct regression, male infertility, partially penetrant Leydig cell hyperplasia**	**261550***	(Behringer et al., 1994; Mishina et al., 1996)

ENSMUSG00000037031	Tspan15	Tetraspanin 15	10	-	-	-
ENSMUSG00000021136	Smoc1	SPARC related modular calcium binding 1	10	embryonic optic and limb defects; viable to PN21	206920	(Okada et al., 2011)

Table 3.9. Subset of genes upregulated in 12.5 dpc Sertoli cells ($p < 0.05$).

Classification used the same criteria as Table 3.3. References are the primary report of the null or mutant mouse and any subsequent clarifying reports. (Chr., chromosome; OMIM assoc. = OMIM reference number if the gene is associated with any type of human disorder (* indicates a genitourinary, endocrine or DSD phenotype, **bold** indicates previously described Sertoli cell genes).

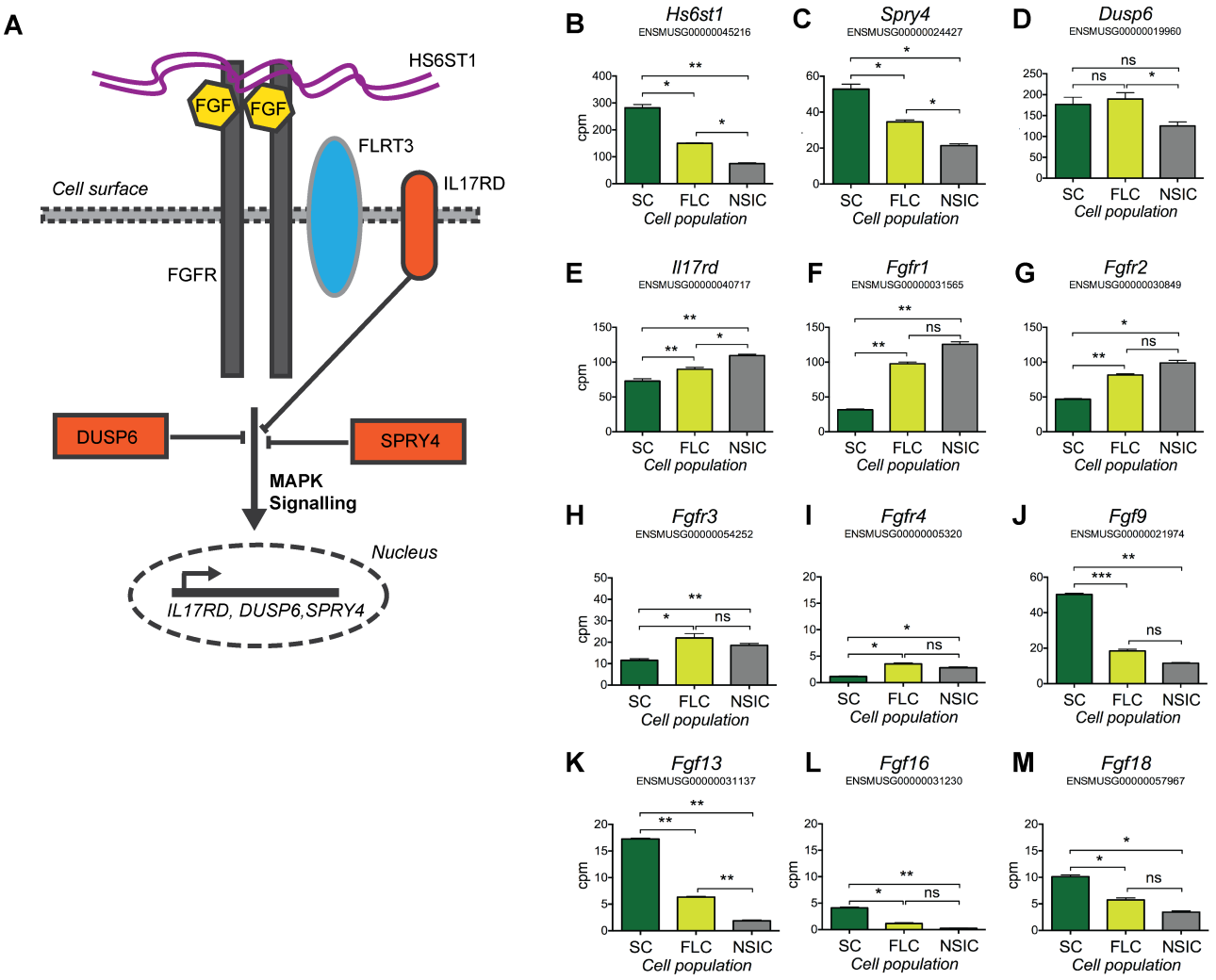

Figure 3.13. DSD genes Hs6st1 and Spry4 are expressed in Sertoli cells and many members of the signaling pathway are also expressed in 12.5 dpc testis.

(A) Cartoon depiction of the FGF-Network associated genes that are mutated in patients with Hypogonadotrophic Hypogonadism (modified from (Miraoui et al., 2013)). The network is comprised of an FGF-Receptor (grey) and FGF ligand (green). IL17RD, DUSP6 and SPRY4 (orange) are inhibitors of the MAPK pathways downstream of FGF signaling and are expressed in the 12.5 dpc testis. HS6ST1 (purple) encodes a HS-modifying enzyme. KAL1 and FLRT3 (blue solid) are known enhancers of FGF signaling in which human mutation causes DSD but that are not expressed in the testis. There is no verified homolog of KAL1 in mouse. (B-H) Counts per million reads (cpm) from RNA-seq data show expression of network genes that are detected in our RNA-seq analysis *Hs6st1* (B) and *Spry4* (C) shows a Sertoli cell enriched expression pattern. Negative regulators of the pathway *Dusp6* (D) and *Il17rd* (E) are expressed in the 12.5 dpc somatic testis. FGF-family members are also expressed, including *Fgfr1* (F) and the dominant receptor ligand pair in Sertoli cells *Fgfr2* (G) and *Fgf9* (J). *Fgfr3* (H) and *Fgfr4* (I) are expressed minimally in the 12.5 dpc testis. Other FGF ligands are also expressed in the Sertoli cells of the 12.5 dpc testis: *Fgf13* (K); *Fgf16* (L) and *Fgf18* (M). Error: S.E.M., * = p = 0.05, ** = p = 0.001, *** = p = 0.0001, **** = p = 0.00001, ns = not statistically significant.

3.7 The ovary: investigating subpopulations of somatic cells

In contrast to the cord-level structural organisation seen in the testis at 12.5 dpc, the ovary is a mixture of somatic and clustered germ cells during fetal life. During postnatal life the ovary regionalises and follicular granulosa cells surround the matured germ cells, oocytes. However, the regionalisation of the fetal ovary and the specification of the different cell lineages is poorly understood.

There are a suite of genes that are important for ovarian development including *Wnt4* (Vainio et al., 1999), *Rspo1* (Chassot et al., 2008; Parma et al., 2006) and *FoxL2* (Ottolenghi et al., 2005; Schmidt et al., 2004). All these genes can be used as markers of pre-granulosa cells and as readouts of the ovarian pathway. Some regionalisation of ovarian gene expression has been reported in the 13.5 dpc mouse ovary. Chen et al. (2012) identified three spatial expression patterns displayed by somatically-expressed ovarian genes. In one category were genes including *Fst, FoxL2* and *Wnt4*, with expression of genes such as *Rspo1* and *Irx3* being regionally distinct. Expression of genes such as *Bmp2* formed a third regionalised expression domain.

Recent studies have shown that the fetal mouse ovary contains a three distinct somatic cell types. Theses are classified as: precursors for medullary granulosa cells, which are FOXL2-positive cells; precursors for cortical granulosa cells, which are FOXL2-negative/LGR5-positive cells and presumptive precursors for steroidogenic theca cells, which are FOXL2-negative/NR2F2-positive (Chen et al., 2012; Mork et al., 2011; Rastetter et al., 2014; Zheng et al., 2014). Interestingly, although *Wnt4* and *Rspo1* are expressed in FOXL2-positive cells, *Lgr5* is not expressed in *Rspo1-/-* or *Wnt4-/-* ovaries (Rastetter et al., 2014). The study described herein was conducted before the identification of *Lgr5* and *Nr2f2* as linage markers in the fetal ovary. As a result, this analysis primarily focuses on separating FOXL2-positive and FOXL2-negative somatic cell lineages, based on expression of GFP in the *Sf1*-eGFP ovary (Mork et al., 2011; Zheng et al., 2014).

Evaluation of GFP in Sf1-eGFP mouse fetal ovaries

In the manuscript contained within this chapter, we exploited a published observation that the somatic cells of the early XY gonad differentially express NR5A1 (Schmahl et al., 2000). We determined that FLCs ("low-GFP"), Sertoli cells ("high-GFP") and NSICs ("GFP-negative") could be isolated based on the expression level of GFP in the XY *Sf1*-eGFP transgenic gonad. In characterising the XY somatic cell populations I also isolated "high-GFP", "low-GFP" and "GFP-negative" XX somatic cell populations and profiled them to determine if we could separate FOXL2-positive and FOXL2-negative pre-granulosa cells.

The 674 bp-fragment of the *Nr5a1* promoter used to drive GFP expression in the *Sf1*-eGFP transgenic gonad marks a subpopulation of somatic cells of the developing XX and XY gonads at 10.5-11.5 dpc (Beverdam and Koopman, 2006). Previously, Beverdam et al. (2006) profiled gene expression in the GFP-positive ovarian cell population at 10.5 and 11.5 dpc to characterise the pre-granulosa cell and identify genes that may play a role in female sex determination. However, the expression of GFP in the XX gonad beyond 11.5 dpc was not reported in that publication (Beverdam and Koopman, 2006).

Previously we showed colocalisation of NR5A1 and GFP at 11.5 dpc in XY gonads (Figure 3.2A,B,G; (Beverdam and Koopman, 2006)); I confirmed that NR5A1 and GFP also colocalise at 11.5 dpc in the XX gonad (Fig. 3.14A). Immunofluorescence analysis showed that weak expression of nuclear NR5A1 persisted in cytoplasmic GFP-transgene-positive cells at 12.5 dpc; however, the expression of GFP in the XX gonad did not mirror the endogenous expression profile of NR5A1 beyond 12.5 dpc. (Fig. 3.14B-D). After 12.5 dpc, NR5A1-protein expression in the ovary wanes although *Nr5a1* expression is maintained at a transcript level ((Hatano et al., 1994; Ikeda et al., 1994; Morohashi et al., 1995); Fig. 3.14B-B,L-L''). At 13.5-14.5 dpc, as expected I observed a loss of endogenous NR5A1 protein expression, however, the expression of the cytoplasmic GFP-transgene persisted (Fig. 3.14C,D). The GFP transgene is not expressed in germ cells ((Beverdam and Koopman, 2006); this study). I used an antibody to FOXL2 to determine if FOXL2-positive pre-granulosa cells persisted in expressing GFP. Co-staining for FOXL2 and GFP demonstrated that a proportion of GFP-positive cells co-localised with nuclear FOXL2 at 12.5-13.5 dpc, indicating that the transgene was expressed in FOXL2-positive pre-granulosa cells (Fig. 3.14E,F). GFP expression in NR2F2-positive and/or LGR5-positive XX somatic cells remains to be established.

The presence of numerous GFP-positive/FOXL2-negative cells indicates that the *Sf1*-eGFP transgene may mark multiple ovarian somatic cell lineages, therefore I investigated the expression profile of the high-GFP and low-GFP population by qRT-PCR.

Isolation and characterisation of fetal ovary somatic cell populations

As in the XY gonad, cell populations from 11.5-14.5 dpc *Sf1*-eGFP transgenic ovaries were isolated based on GFP fluorescence: a strongly GFP-positive ("high-GFP") cell population, a weakly GFP-positive ("low-GFP") cell population and a GFP-negative population. Germ cells were removed using antibodies to cell surface markers. Dissociated cells were incubated with antibodies to either SSEA-1 (recognising germ cells only) or CD31 (recognising germ and endothelial cells), and FACS was then used to separate the four cell populations (Fig. 3.4A). I profiled the expression of key ovarian somatic cell marker genes by qRT-PCR in XX and XY sorted cells. In the analysis of the XX cell populations I primarily characterised the "high-GFP" and "low-GFP" cell populations, which represent Sertoli cells and FLCs in the XY gonad, to investigate if the GFP transgene could be used to separate FOXL2-positive and FOXL2-negative somatic subpopulations in the XX gonad.

At 11.5 dpc, the XX high-GFP population (Fig. 3.14, dark green stripe) expressed higher levels of the genes encoding *Wt1* and *Nr0b1,* which are expressed in the somatic cells of the XX and XY gonad (Fig. 3.14G,H). Expression of the genes encoding ovarian granulosa cell markers *Wnt4* and *Rspo1* in the high-GFP cell population indicated that the high-GFP expressing population of the XX gonad was enriched for granulosa cells, the female equivalent of Sertoli cells (Fig. 3.14I,J). Interestingly, expression of the gene encoding *Cyp11a1* was significantly upregulated in the high-GFP somatic cells of the ovary compared to the low-GFP XX population and the XY gonad at 11.5 dpc (Fig. 3.14K).

In the XX cell populations, the high-GFP population robustly expressed genes characteristic of the FOXL2-positive pre-granulosa cell population including *FoxL2* itself, along with granulosa cell marker genes *Nr0b1*, *Wnt4, Fst* and *Rspo1* (Fig. 3.14M-Q). At 13.5-14.5 dpc the high-GFP population continued to express higher levels of *FoxL2* and *Fst* than expressed by the low-GFP cell population (Fig. 3.14M',Q',M'',Q''). However, expression of *Nr0b1* and *Wnt4* was equivalent between the low-GFP and high-GFP expressing cell populations (Fig. 3.14N',N'',O',O'') and expression of *Rspo1* in the low-GFP cell population was increased from 13-5-14.5 dpc (Fig.

3.14P’’). The high-GFP population expressed levels of *Nr5a1* equivalent to that observed in FLCs from 12.5 dpc (Fig. 3.14L,L’,L’’). These data indicate that the high-GFP expressing population is enriched for *FoxL2*-expressing pre-granulosa cells at 12.5 dpc.

The low-GFP cell population of the XX gonad consisted of somatic cells characterised by low-level expression of the genes encoding *FoxL2,* other classic ovarian markers and *Nr5a1* (Fig. 3.14L-Q,L’-Q’,L’’-Q’’). Recently, FOXL2-negative populations of somatic ovarian cells have been identified (Rastetter et al., 2014), these data suggest that the XX low-GFP somatic cell population may instead express the newly identified pre-granulosa somatic ovarian marker *Lgr5*. This was not investigated in this study. Therefore, the low-GFP expressing population is enriched for FOXL2-negative pre-granulosa somatic cells.

The germ cell-depleted, GFP-negative, putative interstitial cell population (Fig. 3.14, grey) showed minimal expression of *Nr5a1* and *FoxL2* indicating that, like the low-GFP fraction, it consisted of FOXL2-negative somatic cells (Fig. 3.14S,T,V). In the XY gonad the germ cell-depleted, GFP-negative population was enriched for NSICs. As NSICs in the XY gonad express NR2F2, I propose that the XX GFP-negative population may represent an *Nr2f2*-positive non-supporting somatic cells population

As in the XY gonad, germ cells were not the focus of this analysis. However, I also examined the expression of *Ddx4* in the XX sorted cells to determine the efficiency of germ cell depletion from the GFP-negative fraction. As expected, expression of *Ddx4* was robust in the antibody-selected cell population at 12.5-13.5 dpc (Fig. 3.14R,U). Low-level expression of *Ddx4* was detected in the GFP-negative fraction (Fig. 3.14R,U), indicating a low level of germ cell contamination.

The robust expression of *FoxL2* at 12.5-13.5 dpc in the high-GFP population indicates that the *Sf1*-eGFP line can be used to separate FOXL2-positive and FOXL2-negative somatic cells. It will be particularly interesting to profile the expression of *Lgr5* and *Nr2f2* in the sorted cell populations to determine if the isolated low-GFP and GFP-negative populations represent distinct cell lineages. Therefore, the *Sf1*-eGFP transgenic may also prove useful in characterising the subpopulations of the somatic cells of the ovary.

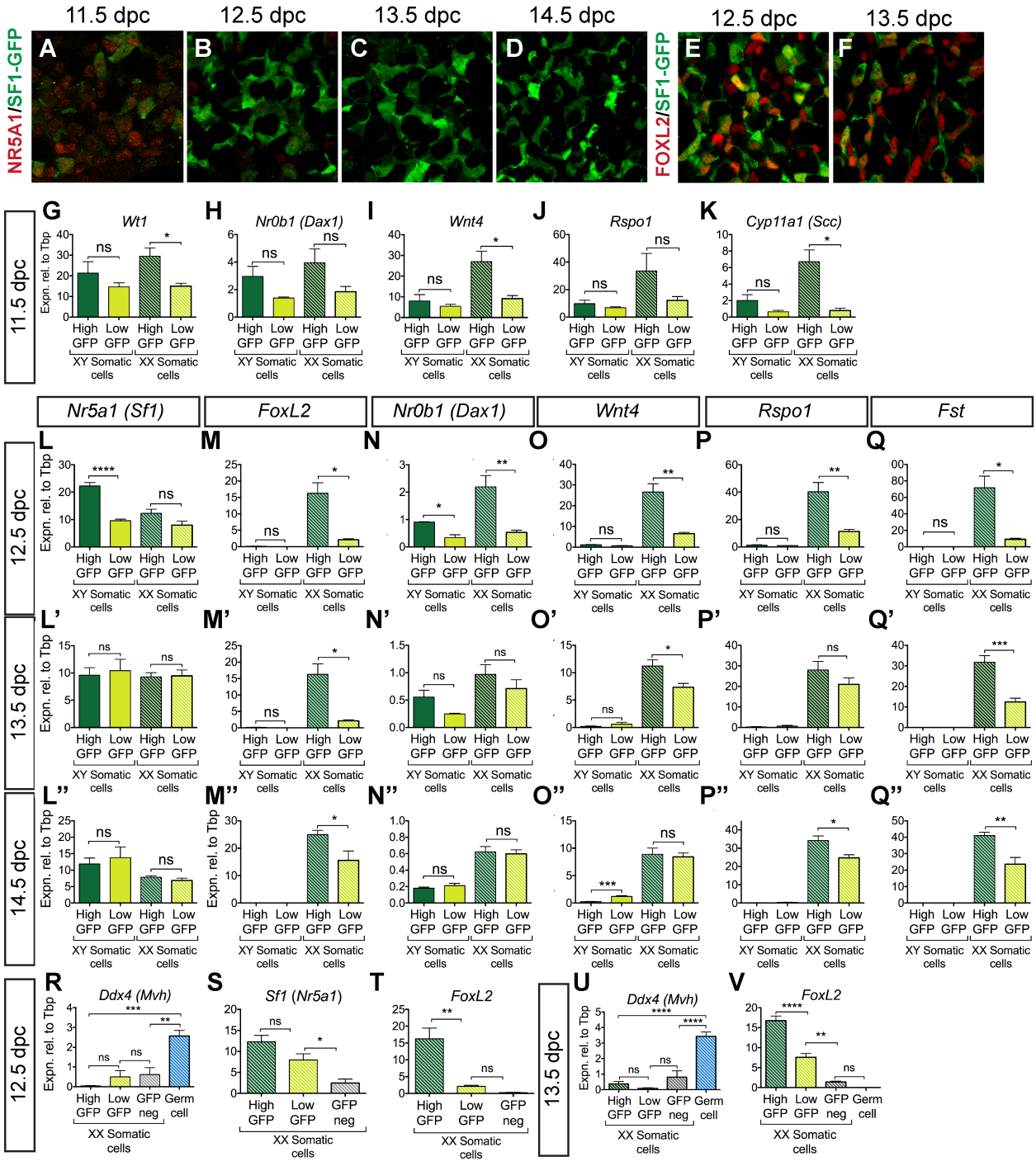
11.5 dpc
12.5 dpc
13.5 dpc
14.5 dpc
NR5A1/SF1-GFP
FOXL2/SF1-GFP
A
B
C
D
E
F
G Wt1
H Nr0b1 (Dax1)
I Wnt4
J Rspo1
K Cyp11a1 (Scc)
Nr5a1 (Sf1)
FoxL2
Nr0b1 (Dax1)
Wnt4
Rspo1
Fst
L
M
N
O
P
Q
L'
M'
N'
O'
P'
Q'
L''
M''
N''
O''
P''
Q''
R Ddx4 (Mvh)
S Sf1 (Nr5a1)
T FoxL2
U Ddx4 (Mvh)
V FoxL2
Expn. rel. to Tbp
High GFP
Low GFP
GFP neg
Germ cell
XY Somatic cells
XX Somatic cells
ns

Figure 3.14. Some GFP-positive cells are FOXL2-positive at 12.5 dpc XX gonads. High-GFP population represents FoxL2-high cells and the low-GFP population represents FoxL2-low in 12.5 dpc XX Sf1-eGFP gonads.

(A-F) IF of *Sf1*-eGFP gonads demonstrates that nuclear NR5A1 is expressed in the same cells that express cytoplasmic GFP in the 11.5-12.5 dpc XX gonad. (A) GFP/NR5A1-positive cells are present in the XX 11.5 dpc gonad. (B) Some NR5A1-positive cells persist at 12.5 dpc and colocalise with GFP-positive cells. (C-D) GFP-expression is maintained at 13.5-14.5 dpc but nuclear endogenous NR5A1-expression is absent. (E-F) Nuclear FOXL2 staining resides in GFP-positive cells, indicating that GFP marks FOXL2-positive cells, although not all GFP-positive cells have a FOXL2-positive nuclei. (G-V) As described in Fig. 3.3. four cell populations were isolated by FACS using a germ (GC) or germ cell/endothelial cell (GC/EC) depleted sorting method. This analysis predominately focused on the high-GFP and low-GFP populations. (G-K) At 11.5 dpc, qRT-PCR for somatic marker *Nr5a1* (Fig. 3.3B) and Sertoli cell marker *Sox9* (Fig. 3.3C), showed that the high-GFP expressing cell population in XY gonads was enriched for Sertoli cells. In sorted cell populations from the 11.5 dpc XX gonad the high-GFP population expressed higher levels of somatic (granulosa) cell markers *Wt1* (G), *Nr0b1* (H), *Wnt4* (I) and *Rspo1* (J). Surprisingly, expression of *Cyp11a1* (K) was also significantly higher in the high-GFP population of the XX gonad at 11.5 dpc. In sorted cell populations from the 12.5 dpc XX gonad the high-GFP population expressed similar levels of *Nr5a1* (L) and higher levels of somatic (granulosa) cell markers *FoxL2* (M), *Nr0b1* (N), *Wnt4* (O), *Rspo1* (P) and *Fst* (Q). From 13.5-14.5 dpc higher levels of somatic (granulosa) cell markers *FoxL2* (M', M'') and *Fst* (Q',Q'') in the high-GFP population was maintained, however, expression of *Nr0b1* (N',N''), *Wnt4* (O',O'') and *Rspo1* (P',P'') were similar between the high-GFP and low-GFP populations. Expression of *Nr5a1* remained equivalent at 13.5-14.5 dpc (Fig. 3.3J,3.4H,L',L"). Removal of germ cells with a CD31 antibody resulted in removal of the majority of *Ddx4*- expessing cells at 12.5-13.5 dpc (R,U). Examination of *Nr5a1* (S) and *FoxL2* (T,V) expression in the GFP-negative and germ cell faction by qRTPCR showed that *Nr5a1/FoxL2*-positive cells are restricted to the GFP-positive populations. *n* values for G-K,M''-Q'',R,U: *n*= 4, 4, 4, 4; M,N,Q: *n*= 3, 3, 3, 3; L: *n*=4, 5, 4, 5; O,P: *n*= 3, 3, 5, 5; L': *n*= 8, 8, 5, 5; M',O': *n*= 8, 8, 9, 9; N',P',Q': *n*= 4, 4, 5, 5; L",V: *n*= 8, 8, 4, 4; S: *n*=5, 4, 4; T: *n*= 3, 3, 3, 4. For all qRT-PCR: levels are shown relative to *Tbp,* error = S.E.M., * = p = 0.05, ** = p = 0.001, *** = p = 0.0001, **** = p = 0.00001, ns = not statistically. Scale bar: 100 μM.

3.8 NR2F2 in the developing testis: a brief expression report

Expression of *Nr2f2* in the interstitium of the testis has been noted from 13.5 dpc (Pereira et al., 1999; Pereira et al., 1995), however, whether NR2F2 is expressed in the FLC or NSIC populations in the early gonad is unknown. Recently, it has been demonstrated that NR2F2 is expressed in the NSIC population of the 18.5 dpc testis and that these fetal NR2F2-positive interstitial cells give rise to ALCs (Kilcoyne et al., 2014). The existence of interstitial NR2F2-positive cells in the developing testis provides the first suggestion that molecular events occurring during fetal gonadogenesis and masculinisation can affect the final levels of testosterone in the adult individual by affecting the NR2F2-positive ALC progenitor cells, ALCs being the source of testosterone after puberty. *Nr2f2-/-* embryos die at 10 dpc from cardiovascular defects (Pereira et al., 1999), and so examination of NR2F2 in gonadogenesis requires a suitable conditional/inducible system. Conditional ablation of NR2F2 two weeks after birth results in infertility, hypogonadism, and a severe reduction in testosterone production (Qin et al., 2008). Ablation of NR2F2 in mature ALCs did not result in any dysfunction in Leydig cells or any reproductive defects (Qin et al., 2008). Therefore, expression of NR2F2 is required for formation and maturation, but not maintenance, of functional ALCs.

In XX animals, *Nr2f2*-/+ ovaries have a reduced ability to produce sex steroids (Takamoto et al., 2005). Together these data support the hypothesis that NR2F2 is important for general postnatal steroidogenic cell function in the testis and the ovary. Whether NR2F2 has a critical role in fetal gonadogenesis is yet to be determined. At the time this study was conducted it had not been published that NR2F2 was expressed in the embryonic XX gonad. Therefore, this analysis focuses on the XY gonad. Subsequently it has been shown that NR2F2 marks a distinct somatic cell population in the ovary at 14.5 dpc (Rastetter et al., 2014).

In the manuscript I showed that NR2F2 cells were ARX-positive but negative for NR5A1 (Fig. 3.10B-D) with few exceptions where NR2F2/ARX-positive cells were also NR5A1-positive (grey arrow, Fig. 3.10B-D). I performed qRT-PCR on 12.5-14.5 dpc XY *Sf1*-eGFP sorted cell populations. Expression of the gene encoding *Nr2f2* was expressed at higher levels in the NSIC population compared to the FLC population at 12.5 dpc only (Fig. 3.15A). To confirm that NR2F2-positive cells were NSICs at 12.5 dpc I examined expression of NR2F2, NR5A1 and GFP in the *Sf1*-eGFP mouse. As observed in Fig. 3.10 there were a few NR2F2/NR5A1-positive cells that were

also GFP-positive (yellow arrow, Fig. 3.15B-E). The majority of the NR2F2-positive cells were not marked by the *Sf1*-eGFP transgene (grey arrow, Fig. 3.15B-E). I examined whether NR5A1/NR2F2-positive cells could be HSD3β positive. While NR2F2/NR5A1-positive cells were observed (Fig. 3.10; Fig. 3.15B-E) NR2F2-positive and HSD3β-positive cells appeared to be mutually exclusive (Fig. 3.15F,G).

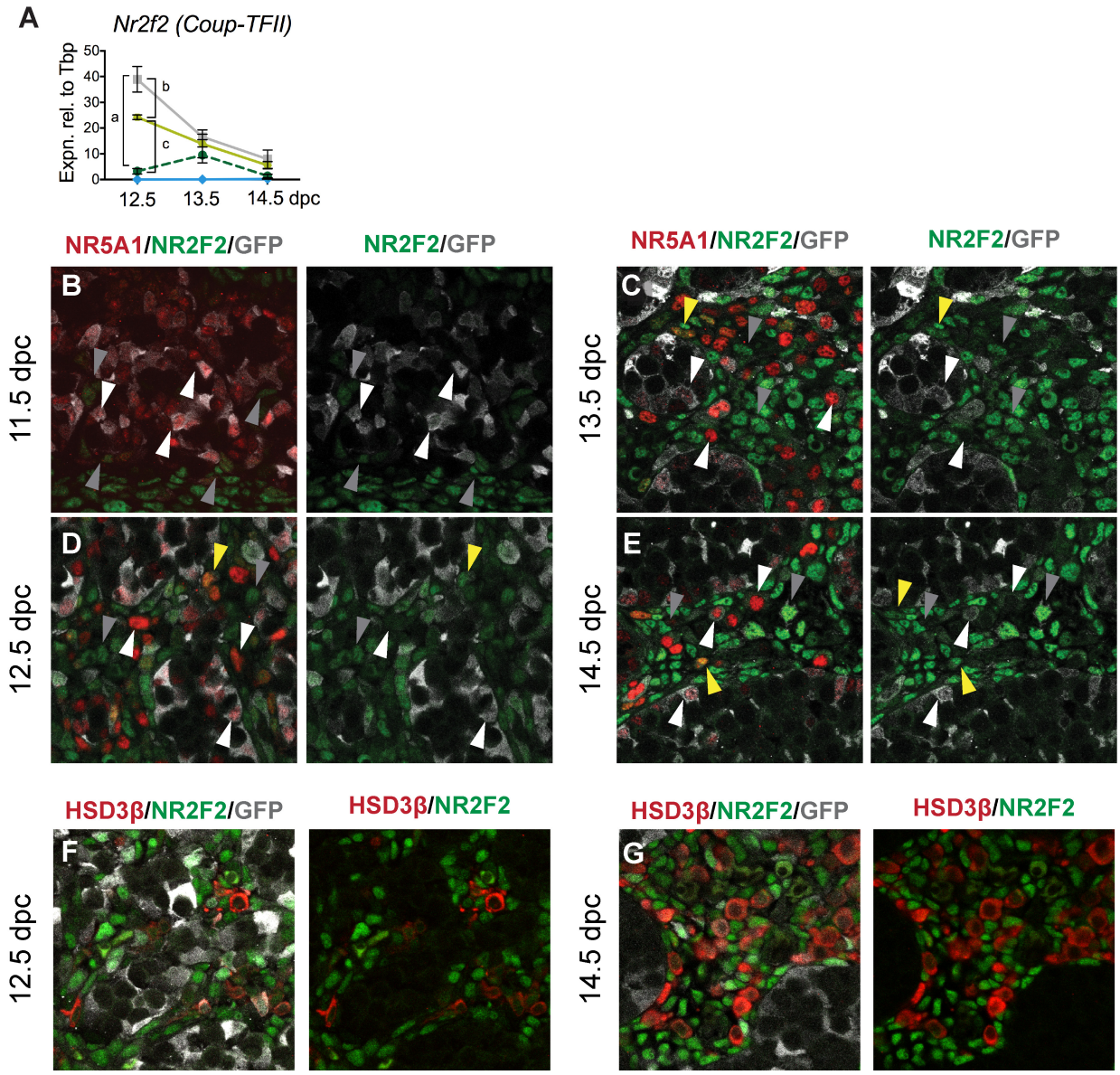

Figure 3.15. NR2F2-positive cells are predominately NR5A1/HSD3B-negative interstitial cells.

(A) qRT-PCR for *Nr2f2* in *Sf1*-eGFP aorted XY gonadal cells from 12.5-14.5 dpc indicated that *Nr2f2* was expressed significantly higher in NSICs compared to FLCs at 12.5 dpc only (a, ****; b, **; c, ****; all other comparisons were "ns"). IF for NF2R2 demonstrates that the majority of NR2F2-positive cells are NR5A1-negative. (B-E) At 11.5 dpc some NR2F2 cells can be observed in the XY gonad (B). From 12.5-14.5 dpc in XY gonads, only a few NR2F2/ARX/NR5A1-positive cells are present; the majority of NR2F2-positive cells are NR5A1-negative/GFP-negative (C-E). (F,G) A few NR2F2-positive cells are GFP-positive but no HSD3β-positive cells are NR2F2-positive. Scale bar: 100 μM. Arrows= yellow: NR5A1/NR2F2-positive; white: NR5A1-positive; gray: NR2F2-positive. For all qRT-PCR: levels are shown relative to *Tbp,* error = S.E.M., * = p = 0.05, ** = p = 0.001, *** = p = 0.0001, **** = p = 0.00001, ns = not statistically.

3.9 Chapter Conclusion

This chapter demonstrates the utility of the *Sf1*-eGFP line in understanding somatic gonad cell lineage development. These data show that in the *Sf1*-eGFP XY gonad Sertoli cell, FLC and NSIC populations can be isolated at 12.5 dpc. In the *Sf1*-eGFP XX gonad, FOXL2-positive and FOXL2-negative somatic cell populations can be isolated at 12.5 dpc. Having isolated the three somatic cell populations in the XY gonad at 12.5 dpc I performed RNA-seq. Using differentially expressed gene analysis I identified a suite of genes whose expression precedes the upregulation of steroidogenic pathway components in the FLC population. These data showed that neuroactive ligand-receptor components were overrepresented in the FLC lineage at 12.5 dpc. The expression of these components in the fetal testis preceded the expression of neuroactive ligand-receptor components in the HPG axis. This observation indicated that in cases of DSD caused by mutation of genes involved in the HPG axis, a fetal testicular phenotype may precede the gonadotropin-dependent HPG-axis driven phenotype that arises later in development.

In addition, this analysis provided the first comparative characterisation of FLCs and enriched NSICs. This analysis highlighted that the NSIC population has a distinct transcriptomic profile when compared to FLCs. The subtractive approach taken to isolate the NSIC population meant that it also contained cell types such as blood cells and macrophages; these ontologies were identified by DAVID analysis. The NSIC lineage has recently been shown to give rise to the ALC lineage that produces testosterone postnatally (Kilcoyne et al., 2014). I found that DSD gene *Frem2* was expressed in 12.5 dpc NSICs, which may help to explain the Fraser Syndrome testicular phenotype of ambiguous genitalia.

ARX marks the NSIC enriched cell lineage in the fetal testis. Interestingly the expression of ARX is not restricted to the XY gonad, expression of ARX is also observed throughout the XX gonad (Kitamura et al., 2002; Miyabayashi et al., 2013). ARX is expressed in a small population of NR5A1-positive/HSD3β-positive FLCs cells but predominately marks the NSIC population (this study; (Miyabayashi et al., 2013)). In this chapter I provide the first in depth characterisation of a new NSIC-enriched cell lineage marker, NR2F2. I show that expression of NR2F2 is very similar to the behaviour of ARX. The majority of NR2F2-positive cells colocalises with ARX from 12.5 dpc .A small population of NR2F2-positive cells are apparently NR5A1-positive FLCs. Additionally, NR2F2 has been shown to be expressed in XX somatic cells (Rastetter et al., 2014).

Chapter 4: Concluding Remarks

How the testis interstitium influences testicular development and how FLCs differ from NSICs have been long-standing questions in the field. In order to understand the role of the different interstitial cell types, I characterised the transcriptomes of the various somatic cell populations of the testis using RNA-seq. In addition, my project aimed to provide a methodology to handle and prioritise the outputs from transcriptomic screens and rare disease cohort studies. To do this, I developed an *ex vivo* gene knockdown strategy suitable for screening genes of interest for potential roles in organogenesis. Collectively, this work revealed transcriptomic differences between the FLC and NSIC populations and provided a method with which to assess functionality of the genes-of-interest coming out of this comparative screen. This work aims to help us develop a greater understanding of the influence of the testis interstitium on gonadogenesis.

In this project, in order to gain insight into the function of novel target genes in organogenesis, I developed a first-pass screening method that enables the knockdown of genes, singularly or in combination. This methodology can be used to assist in assessing whether or not performing a complex genetic loss-of-function experiment is likely to be informative and to prioritise candidates for functional validation. By injecting the MO into the heart, this technique utilised the vascular network of the embryo, thereby delivering the MO to target tissues; these were then explanted, cultured and analysed. I demonstrated that MO injection could partially reproduce known gene knockout phenotypes in the fetal gonads and pancreas, and be used to obtain preliminary data regarding the function of DSD candidate genes during gonadogenesis. The discussion of the proof-of-principle experiments designed to knockdown known gonadogenesis genes, and novel genes identified from DSD patient cohorts, is outlined in detail in Chapter 2. We anticipate that this relatively simple method will allow those in the field to dissect gene function during organogenesis more swiftly.

In the lead up to the XY gonad somatic cell transcriptomics project I performed an in-depth analysis of the *Sf1*-eGFP mouse line, generated previously in our lab. I identified three key differences between GFP expression and endogenous SFI expression in transgenic *Sf1*-eGFP gonads. These differences indicate that the 674 bp fragment used to direct GFP expression in the *Sf1*-eGFP line is insufficient to faithfully replicate the endogenous expression pattern of NR5A1. The fact that a

known fetal Leydig enhancer 3.1 kb upstream of the *Nr5a1* transcription site (Shima et al., 2012) is not present in the *Sf1*-eGFP construct may explain why, unlike endogenous NR5A1, GFP does not become robustly expressed in FLCs as they differentiate. Similarly, I propose that the normal endogenous downregulation of NR5A1 in Sertoli cells and XX somatic cells, neither of which occurs in our mouse line, is controlled by a mechanism that involves *Nr5a1* regulatory sequences outside the 674bp *Nr5a1* promoter fragment used in this model. Despite the fact that the *Sf1*-eGFP mouse line does not recapitulate endogenous NR5A1 expression at later timepoints, it proved suitable for our purpose - the FACS-based separation of Sertoli cell ("NR5A1/GFP-high") and pre-FLCs ("NR5A1/GFP-low") at 12.5 dpc.

I used the *Sf1*-eGFP line to isolate enriched populations of four distinct fetal testis cell lineages using a FACS-based technique: Sertoli, Leydig, interstitial and germ cells were each isolated. This technique allowed the isolation of the purest and best-validated population of pre-FLCs yet reported. In the fetal gonad, identifying which cell type/s express a novel gene-of-interest is a labour-intensive task (Svingen et al., 2011; Wainwright et al., 2013). In addition to being used for transcriptomic analysis, as demonstrated here, this sorting method will facilitate the rapid determination of expression of novel genes in the XY gonad using qRT-PCR.

Among the most important criteria for assessing whether a pathway is potentially functional in the system is demonstrating that a resident cell population is producing the secreted protein, expression of specific receptors in the surrounding cell population/s, and evidence that signaling activity is taking place in the cell or its neighbours. Therefore, transcriptomic approaches such as RNA-seq provide the ideal starting point from which to uncover signaling dynamics and design future functional studies. The comprehensive molecular characterisation of each somatic cell population revealed which genes are expressed in both the FLC and NSIC populations early in gonadogenesis. My transcriptomic analysis found that in the FLC and Sertoli cell populations numerous factors that are essential for the development and functionality of the neuroendocrine system are expressed. Although the genes encoding receptors associated with neuroactive ligand signaling are known to be essential for proper sexual development they have not been implicated previously in early testicular development. Using my RNA-seq dataset in combination with reanalysed microarray data (Jameson et al., 2012b) for each neuroactive ligand receptor identified I was able to show that at 12.5-13.5 dpc in the XY gonad the relevant secreted ligand was expressed (Fig. 3.11). These data provide the ideal starting point from which to uncover signaling dynamics and design functional

studies to investigate the role of the various signaling pathways in gonadogenesis. My results also revealed that the NSIC population, which has been shown to contribute to the ALC population postnatally (Kilcoyne et al., 2014), is transcriptomically distinct from the FLC population. These data suggest that NSICs may play an important functional role in fetal testis development. The differences we have identified between transcriptomic profiles in FLC- and NSIC-enriched populations may provide leads as to how pre-FLCs are specified, or how NSICs resist specification within the total interstitial population.

Many of the neuropeptide factors involved in neuroendocrine development are also involved in mediating cellular function in the testis. This has led to an interest in so called "neuroendocrine gonadal peptides" which are produced locally by the testis and act as mediators of gonadal function. The role of neuroendocrine peptides in the adult testis and reproductive system is well established, but a role for these factors in fetal gonadogenesis has not been clearly established. In part this is due to the fact that most of the early work on neuroendocrine gonadal peptides was done in *in vitro* systems, and has not been followed up with work in *in vivo* systems. Nevertheless, this early work indicates that neuroendocrine components could operate in the fetal testis. Indeed, a review by Gnessi et al. (1997) argued that in the developing testis an "intratesticular network of regulators … might participate first in the development of the male gonad and later in the initiation and maintenance of testicular function". It was argued that a fetal role was likely to exist for many of the neuroendocrine components that are essential for reproductive function later in life. My findings support this theory by demonstrating that there are a number of neuroendocrine components expressed in the developing testis. Functional validation of these novel genes will need to be investigated to assess whether they may play unappreciated roles early in gonadogenesis.

I also investigated if any DSD-causing genes were expressed in the fetal testis. Expression of known DSD genes in fetal somatic cell populations might indicate that the gene has an unappreciated role in fetal development of the testis. The transcriptomic analysis of the XY somatic cell populations identified a number of DSD genes (*TACR3*, *SPRY4*, *HS6ST1*, *FREM2*) that have not previously been associated with gonadogenesis. I propose that mutations in these genes may have a role in fetal testis development and that mutation of these genes may therefore result in early masculinisation defects.

Collectively, these results provide a comprehensive characterisation of the various somatic cell types of the testis, in particular the FLC and NSIC populations. This work highlights that the interstitium is a complex mix of cells that can affect testicular development and masculinisation during fetal development and beyond. This work splits the interstitial cell population into FLCs and the broad category of the remaining interstitium, which in this analysis contains cells such as macrophages in addition to NSICs. While this work is the first to separate FLCs from the rest of the interstitium and compare the characteristics of the FLC versus the NSIC population, further fractionation of the interstitial space in future characterisation studies would provide us with a deeper understanding of the important cellular processes that shape masculinisation of the embryo. Expression and functional validation will be needed to gain a clearer understanding of how the interstitium responds to cues and how different sub-populations gain identity. In addition, these results provide a methodology to tackle functional characterisation of genes of interest. Understanding how cells residing in the fetal interstitium contribute to masculinisation will help us to understand the impact of this population on health and disease/dysfunction in conditions ranging from DSD to infertility.

References

Abeliovich, A., Schmitz, Y., Fariñas, I., Choi-Lundberg, D., Ho, W. H., Castillo, P. E., Shinsky, N., Verdugo, J. M., Armanini, M., Ryan, A., et al. (2000). Mice lacking alpha-synuclein display functional deficits in the nigrostriatal dopamine system. *Neuron* **25**, 239–252.

Achermann, J. C., Ito, M., Ito, M., Hindmarsh, P. C. and Jameson, J. L. (1999). A mutation in the gene encoding steroidogenic factor-1 causes XY sex reversal and adrenal failure in humans. *Nat. Genet.* **22**, 125–126.

Achermann, J. C., Ozisik, G., Ito, M., Orun, U. A., Harmanci, K., Gurakan, B. and Jameson, J. L. (2002). Gonadal determination and adrenal development are regulated by the orphan nuclear receptor steroidogenic factor-1, in a dose-dependent manner. *J. Clin. Endocrinol. Metab.* **87**, 1829–1833.

Acquaah-Mensah, G. K., Taylor, R. C. and Bhave, S. V. (2012). PACAP interactions in the mouse brain: implications for behavioral and other disorders. *Gene* **491**, 224–231.

Adams, I. R. and McLaren, A. (2002). Sexually dimorphic development of mouse primordial germ cells: switching from oogenesis to spermatogenesis. *Development* **129**, 1155–1164.

Akakura, S., Huang, C., Nelson, P. J., Foster, B. and Gelman, I. H. (2008). Loss of the SSeCKS/Gravin/AKAP12 gene results in prostatic hyperplasia. *Cancer Res* **68**, 5096–5103.

Albrecht, K. H. and Eicher, E. M. (2001). Evidence that Sry is expressed in pre-Sertoli cells and Sertoli and granulosa cells have a common precursor. *Dev. Biol.* **240**, 92–107.

Anders, S., Pyl, P. T. and Huber, W. (2014). HTSeq-a Python framework to work with high-throughput sequencing data. *Bioinformatics* btu638.

Anderson, E. L., Baltus, A. E., Roepers-Gajadien, H. L., Hassold, T. J., de Rooij, D. G., van Pelt, A. M. M. and Page, D. C. (2008). Stra8 and its inducer, retinoic acid, regulate meiotic initiation in both spermatogenesis and oogenesis in mice. *Proc. Natl. Acad. Sci. U. S. A.* **105**, 14976–14980.

Arango, N. A., Lovell-Badge, R. and Behringer, R. R. (1999). Targeted Mutagenesis of the Endogenous Mouse Mis Gene Promoter: In Vivo Definition of Genetic Pathways of Vertebrate Sexual Development. *Cell* **99**, 409–419.

Asrar, S., Meng, Y., Zhou, Z., Todorovski, Z., Huang, W. W. and Jia, Z. (2009). Regulation of hippocampal long-term potentiation by p21-activated protein kinase 1 (PAK1). *Neuropharmacology* **56**, 73–80.

Aubert, M. L., Begeot, M., Winiger, B. P., Morel, G., Sizonenko, P. C. and Dubois, P. M. (1985). Ontogeny of hypothalamic luteinizing hormone-releasing hormone (GnRH) and pituitary GnRH receptors in fetal and neonatal rats. *Endocrinology* **116**, 1565–1576.

Baba, T., Otake, H., Sato, T., Miyabayashi, K., Shishido, Y., Wang, C.-Y., Shima, Y., Kimura, H., Yagi, M., Ishihara, Y., et al. (2014). Glycolytic genes are targets of the nuclear receptor Ad4BP/SF-1. *Nat Commun* **5**, 3634.

Bagheri-Fam, S., Sim, H., Bernard, P., Jayakody, I., Taketo, M. M., Scherer, G. and Harley, V. R. (2008). Loss of Fgfr2 leads to partial XY sex reversal. *Dev. Biol.* **314**, 71–83.

Bai, D. (2014). Atrial fibrillation-linked GJA5/connexin40 mutants impaired gap junctions via different mechanisms. *FEBS Lett.* **588**, 1238–1243.

Baker, P. J. and O'Shaughnessy, P. J. (2001). Role of gonadotrophins in regulating numbers of Leydig and Sertoli cells during fetal and postnatal development in mice. *Reproduction* **122**, 227–234.

Baltus, A. E., Menke, D. B., Hu, Y. C., Goodheart, M. L., Carpenter, A. E., de Rooij, D. G. and Page, D. C. (2006). In germ cells of mouse embryonic ovaries, the decision to enter meiosis precedes premeiotic DNA

replication. *Nat. Genet.* **38**, 1430–1434.

Bardoni, B., Zanaria, E., Guioli, S., Floridia, G., Worley, K. C., Tonini, G., Ferrante, E., Chiumello, G., McCabe, E. R. B., Fraccaro, M., et al. (1994). A dosage sensitive locus at chromosome Xp21 is involved in male to female sex reversal. *Nat. Genet.* **7**, 497–501.

Barrionuevo, F., Bagheri-Fam, S., Klattig, J., Kist, R., Taketo, M. M., Englert, C. and Scherer, G. (2006). Homozygous inactivation of Sox9 causes complete XY sex reversal in mice. *Biol. Reprod.* **74**, 195–201.

Barsoum, I. and Yao, H. H. (2011). Redundant and differential roles of transcription factors gli1 and gli2 in the development of mouse fetal Leydig cells. *Biol. Reprod.* **84**, 894–899.

Barsoum, I. B. and Yao, H. H. (2010). Fetal Leydig cells: progenitor cell maintenance and differentiation. *J. Androl.* **31**, 11–15.

Barsoum, I. B., Bingham, N. C., Parker, K. L., Jorgensen, J. S. and Yao, H. H. C. (2009). Activation of the Hedgehog pathway in the mouse fetal ovary leads to ectopic appearance of fetal Leydig cells and female pseudohermaphroditism. *Dev. Biol.* **329**, 96–103.

Barsoum, I. B., Kaur, J., Ge, R. S., Cooke, P. S. and Yao, H. H.-C. (2013). Dynamic changes in fetal Leydig cell populations influence adult Leydig cell populations in mice. *FASEB J.* **27**, 2657–2666.

Basciani, S., Mariani, S., Arizzi, M., Ulisse, S., Rucci, N., Jannini, E. A., Rocca, C. D., Manicone, A., Carani, C., Spera, G., et al. (2002). Expression of Platelet-Derived Growth Factor-A (PDGF-A), PDGF-B, and PDGF Receptor-α and -β during Human Testicular Development and Disease. *The Journal of Clinical Endocrinology & Metabolism* **87**, 2310–2319.

Bashamboo, A., Ferraz-de-Souza, B., Lourenço, D., Lin, L., Sebire, N. J., Montjean, D., Bignon-Topalovic, J., Mandelbaum, J., Siffroi, J.-P., Christin-Maitre, S., et al. (2010). Human male infertility associated with mutations in NR5A1 encoding steroidogenic factor 1. *Am. J. Hum. Genet.* **87**, 505–512.

Bazigou, E., Xie, S., Chen, C., Weston, A., Miura, N., Sorokin, L., Adams, R., Muro, A. F., Sheppard, D. and Makinen, T. (2009). Integrin-alpha9 is required for fibronectin matrix assembly during lymphatic valve morphogenesis. *Dev. Cell* **17**, 175–186.

Behringer, R. R., Finegold, M. J. and Cate, R. L. (1994). Mullerian-inhibiting substance function during mammalian sexual development. *Cell* **79**, 415–425.

Benjamini, Y. and Hochberg, Y. (1995). Controlling the False Discovery Rate: A Practical and Powerful Approach to Multiple Testing**.** *Journal of the Royal Statistical Society* **57**, 289–300.

Bettahi, I., Marker, C. L., Roman, M. I. and Wickman, K. (2002). Contribution of the Kir3.1 subunit to the muscarinic-gated atrial potassium channel IKACh. *J. Biol. Chem.* **277**, 48282–48288.

Beverdam, A. and Koopman, P. (2006). Expression profiling of purified mouse gonadal somatic cells during the critical time window of sex determination reveals novel candidate genes for human sexual dysgenesis syndromes. *Hum. Mol. Genet.* **15**, 417–431.

Bi, W., Huang, W., Whitworth, D. J., Deng, J. M., Zhang, Z., Behringer, R. R. and de Crombrugghe, B. (2001). Haploinsufficiency of Sox9 results in defective cartilage primordia and premature skeletal mineralization. *Proc. Natl. Acad. Sci. U. S. A.* **98**, 6698–6703.

Bianco, S. D. C. and Kaiser, U. B. (2009). The genetic and molecular basis of idiopathic hypogonadotropic hypogonadism. *Nat. Rev. Endocrinol.* **5**, 569–576.

Biason-Lauber, A. and Schoenle, E. J. (2000). Apparently normal ovarian differentiation in a prepubertal girl with transcriptionally inactive steroidogenic factor 1 (NR5A1/SF-1) and adrenocortical insufficiency. *Am. J. Hum. Genet.* **67**, 1563–1568.

Bingham, N. C., Verma-Kurvari, S., Parada, L. F. and Parker, K. L. (2006). Development of a steroidogenic factor

1/Cre transgenic mouse line. *Genesis* **44**, 419–424.

Bishop, C. E., Whitworth, D. J., Qin, Y., Agoulnik, A. I., Agoulnik, I. U., Harrison, W. R., Behringer, R. R. and Overbeek, P. A. (2000). A transgenic insertion upstream of Sox9 is associated with dominant XX sex reversal in the mouse. *Nat. Genet.* **26**, 490–494.

Bitgood, M. J. and McMahon, A. P. (1995). Hedgehog and Bmp genes are coexpressed at many diverse sites of cell-cell interaction in the mouse embryo. *Dev. Biol.* **172**, 126–138.

Bitgood, M. J., Shen, L. and McMahon, A. P. (1996). Sertoli cell signaling by Desert hedgehog regulates the male germline. *Curr. Biol.* **6**, 298–304.

Bland, M. L., Fowkes, R. C. and Ingraham, H. A. (2004). Differential requirement for steroidogenic factor-1 gene dosage in adrenal development versus endocrine function. *Mol. Endocrinol.* **18**, 941–952.

Bonneau, D., Toutain, A., Laquerrière, A., Marret, S., Saugier-Veber, P., Barthez, M.-A., Radi, S., Biran-Mucignat, V., Rodriguez, D. and Gélot, A. (2002). X-linked lissencephaly with absent corpus callosum and ambiguous genitalia (XLAG): clinical, magnetic resonance imaging, and neuropathological findings. *Ann. Neurol.* **51**, 340–349.

Bouma, G. J., Affourtit, J. P., Bult, C. J. and Eicher, E. M. (2007). Transcriptional profile of mouse pre-granulosa and Sertoli cells isolated from early-differentiated fetal gonads. *Gene Expr. Patterns* **7**, 113–123.

Bouma, G. J., Albrecht, K. H., Washburn, L. L., Recknagel, A. K., Churchill, G. A. and Eicher, E. M. (2005). Gonadal sex reversal in mutant Dax1 XY mice: a failure to upregulate Sox9 in pre-Sertoli cells. *Development* **132**, 3045–3054.

Bouma, G. J., Hudson, Q. J., Washburn, L. L. and Eicher, E. M. (2010). New Candidate Genes Identified for Controlling Mouse Gonadal Sex Determination and the Early Stages of Granulosa and Sertoli Cell Differentiation. *Biol. Reprod.* **82**, 380–389.

Bowles, J., Bullejos, M. and Koopman, P. (2000). A subtractive gene expression screen suggests a role for vanin-1 in testis development in mice. *Genesis* **27**, 124–135.

Bowles, J., Feng, C. W., Spiller, C., Davidson, T. L., Jackson, A. and Koopman, P. (2010). FGF9 suppresses meiosis and promotes male germ cell fate in mice. *Dev. Cell* **19**, 440–449.

Bowles, J., Knight, D., Smith, C., Wilhelm, D., Richman, J., Mamiya, S., Yashiro, K., Chawengsaksophak, K., Wilson, M. J., Rossant, J., et al. (2006). Retinoid signaling determines germ cell fate in mice. *Science* **312**, 596–600.

Boyer, A., Lussier, J. G., Sinclair, A. H., McClive, P. J. and Silversides, D. W. (2004). Pre-sertoli specific gene expression profiling reveals differential expression of Ppt1 and Brd3 genes within the mouse genital ridge at the time of sex determination. *Biol. Reprod.* **71**, 820–827.

Brennan, J., Karl, J. and Capel, B. (2002). Divergent vascular mechanisms downstream of Sry establish the arterial system in the XY gonad. *Dev. Biol.* **244**, 418–428.

Brennan, J., Tilmann, C. and Capel, B. (2003). Pdgfr-α mediates testis cord organization and fetal Leydig cell development in the XY gonad. *Genes Dev.* **17**, 800–810.

Buaas, F. W., Val, P. and Swain, A. (2009). The transcription co-factor CITED2 functions during sex determination and early gonad development. *Hum. Mol. Genet.* **18**, 2989–3001.

Bullejos, M. and Koopman, P. (2001). Spatially dynamic expression of Sry in mouse genital ridges. *Dev. Dyn.* **221**, 201–205.

Bullejos, M., Bowles, J. and Koopman, P. (2002). Extensive vascularization of developing mouse ovaries revealed by caveolin-1 expression. *Dev. Dyn.* **225**, 95–99.

Burgoyne, P. S., Tam, P. P. and Evans, E. P. (1983). Retarded development of XO conceptuses during early pregnancy in the mouse. *J. Reprod. Fertil.* **68**, 387–393.

Buters, J. T. M., Sakai, S., Richter, T., Pineau, T., Alexander, D. L., Savas, U., Doehmer, J., Ward, J. M., Jefcoate, C. R. and Gonzalez, F. J. (1999). Cytochrome P450 CYP1B1 determines susceptibility to 7, 12-dimethylbenz[a]anthracene-induced lymphomas. *P.N.A.S* **96**, 1977–1982.

Canto, P., Soderlund, D., Reyes, E. and Mendez, J. P. (2004). Mutations in the desert hedgehog (DHH) gene in patients with 46,XY complete pure gonadal dysgenesis. *J. Clin. Endocrinol. Metab.* **89**, 4480–4483.

Canto, P., Vilchis, F., Soderlund, D., Reyes, E. and Mendez, J. P. (2005). A heterozygous mutation in the desert hedgehog gene in patients with mixed gonadal dysgenesis. *Mol. Hum. Reprod.* **11**, 833–836.

Carpenter, E. M., Goddard, J. M., Davis, A. P., Nguyen, T. P. and Capecchi, M. R. (1997). Targeted disruption of Hoxd-10 affects mouse hindlimb development. *Development* **124**, 4505–4514.

Carvalho, B. S. and Irizarry, R. A. (2010). A framework for oligonucleotide microarray preprocessing. *Bioinformatics* **26**, 2363–2367.

Chaboissier, M.-C., Kobayashi, A., Vidal, V. I. P., Latzkendorf, S., van de Kant, H. J. G., Wegner, M., de Rooij, D. G., Behringer, R. R. and Schedl, A. (2004). Functional analysis of Sox8 and Sox9 during sex determination in the mouse. **131**, 1891–1901.

Chang, A. C. M., Cha, J., Koentgen, F. and Reddel, R. R. (2005). The murine stanniocalcin 1 gene is not essential for growth and development. *Mol. Cell. Biol.* **25**, 10604–10610.

Chang, H., Gao, F., Guillou, F., Taketo, M. M., Huff, V. and Behringer, R. R. (2008). Wt1 negatively regulates beta-catenin signaling during testis development. *Development* **135**, 1875–1885.

Chassot, A. A., Ranc, F., Gregoire, E. P., Roepers-Gajadien, H. L., Taketo, M. M., Camerino, G., de Rooij, D. G., Schedl, A. and Chaboissier, M. C. (2008). Activation of beta-catenin signaling by Rspo1 controls differentiation of the mammalian ovary. *Hum. Mol. Genet.* **17**, 1264–1277.

Chen, H., Palmer, J. S., Thiagarajan, R. D., Dinger, M. E., Lesieur, E., Chiu, H., Schulz, A., Spiller, C., Grimmond, S. M., Little, M. H., et al. (2012). Identification of novel markers of mouse fetal ovary development. *PLoS ONE* **7**, e41683.

Childs, A. J., Cowan, G., Kinnell, H. L., Anderson, R. A. and Saunders, P. T. (2011). Retinoic Acid signalling and the control of meiotic entry in the human fetal gonad. *PLoS ONE* **6**, e20249.

Choe, C.-U., Nabuurs, C., Stockebrand, M. C., Neu, A., Nunes, P., Morellini, F., Sauter, K., Schillemeit, S., Hermans-Borgmeyer, I., Marescau, B., et al. (2013). L-arginine:glycine amidinotransferase deficiency protects from metabolic syndrome. *Hum. Mol. Genet.* **22**, 110–123.

Christensen, A. K. and Gillim, S. W. (1969). *The correlation of fine structure and function in steroid-secreting cells, with emphasis on those of the gonads*. The gonads.

Chuang, P.-T., Kawcak, T. and McMahon, A. P. (2003). Feedback control of mammalian Hedgehog signaling by the Hedgehog-binding protein, Hip1, modulates Fgf signaling during branching morphogenesis of the lung. *Genes Dev.* **17**, 342–347.

Clark, A. M., Garland, K. K. and Russell, L. D. (2000). Desert hedgehog (Dhh) Gene Is Required in the Mouse Testis for Formation of Adult-Type Leydig Cells and Normal Development of Peritubular Cells and Seminiferous Tubules. *Biol. Reprod.* **63**, 1825–1838.

Clepet, C., Schafer, A. J., Sinclair, A. H., Palmer, M. S., Lovell-Badge, R. and Goodfellow, P. N. (1993). The human SRY transcript. *Hum. Mol. Genet.* **2**, 2007–2012.

Coffey, P. J., Gias, C., McDermott, C. J., Lundh, P., Pickering, M. C., Sethi, C., Bird, A., Fitzke, F. W., Maass, A., Chen, L. L., et al. (2007). Complement factor H deficiency in aged mice causes retinal abnormalities and

visual dysfunction. *P.N.A.S* **104**, 16651–16656.

Cole, L. W., Sidis, Y., Zhang, C., Quinton, R., Plummer, L., Pignatelli, D., Hughes, V. A., Dwyer, A. A., Raivio, T., Hayes, F. J., et al. (2008). Mutations in prokineticin 2 and prokineticin receptor 2 genes in human gonadotrophin-releasing hormone deficiency: molecular genetics and clinical spectrum. *J. Clin. Endocrinol. Metab.* **93**, 3551–3559.

Colvin, J. S., Bohne, B. A., Harding, G. W., McEwen, D. G. and Ornitz, D. M. (1996). Skeletal overgrowth and deafness in mice lacking fibroblast growth factor receptor 3. *Nat. Genet.* **12**, 390–397.

Colvin, J. S., Feldman, B., Nadeau, J. H., Goldfarb, M. and Ornitz, D. M. (1999). Genomic organization and embryonic expression of the mouse fibroblast growth factor 9 gene. *Dev. Dyn.* **216**, 72–88.

Colvin, J. S., Green, R. P., Schmahl, J., Capel, B. and Ornitz, D. M. (2001). Male-to-Female Sex Reversal in Mice Lacking Fibroblast Growth Factor 9. *Cell* **104**, 875–889.

Combes, A. N., Lesieur, E., Harley, V. R., Sinclair, A. H., Little, M. H., Wilhelm, D. and Koopman, P. (2009a). Three-dimensional visualization of testis cord morphogenesis, a novel tubulogenic mechanism in development. *Dev. Dyn.* **238**, 1033–1041.

Combes, A. N., Spiller, C. M., Harley, V. R., Sinclair, A. H., Dunwoodie, S. L., Wilhelm, D. and Koopman, P. (2010). Gonadal defects in Cited2-mutant mice indicate a role for SF1 in both testis and ovary differentiation. *Int. J. Dev. Biol.* **54**, 683–689.

Combes, A. N., Wilhelm, D., Davidson, T., Dejana, E., Harley, V., Sinclair, A. and Koopman, P. (2009b). Endothelial cell migration directs testis cord formation. *Dev. Biol.* **326**, 112–120.

Conover, C. A., Boldt, H. B., Bale, L. K., Clifton, K. B., Grell, J. A., Mader, J. R., Mason, E. J. and Powell, D. R. (2011). Pregnancy-associated plasma protein-A2 (PAPP-A2): tissue expression and biological consequences of gene knockout in mice. *Endocrinology* **152**, 2837–2844.

Cool, J., Carmona, F. D., Szucsik, J. C. and Capel, B. (2008). Peritubular myoid cells are not the migrating population required for testis cord formation in the XY gonad. *Sex. Dev.* **2**, 128–133.

Cool, J., DeFalco, T. J. and Capel, B. (2011). Vascular-mesenchymal cross-talk through Vegf and Pdgf drives organ patterning. *Proc. Natl. Acad. Sci. U. S. A.* **108**, 167–172.

Correa, R. V., Domenice, S., Bingham, N. C., Billerbeck, A. E., Rainey, W. E., Parker, K. L. and Mendonca, B. B. (2004). A microdeletion in the ligand binding domain of human steroidogenic factor 1 causes XY sex reversal without adrenal insufficiency. *J. Clin. Endocrinol. Metab.* **89**, 1767–1772.

Coutant, R., Mallet, D., Lahlou, N., Bouhours-Nouet, N., Guichet, A., Coupris, L., Croue, A. and Morel, Y. (2007). Heterozygous mutation of steroidogenic factor-1 in 46,XY subjects may mimic partial androgen insensitivity syndrome. *J. Clin. Endocrinol. Metab.* **92**, 2868–2873.

Coveney, D., Cool, J., Oliver, T. and Capel, B. (2008a). Four-dimensional analysis of vascularization during primary development of an organ, the gonad. *Proc. Natl. Acad. Sci. U. S. A.* **105**, 7212–7217.

Coveney, D., Ross, A. J., Slone, J. D. and Capel, B. (2008b). A microarray analysis of the XX Wnt4 mutant gonad targeted at the identification of genes involved in testis vascular differentiation. *Gene Expr. Patterns* **8**, 529–537.

Cox, P. R., Fowler, V., Xu, B., Sweatt, J. D., Paylor, R. and Zoghbi, H. Y. (2003). Mice lacking Tropomodulin-2 show enhanced long-term potentiation, hyperactivity, and deficits in learning and memory. *Mol. Cell. Neurosci.* **23**, 1–12.

Cox, S., Smith, L., Bogani, D., Cheeseman, M., Siggers, P. and Greenfield, A. (2006). Sexually dimorphic expression of secreted frizzled-related (SFRP) genes in the developing mouse Müllerian duct. *Mol. Reprod. Dev.* **73**, 1008–1016.

Crawford, P. A., Dorn, C., Sadovsky, Y. and Milbrandt, J. (1998). Nuclear receptor DAX-1 recruits nuclear receptor

corepressor N-CoR to steroidogenic factor 1. *Mol. Cell. Biol.* **18**, 2949–2956.

Crisponi, L., Deiana, M., Loi, A., Chiappe, F., Uda, M., Amati, P., Bisceglia, L., Zelante, L., Nagaraja, R., Porcu, S., et al. (2001). The putative forkhead transcription factor FOXL2 is mutated in blepharophimosis/ptosis/epicanthus inversus syndrome. *Nat. Genet.* **27**, 159–166.

Cui, S., Ross, A., Stallings, N., Parker, K. L., Capel, B. and Quaggin, S. E. (2004). Disrupted gonadogenesis and male-to-female sex reversal in Pod1 knockout mice. *Development* **131**, 4095–4105.

Cupp, A. S., Dufour, J. M., Kim, G., Skinner, M. K. and Kim, K. H. (1999). Action of retinoids on embryonic and early postnatal testis development. *Endocrinology* **140**, 2343–2352.

Daneau, I., Pilon, N., Boyer, A., Behdjani, R., Overbeek, P. A., Viger, R., Lussier, J. and Silversides, D. W. (2002). The porcine SRY promoter is transactivated within a male genital ridge environment. *Genesis* **33**, 170–180.

De Baere, E., Beysen, D., Oley, C., Lorenz, B., Cocquet, J., De Sutter, P., Devriendt, K., Dixon, M., Fellous, M., Fryns, J.-P., et al. (2003). FOXL2 and BPES: mutational hotspots, phenotypic variability, and revision of the genotype-phenotype correlation. *Am. J. Hum. Genet.* **72**, 478–487.

De Baere, E., Dixon, M. J., Small, K. W., Jabs, E. W., Leroy, B. P., Devriendt, K., Gillerot, Y., Mortier, G., Meire, F., Van Maldergem, L., et al. (2001). Spectrum of FOXL2 gene mutations in blepharophimosis-ptosis-epicanthus inversus (BPES) families demonstrates a genotype--phenotype correlation. *Hum. Mol. Genet.* **10**, 1591–1600.

Dean, C. H., Miller, L.-A. D., Smith, A. N., Dufort, D., Lang, R. A. and Niswander, L. A. (2005). Canonical Wnt signaling negatively regulates branching morphogenesis of the lung and lacrimal gland. *Dev. Biol.* **286**, 270–286.

DeFalco, T., Bhattacharya, I., Williams, A. V., Sams, D. M. and Capel, B. (2014). Yolk-sac-derived macrophages regulate fetal testis vascularization and morphogenesis. *Proc. Natl. Acad. Sci. U. S. A.* **111**, E2384–93.

Defalco, T., Saraswathula, A., Briot, A., Iruela-Arispe, M. L. and Capel, B. (2013). Testosterone levels influence mouse fetal leydig cell progenitors through notch signaling. *Biol. Reprod.* **88**, 91.

DeFalco, T., Takahashi, S. and Capel, B. (2011). Two distinct origins for Leydig cell progenitors in the fetal testis. *Dev. Biol.* **In Press, Corrected Proof**.

Deng, C., Bedford, M., Li, C., Xu, X., Yang, X., Dunmore, J. and Leder, P. (1997). Fibroblast growth factor receptor-1 (FGFR-1) is essential for normal neural tube and limb development. *Dev. Biol.* **185**, 42–54.

Deng, C., Wynshaw-Boris, A., Zhou, F., Kuo, A. and Leder, P. (1996). Fibroblast growth factor receptor 3 is a negative regulator of bone growth. *Cell* **84**, 911–921.

Di Giovanni, V., Alday, A., Chi, L., Mishina, Y. and Rosenblum, N. D. (2011). Alk3 controls nephron number and androgen production via lineage-specific effects in intermediate mesoderm. *Development* **138**, 2717–2727.

Diez-Roux, G., Banfi, S., Sultan, M., Geffers, L., Anand, S., Rozado, D., Magen, A., Canidio, E., Pagani, M., Peluso, I., et al. (2011). A High-Resolution Anatomical Atlas of the Transcriptome in the Mouse Embryo. *PLoS Biol.* **9**, e1000582.

Dobyns, W. B., Berry-Kravis, E., Havernick, N. J., Holden, K. R. and Viskochil, D. (1999). X-linked lissencephaly with absent corpus callosum and ambiguous genitalia. *Am. J. Med. Genet.* **86**, 331–337.

Dode, C. and Hardelin, J. P. (2009). Kallmann syndrome. *Eur. J. Hum. Genet.* **17**, 139–146.

Dode, C., Teixeira, L., Levilliers, J., Fouveaut, C., Bouchard, P., Kottler, M. L., Lespinasse, J., Lienhardt-Roussie, A., Mathieu, M., Moerman, A., et al. (2006). Kallmann syndrome: mutations in the genes encoding prokineticin-2 and prokineticin receptor-2. *PLoS Genet.* **2**, 1648–1652.

Dodé, C., Levilliers, J., Dupont, J.-M., De Paepe, A., Le Dû, N., Soussi-Yanicostas, N., Coimbra, R. S.,

Delmaghani, S., Compain-Nouaille, S., Baverel, F., et al. (2003). Loss-of-function mutations in FGFR1 cause autosomal dominant Kallmann syndrome. *Nat. Genet.* **33**, 463–465.

Dubois, C. L., Shih, H.-P., Seymour, P. A., Patel, N. A., Behrmann, J. M., Ngo, V. and Sander, M. (2011). Sox9-haploinsufficiency causes glucose intolerance in mice. *PLoS ONE* **6**, e23131.

Eisen, J. S. and Smith, J. C. (2008). Controlling morpholino experiments: don't stop making antisense. *Development* **135**, 1735–1743.

El-Gehani, F., Zhang, F. P., Pakarinen, P., Rannikko, A. and Huhtaniemi, I. (1998). Gonadotropin-independent regulation of steroidogenesis in the fetal rat testis. *Biol. Reprod.* **58**, 116–123.

Falardeau, J., Chung, W. C. J., Beenken, A., Raivio, T., Plummer, L., Sidis, Y., Jacobson-Dickman, E. E., Eliseenkova, A. V., Ma, J., Dwyer, A., et al. (2008). Decreased FGF8 signaling causes deficiency of gonadotropin-releasing hormone in humans and mice. *J Clin Invest* **118**, 2822–2831.

Fan, X., Molotkov, A., Manabe, S.-I., Donmoyer, C. M., Deltour, L., Foglio, M. H., Cuenca, A. E., Blaner, W. S., Lipton, S. A. and Duester, G. (2003). Targeted disruption of Aldh1a1 (Raldh1) provides evidence for a complex mechanism of retinoic acid synthesis in the developing retina. *Mol. Cell. Biol.* **23**, 4637–4648.

Fatchiyah, Zubair, M., Shima, Y., Oka, S., Ishihara, S., Fukui-Katoh, Y. and Morohashi, K. (2006). Differential gene dosage effects of Ad4BP/SF-1 on target tissue development. *Biochem. Biophys. Res. Commun.* **341**, 1036–1045.

Feng, C.-W., Bowles, J. and Koopman, P. (2014). Control of mammalian germ cell entry into meiosis. *Mol. Cell. Endocrinol.* **382**, 488–497.

Ferraz-de-Souza, B., Lin, L. and Achermann, J. C. (2011). Steroidogenic factor-1 (SF-1, NR5A1) and human disease. *Mol. Cell. Endocrinol.* **336**, 198–205.

Foster, J. W., Dominguez-Steglich, M. A., Guioli, S., Kwok, C., Weller, P. A., Stevanovic, M., Weissenbach, J., Mansour, S., Young, I. D., Goodfellow, P. N., et al. (1994). Campomelic dysplasia and autosomal sex reversal caused by mutations in an SRY-related gene. *Nature* **372**, 525–530.

França, M. M., Ferraz-de-Souza, B., Santos, M. G., Lerario, A. M., Fragoso, M. C. B. V., Latronico, A. C., Kuick, R. D., Hammer, G. D. and Lotfi, C. F. P. (2013). POD-1 binding to the E-box sequence inhibits SF-1 and StAR expression in human adrenocortical tumor cells. *Mol. Cell. Endocrinol.* **371**, 140–147.

Gao, L., Kim, Y., Kim, B., Lofgren, S. M., Schultz-Norton, J. R., Nardulli, A. M., Heckert, L. L. and Jorgensen, J. S. (2011). Two regions within the proximal steroidogenic factor 1 promoter drive somatic cell-specific activity in developing gonads of the female mouse. *Biol. Reprod.* **84**, 422–434.

Geissler, W. M., Davis, D. L., Wu, L., Bradshaw, K. D., Patel, S., Mendonca, B. B., Elliston, K. O., Wilson, J. D., Russell, D. W. and Andersson, S. (1994). Male pseudohermaphroditism caused by mutations of testicular 17β–hydroxysteroid dehydrogenase 3. *Nat. Genet.* **7**, 34–39.

Gianetti, E., Tusset, C., Noel, S. D., Au, M. G., Dwyer, A. A., Hughes, V. A., Abreu, A. P., Carroll, J., Trarbach, E., Silveira, L. F. G., et al. (2010). TAC3/TACR3 mutations reveal preferential activation of gonadotropin-releasing hormone release by neurokinin B in neonatal life followed by reversal in adulthood. *J. Clin. Endocrinol. Metab.* **95**, 2857–2867.

Glasson, S. S., Askew, R., Sheppard, B., Carito, B., Blanchet, T., Ma, H.-L., Flannery, C. R., Peluso, D., Kanki, K., Yang, Z., et al. (2005). Deletion of active ADAMTS5 prevents cartilage degradation in a murine model of osteoarthritis. *Nature* **434**, 644–648.

Gnessi, L., Emidi, A., Jannini, E. A., Carosa, E., Maroder, M., Arizzi, M., Ulisse, S. and Spera, G. (1995). Testicular development involves the spatiotemporal control of PDGFs and PDGF receptors gene expression and action. *J. Cell Biol.* **131**, 1105–1121.

Gnessi, L., Fabbri, A. and Spera, G. (1997). Gonadal peptides as mediators of development and functional control of

the testis: an integrated system with hormones and local environment. *Endocr. Rev.* **18**, 541–609.

Gonzalez-Brito, M. R. and Bixby, J. L. (2009). Protein tyrosine phosphatase receptor type O regulates development and function of the sensory nervous system. *Mol. Cell. Neurosci.* **42**, 458–465.

Grieshammer, U., Le Ma, Plump, A. S., Wang, F., Tessier-Lavigne, M. and Martin, G. R. (2004). SLIT2-mediated ROBO2 signaling restricts kidney induction to a single site. *Dev. Cell* **6**, 709–717.

Grimmond, S., Van Hateren, N., Siggers, P., Arkell, R., Larder, R., Soares, M. B., de Fatima Bonaldo, M., Smith, L., Tymowska-Lalanne, Z., Wells, C., et al. (2000). Sexually dimorphic expression of protease nexin-1 and vanin-1 in the developing mouse gonad prior to overt differentiation suggests a role in mammalian sexual development. *Hum. Mol. Genet.* **9**, 1553–1560.

Griswold, S. L. and Behringer, R. R. (2009). Fetal Leydig Cell Origin and Development. *Sex. Dev.* **3**, 1–15.

Gross, I., Morrison, D. J., Hyink, D. P., Georgas, K., English, M. A., Mericskay, M., Hosono, S., Sassoon, D., Wilson, P. D., Little, M., et al. (2003). The receptor tyrosine kinase regulator Sprouty1 is a target of the tumor suppressor WT1 and important for kidney development. *J. Biol. Chem.* **278**, 41420–41430.

Gubbay, J., Collignon, J., Koopman, P., Capel, B., Economou, A., Munsterberg, A., Vivian, N., Goodfellow, P. and Lovell-Badge, R. (1990). A gene mapping to the sex-determining region of the mouse Y chromosome is a member of a novel family of embryonically expressed genes. *Nature* **346**, 245–250.

Gupta, P., Soyombo, A. A., Atashband, A., Wisniewski, K. E., Shelton, J. M., Richardson, J. A., Hammer, R. E. and Hofmann, S. L. (2001). Disruption of PPT1 or PPT2 causes neuronal ceroid lipofuscinosis in knockout mice. *P.N.A.S* **98**, 13566–13571.

Gurtner, G. C., Davis, V., Li, H., McCoy, M. J., Sharpe, A. and Cybulsky, M. I. (1995). Targeted disruption of the murine VCAM1 gene: essential role of VCAM-1 in chorioallantoic fusion and placentation. *Genes Dev.* **9**, 1–14.

Habert, R. and Picon, R. (1984). Testosterone, dihydrotestosterone and estradiol-17[beta] levels in maternal and fetal plasma and in fetal testes in the rat. *J. Steroid Biochem.* **21**, 193–198.

Hacker, A., Capel, B., Goodfellow, P. and Lovell-Badge, R. (1995). Expression of Sry, the mouse sex determining gene. *Development* **121**, 1603–1614.

Hajkova, P., Ancelin, K., Waldmann, T., Lacoste, N., Lange, U. C., Cesari, F., Lee, C., Almouzni, G., Schneider, R. and Surani, M. A. (2008). Chromatin dynamics during epigenetic reprogramming in the mouse germ line. *Nature* **452**, 877–881.

Halvorson, L. M. (2014). PACAP modulates GnRH signaling in gonadotropes. *Mol. Cell. Endocrinol.* **385**, 45–55.

Hardelin, J. P. and Dode, C. (2008). The complex genetics of Kallmann syndrome: KAL1, FGFR1, FGF8, PROKR2, PROK2, et al. *Sex. Dev.* **2**, 181–193.

Hartwig, S., Ho, J., Pandey, P., Macisaac, K., Taglienti, M., Xiang, M., Alterovitz, G., Ramoni, M., Fraenkel, E. and Kreidberg, J. A. (2010). Genomic characterization of Wilms' tumor suppressor 1 targets in nephron progenitor cells during kidney development. *Development* **137**, 1189–1203.

Hasegawa, K., Chuma, S., Tada, T., Sakurai, T., Tamura, M., Suemori, H. and Nakatsuji, N. (2006). Testatin transgenic and knockout mice exhibit normal sex-differentiation. *Biochem. Biophys. Res. Commun.* **341**, 369–375.

Hasegawa, T., Fukami, M., Sato, N., Katsumata, N., Sasaki, G., Fukutani, K., Morohashi, K. and Ogata, T. (2004). Testicular dysgenesis without adrenal insufficiency in a 46,XY patient with a heterozygous inactive mutation of steroidogenic factor-1. *J. Clin. Endocrinol. Metab.* **89**, 5930–5935.

Hatano, O., Takayama, K., Imai, T., Waterman, M. R., Takakusu, A., Omura, T. and Morohashi, K. (1994). Sex-dependent expression of a transcription factor, Ad4BP, regulating steroidogenic P-450 genes in the gonads during prenatal and postnatal rat development. *Development* **120**, 2787–2797.

Hazra, R., Jimenez, M., Desai, R., Handelsman, D. J. and Allan, C. M. (2013). Sertoli cell androgen receptor expression regulates temporal fetal and adult Leydig cell differentiation, function, and population size. *Endocrinology* **154**, 3410–3422.

Heikkila, M., Prunskaite, R., Naillat, F., Itaranta, P., Vuoristo, J., Leppaluoto, J., Peltoketo, H. and Vainio, S. (2005). The partial female to male sex reversal in Wnt-4-deficient females involves induced expression of testosterone biosynthetic genes and testosterone production, and depends on androgen action. *Endocrinology* **146**, 4016–4023.

Hines, L. M., Hoffman, P. L., Bhave, S., Saba, L., Kaiser, A., Snell, L., Goncharov, I., LeGault, L., Dongier, M., Grant, B., et al. (2006). A sex-specific role of type VII adenylyl cyclase in depression. *J. Neurosci.* **26**, 12609–12619.

Hirai, H., Pang, Z., Bao, D., Miyazaki, T., Li, L., Miura, E., Parris, J., Rong, Y., Watanabe, M., Yuzaki, M., et al. (2005). Cbln1 is essential for synaptic integrity and plasticity in the cerebellum. *Nat. Neurosci.* **8**, 1534–1541.

Hirai, S., Naito, M., Terayama, H., Qu, N., Kuerban, M., Musha, M., Ikeda, A., Miura, M. and Itoh, M. (2012). The origin of lymphatic capillaries in murine testes. *J. Androl.* **33**, 745–751.

Hiramatsu, R., Harikae, K., Tsunekawa, N., Kurohmaru, M., Matsuo, I. and Kanai, Y. (2010). FGF signaling directs a center-to-pole expansion of tubulogenesis in mouse testis differentiation. *Development* **137**, 303–312.

Hsu, P. D., Lander, E. S. and Zhang, F. (2014). Development and Applications of CRISPR-Cas9 for Genome Engineering. *Cell* **157**, 1262–1278.

Huang, D. W., Sherman, B. T. and Lempicki, R. A. (2009a). Bioinformatics enrichment tools: paths toward the comprehensive functional analysis of large gene lists. *Nucl. Acids Res.* **37**, 1–13.

Huang, D. W., Sherman, B. T. and Lempicki, R. A. (2009b). Systematic and integrative analysis of large gene lists using DAVID bioinformatics resources. *Nat Protoc* **4**, 44–57.

Huang, X. Z., Wu, J. F., Ferrando, R., Lee, J. H., Wang, Y. L., Farese, R. V., Jr and Sheppard, D. (2000). Fatal bilateral chylothorax in mice lacking the integrin alpha9beta1. *Mol. Cell. Biol.* **20**, 5208–5215.

Huhtaniemi, I. and Pelliniemi, L. J. (1992). Fetal Leydig cells: cellular origin, morphology, life span, and special functional features. *Proc. Soc. Exp. Biol. Med.* **201**, 125–140.

Huszar, D., Lynch, C. A., Fairchild-Huntress, V., Dunmore, J. H., Fang, Q., Berkemeier, L. R., Gu, W., Kesterson, R. A., Boston, B. A., Cone, R. D., et al. (1997). Targeted disruption of the melanocortin-4 receptor results in obesity in mice. *Cell* **88**, 131–141.

Hutson, J. C. (1990). Changes in the concentration and size of testicular macrophages during development. *Biol. Reprod.* **43**, 885–890.

Ikeda, Y., Lala, D. S., Luo, X., Kim, E., Moisan, M. P. and Parker, K. L. (1993). Characterization of the mouse FTZ-F1 gene, which encodes a key regulator of steroid hydroxylase gene expression. *Mol. Endocrinol.* **7**, 852–860.

Ikeda, Y., Luo, X., Abbud, R., Nilson, J. H. and Parker, K. L. (1995). The nuclear receptor steroidogenic factor 1 is essential for the formation of the ventromedial hypothalamic nucleus. *Mol. Endocrinol.* **9**, 478–486.

Ikeda, Y., Shen, W. H., Ingraham, H. A. and Parker, K. L. (1994). Developmental expression of mouse steroidogenic factor-1, an essential regulator of the steroid hydroxylases. *Mol. Endocrinol.* **8**, 654–662.

Ingham, P. W. and McMahon, A. P. (2001). Hedgehog signaling in animal development: paradigms and principles. *Genes Dev.* **15**, 3059–3087.

Ingraham, H. A., Lala, D. S., Ikeda, Y., Luo, X., Shen, W. H., Nachtigal, M. W., Abbud, R., Nilson, J. H. and Parker, K. L. (1994). The nuclear receptor steroidogenic factor 1 acts at multiple levels of the reproductive axis. *Genes Dev.* **8**, 2302–2312.

Ivell, R., Wade, J. D. and Anand-Ivell, R. (2013). INSL3 as a biomarker of Leydig cell functionality. *Biol. Reprod.* **88**, 147–147.

Jadeja, S., Smyth, I., Pitera, J. E., Taylor, M. S., van Haelst, M., Bentley, E., McGregor, L., Hopkins, J., Chalepakis, G., Philip, N., et al. (2005). Identification of a new gene mutated in Fraser syndrome and mouse myelencephalic blebs. *Nat. Genet.* **37**, 520–525.

Jadhav, U. and Jameson, J. L. (2011). Steroidogenic factor-1 (SF-1)-driven differentiation of murine embryonic stem (ES) cells into a gonadal lineage. *Endocrinology* **152**, 2870–2882.

Jager, R. J., Anvret, M., Hall, K. and Scherer, G. (1990). A human XY female with a frame shift mutation in the candidate testis-determining gene SRY. *Nature* **348**, 452–454.

Jameson, S. A., Lin, Y.-T. and Capel, B. (2012a). Testis development requires the repression of Wnt4 by Fgf signaling. *Dev. Biol.* **370**, 24–32.

Jameson, S. A., Natarajan, A., Cool, J., Defalco, T., Maatouk, D. M., Mork, L., Munger, S. C. and Capel, B. (2012b). Temporal transcriptional profiling of somatic and germ cells reveals biased lineage priming of sexual fate in the fetal mouse gonad. *PLoS Genet.* **8**, e1002575.

Japon, M. A., Rubinstein, M. and Low, M. J. (1994). In situ hybridization analysis of anterior pituitary hormone gene expression during fetal mouse development. *J. Histochem. Cytochem.* **42**, 1117–1125.

Jeays-Ward, K., Dandonneau, M. and Swain, A. (2004). Wnt4 is required for proper male as well as female sexual development. *Dev. Biol.* **276**, 431–440.

Jeays-Ward, K., Hoyle, C., Brennan, J., Dandonneau, M., Alldus, G., Capel, B. and Swain, A. (2003). Endothelial and steroidogenic cell migration are regulated by WNT4 in the developing mammalian gonad. *Development* **130**, 3663–3670.

Jeske, Y. W., Bowles, J., Greenfield, A. and Koopman, P. (1995). Expression of a linear Sry transcript in the mouse genital ridge. *Nat. Genet.* **10**, 480–482.

Jordan, B. K., Mohammed, M., Ching, S. T., Délot, E., Chen, X. N., Dewing, P., Swain, A., Rao, P. N., Elejalde, B. R. and Vilain, E. (2001). Up-regulation of WNT-4 signaling and dosage-sensitive sex reversal in humans. *Am. J. Hum. Genet.* **68**, 1102–1109.

Jordan, B. K., Shen, J. H., Olaso, R., Ingraham, H. A. and Vilain, E. (2003). Wnt4 overexpression disrupts normal testicular vasculature and inhibits testosterone synthesis by repressing steroidogenic factor 1/beta-catenin synergy. *Proc. Natl. Acad. Sci. U. S. A.* **100**, 10866–10871.

Karl, J. and Capel, B. (1998). Sertoli Cells of the Mouse Testis Originate from the Coelomic Epithelium. *Dev. Biol.* **203**, 323–333.

Karpova, T., Maran, R. R., Presley, J., Scherrer, S. P., Tejada, L. and Heckert, L. L. (2005). Transgenic rescue of SF-1-null mice. *Ann. N. Y. Acad. Sci.* **1061**, 55–64.

Kashimada, K. and Koopman, P. (2010). Sry: the master switch in mammalian sex determination. *Development* **137**, 3921–3930.

Kidd, T., Brose, K., Mitchell, K. J., Fetter, R. D., Tessier-Lavigne, M., Goodman, C. S. and Tear, G. (1998). Roundabout controls axon crossing of the CNS midline and defines a novel subfamily of evolutionarily conserved guidance receptors. *Cell* **92**, 205–215.

Kilcoyne, K. R., Smith, L. B., Atanassova, N., Macpherson, S., McKinnell, C., van den Driesche, S., Jobling, M. S., Chambers, T. J. G., De Gendt, K., Verhoeven, G., et al. (2014). Fetal programming of adult Leydig cell function by androgenic effects on stem/progenitor cells. *Proc. Natl. Acad. Sci. U. S. A.* **111**, E1924–32.

Kim, D., Pertea, G., Trapnell, C., Pimentel, H., Kelley, R. and Salzberg, S. L. (2013). TopHat2: accurate alignment of transcriptomes in the presence of insertions, deletions and gene fusions. *Genome Biol.* **14**, R36.

Kim, Y., Bingham, N., Sekido, R., Parker, K. L., Lovell-Badge, R. and Capel, B. (2007). Fibroblast growth factor receptor 2 regulates proliferation and Sertoli differentiation during male sex determination. *Proc. Natl. Acad. Sci. U. S. A.* **104**, 16558–16563.

Kim, Y., Kobayashi, A., Sekido, R., DiNapoli, L., Brennan, J., Chaboissier, M. C., Poulat, F., Behringer, R. R., Lovell-Badge, R. and Capel, B. (2006). Fgf9 and Wnt4 act as antagonistic signals to regulate mammalian sex determination. *PLoS Biol.* **4**, e187.

Kitamura, K., Yanazawa, M., Sugiyama, N., Miura, H., Iizuka-Kogo, A., Kusaka, M., Omichi, K., Suzuki, R., Kato-Fukui, Y., Kamiirisa, K., et al. (2002). Mutation of ARX causes abnormal development of forebrain and testes in mice and X-linked lissencephaly with abnormal genitalia in humans. *Nat. Genet.* **32**, 359–369.

Knauff, E. A. H., Franke, L., van Es, M. A., van den Berg, L. H., van der Schouw, Y. T., Laven, J. S. E., Lambalk, C. B., Hoek, A., Goverde, A. J., Christin-Maitre, S., et al. (2009). Genome-wide association study in premature ovarian failure patients suggests ADAMTS19 as a possible candidate gene. *Hum. Reprod.* **24**, 2372–2378.

Knebelmann, B., Boussin, L., Guerrier, D., Legeai, L., Kahn, A., Josso, N. and Picard, J. Y. (1991). Anti-Müllerian hormone Bruxelles: a nonsense mutation associated with the persistent Müllerian duct syndrome. *P.N.A.S* **88**, 3767–3771.

Koopman, P., Gubbay, J., Vivian, N., Goodfellow, P. and Lovell-Badge, R. (1991). Male development of chromosomally female mice transgenic for Sry. *Nature* **351**, 117–121.

Koopman, P., Munsterberg, A., Capel, B., Vivian, N. and Lovell-Badge, R. (1990). Expression of a candidate sex-determining gene during mouse testis differentiation. *Nature* **348**, 450–452.

Koubova, J., Menke, D. B., Zhou, Q., Capel, B., Griswold, M. D. and Page, D. C. (2006). Retinoic acid regulates sex-specific timing of meiotic initiation in mice. *Proc. Natl. Acad. Sci. U. S. A.* **103**, 2474–2479.

Köhler, B., Lin, L., Ferraz-de-Souza, B., Wieacker, P., Heidemann, P., Schröder, V., Biebermann, H., Schnabel, D., Grüters, A. and C, A. J. (2008). Five novel mutations in steroidogenic factor 1 (SF1, NR5A1) in 46,XY patients with severe underandrogenization but without adrenal insufficiency. *Hum. Mutat.* **29**, 59–64.

Krishnan, V., Elberg, G., Tsai, M. J. and Tsai, S. Y. (1997a). Identification of a novel sonic hedgehog response element in the chicken ovalbumin upstream promoter-transcription factor II promoter. *Mol. Endocrinol.* **11**, 1458–1466.

Krishnan, V., Pereira, F. A., Qiu, Y., Chen, C. H., Beachy, P. A., Tsai, S. Y. and Tsai, M. J. (1997b). Mediation of Sonic hedgehog-induced expression of COUP-TFII by a protein phosphatase. *Science* **278**, 1947–1950.

Kumar, S., Chatzi, C., Brade, T., Cunningham, T. J., Zhao, X. and Duester, G. (2011). Sex-specific timing of meiotic initiation is regulated by Cyp26b1 independent of retinoic acid signalling. *Nat Commun* **2**, 151.

Lahr, G., Maxson, S. C., Mayer, A., Just, W., Pilgrim, C. and Reisert, I. (1995). Transcription of the Y chromosomal gene, Sry, in adult mouse brain. *Brain Res. Mol. Brain Res.* **33**, 179–182.

Lapatto, R., Pallais, J. C., Zhang, D., Chan, Y.-M., Mahan, A., Cerrato, F., Le, W. W., Hoffman, G. E. and Seminara, S. B. (2007). Kiss1-/- mice exhibit more variable hypogonadism than Gpr54-/- mice. *Endocrinology* **148**, 4927–4936.

Larney, C., Bailey, T. L. and Koopman, P. (2014). Switching on sex: transcriptional regulation of the testis-determining gene Sry. *Development* **141**, 2195–2205.

Law, C. W., Chen, Y., Shi, W. and Smyth, G. K. (2014). voom: Precision weights unlock linear model analysis tools for RNA-seq read counts. *Genome Biol.* **15**, R29.

Le Bouffant, R., Guerquin, M. J., Duquenne, C., Frydman, N., Coffigny, H., Rouiller-Fabre, V., Frydman, R., Habert, R. and Livera, G. (2010). Meiosis initiation in the human ovary requires intrinsic retinoic acid synthesis. *Hum. Reprod.* **25**, 2579–2590.

Lee, C. Y., Lee, S. M., Lewis, S. and Johnson, F. M. (1980). Identification and biochemical analysis of mouse mutants deficient in cytoplasmic malic enzyme. *Biochemistry (Mosc.)* **19**, 5098–5103.

Lin, L., Gu, W. X., Ozisik, G., To, W. S., Owen, C. J., Jameson, J. L. and Achermann, J. C. (2006). Analysis of DAX1 (NR0B1) and steroidogenic factor-1 (NR5A1) in children and adults with primary adrenal failure: ten years' experience. *J. Clin. Endocrinol. Metab.* **91**, 3048–3054.

Lin, L., Philibert, P., Ferraz-de-Souza, B., Kelberman, D., Homfray, T., Albanese, A., Molini, V., Sebire, N. J., Einaudi, S., Conway, G. S., et al. (2007). Heterozygous missense mutations in steroidogenic factor 1 (SF1/Ad4BP, NR5A1) are associated with 46,XY disorders of sex development with normal adrenal function. *J. Clin. Endocrinol. Metab.* **92**, 991–999.

Liu, C. F., Bingham, N., Parker, K. and Yao, H. H. (2009). Sex-specific roles of beta-catenin in mouse gonadal development. *Hum. Mol. Genet.* **18**, 405–417.

Liu, Y., Kim, B. O., Kao, C., Jung, C., Dalton, J. T. and He, J. J. (2004). Tip110, the human immunodeficiency virus type 1 (HIV-1) Tat-interacting protein of 110 kDa as a negative regulator of androgen receptor (AR) transcriptional activation. *J. Biol. Chem.* **279**, 21766–21773.

Liu, Y., Li, J., Kim, B. O., Pace, B. S. and He, J. J. (2002). HIV-1 Tat protein-mediated transactivation of the HIV-1 long terminal repeat promoter is potentiated by a novel nuclear Tat-interacting protein of 110 kDa, Tip110. *J. Biol. Chem.* **277**, 23854–23863.

Loffler, K. A., Zarkower, D. and Koopman, P. (2003). Etiology of ovarian failure in blepharophimosis ptosis epicanthus inversus syndrome: FOXL2 is a conserved, early-acting gene in vertebrate ovarian development. *Endocrinology* **144**, 3237–3243.

Loo, B.-M. and Salmivirta, M. (2002). Heparin/Heparan sulfate domains in binding and signaling of fibroblast growth factor 8b. *J. Biol. Chem.* **277**, 32616–32623.

Lourenco, D., Brauner, R., Lin, L., De Perdigo, A., Weryha, G., Muresan, M., Boudjenah, R., Guerra-Junior, G., Maciel-Guerra, A. T., Achermann, J. C., et al. (2009). Mutations in NR5A1 associated with ovarian insufficiency. *N. Engl. J. Med.* **360**, 1200–1210.

Loveland, K. L., Hedger, M. P., Risbridger, G., Herszfeld, D. and De Kretser, D. M. (1993). Identification of receptor tyrosine kinases in the rat testis. *Mol. Reprod. Dev.* **36**, 440–447.

Loveland, K. L., Zlatic, K., Stein-Oakley, A., Risbridger, G. and deKretser, D. M. (1995). Platelet-derived growth factor ligand and receptor subunit mRNA in the Sertoli and Leydig cells of the rat testis. *Mol. Cell. Endocrinol.* **108**, 155–159.

Lovell-Badge, R. and Robertson, E. (1990). XY female mice resulting from a heritable mutation in the primary testis-determining gene, Tdy. *Development* **109**, 635–646.

Lu, B., Figini, M., Emanueli, C., Geppetti, P., Grady, E., Gerard, N., Ansell, J., Payan, D., Gerard, C. and Bunnett, N. (1997). The control of microvascular permeability and blood pressure by neutral endopeptidase. *Nat Med* **3**, 904–907.

Lu, Q., Gore, M., Zhang, Q., Camenisch, T., Boast, S., Casagranda, F., Lai, C., Skinner, M. K., Klein, R., Matsushima, G. K., et al. (1999). Tyro-3 family receptors are essential regulators of mammalian spermatogenesis. *Nature* **398**, 723–728.

LU, T. (2000). Molecular Basis for Feedback Regulation of Bile Acid Synthesis by Nuclear Receptors. *Molecular Cell* **6**, 507–515.

Lu, W., van Eerde, A. M., Fan, X., Quintero-Rivera, F., Kulkarni, S., Ferguson, H., Kim, H.-G., Fan, Y., Xi, Q., Li, Q.-G., et al. (2007). Disruption of ROBO2 Is Associated with Urinary Tract Anomalies and Confers Risk of Vesicoureteral Reflux. *The American Journal of Human Genetics* **80**, 616–632.

Ludbrook, L. M. and Harley, V. R. (2004). Sex determination: a "window" of DAX1 activity. *Trends in*

endocrinology and metabolism: TEM **15**, 116–121.

Lukyanenko, Carpenter, Boone, Baker, McGunegleHutson (2000). Specificity of a new lipid mediator produced by testicular and peritoneal macrophages on steroidogenesis. *Int. J. Androl.* **23**, 258–265.

Lukyanenko, Y. O., Chen, J. J. and Hutson, J. C. (2001). Production of 25-hydroxycholesterol by testicular macrophages and its effects on Leydig cells. *Biol. Reprod.*

Luo, X., Ikeda, Y. and Parker, K. L. (1994). A cell-specific nuclear receptor is essential for adrenal and gonadal development and sexual differentiation. *Cell* **77**, 481–490.

Ma, X., Dong, Y., Matzuk, M. M. and Kumar, T. R. (2004). Targeted disruption of luteinizing hormone beta-subunit leads to hypogonadism, defects in gonadal steroidogenesis, and infertility. *P.N.A.S* **101**, 17294–17299.

Maatouk, D. M., DiNapoli, L., Alvers, A., Parker, K. L., Taketo, M. M. and Capel, B. (2008). Stabilization of beta-catenin in XY gonads causes male-to-female sex-reversal. *Hum. Mol. Genet.* **17**, 2949–2955.

Maatouk, D. M., Mork, L., Hinson, A., Kobayashi, A., McMahon, A. P. and Capel, B. (2012). Germ cells are not required to establish the female pathway in mouse fetal gonads. *PLoS ONE* **7**, e47238.

MacLean, G., Li, H., Metzger, D., Chambon, P. and Petkovich, M. (2007). Apoptotic extinction of germ cells in testes of Cyp26b1 knockout mice. *Endocrinology* **148**, 4560–4567.

Magre, S. and Jost, A. (1980). The initial phases of testicular organogenesis in the rat. An electron microscopy study. *Arch. Anat. Microsc. Morphol. Exp.* **69**, 297–318.

Maier, E. M., Leitner, C., Lohrs, U. and Kuhnle, U. (2003). True hermaphroditism in an XY individual due to a familial point mutation of the SRY gene. *J. Pediatr. Endocrinol. Metab.* **16**, 575–580.

Mallet, D., Bretones, P., Michel-Calemard, L., Dijoud, F., David, M. and Morel, Y. (2004). Gonadal dysgenesis without adrenal insufficiency in a 46, XY patient heterozygous for the nonsense C16X mutation: a case of SF1 haploinsufficiency. *J. Clin. Endocrinol. Metab.* **89**, 4829–4832.

Manicone, A. M., Birkland, T. P., Lin, M., Betsuyaku, T., van Rooijen, N., Lohi, J., Keski-Oja, J., Wang, Y., Skerrett, S. J. and Parks, W. C. (2009). Epilysin (MMP-28) restrains early macrophage recruitment in Pseudomonas aeruginosa pneumonia. *J. Immunol.* **182**, 3866–3876.

Margarit, E., Coll, M. D., Oliva, R., Gomez, D., Soler, A. and Ballesta, F. (2000). SRY gene transferred to the long arm of the X chromosome in a Y-positive XX true hermaphrodite. *Am. J. Med. Genet.* **90**, 25–28.

Marguet, D., Baggio, L., Kobayashi, T., Bernard, A. M., Pierres, M., Nielsen, P. F., Ribel, U., Watanabe, T., Drucker, D. J. and Wagtmann, N. (2000). Enhanced insulin secretion and improved glucose tolerance in mice lacking CD26. *P.N.A.S* **97**, 6874–6879.

Marioni, J. C., Mason, C. E., Mane, S. M., Stephens, M. and Gilad, Y. (2008). RNA-seq: an assessment of technical reproducibility and comparison with gene expression arrays. *Genome Res.* **18**, 1509–1517.

Mark, M., Jacobs, H., Oulad-Abdelghani, M., Dennefeld, C., Féret, B., Vernet, N., Codreanu, C.-A., Chambon, P. and Ghyselinck, N. B. (2008). STRA8-deficient spermatocytes initiate, but fail to complete, meiosis and undergo premature chromosome condensation. *J. Cell. Sci.* **121**, 3233–3242.

Martin, L. J. and Tremblay, J. J. (2010). Nuclear receptors in Leydig cell gene expression and function. *Biol. Reprod.* **83**, 3–14.

Mastorakos, G., Pavlatou, M. G. and Mizamtsidi, M. (2006). The hypothalamic-pituitary-adrenal and the hypothalamic- pituitary-gonadal axes interplay. *Pediatr. Endocrinol. Rev.* **3 Suppl 1**, 172–181.

Matsumoto, S., Yamazaki, C., Masumoto, K., Nagano, M., Naito, M., Soga, T., Hiyama, H., Matsumoto, M., Takasaki, J., Kamohara, M., et al. (2006). Abnormal development of the olfactory bulb and reproductive system in mice lacking prokineticin receptor PKR2. *Proc. Natl. Acad. Sci. U. S. A.* **103**, 4140–4145.

Mayer, A., Lahr, G., Swaab, D. F., Pilgrim, C. and Reisert, I. (1998). The Y-chromosomal genes SRY and ZFY are transcribed in adult human brain. *Neurogenetics* **1**, 281–288.

McClelland, K., Bowles, J. and Koopman, P. (2012). Male sex determination: insights into molecular mechanisms. *Asian J. Androl.* **14**, 164–171.

McClive, P. J., Hurley, T. M., Sarraj, M. A., van den Bergen, J. A. and Sinclair, A. H. (2003). Subtractive hybridisation screen identifies sexually dimorphic gene expression in the embryonic mouse gonad. *Genesis* **37**, 84–90.

McDowell, E. N., Kisielewski, A. E., Pike, J. W., Franco, H. L., Yao, H. H. and Johnson, K. J. (2012). A transcriptome-wide screen for mRNAs enriched in fetal Leydig cells: CRHR1 agonism stimulates rat and mouse fetal testis steroidogenesis. *PLoS ONE* **7**, e47359.

McLaren, A. (2003). Primordial germ cells in the mouse. *Dev. Biol.* **262**, 1–15.

McLaren, A. and Southee, D. (1997). Entry of mouse embryonic germ cells into meiosis. *Dev. Biol.* **187**, 107–113.

Meeks, J. J., Crawford, S. E., Russell, T. A., Morohashi, K., Weiss, J. and Jameson, J. L. (2003a). Dax1 regulates testis cord organization during gonadal differentiation. *Development* **130**, 1029–1036.

Meeks, J. J., Weiss, J. and Jameson, J. L. (2003b). Dax1 is required for testis determination. *Nat. Genet.* **34**, 32–33.

Menke, D. B. and Page, D. C. (2002). Sexually dimorphic gene expression in the developing mouse gonad. *Gene Expr. Patterns* **2**, 359–367.

Meyer, D. and Birchmeier, C. (1995). Multiple essential functions of neuregulin in development. *Nature* **378**, 386–390.

Miller, S. C., Bowman, B. M. and Rowland, H. G. (1983). Structure, cytochemistry, endocytic activity, and immunoglobulin (Fc) receptors of rat testicular interstitial-tissue macrophages. *American Journal of Anatomy* **168**, 1–13.

Miraoui, H., Dwyer, A. A., Sykiotis, G. P., Plummer, L., Chung, W., Feng, B., Beenken, A., Clarke, J., Pers, T. H., Dworzynski, P., et al. (2013). Mutations in FGF17, IL17RD, DUSP6, SPRY4, and FLRT3 Are Identified in Individuals with Congenital Hypogonadotropic Hypogonadism. *The American Journal of Human Genetics* **92**, 725–743.

Mise, N., Fuchikami, T., Sugimoto, M., Kobayakawa, S., Ike, F., Ogawa, T., Tada, T., Kanaya, S., Noce, T. and Abe, K. (2008). Differences and similarities in the developmental status of embryo-derived stem cells and primordial germ cells revealed by global expression profiling. *Genes Cells* **13**, 863–877.

Mishina, Y., Rey, R., Finegold, M. J., Matzuk, M. M., Josso, N., Cate, R. L. and Behringer, R. R. (1996). Genetic analysis of the Müllerian-inhibiting substance signal transduction pathway in mammalian sexual differentiation. *Genes Dev.* **10**, 2577–2587.

Miura, H., Yanazawa, M., Kato, K. and Kitamura, K. (1997). Expression of a novel aristaless related homeobox gene “Arx” in the vertebrate telencephalon, diencephalon and floor plate. *Mech. Dev.* **65**, 99–109.

Miyabayashi, K., Katoh-Fukui, Y., Ogawa, H., Baba, T., Shima, Y., Sugiyama, N., Kitamura, K. and Morohashi, K. (2013). Aristaless related homeobox gene, Arx, is implicated in mouse fetal Leydig cell differentiation possibly through expressing in the progenitor cells. *PLoS ONE* **8**, e68050.

Monget, P., Bobe, J., Gougeon, A., Fabre, S., Monniaux, D. and Dalbies-Tran, R. (2012). The ovarian reserve in mammals: A functional and evolutionary perspective. *Mol. Cell. Endocrinol.* **356**, 2–12.

Moniot, B., Declosmenil, F., Barrionuevo, F., Scherer, G., Aritake, K., Malki, S., Marzi, L., Cohen-Solal, A., Georg, I., Klattig, J., et al. (2009). The PGD2 pathway, independently of FGF9, amplifies SOX9 activity in Sertoli cells during male sexual differentiation. *Development* **136**, 1813–1821.

Moniot, B., Farhat, A., Aritake, K., Declosmenil, F., Nef, S., Eguchi, N., Urade, Y., Poulat, F. and Boizet-Bonhoure, B. (2011). Hematopoietic prostaglandin D synthase (H-Pgds) is expressed in the early embryonic gonad and participates to the initial nuclear translocation of the SOX9 protein. *Dev. Dyn.* **240**, 2335–2343.

Moniot, B., Ujjan, S., Champagne, J., Hirai, H., Aritake, K., Nagata, K., Dubois, E., Nidelet, S., Nakamura, M., Urade, Y., et al. (2014). Prostaglandin D2 acts through the Dp2 receptor to influence male germ cell differentiation in the foetal mouse testis. *Development* **141**, 3561–3571.

Monyer, H., Burnashev, N., Laurie, D. J., Sakmann, B. and Seeburg, P. H. (1994). Developmental and regional expression in the rat brain and functional properties of four NMDA receptors. *Neuron* **12**, 529–540.

Monyer, H., Sprengel, R., Schoepfer, R., Herb, A., Higuchi, M., Lomeli, H., Burnashev, N., Sakmann, B. and Seeburg, P. H. (1992). Heteromeric NMDA receptors: molecular and functional distinction of subtypes. *Science* **256**, 1217–1221.

Morcos, P. A. (2007). Achieving targeted and quantifiable alteration of mRNA splicing with Morpholino oligos. *Biochem. Biophys. Res. Commun.* **358**, 521–527.

Morcos, P. A., Li, Y. and Jiang, S. (2008). Vivo-Morpholinos: a non-peptide transporter delivers Morpholinos into a wide array of mouse tissues. *Biotechniques* **45**, 613–614.

Mork, L., Maatouk, D. M., McMahon, J. A., Guo, J. J., Zhang, P., McMahon, A. P. and Capel, B. (2011). Temporal Differences in Granulosa Cell Specification in the Ovary Reflect Distinct Follicle Fates in Mice. *Biol. Reprod.*

Morohashi, K., Hatano, O., Nomura, M., Takayama, K., Hara, M., Yoshii, H., Takakusu, A. and Omura, T. (1995). Function and distribution of a steroidogenic cell-specific transcription factor, Ad4BP. *J. Steroid Biochem. Mol. Biol.* **53**, 81–88.

Morohashi, K., Tsuboi-Asai, H., Matsushita, S., Suda, M., Nakashima, M., Sasano, H., Hataba, Y., Li, C. L., Fukata, J., Irie, J., et al. (1999). Structural and functional abnormalities in the spleen of an mFtz-F1 gene-disrupted mouse. *Blood* **93**, 1586–1594.

Moulton, J. D. and Jiang, S. (2009). Gene knockdowns in adult animals: PPMOs and vivo-morpholinos. *Molecules* **14**, 1304–1323.

Murer, V., Spetz, J. F., Hengst, U., Altrogge, L. M., de Agostini, A. and Monard, D. (2001). Male fertility defects in mice lacking the serine protease inhibitor protease nexin-1. *P.N.A.S* **98**, 3029–3033.

Muscatelli, F., Strom, T. M., Walker, A. P., Zanaria, E., Recan, D., Meindl, A., Bardoni, B., Guioli, S., Zehetner, G., Rabl, W., et al. (1994). Mutations in the DAX-1 gene give rise to both X-linked adrenal hypoplasia congenita and hypogonadotropic hypogonadism. *Nature* **372**, 672–676.

Nagase, T., Seki, N., Tanaka, A., Ishikawa, K. and Nomura, N. (1995). Prediction of the coding sequences of unidentified human genes. IV. The coding sequences of 40 new genes (KIAA0121-KIAA0160) deduced by analysis of cDNA clones from human cell line KG-1. *DNA Res.* **2**, 167–74– 199–210.

Nagy, A. (2010). Visualizing Fetal Mouse Vasculature by India Ink Injection. *Cold Spring Harb Protoc* **2010**, pdb.prot5371–pdb.prot5371.

Nakamura, Y., Yamamoto, M. and Matsui, Y. (2002). Introduction and expression of foreign genes in cultured mouse embryonic gonads by electroporation. *Reprod. Fertil. Dev.* **14**, 259–265.

Nef, S., Schaad, O., Stallings, N. R., Cederroth, C. R., Pitetti, J. L., Schaer, G., Malki, S., Dubois-Dauphin, M., Boizet-Bonhoure, B., Descombes, P., et al. (2005). Gene expression during sex determination reveals a robust female genetic program at the onset of ovarian development. *Dev. Biol.* **287**, 361–377.

Nef, S., Shipman, T. and Parada, L. F. (2000). A molecular basis for estrogen-induced cryptorchidism. *Dev. Biol.* **224**, 354–361.

Nes, W. D., Lukyanenko, Y. O., Jia, Z. H. and Quideau, S. (2000). Identification of the Lipophilic Factor Produced by Macrophages That Stimulates Steroidogenesis 1. ....

Nieto, K., Pena, R., Palma, I., Dorantes, L. M., Erana, L., Alvarez, R., Garcia-Cavazos, R., Kofman-Alfaro, S. and Queipo, G. (2004). 45,X/47,XXX/47,XX, del(Y)(p?)/46,XX mosaicism causing true hermaphroditism. *Am. J. Med. Genet. A.* **130A**, 311–314.

Nordqvist, K. and Töhönen, V. (1997). An mRNA differential display strategy for cloning genes expressed during mouse gonad development. *Int. J. Dev. Biol.* **41**, 627–638.

O'Shaughnessy, P. J., Baker, P., Sohnius, U., Haavisto, A. M., Charlton, H. M. and Huhtaniemi, I. (1998). Fetal Development of Leydig Cell Activity in the Mouse Is Independent of Pituitary Gonadotroph Function. *Endocrinology* **139**, 1141–1146.

O'Shaughnessy, P. J., Johnston, H., Willerton, L. and Baker, P. J. (2002). Failure of normal adult Leydig cell development in androgen-receptor-deficient mice. *J. Cell. Sci.* **115**, 3491–3496.

O'Shaughnessy, P. J., Monteiro, A. and Abel, M. (2012). Testicular development in mice lacking receptors for follicle stimulating hormone and androgen. *PLoS ONE* **7**, e35136.

Ogata, T., Matsuo, N., Hiraoka, N. and Hata, J. I. (2000). X-linked lissencephaly with ambiguous genitalia: delineation of further case. *Am. J. Med. Genet.* **94**, 174–176.

Okada, I., Hamanoue, H., Terada, K., Tohma, T., Megarbane, A., Chouery, E., Abou-Ghoch, J., Jalkh, N., Cogulu, O., Ozkinay, F., et al. (2011). SMOC1 is essential for ocular and limb development in humans and mice. *Am. J. Hum. Genet.* **88**, 30–41.

Okigaki, M., Davis, C., Falasca, M., Harroch, S., Felsenfeld, D. P., Sheetz, M. P. and Schlessinger, J. (2003). Pyk2 regulates multiple signaling events crucial for macrophage morphology and migration. *P.N.A.S* **100**, 10740–10745.

Ono, M. and Harley, V. R. (2013). Disorders of sex development: new genes, new concepts. *Nat. Rev. Endocrinol.* **9**, 79–91.

Ornitz, D. M., Xu, J., Colvin, J. S., McEwen, D. G., MacArthur, C. A., Coulier, F., Gao, G. and Goldfarb, M. (1996). Receptor specificity of the fibroblast growth factor family. *J. Biol. Chem.* **271**, 15292–15297.

Orth, J. M. (1982). Proliferation of sertoli cells in fetal and postnatal rats: A quantitative autoradiographic study. *The Anatomical Record* **203**, 485–492.

Ostrer, H. (2014). Disorders of sex development (DSDs): an update. *J. Clin. Endocrinol. Metab.* **99**, 1503–1509.

Ottolenghi, C., Omari, S., Garcia-Ortiz, J. E., Uda, M., Crisponi, L., Forabosco, A., Pilia, G. and Schlessinger, D. (2005). Foxl2 is required for commitment to ovary differentiation. *Hum. Mol. Genet.* **14**, 2053–2062.

Pakarinen, P., Kimura, S., El-Gehani, F., Pelliniemi, L. J. and Huhtaniemi, I. (2002). Pituitary Hormones Are Not Required for Sexual Differentiation of Male Mice: Phenotype of the T/ebp/Nkx2.1 Null Mutant Mice. *Endocrinology* **143**, 4477–4482.

Palermo, R. (2007). Differential actions of FSH and LH during folliculogenesis. *Reprod. Biomed. Online* **15**, 326–337.

Palmer, S. J. and Burgoyne, P. S. (1991). In situ analysis of fetal, prepuberal and adult XX----XY chimaeric mouse testes: Sertoli cells are predominantly, but not exclusively, XY. *Development* **112**, 265–268.

Pan, Y., Bai, C. B., Joyner, A. L. and Wang, B. (2006). Sonic hedgehog signaling regulates Gli2 transcriptional activity by suppressing its processing and degradation. *Mol. Cell. Biol.* **26**, 3365–3377.

Park, S. Y., Meeks, J. J., Raverot, G., Pfaff, L. E., Weiss, J., Hammer, G. D. and Jameson, J. L. (2005). Nuclear receptors Sf1 and Dax1 function cooperatively to mediate somatic cell differentiation during testis development. *Development* **132**, 2415–2423.

Parma, P., Radi, O., Vidal, V., Chaboissier, M. C., Dellambra, E., Valentini, S., Guerra, L., Schedl, A. and Camerino, G. (2006). R-spondin1 is essential in sex determination, skin differentiation and malignancy. *Nat. Genet.* **38**, 1304–1309.

Patek, C. E., Kerr, J. B., Gosden, R. G., Jones, K. W., Hardy, K., Muggleton-Harris, A. L., Handyside, A. H., Whittingham, D. G. and Hooper, M. L. (1991). Sex chimaerism, fertility and sex determination in the mouse. *Development* **113**, 311–325.

Paul, C., Povey, J. E., Lawrence, N. J., Selfridge, J., Melton, D. W. and Saunders, P. T. K. (2007). Deletion of genes implicated in protecting the integrity of male germ cells has differential effects on the incidence of DNA breaks and germ cell loss. *PLoS ONE* **2**, e989.

Pepling, M. E. and Spradling, A. C. (1998). Female mouse germ cells form synchronously dividing cysts. *Development* **125**, 3323–3328.

Pereira, F. A., Qiu, Y., Tsai, M.-J. and Tsai, S. Y. (1995). Chicken ovalbumin upstream promoter transcription factor (COUP-TF): Expression during mouse embryogenesis. *J. Steroid Biochem. Mol. Biol.* **53**, 503–508.

Pereira, F. A., Qiu, Y., Zhou, G., Tsai, M. J. and Tsai, S. Y. (1999). The orphan nuclear receptor COUP-TFII is required for angiogenesis and heart development. *Genes Dev.* **13**, 1037–1049.

Petek, E., Windpassinger, C., Mach, M., Rauter, L., Scherer, S. W., Wagner, K. and Kroisel, P. M. (2003). Molecular characterization of a 12q22-q24 deletion associated with congenital deafness: confirmation and refinement of the DFNA25 locus. *Am. J. Med. Genet. A.* **117A**, 122–126.

Pickering, M. C., Cook, H. T., Warren, J., Bygrave, A. E., Moss, J., Walport, M. J. and Botto, M. (2002). Uncontrolled C3 activation causes membranoproliferative glomerulonephritis in mice deficient in complement factor H. *Nat. Genet.* **31**, 424–428.

Pisarska, M. D., Barlow, G. and Kuo, F. T. (2011). Minireview: roles of the forkhead transcription factor FOXL2 in granulosa cell biology and pathology. *Endocrinology* **152**, 1199–1208.

Polanco, J. C. and Koopman, P. (2007). Sry and the hesitant beginnings of male development. *Dev. Biol.* **302**, 13–24.

Polanco, J. C., Wilhelm, D., Davidson, T.-L., Knight, D. and Koopman, P. (2010). Sox10 gain-of-function causes XX sex reversal in mice: implications for human 22q-linked disorders of sex development. *Hum. Mol. Genet.* **19**, 506–516.

Prakash, S. K., Paylor, R., Jenna, S., Lamarche-Vane, N., Armstrong, D. L., Xu, B., Mancini, M. A. and Zoghbi, H. Y. (2000). Functional analysis of ARHGAP6, a novel GTPase-activating protein for RhoA. *Hum. Mol. Genet.* **9**, 477–488.

Pyun, J.-A., Kim, S., Cha, D. H. and Kwack, K. (2013). Epistasis between IGF2R and ADAMTS19 polymorphisms associates with premature ovarian failure. *Hum. Reprod.* **28**, 3146–3154.

Qin, J., Tsai, M.-J. and Tsai, S. Y. (2008). Essential roles of COUP-TFII in Leydig cell differentiation and male fertility. *PLoS ONE* **3**, e3285.

Qin, Y. and Bishop, C. E. (2005). Sox9 is sufficient for functional testis development producing fertile male mice in the absence of Sry. *Hum. Mol. Genet.* **14**, 1221–1229.

Quaggin, S. E., Schwartz, L., Cui, S., Igarashi, P., Deimling, J., Post, M. and Rossant, J. (1999). The basic-helix-loop-helix protein pod1 is critically important for kidney and lung organogenesis. *Development* **126**, 5771–5783.

Quaggin, S. E., Vanden Heuvel, G. B. and Igarashi, P. (1998). Pod-1, a mesoderm-specific basic-helix-loop-helix protein expressed in mesenchymal and glomerular epithelial cells in the developing kidney. *Mech. Dev.* **71**, 37–48.

Quaggin, S. E., Yeger, H. and Igarashi, P. (1997). Antisense oligonucleotides to Cux-1, a Cut-related homeobox gene, cause increased apoptosis in mouse embryonic kidney cultures. *J Clin Invest* **99**, 718–724.

Rastetter, R. H., Bernard, P., Palmer, J. S., Chassot, A.-A., Chen, H., Western, P. S., Ramsay, R. G., Chaboissier, M.-C. and Wilhelm, D. (2014). Marker genes identify three somatic cell types in the fetal mouse ovary. *Dev. Biol.* **394**, 242–252.

Reuter, A. L., Goji, K., Bingham, N. C., Matsuo, M. and Parker, K. L. (2007). A novel mutation in the accessory DNA-binding domain of human steroidogenic factor 1 causes XY gonadal dysgenesis without adrenal insufficiency. *Eur. J. Endocrinol.* **157**, 233–238.

Richards, J. S. and Pangas, S. A. (2010). The ovary: basic biology and clinical implications. *J. Clin. Invest.* **120**, 963–972.

Risbridger, G. P. (1993). Discrete stimulatory effects of platelet-derived growth factor (PDGF-BB) on Leydig cell steroidogenesis. *Mol. Cell. Endocrinol.* **97**, 125–128.

Robinson, M. D. and Oshlack, A. (2010). A scaling normalization method for differential expression analysis of RNA-seq data. *Genome Biol.* **11**, R25.

Rohatgi, R., Milenkovic, L., Corcoran, R. B. and Scott, M. P. (2009). Hedgehog signal transduction by Smoothened: pharmacologic evidence for a 2-step activation process. *Proc. Natl. Acad. Sci. U. S. A.* **106**, 3196–3201.

Rolland, A. D., Lehmann, K. P., Johnson, K. J., Gaido, K. W. and Koopman, P. (2011). Uncovering gene regulatory networks during mouse fetal germ cell development. *Biol. Reprod.* **84**, 790–800.

Ryan, J., Ludbrook, L., Wilhelm, D., Sinclair, A., Koopman, P., Bernard, P. and Harley, V. R. (2011). Analysis of gene function in cultured embryonic mouse gonads using nucleofection. *Sex. Dev.* **5**, 7–15.

Sadovsky, Y., Crawford, P. A., Woodson, K. G., Polish, J. A., Clements, M. A., Tourtellotte, L. M., Simburger, K. and Milbrandt, J. (1995). Mice deficient in the orphan receptor steroidogenic factor 1 lack adrenal glands and gonads but express P450 side-chain-cleavage enzyme in the placenta and have normal embryonic serum levels of corticosteroids. *Proc. Natl. Acad. Sci. U. S. A.* **92**, 10939–10943.

Sagane, K., Hayakawa, K., Kai, J., Hirohashi, T., Takahashi, E., Miyamoto, N., Ino, M., Oki, T., Yamazaki, K. and Nagasu, T. (2005). Ataxia and peripheral nerve hypomyelination in ADAM22-deficient mice. *BMC Neurosci* **6**, 33.

Saigoh, K., Wang, Y. L., Suh, J. G., Yamanishi, T., Sakai, Y., Kiyosawa, H., Harada, T., Ichihara, N., Wakana, S., Kikuchi, T., et al. (1999). Intragenic deletion in the gene encoding ubiquitin carboxy-terminal hydrolase in gad mice. **23**, 47–51.

Sandilands, A., Smith, F. J. D., Lunny, D. P., Campbell, L. E., Davidson, K. M., MacCallum, S. F., Corden, L. D., Christie, L., Fleming, S., Lane, E. B., et al. (2013). Generation and Characterisation of Keratin 7 (K7) Knockout Mice. *PLoS ONE* **8**, e64404.

Sanes, J. R., Rubenstein, J. L. and Nicolas, J. F. (1986). Use of a recombinant retrovirus to study post-implantation cell lineage in mouse embryos. *EMBO J.* **5**, 3133–3142.

Sarraj, M. A., Chua, H. K., Umbers, A., Loveland, K. L., Findlay, J. K. and Stenvers, K. L. (2007). Differential expression of TGFBR3 (betaglycan) in mouse ovary and testis during gonadogenesis. *Growth Factors* **25**, 334–345.

Sarraj, M. A., Escalona, R. M., Umbers, A., Chua, H. K., Small, C., Griswold, M., Loveland, K., Findlay, J. K. and Stenvers, K. L. (2010). Fetal testis dysgenesis and compromised Leydig cell function in Tgfbr3 (beta glycan) knockout mice. *Biol. Reprod.* **82**, 153–162.

Satoh, W., Gotoh, T., Tsunematsu, Y., Aizawa, S. and Shimono, A. (2006). Sfrp1 and Sfrp2 regulate anteroposterior axis elongation and somite segmentation during mouse embryogenesis. *Development* **133**, 989–999.

Scarff, K. L., Ung, K. S., Nandurkar, H., Crack, P. J., Bird, C. H. and Bird, P. I. (2004). Targeted disruption of SPI3/Serpinb6 does not result in developmental or growth defects, leukocyte dysfunction, or susceptibility to stroke. *Mol. Cell. Biol.* **24**, 4075–4082.

Schack, von, D., Casademunt, E., Schweigreiter, R., Meyer, M., Bibel, M. and Dechant, G. (2001). Complete ablation of the neurotrophin receptor p75NTR causes defects both in the nervous and the vascular system. *Nat. Neurosci.* **4**, 977–978.

Schally, A. V., Arimura, A., Baba, Y., Nair, R. M. G., Matsuo, H., Redding, T. W., Debeljuk, L. and White, W. F. (1971). Isolation and properties of the FSH and LH-releasing hormone. *Biochem. Biophys. Res. Commun.* **43**, 393–399.

Schmahl, J. and Capel, B. (2003). Cell proliferation is necessary for the determination of male fate in the gonad. *Dev. Biol.* **258**, 264–276.

Schmahl, J., Eicher, E. M., Washburn, L. L. and Capel, B. (2000). Sry induces cell proliferation in the mouse gonad. *Development* **127**, 65–73.

Schmahl, J., Kim, Y., Colvin, J. S., Ornitz, D. M. and Capel, B. (2004). Fgf9 induces proliferation and nuclear localization of FGFR2 in Sertoli precursors during male sex determination. *Development* **131**, 3627–3636.

Schmahl, J., Rizzolo, K. and Soriano, P. (2008). The PDGF signaling pathway controls multiple steroid-producing lineages. *Genes Dev.* **22**, 3255–3267.

Schmidt, D., Ovitt, C. E., Anlag, K., Fehsenfeld, S., Gredsted, L., Treier, A. C. and Treier, M. (2004). The murine winged-helix transcription factor Foxl2 is required for granulosa cell differentiation and ovary maintenance. *Development* **131**, 933–942.

Schulte-Merker, S. and Stainier, D. Y. R. (2014). Out with the old, in with the new: reassessing morpholino knockdowns in light of genome editing technology. *Development* **141**, 3103–3104.

Schwanzel-Fukuda, M. and Pfaff, D. W. (1989). Origin of luteinizing hormone-releasing hormone neurons. *Nature* **338**, 161–164.

Schwanzel-Fukuda, M., Bick, D. and Pfaff, D. W. (1989). Luteinizing hormone-releasing hormone (LHRH)-expressing cells do not migrate normally in an inherited hypogonadal (Kallmann) syndrome. *Brain Res. Mol. Brain Res.* **6**, 311–326.

Sedita, J., Izvolsky, K. and Cardoso, W. V. (2004). Differential expression of heparan sulfate 6-O-sulfotransferase isoforms in the mouse embryo suggests distinctive roles during organogenesis. *Dev. Dyn.* **231**, 782–794.

Sekido, R. and Lovell-Badge, R. (2008). Sex determination involves synergistic action of SRY and SF1 on a specific Sox9 enhancer. *Nature* **453**, 930–934.

Sekido, R., Bar, I., Narvaez, V., Penny, G. and Lovell-Badge, R. (2004). SOX9 is up-regulated by the transient expression of SRY specifically in Sertoli cell precursors. *Dev. Biol.* **274**, 271–279.

Seymour, P. A., Freude, K. K., Dubois, C. L., Shih, H.-P., Patel, N. A. and Sander, M. (2008). A dosage-dependent requirement for Sox9 in pancreatic endocrine cell formation. **323**, 19–30.

Seymour, P. A., Freude, K. K., Tran, M. N., Mayes, E. E., Jensen, J., Kist, R., Scherer, G. and Sander, M. (2007). SOX9 is required for maintenance of the pancreatic progenitor cell pool. **104**, 1865–1870.

Shafeghati, Y., Kniepert, A., Vakili, G. and Zenker, M. (2008). Fraser syndrome due to homozygosity for a splice site mutation of FREM2. *Am. J. Med. Genet. A.* **146A**, 529–531.

Sharp, A., Kusz, K., Jaruzelska, J., Tapper, W., Szarras-Czapnik, M., Wolski, J. and Jacobs, P. (2005). Variability of sexual phenotype in 46,XX(SRY+) patients: the influence of spreading X inactivation versus position effects. *J. Med. Genet.* **42**, 420–427.

Shima, Y., Miyabayashi, K., Baba, T., Otake, H., Katsura, Y., Oka, S., Zubair, M. and Morohashi, K.-I. (2012). Identification of an enhancer in the Ad4BP/SF-1 gene specific for fetal Leydig cells. *Endocrinology* **153**, 417–425.

Shima, Y., Miyabayashi, K., Haraguchi, S., Arakawa, T., Otake, H., Baba, T., Matsuzaki, S., Shishido, Y.,

Akiyama, H., Tachibana, T., et al. (2013). Contribution of Leydig and Sertoli cells to testosterone production in mouse fetal testes. **27**, 63–73.

Shima, Y., Zubair, M., Ishihara, S., Shinohara, Y., Oka, S., Kimura, S., Okamoto, S., Minokoshi, Y., Suita, S. and Morohashi, K. (2005). Ventromedial hypothalamic nucleus-specific enhancer of Ad4BP/SF-1 gene. *Mol. Endocrinol.* **19**, 2812–2823.

Shima, Y., Zubair, M., Komatsu, T., Oka, S., Yokoyama, C., Tachibana, T., Hjalt, T. A., Drouin, J. and Morohashi, K.-I. (2008). Pituitary Homeobox 2 Regulates Adrenal4 Binding Protein/Steroidogenic Factor-1 Gene Transcription in the Pituitary Gonadotrope through Interaction with the Intronic Enhancer. *Mol. Endocrinol.* **22**, 1633–1646.

Shinoda, K., Lei, H., Yoshii, H., Nomura, M., Nagano, M., Shiba, H., Sasaki, H., Osawa, Y., Ninomiya, Y. and Niwa, O. (1995). Developmental defects of the ventromedial hypothalamic nucleus and pituitary gonadotroph in the Ftz-F1 disrupted mice. *Dev. Dyn.* **204**, 22–29.

Sleer, L. S. and Taylor, C. C. (2007). Cell-type localization of platelet-derived growth factors and receptors in the postnatal rat ovary and follicle. *Biol. Reprod.* **76**, 379–390.

Small, C. L., Shima, J. E., Uzumcu, M., Skinner, M. K. and Griswold, M. D. (2005). Profiling gene expression during the differentiation and development of the murine embryonic gonad. *Biol. Reprod.* **72**, 492–501.

Smith, L., Willan, J., Warr, N., Brook, F. A., Cheeseman, M., Sharpe, R., Siggers, P. and Greenfield, A. (2008). The Maestro (Mro) Gene Is Dispensable for Normal Sexual Development and Fertility in Mice. *PLoS ONE* **3**, e4091.

Smyth, G. K. (2004). Linear models and empirical bayes methods for assessing differential expression in microarray experiments. *Stat Appl Genet Mol Biol* **3**, Article3.

Smyth, I. and Scambler, P. (2005). The genetics of Fraser syndrome and the blebs mouse mutants. *Hum. Mol. Genet.* **14 Spec No. 2**, R269–74.

Srivastava, D., Thomas, T., Lin, Q., Kirby, M. L., Brown, D. and Olson, E. N. (1997). Regulation of cardiac mesodermal and neural crest development by the bHLH transcription factor, dHAND. *Nat. Genet.* **16**, 154–160.

Stallings, N. R., Hanley, N. A., Majdic, G., Zhao, L., Bakke, M. and Parker, K. L. (2002). Development of a transgenic green fluorescent protein lineage marker for steroidogenic factor 1. *Mol. Endocrinol.* **16**, 2360–2370.

Stanton, H., Rogerson, F. M., East, C. J., Golub, S. B., Lawlor, K. E., Meeker, C. T., Little, C. B., Last, K., Farmer, P. J., Campbell, I. K., et al. (2005). ADAMTS5 is the major aggrecanase in mouse cartilage in vivo and in vitro. *Nature* **434**, 648–652.

Sultan, M., Schulz, M. H., Richard, H., Magen, A., Klingenhoff, A., Scherf, M., Seifert, M., Borodina, T., Soldatov, A., Parkhomchuk, D., et al. (2008). A global view of gene activity and alternative splicing by deep sequencing of the human transcriptome. *Science* **321**, 956–960.

Sun, B., Qi, N., Shang, T., Wu, H., Deng, T. and Han, D. (2010). Sertoli Cell-Initiated Testicular Innate Immune Response through Toll-Like Receptor-3 Activation Is Negatively Regulated by Tyro3, Axl, and Mer Receptors. *Endocrinology* **151**, 2886–2897.

Svechnikov, K., Landreh, L., Weisser, J., Izzo, G., Colón, E., Svechnikova, I. and Söder, O. (2010). Origin, development and regulation of human Leydig cells. *Horm Res Paediatr* **73**, 93–101.

Svingen, T. and Koopman, P. (2013). Building the mammalian testis: origins, differentiation, and assembly of the component cell populations. *Genes Dev.* **27**, 2409–2426.

Svingen, T., François, M., Wilhelm, D. and Koopman, P. (2012). Three-dimensional imaging of Prox1-EGFP transgenic mouse gonads reveals divergent modes of lymphangiogenesis in the testis and ovary. *PLoS ONE* **7**, e52620.

Svingen, T., McClelland, K. S., Masumoto, K., Sujino, M., Nagano, M., Shigeyoshi, Y. and Koopman, P. (2011). Prokr2-deficient mice display vascular dysmorphology of the fetal testes: potential implications for Kallmann syndrome aetiology. *Sex. Dev.* **5**, 294–303.

Svingen, T., Spiller, C. M., Kashimada, K., Harley, V. R. and Koopman, P. (2009a). Identification of suitable normalizing genes for quantitative real-time RT-PCR analysis of gene expression in fetal mouse gonads. *Sex. Dev.* **3**, 194–204.

Svingen, T., Wilhelm, D., Combes, A. N., Hosking, B., Harley, V. R., Sinclair, A. H. and Koopman, P. (2009b). Ex vivo magnetofection: A novel strategy for the study of gene function in mouse organogenesis. *Dev. Dyn.* **238**, 956–964.

Swain, A., Narvaez, V., Burgoyne, P., Camerino, G. and Lovell-Badge, R. (1998). Dax1 antagonizes Sry action in mammalian sex determination. *Nature* **391**, 761–767.

Swain, A., Zanaria, E., Hacker, A., Lovell-Badge, R. and Camerino, G. (1996). Mouse Dax1 expression is consistent with a role in sex determination as well as in adrenal and hypothalamus function. *Nat. Genet.* **12**, 404–409.

Sykiotis, G. P., Hoang, X.-H., Avbelj, M., Hayes, F. J., Thambundit, A., Dwyer, A., Au, M., Plummer, L., Crowley, W. F. and Pitteloud, N. (2010). Congenital idiopathic hypogonadotropic hypogonadism: evidence of defects in the hypothalamus, pituitary, and testes. *J. Clin. Endocrinol. Metab.* **95**, 3019–3027.

Takamoto, N., Kurihara, I., Lee, K., Demayo, F. J., Tsai, M.-J. and Tsai, S. Y. (2005). Haploinsufficiency of chicken ovalbumin upstream promoter transcription factor II in female reproduction. *Mol. Endocrinol.* **19**, 2299–2308.

Tamura, M., Kanno, Y., Chuma, S., Saito, T. and Nakatsuji, N. (2001). Pod-1/Capsulin shows a sex- and stage-dependent expression pattern in the mouse gonad development and represses expression of Ad4BP/SF-1. *Mech. Dev.* **102**, 135–144.

Tang, H., Brennan, J., Karl, J., Hamada, Y., Raetzman, L. and Capel, B. (2008). Notch signaling maintains Leydig progenitor cells in the mouse testis. *Development* **135**, 3745–3753.

Tapanainen, J., Kellokumpu-Lehtinen, P., Pelliniemi, L. and Huhtaniemi, I. (1981). Age-Related Changes in Endogenous Steroids of Human Fetal Testis during Early and Midpregnancy. *J. Clin. Endocrinol. Metab.* **52**, 98–102.

Tevosian, S. G. and Manuylov, N. L. (2008). To beta or not to beta: canonical beta-catenin signaling pathway and ovarian development. *Dev. Dyn.* **237**, 3672–3680.

The Leydig Cell in Health and Disease (2007). *The Leydig Cell in Health and Disease*. Totowa, NJ: Springer Science & Business Media.

Tomizuka, K., Horikoshi, K., Kitada, R., Sugawara, Y., Iba, Y., Kojima, A., Yoshitome, A., Yamawaki, K., Amagai, M., Inoue, A., et al. (2008). R-spondin1 plays an essential role in ovarian development through positively regulating Wnt-4 signaling. *Hum. Mol. Genet.* **17**, 1278–1291.

Topaloglu, A. K., Reimann, F., Guclu, M., Yalin, A. S., Kotan, L. D., Porter, K. M., Serin, A., Mungan, N. O., Cook, J. R., Ozbek, M. N., et al. (2009). TAC3 and TACR3 mutations in familial hypogonadotropic hypogonadism reveal a key role for Neurokinin B in the central control of reproduction. *Nat. Genet.* **41**, 354–358.

Tornberg, J., Sykiotis, G. P., Keefe, K., Plummer, L., Hoang, X., Hall, J. E., Quinton, R., Seminara, S. B., Hughes, V., Van Vliet, G., et al. (2011). Heparan sulfate 6-O-sulfotransferase 1, a gene involved in extracellular sugar modifications, is mutated in patients with idiopathic hypogonadotrophic hypogonadism. *Proc. Natl. Acad. Sci. U. S. A.* **108**, 11524–11529.

Tsukiyama, T. and Yamaguchi, T. P. (2012). Mice lacking Wnt2b are viable and display a postnatal olfactory bulb phenotype. *Neuroscience Letters* **512**, 48–52.

Uda, M., Ottolenghi, C., Crisponi, L., Garcia, J. E., Deiana, M., Kimber, W., Forabosco, A., Cao, A., Schlessinger, D. and Pilia, G. (2004). Foxl2 disruption causes mouse ovarian failure by pervasive blockage of follicle development. *Hum. Mol. Genet.* **13**, 1171–1181.

Uhlenhaut, N. H., Jakob, S., Anlag, K., Eisenberger, T., Sekido, R., Kress, J., Treier, A. C., Klugmann, C., Klasen, C., Holter, N. I., et al. (2009). Somatic sex reprogramming of adult ovaries to testes by FOXL2 ablation. *Cell* **139**, 1130–1142.

Umehara, F., Tate, G., Itoh, K., Yamaguchi, N., Douchi, T., Mitsuya, T. and Osame, M. (2000). A novel mutation of desert hedgehog in a patient with 46,XY partial gonadal dysgenesis accompanied by minifascicular neuropathy. *Am. J. Hum. Genet.* **67**, 1302–1305.

Vainio, S., Heikkila, M., Kispert, A., Chin, N. and McMahon, A. P. (1999). Female development in mammals is regulated by Wnt-4 signalling. *Nature* **397**, 405–409.

Val, P., Martinez-Barbera, J.-P. and Swain, A. (2007). Adrenal development is initiated by Cited2 and Wt1 through modulation of Sf-1 dosage. *Development* **134**, 2349–2358.

Valdes-Socin, H., Rubio Almanza, M., TomÃ FernÃ ndez-Ladreda, M., Debray, F. O. G., Bours, V. and Beckers, A. (2014). Reproduction, Smell, and Neurodevelopmental Disorders: Genetic Defects in Different Hypogonadotropic Hypogonadal Syndromes. *Front. Endocrinol.* **5**.

van den Driesche, S., Walker, M., McKinnell, C., Scott, H. M., Eddie, S. L., Mitchell, R. T., Seckl, J. R., Drake, A. J., Smith, L. B., Anderson, R. A., et al. (2012). Proposed Role for COUP-TFII in Regulating Fetal Leydig Cell Steroidogenesis, Perturbation of Which Leads to Masculinization Disorders in Rodents. **7**, e37064.

Vega, A., Martinot, E., Baptissart, M., de Haze, A., Saru, J.-P., Baron, S., Caira, F., Schoonjans, K., Lobaccaro, J.-M. A. and Volle, D. H. (2014). Identification of the link between the hypothalamo-pituitary axis and the testicular orphan nuclear receptor NR0B2 in adult male mice. *Endocrinology* en20141418.

Vergouwen, R. P., Huiskamp, R., Bas, R. J., Roepers-Gajadien, H. L., Davids, J. A. and de Rooij, D. G. (1993). Postnatal development of testicular cell populations in mice. *J. Reprod. Fertil.* **99**, 479–485.

Vidal, V. P. I., Chaboissier, M.-C., de Rooij, D. G. and Schedl, A. (2001). Sox9 induces testis development in XX transgenic mice. *Nat. Genet.* **28**, 216–217.

Volle, D. H., Duggavathi, R., Magnier, B. C., Houten, S. M., Cummins, C. L., Lobaccaro, J.-M. A., Verhoeven, G., Schoonjans, K. and Auwerx, J. (2007). The small heterodimer partner is a gonadal gatekeeper of sexual maturation in male mice. *Genes Dev.* **21**, 303–315.

Wagner, T., Wirth, J., Meyer, J., Zabel, B., Held, M., Zimmer, J., Pasantes, J., Bricarelli, F. D., Keutel, J., Hustert, E., et al. (1994). Autosomal sex reversal and campomelic dysplasia are caused by mutations in and around the SRY-related gene SOX9. *Cell* **79**, 1111–1120.

Wainwright, E. N. and Wilhelm, D. (2010). The game plan: cellular and molecular mechanisms of mammalian testis development. *Curr. Top. Dev. Biol.* **90**, 231–262.

Wainwright, E. N., Jorgensen, J. S., Kim, Y., Truong, V., Bagheri-Fam, S., Davidson, T., Svingen, T., Fernandez-Valverde, S. L., McClelland, K. S., Taft, R. J., et al. (2013). SOX9 Regulates MicroRNA miR-202-5p/3p Expression During Mouse Testis Differentiation. *Biol. Reprod.* **89**, 34.

Wainwright, E. N., Svingen, T., Ng, E. T., Wicking, C. and Koopman, P. (2014). Primary cilia function regulates the length of the embryonic trunk axis and urogenital field in mice. *Dev. Biol.* **395**, 342–354.

Wang, Q., Lu, J., Zhang, S., Wang, S., Wang, W., Wang, B., Wang, F., Chen, Q., Duan, E., Leitges, M., et al. (2013). Wnt6 Is Essential for Stromal Cell Proliferation During Decidualization in Mice. *Biol. Reprod.* **88**, 5–5.

Warman, D. M., Costanzo, M., Marino, R., Berensztein, E., Galeano, J., Ramirez, P. C., Saraco, N., Baquedano, M. S., Ciaccio, M., Guercio, G., et al. (2011). Three new SF-1 (NR5A1) gene mutations in two unrelated families with multiple affected members: within-family variability in 46,XY subjects and low ovarian reserve in fertile

46,XX subjects. *Horm Res Paediatr* **75**, 70–77.

Warr, N., Siggers, P., Bogani, D., Brixey, R., Pastorelli, L., Yates, L., Dean, C. H., Wells, S., Satoh, W., Shimono, A., et al. (2009). Sfrp1 and Sfrp2 are required for normal male sexual development in mice. *Dev. Biol.* **326**, 273–284.

Warren, D. W., Haltmeyer, G. C. and Eik-Nes, K. B. (1972). Synthesis and metabolism of testosterone in the fetal rat testis. *Biol. Reprod.* **7**, 94–99.

Warren, D. W., Huhtaniemi, I. T., Tapanainen, J., Dufau, M. L. and Catt, K. J. (1984). Ontogeny of gonadotropin receptors in the fetal and neonatal rat testis. *Endocrinology* **114**, 470–476.

Watase, K., Hashimoto, K., Kano, M., Yamada, K., Watanabe, M., Inoue, Y., Okuyama, S., Sakagawa, T., Ogawa, S., Kawashima, N., et al. (1998). Motor discoordination and increased susceptibility to cerebellar injury in GLAST mutant mice. *Eur. J. Neurosci.* **10**, 976–988.

Weidinger, G., Thorpe, C. J., Wuennenberg-Stapleton, K., Ngai, J. and Moon, R. T. (2005). The Sp1-Related Transcription Factors sp5 and sp5-like Act Downstream of Wnt/β-Catenin Signaling in Mesoderm and Neuroectoderm Patterning. *Curr. Biol.* **15**, 489–500.

Weinstein, M., Xu, X., Ohyama, K. and Deng, C. X. (1998). FGFR-3 and FGFR-4 function cooperatively to direct alveogenesis in the murine lung. *Development* **125**, 3615–3623.

Wertz, K. and Herrmann, B. G. (1999). Kidney-specific cadherin (cdh16) is expressed in embryonic kidney, lung, and sex ducts. *Mech. Dev.* **84**, 185–188.

Wharram, B. L., Goyal, M., Gillespie, P. J., Wiggins, J. E., Kershaw, D. B., Holzman, L. B., Dysko, R. C., Saunders, T. L., Samuelson, L. C. and Wiggins, R. C. (2000). Altered podocyte structure in GLEPP1 (Ptpro)-deficient mice associated with hypertension and low glomerular filtration rate. *J Clin Invest* **106**, 1281–1290.

Wigle, J. T. and Oliver, G. (1999). Prox1 Function Is Required for the Development of the Murine Lymphatic System. *Cell* **98**, 769–778.

Wilhelm, D. and Englert, C. (2002). The Wilms tumor suppressor WT1 regulates early gonad development by activation of Sf1. *Genes Dev.* **16**, 1839–1851.

Wilhelm, D., Hiramatsu, R., Mizusaki, H., Widjaja, L., Combes, A. N., Kanai, Y. and Koopman, P. (2007). SOX9 regulates prostaglandin D synthase gene transcription in vivo to ensure testis development. *J. Biol. Chem.* **282**, 10553–10560.

Wilhelm, D., Martinson, F., Bradford, S., Wilson, M. J., Combes, A. N., Beverdam, A., Bowles, J., Mizusaki, H. and Koopman, P. (2005). Sertoli cell differentiation is induced both cell-autonomously and through prostaglandin signaling during mammalian sex determination. *Dev. Biol.* **287**, 111–124.

Wilhelm, D., Washburn, L. L., Truong, V., Fellous, M., Eicher, E. M. and Koopman, P. (2009). Antagonism of the testis- and ovary-determining pathways during ovotestis development in mice. *Mech. Dev.* **126**, 324–336.

Wray, S. (2002). Development of gonadotropin-releasing hormone-1 neurons. *Front Neuroendocrinol* **23**, 292–316.

Wray, S., Grant, P. and Gainer, H. (1989a). Evidence that cells expressing luteinizing hormone-releasing hormone mRNA in the mouse are derived from progenitor cells in the olfactory placode. *Proc. Natl. Acad. Sci. U. S. A.* **86**, 8132–8136.

Wray, S., Nieburgs, A. and Elkabes, S. (1989b). Spatiotemporal cell expression of luteinizing hormone-releasing hormone in the prenatal mouse: evidence for an embryonic origin in the olfactory placode. *Brain Res. Dev. Brain Res.* **46**, 309–318.

Wu, B., Li, Y., Morcos, P. A., Doran, T. J., Lu, P. and Lu, Q. L. (2009). Octa-guanidine morpholino restores dystrophin expression in cardiac and skeletal muscles and ameliorates pathology in dystrophic mdx mice. *Mol. Ther.* **17**, 864–871.

Wu, X., Wan, S. and Lee, M. M. (2007). Key factors in the regulation of fetal and postnatal Leydig cell development. *J. Cell. Physiol.* **213**, 429–433.

Yang, D., Nakao, M., Shichijo, S., Sasatomi, T., Takasu, H., Matsumoto, H., Mori, K., Hayashi, A., Yamana, H., Shirouzu, K., et al. (1999). Identification of a gene coding for a protein possessing shared tumor epitopes capable of inducing HLA-A24-restricted cytotoxic T lymphocytes in cancer patients. *Cancer Res* **59**, 4056–4063.

Yang, F., Eckardt, S., Leu, N. A., McLaughlin, K. J. and Wang, P. J. (2008). Mouse TEX15 is essential for DNA double-strand break repair and chromosomal synapsis during male meiosis. *J. Cell Biol.* **180**, 673–679.

Yang, J. J., Caligioni, C. S., Chan, Y.-M. and Seminara, S. B. (2012). Uncovering novel reproductive defects in neurokinin B receptor null mice: closing the gap between mice and men. *Endocrinology* **153**, 1498–1508.

Yang, J. T., Rayburn, H. and Hynes, R. O. (1995). Cell adhesion events mediated by alpha 4 integrins are essential in placental and cardiac development. *Development* **121**, 549–560.

Yao, H. H. and Capel, B. (2002). Disruption of testis cords by cyclopamine or forskolin reveals independent cellular pathways in testis organogenesis. *Dev. Biol.* **246**, 356–365.

Yao, H. H. C., Matzuk, M. M., Jorgez, C. J., Menke, D. B., Page, D. C., Swain, A. and Capel, B. (2004). Follistatin operates downstream of Wnt4 in mammalian ovary organogenesis. *Dev. Dyn.* **230**, 210–215.

Yao, H. H., Aardema, J. and Holthusen, K. (2006). Sexually dimorphic regulation of inhibin beta B in establishing gonadal vasculature in mice. *Biol. Reprod.* **74**, 978–983.

Yao, H. H.-C., Whoriskey, W. and Capel, B. (2002). Desert Hedgehog/Patched 1 signaling specifies fetal Leydig cell fate in testis organogenesis. *Genes Dev.* **16**, 1433–1440.

Yates, L. L., Schnatwinkel, C., Murdoch, J. N., Bogani, D., Formstone, C. J., Townsend, S., Greenfield, A., Niswander, L. A. and Dean, C. H. (2010). The PCP genes Celsr1 and Vangl2 are required for normal lung branching morphogenesis. *Hum. Mol. Genet.* **19**, 2251–2267.

Yochum, C. L., Bhattacharya, P., Patti, L., Mirochnitchenko, O. and Wagner, G. C. (2010). Animal model of autism using GSTM1 knockout mice and early post-natal sodium valproate treatment. *Behav. Brain Res.* **210**, 202–210.

Yoon, S.-J., Kim, K.-H., Chung, H.-M., Choi, D.-H., Lee, W.-S., Cha, K.-Y. and Lee, K.-A. (2006). Gene expression profiling of early follicular development in primordial, primary, and secondary follicles. *Fertil. Steril.* **85**, 193–203.

Young, J. M. and McNeilly, A. S. (2010). Theca: the forgotten cell of the ovarian follicle. *Reproduction* **140**, 489–504.

Zhang, F. P., Poutanen, M., Wilbertz, J. and Huhtaniemi, I. (2001). Normal prenatal but arrested postnatal sexual development of luteinizing hormone receptor knockout (LuRKO) mice. *Mol. Endocrinol.* **15**, 172–183.

Zhang, X., Chou, W., Haig-Ladewig, L., Zeng, W., Cao, W., Gerton, G., Dobrinski, I. and Tseng, H. (2012). BNC1 is required for maintaining mouse spermatogenesis. *Genesis* **50**, 517–524.

Zhao, L., Neumann, B., Murphy, K., Silke, J. and Gonda, T. J. (2008). Lack of reproducible growth inhibition by Schlafen1 and Schlafen2 in vitro. *Blood Cells Mol. Dis.* **41**, 188–193.

Zheng, W., Zhang, H., Gorre, N., Risal, S., Shen, Y. and Liu, K. (2014). Two classes of ovarian primordial follicles exhibit distinct developmental dynamics and physiological functions. *Hum. Mol. Genet.* **23**, 920–928.

Zubair, M., Ishihara, S., Oka, S., Okumura, K. and Morohashi, K. (2006). Two-step regulation of Ad4BP/SF-1 gene transcription during fetal adrenal development: initiation by a Hox-Pbx1-Prep1 complex and maintenance via autoregulation by Ad4BP/SF-1. *Mol. Cell. Biol.* **26**, 4111–4121.

Zubair, M., Oka, S., Parker, K. L. and Morohashi, K.-I. (2009). Transgenic Expression of Ad4BP/SF-1 in Fetal Adrenal Progenitor Cells Leads to Ectopic Adrenal Formation. *Mol. Endocrinol.* **23**, 1657–1667.

Appendices

Supplemental Tables Associated With This Thesis

Supplemental Table 1: Splice site MO sequences targeting exon/intron boundaries of target genes.

Morpholino sequences for targets described in manuscript.

Gene target	**Antisense Sequence**
Adamts19	5'AGCTGTGGATGCTTACCAGGCCACC
Ctrb1	5'CAACGTAGCCTGGGACTCACTTGAC
Gli1	5'GGGATTGCCCCAGTGCTCACCTTCA
Gli2	5'CCACTGTCACAGGAGGCAAGAGAAA
Gli3	5’AATCCCTATAAAACACCACAGTGCC
Nr0b1 (Dax1)	5’GCCTGAGGCTCCTGTAGCTCGTTCT
Nr0b2	5’AGCTCATGGTTAGTATCTTGTTCCT
Sart3	5’GGACCTAAAAGACAAGAAGCGATCT
Sox9	5’GACCACTCGCGCCTTGCTCACCAGA
Stra8	5’ACTATCCCCAAGTCCCTGTACCTTT
Wnt4	5’CCTAGACCAACCCTCCTCACCTTGT
Standard Control	5'CCTCTTACCTCAGTTACAATTTATA

Supplemental Table 2: Taqman gene expression sets for qRT-PCR.

TaqMan Gene Expression Assay catalogue numbers described in this thesis. *Tbp* (*) was used an a normalising gene in all experiments.

Gene	Catalogue Code	Gene	Catalogue Code
Adamts 16	Mm00468144_m1	*Nr5a1 (Sf1)*	Mm00446826_m1
Adamts19	Mm00558559_m1	*Pax6*	Mm00443081_m1
Adcy7	Mm00545780_m1	*Pdx1*	Mm00435565_m1
Amh	Mm03023963_m1	*Pdzk1*	Mm00451926_m1
Arx	Mm00545903_m1	*Pou5f1 (Oct3/4)*	Mm00658129_gH
Car2	Mm00501576_m1	*Ppy*	Mm00435889_m1
Cdh1 (E-cad)	Mm01247357_m1	*Prlr*	Mm04336676_m1
Clca1	Mm00777368_m1	*Ptch1*	Mm00436026_m1
Cyp11a1 (Scc)	Mm00490735_m1	*Ptgds*	Mm01330613_m1
Ddx4 (Mvh)	Mm00802445_m1	*Rec8*	Mm00490939_m1
Dhh	Mm01310203_m1	*Robo2*	Mm00620713_m1
Dmc1	Mm00494485_m1	*Rspo1*	Mm00507076_m1
FoxL2	Mm00843544_s1	*Scp3*	Mm00488519_m1
Fras1	Mm00663578_m1	*Sox18*	Mm00656049_gH
Frem2	Mm00556222_m1	*Sox9*	Mm00448840_m1
Fst	Mm00514982_m1	*Sst*	Mm00436671_m1
Ghrl	Mm00445450_m1	*Star*	Mm00441558_m1
Glug	Mm00801712_m1	*Stra8*	Mm00486473_m1
Gstm7	Mm00499573_g1	*Tac2*	Mm01160362_m1
Hsd3b	Mm01261921_mH	*Tacr3*	Mm00445346_m1
Ins1	Mm01950294_s1	*Tbp**	Mm00446973_m1
Ins2	Mm00731595_gH	*Trank1*	Mm01245649_m1
Irx3	Mm00500463_m1	*Wnt4*	Mm00437341_m1
Mc2r	Mm00434865_s1	*Wt1*	Mm01337048_m1
Notch2	Mm00803077_m1	*Xlr3*	Mm00496001_m1
Nr0b1 (Dax1)	Mm00431729_m1		

Supplemental Table 3: Primary Antibodies for Immunofluorescence and Western Blot

Dilutions and catalogue numbers for primary antibodies described in this thesis.

Primary Antibody	Company	Catalogue Code	Species	Dilution
A-TUB	Sigma	T5168	mouse	1:5000 (WB)
AMH	Santa Cruz Biotechnology	sc-6886 (MIS C-20)	goat	1:200
ARX	Gift from K. Morohashi, Kyushu Uni, Japan: (Miyabayashi et al., 2013)		rabbit	1:200
CDH1 (ECAD)	BD Pharmingen 610182	610182	mouse	1:200
DDX4 (MVH)	mAB Abcam	ab27591	mouse	1:500
FOXL2	Gift from Dagmar Wilhelm, Monash University, Australia: (Polanco et al., 2010)		rabbit	1:800
GFP	Abcam	ab5450	goat	1:400
gH2AX	Millipore	05-636	mouse	1:200
HSD3B	Transgenic Inc	KAL-KO607	rabbit	1:600
iB4-biotin conjugate	Sigma Aldrich	L2140	biotin	1:200
INS	Sigma Aldrich	12018	mouse	1:200
NR2F2 (COUPTFII)	Perseus Proteomics Inc.	PP-H7147-00	mouse	1:400
NR5A1	Transgenic Inc	KAL-KO610	rat	1:600
PAX2	Invitrogen	71-6000	rabbit	1:200
PAX6	Covance Research Products Inc	PRB278P	rabbit	1:200
POU5F1 (OCT4)	Santa Cruz Biotechnology	sc-5279	mouse	1:200
SCP3	Abcam ab15093	ab15093	rabbit	1:200
SOX9	Abnova	H00006662-M01	mouse	1:200 (IF) 1:1000 (WB)
STRA8	Abcam	ab49405	rabbit	1:200

Supplemental Table 4: Secondary Antibodies for Immunofluorescence and Western Blot

Dilutions and catalogue numbers for secondary antibodies described in this thesis.

Conjugate	**Invitrogen Catalogue Code (all used at 1:200)**	
anti-goat 488	A11055	
anti-mouse 488	A11001/A11017	
anti-mouse 594	A11032/A11005	
anti-mouse 647	A31571	
anti-mouse HRP	Sigma: A8924	
anti-rabbit 488	A11034	
anti-rabbit 568	A10042	
anti-rabbit 594	A11037	
anti-rabbit 647	A31573	
anti-rat 488	A11006	
anti-rat 594	A11007	
Probe	**Company**	**Dilution**
DAPI	Molecular Probes	2 ng/µl in PBS at 1:5000

Supplemental Table 5: List of previously published data on testis expression for 84 FLC-enriched genes.

List of genes that have been previously reported to be expressed in the adult or fetal mouse testis or in human testis/DSD in PubMed. This list is current as of 12 Nov 2014. In most cases where fetal expression was detected this was not at 12.5 dpc and no further expression analysis was performed. (* indicates that there is a published expression pattern for this gene at 12.5 dpc)

Human testis	**DSD association**	**Adult testis**	**Fetal testis**	**Not reported**	
Art3	*Lars2*	*Adamts5*	*Adcy7*	*Arhgap6*	*Itga9*
Ffar2		*Btnl9*	*Cbln1*	*Armcx6*	*Kcns2*
Hoxd10		*Cyp1b1*	*Crhr1*	*Bmp2*	*Lrrtm3*
Mmp28		*Gpr153*	*Gja5*	*C7*	*Mme*
Ptpro		*Hspa12a*	*Hhip*	*Casq2*	*Myh7*
Rad51ap2		*Kcnj3*	*Hsd11b2*	*Chst1*	*Oit3*
Vipr1		*Kcnk3*	*Htra3*	*Chst2*	*Pcp4l1*
		Myh11	*Inhba**	*Clca1*	*Plcxd3*
		Myl4	*Itih5**	*Clec1b*	*Pnmal1*
		Myoc	*Mc2r*	*Col23a1*	*Robo2*
		Nts	*Mc4r*	*Gm11549*	*Serpina3g*
		Otof	*Ngfr**	*Gm13659*	*Sertm1*
		Pdyn	*Nrg1*	*Gm14396*	*Sox18*
		Slitrk2	*Ppp1r14a*	*Gm5067*	*Speer7-ps1*
		Syt15	*Prlr*	*Gpr174*	*Sstr4*
		Tac2	*Prokr2**	*Gpr20*	*Stc1*
		Tacr3	*Srpx2*	*Grin2a*	*Tg*
			*Vcam1**	*Grrp1*	*Trac*
			Vgll3	*Irf8*	
			Vsnl1	*Itga4*	

Supplemental Table 6: Genes putatively regulated by NR5A1

We identified overlap between the upregulated and downregulated gene lists produced by Baba et al., (2014) and our three lists of genes upregulated in FLCs, NSICs and Sertoli cells (SData File 2). Genes that overlap in the data sets are putatively regulated by NR5A1 and are listed under each cell type as either being putatively up- or down-regulated by NR5A1. Sertoli cell genes are listed in Table 3.8.

Genes putatively upregulated by NR5A1	Genes putatively downregulated by NR5A1
FLCs:	FLCs:
Htra3	*Bmp2*
Vcam1	*Kcnk3*
NSICs:	NSICs:
B4galnt1	*9630033F20Rik*
C1s	*Bspry*
Car2	*Cyth4*
Ecm1	*Gypa*
Foxp2	*Myo15b*
Hr	*Trib3*
Ifitm3	*9630033F20Rik*
Lrp11	*Bspry*
Ly6a	*Cyth4*
Ogn	*Gypa*
Prss23	*Myo15b*
S100a6	*Trib3*
Slc9a3r1	

Supplemental Table 7: Eurexpress IDs.

List of Eurexpress and Ref Seq IDs for the ISHs in this thesis. (*= *Trank1* is annotated in the Eurexpress database as *Lba1* (*lupus brain antigen 1*)).

Gene	Population	Eurexpress ID	MGI ID	Ref Seq ID
Cyp11a1	FLC	euxassay_006083	MGI:88582	NM_019779
Nr2f2	NSIC	euxassay_011662	MGI:1352452	NM_183261
Amh	SC	euxassay_019122	MGI:88006	NM_007445
Adcy7	FLC	euxassay_018247	MGI:102891	NM_007406
Clca1	FLC	euxassay_011993	MGI:1316732	NM_009899
Itga9	FLC	euxassay_011292	MGI:104756	NM_133721
Nrg	FLC	euxassay_007625	MGI:96083	XM_893383
Nts	FLC	euxassay_007634	MGI:1328351	NM_024435
Prlr	FLC	euxassay_007856	MGI:97763	NM_011169
Srpx2	FLC	euxassay_002179	MGI:1916042	NM_026838
Tacr3	FLC	euxassay_004597	MGI:892968	NM_021382
Car2	NSIC	euxassay_004081	MGI:88269	NM_009801
Slc6a18	NSIC	euxassay_007790	MGI:1336892	NM_011730
Ermpa	NSIC	euxassay_005148	MGI:1349816	NM_013848
Adamts16	SC	euxassay_001489	MGI:2429637	NM_172053
Adhfe1	SC	euxassay_001519	MGI:1923437	NM_175236
Arhgdig	SC	euxassay_000468	MGI:108430	NM_008113
Clcn2	SC	euxassay_008248	MGI:105061	NM_009900
Gsta4	SC	euxassay_004740	MGI:1309515	NM_010357
Gstm1	SC	euxassay_000731	MGI:95860	NM_010358
Gstm7	SC	euxassay_018910	MGI:1915562	XM_289885
Hcrtr1	SC	euxassay_017929	MGI:2385650	AF394596
Hs6st1	SC	euxassay_006185	MGI:1354958	NM_015818
Kctd14	SC	euxassay_012606	MGI:1289222	NM_001010826
Npr1	SC	euxassay_007624	MGI:97371	NM_008727
Pak3	SC	euxassay_017534	MGI:1339656	NM_008778
Ppt1	SC	euxassay_013980	MGI:1298204	NM_008917
Rgs11	SC	euxassay_000824	MGI:1354739	XM_128488
Smoc1	SC	euxassay_003378	MGI:1929878	NM_022316
Stc2	SC	euxassay_003589	MGI:1316731	NM_011491
Tle6	SC	euxassay_001017	MGI:2149593	NM_053254
*Trank1**	SC	euxassay_013745	MGI:1341834	XM_001005347
Tyro3	SC	euxassay_006322	MGI:104294	NM_019392

Supplemental Table 8: Genes detected as upregulated in each population that have an annotation in OMIM.

The following information is drawn from the Online Mendelian Inheritance in Man, OMIM® data base currated by McKusick-Nathans Institute of Genetic Medicine, Johns Hopkins University (Baltimore, MD), accessed on 12 November 2014. URL: http://omim.org/. This workbook shows whether there is any known association between upregulated genes in each population and an OMIM phenotype. The nomenclature and symbols used in the list are indicated below

The following information is drawn from the Online Mendelian Inheritance in Man, OMIM® data base currated by McKusick-Nathans Institute of Genetic Medicine, Johns Hopkins University (Baltimore, MD), accessed on 12 November 2014. URL: http://omim.org/

Note that not every gene with a phenotype identified has a corresponding MIM number in the OMIM data base.

Additional information from the descriptions from the OMIM database can be interpreted as follows:

Brackets, "[ ]", indicate "nondiseases," mainly genetic variations that lead to apparently abnormal laboratory test values (e.g., dysalbuminemic euthyroidal hyperthyroxinemia).

Braces, "{ }", indicate mutations that contribute to susceptibility to multifactorial disorders (e.g., diabetes, asthma) or to susceptibility to infection (e.g., malaria).

A question mark, "?", before the disease name indicates an unconfirmed or possibly spurious mapping.

The number in parentheses after the name of each disorder indicates the following: (1) the disorder was positioned by mapping of the wildtype gene; (2) the disease phenotype itself was mapped; (3) the molecular basis of the disorder is known; (4) the disorder is a chromosome deletion or duplication syndrome.

Each OMIM entry is given a unique six-digit number. The first digit of the number provides the following information summarized below:

1----- (100000-) 2----- (200000-) Autosomal loci or phenotypes (entries created before May 15, 1994)

3----- (300000-) X-linked loci or phenotypes

4----- (400000-) Y-linked loci or phenotypes

5----- (500000-) Mitochondrial loci or phenotypes

6----- (600000-) Autosomal loci or phenotypes (entries created after May 15, 1994)

Supplemental Table 8.1: OMIM FLC genes

Symbol	MIM number	OMIM Description
SRPX2	300643	?Rolandic epilepsy, mental retardation, and speech dyspraxia (3)
MME		[Neutral endopeptidase deficiency] (1); Membranous glomerulonephritis, antenatal (1)
NRG1	603013	{?Schizophrenia, susceptibility to} (1)
BMP2	235200, 112600	{HFE hemochromatosis, modifier of} (3); Brachydactyly, type A2 (3)
MYH11	132900	Aortic aneurysm, familial thoracic 4 (3)
HSD11B2	218030	Apparent mineralocorticoid excess (3)
GJA5	614049, 108770	Atrial fibrillation, familial, 11 (3); Atrial standstill, digenic (GJA5/SCN5A) (3)
C7	610102	C7 deficiency (3)
MYH7	192600, 613426, 608358, 160500, 181430, 613426	Cardiomyopathy, familial hypertrophic, 1 (3); Cardiomyopathy, dilated, 1S (3); Myopathy, myosin storage (3); Laing distal myopathy (3); Scapuloperoneal syndrome, myopathic type (3); Left ventricular noncompaction 5 (3)
OTOF	601071, 601071	Deafness, autosomal recessive 9 (3); Auditory neuropathy, autosomal recessive, 1 (3)
GRIN2A	245570	Epilepsy, focal, with speech disorder and with or without mental retardation (3)
MYOC	137750	Glaucoma 1A, primary open angle (3)
CYP1B1	231300, 604229	Glaucoma 3A, primary open angle, congenital, juvenile, or adult onset (3); Peters anomaly (3)
MC2R	202200	Glucocorticoid deficiency, due to ACTH unresponsiveness (3)
TACR3	614840	Hypogonadotropic hypogonadism 11 with or without anosmia (3)
PROKR2	244200	Hypogonadotropic hypogonadism 3 with or without anosmia (3)
SOX18	607823	Hypotrichosis-lymphedema-telangiectasia syndrome (3)
IRF8	614893, 614894	Immunodeficiency 32A, mycobacteriosis, autosomal dominant (3); Immunodeficiency 32B, monocyte and dendritic cell deficiency, autosomal recessive (3)
TRAC	615387	Immunodeficiency 7, TCR-alpha/beta deficient (3)
PRLR	615554, 615555	Multiple fibroadenomas of the breast (3); ?Hyperprolactinemia (3)
PTPRO	614196	Nephrotic syndrome, type 6 (3)
MC4R	601665	Obesity, autosomal dominant (3)
LARS2	615300	Perrault syndrome 4 (3)
KCNK3	615344	Pulmonary hypertension, primary, 4 (3)
PDYN	610245	Spinocerebellar ataxia 23 (3)
TG	274700, 608175	Thyroid dyshormonogenesis 3 (3); {Autoimmune thyroid disease, susceptibility to, 3} (3)
CASQ2	611938	Ventricular tachycardia, catecholaminergic polymorphic, 2 (3)
HOXD10	192950, 192950	Vertical talus, congenital (3); Charcot-Marie-Tooth disease, foot deformity of (3)
ROBO2	610878	Vesicoureteral reflux 2 (3)
HTRA3	193235	Vitreoretinopathy, neovascular inflammatory (3)

Supplemental Table 8.2: OMIM NSIC genes

Symbol	MIM number	OMIM Description
NEFH	105400	?{Amyotrophic lateral sclerosis, susceptibility to} (3)
UCHL1	613643, 615491	?{Parkinson disease 5, susceptibility to} (3); ?Neurodegeneration with optic atrophy, childhood onset (3)
ACTN2	612158	?Cardiomyopathy, dilated, 1AA (3)
ALX1	613456	?Frontonasal dysplasia 3 (3)
PHC1	615414	?Microcephaly 11, primary, autosomal recessive (3)
HOXA2	612290, 612290	?Microtia, hearing impairment, and cleft palate (AR) (3); ?Microtia with or without hearing impairment (AD) (3)
PCK1	261680	?Phosphoenolpyruvate carboxykinase-1, cytosolic, deficiency (1)
STAG3	615723	?Premature ovarian failure 8 (3)
KCNJ8		?Prinzmetal angina (1)
TAF4B	615841	?Spermatogenic failure 13 (3)
AMPD3	612874	[AMP deaminase deficiency, erythrocytic] (3)
GCNT2	110800, 110800, 110800	[Blood group, Ii] (3); Cataract 13 with adult i phenotype (3); Adult i phenotype without cataract (3)
KEL	110900	[Blood group, Kell] (3)
GYPA	611162	[Blood group, MN] (3); {Malaria, resistance to} (3)
ERMAP	111750, 111620	[Blood group, Scianna system] (3); [Blood group, Radin] (3)
RGS5	145500	[Blood pressure regulation QTL] (2)
AFP	615970, 615969	[Hereditary persistence of alpha-fetoprotein] (3); Alpha-fetoprotein deficiency (3)
RHD		[Rh-negative blood type] (3)
XPNPEP2	300909	{Angioedema induced by ACE inhibitors, susceptibility to} (3)
HMGA1	125853	{Diabetes mellitus, noninsulin-dependent, susceptibility to} (3)
PTPN22	222100, 180300, 152700	{Diabetes, type 1, susceptibility to} (3); {Rheumatoid arthritis, susceptibility to} (3); {Systemic lupus erythematosus susceptibility to} (3)
HBEGF		{Diphtheria, susceptibility to} (1)
CFH	235400, 609814, 610698, 126700	{Hemolytic uremic syndrome, atypical, susceptibility to, 1} (3); Complement factor H deficiency (3); {Macular degeneration, age-related, 4} (3); Basal laminar drusen (3)
PTPRC	609532, 608971	{Hepatitic C virus, susceptibility to} (3); Severe combined immunodeficiency, T cell-negative, B-cell/natural killer-cell positive (3)
CCL3	609423	{HIV infection, resistance to} (2)
CCR2		{HIV infection, susceptibility/resistance to} (3)
IFITM3	614680	{Influenza, severe, susceptibility to} (3)
TLR2	246300, 114500, 607948	{Leprosy, susceptibility to} (3); {Colorectal cancer, susceptibility to} (3); {Mycobacterium tuberculosis, susceptibility to} (3)
CDKN2A	155601, 155755, 606719	{Melanoma, cutaneous malignant, 2} (3); Melanoma and neural system tumor syndrome (3); Pancreatic cancer/melanoma syndrome (3); Orolaryngeal cancer, multiple, (3)
SLC11A1	607948, 610446	{Mycobacterium tuberculosis, susceptibility to infection by} (3); {Buruli ulcer, susceptibility to} (3)
GCLM	608446	{Myocardial infarction, susceptibility to} (3)
MIAT	608446	{Myocardial infarction, susceptibility to} (3)
ADRB3	601665	{Obesity, susceptibility to} (3)
CX3CR1	609423, 607339, 613784	{Rapid progression to AIDS from HIV1 infection} (3); {Coronary artery disease, resistance to} (3); {Macular degeneration, age-related, 12} (3)
SLC22A4	180300	{Rheumatoid arthritis, susceptibility to} (3)
DAO	181500	{Schizophrenia} (2)

DAZL		{Spermatogenic failure, susceptibility to} (3)
ALOX5AP	601367	{Stroke, susceptibility to} (3)
ITGAM	609939	{Systemic lupus erythematous, association with susceptibility to, 6} (3)
MYB		{T-cell acute lymphoblastic leukemia} (3)
GNAT2	613856	Achromatopsia-4 (3)
SLC39A4	201100	Acrodermatitis enteropathica (3)
IGHM	601495	Agammaglobulinemia 1 (3)
BLNK	613502	Agammaglobulinemia 4 (3)
PRRX1	202650	Agnathia-otocephaly complex (3)
HR	203655, 209500, 146550	Alopecia universalis (3); Atrichia with papular lesions (3); Hypotrichosis 4 (3)
RHAG	268150	Anemia, hemolytic, Rh-null, regulator type (3); Rh-mod syndrome (3)
ALAS2	300751, 300752	Anemia, sideroblastic, X-linked (3); Protoporphyria, erythropoietic, X-linked (3)
PAX6	106210, 604229, 106210, 148190, 136520, 120430, 165550, 120200, 120430, 206700	Aniridia (3); Peters anomaly (3); Cataract with late-onset corneal dystrophy (3); Keratitis (3); Foveal hypoplasia 1 (3); ?Morning glory disc anomaly (3); Optic nerve hypoplasia (3); Coloboma, ocular (3); Coloboma of optic nerve (3); Gillespie syndrome (3)
MYBPC1	614335, 614915	Arthrogryposis, distal, type 1B (3); Lethal congenital contracture syndrome 4 (3)
TTPA	277460	Ataxia with isolated vitamin E deficiency (3)
NLRC4	616050	Autoinflammation with infantile enterocolitis (3)
PITX2	180500, 137600, 180550, 604229	Axenfeld-Rieger syndrome, type 1 (3); Iridogoniodysgenesis, type 2 (3); Ring dermoid of cornea (3); Peters anomaly (3)
OCLN	251290	Band-like calcification with simplified gyration and polymicrogyria (3)
CTHRC1	614266	Barrett esophagus/esophageal adenocarcinoma (3)
CYP7B1	613812, 270800	Bile acid synthesis defect, congenital, 3 (3); Spastic paraplegia 5A, autosomal recessive (3)
SIX1	608389, 605192	Brachiootic syndrome 3 (3); Deafness, autosomal dominant 23 (3)
BMPR1B	112600, 609441	Brachydactyly, type A2 (3); Chrondrodysplasia, acromesomelic, with genital anomalies (3)
C1QA	613652	C1q deficiency (3)
C1QB	613652	C1q deficiency (3)
C1QC	613652	C1q deficiency (3)
C1S	613783	C1s deficiency (3)
RBM20	613172	Cardiomyopathy, dilated, 1DD (3)
SLC16A12	612018	Cataract, juvenile, with microcornea and glucosuria (3)
NEFL	607684, 607734	Charcot-Marie-Tooth disease, type 2E (3); Charcot-Marie-Tooth disease, type 1F (3)
VIL1		Cholestasis, progressive canalicular (1)
NCF1	233700	Chronic granulomatous disease due to deficiency of NCF-1 (3)
NCF2	233710	Chronic granulomatous disease due to deficiency of NCF-2 (3)
CYBB	306400, 300645	Chronic granulomatous disease, X-linked (3); Immunodeficiency 34, mycobacteriosis, X-linked (3)
DNAAF3	606763	Ciliary dyskinesia, primary, 2 (3)
RSPH1	615481	Ciliary dyskinesia, primary, 24 (3)
CIRH1A	604901	Cirrhosis, North American Indian childhood type (3)
RUNX2	119600, 119600, 119600, 156510	Cleidocranial dysplasia (3); Cleidocranial dysplasia, forme fruste, with brachydactyly (3); Cleidocranial dysplasia, forme fruste, dental anomalies only (3); Metaphyseal dysplasia with maxillary hypoplasia with or without brachydactyly (3)

MSH2	120435, 158320, 276300	Colorectal cancer, hereditary nonpolyposis, type 1 (3); Muir-Torre syndrome (3); Mismatch repair cancer syndrome (3)
MSH6	614350, 608089, 276300	Colorectal cancer, hereditary nonpolyposis, type 5 (3); Endometrial cancer, familial (3); Mismatch repair cancer syndrome (3)
CDHR1	613660, 613660	Cone-rod dystrophy 15 (3); Retinitis pigmentosa 65 (3)
ALG13	300884	Congenital disorder of glycosylation, type Is (3)
MSX2	604757, 168500, 168550	Craniosynostosis, type 2 (3); Parietal foramina 1 (3); Parietal foramina with cleidocranial dysplasia (3)
GRHL2	608641, 616029	Deafness, autosomal dominant 28 (3); Ectodermal dysplasia/short stature syndrome (3)
ESRRB	608565	Deafness, autosomal recessive 35 (3)
ILDR1	609646	Deafness, autosomal recessive 42 (3)
SYNE4	615540	Deafness, autosomal recessive 76 (3)
TPRN	613307	Deafness, autosomal recessive 79 (3)
GLIS3	610199	Diabetes mellitus, neonatal, with congenital hypothyroidism (3)
EPCAM	613217, 613244	Diarrhea 5, with tufting enteropathy, congenital (3); Colorectal cancer, hereditary nonpolyposis, type 8 (3)
LRP2	222448	Donnai-Barrow syndrome (3)
EFEMP1	126600	Doyne honeycomb degeneration of retina (3)
SALL4	607323, 147750	Duane-radial ray syndrome (3); IVIC syndrome (3)
NHP2	613987	Dyskeratosis congenita, autosomal recessive 2 (3)
SPTA1	130600, 266140, 270970	Elliptocytosis-2 (3); Pyropoikilocytosis (3); Spherocytosis, type 3 (3)
SPTB		Elliptocytosis-3 (3); Spherocytosis, type 2 (3); Anemia, neonatal hemolytic, fatal and near-fatal (3)
CDH1	608089, 167000, 114480, 137215, 176807	Endometrial carcinoma, somatic (3); Ovarian carcinoma, somatic (3); {Breast cancer, lobular} (3); Gastric cancer, familial diffuse, with or without cleft lip and/or palate (3); {Prostate cancer, susceptibility to} (3)
ITGB4	226730, 226650, 131800	Epidermolysis bullosa, junctional, with pyloric atresia (3); Epidermolysis bullosa, junctional, non-Herlitz type (3); Epidermolysis bullosa of hands and feet (3)
SLC1A3	612656	Episodic ataxia, type 6 (3)
KCNA1	160120	Episodic ataxia/myokymia syndrome (3)
BPGM	222800	Erythrocytosis due to bisphosphoglycerate mutase deficiency (3)
GJB3	133200, 612644, 220290	Erythrokeratodermia variabilis et progressiva (3); Deafness, autosomal dominant 2B (3); Deafness, autosomal recessive (3); Deafness, autosomal dominant, with peripheral neuropathy (3); Deafness, digenic, GJB2/GJB3 (3)
F13A1	613225, 608446, 188050	Factor XIIIA deficiency (3); {Myocardial infarction, protection against} (3); {Venous thrombosis, protection against} (3)
PLCG2	614468, 614878	Familial cold autoinflammatory syndrome 3 (3); Autoinflammation, antibody deficiency, and immune dysregulation syndrome (3)
RAD51C	613390, 613399	Fanconi anemia, complementation group O (3); {Breast-ovarian cancer, familial, susceptibility to, 3} (3)
GPR98	604352, 605472, 605472	Febrile seizures, familial, 4 (3); Usher syndrome, type 2C (3); Usher syndrome, type 2C, GPR98/PDZD7 digenic (3)
TWIST2	227260	Focal facial dermal dysplasia 3, Setleis type (3)
TDGF1		Forebrain defects (3)
FREM2	219000	Fraser syndrome (3)
ALDOB	229600	Fructose intolerance (3)
TBXAS1	231095, 614158	Ghosal hematodiaphyseal syndrome (3); ?Thromboxane synthase deficiency (1)
ITGB3	273800, 608446, 187800	Glanzmann thrombasthenia (3); Thrombocytopenia, neonatal alloimmune (3); {Myocardial infarction, susceptibility to} (3); Purpura, posttransfusion (3); Bleeding disorder, platelet-type, 16, autosomal

		dominant (3)
SATB2	612313	Glass syndrome (3)
FGD2	607398	Glucocorticoid deficiency 2 (3)
GGT1		Glutathioninuria (1),
AMT	605899	Glycine encephalopathy (3)
GLDC	605899	Glycine encephalopathy (3)
NCF4	613960	Granulomatous disease, chronic, autosomal recessive, cytochrome b-positive, type III (3)
NBEAL2	139090	Gray platelet syndrome (3)
RAB27A	607624	Griscelli syndrome, type 2 (3)
MLPH	609227	Griscelli syndrome, type 3 (3)
GCLC	230450, 608446	Hemolytic anemia due to gamma-glutamylcysteine synthetase deficiency (3); {Myocardial infarction, susceptibility to} (3)
GPX1	614164	Hemolytic anemia due to glutathione peroxidase deficiency (1)
ZIC3	306955, 306955, 314390	Heterotaxy, visceral, 1, X-linke (3); Congenital heart defects, nonsyndromic, 1, X-linked (3); VACTERL association, X-linked (3)
NODAL	270100	Heterotaxy, visceral, 5 (3)
L1CAM	307000, 303350, 303350, 307000, 307000, 304100	Hydrocephalus due to aqueductal stenosis (3); MASA syndrome (3); CRASH syndrome (3); Hydrocephalus with Hirschsprung disease (3); Hydrocephalus with congenital idiopathic intestinal pseudoobstruction (3); Corpus callosum, partial agenesis of (3)
CCDC88C	236600, 616053	Hydrocephalus, nonsyndromic, autosomal recessive (3); ?Spinocerebellar ataxia 40 (3)
GATA3	146255	Hypoparathyroidism, sensorineural deafness, and renal dysplasia (3)
APCDD1	605389	Hypotrichosis 1 (3)
LIPH	604379, 604379, 612797, 125853, 614025	Hypotrichosis 7 (3); Woolly hair, autosomal recessive 2 with or without hypotrichosis (3), [High density lipoprotein cholesterol level QTL 12] (3); {Diabetes mellitus, noninsulin-dependent} (3); Hepatic lipase deficiency (3)
ST14	602400	Ichthyosis, congenital, autosomal recessive 11 (3)
CLDN1	607626	Ichthyosis, leukocyte vacuoles, alopecia, and sclerosing cholangitis (3)
PIK3CD	615513	Immunodeficiency 14 (3)
GATA2	614172, 614038, 614286, 601626	Immunodeficiency 21 (3); Emberger syndrome (3); {Myelodysplastic syndrome, susceptibility to} (3); {Leukemia, acute myeloid, susceptibility to} (3)
CORO1A	615401	Immunodeficiency 8 (3)
GDF6	118100, 613094, 613703, 615360	Klippel-Feil syndrome 1, autosomal dominant (3); Microphthalmia, isolated 4 (3); Microphthalmia with coloboma 6, digenic (3); Leber congenital amaurosis 17 (3)
GDF3	613702, 613703, 613704	Klippel-Feil syndrome 3, autosomal dominant (3); Microphthalmia with coloboma 6 (3); Microphthalmia, isolated 7 (3)
LEFTY2		Left-right axis malformations (3)
TAL1		Leukemia-1, T-cell acute lymphocytic (3)
IKZF1		Leukemia, acute lymphoblastic (3)
LMO1		Leukemia, T-cell acute lymphoblastic (2)
LYL1		Leukemia, T-cell acute lymphoblastoid (2)
FERMT3	612840	Leukocyte adhesion deficiency, type III (3)
CSF1R	221820	Leukoencephalopathy, diffuse hereditary, with spheroids (3)
DCX	300067, 300067	Lissencephaly, X-linked (3); Subcortical laminal heteropia, X-linked (3)
SCN5A	603830, 601144, 113900, 113900, 603829, 608567, 601154, 272120,	Long QT syndrome-3 (3); Brugada syndrome 1 (3); Heart block, progressive, type IA (3); Heart block, nonprogressive (3); Ventricular fibrillation, familial, 1 (3); Sick sinus syndrome 1 (3); Cardiomyopathy, dilated, 1E (3); {Sudden infant death syndrome, susceptibility to} (3);

	614022	Atrial fibrillation, familial, 10 (3)
SLC7A7	222700	Lysinuric protein intolerance (3)
CUBN	261100	Megaloblastic anemia-1, Finnish type (3)
ORC1	224690	Meier-Gorlin syndrome 1 (3)
FOXP1	613670	Mental retardation with language impairment and autistic features (3)
SPN	615828	Mental retardation, autosomal dominant 24 (3),
IL1RAPL1	300143	Mental retardation, X-linked 21/34 (3)
RAB39B	300271	Mental retardation, X-linked 72 (3)
RARB	615524	Microphthalmia, syndromic 12 (3)
SOX2	206900, 206900	Microphthalmia, syndromic 3 (3); Optic nerve hypoplasia and abnormalities of the central nervous system (3)
OTX2	610125, 613986, 610125	Microphthalmia, syndromic 5 (3); Pituitary hormone deficiency, combined, 6 (3); Retinal dystrophy, early-onset, and pituitary dysfunction (3)
HNF4A	125850, 125853, 616026	MODY, type I (3); {Diabetes mellitus, noninsulin-dependent} (3); Fanconi renotubular syndrome 4, with maturity-onset diabetes of the young (3)
TRIM37	253250	Mulibrey nanism (3)
RET	171400, 155240, 162300, 209880, 171300, 191830, 142623	Multiple endocrine neoplasia IIA (3); Medullary thyroid carcinoma (3); Multiple endocrine neoplasia IIB (3); Central hypoventilation syndrome, congenital (3); Pheochromocytoma (3); Renal agenesis (3); {Hirschsprung disease, susceptibility to, 1} (3)
IRF1	613659, 211980	Myelodysplastic syndrome, preleukemic (3); Myelogenous leukemia, acute (3); Gastric cancer, somatic (3); Nonsmall cell lung cancer, somatic (3)
MPO	254600, 104300	Myeloperoxidase deficiency (3); {Alzheimer disease, susceptibility to} (3); {Lung cancer, protection against, in smokers} (3)
TYROBP	221770	Nasu-Hakola disease (3)
SLC34A1	612286, 613388	Nephrolithiasis/osteoporosis, hypophosphatemic, 1 (3); Fanconi renotubular syndrome 2 (3)
SLC9A3R1	612287	Nephrolithiasis/osteoporosis, hypophosphatemic, 2 (3)
NPHS1	256300	Nephrotic syndrome, type 1 (3)
NALCN	615419	Neuroaxonal neurodegeneration, infantile, with facial dysmophism (3)
FAM134B	613115	Neuropathy, hereditary sensory and autonomic, type IIB (3)
RAC2	608203	Neutrophil immunodeficiency syndrome (3)
NTRK2	613886	Obesity, hyperphagia, and developmental delay (3)
SIM1	601665	Obesity, severe (3)
PLEKHM1	611497	Osteopetrosis, autosomal recessive 6 (3)
SLC4A1	612653, 611162, 179800, 611590, 110500, 112010, 112050, 601551, 601550	Ovalocytosis (3); Spherocytosis, type 4 (3); [Malaria, resistance to] (3); Renal tubular acidosis, distal, AD (3); Renal tubular acidosis, distal, AR (3); [Blood group, Diego] (3); [Blood group, Waldner] (3); [Blood group, Wright] (3); [Blood group, Froese] (3); [Blood group, Swann] (3)
PAX2	120330, 191830, 616002	Papillorenal syndrome (3); Renal hypoplasia, isolated (3); Glomerulosclerosis, focal segmental, 7 (3)
ALX4	609597, 613451, 615529	Parietal foramina 2 (3); Frontonasal dysplasia 2 (3); {Craniosynostosis 5, susceptibility to} (3)
SNCA	605543, 127750, 168601	Parkinson disease 4 (3); Dementia, Lewy body (3); Parkinson disease 1 (3)
KIT	172800, 606764, 154800, 601626, 273300	Piebaldism (3); Gastrointestinal stromal tumor, familial (3); Mast cell disease (3); Leukemia, acute myeloid (3); Germ cell tumors (3)
PKHD1	263200	Polycystic kidney and hepatic disease (3)
SLA	613811	Pontocerebellar hypoplasia type 2D (3),

HFM1	615724	Premature ovarian failure 9 (3)
FECH	177000	Protoporphyria, erythropoietic, autosomal recessive (3)
PNPO	610090	Pyridoxamine 5'-phosphate oxidase deficiency (3)
PKLR	266200, 102900	Pyruvate kinase deficiency (3); Adenosine triphosphate, elevated, of erythrocytes (3)
MET	605074, 114550	Renal cell carcinoma, papillary, 1, familial and somatic (3); Hepatocellular carcinoma, childhood type (3),
HNF1B	137920, 125853, 144700	Renal cysts and diabetes syndrome (3); Diabetes mellitus, noninsulin-dependent (3); {Renal cell carcinoma} (3)
SLC4A5	604278	Renal tubular acidosis, proximal, with ocular abnormalities (3)
ESCO2	268300, 269000	Roberts syndrome (3); SC phocomelia syndrome (3)
HESX1	182230, 182230, 182230	Septooptic dysplasia (3); Pituitary hormone deficiency, combined, 5 (3); Growth hormone deficiency with pituitary anomalies (3)
TBX4	147891	Small patella syndrome (3)
B4GALNT1	609195	Spastic paraplegia 26, autosomal recessive (3)
FOXP2	602081	Speech-language disorder-1 (3)
SYCP3	270960	Spermatogenic failure 4 (3); {Pregnancy loss, susceptibility to} (3)
SPTBN2	600224, 615386	Spinocerebellar ataxia 5 (3); Spinocerebellar ataxia, autosomal recessive 14 (3)
SYNE1	610743, 612998	Spinocerebellar ataxia, autosomal recessive 8 (3); Emery-Dreifuss muscular dystrophy 4, autosomal dominant (3)
DLL3	277300	Spondylocostal dysostosis 1, autosomal recessive (3)
DDR2	271665	Spondylometaepiphyseal dysplasia, short limb-hand type (3)
CSF2RB	614370	Surfactant metabolism dysfunction, pulmonary, 5 (3)
WNT3	273395	Tetra-amelia, autosomal recessive (3)
PROC	176860, 612304	Thrombophilia due to protein C deficiency, autosomal dominant (3); Thrombophilia due to protein C deficiency, autosomal recessive (3)
TRH	275120	Thyrotropin-releasing hormone deficiency (1)
SALL1	107480, 107480	Townes-Brocks syndrome (3); Townes-Brocks branchiootorenal-like syndrome (3)
TEC		Transient erythroblastopenia of childhood (2)
FGF5	190330	Trichomegaly (3)
GALNT3	211900	Tumoral calcinosis, hyperphosphatemic, familial (3)
WNT7A	276820, 228930	Ulna and fibula, absence of, with severe limb deficiency (3); Fuhrmann syndrome (3)
TBX3	181450	Ulnar-mammary syndrome (3)
ECM1	247100	Urbach-Wiethe disease (3)
IRF6	119300, 119500, 608864	van der Woude syndrome (3); Popliteal pterygium syndrome 1 (3); Orofacial cleft 6 (3)
GRHL3	606713	Van der Woude syndrome 2 (3)
WAS	301000, 313900, 300299, 313900	Wiskott-Aldrich syndrome (3); Thrombocytopenia, X-linked (3); Neutropenia, severe congenital, X-linked (3); Thrombocytopenia, X-linked, intermittent (3)

Supplemental Table 8.3: OMIM Sertoli genes

Symbol	MIM number	OMIM Description
AAGAB	148600	Keratoderma, palmoplantar, punctate type IA (3)
AASS	238700, 268700	Hyperlysinemia (3); Saccharopinuria (1)
ABAT	613163	GABA-transaminase deficiency (3)
ABCA12	601277, 242500	Ichthyosis, congenital, autosomal recessive 4A (3); Ichthyosis, autosomal recessive 4B (harlequin) (3)
ACSM3		{?Hypertension, essential} (1)
ACVR1B		Pancreatic cancer, somatic (3)
ADAM10	615537, 615590	Reticulate acropigmentation of Kitamura (3); {Alzheimer disease 18, susceptibility to} (3)
AFF2	309548	Mental retardation, X-linked, FRAXE type (3)
AHCY	613752	Hypermethioninemia with deficiency of S-adenosylhomocysteine hydrolase (3)
AK3		,
ALDH2	610251, 610251	Alcohol sensitivity, acute (3); {Hangover, susceptibility to} (3); {Sublingual nitroglycerin, susceptibility to poor response to} (3); {Esophageal cancer, alcohol-related, susceptibility to} (3)
ALDOA	611881	Glycogen storage disease XII (3)
AMH	261550	Persistent Mullerian duct syndrome, type I (3)
AMHR2	261550	Persistent Mullerian duct syndrome, type II (3)
AQP5	600231	Palmoplantar keratoderma, Bothnian type (3)
ARHGAP26	607785	Leukemia, juvenile myelomonocytic (3)
ART4	616060	[Blood group, Dombrock] (3)
ASAH1	228000, 159950	Farber lipogranulomatosis (3); Spinal muscular atrophy with progressive myoclonic epilepsy (3)
ASL	207900	Argininosuccinic aciduria (3)
ASS1	215700	Citrullinemia (3)
ATP1A2	602481, 104290, 602481	Migraine, familial hemiplegic, 2 (3); Alternating hemiplegia of childhood (3); Migraine, familial basilar (3)
ATP2A2	124200, 101900	Darier disease (3); Acrokeratosis verruciformis (3)
ATP2B3	302500	?Spinocerebellar ataxia, X-linked 1 (3)
ATP8A2	615268	?Cerebellar ataxia, mental retardation, and dysequilibrium syndrome 4 (3)
ATP8B1	211600, 243300, 147480	Cholestasis, progressive familial intrahepatic 1 (3); Cholestasis, benign recurrent intrahepatic (3); Cholestasis, intrahepatic, of pregnancy, 1 (3)
ATXN1	164400	Spinocerebellar ataxia 1 (3)
BCAT2		?Hypervalinemia or hyperleucine-isoleucinemia (1)
BCHE		Apnea, postanesthetic (3)
BHLHE41	612975	[Short sleeper] (3)
BLOC1S3	614077	Hermansky-Pudlak syndrome 8 (3)
BLVRA	614156	Hyperbiliverdinemia (3)
CACNA1C	601005, 611875	Timothy syndrome (3); Brugada syndrome 3 (3)
CD151	609057, 179620	Nephropathy with pretibial epidermolysis bullosa and deafness (3); [Blood group, Raph] (3)
CD2AP	607832	Glomerulosclerosis, focal segmental, 3 (3)
CD320	613646	Methylmalonic aciduria due to transcobalamin receptor defect (3)
CDH19	601390	Van Maldergem syndrome 1 (3),
CDH23	601067, 601386, 601067	Usher syndrome, type 1D (3); Deafness, autosomal recessive 12 (3); Usher syndrome, type 1D/F digenic (3)
CEBPA	601626	Leukemia, acute myeloid (3)

CHCHD10	615911	Frontotemporal dementia and/or amyotrophic lateral sclerosis 2 (3)
CISH	607948, 611162, 614383	{Tuberculosis, susceptibility to} (3); {Malaria, susceptibility to} (3); {Bacteremia, susceptibility to} (3)
CLCN2	607628, 607628, 607628, 615651	{Epilepsy, juvenile myoclonic, susceptibility to, 8} (3); {Epilepsy, juvenile absence, susceptibility to, 2} (3); {Epilepsy, idiopathic generalized, susceptibility to, 11} (3); Leukoencephalopathy with ataxia (3)
CNGA1	613756	Retinitis pigmentosa 49 (3)
COCH	601369	Deafness, autosomal dominant 9 (3)
COL17A1	226650	Epidermolysis bullosa, junctional, non-Herlitz type (3)
COL18A1	267750	Knobloch syndrome, type 1 (3)
COL27A1	615155	?Steel syndrome (3)
COL2A1	108300, 156550, 200610, 183900, 184250, 132450, 271700, 604864, 151210, 215150, 608805, 150600, 609508, 609162	Stickler syndrome, type I (3); Kniest dysplasia (3); Achondrogenesis, type II or hypochondrogenesis (3); SED congenita (3); SMED Strudwick type (3); Epiphyseal dysplasia, multiple, with myopia and deafness (3); Spondyloperipheral dysplasia (3); SED, Namaqualand type (3); Osteoarthritis with mild chondrodysplasia (3); Vitreoretinopathy with phalangeal epiphyseal dysplasia (3); Platyspondylic skeletal dysplasia, Torrance type (3); Otospondylomegaepiphyseal dysplasia (3); Avascular necrosis of the femoral head (3); Legg-Calve-Perthes disease (3); Stickler sydrome, type I, nonsyndromic ocular (3); Czech dysplasia (3)
COL8A2	136800, 609140	Corneal dystrophy, Fuchs endothelial, 1 (3); Corneal dystrophy, posterior polymorphous 2 (3)
COL9A1	614135, 614134	Epiphyseal dysplasia, multiple, 6 (3); Stickler syndrome, type IV (3)
COL9A2	600204, 603932, 614284	Epiphyseal dysplasia, multiple, 2 (3); {Intervertebral disc disease, susceptibility to} (3); Stickler syndrome, type V (3)
COL9A3	600969, 603932	Epiphyseal dysplasia, multiple, 3 (3); Epiphyseal dysplasia, multiple, with myopathy (3); {Intervertebral disc disease, susceptibility to} (3)
CORIN	614595	Preeclampsia/eclampsia 5 (3)
CP	604290, 604290, 604290	[Hypoceruloplasminemia, hereditary] (3); Cerebellar ataxia (3); Hemosiderosis, systemic, due to aceruloplasminemia (3)
CST3	105150, 611953	Cerebral amyloid angiopathy (3); Macular degeneration, age-related, 11 (3)
CTNNA3	615616	Arrhythmogenic right ventricular dysplasia, familial, 13 (3)
CTSF	615362	Ceroid lipofuscinosis, neuronal, 13, Kufs type (3)
CYBA	233690	Chronic granulomatous disease, autosomal, due to deficiency of CYBA (3)
CYP26B1	614416	Craniosynostosis with radiohumeral fusions and other skeletal and craniofacial anomalies (3)
DAG1	613818	Muscular dystrophy-dystroglycanopathy (limb-girdle), type C, 9 (3)
DBP		,
DHH	607080, 233420	46XY partial gonadal dysgenesis, with minifascicular neuropathy (3); 46XY sex reversal 7 (3)
DNMT3B	242860	Immunodeficiency-centromeric instability-facial anomalies syndrome 1 (3)
DOK1	616060	, [Blood group, Dombrock] (3)
DOK7	254300, 208150	Myasthenia, limb-girdle, familial (3); Fetal akinesia deformation sequence (3)
DSC2	610476, 610476	Arrhythmogenic right ventricular dysplasia 11 (3); Arrhythmogenic right ventricular dysplasia 11 with mild palmoplantar keratoderma and woolly hair (3)
DSG2	610193, 612877	Arrhythmogenic right ventricular dysplasia 10 (3); Cardiomyopathy, dilated, 1BB (3)
DSP	612908, 605676, 607450, 607655, 609638	Keratosis palmoplantaris striata II (3); Dilated cardiomyopathy with woolly hair and keratoderma (3); Arrhythmogenic right ventricular dysplasia 8 (3); Skin fragility-woolly hair syndrome (3); Epidermolysis bullosa, lethal acantholytic (3)

DST	614653, 615425	?Neuropathy, hereditary sensory and autonomic, type VI (3); Epidermolysis bullosa simplex, sutosomal recessive 2 (3)
DTNA	604169	Left ventricular noncompaction 1, with or without congenital heart defects (3)
DUOX2	607200	Thryoid dyshormonogenesis 6 (3)
EBP	302960	, Chondrodysplasia punctata, X-linked dominant (3)
EDN1	615706, 612798	Auriculocondylar syndrome 3 (3); Question mark ears, isolated (3); {High density lipoprotein cholesterol level QTL 7} (3)
ENO1		Enolase deficiency (1)
ENPP1	125853, 601665, 208000, 613312, 615522	{Diabetes mellitus, non-insulin-dependent, susceptibility to} (3); {Obesity, susceptibility to} (3); Arterial calcification, generalized, of infancy, 1 (3); Hypophosphatemic rickets, autosomal recessive, 2 (3); Cole disease (3)
EPS8	615974	?Deafness, autosomal recessive 102 (3)
ERBB2	211980, 137800, 613659	Adenocarcinoma of lung, somatic (3); Glioblastoma, somatic (3); Gastric cancer, somatic (3); Ovarian cancer, somatic, (3)
ERBB3	607598	Lethal congenital contractural syndrome 2 (3)
ERBB4	615515	Amyotrophic lateral sclerosis 19 (3)
ESPN	609006	Deafness, autosomal recessive 36 (3); Deafness, neurosensory, without vestibular involvement, autosomal dominant (3)
FAM83H	130900	Amelogenesis imperfecta, type III (3)
FGF16	309630	Metacarpal 4-5 fusion (3)
FGF9	612961	Multiple synostoses syndrome 3 (3)
FOLR1	613068	Neurodegeneration due to cerebral folate transport deficiency (3)
FUCA1	230000	Fucosidosis (3)
GALE	230350	Galactose epimerase deficiency (3)
GAMT	612736	Cerebral creatine deficiency syndrome 2 (3)
GATA4	607941, 614429, 614430, 615542, 187500	Atrial septal defect 2 (3); Ventricular septal defect 1 (3); Atrioventricular septal defect 4 (3); ?Testicular anomalies with or without congenital heart disease (3); Tetralogy of Fallot (3)
GATM	612718	Cerebral creatine deficiency syndrome 3 (3)
GCDH	231670	Glutaricaciduria, type I (3)
GDNF	209880, 171300, 613711	Central hypoventilation syndrome (3); {Pheochromocytoma, modifier of} (3); {Hirschsprung disease, susceptibility to, 3} (3)
GJA1	164200, 186100, 241550, 600309, 257850, 218400	Oculodentodigital dysplasia (3); Syndactyly, type III (3); Hypoplastic left heart syndrome 1 (3); Atrioventricular septal defect 3 (3); Oculodentodigital dysplasia, autosomal recessive (3); Craniometaphyseal dysplasia, autosomal recessive (3)
GJB1	302800	Charcot-Marie-Tooth neuropathy, X-linked dominant, 1 (3)
GJB2	220290, 601544, 124500, 148350, 148210, 602540, 149200	Deafness, autosomal recessive 1A (3); Deafness, autosomal dominant 3A (3); Vohwinkel syndrome (3); Keratoderma, palmoplantar, with deafness (3); Keratitis-ichthyosis-deafness syndrome (3); Hystrix-like ichthyosis with deafness (3); Bart-Pumphrey syndrome (3)
GLB1	230500, 230600, 230650, 253010	GM1-gangliosidosis, type I (3); GM1-gangliosidosis, type II (3); GM1-gangliosidosis, type III (3); Mucopolysaccharidosis type IVB (Morquio) (3)
GM2A	272750	GM2-gangliosidosis, AB variant (3)
GNB3	145500	{Hypertension, essential, susceptibility to} (3)
GPR179	614565	Night blindness, congenital stationary (complete), 1E, autosomal recessive (3)
GPR56	606854, 615752	Polymicrogyria, bilateral frontoparietal (3); Polymicrogyria, bilateral perisylvian (3)
HFE	235200, 612635, 176200, 176100, 104300, 614193	Hemochromatosis (3); {Microvascular complications of diabetes 7} (3); {Porphyria variegata, susceptibility to} (3); {Porphyria cutanea tarda, susceptibility to} (3); {Alzheimer disease, susceptibility to} (3); [Transferrin serum level QTL2] (3)

HK1	235700, 605285	, Hemolytic anemia due to hexokinase deficiency (3); Neuropathy, hereditary motor and sensory, Russe type (3),
HK2		,
HMGCS2	605911	HMG-CoA synthase-2 deficiency (3)
HOGA1	613616	Hyperoxaluria, primary, type III (3)
HPS3	614072	Hermansky-Pudlak syndrome 3 (3)
HS6ST1	614880	{Hypogonadotropic hypogonadism 15 with or without anosmia} (3)
HSD17B3	264300	Pseudohermaphroditism, male, with gynecomastia (3)
HSPB1	608634, 606595	Neuropathy, distal hereditary motor, type IIB (3); Charcot-Marie-Tooth disease, axonal, type 2F (3)
HTRA1	610149, 610149, 600142	{Macular degeneration, age-related, 7} (3); {Macular degeneration, age-related, neovascular type} (3); CARASIL syndrome (3)
IDH1	137800	{Glioma, susceptibility to, somatic} (3)
IFNGR2	614889	Immunodeficiency 28, mycobacteriosis (3)
IGSF1	300888	Hypothyroidism, central, and testicular enlargement (3)
IL10RA	613148	Inflammatory bowel disease 28, early onset, autosomal recessive (3)
ITGA6	226730	Epidermolysis bullosa, junctional, with pyloric stenosis (3)
KBTBD13	609273	Nemaline myopathy 6, autosomal dominant (3)
KCNE1	612347, 613695	Jervell and Lange-Nielsen syndrome 2 (3); Long QT syndrome 5 (3)
KCNQ1	192500, 220400, 607554, 609621, 192500	Long QT syndrome 1 (3); Jervell and Lange-Nielsen syndrome (3); Atrial fibrillation, familial, 3 (3); Short QT syndrome 2 (3); {Long QT syndrome 1, acquired, susceptibility to} (3)
KCNT1	614959, 615005	Epileptic encephalopathy, early infantile, 14 (3); Epilepsy, nocturnal frontal lobe, 5 (3)
KIF21A	135700, 135700	Fibrosis of extraocular muscles, congenital, 1 (3); Fibrosis of extraocular muscles, congenital, 3B (3)
KLK1	615953	[Kallikrein, decreased urinary activity of] (3)
KRT8	215600, 215600	Cirrhosis, cryptogenic (3); {Cirrhosis, noncryptogenic, susceptibility to} (3)
LAMA3	615235, 226700, 226650, 245660	Cardiomyopathy, dilated, 1JJ (3), Epidermolysis bullosa, junctional, Herlitz type (3); Epidermolysis bullosa, generalized atrophic benign (3); Laryngoonychocutaneous syndrome (3)
LDHB	614128	Lactate dehydrogenase-B deficiency (3)
LMF1	246650	Lipase deficiency, combined (3)
LPL	238600, 144250	Lipoprotein lipase deficiency (3); Combined hyperlipidemia, familial (3); [High density lipoprotein cholesterol level QTL 11] (3)
LRP4	212780, 614305	Cenani-Lenz syndactyly syndrome (3); Sclerosteosis 2 (3)
LTBP2	613097, 613086, 251750, 614819	Tooth agenesis, selective, 6 (3), Glaucoma 3, primary congenital, D (3); Microspherophakia and/or megalocornea, with ectopia lentis and with or without secondary glaucoma (3); Weill-Marchesani syndrome 3, recessive (3)
LZTS1	133239	Esophageal squamous cell carcinoma (3)
MAMLD1	300758	Hypospadias 2, X-linked (3)
MAN2B1	248500	Mannosidosis, alpha-, types I and II (3)
MANBA	248510	Mannosidosis, beta (3)
MAP2K1	615279	Cardiofaciocutaneous syndrome 3 (3)
MASP1	257920	3MC syndrome 1 (3)
MBP		,
MEF2A	608320	{Coronary artery disease, autosomal dominant, 1} (3)
MID2	300928	?Mental retardation, X-linked 101 (3)
MINPP1	188470	Thyroid carcinoma, follicular (3)
MMD2		, Miyoshi muscular dystrophy 2 (2)

MPI	602579	Congenital disorder of glycosylation, type Ib (3)
MTM1	310400	Myotubular myopathy, X-linked (3)
MYBPC3	115197, 615396, 615396	Cardiomyopathy, familial hypertrophic, 4 (3); Cardiomyopathy, dilated, 1MM (3); Left ventricular noncompaction 10 (3)
MYH14	600652, 614369	Deafness, autosomal dominant 4A (3); Peripheral neuropathy, myopathy, hoarseness, and hearing loss (3),
MYH6	613251, 614089, 613252, 614090	Cardiomyopathy, familial hypertrophic, 14 (3); Atrial septal defect 3 (3); Cardiomyopathy, dilated, 1EE (3); {Sick sinus syndrome 3} (3)
MYO7A	276900, 600060, 601317	Usher syndrome, type 1B (3); Deafness, autosomal recessive 2 (3); Deafness, autosomal dominant 11 (3)
NAGLU	252920	Mucopolysaccharidosis type IIIB (Sanfilippo B) (3)
NOS1	615413	Spermatogenic failure 12 (3),
NQO1		{Benzene toxicity, susceptibility to} (3); {Leukemia, post-chemotherapy, susceptibility to} (3); {Breast cancer, poor survival after chemotherapy for} (3)
NR0B1	300200, 300018	Adrenal hypoplasia, congenital, with hypogonadotropic hypogonadism (3); 46XY sex reversal 2, dosage-sensitive (3)
NR0B2	601665	Obesity, mild, early-onset (3)
NR3C2	177735, 605115	Pseudohypoaldosteronism type I, autosomal dominant (3); Hypertension, early-onset, autosomal dominant, with exacerbation in pregnancy (3)
NR5A1	612965, 612964, 613957	46XY sex reversal 3 (3); Premature ovarian failure 7 (3); Adrenocortical insufficiency (3); Spermatogenic failure 8 (3)
NSDHL	308050, 300831	CHILD syndrome (3); CK syndrome (3)
NT5E	211800	Calcification of joints and arteries (3)
OPLAH	260005	5-oxoprolinase deficiency (3)
P2RX2	608224	Deafness, autosomal dominant 41 (3)
PAK3	300558	Mental retardation, X-linked 30/47 (3)
PAPSS2	612847	Brachyolmia 4 with mild epiphyseal and metaphyseal changes (3)
PDE11A	610475	Pigmented nodular adrenocortical disease, primary, 2 (3)
PDE8B	614190, 609161	Pigmented nodular adrenocortical disease, primary, 3 (3); Striatal degeneration, autosomal dominant (3)
PGAM2	261670	Glycogen storage disease X (3)
PGAP2	614207	Hyperphosphatasia with mental retardation syndrome 3 (3)
PGAP3	615716	Hyperphosphatasia with mental retardation syndrome 4 (3)
PGM3	615816	Immunodeficiency 23 (3)
PGP		,
PHF8	300263	Mental retardation syndrome, X-linked, Siderius type (3)
PHGDH	601815, 256520	Phosphoglycerate dehydrogenase deficiency (3); Neu-Laxova syndrome1 (3)
PINK1	605909	Parkinson disease 6, early onset (3)
PITPNM3	600977	Cone-rod dystrophy 5 (3)
PLA2G5	228980	Fleck retina, familial benign (3)
PLA2G6	256600, 610217, 612953	Infantile neuroaxonal dystrophy 1 (3); Neurodegeneration with brain iron accumulation 2B (3); Parkinson disease 14 (3)
PLCB2		Platelet PLC beta-2 deficiency (1)
PLEC	226670, 131950, 612138, 613723	Muscular dystrophy with epidermolysis bullosa simplex (3); Epidermolysis bullosa simplex, Ogna type (3); Epidermolysis bullosa simplex with pyloric atresia (3); Muscular dystrophy, limb-girdle, type 2Q (3)
PLOD2	609220	Bruck syndrome 2 (3)
PPT1	256730	Ceroid lipofuscinosis, neuronal, 1 (3)
PRSS12	249500	Mental retardation, autosomal recessive 1 (3)
PSAP	249900, 610539,	, Metachromatic leukodystrophy due to SAP-b deficiency (3); Gaucher

	611721, 611722	disease, atypical (3); Combined SAP deficiency (3); Krabbe disease, atypical (3)
PTPRF	616001	?Breasts and/or nipples, aplasia or hypoplasia of, 2 (3)
PVRL1	225060, 225060	Cleft lip/palate-ectodermal dysplasia syndrome (3); Orofacial cleft 7 (3)
REEP1	610250, 614751	Spastic paraplegia 31, autosomal dominant (3); Neuronopathy, distal hereditary motor, type VB (3)
REEP2	615625, 615625	?Spastic paraplegia 72, autosomal recessive (3); ?Spastic paraplegia 72, autosomal dominant (3)
RGS2		, Rieger syndrome, type 2 (2)
RGS9BP	608415	Bradyopsia (3)
RHBDF2	148500	Tylosis with esophageal cancer (3)
RILP	612437	Epilepsy, progressive myoclonic 1B (3)
RIN2	613075	Macrocephaly, alopecia, cutis laxa, and scoliosis (3)
RNF135	614192	Macrocephaly, macrosomia, facial dysmorphism syndrome (3)
RNF213	607151	{Moyamoya disease 2, susceptibility to} (3)
ROBO3	607313	Gaze palsy, horizontal, with progressive scoliosis (3)
RP9	180104	?Retinitis pigmentosa 9 (3)
RUNX1	601626, 601399	Leukemia, acute myeloid (3); Platelet disorder, familial, with associated myeloid malignancy (3)
SEMA4A	610282, 610283	Retinitis pigmentosa 35 (3); Cone-rod dystrophy 10 (3)
SEMA7A	614745	[Blood group, John-Milton-Hagen system] (3)
SERPINI1	604218	Encephalopathy, familial, with neuroserpin inclusion bodies (3)
SGSH	252900	Mucopolysaccharidisis type IIIA (Sanfilippo A) (3)
SH3TC2	601596, 613353	Charcot-Marie-Tooth disease, type 4C (3); Mononeuropathy of the median nerve, mild (3)
SIAE	613551	{Autoimmune disease, susceptibility to, 6} (3)
SIL1	248800	Marinesco-Sjogren syndrome (3)
SLC13A2		,
SLC13A5	615905	Epileptic encephalopathy, early infantile, 25 (3)
SLC17A9	616063	Porokeratosis 8, disseminated superficial actinic type (3)
SLC30A2	608118	Zinc deficiency, transient neonatal (3)
SLC34A2	265100, 610441	Pulmonary alveolar microlithiasis (3); ?Testicular microlithiasis (3)
SLC52A3	211530, 211500	Brown-Vialetto-Van Laere syndrome 1 (3); Fazio-Londe disease (3)
SLC6A14	300306	{Obesity, susceptibility to, BMIQ11} (3)
SLC6A4	607834, 164230	{Anxiety-related personality traits} (3); {Obsessive-compulsive disorder} (3)
SLC6A8	300352	Cerebral creatine deficiency syndrome 1 (3)
SMOC1	206920	Microphthalmia with limb anomalies (3)
SMPX	300066	Deafness, X-linked 4 (3)
SOBP	613671	Mental retardation, anterior maxillary protrusion, and strabismus (3)
SORT1	613589	[Low density lipoprotein cholesterol level QTL6] (3)
SOX10	613266, 611584, 609136	Waardenburg syndrome, type 4C (3); Waardenburg syndrome, type 2E, with or without neurologic involvement (3); PCWH syndrome (3)
SOX9	114290, 114290, 114290	Campomelic dysplasia with autosomal sex reversal (3); Acampomelic campomelic dysplasia (3); Campomelic dysplasia (3)
SPINT2	270420	Diarrhea 3, secretory sodium, congenital, syndromic (3)
SPRY4	615266	Hypogonadotropic hypogonadism 17 with or without anosmia (3)
SRC		Colon cancer, advanced, somatic (3)
STEAP3	615234	?Anemia, hypochromic microcytic, with iron overload 2 (3)
STIM1	612783, 160565, 185070	Immunodeficiency 10 (3); Myopathy, tubular aggregate, (3); Stormorken syndrome (3)

SYT2	616040	Myasthenic syndrome, presynaptic, congenital, with or without motor neuropathy (3)
TAPBP	604571	Bare lymphocyte syndrome, type I (3)
TCN2	275350	Transcobalamin II deficiency (3)
TCTN2	613885	Meckel syndrome 8 (3)
THRA	614450	Hypothyroidism, congenital, nongoitrous, 6 (3)
TLR3	613002, 609423	{Herpes simplex encephalitis, susceptibility to, 2 (3); {HIV1 infection, resistance to} (3)
TMIE	600971	Deafness, autosomal recessive 6 (3)
TNNC1	611879, 613243	Cardiomyopathy, dilated, 1Z (3); Cardiomyopathy, familial hypertrophic, 13 (3)
TNNI3	613690, 115210, 611880, 613286	Cardiomyopathy, familial hypertrophic, 7 (3); Cardiomyopathy, familial restrictive, 1 (3); Cardiomyopathy, dilated, 2A (3); Cardiomyopathy, dilated, 1FF (3)
TNNT2	115195, 601494, 612422, 601494	Cardiomyopathy, familial hypertrophic, 2 (3); Cardiomyopathy, dilated, 1D (3); Cardiomyopathy, familial restrictive, 3 (3); Left ventricular noncompaction 6 (3)
TRIM32	254110, 615988	Muscular dystrophy, limb-girdle, type 2H (3); ?Bardet-Biedl syndrome 11 (3)
TRPV3	614594	Olmsted syndrome (3)
TSPAN7	300210	Mental retardation, X-linked 58 (3)
TUBB2B	610031	Polymicrogyria, symmetric or asymmetric (3)
UCP2	607447	{Obesity, susceptibility to, BMIQ4} (3)
UNC119	615518	?Cone-rod dystrophy (3); ?Immunodeficiency 13 (3)
USP9X	300919	Mental retardation, X-linked 99 (3)
VAMP1	108600	Spastic ataxia 1, autosomal dominant (3)
VAT1		,
VNN1		[High density lipoprotein cholesterol level QTL 8] (3)
WDR72	613211	Amelogenesis imperfecta, type IIA3 (3)
XYLT1	264800, 615777	{Pseudoxanthoma elasticum, modifier of severity of} (3); Desbuquois dysplasia 2 (3)
ZBTB18	612337	?Mental retardation, autosomal dominant 22 (3)
ZBTB20	259050	Primrose syndrome (3)

Supplemental Data associated with this thesis

Refer to accompanying .xls, .pdf and movie files associated with the thesis.

Supplemental Video 1. Demonstration of heart injection of constructs in 11.5 dpc embryo. This video demonstrates the injection of a construct (marked by blue dye) into the left ventricle of the beating embryo heart at 11.5 dpc. After several heartbeats the dye can be seen in more distal parts of the embryo and finally in the head vein indicating successful injection. After injection the embryo is incubated with the heart still beating for 30 min before dissection for organ culture. For more detailed information see Fig. 2.1 and Materials and Methods Chapter 2.

Supplemental Data 1: RNA-seq expression data.

Somatic cells isolated from the *Sf1*-eGFP testis (Sertoli, FLC and NSICs) at 12.5 dpc. This workbook contains the cpm data from this gonad cell lineage RNA-seq paper. Only genes with at least 1 count per million in three or more samples were retained (features= 14,307). The "cpm" sheet of the workbook provides results for all retained ENSMUSG transcripts. The counts for a transcript can be graphed using this data file in the “graph cpm” sheet.

Supplemental Data 2: Genes upregulated in enriched cell populations at 12.5 dpc.

This workbook contains the genes that were upregulated in each enriched cell population.:

1) Genes upregulated in a Sertoli specific manner ("Sertoli_Specific_UP")

2) Genes upregulated in a FLC specific manner ("FLC_Specific_UP")

3) Genes upregulated in a NSIC manner ("NSIC_Specific_UP_incl_gc")

4) Genes upregulated in a NSIC manner with any gene that is annotated as a germ cell genes in the Jameson et al. (2012) dataset removed ("NSIC_Specific_UP_no_gc")

This workbook also contains the results of the direct comparisons between “Leydig vs Sertoli” (5), “Leydig vs NSIC” (6) and “Sertoli vs NSIC”(7).

Supplemental Data 3: GO of genes upregulated in enriched cell populations at 12.5 dpc.

Gene ontology analysis was performed using the DAVID Bioinformatics Package (v6.7) (http://david.abcc.ncifcrf.gov; (Huang et al., 2009a; Huang et al., 2009b)) The genes identified for each TF, TM and SF GO term category were then mapped back to the respective file in Supplemental Data 2 and ranked by the moderated F-statistic. The top 10 genes are listed in Fig. 3.9. The cluster and chart results for each population are also listed in their entirety in this file.

Supplemental Data 4: Genes "on" at 11.5dpc in gonadal microarray screens that are detected as upregulated in the FLC enriched population by RNA-seq at 12.5 dpc. Leydig cell enriched genes at 12.5 dpc that also show differential expression between interstitial and supporting cell of 11.5 dpc XY gonad are putative pre-FLC marker genes. Table 3.4 summarises top results. The logFC, P.Value, and adj.P.Val columns indicate results from differential expression analysis. Int. Exp (interstitial) and Sup. Exp (supporting) show median normalised expression of the gene in each of these two cell types, while Int. Rank (interstitial) and Sup. Rank (supporting) indicate the position of the gene in a list ranked by expression in that cell type (0=lowest expression, 100=highest expression).

Published Papers Forming Part Of This Thesis

Peer-reviewed papers

McClelland KS, Wainwright EN, Bowles J and Koopman P. (2014) Rapid screening of gene function by systemic delivery of morpholino oligonucleotides to live mouse embryos. *PLOS ONE* 10(1): e0114932. doi:10.1371/journal.pone.0114932

McClelland KS, Bell K, Larney C, Harley VR, Sinclair A, Oshlack A, Koopman P and Bowles J (2015) Purification and transcriptomic analysis of mouse fetal Leydig cells reveals candidate genes for disorders of sex development. *Biology of Reproduction,* doi:10.1095/biolreprod.115.128918

Review paper

McClelland K, Bowles J and Koopman P. (2012) "Male sex determination: insights into molecular mechanisms." *Asian Journal of Andrology*, 14(1): 164-71

Jointly-Authored Paper Not Forming Part Of The Thesis

Peer-reviewed paper

Wainwright EN, Jorgensen JS, Kim Y, Truong V, Bagheri-Fam S, Davidson T, Svingen T, Fernandez-Valverde SL, **McClelland KS,** Taft RJ, Harley VR, Koopman P, Wilhelm D. (2013) SOX9 regulates microRNA miR-202-5p/3p expression during mouse testis differentiation. *Biology of Reproduction*, 89: 34, 1-12

PLOS ONE

RESEARCH ARTICLE

Rapid Screening of Gene Function by Systemic Delivery of Morpholino Oligonucleotides to Live Mouse Embryos

Kathryn S. McClelland, Elanor N. Wainwright, Josephine Bowles*, Peter Koopman

Institute for Molecular Bioscience, The University of Queensland, Brisbane, Queensland, Australia

* j.bowles@imb.uq.edu.au

Citation: McClelland KS, Wainwright EN, Bowles J, Koopman P (2015) Rapid Screening of Gene Function by Systemic Delivery of Morpholino Oligonucleotides to Live Mouse Embryos. PLoS ONE 10(1): e0114932. doi:10.1371/journal.pone.0114932

Academic Editor: Michael Schubert, Laboratoire de Biologie du Développement de Villefranche-sur-Mer, FRANCE

Received: September 29, 2014

Accepted: November 16, 2014

Published: January 28, 2015

Data Availability Statement: All relevant data are within the paper and its Supporting Information files.

Funding: This work was supported by the Australian Research Council and the National Health and Medical Research Council (NHMRC) of Australia. P. K. is a Senior Principal Research Fellow of the NHMRC.

Competing Interests: The authors have declared that no competing interests exist.

Abstract

Traditional gene targeting methods in mice are complex and time consuming, especially when conditional deletion methods are required. Here, we describe a novel technique for assessing gene function by injection of modified antisense morpholino oligonucleotides (MOs) into the heart of mid-gestation mouse embryos. After allowing MOs to circulate through the embryonic vasculature, target tissues were explanted, cultured and analysed for expression of key markers. We established proof-of-principle by partially phenocopying known gene knockout phenotypes in the fetal gonads (*Stra8*, *Sox9*) and pancreas (*Sox9*). We also generated a novel double knockdown of *Gli1* and *Gli2*, revealing defects in Leydig cell differentiation in the fetal testis. Finally, we gained insight into the roles of *Adamts19* and *Ctrb1*, genes of unknown function in sex determination and gonadal development. These studies reveal the utility of this method as a means of first-pass analysis of gene function during organogenesis before committing to detailed genetic analysis.

Introduction

One of the central challenges in the era of functional genomics is to understand gene function and unravel the complex networks in which proteins operate to determine phenotype. With RNA-seq data amassing on top of an already large list of genes gleaned from microarray screens, many candidate genes now require functional assessment. In addition, possible causative genes for human developmental diseases are being identified rapidly in rare disease cohorts as a result of whole exome and whole genome sequencing.

Much of the functional genomics effort focuses on the mouse model because of its relevance to human development, physiology and disease. Investigation of gene function in mouse has traditionally involved the generation and breeding of complete or conditional loss-of-function alleles via homologous recombination, involving a complex and time-consuming experimental pipeline. Even with advances in genome editing technologies such as the CRISPR/Cas-9 system (for review see [1]), the generation of knockout animals for every promising gene candidate is impractical. Moreover, it is often the case that, after investing the time and resources required to generate a conventional or conditional gene knockout, little or no phenotype results.

Therefore, there is a pressing need to develop methods that provide insight into developmental gene function either as a pre-screen before committing to genome manipulation approaches *in vivo*, or as a means of prioritizing candidates for further analysis.

With this goal in mind, a variety of methods for accelerated *ex vivo* functional analysis have been reported. In the field of gonadal development, these methods have included injection, electroporation or liposome-based delivery of viral-based or siRNA-based constructs into explanted tissue [2–4], followed by organ culture and histological or molecular analysis. Typically, these approaches have caused damage to the target tissue as well as being limited in delivery area. For other developing organs, such as mouse lung and kidney, morpholino antisense oligonucleotides (MOs) have been added to the culture media, but these experiments show high variability due to limited passive uptake of the MO [5–9].

We aimed to develop a method whereby gene function could be perturbed *ex vivo*, rapidly and without injury to the target organ. Here we show that injection of commercially available MOs into the beating heart of a 11.5 dpc (days *post coitum*) mouse embryo results in delivery via the vasculature to the gonads and pancreas. We demonstrate knockdown of protein expression for a number of target genes, leading to predicted downstream effects for known genes and novel functional insights for other genes or combinations of genes. This method offers a rapid, reproducible, efficient means of rapidly pre-screening gene candidates for likely function, as a prelude to more rigorous functional studies in mice.

Materials and Methods

Morpholino design

Splice site MOs were designed to target exon/intron boundaries of target genes (for sequences see S1 Table). All MOs were vivo-MOs which incorporate a dendrimeric octaguanidine delivery moiety end modification, with the exception shown in Fig. 1H, I, where a carboxyfluorescein-labelled standard control MO (F-MO) was used.

Heart injections

For ease of sexing embryos, we used the X-linked GFP line (Hadjantonakis et al., 1998), maintained on an outbred Swiss albino background (Quackenbush strain). Noon on the day on which the mating plug was detected was designated as 0.5 days *post coitum* (dpc). All animal work was conducted according to protocols approved by the University of Queensland Animal Ethics Committee. This study was approved by the University of Queensland Animal Ethics Committee (Permit Number: IMB/176/13/NHMRC/ARC).

Embryos were explanted at 11.5 dpc and placed into PBS (phosphate buffered saline) at 37°C with the amniotic sac intact and the placenta attached. If required, embryos were sexed by GFP expression. The amniotic sac was opened, taking care not to damage any major blood vessels. The left ventricle of the beating heart of the embryo was injected with a MO-cocktail (20 ng/μL (single target) or 15 ng/μL (per MO, two targets) and 6% commercial food dye (Queen Fine Foods Pty. Ltd.)). For each embryo either control or MO targeted against gene of interest (Gene Tools, LLC) was delivered using a Sutter-pulled glass capillary needle. Injection was continued until the marker dye was observed in the head vein (approx. 6–8 heart beats, equivalent to ~20–27 ng MO/embryo (single MO) or ~30–40 ng MO/embryo (combination of two MOs); see S1 Video and Fig. 1). Embryos with non-beating or weakly beating hearts, or where injection was unsuccessful as judged by lack of circulation of the dye (about 1 in 15 embryos), were excluded from further study. Embryos were left to recover for 30 min in pre-warmed PBS in an incubator at 37°C, 5% CO_2; hearts were still beating at the end of this period.

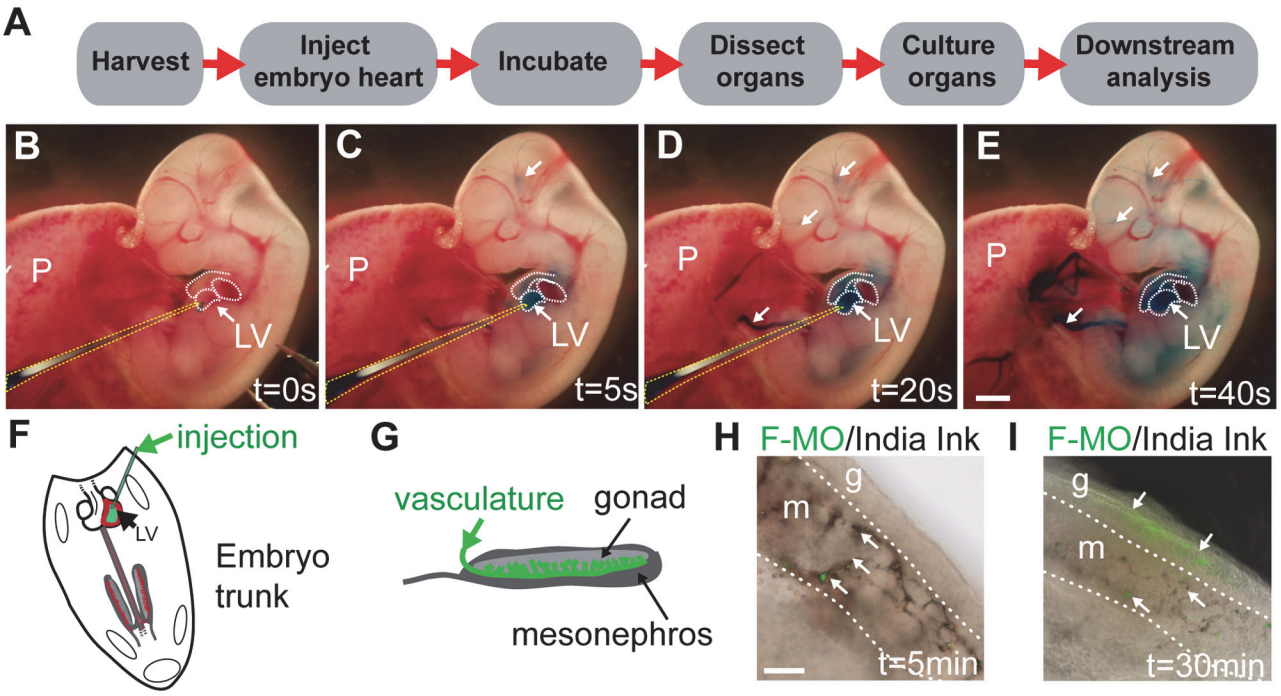

Fig 1. Overview of method: MO delivery by heart injection. (A) Experimental pipeline from harvest of embryos through to injection, culture and downstream analyses. Visualisation of heart injection protocol can be seen in S1 Video and images B–E. The cocktail of dye and MO in PBS is delivered via injection into the left ventricle of the beating heart at 11.5 dpc (B). Dye can be visualised going around the embryonic vasculature (indicated by white arrows) (C, D) and into the head vasculature (D) before the whole embryo is coloured (E). Schematic of ventricle injection (F) and the embryonic gonad which is highly vascularised (G). Delivery of India ink and F-MO (indicated by white arrows) shows the compounds reaching the mesonephric plexus at 5 min post-injection (H; $n = 3$); after 30 min F-MO positive cells were observed in the gonad proper (I; $n = 3$). s = seconds; min = minutes; g = gonad; m = mesonephros; F-MO = carboxyfluorescein-labelled standard control morpholino oligonucleotide. Scale bars: E = 1 mm, H = 0.5 mm.

doi:10.1371/journal.pone.0114932.g001

Video of the above procedure was captured on an Olympus SZX-12 Stereomicroscope (see S1 Video).

For assessing delivery area using a F-MO: 20 μg/mL F-MO (20–27 ng/embryo) and 2% India ink was delivered by heart injection as described above ($n = 3$). After 5 and 30 min recovery the genital ridge was imaged on an Olympus BX-51 Upright Fluorescence/Brightfield microscope.

For gonad culture, UGR (urogenital ridge: gonad plus mesonephros) was dissected out and hanging drops were prepared by pipetting 40 μL of media (BJGB media (Gibco) with 4% Serum Supreme (Lonza), 1% penicillin/streptomycin (Gibco) and 200 mg/mL ascorbic acid (Sigma Aldrich)) containing a single UGR onto the inner face of the lid of a 24 well tissue culture plate. PBS (500 μL) was added to each well and the lid was then inverted to close the plate. After 48 h, cultured gonads were washed in PBS for 5 min and processed for qRT-PCR, Western blot or immunohistochemistry.

For pancreas culture, the foregut endoderm was isolated and any non-affiliated organs removed. The foregut was placed on a Millipore (5 μM TPMT) filter floating on 600 μl of culture medium (M199 media (Gibco) with 10% Serum Supreme (Lonza) and 2% penicillin/streptomycin (Gibco)) and cultured for 4–6 days at 37°C, 5% CO_2 with the media changed every other day. After culture, tissues were washed in PBS for 5 min and processed for qRT-PCR or immunohistochemistry.

Quantitative RT-PCR analysis

Total RNA was extracted and cDNA generated from cultured gonad or pancreas as previously described (Bowles et al., 2010). Duplicate assays were carried out on an ABI Prism 7500 Sequence Detector System. *Tbp* (TATA box binding protein) was used as an endogenous control to normalize gene expression levels [10]. Taqman gene expression sets were as listed in S2 Table.

Relative transcript abundance was calculated using the $2^{-\Delta CT}$ method. Error bars represent S.E.M. calculated from independent biological replicates; statistical significance was assessed using unpaired (two-tailed) Student's *t*-test.

Immunofluorescence

Analyses were carried out on fixed, paraffin-embedded 7 μm sections using standard methods. Briefly, gonad plus mesonephros complexes or foreguts were fixed in 4% paraformaldehyde in phosphate buffered saline overnight at 4°C. Tissues were embedded in 1.5% low melt agarose, ethanol dehydrated, paraffin-embedded and 7 μm sections were cut using a Leica Microtome. Slides were dewaxed by 2 x 10 min washes in xylene, re-hydrated and boiled for 5 min in Antigen Unmasking Solution (Vector Laboratories), then incubated at room temperature for 60 min. The slides were washed for 3 x 10 min in 0.1% Triton-X in PBS (PBTX). The sections were incubated with primary antibodies, which were diluted in blocking buffer at 4°C overnight (for primary antibodies see S3 Table). Antibodies were removed with three washes in PBTX, and the slides re-blocked for 30 min at room temperature. Secondary antibodies were incubated at room temperature for 2 h. The secondary antibodies were removed with three PBS washes before DAPI staining and mounting with a 60% glycerol/PBS solution. Secondary antibodies were all from Invitrogen Molecular Probes (see S4 Table). Sections were examined by confocal microscopy using a Zeiss LSM-510 META or LSM-710 META confocal microscope.

Whole-mount immunofluorescence

Whole mount immunofluorescence was performed as detailed in [11].

Cell quantification

For quantification of the number of INS- and PAX6-positive cells in the pancreas, and HSD3β, NR5A1, SOX9-positive cells in the XY gonad, de-identified gonads or foreguts were serially sectioned at 7 μm and processed as per the immunofluorescence protocol. Quantification was performed on all sections per sample using the ImageJ64 "Cell Counter" plugin. Error bars depict S.E.M. calculated from independent biological replicates; statistical significance was determined using unpaired (two-tailed) Student's *t*-test. Asterisks indicate level of statistical significance in pertinent comparisons.

Western blot

Western blots were carried out as described previously [12], with slight modifications. Briefly, gonad pairs were dissociated with a 13-gauge needle and lysed in 1× SDS sample buffer (62.5 mM Tris—HCl (pH 6.8), 2% SDS, 10% glycerol, 50 mM dithiothreitol, and 0.01% w/v bromophenol blue), separated on SDS-PAGE and transferred to a PVDF membrane (Millipore). SOX9 primary antibody was incubated for 2 h at room temperature and then overnight at 4°C with 13.5 dpc testis as a positive control and 13.5 dpc ovary as a negative control. For primary antibodies see S3 Table, for secondary antibodies see S4 Table. Proteins were visualized using Clarity Western ECL Substrate (Bio-Rad) on a ChemiDoc machine (Bio-Rad). Raw intensity of

bands was determined using Image Lab Software (version 4.0). SOX9 intensity units were calculated relative to α-TUB or β-ACT loading control and relative downregulation calculated with cMO sample set to 1 for individual cMO vs. Sox9MO-treated samples on each of 3 blots. Error bars represent S.E.M. calculated from independent biological replicates; statistical significance was assessed using unpaired (two-tailed) Student's *t*-test.

Flow cytometry and cell sorting

Flow cytometry and cell sorting was carried out as described previously [13]. Briefly, 12.5 dpc *Sf1*-eGFP [14] litters were dissected, gonads sexed by eye and separated from the mesonephros before being dissociated. Cells were incubated with SSEA1-PE antibody (BD Biosciences) to tag germ cells. FACS was performed using a BD FACS Aria cell sorter. Pools of germ (SSEA1-positive) and eGFP-positive cells were collected separately and total RNA was extracted and cDNA prepared as described [15]. Cells from three or four independent litters and sorting experiments were used for qRT-PCR analysis.

Results

Method development: Delivering morpholinos to fetal organs

Initially, we trialled the inclusion of standard 'naked' MOs or vivo-MOs (in which the MO is linked to a dendrimeric octaguanidine delivery moiety) in the media for *ex vivo* organ culture from 11.5 dpc for 48h (data not shown), using a protocol similar to those previously published for lungs and kidneys [7,9], but were unable to achieve widespread tissue uptake and hence efficacy. Therefore, we developed a novel protocol that relied on a combination of two approaches.

First, in order to deliver the compounds uniformly through the organs of interest in the mid-gestation embryo, we looked to classic experiments in mouse and chick, where India ink was used to visualise the early vasculature (for review see [16]). This approach has also been utilised to deliver siRNA and viral constructs to the embryo [17], and to deliver lectin to the 11.5 dpc gonad via the vasculature [18]. These studies relied on injection of compounds into the beating embryonic heart, and so we reasoned that this approach might offer a way to successfully deliver MOs to vascularised tissues in the mouse embryo.

Second, Vivo-Morpholinos (Gene Tools, LLC) were chosen for injection as they reportedly show improved systemic delivery efficacy compared to standard MOs [19–21]. Oligonucleotides were designed to span intron/exon boundaries within the pre-mRNA to produce non-functional, mis-spliced gene products. A standard commercial 25-mer MO (see Materials and Methods) was used as a control for the specificity of MO effects.

We trialled our knockdown procedure using the developing ovaries, testes and pancreas as a test-bed. These organs are well suited to vascular delivery of compounds, are readily explanted, develop normally in organ culture, and are well characterised in terms of morphological and molecular markers of differentiation and morphogenesis. Examination of organogenesis allows specificity and off-target effects of the MO to be assessed by testing for markers of differentiation of the targeted cell type and multiple non-targeted other cell types. Inclusion of developing gonads in these studies offers the additional advantage that known differences in sexually dimorphic gene expression can be used as a further control for general toxicity and/or off-target effects.

A summary of the workflow is shown in Fig. 1A, and the detailed protocol is described in Materials and Methods. Conceptuses were explanted at 11.5 dpc and the amniotic sac of individual embryos opened, taking care not to disrupt major amniotic blood vessels. A MO/food dye cocktail was injected into the left ventricle of the beating heart (Fig. 1B, F) until the dye was

observed to travel around the embryo and into the vessels in the head, typically after 6–10 heart beats (Fig. 1C–E; S1 Video). After injection, embryos were allowed to recover for ~30 min to enable delivery of MO throughout the vasculature. Subsequently, tissues of interest were explanted, and cultured *ex vivo*, before detailed analysis of gene and protein marker expression. In preliminary experiments, we used carboxyfluorescein-labelled MO (F-MO) to assess the extent of delivery to tissues ($n = 3$). In the case of the developing gonads, F-MO and India ink were observed in the nascent mesonephric vasculature at 5 min post-injection (Fig. 1G, H) and were clearly visible in the gonadal tissue after 30 min (Fig. 1I), suggesting that the dye and MO had accessed the target tissue.

Proof of principle: STRA8 in the developing ovary

The germ cells of the gonad are the precursors of sperm (XY) or oocytes (XX): whether they adopt the male or female developmental pathway is determined by their somatic environment (for review see [22]). Upregulation of the gatekeeping gene *Stra8* (*stimulated by retinoic acid gene 8*) at 12.5 dpc is essential for germ cell entry into meiosis in the developing ovary, as demonstrated by the blockade of meiosis in XX *Stra8*$^{-/-}$ gonads (Baltus et al., 2006; for review see [23]). Since *Stra8*$^{-/-}$ gonads have a well-defined phenotype, we tested MO knockdown of *Stra8* as a proof-of-principle experiment.

Although *Stra8* transcript could still be detected after MO treatment (Part A in S1 Fig.), expression of STRA8 protein was greatly decreased as measured by immunofluorescence in Stra8MO-treated XX gonads, indicating successful knockdown (Fig. 2A). Strikingly, meiotic markers γ-H2AX (H2A histone family, member X; Fig. 2A) and SCP3 (synaptonemal complex protein 3; Fig. 2B) were not localised to the nucleus in XX Stra8MO samples, in contrast to control ovaries, where germ cells began to show these hallmark signs of entry into meiosis. Stra8MO knockdown did not have a direct effect on qRT-PCR expression of other meiosis markers (Part C–E in S1 Fig.). However, functional aspects of meiosis, such as SCP3 nuclear localisation, were clearly affected by Stra8MO treatment (Fig. 2 A, B).

We tested for possible effects of generalised toxicity in MO-treated gonads by examining expression of a range of cell lineage markers. Immunofluorescence and qRT-PCR for markers of germ cells—OCT4/POU5F1 (POU domain, class 5, transcription factor 1; Fig. 2B, Part G in S1 Fig.), *Mvh/Ddx4* (Deadbox polypeptide 4; Part F in S1 Fig.) and CDH1 (Cadherin 1; Part H, I in S1 Fig.) indicated that the number of germ cells was unaffected in Stra8MO treated gonads, suggesting no qualitative or quantitative detrimental effect on germ cells. Furthermore, expression of the somatic marker FOXL2 (Forkhead box L2; Part B, I in S1 Fig.) was unchanged in Stra8MO XX gonads, indicating that gonadogenesis in general was not impaired by MO-treatment. Combined, these data show that the reduced meiotic marker expression was likely a specific consequence of MO antagonism of STRA8 expression, rather than generalised toxicity.

In summary, the suppression of markers associated with meiotic entry suggests that germ cells failed to successfully enter meiosis in Stra8MO knockdown XX gonads. Thus, the Stra8MO knockdown partially phenocopied the *Stra8*$^{-/-}$ gonad phenotype.

Proof of principle: SOX9 in the developing testis

To test whether MO treatment can influence phenotype when the protein of interest is already abundant at the time of treatment, we performed MO knockdown of SOX9 (SRY (sex determining region Y)-box 9) at 11.5 dpc. SOX9 expression stimulates the male pathway by promoting Sertoli cell differentiation [24]. In *Sox9*$^{-/-}$ XY embryos, gonadal sex reversal occurs as SOX9 is both necessary and sufficient for male sex determination [25,26]. However, in heterozygous *Sox9*-mutant XY embryos, Sertoli cells are able to differentiate and the SOX9 downstream

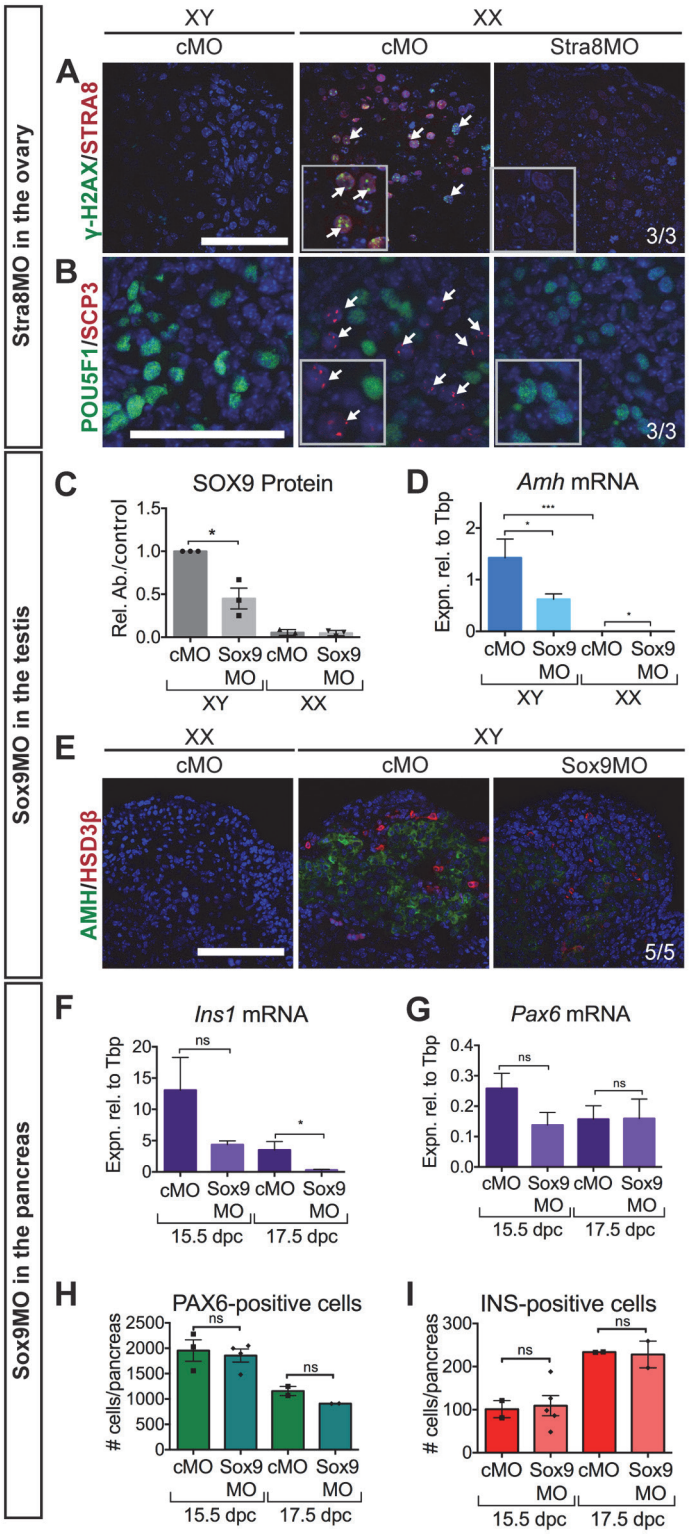

Fig 2. Partial phenocopy of known gene knockouts in gonad and pancreas. (A, B) STRA8 knockdown: IF showed knockdown of STRA8 (A) in Stra8MO-treated XX gonads. Nuclear localisation of meiosis markers (γH2AX (A) and SCP3 (B); indicated by white arrows; see inserts) was absent but germ cells were present (POU5F1 (B); see inserts) in XX Stra8MO-treated gonads. (C–E) Knockdown of SOX9 in the gonad: Western blot for SOX9 (relative to α-TUBULIN or β-ACTIN) showed a downregulation of SOX9 (C) after Sox9MO

treatment in XY gonads (n = 3). Downregulation of expression of SOX9 target gene *Amh* (D) expression was observed by qRT-PCR (n = 8, 15, 11, 4). IF for AMH and HSD3β (E) showed that AMH staining was weaker in XY Sox9MO samples compared to XY controls and that HSD3β-positive FLCs were present but staining was weaker in XY Sox9MO-treated gonads. (F–I) Knockdown of SOX9 in the pancreas: qRT-PCR of Sox9Mo treated pancreata showed *Ins1* (F) was downregulated but *Pax6* (G) was unchanged (n = 5, 5, 5, 5). Quantification of PAX6/INS-positive cells revealed that PAX6-positive (H) and INS-positive (I) cell number was unaltered by Sox9MO treatment (n = 3, 4, 2, 2). Scale bars = 100 μM; cMO = control morpholino; xMO = morpholino targeting gene x. For Western blots SOX9 levels were normalised to α-TUBULIN or β-ACTIN loading controls and Sox9MO-treated XY gonads measured relative to cMO treated XY gonads with expression for each blot set to 1. Rel. Ab./control = Relative Abundance of SOX9 to α-TUBULIN or β-ACTIN. For all qRT-PCR levels are shown relative to *Tbp*, error = S.E.M. For cell quantification error = S.E.M. with individual counts plotted. * = p = 0.05, ** = p = 0.001, *** = p = 0.0001, ns = not statistically significant.

doi:10.1371/journal.pone.0114932.g002

target anti-Müllerian hormone (AMH) is still produced [27,28]. Since SOX9 protein is already abundant in the XY genital ridge at 11.5 dpc, the time of MO treatment, we asked whether MO treatment might result in no effect, full gonadal sex reversal, or an intermediate phenotype.

We found that SOX9 protein abundance was significantly decreased in the Sox9MO treated gonads, as assessed by Western blot (Fig. 2C, for blots see S3 Fig.) and immunofluorescence (Part H in S2 Fig.), although the expression of *Sox9* transcript was unchanged (Part A in S2 Fig.). Moreover, the expression of *bona fide* direct SOX9 target genes *Amh* [29] and *Ptgds* (*prostaglandin D2 synthase*; [30]) were significantly reduced (Fig. 2D, Part B in S2 Fig.) in Sox9MO treated XY gonads compared to XY controls, and AMH protein expression levels were also reduced compared to the control XY gonad (Fig. 2E).

In Sox9MO-treated gonads, residual SOX9 and therefore AMH expression was sufficient to initiate Müllerian duct regression by 13.5 dpc (Part J in S2 Fig.). Consistent with this finding, we showed that SOX9 levels were not sufficiently suppressed as to allow upregulation of the female somatic pathway; FOXL2-positive cells were not observed (Part H in S2 Fig.) and expression of *Fst* (*follistatin*), a female somatic marker, was not upregulated in XY Sox9MO samples compared to XY cMO samples as assessed by qRT-PCR (Part F in S2 Fig.).

The expression of another Sertoli expressed gene, *Dhh* (*desert hedgehog*; [31]) was not significantly downregulated (Part C in S2 Fig.). Accordingly, fetal Leydig cell (FLC) differentiation occurred in the knockdown of SOX9 in XY gonads, as assessed by expression of FLC markers *Cyp11a1* (*cytochrome P450*, *family 11*, *subfamily a*, *polypeptide 1*; Part E in S2 Fig.), *Nr5a1*/NR5A1 (nuclear receptor subfamily 5, group A, member 1; Part D, I in S2 Fig.) and HSD3β (hydroxy-delta-5-steroid dehydrogenase, 3 beta- and steroid delta-isomerase 1; Fig. 2E). As expected, germ cells were unaffected by Sox9MO treatment in both XX and XY gonads, as assessed by the expression of *Ddx4* (Part G in S2 Fig.) and CDH1 (cadherin 1; Part I in S2 Fig.).

In summary, treatment with Sox9MO at 11.5 dpc resulted in a phenotype similar to that of the heterozygous *Sox9* genetic knockout, with reduced target gene expression but no gonadal sex reversal. There was no effect of Sox9MO treatment on germ cells, suggesting the phenotype observed was not due to off-target or toxic effects of the MO.

Proof of principle: SOX9 in the developing pancreas

To demonstrate the utility of MO heart injections for functional assay in other developing organs, we knocked down SOX9 in the developing pancreas. In addition to its roles in gonadogenesis, SOX9 also plays a role endocrine cell differentiation in the pancreas [32,33]. Heterozygous *Sox9*-mutant mice (most closely phenocopied by the Sox9MO effects on gonadal development described above) form fewer endocrine islets, but insulin- and glucagon-positive daughter cells still differentiate [32]. Additionally, heterozygous *Sox9*-mutant mice have

decreased expression of *Pdx1* (*pancreatic and duodenal homeobox 1*; expressed in SOX9-positive multipotent progenitor cells) and *Ngn3* (*neurogenin 3*; endocrine progenitor cells) [34]. We therefore investigated whether treatment with Sox9MO at 11.5 dpc would cause a decrease in expression of *Pdx1/Ngn3* and genes associated with insulin production and/or a decrease in the number of endocrine insulin-positive cells.

We conducted our analyses at 4 days and 6 days post-treatment (the equivalent of 15.5 dpc and 17.5 dpc, respectively). By immunofluorescence we saw a decrease in SOX9 expression (Part K, L in S4 Fig.) in Sox9MO treated pancreata at 15.5 dpc. Importantly, PAX6-positive (Part I, J in S4 Fig.; Fig. 2H) and INS-positive (Fig. 2I) endocrine cells were present in Sox9MO treated pancreata, indicating that the residual SOX9 expression after MO treatment at 11.5 dpc is sufficient to allow endocrine cell types to differentiate. We observed a significant decrease in the expression of *Ins1* (*insulin 1*) and *Ins2* (*insulin 2*) in Sox9MO treated pancreata at 17.5 dpc (Fig. 2F, Part D in S4 Fig.), however the number of INS-positive (Insulin I/II) cells was unperturbed (Fig. 2I). We also investigated the expression of *Pax6* (*paired box 6*), which marks endocrine cells, and found no change in *Pax6* expression (Fig. 2G) or the number of PAX6-positive cells (Fig. 2H) in response to Sox9MO treatment in the cultured pancreata. We found by qRT-PCR that expression of putative direct SOX9 target *Pdx1* (Part C in S4 Fig.; [34]) was unaltered but *Ngn3* (Part B in S4 Fig.; [34]) expression was significantly decreased at 17.5 dpc.

SOX9 knockdown partially mimicked the heterozygous *Sox9*-mutant mouse phenotype as the effect we saw on endocrine cells was restricted to expression of *Ins1*, *Ins2* and *Ngn3*. Expression of *Sox9* was unaltered (Part A in S4 Fig.), as was expression of non-β cell sub-type markers including *Glug* (*glucagon*; α-cells, Part E in S4 Fig.), *Ghrl* (*Ghrelin*; ε-cells, Part F in S4 Fig.), *Ppy* (*Pancreatic polypeptide*; PP-cells, Part G in S4 Fig.) and *Sst* (*Somatostatin*; δ-cells, Part H in S4 Fig.) at both timepoints.

Together, these results suggest that *Ins1*, *Ins2* and *Ngn3* transcription in the pancreas was specifically suppressed by Sox9MO treatment which, therefore, partially phenocopied the heterozygous *Sox9*-mutant mice [32,34]. The specificity of these effects suggests that MO treatment did not result in off-target effects or generalised toxicity in the pancreas. Moreover, the effects of MO knockdown were detectable for at least 6 days post treatment.

MO-mediated double knockdown of GLI transcription factors

We next investigated whether this approach could be used to knock down multiple genes simultaneously, as is commonplace in zebrafish and *Xenopus* studies. To this end we created a double knockdown of the downstream Hedgehog pathway activators GLI1 (GLI-Kruppel family member 1) and GLI2 (GLI-Kruppel family member 2). The Hedgehog signaling pathway promotes the differentiation of the steroidogenic FLC population during testis development. During this process, the ligand DHH (Desert hedgehog) is secreted by Sertoli cells. Hedgehog receptor, PTCH1 (Patched homolog 1), which is induced by Hedgehog signaling, as well as Hedgehog targets GLI1 and GLI2, are expressed by cells of the entire interstitial space that surrounds the testis cords [31,35,36]. In *Dhh*-knockout XY gonads, there are greatly reduced numbers of steroidogenic FLCs [31,36]. However, the differentiation of the FLC population is unaffected in XY gonads of either of *Gli1* or *Gli2* single-knockout embryos, suggesting that GLI factors act redundantly in the testis [35].

To address this potential redundancy, we generated a double knockdown of *Gli1/Gli2* using MO heart injection at 11.5 dpc and examined the effects 48h post-injection equivalent to 13.5 dpc. As a result, we detected by qRT-PCR a decrease in expression of steroidogenic pathway genes *Nr5a1*, *Star* (*steroidogenic acute regulatory protein*), *Cyp11a1* and *Hsd3β* (Fig. 3A–D), indicating a reduction in steroidogenic cell number or capacity. The decrease in *Nr5a1*

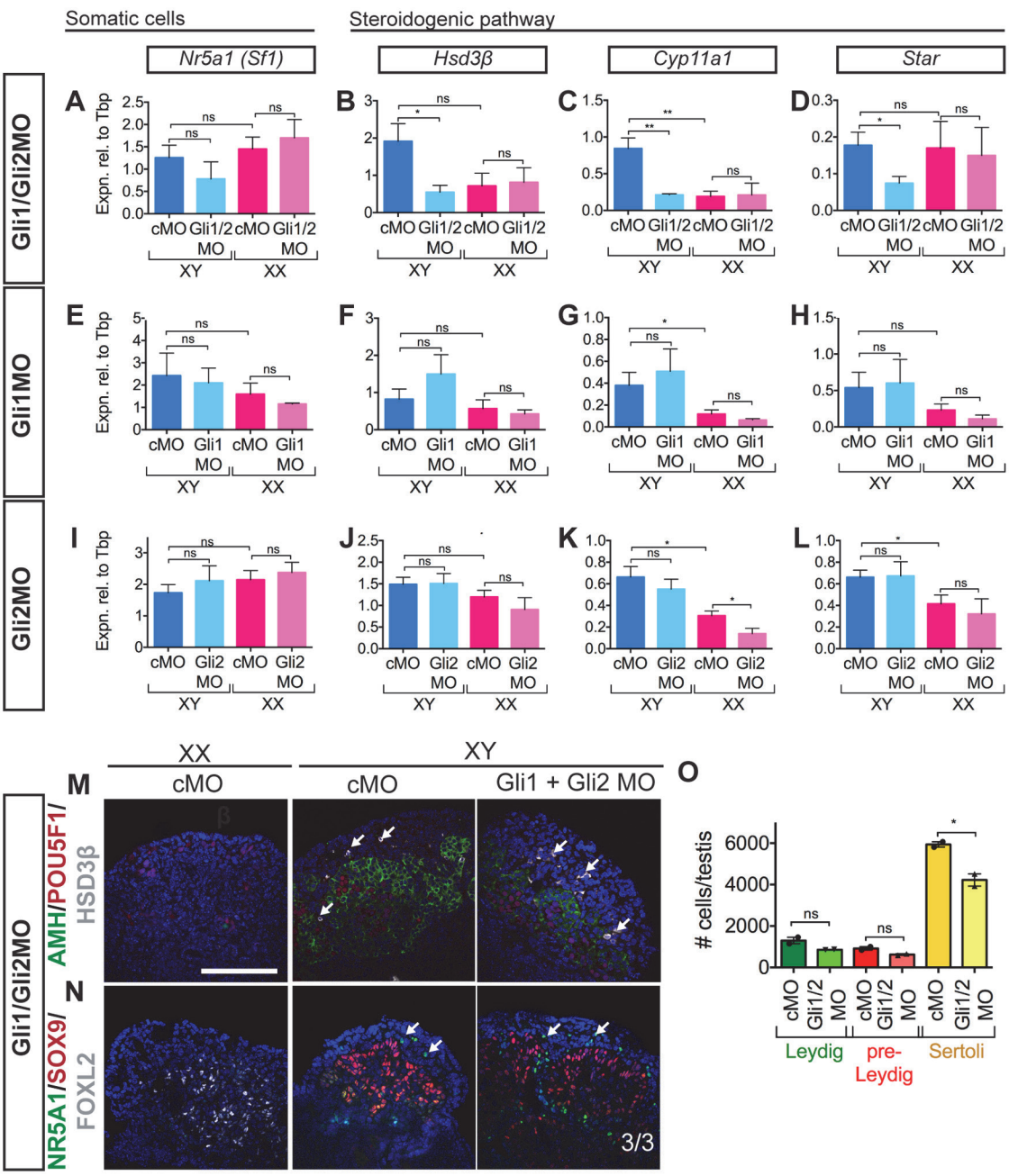

Fig 3. Double knockdown of *Gli1/Gli2* in XY gonads. (A–D) Knockdown of GLI1/GLI2 in the gonad: qRT-PCR showed that treatment with Gli1/Gli2MO (n = 6, 5, 5, 8) resulted in no significant downregulation in steroidogenic regulator *Sf1/Nr5a1* (A) but a significant downregulation in expression of steroidogenic pathway enzymes *Hsd3β* (B), *Cyp11a1* (C) and *Star* (D). No change was observed in *Nr5a1* expression in Gli1MO or Gli2MO knockdown (E, I). Similarly, there were no changes in expression of steroidogenic pathway enzymes *Hsd3β* (F, J), *Cyp11a1* (G, K) and *Star* (H, L) in Gli1MO (E–H; n = 6, 6, 7, 5) or Gli2MO (I–L; n = 8, 7, 4, 3) single knockdowns. IF showed Sertoli cells (AMH (M) and SOX9 (N)) and germ cells (POU5F1 (M)) were present in XY Gli1/Gli2MO treated gonads and no FOXL2-positive cells were observed (N). Steroidogenic *Hsd3β*-positive (M) and *Nr5a1*-positive (N) cells were still present in Gli1/Gli2MO treated XY gonads. Quantification (n = 2) of steroidogenic cells revealed no change in the number of HSD3β-positive Leydig cells (O; green) or SF1-positive/SOX9-negative pre-Leydig cells (O; red). There was a decrease in the number of SOX9-positve Sertoli cells in the Gli1/2MO treated XY gonads (O; yellow). Scale bars = 100 μM; cMO = control morpholino; xMO = morpholino targeting gene x. For all qRT-PCR levels are shown relative to *Tbp*, error = S.E.M. For cell quantification error = S.E.M. with individual counts plotted. * = p = 0.05, ** = p = 0.001, ns = not statistically significant.

doi:10.1371/journal.pone.0114932.g003

expression was consistent but not statistically significant. Notably, no change in the expression of these genes was detected in single Gli1MO (Fig. 3E–H) or Gli2MO (Fig. 3I–L) knockdowns. Thus, the attenuation of steroidogenic gene expression was specific to the Gli1/2MO double knockdown. No difference was observed in levels of the Hedgehog receptor gene *Ptch1* by qRT-PCR in the double or single knockdowns relative to controls (Part C, F, I in S5 Fig.), indicating that the extent of GLI knockdown was not sufficient to perturb expression of at least one known GLI target.

We quantified the number of steroidogenic cells to determine whether the decrease in steroidogenic gene expression was due to a decrease in cell number or to an impediment to cell maturation. There was no significant difference in the number of NR5A1-positive/SOX9-negative (immature FLC) or HSD3β-positive (FLC) cells between Gli1/2MO treated XY gonads and controls (Fig. 3M, N, O), suggesting that the observed phenotype is due to a decrease in steroidogenic capacity of the Leydig cell population. Testis cords formed properly and expression of Sertoli cell marker *Amh*/AMH (Part A, D, G in S5 Fig.) and germ cell markers *Ddx4*/POU5F1 (Fig. 2M, Part B, E, H in S5 Fig.) appeared unaffected by the Gli1/2MO treatment (Fig. 3C, D), consistent with a lack of off-target or broadly toxic effects. Our results support functional redundancy between *Gli1* and *Gli2* in FLCs, and demonstrate proof-of-principle that heart injection of MO can be used to target multiple genes simultaneously to assess possible genetic interactions.

Addressing novel gene function: Adamts19 and Ctrb1

Finally, we characterised the knockdown of two genes to which functions have not previously been ascribed, so as to test the utility of the system for first-pass functional characterisation of novel genes. We focused first on the ovarian gene *Adamts19* (*a disintegrin-like and metallopeptidase [reprolysin type] with thrombospondin type 1 motif, 19*), identified in a PCR-based cDNA subtraction screen, and in which polymorphisms have since been associated with premature ovarian failure (POF; [37–39]. The function of this gene remains unknown at the molecular, cellular or whole organism levels.

We performed qRT-PCR on FACS-sorted somatic cells at 12.5 dpc and confirmed that *Adamts19* was expressed in FOXL2-positive somatic cells, and not in the XX germ cells (Fig. 4A). MO knockdown of *Adamts19* resulted in no change in XX granulosa somatic markers *Fst* or *Irx3* (*Iroquois related homeobox 3*; Fig. 4B, C) and slight but not statistically significant decrease in expression of the germ cell marker *Ddx4* (Fig. 4D). However, there were no observed gross changes in the ratio of the number of FOXL2-positive (somatic) to MVH-positive (germ) cells by immunofluorescence (Fig. 4H). qRT-PCR expression of male markers *Amh* (Fig. 4E) and *Cyp11a1* (Fig. 4G) and somatic marker *Nr5a1* (Fig. 4F) were unperturbed by Adamts19MO treatment indicating there were no broad off-target effects of MO treatment. These results do not indicate a clear role for *Adamts19* in the developing ovary. Importantly, these data illustrate that treatment with a MO does not always perturb gonadogenesis, pointing to a lack of generalized non-specific artefacts.

We also examined the Sertoli-expressed gene *Ctrb1* (*chymotrypsinogen B1*), which has been implicated in gonadal development. In a screen of XX *Wnt4*-knockout (*wingless-related MMTV integration site 4*) mice, which exhibit partial sex reversal, expression of *Ctrb1* was increased, suggesting an association with the testis development pathway [40]. Differential expression data sets indicate that *Ctrb1* is testis-specific from 12.5 dpc and that it is expressed in the Sertoli cell lineage [41].

Knockdown of *Ctrb1* resulted in no change to Sertoli cell markers *Sox9* and *Amh*, but a statistically significant increase in the expression of *Ptgds* in the testis by qRT-PCR (Fig. 4I, J, K).

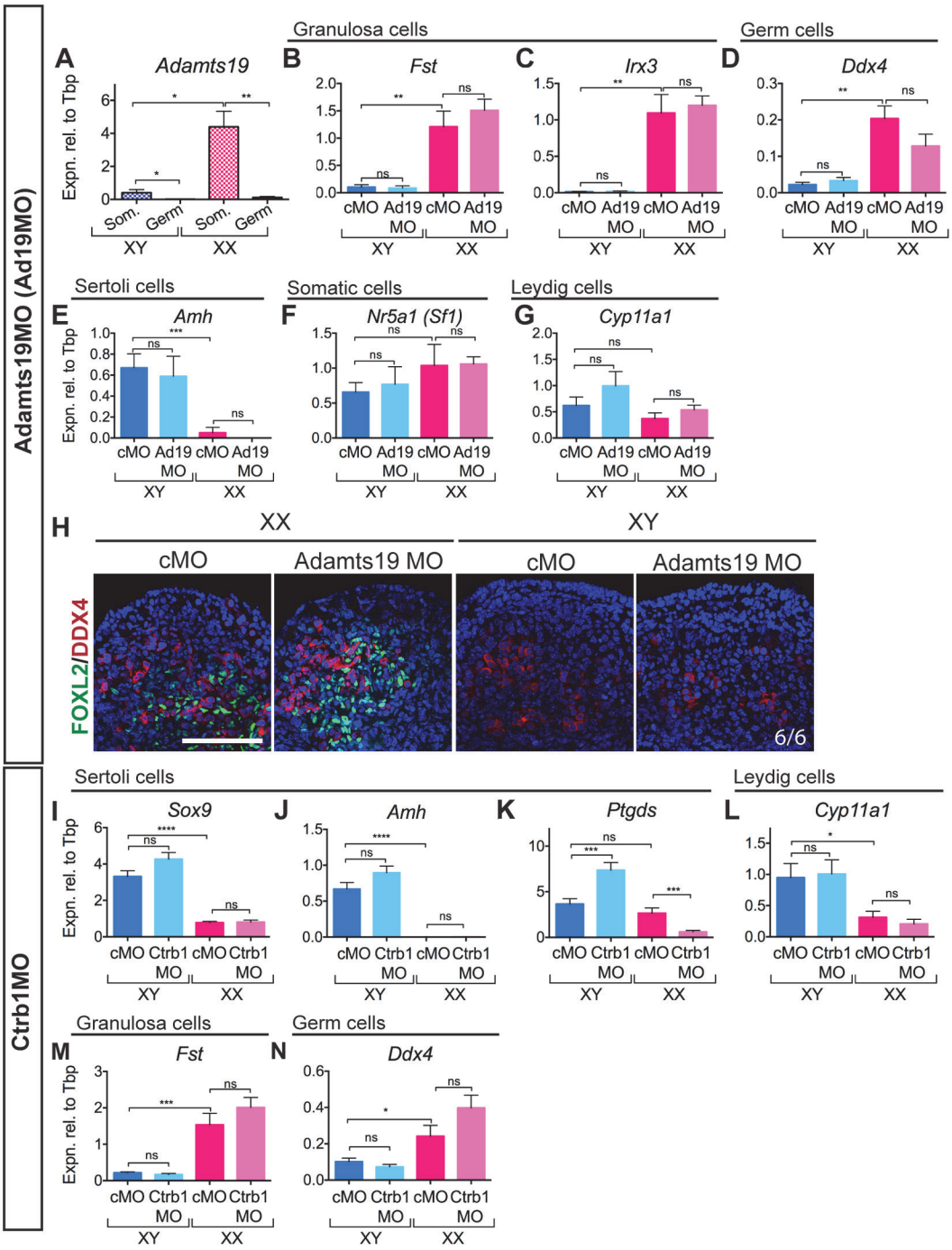

Fig 4. Knockdown of *Adamts19* in XX gonads and *Ctrb1* in XY gonads. (A) qRT-PCR on FACS-sorted somatic and germ cells (n = 3, 4, 3, 4) shows that *Adamts19* is expressed in the somatic cells of the ovary at 12.5 dpc and at much lower levels in somatic cells of the testis. Knockdown of ADAMTS19 in the XX gonad (n = 7, 8, 5, 5) showed no change in female somatic markers *Fst* (B) and *Irx3* (C) and a slight decrease in expression of germ cell marker *Ddx4* (D). Male markers, *Amh* (Sertoli cells; E), *Nr5a1* (Somatic cells; F) and *Cyp11a1* (Leydig cells; G) were unperturbed. IF showed no discernable difference in the ratios of FOXL2-positive/DDX4-positive cells in the Adamts19MO-treated XX gonad compared to the control (H). Knockdown of CTRB1 in the XY gonad (n = 19, 16, 14, 14) resulted in no change to male somatic markers *Sox9* (I) or *Amh* (J) but an increase in *Ptgds* (K) was observed in the Ctrb1MO-treated XY gonad. Expression of Leydig cell marker *Cyp11a1* (L), female somatic marker *Fst* (M) and germ cell marker *Ddx4* (N) was unchanged. Germ = germ cells, Som. = somatic cells. Scale bars = 100 μM; cMO = control morpholino; xMO = morpholino targeting gene x. For all qRT-PCR: levels are shown relative to *Tbp*, error = S.E.M., * = p = 0.05, ** = p = 0.001, *** = p = 0.0001, **** = p = 0.00001, ns = not statistically significant.

doi:10.1371/journal.pone.0114932.g004

In the XX Ctrb1MO treated gonad, *Ptgds* expression was decreased compared to the XX control. No changes were observed in the expression of the steroidogenic gene *Cyp11a1*, granulosa cell marker *Fst* or germ cell marker *Ddx4* (Fig. 4L, M, N) in the XY Ctrb1MO treated gonad, suggesting that the other testis cell lineages are unperturbed. The increase in *Ptgds* expression resulting from knockdown of *Ctrb1* implicates *Ctrb1* in processes downstream of SOX9, such as *Ptgds* regulation and as such provides a basis for the instigation of further genetic studies.

Discussion

We describe here a novel first-pass screening method that can provide insights into the function of candidate organogenesis genes, singly or in combination, either to assist with the design of in-depth genetic and biochemical investigations, or to prioritize lists of candidate genes for these investigations. By injection of MOs into the heart of mouse embryos, we exploited the embryonic vasculature to deliver the MO to the target tissues, which were then explanted, cultured and analysed. Using this technique we partially reproduced known gene knockout phenotypes in the fetal gonads and pancreas, created a novel double knockdown of GLI1 and GLI2, and screened *Adamts19* and *Ctrb1* for potential function in early gonadal development. These studies reveal the utility of this method to obtain insights into gene function during organogenesis rapidly and relatively simply.

The method described here provides a significant improvement on previous injection- and electroporation-based delivery strategies, which suffered from limited delivery area and/or uptake, tendency for tissue damage and lack of reproducibility. Published methods of gain-of-function (cDNA) or loss-of-function (shRNA) construct delivery by magnetofection, nucleofection or liposome-mediated methods in cultured gonads have shown delivery of the effector construct to 2–20% of cells in the target tissue [2–4,42]. In contrast, we visualized delivery of fluorescent MO throughout the tissue of interest, saw consistent knockdown of downstream target genes throughout the cultured organ, and showed in the XY gonad that the MO could target genes in multiple cell lineages. Secondly, injection of the MO into the heart avoids compromising the integrity of the target tissue by direct contact with needles and/or electrodes. Finally, relying on systemic delivery rather than direct injection of the effector construct avoids experimental error and instead produced consistent gene knockdown for the target gene in multiple experiments performed over a two-year period.

Encouragingly, in our proof-of-principle and double-knockdown experiments, it was the capacity of a cell population to express downstream target genes and proteins, rather than the number of expressing cells, that was altered by MO treatment. The knockdown of the target protein was incomplete in all cases; this allowed differentiation of the target cells but their functionality was reduced. For example, FLCs still differentiated in normal numbers in the *Gli1/Gli2* MO treated XY gonads, but they did not produced steroid enzymes at the same capacity as the controls. This indicates that the processes controlled by GLI factors were being perturbed by MO treatment, similarly to the Sox9MO treated XY gonads and pancreata. Importantly, the subtle outcomes of MO treatment were highly reproducible, as shown by our qRT-PCR analyses, suggesting that the information generated provides a robust basis on which to base mechanistic hypotheses and further experiments.

In addition to partially reproducing several established null mouse models, using MO injection we strengthened the case for creating a complex genetic conditional double knockout of GLI1 and GLI2 in FLCs [35]. Our findings suggest that there is functional redundancy between GLI1 and GLI2 in the developing testis and that further genetic analysis is likely to be fruitful.

With any experiments involving MOs, careful attention to controls is required [43]. By careful examination of untargeted cell populations in the organ of interest, we were able to identify

and exclude off-target effects and toxicity. Nonetheless, concerns have been raised regarding the difference between MO knockdown phenotypes and other functional analysis methods [44]. This difference is at least partly explained by the fact that MO knockdown only partially reduces overall activity of the target protein; certainly, in our Sox9MO experiments, the phenotypes obtained more closely resembled heterozygous than homozygous knockouts. All things considered, it is clear that genetic targeting by homologous recombination or CRISPR/Cas9 approaches will remain the gold standard for functional analysis. Therefore, we suggest that, once a likely effect is revealed by MO studies, it would be more useful to advance to definitive functional experiments, rather than to devote additional resources to definitively excluding off-target effects (for example by assaying multiple MOs for each gene of interest).

Supporting Information

S1 Video. Demonstration of heart injection of constructs in 11.5 dpc embryo. This video demonstrates the injection of a construct (marked by blue dye) into the left ventricle of the beating embryo heart at 11.5 dpc. After several heartbeats the dye can be seen in more distal parts of the embryo and finally in the head vein indicating successful injection. After injection the embryo is incubated with the heart still beating for 30 min before dissection for organ culture. For more detailed information see Fig. 1 and Materials and Methods.
(MP4)

S1 Fig. Knockdown of STRA8 does not affect general markers of gonadal or germ cell development. Gene expression profiled by qRT-PCR in cMO-treated (XX and XY) versus Stra8MO- treated XX gonads (n = 4, 4, 10, 14) showed that target gene *Stra8* (A) and female marker gene *FoxL2* (B) were unchanged. Similarly, meiosis marker genes *Dmc1* (DMC1 dosage suppressor of mck1 homolog, meiosis-specific homologous recombination; C) *Scp3*, (D) and *Rec8* (REC8 meiotic recombination protein; E) and germ cell marker genes *Ddx4* (F), *Pou5f1* (G) and *Cdh1* (H) were unperturbed. IF for CDH1 and FOXL2 indicated that germ cells and somatic cells are present in Stra8MO-treated XX gonads (I; n = 3). Scale bars = 100 μM; cMO = control morpholino; xMO = morpholino targeting gene x. For all qRT-PCR levels are shown relative to *Tbp*, error = S.E.M., ∗ = p = 0.05, ∗∗ = p = 0.001, ns = not statistically significant.
(TIF)

S2 Fig. Knockdown of SOX9 using Sox9MO in gonad is specific to Sertoli cells but does not cause sex reversal. qRT-PCR showed that knockdown of SOX9 in the gonad (A, B: n = 8, 15, 11, 4; C–G: n = 5, 9, 6, 4) had no apparent effect on target gene *Sox9* (A), however, downregulation of expression of SOX9 target gene *Ptgds* (B) was observed. Levels of Sertoli gene *Dhh* (C), somatic gene *Nr5a1* (D), FLC marker *Cyp11a1* (E) were unperturbed in Sox9MO-treated gonads. While expressed at very low levels in XY gonads, ovarian marker *Fst* (F) was significantly decreased in XY Sox9MO-treated gonads. Expression of germ cell marker *Ddx4* (G) was unperturbed. IF of XY Sox9MO treated gonads showed a decrease in SOX9 expression with no evidence of sex reversal (FOXL2-positive cells) (H; n = 5). Germ cells (CDH1) and FLCs (NR5A1) could be observed in XY Sox9MO treated gonads by IF (I). Whole-mount IF of gonad mesonephroi staining (J; n = 3): PAX2 (paired box 2), marks the Müllerian duct (MD), Wolffian duct (WD) and mesonephric tubules, and CDH1, marks the Wolffian duct and mesonephric tubules. The Müllerian duct is not retained in XY Sox9MO-treated mesonephroi indicating that the low level of AMH present can regress the duct as normal. Scale bars = 100 μM; cMO = control morpholino; xMO = morpholino targeting gene x. For all qRT-PCR: levels are shown

relative to *Tbp*, error = S.E.M., ∗ = p = 0.05, ∗∗ = p = 0.001, ∗∗∗ = p = 0.0001, ∗∗∗∗ = p = 0.00001, ns = not statistically significant.
(TIF)

S3 Fig. Raw Western blots showing knockdown of SOX9 in the Sox9MO treated XY gonad. (AF) Western blot for SOX9 (relative to α-TUBULIN or β-ACTIN) showed a downregulation of SOX9 upon Sox9MO treatment in XY gonads (n = 3) quantified in Fig. 2C. For Western blots SOX9 levels (B, D, F) were normalised to α-TUBULIN or β-ACTIN loading controls for each blot (A, C, E) and Sox9MO-treated XY gonads measured relative to cMO treated XY gonads with expression for each blot set to 1. 13.5 dpc XY gonads were used as a positive control and 13.5 dpc XX gonads were used as a negative control for SOX9 antibody specificity. cMO = control morpholino; xMO = morpholino targeting gene x.
(TIF)

S4 Fig. Knockdown controls for in Sox9MO treated pancreata. qRT-PCR (n = 5, 5, 5, 5) showed that *Sox9* (A) expression was unperturbed by Sox9MO-treatment. Expression of *Ngn3* (B; marker of multipotent progenitor cells (MPCs)) was significantly decreased at 17.5 dpc. Expression of *Pdx1* (C; marker of endocrine progenitor cells (EPCs)) was unaltered, but *Ins2* (D) expression was significantly decreased in the Sox9MO-treated pancreata at 17.5 dpc. Expression of non-β-cell sub-type markers: α-cells *Glug* (E), ε-cells *Ghrl* (F), PP-cells *Ppy* (G) and δ-cells *Sst* (H) were all unaltered by treatment with Sox9MO. IF at 15.5 dpc showed that as in the cMO-treated pancreata (I), PAX6-positive cells (indicated by white arrows) differentiate when treated with Sox9MO (J), however, SOX9 expression (K, L; indicated by white arrows) is diminished when treated with Sox9MO. cMO = control morpholino; xMO = morpholino targeting gene x. For all qRT-PCR: levels are shown relative to *Tbp*, error = S.E.M., ∗ = p = 0.05, ∗∗ = p = 0.001, ns = not statistically significant.
(TIF)

S5 Fig. Gli1/2MO treatment has no effect of Sertoli or germ cells. (A-C) Knockdown of GLI1/GLI2 in the gonad (n = 6, 5, 5, 8): qRT-PCR for Sertoli cells marked by *Amh* (A), germ cells marked by *Ddx4* (B) and hedgehog receptor *Ptch1* (C) showed no change after Gli1/Gli2MO treatment. The same trend was observed in the Gli1MO knockdown (n = 6, 6, 7, 5; *Amh* (D); *Mvh* (E); *Ptch1* (F)) and the Gli2MO knockdown (n = 8, 7, 4, 3; *Amh* (G); *Mvh* (H); *Ptch1* (I)). cMO = control morpholino; xMO = morpholino targeting gene x. For all qRT-PCR levels are shown relative to *Tbp*, error = S.E.M., ∗ = p = 0.05, ns = not statistically significant.
(TIF)

S1 Table. Splice site MO sequences targeting exon/intron boundaries of target genes. Morpholino sequences for targets described in manuscript.
(DOCX)

S2 Table. Taqman gene expression sets for qRT-PCR. TaqMan Gene Expression Assay catalogue numbers described in manuscript.
(DOCX)

S3 Table. Primary Antibodies for Immunofluorescence and Western Blot. Dilutions and catalogue numbers for primary antibodies described in manuscript.
(DOCX)

S4 Table. Secondary Antibodies for Immunofluorescence and Western Blot. Dilutions and catalogue numbers for secondary antibodies described in manuscript.
(DOCX)

Acknowledgments

We thank Tara-Lynne Davidson, Kim Miles and Virginia Nink for technical assistance, Peter Thorn and Brandon Wainwright for antibodies, and Lori Sussel, Ben Hogan and Annemiek Beverdam for helpful discussions. Confocal microscopy was performed at the Australian Cancer Research Foundation (ACRF)/Institute for Molecular Bioscience Dynamic Imaging Facility for Cancer Biology. Flow cytometry and cell sorting was performed at the ACRF Brain Tumour Research Centre at the Queensland Brain Institute. This work was supported by the Australian Research Council and the National Health and Medical Research Council (NHMRC) of Australia. P. K. is a Senior Principal Research Fellow of the NHMRC.

Author Contributions

Conceived and designed the experiments: KSM JB PK. Performed the experiments: KSM ENW JB. Analyzed the data: KSM JB. Wrote the paper: KSM ENW JB PK.

References

1. Hsu PD, Lander ES, Zhang F (2014) Development and Applications of CRISPR-Cas9 for Genome Engineering. Cell 157: 1262–1278. doi: 10.1016/j.cell.2014.05.010 PMID: 24906146
2. Nakamura Y, Yamamoto M, Matsui Y (2002) Introduction and expression of foreign genes in cultured mouse embryonic gonads by electroporation. Reprod Fertil Dev 14: 259–265. doi: 10.1071/RD01130 PMID: 12467349
3. Ryan J, Ludbrook L, Wilhelm D, Sinclair A, Koopman P, et al. (2011) Analysis of gene function in cultured embryonic mouse gonads using nucleofection. Sex Dev 5: 7–15. doi: 10.1159/000322162 PMID: 21099207
4. Svingen T, Wilhelm D, Combes AN, Hosking B, Harley VR, et al. (2009) Ex vivo magnetofection: A novel strategy for the study of gene function in mouse organogenesis. Dev Dyn 238: 956–964. doi: 10.1002/dvdy.21919 PMID: 19301396
5. Dean CH, Miller L-AD, Smith AN, Dufort D, Lang RA, et al. (2005) Canonical Wnt signaling negatively regulates branching morphogenesis of the lung and lacrimal gland. Dev Biol 286: 270–286. doi: 10.1016/j.ydbio.2005.07.034 PMID: 16126193
6. Gross I, Morrison DJ, Hyink DP, Georgas K, English MA, et al. (2003) The receptor tyrosine kinase regulator Sprouty1 is a target of the tumor suppressor WT1 and important for kidney development. J Biol Chem 278: 41420–41430. doi: 10.1074/jbc.M306425200 PMID: 12882970
7. Hartwig S, Ho J, Pandey P, Macisaac K, Taglienti M, et al. (2010) Genomic characterization of Wilms' tumor suppressor 1 targets in nephron progenitor cells during kidney development. Development 137: 1189–1203. doi: 10.1242/dev.045732 PMID: 20215353
8. Quaggin SE, Vanden Heuvel GB, Igarashi P (1998) Pod-1, a mesoderm-specific basic-helix-loop-helix protein expressed in mesenchymal and glomerular epithelial cells in the developing kidney. Mech Dev 71: 37–48. doi: 10.1016/S0925–4773(97)00201–3 PMID: 9507058
9. Yates LL, Schnatwinkel C, Murdoch JN, Bogani D, Formstone CJ, et al. (2010) The PCP genes Celsr1 and Vangl2 are required for normal lung branching morphogenesis. Hum Mol Genet 19: 2251–2267. doi: 10.1093/hmg/ddq104 PMID: 20223754
10. Svingen T, Spiller CM, Kashimada K, Harley VR, Koopman P (2009) Identification of suitable normalizing genes for quantitative real-time RT-PCR analysis of gene expression in fetal mouse gonads. Sex Dev 3: 194–204. doi: 10.1159/000228720 PMID: 19752599
11. Combes AN, Lesieur E, Harley VR, Sinclair AH, Little MH, et al. (2009) Three-dimensional visualization of testis cord morphogenesis, a novel tubulogenic mechanism in development. Dev Dyn 238: 1033–1041. doi: 10.1002/dvdy.21925 PMID: 19334288
12. Zhao L, Neumann B, Murphy K, Silke J, Gonda TJ (2008) Lack of reproducible growth inhibition by Schlafen1 and Schlafen2 in vitro. Blood Cells Mol Dis 41: 188–193. doi: 10.1016/j.bcmd.2008.03.006 PMID: 18479948
13. Wainwright EN, Jorgensen JS, Kim Y, Truong V, Bagheri-Fam S, et al. (2013) SOX9 Regulates MicroRNA miR-202–5p/3p Expression During Mouse Testis Differentiation. Biol Reprod 89: 34. doi: 10.1095/biolreprod.113.110155 PMID: 23843232

14. Beverdam A (2006) Expression profiling of purified mouse gonadal somatic cells during the critical time window of sex determination reveals novel candidate genes for human sexual dysgenesis syndromes. Hum Mol Genet 15: 417–431. doi: 10.1093/hmg/ddi463 PMID: 16399799

15. Bowles J, Feng CW, Spiller C, Davidson TL, Jackson A, et al. (2010) FGF9 suppresses meiosis and promotes male germ cell fate in mice. Dev Cell 19: 440–449. doi: 10.1016/j.devcel.2010.08.010 PMID: 20833365

16. Nagy A (2010) Visualizing fetal mouse vasculature by India ink injection. Cold Spring Harb Protoc 2010: pdb.prot5371–pdb.prot5371. doi: 10.1101/pdb.prot5371 PMID: 20150134

17. Sanes JR, Rubenstein JL, Nicolas JF (1986) Use of a recombinant retrovirus to study post-implantation cell lineage in mouse embryos. EMBO J 5: 3133–3142. doi: 10.1093/emboj/20.6.1215 PMID: 3102226

18. Cool J, DeFalco TJ, Capel B (2011) Vascular-mesenchymal cross-talk through Vegf and Pdgf drives organ patterning. Proc Natl Acad Sci U S A 108: 167–172. doi: 10.1073/pnas.1010299108 PMID: 21173261

19. Morcos PA, Li Y, Jiang S (2008) Vivo-Morpholinos: a non-peptide transporter delivers Morpholinos into a wide array of mouse tissues. Biotechniques 45: 613–614. doi: 10.2144/000113005 PMID: 19238792

20. Moulton JD, Jiang S (2009) Gene knockdowns in adult animals: PPMOs and vivo-morpholinos. Molecules 14: 1304–1323. doi: 10.3390/molecules14031304 PMID: 19325525

21. Wu B, Li Y, Morcos PA, Doran TJ, Lu P, et al. (2009) Octa-guanidine morpholino restores dystrophin expression in cardiac and skeletal muscles and ameliorates pathology in dystrophic mdx mice. Mol Ther 17: 864–871. doi: 10.1038/mt.2009.38 PMID: 19277018

22. McLaren A (2003) Primordial germ cells in the mouse. Dev Biol 262: 1–15. doi: 10.1016/S0012–1606(03)00214–8 PMID: 14512014

23. Feng C-W, Bowles J, Koopman P (2014) Control of mammalian germ cell entry into meiosis. Mol Cell Endocrinol 382: 488–497. doi: 10.1016/j.mce.2013.09.026 PMID: 24076097

24. Wainwright EN, Wilhelm D (2010) The game plan: cellular and molecular mechanisms of mammalian testis development. Curr Top Dev Biol 90: 231–262. doi: 10.1016/S0070–2153(10)90006–9 PMID: 20691851

25. Barrionuevo F, Bagheri-Fam S, Klattig J, Kist R, Taketo MM, et al. (2006) Homozygous inactivation of Sox9 causes complete XY sex reversal in mice. Biol Reprod 74: 195–201. doi: 10.1095/biolreprod.105.045930 PMID: 16207837

26. Bishop CE, Whitworth DJ, Qin Y, Agoulnik AI, Agoulnik IU, et al. (2000) A transgenic insertion upstream of Sox9 is associated with dominant XX sex reversal in the mouse. Nat Genet 26: 490–494. doi: 10.1038/82652 PMID: 11101852

27. Chaboissier M-C, Kobayashi A, Vidal VIP, Latzkendorf S, van de Kant HJG, et al. (2004) Functional analysis of Sox8 and Sox9 during sex determination in the mouse. 131: 1891–1901. Available: http://dev.biologists.org/content/131/9/1891.abstract. PMID: 15056615

28. Bi W, Huang W, Whitworth DJ, Deng JM, Zhang Z, et al. (2001) Haploinsufficiency of Sox9 results in defective cartilage primordia and premature skeletal mineralization. Proc Natl Acad Sci U S A 98: 6698–6703. doi: 10.1073/pnas.111092198 PMID: 11371614

29. Arango NA, Lovell-Badge R, Behringer RR (1999) Targeted Mutagenesis of the Endogenous Mouse Mis Gene Promoter: In Vivo Definition of Genetic Pathways of Vertebrate Sexual Development. Cell 99: 409–419. doi: 10.1016/S0092–8674(00)81527–5 PMID: 10571183

30. Wilhelm D, Hiramatsu R, Mizusaki H, Widjaja L, Combes AN, et al. (2007) SOX9 regulates prostaglandin D synthase gene transcription in vivo to ensure testis development. J Biol Chem 282: 10553–10560. doi: 10.1074/jbc.M609578200 PMID: 17277314

31. Bitgood MJ, Shen L, McMahon AP (1996) Sertoli cell signaling by Desert hedgehog regulates the male germline. Curr Biol 6: 298–304. doi: 10.1016/S0960–9822(02)00480–3 PMID: 8805249

32. Seymour PA, Freude KK, Dubois CL, Shih H-P, Patel NA, et al. (2008) A dosage-dependent requirement for Sox9 in pancreatic endocrine cell formation. 323: 19–30. Available: http://linkinghub.elsevier.com/retrieve/pii/S0012160608010828. doi: 10.1016/j.ydbio.2008.07.034 PMID: 18723011

33. Seymour PA, Freude KK, Tran MN, Mayes EE, Jensen J, et al. (2007) SOX9 is required for maintenance of the pancreatic progenitor cell pool. 104: 1865–1870. Available: http://www.pnas.org/cgi/doi/10.1073/pnas.0609217104. PMID: 17267606

34. Dubois CL, Shih H-P, Seymour PA, Patel NA, Behrmann JM, et al. (2011) Sox9-haploinsufficiency causes glucose intolerance in mice. PLoS ONE 6: e23131. doi: 10.1371/journal.pone.0023131 PMID: 21829703

35. Barsoum I, Yao HH (2011) Redundant and differential roles of transcription factors gli1 and gli2 in the development of mouse fetal Leydig cells. Biol Reprod 84: 894–899. doi: 10.1095/biolreprod.110.088997 PMID: 21209421

36. Yao HH-C, Whoriskey W, Capel B (2002) Desert Hedgehog/Patched 1 signaling specifies fetal Leydig cell fate in testis organogenesis. Genes Dev 16: 1433–1440. doi: 10.1101/gad.981202 PMID: 12050120

37. Menke DB, Page DC (2002) Sexually dimorphic gene expression in the developing mouse gonad. Gene Expr Patterns 2: 359–367. doi: 10.1016/S1567–133X(02)00022–4 PMID: 12617826

38. Pyun J-A, Kim S, Cha DH, Kwack K (2013) Epistasis between IGF2R and ADAMTS19 polymorphisms associates with premature ovarian failure. Hum Reprod 28: 3146–3154. doi: 10.1093/humrep/det365 PMID: 24014609

39. Knauff EAH, Franke L, van Es MA, van den Berg LH, van der Schouw YT, et al. (2009) Genome-wide association study in premature ovarian failure patients suggests ADAMTS19 as a possible candidate gene. Hum Reprod 24: 2372–2378. doi: 10.1093/humrep/dep197 PMID: 19508998

40. Coveney D, Ross AJ, Slone JD, Capel B (2008) A microarray analysis of the XX Wnt4 mutant gonad targeted at the identification of genes involved in testis vascular differentiation. Gene Expr Patterns 8: 529–537. PMID: 18953701

41. Jameson SA, Natarajan A, Cool J, Defalco T, Maatouk DM, et al. (2012) Temporal transcriptional profiling of somatic and germ cells reveals biased lineage priming of sexual fate in the fetal mouse gonad. PLoS Genet 8: e1002575. doi: 10.1371/journal.pgen.1002575 PMID: 22438826

42. Gao L, Kim Y, Kim B, Lofgren SM, Schultz-Norton JR, et al. (2011) Two regions within the proximal steroidogenic factor 1 promoter drive somatic cell-specific activity in developing gonads of the female mouse. Biol Reprod 84: 422–434. doi: 10.1095/biolreprod.110.084590 PMID: 20962249

43. Eisen JS, Smith JC (2008) Controlling morpholino experiments: don't stop making antisense. Development 135: 1735–1743. doi: 10.1242/dev.001115 PMID: 18403413

44. Schulte-Merker S, Stainier DYR (2014) Out with the old, in with the new: reassessing morpholino knockdowns in light of genome editing technology. Development 141: 3103–3104. doi: 10.1242/dev.112003 PMID: 25100652

BIOLOGY OF REPRODUCTION (2015) **92**(6):145, 1–17
Published online before print 8 April 2015.
DOI 10.1095/biolreprod.115.128918

Purification and Transcriptomic Analysis of Mouse Fetal Leydig Cells Reveals Candidate Genes for Specification of Gonadal Steroidogenic Cells[1]

Kathryn S. McClelland,[3] Katrina Bell,[4] Christian Larney,[3] Vincent R. Harley,[5] Andrew H. Sinclair,[4] Alicia Oshlack,[4] Peter Koopman,[2,3] and Josephine Bowles[3]

[3]*Institute for Molecular Bioscience, The University of Queensland, Brisbane, Queensland, Australia*
[4]*Murdoch Childrens Research Institute, Royal Children's Hospital, Melbourne, Victoria, Australia*
[5]*Monash Institute of Medical Research-Prince Henry's Institute (MIMR-PHI) Institute of Medical Research, Melbourne, Victoria, Australia*

ABSTRACT

Male sex determination hinges on the development of testes in the embryo, beginning with the differentiation of Sertoli cells under the influence of the Y-linked gene *SRY*. Sertoli cells then orchestrate fetal testis formation including the specification of fetal Leydig cells (FLCs) that produce steroid hormones to direct virilization of the XY embryo. As the majority of XY disorders of sex development (DSDs) remain unexplained at the molecular genetic level, we reasoned that genes involved in FLC development might represent an unappreciated source of candidate XY DSD genes. To identify these genes, and to gain a more detailed understanding of the regulatory networks underpinning the specification and differentiation of the FLC population, we developed methods for isolating fetal Sertoli, Leydig, and interstitial cell-enriched subpopulations using an *Sf1*-eGFP transgenic mouse line. RNA sequencing followed by rigorous bioinformatic filtering identified 84 genes upregulated in FLCs, 704 genes upregulated in nonsteroidogenic interstitial cells, and 1217 genes upregulated in the Sertoli cells at 12.5 days postcoitum. The analysis revealed a trend for expression of components of neuroactive ligand interactions in FLCs and Sertoli cells and identified factors potentially involved in signaling between the Sertoli cells, FLCs, and interstitial cells. We identified 61 genes that were not known previously to be involved in specification or differentiation of FLCs. This dataset provides a platform for exploring the biology of FLCs and understanding the role of these cells in testicular development. In addition, it provides a basis for targeted studies designed to identify causes of idiopathic XY DSD.

differentiation, gonadogenesis, Leydig cell, neuroactive, RNA-seq, Sertoli cell, sex determination, steroidogenesis, transcriptome

INTRODUCTION

The morphogenesis of the testes involves the coordinated differentiation of a number of bipotential cell lineages in the gonadal primordium into testis-specific cell types (for review, see [1]). This process begins with the expression of the Y-linked gene *Sry* (sex determining region of Chr Y), which directs differentiation of Sertoli cells that assemble into cords encapsulating the germ cells. Sertoli cells then influence the differentiation of other cell types within the testes, including the fetal Leydig cells (FLCs), which arise in the interstitium and act as factories for the production of steroid hormones (androgens) that play a major role in masculinization of the XY individual. Other cell types also arise in the testicular interstitium, the nature and function(s) of which are mostly unclear. Some interstitial cells that do not differentiate as FLCs are thought to give rise to adult Leydig cells (ALCs), which maintain androgen production throughout life [2]. The differentiation, function, and interaction of the various cellular subcompartments of the developing testis need to be carefully orchestrated in a spatiotemporal manner, but how this regulation is achieved remains poorly understood.

Disorders of sex development (DSDs) are congenital birth defects characterized by development of atypical chromosomal, gonadal, or anatomical sex. Although the term DSD includes a wide spectrum of conditions, loss or compromised function of genes directing gonadal development during fetal life is a common cause (for review see [3]). As many of the known genes at fault in XY DSD are those regulating gonadogenesis, we hypothesized that defects in specification and differentiation of FLCs or nonsteroidogenic interstitial cells (NSICs) may underlie some classes of human DSD. Currently, few genes and encoded factors are known to direct FLC fate determination and differentiation [4], and even less is known regarding how ALC progenitors are specified from interstitial cells during fetal life [2]. Hedgehog signaling is evidently a positive regulator of FLC differentiation, given that $Dhh^{-/-}$ (Desert hedgehog) XY gonads have reduced FLC numbers [5–7], and that constitutively active hedgehog signaling in the ovary is sufficient to induce some interstitial cells to differentiate along the steroidogenic pathway [8]. Similarly, $Pdgfra^{-/-}$ (platelet derived growth factor receptor, α-polypeptide) XY gonads show abnormal FLC differentiation [9]. Additionally, the aristaless-related homeobox gene (ARX) plays some role in FLC specification based on the fact that $Arx^{-/-}$ XY mouse gonads have reduced FLC numbers. Interestingly, *Arx* is not expressed in FLCs, although it may be expressed in their progenitors [10, 11].

Previous transcriptomic studies aimed at identifying genes important for development of the fetal gonads in mice, or for establishing the molecular signatures of the component cell lineages, have been performed using microarrays [12–16]. Although this method reveals the expression dynamics of thousands of genes simultaneously, it is limited by the incomplete representation of genes on the array and also by the relatively low sensitivity and dynamic range offered [17].

[1]Supported by the Australian Research Council (ARC; grant DP140104059) and the National Health and Medical Research Council (NHMRC) of Australia (grant 546517). P.K. is a Senior Principal Research Fellow of the NHMRC (APP1059006). Data have been submitted to GEO under the accession number GSE65498.
[2]Correspondence: E-mail: p.koopman@imb.uq.edu.au

Received: 6 February 2015.
First decision: 28 February 2015.
Accepted: 2 April 2015.

eISSN: 1529-7268 http://www.biolreprod.org
ISSN: 0006-3363

Additionally, the non-Sertoli gonadal somatic populations studied in previous microarray screens have included a mixture of FLCs and NSICs because of an inability to separate these two populations. Hence, using available microarray datasets, it has been difficult to address the specific question of how FLCs arise and to determine the molecular characteristics of these cells at 12.5 days postcoitum (dpc), prior to the expression of steroidogenic pathway genes.

In this study, we designed and implemented a strategy to separate mouse fetal gonadal cells into four distinct subpopulations—Sertoli cells, germ cells, FLCs, and heterogeneous NSICs—using a fluorescence-activated cell sorting (FACS)-based protocol in combination with a *Sf1*-enhanced green fluorescent protein (eGFP) transgenic mouse line [12]. We used massively parallel sequencing (RNA-seq) to carry out differential gene expression analysis and construct a molecular portrait of FLCs at 12.5 dpc, just at the onset of steroidogenesis. The aim of this study was to identify early lineage markers of the FLC and NSIC populations in order to provide insight into the signaling interactions in the early gonad. The output generated by our approach reveals potential markers for presteroidogenic FLCs, suggests likely signaling relationships among Sertoli cells, FLCs, and NSICs, and reveals new candidate genes that may underlie the fetal origins of DSDs.

MATERIALS AND METHODS

Mouse Strains

Embryos were collected from timed matings of *Sf1*-eGFP (*Nr5a1*)-strain mice [12], with noon of the day on which the mating plug was observed, designated 0.5 dpc. All animal protocols were approved by the University of Queensland Animal Ethics Committee.

Immunofluorescence

Section. Embryos were fixed in 4% paraformaldehyde in PBS overnight at 4°C, dehydrated, and embedded in paraffin; 7-μm sections were cut using a Leica microtome. Slides were dewaxed by 2 × 10 min washes in xylene, rehydrated, boiled for 5 min in Antigen Unmasking Solution (Vector Laboratories), and incubated in the unmasking solution at room temperature for 60 min. The slides were washed for 3 × 10 min in 0.1% Triton-X in PBS (PBTx) and incubated with primary antibodies diluted in blocking buffer (10% heat-inactivated serum supreme in PBTx) at 4°C overnight, followed by washing and reblocking for 30 min at room temperature. Slides were incubated with secondary antibodies in blocking buffer at room temperature for 2 h, washed, and mounted in 60% glycerol/PBS. Sections were imaged by confocal microscopy using a Zeiss LSM-510 META or LSM-710 META confocal microscope. For details of primary and secondary antibodies see Supplemental Tables S1 and S2 (Supplemental Data are available online at www.biolreprod.org).

FACS cells. The protocol was modified from online methods [18]. Briefly, cells were sorted as described below from 12.5-dpc gonad-only samples into ice-cold PBS and kept on ice. A volume of PBS containing between 3000 and 10 000 "events" (~200 μl) was plated into an area demarcated on a Tissue Tack slide (24216; Polysciences Inc.) and allowed to adhere for 15 min before being fixed in 4% paraformaldehyde for 15 min at room temperature and washed with PBS. Slides were blocked in permeabilization/blocking buffer (P/B buffer; 1% bovine serum albumin in PBTx) for 30 min at RT and incubated at 4°C overnight with the primary antibody diluted in P/B buffer. The slides were washed for 1 × 5 min in P/B buffer and then 3 × 10 min in PBTx and incubated with secondary antibodies diluted in P/B buffer for 1 h at room temperature. Slides were DAPI stained, washed, and mounted in 60% glycerol/PBS. Fields of cells were imaged by fluorescent microscopy using a Olympus BX-51 microscope and counted in ImageJ using the CellCounter plug-in. For details of primary and secondary antibodies see Supplemental Tables S1 and S2.

FACS Sorting of Cell Populations

Sf1-eGFP litters (11.5–14.5 dpc) were dissected in cold PBS and gonads sexed by eye, based on the presence of testis cords (12.5–14.5 dpc) or by presence of Barr bodies (11.5 dpc; [19]). For 11.5-dpc samples the mesonephros was left attached, but it was removed for 12.5–14.5-dpc samples. It should be noted that GFP-transgene expression is restricted to the somatic cells of gonad, exclusive of the mesonephros ([12]; this study). As only GFP-positive cells were profiled at 11.5 dpc, there was no mesonephric contamination. Stage-matched CD1 gonads, with mesonephros removed, were used as a negative control to determine GFP-positive populations.

Gonads were enzymatically dissociated using 0.25% Trypsin EDTA (Gibco) or TryplE Express (12604-013; Gibco) with 5 U/ml DNase1 (Sigma) for 20 min at 37°C and then mechanically dissociated using 18- and 23-gauge syringes. PBS (1 ml) was added to the cells that were then pelleted by centrifugation (900 × *g* at 4°C for 10 min); after supernatant was removed the cells were resuspended in 400 μl of ice-cold PBS and stored on ice. Cells were then incubated with anti-SSEA1-PE (#FAB2155P; R&D Systems; specific for germ cells, fucosyltransferase 4 [FUT4]) or anti-CD31-APC (#551262; Becton Dickinson; specific for germ and endothelial cells, platelet/endothelial cell adhesion molecule 1 [PECAM1]) antibody for 20 min and washed with ice-cold PBS. Cells were resuspended in 400 μl PBS for sorting. Anti-SSEA1-PE was used in characterization of cell population studies and anti-CD31-APC was used to remove germ and endothelial cells prior to RNA-seq. Cells were fractionated using a BD FACSAria Cell Sorter; Supplemental Figure S1 shows FACS plots illustrating how gating parameters were derived. Specifically, GFP-negative CD1 stage-matched controls (Supplemental Fig. S1, A and B) and GFP-positive but antibody-negative controls (Supplemental Fig. S1C) were used to place gates for sorting GFP-high, GFP-low, GFP-neg, and antibody-sorted (SSEA1-PE or CD31-APC) populations (Supplemental Fig. S1D). These populations were collected in PBS and kept on ice before further processing.

Quantitative RT-PCR Analysis

Total RNA was extracted (Micro RNeasy kit with carrier RNA; Qiagen) and cDNA generated (High Capacity cDNA Reverse Transcription Kit; Invitrogen) from isolated populations of FACS-sorted cells as previously described [20]. Duplicate assays were conducted on an ABI Prism 7500 Sequence Detector System. The cycle conditions for quantitative RT-PCR (qRT-PCR) were 2 min at 50°C, then 10 min at 95°C, followed by 40 cycles of 92°C for 15 sec then 60°C for 60 sec.

Expression levels of mRNA were normalized to *Tbp* (TATA box binding protein; [21]) and relative transcript abundance was determined using the $2^{-\Delta CT}$ method. *Tbp* was used as a normalizing gene on the assumption that there were equal amounts of *Tbp* in each cell population as in the whole gonad [21]. For Taqman Gene Expression Assay reference numbers, see Supplemental Table S3. SEM was calculated from independent biological replicates ($n \geq 3$) and statistical significance was determined using one-way ANOVA with Bonferroni multiple comparisons test to compare the four sample groups, with the exception of populations sorted at 11.5 dpc, where only two groups were compared and so statistical significance was determined using unpaired (two-tailed) Student *t*-test.

RNA Extraction and Library Preparation for Deep Sequencing

Total RNA was extracted (Micro RNeasy kit without carrier RNA; Qiagen) from CD31-treated FACS-sorted cells. Each sample represented approximately 10 sorting experiments conducted on different days with 4–10 litters of *Sf1*-eGFP embryos in each experiment. We prepared, for each of 3 cell types (high-GFP, low-GFP, GFP-negative with GC/EC removed), replicate A, replicate B, and replicate C (C was an equal mix of samples A and B), resulting in nine samples for sequencing. A cDNA library was prepared from each sample using TruSeq Stranded Total RNA Libraries (RS-122-2201, Truseq stranded Total RNA LT [with Ribo-Zero Human/Mouse/Rat], Set A; Illumina protocol 15031048 Rev C, September 2012). The nine samples were run on four lanes of an Illumina HiSeq 1500, with all samples run over all lanes, generating 100-bp paired end reads after ribosomal depletion. Sequencing and library preparation were completed by the Monash Health Translation Precinct Medical Genomics Facility, Australia. Data have been submitted to GEO, accession GSE65498.

RNA-Seq Analysis

An average of 65 million raw reads were generated per sample. The quality of the sequencing files was examined using the FastQC program (FastQC; www.bioinformatics.babraham.ac.uk/projects/). Tophat2 [22] was used to map reads to the mouse genome (mm10), with mouse gene model annotations (mm10, downloaded from Ensembl [http://www.ensembl.org/info/data/ftp/index.html]) supplied via the -G option. On average over 85% of the reads mapped to the mouse genome. Read counts were then summarized across genes using HTSeq-count [23], with Ensembl mm10 gene annotation. No lane-

specific technical effects were observed; therefore, all lane files per sample were merged into one file per sample for differential gene expression analysis.

Differential Gene Expression Analysis

The count data were analyzed within the R statistical computing environment. Only genes with at least one count per million (cpm) in three or more samples were retained for further analysis. This reduced the number of features to 14 307 for the differential gene expression analysis (complete data in Supplemental Data S1). The count data of reads per gene feature were analyzed using TMM [24] and voom [25] for normalization and limma [26] for differential expression analysis, which applies empirical Bayes methods to compute moderated *t*-tests and *P* values adjusted for multiple testing using the Benjamini-Hochberg method [27]. Lists of the differentially expressed genes between each pair (contrast) of the three cell types were generated and annotated based on Ensembl mm10 annotation. Genes that were upregulated in one cell type compared to the other two cell types (adjusted *P* value <0.05 and log fold change of at least 1 or 0.6 for each contrast) formed the upregulated gene lists for each of the cell types. The adjusted *P* value of the moderated *F* statistic (*F*), which combines the *t* statistics for all the contrasts into an overall test of significance for each gene, was used to rank the cell-specific gene lists for discussion. The full gene lists for all comparisons are in Supplemental Data S2.

To validate the RNA-seq data, we used the normalized sequence cpm to indicate expression of various marker genes (Supplemental Data S1). SEM was calculated from the three sequencing replicates and statistical significance was determined using one-way ANOVA with Bonferroni multiple comparisons test.

Previously Reported Genes

Genes that have testicular expression previously reported as having expression in the testis in articles on PubMed are listed in Supplemental Data S3.

Eurexpress Database In Situ Hybridization Mining

We searched the 14.5-dpc dataset from Eurexpress Transcriptome Atlas Database for Mouse Embryo (http://www.eurexpress.org) for in situ hybridization (ISH) data that might verify testicular expression for genes of interest identified in our RNA-seq analysis. Representative section images were downloaded and the testis region selected in Photoshop. Gene IDs and Eurexpress IDs are listed in Supplemental Table S4.

Gene Ontology Analysis

Gene ontology (GO) analysis was performed using the DAVID Bioinformatics Package (v6.7) (http://david.abcc.ncifcrf.gov; [28, 29]). The following three GO terms were used to categorize each population:

Transmembrane factor: SP_PIR_KEYWORDS transmembrane (GO:0016021; TM)
Secreted factor: SP_PIR_KEYWORDS secreted (GO:0005576; SF)
Transcription factor: GOTERM_MF_FAT transcription factor activity (GO:0003700; TF)

For details of additional GO terms used, see Supplemental Data S4 and Supplemental Tables S5 and S6. The genes identified in each GO term category were then mapped back to the differentially expressed gene lists and ranked by *F* statistic.

Genes Putatively Regulated by NR5A1

The list of genes putatively regulated by NR5A1 is from Baba et al. [30]. The full list of overlapping genes is in Supplemental Data S5.

11.5-dpc Expression of FLC Genes

From our list of genes preferentially expressed in Leydig cells at 12.5 dpc, we sought to determine if any might potentially also mark Leydig cells at 11.5 dpc. To do this, we considered the data available for these genes at 11.5 dpc [15]. Genes found to be enriched in Leydig cells at 12.5 dpc that also show differing expression between the interstitial and supporting cell compartments of 11.5-dpc testes are putative pre-FLC marker genes. Data were obtained from GEO (GSE27715) and analyzed with R and Bioconductor. Raw data were normalized using oligo [31] and differential expression analysis was carried out with limma [26]. Int. Exp (interstitial) and Sup. Exp (supporting) show median normalized expression of the gene in each of these two cell types, and Int. Rank (interstitial) and Sup. Rank (supporting) indicate the position of the gene in a list ranked by expression in that cell type (0 = lowest expression, 100 = highest expression; Supplemental Data S6). For our final list of genes of interest we noted those genes with expression in interstitial cells more than four times that in supporting cells (log fold change ≥ 2). Of particular interest in predicting putative markers for FLCs are the 10 genes with low expression in supporting cells (Sup. Exp ≤ 6; marked in gray in Supplemental Table S7).

Genes Identified in Online Mendelian Inheritance in Man Database

A full list of genes associated with human disease from the Online Mendelian Inheritance in Man (OMIM) database (accessed 12 November 2014; http://omim.org/) is shown in Supplemental Data S7.

RESULTS

Evaluation of GFP as a Proxy for NR5A1/SF1 Expression in Sf1-*eGFP* Mouse Fetal Testes

We previously used a 674-bp fragment of the *Sf1*/*Nr5a1* (steroidogenic factor 1/nuclear receptor subfamily 5, group A, member 1) promoter to drive GFP expression in a subpopulation of somatic cells of the developing gonad in *Sf1*-eGFP transgenic mice (throughout this study we will refer to the this mouse line using the common name SF1/*Sf1*-eGFP) [12]. In that study, we profiled gene expression in the GFP-positive cell population at 10.5 and 11.5 dpc with the aim of identifying genes expressed in the Sertoli/granulosa cell lineage that may play a role in male or female sex determination. In the present study, we exploited a published observation that the NR5A1-positive cell population of the early male gonad can be subdivided into a high-NR5A1-expressing population that differentiates into pre-Sertoli cells and a low-NR5A1-expressing population that differentiates into a subset of the interstitial cells (presumptive FLCs) between 11.25 and 11.75 dpc [32]. Specifically, we sought to determine whether FLCs could be isolated from fetal testes based on GFP expression level in *Sf1*-eGFP transgenic mice. We reasoned that this strategy might allow molecular characterization of the FLC lineage at 12.5 dpc, a time point that would allow identification of genes involved in FLC specification prior to large-scale upregulation of steroidogenesis genes.

In our previous study we established colocalization of NR5A1 and GFP at 11.5 dpc and we confirmed this here (Supplemental Fig. S2, A, B, and G; [12]). We showed that NR5A1/GFP-positive cells were SOX9 positive and ARX/DDX4 negative at 11.5 dpc (DEAD box polypeptide 4; MVH; Supplemental Fig. S2, A, B, and G). We then demonstrated that endogenous expression profile of NR5A1 was mirrored by GFP expression in XY gonads at 12.5 dpc. Immunofluorescence analysis showed that cells with nuclear NR5A1 expression showed cytoplasmic expression of the GFP transgene (Fig. 1, first column). As this analysis was performed using single confocal slices on sectioned embryos, not all cells in an image would be expected to have both nuclear and cytoplasmic staining. We then used lineage-specific marker antibodies to determine which cell types expressed GFP/NR5A1 in our transgenic line. GFP/NR5A1-positive cells lined the testis cords and NR5A1-positive nuclei in ''strongly'' GFP-positive cells colocalized with nuclear SOX9 at 12.5 dpc and later, indicating that the transgene was expressed in Sertoli cells (Fig. 1A; Supplemental Fig. S2, B, D, and F). We deduced that interstitial ''weakly'' GFP-positive cells were presteroidogenic FLCs by virtue of their nuclear expression of NR5A1 (Fig. 1, A–C, first column; [33, 34]). This was confirmed by immunofluorescence for ARX, a nuclear marker

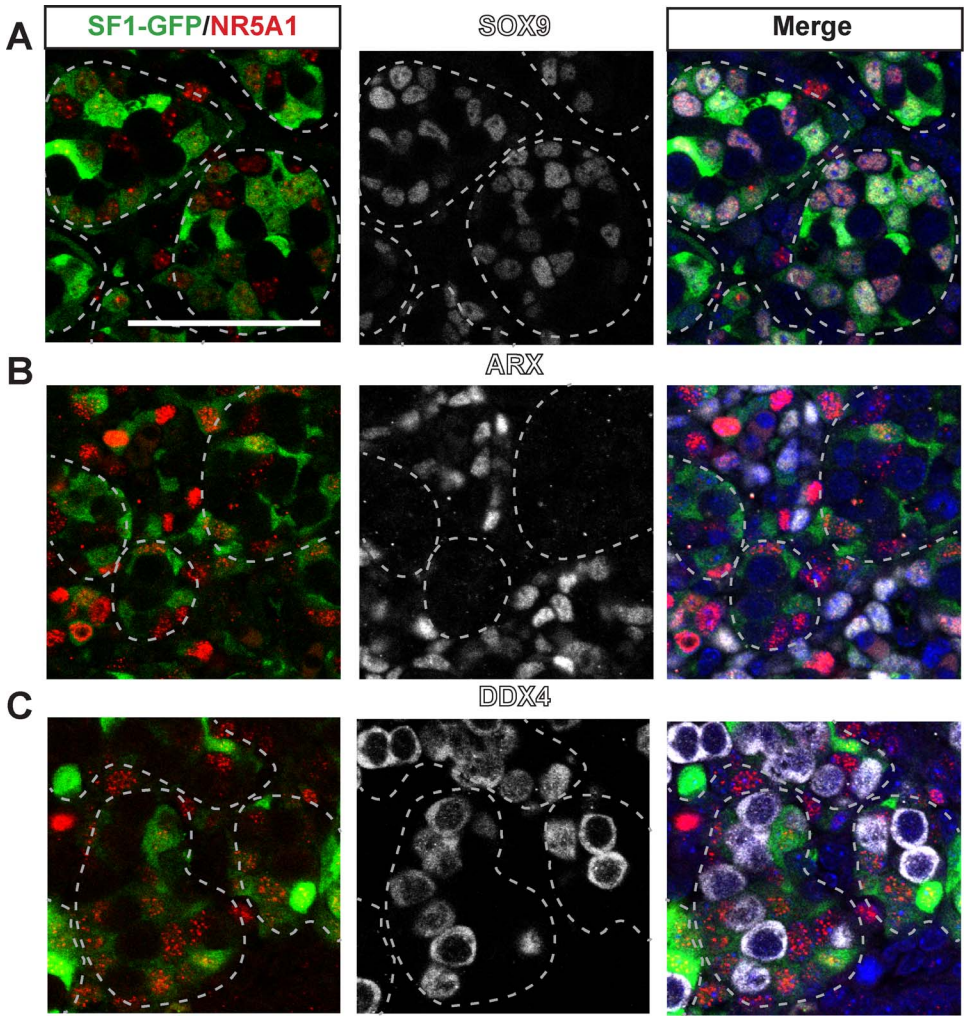

FIG. 1. GFP-positive cells mark FLCs and SCs in *Sf1*-eGFP 12.5 dpc XY gonads. **A**–**C**) Immunofluorescence of *Sf1*-eGFP gonads demonstrates that nuclear NR5A1 is expressed in the same cells that express cytoplasmic GFP in the 12.5-dpc XY gonad. **A**) GFP/NR5A1-positive cells line the cords; nuclear SOX9 and NR5A1 colocalize in GFP-positive cells, indicating that GFP marks Sertoli cells. **B**) Some GFP/NR5A1 cells reside interstitially; these NR5A1-positive cells do not costain with ARX, a marker of non-FLCs, indicating that interstitial GFP/NR5A1-positive cells are presteroidogenic FLCs. **C**) DDX4-positive germ cells are GFP/NR5A1 negative. Bar = 100 μm.

of non-FLC interstitial cells at 12.5 dpc: ARX did not colocalize with the NR5A1-positive nuclei of GFP-positive interstitial cells (Fig. 1B). Additional analysis at 13.5–14.5 dpc showed that GFP/NR5A1-positive cells in the interstitium that were exclusive of ARX-positive nuclei expressed cytoplasmic HSD3β, confirming that FLCs expressed the GFP transgene (Supplemental Fig. S2, C, E, H, and J). We also confirmed that the transgene was not expressed in germ cells: GFP/NR5A1-positive cells were negative for germ cell marker DDX4 (Fig. 1C; Supplemental Fig. S2, G, I, and K). These results demonstrate that GFP, like endogenous NR5A1, is expressed in the Sertoli cell and FLC populations in *Sf1*-eGFP transgenic testes at 12.5 dpc and beyond.

Isolation and Characterization of Fetal Testis Cell Populations

The above observations suggested that it might be possible to separate three populations of somatic cells from 12.5 dpc *Sf1*-eGFP transgenic testes based on GFP fluorescence: strongly GFP-positive (''high-GFP'') Sertoli cells, weakly GFP-positive (''low-GFP'') FLCs, and a GFP-negative population of NSICs. In addition, a fourth cell population, the germ cells, could be isolated using well-characterized antibodies to cell surface markers. To this end, we explanted and dissociated *Sf1*-eGFP testes, incubated the cells with antibodies to either SSEA-1 (recognizing germ cells only) or CD31 (recognizing germ and endothelial cells), and used FACS to separate the four cell populations (Fig. 2A).

We profiled expression of key marker genes by qRT-PCR in the four populations of cells to investigate their composition. As expected, the high-GFP population (Fig. 2, dark green) robustly expressed Sertoli cell hallmarks including *Nr5a1*, *Sox9*, *Amh* (anti-Müllerian hormone), and *Ptgds* (prostaglandin D2 synthase; Fig. 2, B–E). These cells expressed low levels of Leydig cell markers *Star* (steroidogenic acute regulatory protein) and *Cyp11a1* (cytochrome P450, family 11, subfamily a, polypeptide 1; Fig. 2, F and G). This pattern of marker expression was established at 11.5 dpc (Supplemental Fig. S3, A and B) and retained until at least 14.5 dpc (Fig. 2, J–L; Supplemental Fig. S3, C–E and H–M). Therefore, we concluded that the high-GFP-expressing population is enriched for Sertoli cells. Surprisingly, *Ptch1* was expressed at similar levels in the high-GFP (putative Sertoli) and low-GFP (putative FLC) populations (Fig. 2H): despite reports that *Ptch1* expression is characteristic of FLCs [6, 35], high-quality

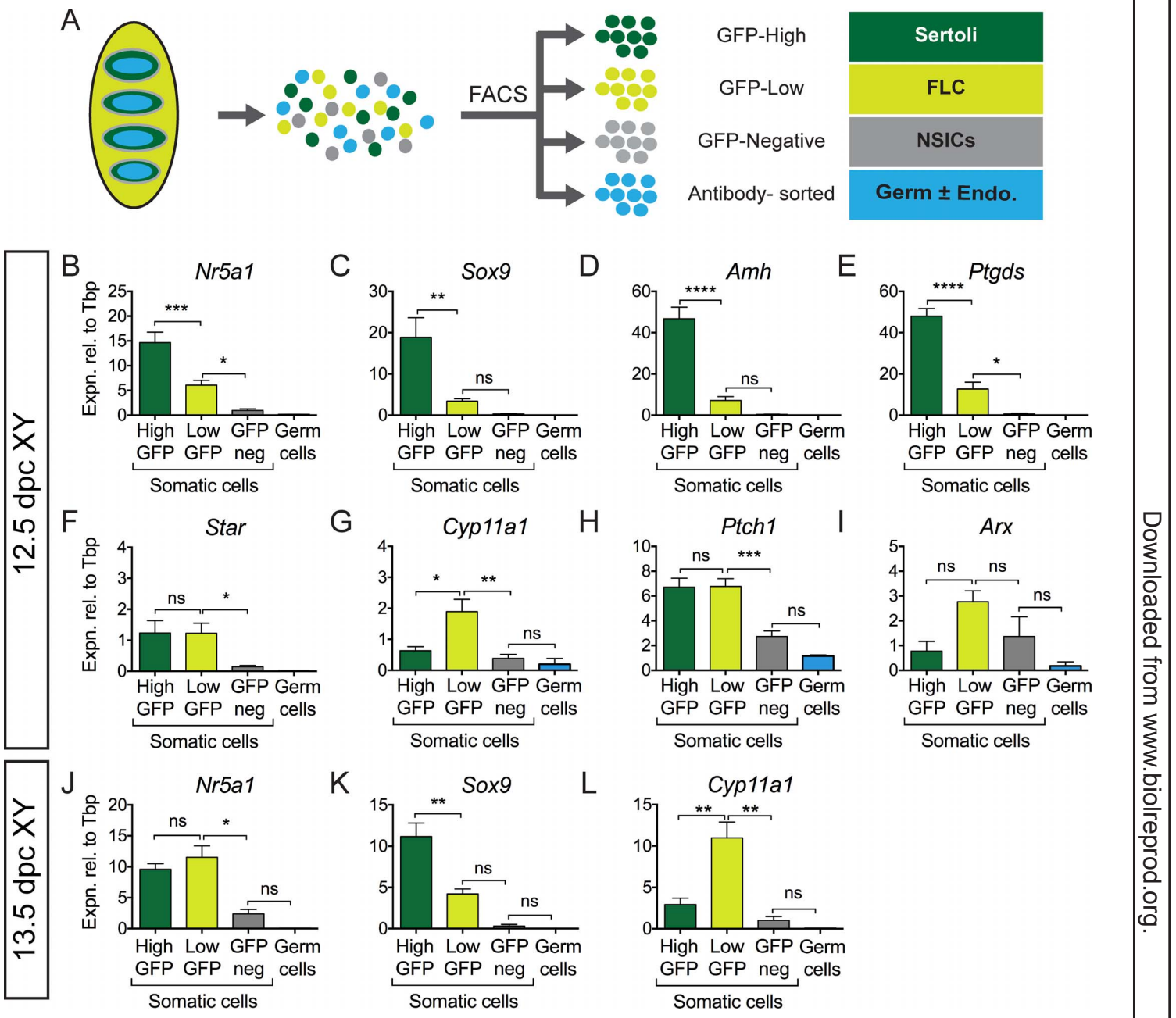

FIG. 2. The high-GFP population represents Sertoli cells and the low-GFP population represents FLCs in 12.5-dpc XY *Sf1*-eGFP gonads. **A**) Schematic of FACS protocol for the XY *Sf1*-eGFP gonads; four cell populations were isolated by FACS using a germ (GC)- or germ cell/endothelial cell (GC/EC)-depleted sorting method. **B**–**I**) At 12.5 dpc, qRT-PCR for somatic marker *Nr5a1* (**B**) and Sertoli cell markers, *Sox9* (**C**), *Amh* (**D**), and *Ptgds* (**E**) showed that the high-GFP-expressing cell population was enriched for Sertoli cells. The low-GFP expressing cell population expressed low levels of Sertoli cell markers. Early FLC marker *Star* (**F**) was similar in the two GFP-positive populations; however, *Cyp11a1* (**G**) was elevated in the low-GFP population. Interstitial markers *Ptch1* (**H**) and *Arx* (**I**) are the only markers expressed in the GFP-negative population. The same trend was observed at 13.5 dpc: high-GFP expressing cells expressed *Nr5a1* (**J**) and high levels of *Sox9* (**K**), whereas low-GFP expressing cells were confirmed to be enriched for FLCs, as they expressed high levels of *Cyp11a1* (**L**). For all qRT-PCR: levels are shown relative to *Tbp*; error = SEM; $*P = 0.05$, $**P = 0.001$, $***P = 0.0001$, $****P = 0.00001$, ns = not statistically significant. For 12.5 dpc, for *Nr5a1*, *Sox9* n = 4, 5, 4, 4 (GC/EC); *Star* n = 4, 5, 5, 5 (GC/EC); *Cyp11a1* n = 3, 4, 4, 4 (GC); *Amh*, *Ptgds*, *Arx* n = 4, 4, 4, 4; *Ptch1* n = 3, 5, 5, 5 (GC/EC). For 13.5 dpc, for *Nr5a1* n = 8, 8, 5, 5; *Sox9* n = 7, 7, 4, 4; *Cyp11a1* n = 8, 8, 4, 4 (GC).

expression data agree with our findings and indicate that *Ptch1* is expressed at similar levels in Sertoli and testicular interstitial cell populations at 12.5 dpc ([16]; this study).

The low-GFP-expressing population (Fig. 2, light green) was characterized by reduced expression of *Nr5a1* at 12.5 dpc and weak expression of *Sox9*, *Amh*, and *Ptgds* (Fig. 2, B–E). At this stage of testis development, expression of steroidogenic genes begins at a low level in the FLCs. Accordingly, expression of early FLC marker *Star* was similar between GFP-positive populations; however, elevated levels of early steroidogenic pathway member *Cyp11a1* were detected in the low-GFP population (Fig. 2, F and G). These and other steroidogenic markers became more highly expressed in the low-GFP population at 13.5 and 14.5 dpc (Fig. 2L; Supplemental Fig. S3, D, E, and K–M). Therefore, we conclude that the low-GFP expressing population is enriched for FLCs at 12.5 dpc.

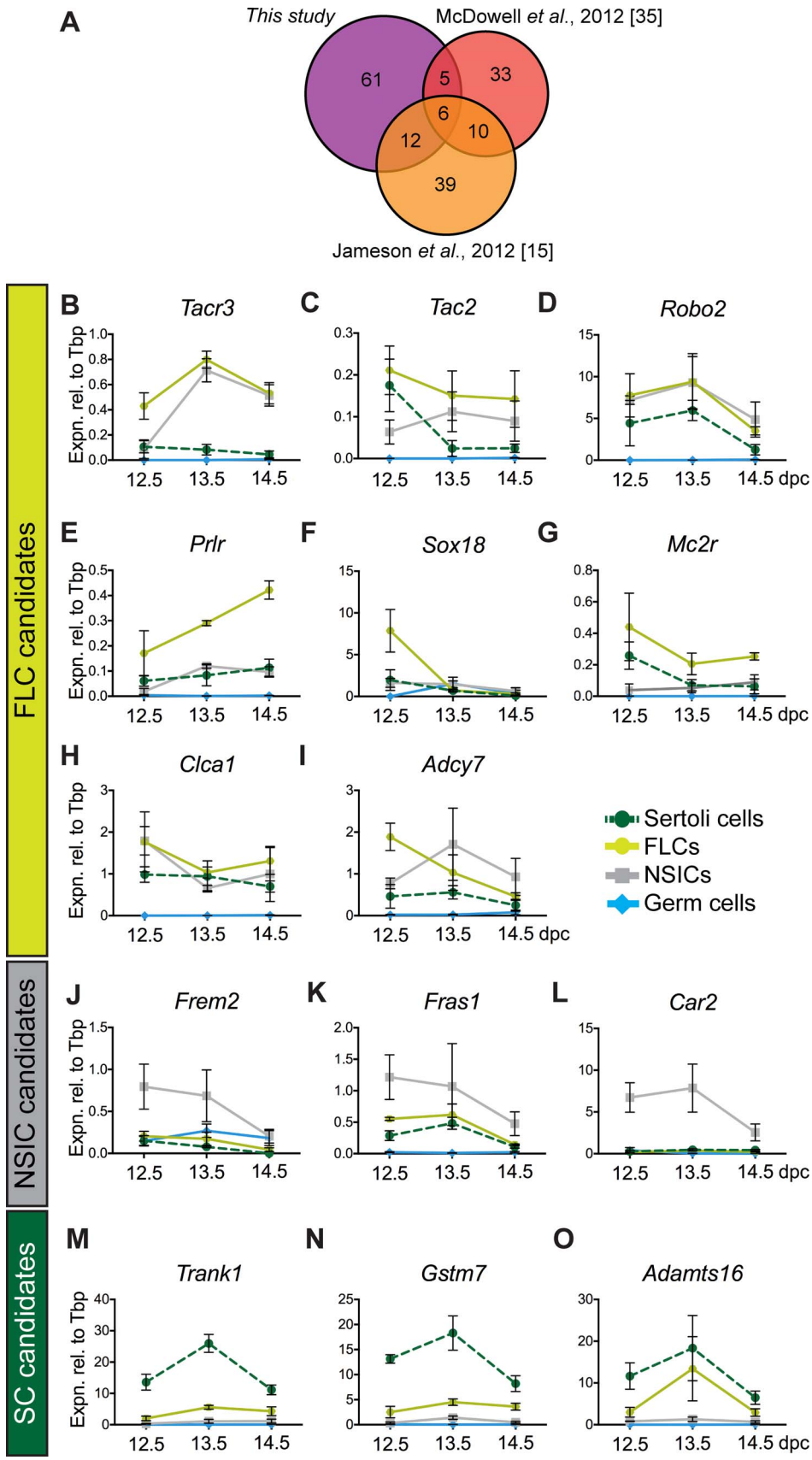

FIG. 3. Validation by qRT-PCR of cell lineage expression of novel candidate genes from 12.5 to 14.5 dpc. **A**) Comparison between our dataset of genes upregulated in the FLC-enriched population and the McDowell et al. [35] and Jameson et al. [15] datasets is represented; only six genes are present in all three datasets. See Table 1 for lists of genes in each category. **B**–**O**) The qRT-PCR for candidate genes identified as being differentially expressed between cell types on sorted cell populations from the 12.5–14.5-dpc *Sf1*-eGFP XY gonad. Novel genes identified as being highly expressed in enriched FLC: *Tacr3* (**B**), *Tac2* (**C**), *Robo2* (**D**), *Prlr* (**E**), *Sox18* (**F**), *Mc2r* (**G**), *Clca1* (**H**), and *Adcy7* (**I**). Novel genes highly expressed in enriched NSICs: *Frem2* (**J**), *Fras1* (**K**), and

The germ cell-depleted, GFP-negative, putative NSIC population (Fig. 2, gray) showed minimal expression of *Nr5a1*; Sertoli cell markers *Amh*, *Ptgds*, and *Dhh*; and FLC markers *Star*, *Cyp11a1*, and *Hsd3β* (hydroxy-delta-5-steroid dehydrogenase, 3 beta- and steroid delta-isomerase 1), indicating that it was devoid of Sertoli cells and FLCs (Fig. 2, B–G and J–L; Supplemental Fig. S3, C–E and H–M). Among the genes we examined, only the DHH receptor *Ptch1* (patched homolog 1) and *Arx* were expressed in the GFP-negative population (Fig. 2, H and I; Supplemental Fig. S3, F–H, N, and O). These data indicated that the germ cell-depleted, GFP-negative population was enriched for NSICs that did not express NR5A1/*Nr5a1* or any other Sertoli or FLC markers.

Although germ cells were not the focus of this analysis, we also examined the expression of *Ddx4* to examine the efficiency of germ cell depletion from the GFP-negative fraction. As expected, expression of *Ddx4* was robust in this cell population from 12.5 to 14.5 dpc (Supplemental Fig. S3, P–R), but some expression was also in the GFP-negative fraction at 12.5 dpc (Supplemental Fig. S3P), indicating a low level of germ cell contamination.

To validate the purity of the high-GFP and low-GFP cell populations using the high-GFP/low-GFP FACS separation strategy described above, we performed immunofluorescence on FACS-sorted cell populations for NR5A1, Sertoli cell marker SOX9, germ cell marker DDX4, and vascular endothelial cell marker iB4 (isolectin B4; Supplemental Fig. S1, E–G). We found that virtually all cells in both the high-GFP and low-GFP populations were NR5A1 positive, as expected, whereas the GFP-negative population was devoid of NR5A1-positive cells (Supplemental Fig. S1E). Results of this analysis were consistent with those obtained by qRT-PCR and indicate that virtually all cells in the high-GFP population (putative Sertoli cells) were SOX9-positive; therefore, this population was a relatively pure population of Sertoli cells (Fig. 2C; Supplemental Fig. S1F). On the other hand, about 7.6% of cells isolated in the low-GFP population (putative FLCs) were SOX9-positive, indicating that a low level of Sertoli cell contamination was present in the FLC population (Fig. 2G; Supplemental Fig. S1F). Although our strategy attempted to remove the majority of germ and endothelial cells using a CD31 antibody, we found that about 22% of cells in the GFP-negative fraction were DDX4-positive germ cells and that approximately 6.4% of the GFP-negative population of cells were iB4-positive endothelial cells (Fig. 2A; Supplemental Fig. S1G). We also tested for staining of Leydig cell markers CYP11A1 and HSD3β, but, as in section immunofluorescence, these markers proved uninformative at 12.5 dpc. These data indicated that the population purity of the three FACS isolated somatic cell populations was sufficient to represent the different enriched fetal testis cell populations.

Generation and Quality of RNA-Seq Data

We next analyzed the transcriptomes of the sorted testicular cell populations by RNA-seq. Cells were collected from 12.5-dpc *Sf1*-eGFP XY gonads, depleted of germ and endothelial cells using a CD31 antibody, and fractionated into three populations using the methods described above (Fig. 2A). Triplicate samples of each somatic cell population were generated, RNA was isolated and reverse transcribed, and the resulting cDNA deep sequenced using a paired-end 100-bp stranded sequencing format on Illumina HiSeq 1500. An average of 65 million raw reads were generated per sample. Supplemental Data S1 provide a spreadsheet of cpm RNA-seq data for all Ensembl gene IDs detected at >1 cpm in 3 or more samples (data can be accessed from GEO; GSE65498).

To validate the RNA-seq data, we examined the normalized sequence cpm as an indicator of expression of various marker genes (Supplemental Fig. S4, A–I; Supplemental Data S1). The results of this analysis were consistent with results obtained by qRT-PCR, with the exception of *Star*, where transcripts were detected in the NSIC population at low levels in the RNA-seq data (Fig. 2, B–I; Supplemental Fig. S4, A–I). These data indicated that the RNA-seq output accurately represented the transcriptomes of the different enriched fetal testis cell populations.

Differentially Expressed Gene Analysis

Genes were identified as being upregulated in a cell population if they showed >1 log fold change and adjusted *P* value <0.05 in the differential expression analysis compared to either of the other cell types. As expected, the GFP-negative fraction isolated by FACS was negative for Sertoli and FLC markers. However, each of the GFP-positive populations contained some transcripts characteristic of other populations, consistent with results obtained by qRT-PCR (Fig. 2, B–L; Supplemental Figs. S3 and S4). That is, some FLCs were likely to have contaminated the Sertoli cell-enriched fraction (Fig. 2G, low-level expression of *Cyp11a1*) and some Sertoli cells were likely to have been present in the FLC-enriched fraction (Fig. 2C, low-level expression of *Sox9*). For this reason, the log fold cutoff off was lowered to >0.6 for these samples, to reduce the potential of obtaining false negatives when compiling lists of cell type-specific genes. In this way, we identified a group of genes upregulated in each enriched cell population: 84 FLC-enriched genes, 704 NSIC-enriched genes, and 1217 Sertoli cell-enriched genes (Supplemental Data S2). Validation of a subset of the genes from the lists of upregulated transcripts demonstrates that a gene in these lists is likely to be expressed in a single testicular cell population at 12.5 dpc.

Validation of the FLC-Enriched Gene Dataset

As a first step in validating the 84 candidate FLC genes, we compared them to results of published studies. Of these genes, 72% (61 genes) were previously unreported in the two published microarray datasets that have provided lists of candidate FLC genes at 12.5 dpc ([15, 35]; Fig. 3A; Table 1). A number of genes had been identified as being expressed in whole adult testis, although for most no further gonadal or fetal gonadal characterization has been performed (Supplemental Data S3). Four of the 84 genes (*Htra3*, *Vcam1*, *Bmp2*, and *Kcnk3*) overlapped with a list of 567 genes identified as putatively regulated by NR5A1 by performing RNA-seq on Y-1 cells treated with *Nr5a1*-siRNA [30] consistent with *Nr5a1*'s pivotal role in FLC specification and differentiation.

We next analyzed temporal and cell-specific gene expression of candidate FLC genes by qRT-PCR on sorted *Sf1*-eGFP cell populations at 12.5–14.5 dpc. These analyses confirmed FLC-enriched expression of *Tacr3*, *Tac2*, *Prlr*, *Sox18*, *Mc2r*,

Car2 (**L**). Novel genes identified as being highly expressed in enriched Sertoli cells: *Trank1* (**M**), *Gstm7* (**N**), and *Adamt16* (**O**) (**B**, **C**, **E**, **G**, **L**, **M**, **N**: 12.5/13.5 dpc, n = 3, 3, 3, 3, 14.5 dpc, n = 4, 4, 4, 3; **D**, **F**, **H**, **I**, **J**, **K**, **O**: 12.5/13.5 dpc, n = 3, 3, 3, 3, 14.5 dpc, n = 3, 4, 4, 3). For all qRT-PCR, levels are shown relative to *Tbp*; error = SEM.

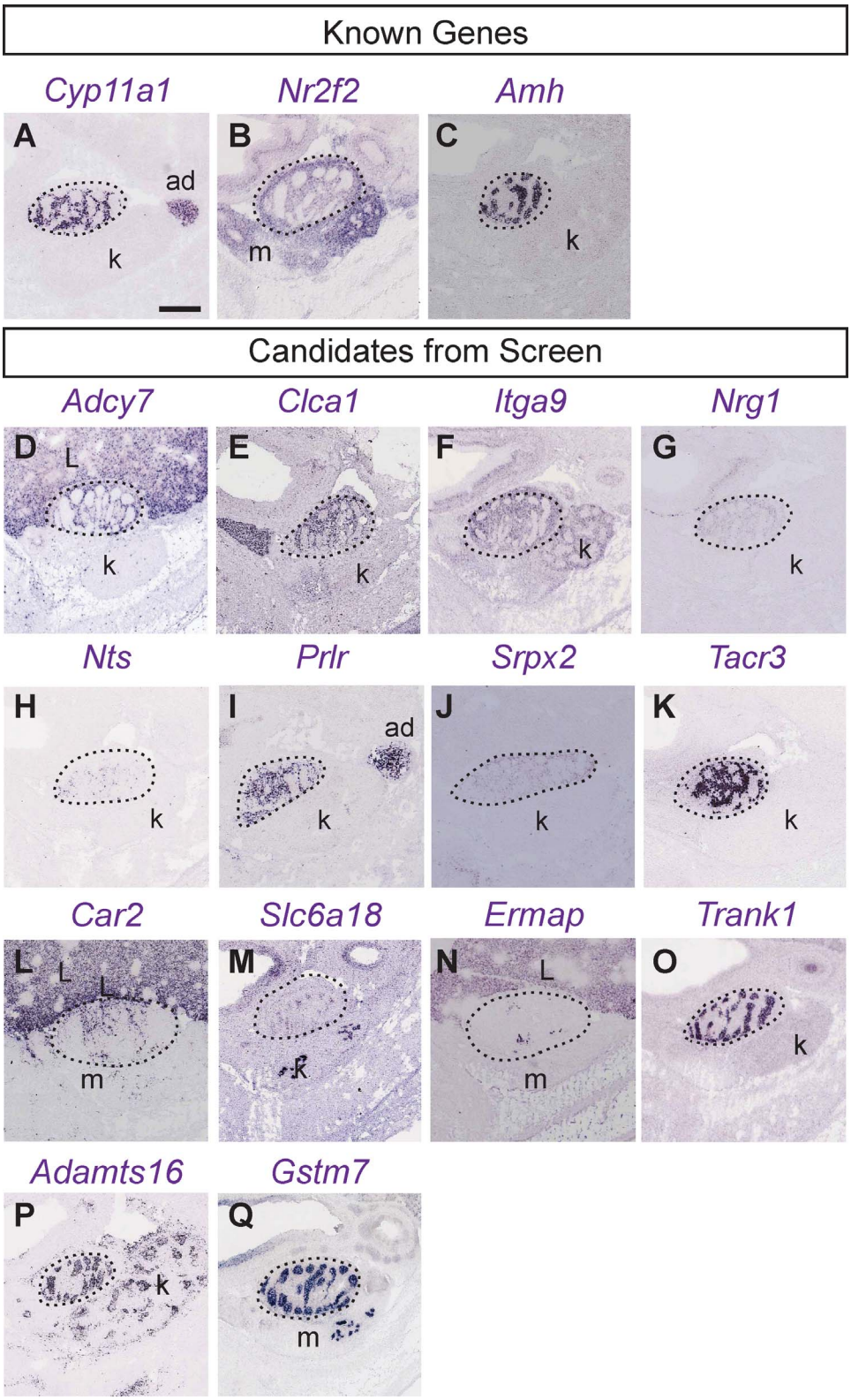

FIG. 4. ISH for genes identified by RNA-seq to be overexpressed in FLCs, NSICs, and Sertoli cells. ISHs for newly identified candidate genes at 14.5 dpc from Eurexpress Transcriptome Atlas Database for Mouse Embryo (http://www.eurexpress.org). Marker genes: *Cyp11a1* (**A**) shows FLC expression pattern, *Nr2f2* (**B**; nuclear receptor subfamily 2, group F, member 2) shows an interstitial pattern, and *Amh* (**C**) shows a Sertoli cell expression pattern. Novel FLC genes *Adcy7* (**D**), *Clca1* (**E**), *Itga9* (**F**), *Nrg1* (**G**), *Nts* (**H**), *Prlr* (**I**), *Srpx2* (**J**), and *Tacr3* (**K**; also shows adrenal expression [data not shown]) show expression in cells distributed outside the testis cords indicating that FLC-expressed genes are being detected. Novel NSIC genes *Car2* (**L**), *Slc6a18* (**M**), and *Ermap* (**N**) show expression in cells distributed outside the testis cords indicating the NSIC expressed genes are being detected. Novel Sertoli cell genes *Trank1* (**O**), *Adamts16* (**P**), and *Gstm7* (**Q**) show expression in cells distributed around the border of the testis cords indicating Sertoli cell expression. The testis region is demarcated by a dotted line. Bar = 0.5 mm. k, kidney; ad, adrenal; L, liver; m, mesonephros; Eurexpress probe IDs can be found in Supplemental Data S4.

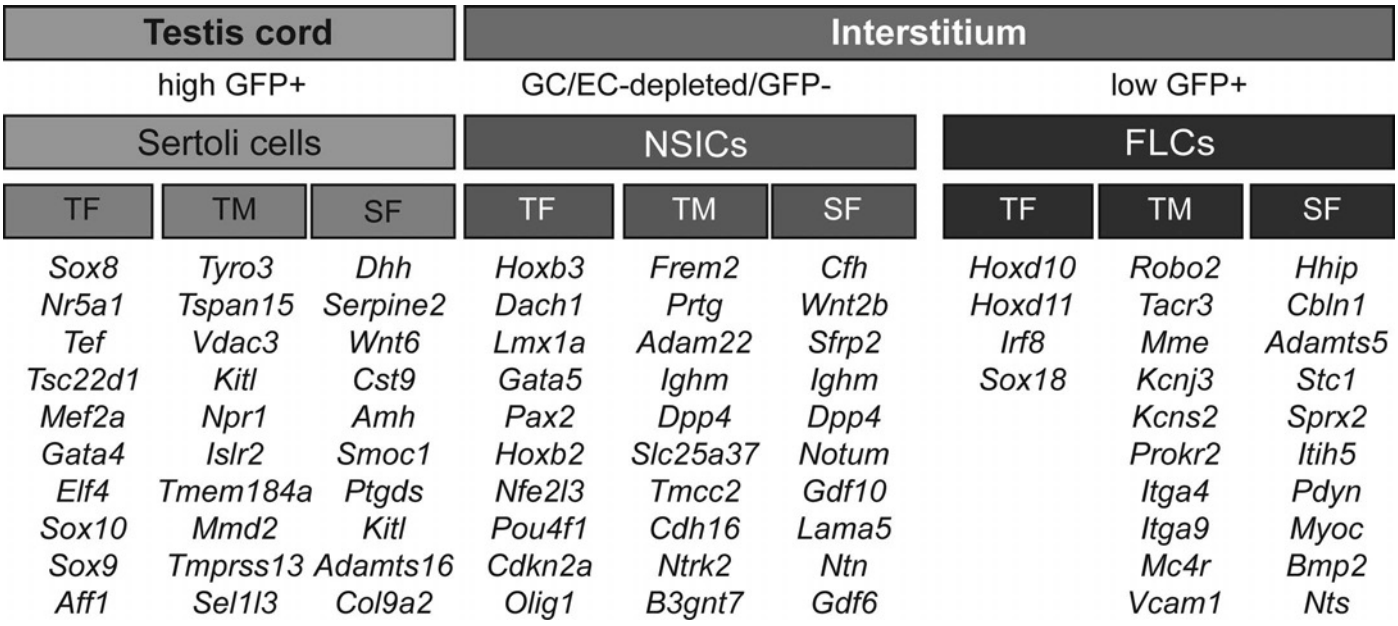

FIG. 5. Subset of transcription factors, transmembrane factors, and secreted factors identified by GO analysis in each cell population. Using DAVID pathway analysis the transcription factors (TF), transmembrane factors (TM), and secreted factors (SF) present in each cell-enriched population were identified. A subset of genes identified in each category are listed (for full listing of GO terms and data see Supplemental Data S4; for overrepresentation analysis for FLCs and NSICs see Supplemental Tables S5 and S6).

and *Adcy7* compared to NSICs (Fig. 3, B, C, E–G, and I). *Prlr* was expressed in the FLC population with expression increasing from 12.5 dpc (Fig. 3E). *Robo2* and *Clca1* appeared to be expressed equally in FLCs and NSICs by qRT-PCR (Fig. 3, D and H). Expression of *Tacr3* was elevated in the FLC-enriched population at 12.5 dpc and was subsequently expressed in the FLC and NSIC populations (Fig. 3B). Interestingly, *Tac2*, *Sox18*, and *Adcy7* were expressed more highly in the FLC than in the NSIC population at 12.5 dpc only before becoming either expressed in multiple populations or downregulated (Fig. 3, C, F, and I).

Lastly, we examined the ISH staining patterns of the FLC genes identified by RNA-seq at 14.5 dpc, when FLCs have upregulated steroid production, using the Eurexpress whole embryo section ISH database [36]. Of the eight expression profiles analyzed in this way (*Adcy7*, *Clca1*, *Itga9*, *Nrg1*, *Nts*, *Prlr*, *Srpx2*, and *Tacr3*), all showed the expected expression in the interstitial space, similar to the known FLC marker *Cyp11a1* (Fig. 4, A and D–K), and distinct from the cord-associated expression of the Sertoli cell marker *Amh* (Fig. 4C). Taken together, these validation steps confirmed that the putative FLC gene dataset generated in this study represents an accurate subset of the FLC transcriptome.

Mining of the FLC-Enriched Gene Dataset

We sought to generate a transcriptional portrait of the FLCs based on the RNA-sequencing dataset. We performed GO analysis, using the DAVID Bioinformatics Package, for each of the three outputs of the differentially expressed gene analysis.

TABLE 1. Genes represented in three different characterizations of the FLC population (see Fig. 3A).

FLC genes found in	Gene lists
This study, Jameson et al. [15], and McDowell et al. [35]	*Inhba, Ppp1r14a, Prlr, Prokr2, Robo2, Vsnl1*
This study and Jameson et al. [15]	*C7, Casq2, Cbln1, Grin2a, Hhip, Hspa12a, Itga9, Kcnj3, Mc2r, Nts, Stc1, Vcam1*
This study and McDowell et al. [35]	*Crhr1, Htra3, Itih5, Srpx2, Vgll3*
Jameson et al. [15] and McDowell et al. [35]	*Aebp1, AI427809, Cyp11a1, Cyp17a1, Fads1, Gramd1b, Hsd3b1, Lhcgr, Npy, Star*
This study only	*Adamts5, Adcy7, Arhgap6, Armcx6, Art3, Bmp2, Btnl9, Chst1, Chst2, Clca1, Clec1b, Col23a1, Cyp1b1, Ffar2, Gja5, Gm11549, Gm13659, Gm14396, Gm5067, Gpr153, Gpr174, Gpr20, Grrp1, Hoxd10, Hoxd11, Hsd11b2, Irf8, Itga4, Kcnk3, Kcns2, Lars2, Lrrtm3, Mc4r, Mme, Mmp28, Myh11, Myh7, Myl4, Myoc, Ngfr, Nrg1, Oit3, Otof, Pcp4l1, Pdyn, Plcxd3, Pnmal1, Ptpro, Rad51ap2, Serpina3g, Sertm1, Slitrk2, Sox18, Speer7-ps1, Sstr4, Syt15, Tac2, Tacr3, Tg, Trac, Vipr1*
Jameson only [15]	*A430107O13Rik, Ace2, Adam12, Alas1, Armcx2, Atp1a3, Clca2, Col6a1, Copz2, Cxcr7, Cyp51, Enpep, Ephx1, Fat3, Fdps, Fdx1, Gpc3, Gpm6a, Grk5, Hsd17b7, Jag1, Mobkl3, Osr2, Pltp, Prkar2b, Pros1, Rbp4, Ren1, Sc4mol, Scarb1, Sct, Slc6a15, Smoc2, Ssfa2, Tgfbr3, Tnc, Tpm2, Trib2, Zeb2*
McDowell only [35]	*1200009O22Rik, 4930474M22Rik, 5031410I06Rik, Abcc9, Adamts7, Alcam, Arx, B3galt1, Cd36, Cdkn2c, Dlc1, Fbn1, Glipr2, Gpx3, Gria4, Gsta2, Gucy1b3, Inha, Insl3, Itgb8, Itm2a, Lrrk2, Ltbp4, Ng23, Nuak1, Pi15, Ptrf, Scd1, Sec24d, Slc29a1, Speer4d, Thbd, Tm7sf2*

List of FLC genes identified in this study, the McDowell et al. dataset [35], and the Jameson et al. dataset [15] at 12.5 dpc indicating unique and overlapping genes between datasets.

TABLE 2. Subset of genes upregulated in 12.5-dpc FLCs ($P < 0.05$).

ID	Gene symbol	Gene name	Chr[a]	Phenotype[b]	OMIM assoc.[c]	Reference[d]
ENSMUSG00000052516	*Robo2*	Roundabout homolog 2	16	Urogenital and organ patterning defects	610878	[40]
ENSMUSG00000056025	*Clca1*	Chloride channel calcium activated 1	3	—	—	—
ENSMUSG00000028172	*Tacr3*	Tachykinin receptor 3/neuromedin K receptor (Nk3r)	3	Postnatal defects; males have small testes and low FSH	614840*	[42, 65]
ENSMUSG00000062991	*Nrg1*	Neuregulin 1	8	Embryonic lethal at 10.5 dpc; cardiac defect	603013	[37]
ENSMUSG00000024087	*Cyp1b1*	Cytochrome P450, family 1, subfamily b, polypeptide 1	17	No lethal developmental defects	231300	[71]
ENSMUSG00000027820	*Mme*	Membrane metallo endopeptidase/NEP	3	No lethal developmental defects	—	[72]
ENSMUSG00000026824	*Kcnj3*	Potassium inwardly-rectifying channel, subfamily J, member 3	2	No lethal developmental defects	—	[73]
ENSMUSG00000064325	*Hhip*	Hedgehog-interacting protein	8	Lethal at P0; respiratory defects	—	[38]
ENSMUSG00000050963	*Kcns2*	K+ voltage-gated channel, subfamily S, 2	15	—	—	—
ENSMUSG00000031654	*Cbln1*	Cerebellin 1 precursor protein	8	No lethal developmental defects; postnatal cerebellum defects	—	[74]
ENSMUSG00000050558	*Prokr2*	Prokineticin receptor 2	2	No gross FLC phenotype; postnatal atrophy of the reproductive system and olfactory bulb defects	244200*	[41, 46, 64]
ENSMUSG00000027009	*Itga4*	Integrin alpha 4	2	Embryonic lethal; placentation defect and cardiac hemorrhage	—	[75]
ENSMUSG00000020682	*Mmp28*	Matrix metallopeptidase 28 (Epilysin)	11	No lethal developmental defects	—	[76]
ENSMUSG00000039115	*Itga9*	Integrin alpha 9	9	No lethal developmental defects; postnatal thorax and lymphatic valve defects	—	[77, 78]
ENSMUSG00000030223	*Ptpro*	Protein tyrosine phosphatase, receptor type, O	6	No lethal developmental defects; sensory and glomerular defects postnatally	614196	[79, 80]
ENSMUSG00000050368	*Hoxd10*	Homeobox D10	2	Nervous system, hind limb, and musculoskeletal defects	192950	[81]
ENSMUSG00000047259	*Mc4r*	Melanocortin 4 receptor	18	No lethal developmental defects; obesity	601665	[82]
ENSMUSG00000022894	*Adamts5*	A disintegrin-like and metallopeptidase with thrombospondin type 1 motif, 5	16	No lethal developmental defects; postnatal cartilage aggrecanase	—	[83, 84]
ENSMUSG00000027962	*Vcam1*	Vascular cell adhesion molecule 1	3	Embryonic lethal at 12.5 dpc; required for chorioallantoic fusion and placentation	—	[85]
ENSMUSG00000025092	*Hspa12a*	Heat shock protein 12A	19	—	—	—
ENSMUSG00000040283	*Btnl9*	Butyrophilin-like 9	11	—	—	—
ENSMUSG00000014813	*Stc1*	Stanniocalcin 1	14	No lethal developmental defects	—	[86]
ENSMUSG00000031659	*Adcy7*	Adenylate cyclase 7	8	Embryonic lethal; −/+ survive	—	[87]
ENSMUSG00000000120	*Ngfr*	P75 NTR/nerve growth factor receptor	11	40% perinatal loss of −/− between 15.5 dpc and birth due to vascular defects	—	[39]
ENSMUSG00000031355	*Arhgap6*	Rho gtpase activating protein 6	X	No lethal developmental defects	—	[88]

[a] Chr., chromosome.
[b] Phenotype indicates the embryonic or postnatal phenotype of the null animal. Information from published reports where there was postnatal survival mutations were classified as "no lethal developmental defects" (indicates that the null offspring were obtained as adults at the expected Mendelian ratios) or "fertile" (indicates that the mice were able to reproduce normally). FSH, follicle-stimulating hormone.
[c] OMIM assoc. = OMIM reference number if the gene is associated with any type of human disorder (* indicates a genitourinary, endocrine, or DSD phenotype).
[d] References are the primary report of the null or mutant mouse and any subsequent clarifying reports.

Ten of the identified genes for each of three ontologies (transmembrane factors, secreted factors, and transcription factors) for each sorted cell population are listed in Fig. 5. Among the 84 candidate FLC genes, we identified 35 genes encoding transmembrane components ($P = 2.33E{-}03$); of these, there was an overrepresentation of genes involved in neurogenesis/neurotransmission (Supplemental Table S5), with eight encoding receptors, or receptor components, for neuroactive ligands (*Tacr3*, *Mc4r*, *Prlr*, *Crhr1*, *Mc2r*, *Sstr4*, *Grin2a*, and *Vipr1*; $P = 2.96E{-}03$). Additionally, five receptors were identified as being involved in cell adhesion (*Robo2*, *Itga4*, *Itga9*, *Vcam1*, and *Arhgap6*; $P = 9.86E{+}01$). Secreted factors were also overrepresented, with 14 secreted factors upregulated in the enriched FLC population including, *Tac2*, *Hhip*, *Pdyn*, and *Inhba* ($P = 9.98E{-}02$). Finally, we identified four genes encoding transcription factors in the FLC enriched population: *Hoxd10*, *Hoxd11*, *Irf8*, and *Sox18* ($P = 1.00E{+}02$).

We queried the OMIM Database and found that 30 of the candidate FLC genes are associated with human disease phenotypes (26 where the molecular basis is known; eight listed in Table 2; full list in Supplemental Data S7). Analysis of published literature revealed that genetic deletion of some of

the genes upregulated in the FLC-enriched population results in embryonic lethality (Table 2) from a variety of causes, including cardiac (*Nrg1* [37]), respiratory (*Hhip* [38]), and vascular defects (*Ngfr* [39]). Among these, gene knockout of *Robo2*, *Prokr2*, and *Tacr3* in mice resulted in defects in postnatal urogenital and reproductive system development [40–42]. Interestingly, these three genes encode transmembrane receptors important for neuroactive-ligand signaling.

Finally, we sought to determine if any FLC genes at 12.5 dpc might also mark pre-FLCs at 11.5 dpc and might therefore be useful in clarifying the developmental origin of FLCs. We reanalyzed a previously published microarray dataset [15] and considered whether genes we found to be enriched in FLCs at 12.5 dpc were also robustly upregulated in the ''interstitial'' population (which includes pre-FLCs) compared with the ''supporting'' (pre-Sertoli) population at 11.5 dpc: we reasoned that such genes may mark FLCs even before they attain steroidogenic capacity. This analysis resulted in the identification of 10 genes of interest: *Prokr2*, *Itga9*, *Ptpro*, *Ngfr*, *Clca1*, *Adamts5*, *Nrg1*, *Arhgap6*, *Myl4*, and *Hsd11b2* (Supplemental Table S7 and Supplemental Data S6). These genes, characterizing non-Sertoli NR5A1-positive cells prior to FLC maturation (which occurs between 12.5 and 13.5 dpc), may act as early markers for the FLC lineage and, therefore, may aid our understanding of FLC specification and differentiation.

NSICs Versus FLC Transcriptomes: Clues to the Origin of FLCs

It is clear that signaling from Sertoli cells to interstitial cells plays a critical role in the specification of FLCs [4]. Early expression of NR5A1 in pre-FLCs precedes steroidogenesis and is likely important for their future steroidogenic capacity. However, it is not clear why only some interstitial cells respond to signals such as DHH by initiating steroidogenesis; this is especially puzzling because non-FLCs of the interstitium are apparently capable of responding to DHH as they express the receptor PTCH1 [6]. Here we confirm that NSICs express PTCH1 (Fig. 2H and Supplemental Fig. S3, F and N): previous studies have demonstrated that PTCH1, along with receptors for other Sertoli-produced factors such as PDGFα, are expressed in a pan-interstitial manner [9]. We reasoned that knowledge of early markers that do discriminate NSICs from FLCs may help explain why only FLCs differentiate in response to Sertoli-derived cues.

NSICs that express NR2F2 at 18.5 dpc are considered progenitor cells for the ALC population [2], but it is not known whether these cells also express NR5A1 [43]. To help clarify this issue, we examined whether NR2F2-positive cells in the fetal testis were also positive for NR5A1. At 11.5 dpc most NR2F2-positive cells also expressed ARX, a smaller proportion expressed NR5A1, and some triple-positive cells were seen (Supplemental Fig. S5A). From 12.5 to 14.5 dpc, NR2F2 cells were ARX positive but negative for NR5A1 (Supplemental Fig. S5, B–D) with few exceptions (gray arrow, Supplemental Fig. S5, B–D). Unless NR2F2 cells begin to express NR5A1 at later time points, these data would suggest that ALC progenitors do not express NR5A1 during fetal life.

We looked at the heterogeneity of the isolated NSIC population by performing DAVID analysis on the upregulated genes (704 genes). We established that the NSIC population contained both blood cells and macrophages, which have been shown to be important for testis morphogenesis and vascularization [44]. We identified a subset of genes involved in hematopoiesis (29 genes; $P = 1.26E{-}04$), leukocyte activation (24; $P = 3.02E{-}04$), and immune response (32; $P = 1.99E{-}05$) in the gene list (Supplemental Data S4).

Subsequently, we performed qRT-PCR on sorted *Sf1*-eGFP cell populations to verify the NSIC-enriched expression of genes upregulated in the NSIC list. We detected expression of *Car2* in NSICs but not FLCs by qRT-PCR (Fig. 3L), whereas expression of *Car2*, *Slc6a18*, and *Ermap* by ISH was consistent with the predicted interstitial expression pattern for the candidate genes (Fig. 4, B and L–N) and distinct from the cord-associated expression of the Sertoli cell marker *Amh* (Fig. 4C). Therefore, at least *Car2* appears to be a novel marker for NSICs that warrants further investigation.

Next, we looked to identify additional factors that set NSICs apart from FLCs. We observed an overrepresentation of genes associated with developmental processes (Supplemental Table S6) in the NSIC-enriched population. Interestingly, the NSIC population was marked by expression of transcription factors, including *Hoxd3*, *Hoxb2*, *Olig1*, and *Gata5* (57 genes; $P = 1.49E{-}05$; Supplemental Table S6), suggesting that this population is involved in active developmental processes at this critical stage of gonadal development; we found very few transcription factors characteristic of the FLC population. In addition, GO analysis identified numerous transmembrane component genes not expressed in the FLC population that may be involved in Sertoli-NSIC cell signaling (including *Frem2*, *Prokr1*, *Ntrk2*, *Cdh16*, and *Adam22*; 177 genes; $P = 2.22E{-}04$; Supplemental Table S6 and Fig. 5). Two hundred three of the genes identified as being upregulated in the NSIC-enriched population have been associated with a phenotype in OMIM, and for 162 of these the molecular basis is known (eight listed in Table 3; full list in Supplemental Data S7).

One of the transmembrane components identified in NSICs but not FLCs was *Frem2*/*FREM2* (Fras1-related extracellular matrix protein 2), a cell surface receptor that is a known DSD gene causing Fraser syndrome (OMIM: 219000; Table 3; [45]). Expression of *Frem2* has not been reported previously in the fetal gonad. By qRT-PCR we established that *Frem2* and its close family member *Fras1* (Fraser syndrome 1 homolog), which is also involved in Fraser syndrome, are expressed in the NSIC-enriched population of the testis at 12.5–13.5 dpc (Fig. 3, J and K). These data established that there is a large group of factors, some of which are known to be relevant to human DSD, which set NSICs apart from FLCs during early development. These genes may be relevant to the fate decisions made by NSICs at the time of FLC specification.

Sertoli Cells: Signaling to the FLCs and NSICs

Understanding of the process of interstitial cell specification requires knowledge of all potential paracrine factors produced by newly specified Sertoli cells. In addition to published microarray data from enriched Sertoli cells, we used RNA-seq to survey the Sertoli cells in greater detail [15]. Our RNA-seq analysis identified 1217 genes upregulated in the Sertoli cell-enriched population (Supplemental Data S2), and these included a number of previously described fetal Sertoli cell genes (*Aard*, *Dhh*, *Mro*, *Ptk2b*, *Cst9*, *Col9a3*, *Aldh1a1*, and *Amh*), thereby validating our approach. We identified *Trank1*, *Gstm7*, and *Adamts16* as novel genes expressed in the Sertoli cell population by qRT-PCR and ISH (Fig. 3, M–O, and Fig. 4, C and O–Q). DAVID analysis identified genes that encoded transmembrane factors (330 genes; $P = 3.19E{-}10$), and 44 genes with transcription factor activity ($P = 6.7E{-}1$) were upregulated in the Sertoli cell-enriched population (Fig. 5).

Interestingly, as in the FLC-enriched population list, we found a number of gonadotropin-releasing hormone (GnRH)-

TABLE 3. Subset of genes upregulated in 12.5-dpc NSICs ($P < 0.05$).[a]

ID	Gene symbol	Gene name	Chr.[b]	Phenotype	OMIM assoc.[c]	Reference[d]
ENSMUSG00000025105	*Bnc1*	Basonuclin 1	7	Subferiltle; postnatal spermatid expression	—	[89]
ENSMUSG00000037016	*Frem2*	Fras1 related extracellular matrix protein 2	3	Syndactyly, cryptophthalmos and urogential defects, ambiguous genitalia	219000*	[45]
ENSMUSG00000026365	*Cfh*	Complement component factor h	1	No lethal developmental defects; fertile	126700/609814/235400/610698	[90, 91]
ENSMUSG00000073530	*Pappa2*	Pappalysin 2	1	Postnatal growth retardation; fertile, with compromised fecundity	N/A	[92]
ENSMUSG00000027840	*Wnt2b*	Wingless-type MMTV integration site family, member 2B	3	No lethal developmental defects; fertile; olfactory bulb defect	—	[93]
ENSMUSG00000038587	*Akap12*	A kinase anchor protein12	10	Delayed fertility; urogenital hyperplasia	—	[94]
ENSMUSG00000023039	*Krt7*	Keratin 7	15	No lethal developmental defects; fertile	—	[95]
ENSMUSG00000027996	*Sfrp2*	Secreted frizzled-related protein 2	3	*Sfrp2*$^{-/-}$ viable and fertile; *Sfrp2*$^{-/-}$ / *Sfrp1*$^{-/-}$ gonadal defects, embryonic lethal at 16.5 dpc	—	[96–98]
ENSMUSG00000030774	*Pak1*	p21 protein (Cdc42/Rac)-activated kinase 1	7	No lethal developmental defects; fertile	—	[99]
ENSMUSG00000018659	*Pnpo*	Protogenin homolog	11	—	610090	—
ENSMUSG00000036030	*Prtg*	Pyridoxine 5′-phosphate oxidase	9	—	—	—
ENSMUSG00000029223	*Uchl1*	Ubiquitin carboxy-terminal hydrolase L1	5	No lethal developmental defects; fertile; develops ataxia	615491/613643	[100]
ENSMUSG00000040537	*Adam22*	α disintegrin and metallopeptidase domain 22	5	No lethal developmental defects; fertile	—	[101]
ENSMUSG00000035000	*Dpp4*	Dipeptidylpeptidase 4 (CD26)	2	No lethal developmental defects	—	[102]
ENSMUSG00000025889	*Snca*	Synuclein, alpha	6	No lethal developmental defects	127750/168601/605543	[103]
ENSMUSG00000021182	*Ccdc88c*	Coiled-coil domain containing 88C	12	—	236600	—
ENSMUSG00000009628	*Tex15*[e]	Testis expressed gene 15	8	Germ cell expression; males infertile	—	[104]
ENSMUSG00000041605	*5730559C18Rik*	RIKEN cDNA 5730559C18 gene	1	—	—	—
ENSMUSG00000034248	*Slc25a37*	Solute carrier family 25, member 37	14	—	—	—
ENSMUSG00000005360	*Slc1a3*	Solute carrier family 1, member 3	15		612656	
ENSMUSG00000042066	*Tmcc2*	Transmembrane and coiled-coil domains 2	1	No lethal developmental defects	N/A	[105]
ENSMUSG00000031881	*Cdh16*[e]	Cadherin 16	8	—	—	[106]
ENSMUSG00000038193	*Hand2*	Heart and neural crest derivatives expressed transcript 2	8	Embryonic lethal at 10.5 dpc; cardiac defects	—	[107]
ENSMUSG00000050244	*Heatr1*	HEAT repeat containing 1	13	—	N/A	—
ENSMUSG00000024151	*Msh2*[e]	MutS homolog 2 (E. coli)	17	No lethal developmental defects; fertile	120435/276300/158320	[108]
ENSMUSG00000063506	*Arhgap22*	Rho GTPase activating protein 22	14	—	—	—

TABLE 3. *Continued.*

ID	Gene symbol	Gene name	Chr.[b]	Phenotype	OMIM assoc.[c]	Reference[d]
ENSMUSG00000032186	*Tmod2*	Tropomodulin 2	9	No lethal developmental defects; fertile	—	[109]

[a] Classification used the same criteria as Table 2. We manually removed high-ranking known hematopoiesis-related genes to display 25 genes (8 genes removed; see Supplemental Data S2).
[b] Chr., chromosome.
[c] OMIM assoc. = OMIM reference number if the gene is associated with any type of human disorder (* indicates a genitourinary, endocrine, or DSD phenotype).
[d] References are the primary report of the null or mutant mouse and any subsequent clarifying reports.
[e] Indicates reported expression in germ cells.

signaling pathway components (11, including *Ptk2b*, *Src*, *Adcy9*, and *Plcb2*; $P = 3.50E{-}01$) and neurogenesis-related genes (20, including *Islr2*, *Robo1*, *Hes5*, *Sema6c*, and *Serpine2*; $P = 2.30E{-}02$). This abundance of neuroactive signaling-related genes further hints at a potential role for neuroactive ligand/receptor pairs in gonadogenesis.

Signals, such as DHH, from the Sertoli cells to the interstitium are essential for FLC development. In our group of Sertoli-enriched genes we identified an overrepresentation of 128 secreted factors ($P = 2.24E{-}17$; Fig. 4) including *Dhh*. We looked for known ligand pairs for the 35 FLC receptors identified in our RNA-seq data and the reprocessed Jameson et al. [15] data. We identified expression of the genes encoding known ligands to the neuroactive receptors (*Mc2r*, *Mc4r*, *Crhr*, *Vipr1*, *Prlr*, *Sstr4*, and *Tacr3*), a related receptor (*Adcy7*), and two neurogenesis-related receptors (*Prokr2*/*Robo2*) in our RNA-seq data and/or the reanalyzed Jameson dataset (Fig. 6).

DISCUSSION

We used RNA-seq to define the transcriptome of FLCs and compare it to those of NSICs and Sertoli cells in mice at 12.5 dpc in order to identify novel early markers of individual cell types in the developing testis, with particular focus on the FLC population. We anticipated that a detailed portrait of the genes expressed in FLC just prior to the onset of steroidogenesis, in comparison to a similar picture of the Sertoli and NSIC transcriptomes, would prove informative in terms of understanding how FLCs come to be specified and how they differentiate to become functional hormone-producing cells. Although previous studies have profiled somatic cells early in gonadogenesis [15, 35], the present study provides the first

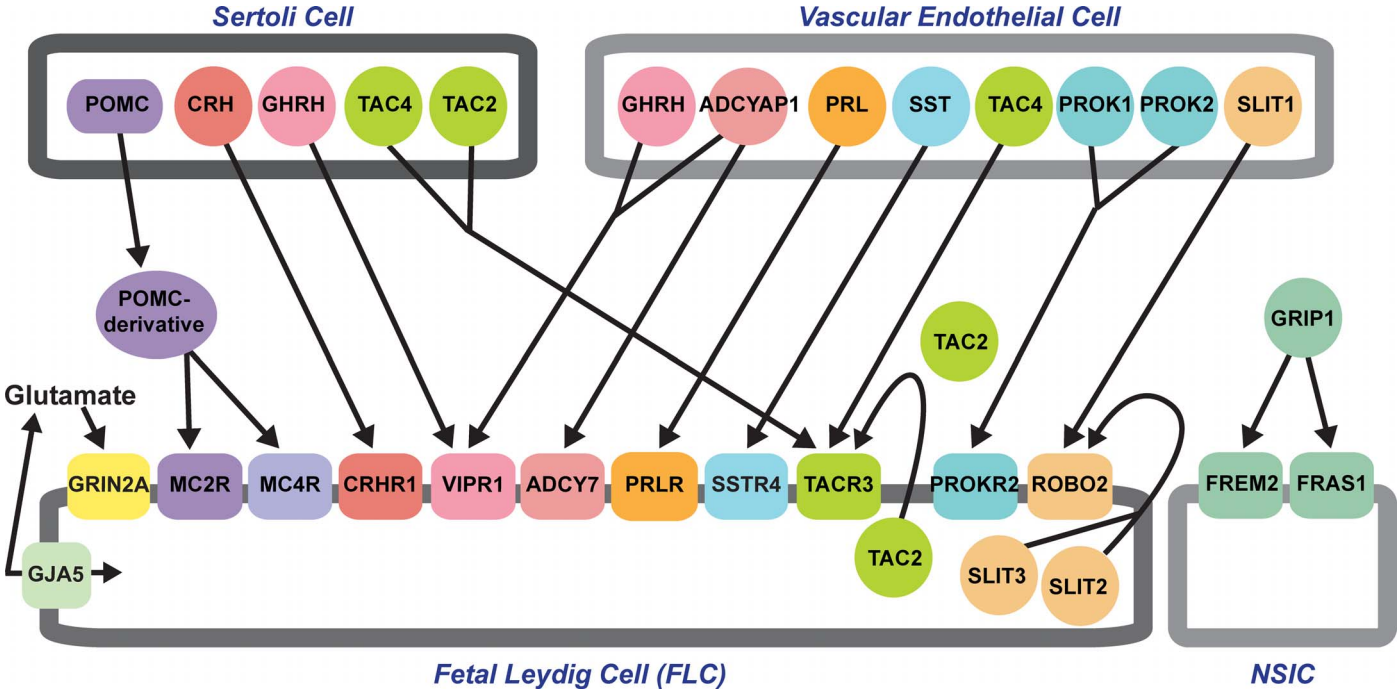

FIG. 6. Schematic of putative receptor-ligand interactions focusing on the receptors overexpressed on FLCs and NSICs. Receptors associated with neuroactive ligand signaling and/or DSD are represented. Ligands were identified from the literature and expression of ligands in cell types of the testis at 12.5 dpc was determined using data from this study and reprocessed Jameson et al. [15] data. The resulting schematic details proposed receptor-ligand interactions inferred from data at 12.5 dpc in the XY gonad. GJA5 shuttles glutamate, which is a ligand for the NMDA receptor of which GRIN2A is a subunit. The POMC complex is produced by Sertoli cells and its derivatives activate MC2R and MC4R. CRH is a ligand for CRHR1, whereas GHRH and ADCYAP1 (or PACAP) are ligands for VIPR1. ADCYAP1 can also activate ADCY7. PRL and SST are the ligands for PRLR and SSTR4 respectively and are expressed by vascular endothelial cells (VECs). TAC2 is predominately expressed by FLCs but also by Sertoli cells, whereas VECs and Sertoli cells express TAC4. Both TAC2 and TAC4 can activate TACR3. PROK1 and PROK2 can activate PROKR2. SLIT1/2/3 can activate ROBO2 and are expressed in the testis. The ligand GRIP1 is responsible for activating FREM2 and its close family member FRAS1.

RNA-seq analysis of enriched FLC, NSIC, and Sertoli cell populations in the XY gonad.

The method we developed for separating cell types has yielded the purest and most validated population of pre-FLCs yet reported. Determining which cell types a given gene is expressed in has hitherto been typically a labor-intensive task [46, 47]. Aside from providing the basis for our transcriptomic analysis, the system we developed will be useful in future studies designed to assign expression of any novel gene to a particular cell lineage using qRT-PCR.

We found that 61 of the overexpressed genes in the FLC-enriched population were previously unreported in the fetal gonad and therefore represent novel candidates for involvement in FLC specification. By checking previously published 11.5-dpc microarray data for genes we identified as FLC-upregulated at 12.5 dpc, we identified 10 robustly expressed putative presteroidogenic FLC marker genes. One of these is *Prokr2*, which we have previously shown to be expressed in the XY 11.5-dpc genital ridge [46], thereby validating this approach. Some of these 10 genes may prove useful in identifying pre-FLCs before they begin to express characteristic steroidogenic enzyme genes.

Hormones produced by the FLCs direct the masculinization of the embryo. Even though key components of the hypothalamic-pituitary-gonadal (HPG) axis are in place from around 16.5 dpc, the production of hormones by FLCs is thought to be independent of the HPG axis [48–52]. The GnRH-neural circuitry is a key component of the HPG; the formation and activation of the GnRH-neural circuitry involves a series of neuroactive ligand/receptor pairs; mutation of genes involved in this circuitry often results in DSD, which, it has been assumed, is primarily associated with HPG axis dysfunction [53–55]. Oddly, we found that a number of genes associated with these processes, which occur after the differentiation of FLCs, are expressed in the Sertoli cells and FLCs at 12.5 dpc. Of the 35 genes that encode receptors, in the FLC upregulated list, DAVID analysis identified 8 factors associated with neuroactive-ligand signaling (*Mc2r*, *Mc4r*, *Grin2a*, *Crhr1*, *Vipr1*, *Prlr*, *Sstr4*, and *Tacr3*; Fig. 6). In addition, we identified *Adcy7*, which encodes a receptor that is a regulator of intracellular cAMP concentration and that shares the ligand PACAP, encoded by the gene *Adcyap1*, with VIPR1 [56, 57]. Also of interest was the expression of *Gja5*, which encodes a gap junction protein CX40 involved in shuttling glutamate, an activator of the *N*-methyl-D-aspartate (NMDA) glutamate receptor, of which GRIN2A is a subunit (Fig. 6; [58–60]). Furthermore, *Robo2* and *Prokr2* were of interest, as both are implicated in neuronal processes and GnRH signaling [41, 61–63]. Assessment of the known ligands for the 11 receptors of interest indicated that putative ligand pairs were expressed in the FLCs, Sertoli cells, or vascular endothelial cells (Fig. 5; this study; [15]). Whether the testicular expression of these genes plays a role in gonadogenesis is yet to be determined, but the observation that they dominate the subgroup of FLC-upregulated genes that are not associated with steroidogenesis may be significant.

These findings also have implications for identifying the causes of DSD. Of the neuroactive genes identified, some that are upregulated in FLCs have previously been associated with DSDs that have urogenital phenotypes, for example *PROKR2* and *TACR3*. Mutations in *PROKR2* (OMIM: 244200; [64]) and *TACR3* (OMIM: 614840; [65, 66]) are associated with hypogonadotrophic hypogonadism in humans and mice. As many of the factors associated with neuroactive-ligand receptor activation and other neuronal processes are expressed robustly in the FLCs or the Sertoli cells of the developing testis (this study; [21]) it is tempting to speculate that gonadal production of these factors may precede HPG-driven production and explain male bias in individuals affected by hypogonadotrophic hypogonadism [46, 55, 64, 67].

Prokr2$^{-/-}$ mice have reproductive defects, and we have previously shown that there was no change in expression of FLC marker HSD3β/*Hsd3β* in *Prokr2*$^{-/-}$ embryos compared to *wild-type* littermates [41, 46]. However, embryonic *Prokr2*$^{-/-}$ testes display vasculature dysmorphology, a phenotype often associated with FLC impairment [10, 46]. *Tacr3*$^{-/-}$ mice have a variety of reproductive and fertility defects and a postnatal hormone profile similar to that of several other GnRH-deficient mouse models [41, 42, 68]. Our results suggest that more detailed analysis of the postnatal and embryonic gonadal phenotype of the *Tacr3*$^{-/-}$ mouse is needed to assess the effect of TACR3 loss before HPG axis activation occurs.

We identified that *Frem2* and *Fras1*, known DSD genes, are overexpressed in the NSIC population of the XY gonad from 12.5 to 13.5 dpc. Mutations in *Frem2* and *Fras1* result in Fraser syndrome (OMIM: 219000; [45, 69]) a multisystem disorder with ambiguous genitalia in 20% of patients (for review see [70]). *Frem2* knockout mice also have multiple developmental defects; however, the ambiguous genitalia phenotype seen in patients has not been characterized in mouse [45]. We postulate that a requirement for expression of *Frem2* and *Fras1* in NSICs early in gonadogenesis may contribute to the ambiguous genitalia phenotype seen in this model. This finding supports the idea that NSICs, not just Sertoli and FLCs, may play an important role in masculinization during fetal life.

It has recently been shown that some non-FLC of the interstitium differentiate into ALCs postnatally [2], establishing that a functional fetal NSIC population is important for postnatal masculinization of the individual. We find that early in gonadogenesis the NSIC population is characterized by expression of NR2F2 and a set of transcription factors and transmembrane receptors that are distinct from those of the FLC population. The differences we have identified between transcriptomic profiles in FLC- and NSIC-enriched populations may provide leads as to how pre-FLCs are selected or how NSICs resist selection from within the total interstitial population.

Functional investigation into individual genes shown to be upregulated in the various cell types, and processes highlighted as likely to be active within and between cells, will be needed if we are to gain a clearer understanding of gonadogenesis and postnatal sexual development, particularly as they relate to steroid production. We envisage that this dataset will be a resource to identify genes involved in normal gonadogenesis, in mouse and human, and to pinpoint genes likely to underlie some cases of human DSD.

ACKNOWLEDGMENT

We thank Tara-Lynne Davidson, Cassy Spiller, Janelle Ryan, and Virginia Nink for technical assistance; Ken-Ichirou Morohashi for the ARX antibody; Elanor Wainwright and Liang Zhao for critical reading of the manuscript; and Ben Hogan and Annemiek Beverdam for helpful discussions. Confocal microscopy was performed at the Australian Cancer Research Foundation (ACRF)/Institute for Molecular Bioscience Dynamic Imaging Facility for Cancer Biology. Flow cytometry and cell sorting was performed at the ACRF Brain Tumour Research Centre at the Queensland Brain Institute. Sequencing and library preparation was completed by the Monash Health Translation Precinct (MHTP) Medical Genomics Facility.

REFERENCES

1. Svingen T, Koopman P. Building the mammalian testis: origins,

differentiation, and assembly of the component cell populations. Genes Dev 2013; 27:2409–2426.
2. Kilcoyne KR, Smith LB, Atanassova N, Macpherson S, McKinnell C, van den Driesche S, Jobling MS, Chambers TJG, De Gendt K, Verhoeven G, O'Hara L, Platts S, et al. Fetal programming of adult Leydig cell function by androgenic effects on stem/progenitor cells. Proc Natl Acad Sci U S A 2014; 111:E1924–E1932.
3. Ono M, Harley VR. Disorders of sex development: new genes, new concepts. Nat Rev Endocrinol 2013; 9:79–91.
4. Griswold SL, Behringer RR. Fetal Leydig cell origin and development. Sex Dev 2009; 3:1–15.
5. Bitgood MJ, Shen L, McMahon AP. Sertoli cell signaling by desert hedgehog regulates the male germline. Curr Biol 1996; 6:298–304.
6. Yao HH-C, Whoriskey W, Capel B. Desert Hedgehog/Patched 1 signaling specifies fetal Leydig cell fate in testis organogenesis. Genes Dev 2002; 16:1433–1440.
7. Clark AM, Garland KK, Russell LD. Desert hedgehog (Dhh) gene is required in the mouse testis for formation of adult-type Leydig cells and normal development of peritubular cells and seminiferous tubules. Biol Reprod 2000; 63:1825–1838.
8. Barsoum IB, Bingham NC, Parker KL, Jorgensen JS, Yao HHC. Activation of the Hedgehog pathway in the mouse fetal ovary leads to ectopic appearance of fetal Leydig cells and female pseudohermaphroditism. Dev Biol 2009; 329:96–103.
9. Brennan J, Tilmann C, Capel B. Pdgfr-α mediates testis cord organization and fetal Leydig cell development in the XY gonad. Genes Dev 2003; 17: 800–810.
10. Miyabayashi K, Katoh-Fukui Y, Ogawa H, Baba T, Shima Y, Sugiyama N, Kitamura K, Morohashi K. Aristaless related homeobox gene, Arx, is implicated in mouse fetal Leydig cell differentiation possibly through expressing in the progenitor cells. PLoS One 2013; 8:e68050.
11. Kitamura K, Yanazawa M, Sugiyama N, Miura H, Iizuka-Kogo A, Kusaka M, Omichi K, Suzuki R, Kato-Fukui Y, Kamiirisa K, Matsuo M, Kamijo S, et al. Mutation of ARX causes abnormal development of forebrain and testes in mice and X-linked lissencephaly with abnormal genitalia in humans. Nat Genet 2002; 32:359–369.
12. Beverdam A, Koopman P. Expression profiling of purified mouse gonadal somatic cells during the critical time window of sex determination reveals novel candidate genes for human sexual dysgenesis syndromes. Hum Mol Genet 2006; 15:417–431.
13. Nef S, Schaad O, Stallings NR, Cederroth CR, Pitetti JL, Schaer G, Malki S, Dubois-Dauphin M, Boizet-Bonhoure B, Descombes P, Parker KL, Vassalli JD. Gene expression during sex determination reveals a robust female genetic program at the onset of ovarian development. Dev Biol 2005; 287:361–377.
14. Bouma GJ, Affourtit JP, Bult CJ, Eicher EM. Transcriptional profile of mouse pre-granulosa and Sertoli cells isolated from early-differentiated fetal gonads. Gene Expr Patterns 2007; 7:113–123.
15. Jameson SA, Natarajan A, Cool J, Defalco T, Maatouk DM, Mork L, Munger SC, Capel B. Temporal transcriptional profiling of somatic and germ cells reveals biased lineage priming of sexual fate in the fetal mouse gonad. PLoS Genet 2012; 8:e1002575.
16. Bouma GJ, Hudson QJ, Washburn LL, Eicher EM. New Candidate genes identified for controlling mouse gonadal sex determination and the early stages of granulosa and Sertoli cell differentiation. Biol Reprod 2010; 82: 380–389.
17. Marioni JC, Mason CE, Mane SM, Stephens M, Gilad Y. RNA-seq: an assessment of technical reproducibility and comparison with gene expression arrays. Genome Res 2008; 18:1509–1517.
18. Hajkova P, Ancelin K, Waldmann T, Lacoste N, Lange UC, Cesari F, Lee C, Almouzni G, Schneider R, Surani MA. Chromatin dynamics during epigenetic reprogramming in the mouse germ line. Nature 2008; 452:877–881.
19. Burgoyne PS, Tam PP, Evans EP. Retarded development of XO conceptuses during early pregnancy in the mouse. J Reprod Fertil 1983; 68:387–393.
20. Bowles J, Feng CW, Spiller C, Davidson TL, Jackson A, Koopman P. FGF9 suppresses meiosis and promotes male germ cell fate in mice. Dev Cell 2010; 19:440–449.
21. Svingen T, Spiller CM, Kashimada K, Harley VR, Koopman P. Identification of suitable normalizing genes for quantitative real-time RT-PCR analysis of gene expression in fetal mouse gonads. Sex Dev 2009; 3:194–204.
22. Kim D, Pertea G, Trapnell C, Pimentel H, Kelley R, Salzberg SL. TopHat2: accurate alignment of transcriptomes in the presence of insertions, deletions and gene fusions. Genome Biol 2013; 14:R36.
23. Anders S, Pyl PT, Huber W. HTSeq—a Python framework to work with high-throughput sequencing data. Bioinformatics 2014. btu638.
24. Robinson MD, Oshlack A. A scaling normalization method for differential expression analysis of RNA-seq data. Genome Biol 2010; 11:R25.
25. Law CW, Chen Y, Shi W, Smyth GK. voom: Precision weights unlock linear model analysis tools for RNA-seq read counts. Genome Biol 2014; 15:R29.
26. Smyth GK. Linear models and empirical Bayes methods for assessing differential expression in microarray experiments. Stat Appl Genet Mol Biol 2004; 3:Article3.
27. Benjamini Y, Hochberg Y. Controlling the false discovery rate: a practical and powerful approach to multiple testing. J R Statist Soc B 1995; 57:289–300.
28. Huang DW, Sherman BT, Lempicki RA. Bioinformatics enrichment tools: paths toward the comprehensive functional analysis of large gene lists. Nucl Acids Res 2009; 37:1–13.
29. Huang DW, Sherman BT, Lempicki RA. Systematic and integrative analysis of large gene lists using DAVID bioinformatics resources. Nat Protoc 2009; 4:44–57.
30. Baba T, Otake H, Sato T, Miyabayashi K, Shishido Y, Wang C-Y, Shima Y, Kimura H, Yagi M, Ishihara Y, Hino S, Ogawa H, et al. Glycolytic genes are targets of the nuclear receptor Ad4BP/SF-1. Nat Commun 2014; 5:3634.
31. Carvalho BS, Irizarry RA. A framework for oligonucleotide microarray preprocessing. Bioinformatics 2010; 26:2363–2367.
32. Schmahl J, Eicher EM, Washburn LL, Capel B. Sry induces cell proliferation in the mouse gonad. Development 2000; 127:65–73.
33. Hatano O, Takayama K, Imai T, Waterman MR, Takakusu A, Omura T, Morohashi K. Sex-dependent expression of a transcription factor, Ad4BP, regulating steroidogenic P-450 genes in the gonads during prenatal and postnatal rat development. Development 1994; 120: 2787–2797.
34. Morohashi K, Hatano O, Nomura M, Takayama K, Hara M, Yoshii H, Takakusu A, Omura T. Function and distribution of a steroidogenic cell-specific transcription factor, Ad4BP. J Steroid Biochem Mol Biol 1995; 53:81–88.
35. McDowell EN, Kisielewski AE, Pike JW, Franco HL, Yao HH, Johnson KJ. A transcriptome-wide screen for mRNAs enriched in fetal Leydig cells: CRHR1 agonism stimulates rat and mouse fetal testis steroidogenesis. PLoS One 2012; 7:e47359.
36. Diez-Roux G, Banfi S, Sultan M, Geffers L, Anand S, Rozado D, Magen A, Canidio E, Pagani M, Peluso I, Lin-Marq N, Koch M, et al. A high-resolution anatomical atlas of the transcriptome in the mouse embryo. PLoS Biol 2011; 9:e1000582.
37. Meyer D, Birchmeier C. Multiple essential functions of neuregulin in development. Nature 1995; 378:386–390.
38. Chuang P-T, Kawcak T, McMahon AP. Feedback control of mammalian Hedgehog signaling by the Hedgehog-binding protein, Hip1, modulates Fgf signaling during branching morphogenesis of the lung. Genes Dev 2003; 17:342–347.
39. Schack von D, Casademunt E, Schweigreiter R, Meyer M, Bibel M, Dechant G. Complete ablation of the neurotrophin receptor p75NTR causes defects both in the nervous and the vascular system. Nat Neurosci 2001; 4:977–978.
40. Grieshammer U, Le M, Plump AS, Wang F, Tessier-Lavigne M, Martin GR. SLIT2-mediated ROBO2 signaling restricts kidney induction to a single site. Dev Cell 2004; 6:709–717.
41. Matsumoto S, Yamazaki C, Masumoto K, Nagano M, Naito M, Soga T, Hiyama H, Matsumoto M, Takasaki J, Kamohara M, Matsuo A, Ishii H, et al. Abnormal development of the olfactory bulb and reproductive system in mice lacking prokineticin receptor PKR2. Proc Natl Acad Sci U S A 2006; 103:4140–4145.
42. Yang JJ, Caligioni CS, Chan Y-M, Seminara SB. Uncovering novel reproductive defects in neurokinin B receptor null mice: closing the gap between mice and men. Endocrinology 2012; 153:1498–1508.
43. Barsoum IB, Yao HH. Fetal Leydig cells: progenitor cell maintenance and differentiation. J Androl 2010; 31:11–15.
44. DeFalco T, Bhattacharya I, Williams AV, Sams DM, Capel B. Yolk-sac-derived macrophages regulate fetal testis vascularization and morphogenesis. Proc Natl Acad Sci U S A 2014; 111:E2384–93.
45. Jadeja S, Smyth I, Pitera JE, Taylor MS, van Haelst M, Bentley E, McGregor L, Hopkins J, Chalepakis G, Philip N, Perez Aytes A, Watt FM, et al. Identification of a new gene mutated in Fraser syndrome and mouse myelencephalic blebs. Nat Genet 2005; 37:520–525.
46. Svingen T, McClelland KS, Masumoto K, Sujino M, Nagano M, Shigeyoshi Y, Koopman P. Prokr2-deficient mice display vascular

dysmorphology of the fetal testes: potential implications for Kallmann syndrome aetiology. Sex Dev 2011; 5:294–303.
47. Wainwright EN, Jorgensen JS, Kim Y, Truong V, Bagheri-Fam S, Davidson T, Svingen T, Fernandez-Valverde SL, McClelland KS, Taft RJ, Harley VR, Koopman P, et al. SOX9 regulates microRNA miR-202-5p/3p expression during mouse testis differentiation. Biol Reprod 2013; 89:34.
48. Japon MA, Rubinstein M, Low MJ. In situ hybridization analysis of anterior pituitary hormone gene expression during fetal mouse development. J Histochem Cytochem 1994; 42:1117–1125.
49. O'Shaughnessy PJ, Baker P, Sohnius U, Haavisto AM, Charlton HM, Huhtaniemi I. Fetal development of Leydig cell activity in the mouse is independent of pituitary gonadotroph function. Endocrinology 1998; 139:1141–1146.
50. Zhang FP, Poutanen M, Wilbertz J, Huhtaniemi I. Normal prenatal but arrested postnatal sexual development of luteinizing hormone receptor knockout (LuRKO) mice. Mol Endocrinol 2001; 15:172–183.
51. Pakarinen P, Kimura S, El-Gehani F, Pelliniemi LJ, Huhtaniemi I. Pituitary hormones are not required for sexual differentiation of male mice: phenotype of the T/ebp/Nkx2.1 null mutant mice. Endocrinology 2002; 143:4477–4482.
52. Baker PJ, O'Shaughnessy PJ. Role of gonadotrophins in regulating numbers of Leydig and Sertoli cells during fetal and postnatal development in mice. Reproduction 2001; 122:227–234.
53. Mastorakos G, Pavlatou MG, Mizamtsidi M. The hypothalamic-pituitary-adrenal and the hypothalamic-pituitary-gonadal axes interplay. Pediatr Endocrinol Rev 2006; 3(suppl 1):172–181.
54. Bianco SDC, Kaiser UB. The genetic and molecular basis of idiopathic hypogonadotropic hypogonadism. Nat Rev Endocrinol 2009; 5:569–576.
55. Hardelin JP, Dode C. The complex genetics of Kallmann syndrome: KAL1, FGFR1, FGF8, PROKR2, PROK2, et al. Sex Dev 2008; 2: 181–193.
56. Acquaah-Mensah GK, Taylor RC, Bhave SV. PACAP interactions in the mouse brain: implications for behavioral and other disorders. Gene 2012; 491:224–231.
57. Halvorson LM. PACAP modulates GnRH signaling in gonadotropes. Mol Cell Endocrinol 2014; 385:45–55.
58. Monyer H, Burnashev N, Laurie DJ, Sakmann B, Seeburg PH. Developmental and regional expression in the rat brain and functional properties of four NMDA receptors. Neuron 1994; 12:529–540.
59. Monyer H, Sprengel R, Schoepfer R, Herb A, Higuchi M, Lomeli H, Burnashev N, Sakmann B, Seeburg PH. Heteromeric NMDA receptors: molecular and functional distinction of subtypes. Science 1992; 256: 1217–1221.
60. Bai D. Atrial fibrillation-linked GJA5/connexin40 mutants impaired gap junctions via different mechanisms. FEBS Lett 2014; 588:1238–1243.
61. Cole LW, Sidis Y, Zhang C, Quinton R, Plummer L, Pignatelli D, Hughes VA, Dwyer AA, Raivio T, Hayes FJ, Seminara SB, Huot C, et al. Mutations in prokineticin 2 and prokineticin receptor 2 genes in human gonadotrophin-releasing hormone deficiency: molecular genetics and clinical spectrum. J Clin Endocrinol Metab 2008; 93:3551–3559.
62. Kidd T, Brose K, Mitchell KJ, Fetter RD, Tessier-Lavigne M, Goodman CS, Tear G. Roundabout controls axon crossing of the CNS midline and defines a novel subfamily of evolutionarily conserved guidance receptors. Cell 1998; 92:205–215.
63. Lu W, van Eerde AM, Fan X, Quintero-Rivera F, Kulkarni S, Ferguson H, Kim H-G, Fan Y, Xi Q, Li Q-G, Sanlaville D, Andrews W, et al. Disruption of ROBO2 is associated with urinary tract anomalies and confers risk of vesicoureteral reflux. Am J Hum Genet 2007; 80: 616–632.
64. Dode C, Teixeira L, Levilliers J, Fouveaut C, Bouchard P, Kottler ML, Lespinasse J, Lienhardt-Roussie A, Mathieu M, Moerman A, Morgan G, Murat A, et al. Kallmann syndrome: mutations in the genes encoding prokineticin-2 and prokineticin receptor-2. PLoS Genet 2006; 2: 1648–1652.
65. Topaloglu AK, Reimann F, Guclu M, Yalin AS, Kotan LD, Porter KM, Serin A, Mungan NO, Cook JR, Ozbek MN, Imamoglu S, Akalin NS, et al. TAC3 and TACR3 mutations in familial hypogonadotropic hypogonadism reveal a key role for Neurokinin B in the central control of reproduction. Nat Genet 2009; 41:354–358.
66. Gianetti E, Tusset C, Noel SD, Au MG, Dwyer AA, Hughes VA, Abreu AP, Carroll J, Trarbach E, Silveira LFG, Costa EMF, de Mendonça BB, et al. TAC3/TACR3 mutations reveal preferential activation of gonadotropin-releasing hormone release by neurokinin B in neonatal life followed by reversal in adulthood. J Clin Endocrinol Metab 2010; 95: 2857–2867.
67. Dodé C, Levilliers J, Dupont J-M, De Paepe A, Le Dû N, Soussi-Yanicostas N, Coimbra RS, Delmaghani S, Compain-Nouaille S, Baverel F, Pêcheux C, Le Tessier D, et al. Loss-of-function mutations in FGFR1 cause autosomal dominant Kallmann syndrome. Nat Genet 2003; 33: 463–465.
68. Lapatto R, Pallais JC, Zhang D, Chan Y-M, Mahan A, Cerrato F, Le WW, Hoffman GE, Seminara SB. Kiss1−/− mice exhibit more variable hypogonadism than Gpr54−/− mice. Endocrinology 2007; 148: 4927–4936.
69. Shafeghati Y, Kniepert A, Vakili G, Zenker M. Fraser syndrome due to homozygosity for a splice site mutation of FREM2. Am J Med Genet A 2008; 146A:529–531.
70. Smyth I, Scambler P. The genetics of Fraser syndrome and the blebs mouse mutants. Hum Mol Genet 2005; 14(spec no 2):R269–R274.
71. Buters JTM, Sakai S, Richter T, Pineau T, Alexander DL, Savas U, Doehmer J, Ward JM, Jefcoate CR, Gonzalez FJ. Cytochrome P450 CYP1B1 determines susceptibility to 7, 12-dimethylbenz[a]anthracene-induced lymphomas. Proc Natl Acad Sci U S A 1999; 96:1977–1982.
72. Lu B, Figini M, Emanueli C, Geppetti P, Grady E, Gerard N, Ansell J, Payan D, Gerard C, Bunnett N. The control of microvascular permeability and blood pressure by neutral endopeptidase. Nat Med 1997; 3:904–907.
73. Bettahi I, Marker CL, Roman MI, Wickman K. Contribution of the Kir3.1 subunit to the muscarinic-gated atrial potassium channel IKACh. J Biol Chem 2002; 277:48282–48288.
74. Hirai H, Pang Z, Bao D, Miyazaki T, Li L, Miura E, Parris J, Rong Y, Watanabe M, Yuzaki M, Morgan JI. Cbln1 is essential for synaptic integrity and plasticity in the cerebellum. Nat Neurosci 2005; 8: 1534–1541.
75. Yang JT, Rayburn H, Hynes RO. Cell adhesion events mediated by alpha 4 integrins are essential in placental and cardiac development. Development 1995; 121:549–560.
76. Manicone AM, Birkland TP, Lin M, Betsuyaku T, van Rooijen N, Lohi J, Keski-Oja J, Wang Y, Skerrett SJ, Parks WC. Epilysin (MMP-28) restrains early macrophage recruitment in *Pseudomonas aeruginosa* pneumonia. J Immunol 2009; 182:3866–3876.
77. Bazigou E, Xie S, Chen C, Weston A, Miura N, Sorokin L, Adams R, Muro AF, Sheppard D, Makinen T. Integrin-alpha9 is required for fibronectin matrix assembly during lymphatic valve morphogenesis. Dev Cell 2009; 17:175–186.
78. Huang XZ, Wu JF, Ferrando R, Lee JH, Wang YL, Farese RV Jr, Sheppard D. Fatal bilateral chylothorax in mice lacking the integrin alpha9beta1. Mol Cell Biol 2000; 20:5208–5215.
79. Wharram BL, Goyal M, Gillespie PJ, Wiggins JE, Kershaw DB, Holzman LB, Dysko RC, Saunders TL, Samuelson LC, Wiggins RC. Altered podocyte structure in GLEPP1 (Ptpro)-deficient mice associated with hypertension and low glomerular filtration rate. J Clin Invest 2000; 106:1281–1290.
80. Gonzalez-Brito MR, Bixby JL. Protein tyrosine phosphatase receptor type O regulates development and function of the sensory nervous system. Mol Cell Neurosci 2009; 42:458–465.
81. Carpenter EM, Goddard JM, Davis AP, Nguyen TP, Capecchi MR. Targeted disruption of Hoxd-10 affects mouse hindlimb development. Development 1997; 124:4505–4514.
82. Huszar D, Lynch CA, Fairchild-Huntress V, Dunmore JH, Fang Q, Berkemeier LR, Gu W, Kesterson RA, Boston BA, Cone RD, Smith FJ, Campfield LA, et al. Targeted disruption of the melanocortin-4 receptor results in obesity in mice. Cell 1997; 88:131–141.
83. Glasson SS, Askew R, Sheppard B, Carito B, Blanchet T, Ma H-L, Flannery CR, Peluso D, Kanki K, Yang Z, Majumdar MK, Morris EA. Deletion of active ADAMTS5 prevents cartilage degradation in a murine model of osteoarthritis. Nature 2005; 434:644–648.
84. Stanton H, Rogerson FM, East CJ, Golub SB, Lawlor KE, Meeker CT, Little CB, Last K, Farmer PJ, Campbell IK, Fourie AM, Fosang AJ. ADAMTS5 is the major aggrecanase in mouse cartilage in vivo and in vitro. Nature 2005; 434:648–652.
85. Gurtner GC, Davis V, Li H, McCoy MJ, Sharpe A, Cybulsky MI. Targeted disruption of the murine VCAM1 gene: essential role of VCAM-1 in chorioallantoic fusion and placentation. Genes Dev 1995; 9: 1–14.
86. Chang ACM, Cha J, Koentgen F, Reddel RR. The murine stanniocalcin 1 gene is not essential for growth and development. Mol Cell Biol 2005; 25:10604–10610.
87. Hines LM, Hoffman PL, Bhave S, Saba L, Kaiser A, Snell L, Goncharov I, LeGault L, Dongier M, Grant B, Pronko S, Martinez L, et al. A sex-specific role of type VII adenylyl cyclase in depression. J Neurosci 2006; 26:12609–12619.
88. Prakash SK, Paylor R, Jenna S, Lamarche-Vane N, Armstrong DL, Xu B,

Mancini MA, Zoghbi HY. Functional analysis of ARHGAP6, a novel GTPase-activating protein for RhoA. Hum Mol Genet 2000; 9:477–488.
89. Zhang X, Chou W, Haig-Ladewig L, Zeng W, Cao W, Gerton G, Dobrinski I, Tseng H. BNC1 is required for maintaining mouse spermatogenesis. Genesis 2012; 50:517–524.
90. Pickering MC, Cook HT, Warren J, Bygrave AE, Moss J, Walport MJ, Botto M. Uncontrolled C3 activation causes membranoproliferative glomerulonephritis in mice deficient in complement factor H. Nat Genet 2002; 31:424–428.
91. Coffey PJ, Gias C, McDermott CJ, Lundh P, Pickering MC, Sethi C, Bird A, Fitzke FW, Maass A, Chen LL, Holder GE, Luthert PJ, et al. Complement factor H deficiency in aged mice causes retinal abnormalities and visual dysfunction. Proc Natl Acad Sci U S A 2007; 104: 16651–16656.
92. Conover CA, Boldt HB, Bale LK, Clifton KB, Grell JA, Mader JR, Mason EJ, Powell DR. Pregnancy-associated plasma protein-A2 (PAPP-A2): tissue expression and biological consequences of gene knockout in mice. Endocrinology 2011; 152:2837–2844.
93. Tsukiyama T, Yamaguchi TP. Mice lacking Wnt2b are viable and display a postnatal olfactory bulb phenotype. Neurosci Lett 2012; 512:48–52.
94. Akakura S, Huang C, Nelson PJ, Foster B, Gelman IH. Loss of the SSeCKS/Gravin/AKAP12 gene results in prostatic hyperplasia. Cancer Res 2008; 68:5096–5103.
95. Sandilands A, Smith FJD, Lunny DP, Campbell LE, Davidson KM, MacCallum SF, Corden LD, Christie L, Fleming S, Lane EB, McLean WHI. Generation and characterisation of keratin 7 (K7) knockout mice. PLoS One 2013; 8:e64404.
96. Warr N, Siggers P, Bogani D, Brixey R, Pastorelli L, Yates L, Dean CH, Wells S, Satoh W, Shimono A, Greenfield A. Sfrp1 and Sfrp2 are required for normal male sexual development in mice. Dev Biol 2009; 326:273–284.
97. Cox S, Smith L, Bogani D, Cheeseman M, Siggers P, Greenfield A. Sexually dimorphic expression of secreted frizzled-related (SFRP) genes in the developing mouse Müllerian duct. Mol Reprod Dev 2006; 73: 1008–1016.
98. Satoh W, Gotoh T, Tsunematsu Y, Aizawa S, Shimono A. Sfrp1 and Sfrp2 regulate anteroposterior axis elongation and somite segmentation during mouse embryogenesis. Development 2006; 133:989–999.
99. Asrar S, Meng Y, Zhou Z, Todorovski Z, Huang WW, Jia Z. Regulation of hippocampal long-term potentiation by p21-activated protein kinase 1 (PAK1). Neuropharmacology 2009; 56:73–80.
100. Saigoh K, Wang YL, Suh JG, Yamanishi T, Sakai Y, Kiyosawa H, Harada T, Ichihara N, Wakana S, Kikuchi T, Wada K. Intragenic deletion in the gene encoding ubiquitin carboxy-terminal hydrolase in gad mice. 1999; 23:47–51.
101. Sagane K, Hayakawa K, Kai J, Hirohashi T, Takahashi E, Miyamoto N, Ino M, Oki T, Yamazaki K, Nagasu T. Ataxia and peripheral nerve hypomyelination in ADAM22-deficient mice. BMC Neurosci 2005; 6: 33.
102. Marguet D, Baggio L, Kobayashi T, Bernard AM, Pierres M, Nielsen PF, Ribel U, Watanabe T, Drucker DJ, Wagtmann N. Enhanced insulin secretion and improved glucose tolerance in mice lacking CD26. Proc Natl Acad Sci U S A 2000; 97:6874–6879.
103. Abeliovich A, Schmitz Y, Fariñas I, Choi-Lundberg D, Ho WH, Castillo PE, Shinsky N, Verdugo JM, Armanini M, Ryan A, Hynes M, Phillips H, et al. Mice lacking alpha-synuclein display functional deficits in the nigrostriatal dopamine system. Neuron 2000; 25:239–252.
104. Yang F, Eckardt S, Leu NA, McLaughlin KJ, Wang PJ. Mouse TEX15 is essential for DNA double-strand break repair and chromosomal synapsis during male meiosis. J Cell Biol 2008; 180:673–679.
105. Watase K, Hashimoto K, Kano M, Yamada K, Watanabe M, Inoue Y, Okuyama S, Sakagawa T, Ogawa S, Kawashima N, Hori S, Takimoto M, et al. Motor discoordination and increased susceptibility to cerebellar injury in GLAST mutant mice. Eur J Neurosci 1998; 10:976–988.
106. Wertz K, Herrmann BG. Kidney-specific cadherin (cdh16) is expressed in embryonic kidney, lung, and sex ducts. Mech Dev 1999; 84:185–188.
107. Srivastava D, Thomas T, Lin Q, Kirby ML, Brown D, Olson EN. Regulation of cardiac mesodermal and neural crest development by the bHLH transcription factor, dHAND. Nat Genet 1997; 16:154–160.
108. Paul C, Povey JE, Lawrence NJ, Selfridge J, Melton DW, Saunders PTK. Deletion of genes implicated in protecting the integrity of male germ cells has differential effects on the incidence of DNA breaks and germ cell loss. PLoS One 2007; 2:e989.
109. Cox PR, Fowler V, Xu B, Sweatt JD, Paylor R, Zoghbi HY. Mice lacking Tropomodulin-2 show enhanced long-term potentiation, hyperactivity, and deficits in learning and memory. Mol Cell Neurosci 2003; 23:1–12.

Asian Journal of Andrology (2012) 14, 164–171

www.nature.com/aja

REVIEW

Male sex determination: insights into molecular mechanisms

Kathryn McClelland, Josephine Bowles and Peter Koopman

Disorders of sex development often arise from anomalies in the molecular or cellular networks that guide the differentiation of the embryonic gonad into either a testis or an ovary, two functionally distinct organs. The activation of the Y-linked gene *Sry* (*sex-determining region Y*) and its downstream target *Sox9* (*Sry box-containing gene 9*) triggers testis differentiation by stimulating the differentiation of Sertoli cells, which then direct testis morphogenesis. Once engaged, a genetic pathway promotes the testis development while actively suppressing genes involved in ovarian development. This review focuses on the events of testis determination and the struggle to maintain male fate in the face of antagonistic pressure from the underlying female programme.
Asian Journal of Andrology (2012) **14,** 164–171; doi:10.1038/aja.2011.169; published online 19 December 2011

Keywords: gonadal; knockout; mice; sex determination; sex-determining region Y protein; sex disorders; sex reversal; sexual development; testis

INTRODUCTION

Perceptions of sex and sexuality pervade modern culture. However, it is important to recognize that not all members of our society fit comfortably the socially constructed ideas of masculinity and femininity. These people are likely to struggle with a variety of medical and psychosocial issues surrounding their sexuality.[1,2] It is estimated that 1.7% of all live births have a disorder of sex development (DSD).[3,4] These conditions are congenital and are characterized by chromosomal or gonadal sex that does not match outward appearance of maleness or femaleness, or anatomical sex that is in some way ambiguous or intermediate between male and female.[4] Some of these conditions are associated with infertility, predisposition to gonadal tumours and/or other syndromic features.[5,6] Clearly, discovery of the underlying molecular causes of DSDs is an important goal in biomedical research.

Genomic and structure/function studies of human DSDs have revealed a number of genes as being important for sex development, while studies in the mouse have further extended our understanding of the mechanism of action of these genes; these approaches are complementary. Identifying the molecular mechanisms behind sex determination and differentiation will lead to more accurate diagnosis and prognosis, and assist in providing more informed options for psychological, endocrinological, surgical and other clinical management of DSDs, many of which remain uncharacterized at a molecular level. In a broader context, understanding the events of early testis development may also illuminate some of the underlying causes of male infertility.

In this review, we examine the molecular mechanisms behind male sex determination and differentiation, and how impairment of these mechanisms underlies a subset of human DSDs. In particular, we highlight the interplay between the molecular pathways that promote male and female development, and the role of gene dosage and phenotype sensitivity in mice and humans.

SRY AND THE BEGINNINGS OF MALENESS

We each inherit an X or a Y sex chromosome from our father and an X chromosome from our mother during fertilisation. The resulting chromosomal sex (XX or XY) leads to the transformation of the embryo into a male or a female. Before gonadal sex determination in both XX and XY embryos, a bipotential gonadal primordium exists that has the potential to differentiate into either testes or ovaries. Activation of the Y-linked gene *Sry* (*sex-determining region Y*) initiates testicular development. When *Sry* is expressed ectopically in XX mice, the testis pathway is initiated.[7] When *Sry* is not present, as in XX individuals, or non-functional in XY individuals, the bipotential gonads generally do not follow the testicular pathway and instead develop into ovaries.[8,9]

SRY plays a role in a number of DSDs: mutation or loss of function of SRY results in complete male to female sex reversal,[10,11] whereas ectopic expression of SRY in XX individuals due to chromosomal translocation of SRY may result in female to male sex reversal. Indeed, SRY translocation is responsible for 10% of all 46,XX female to male sex reversal.[12] Formation of ovotestes, where ovarian and testicular tissues coexist in the same organ, can also occur in cases of ectopic SRY activity.[13,14]

SRY is a transcription factor with a DNA-binding high-mobility group box domain.[15,16] In mice, expression of *Sry* is both brief and carefully regulated; however, the factors controlling this burst of expression remain unknown. One of the factors postulated to play a role in activation of *Sry* is Wilms' tumour 1 (WT1), which can act as a

Institute for Molecular Bioscience, The University of Queensland, Brisbane, QLD 4072, Australia
Correspondence: Prof P Koopman (p.koopman@imb.uq.edu.au)
Received: 4 September 2011; Revised: 7 October 2011; Accepted: 19 October 2011; Published online: 19 December 2011

transcriptional activator[17,18] or repressor.[19] WT1 has two active isoforms in the gonad, with either an insertion or an omission of three amino acids, lysine (K), tyrosine (T) and serine (S), between two zinc finger motifs.[20,21] Each isoform has distinct functions during mouse testis determination. Knockout mice show that WT1+KTS, although unlikely to be directly regulating *Sry* expression, is required for maintenance of the gonad.[20] However, this WT1 isoform has been shown to be able to transactivate the human *SRY* promoter *in vitro*.[22] Conversely, WT1+KTS-null mice exhibit complete XY sex reversal, presumably due to abnormally low *Sry* expression.[20] In agreement with the mouse model, WT1 haploinsufficiency, resulting in reduced levels of WT1+KTS, results in XY sex reversal in human patients.[23] It is proposed that WT1+KTS is involved in cell-autonomous regulation of *Sry in vivo*, as indicated by reduced SRY levels in cells of WT1+KTS-null mouse gonads.[24] It is important when interpreting these results to take into account the fact that knocking out one WT1 isoform leads to an increase in expression of the other, which may have an impact on the observed phenotype and interaction with SRY.

In addition to sufficiently early onset of expression of *Sry*, a threshold level of expression must be achieved for complete testis differentiation to occur. In mice, expression of *Sry* is initiated at 10.5 days post-coitum (d.p.c.), peaks at 11.5 d.p.c. and is extinguished by 12.5 d.p.c.[25–27] *Sry* expression occurs in a wave-like pattern, beginning in the central region of the gonad and expanding out towards the poles.[28–31] In humans, *SRY* has a broader spatiotemporal expression profile, occurring in multiple tissues such as the adrenal and heart, and being maintained for longer in the testis, apparently through to adulthood.[32] *Sry/SRY* is also expressed in the brain of mice and humans.[32–34] In mice, SRY is expressed in a subset of nigrostriatal doperminergic neurons in the brain and appears to affect the specific motor behaviours they control.[35] However, although SRY is suspected of being involved in sexual dimorphism of the brain, a specific role for SRY outside sex determination has yet to be conclusively demonstrated.

Before turning to the cellular role of SRY, it is important to discuss briefly the course of events that occur as the testis differentiates. The gonads arise from a pair of bipotential primordia known as the genital ridges. In males, differentiation of the bipotential supporting cell lineage into Sertoli cells results in organisation of the developing testis into two main compartments: the testis cords, which comprise aggregates of germ cells surrounded by a layer of Sertoli cells in turn encased by peritubular myoid cells, and the testis interstitium which includes the steroidogenic Leydig cells and the testis vasculature. The development of secondary sexual characteristics in the embryo, such as external genitalia, is directed by the testes. Thus, the morphogenesis of the bipotential gonads into testes dictates the phenotypic sex of the male individual (**Figure 1**).

In mice, the first known cellular difference between the XX and XY gonad after expression of *Sry* is the male-specific proliferation of the epithelium at the coelomic surface of the genital ridges.[36,37] This sex-specific proliferation is thought to amplify the population of cells capable of differentiating into Sertoli cells, the first testicular cell type to differentiate,[38] and is required for the formation of testis cords.[36,37,39] Thus far, the molecular mechanism that induces coelomic epithelial proliferation is unknown. We do know a direct molecular target of SRY: the gene encoding the transcription factor *Sox9* (*Sry box-containing gene 9*).[40] Because testes develop normally in transgenic XX mice overexpressing *Sox9*, it appears that male-specific proliferation of the coelomic epithelium and all other aspects of foetal testis development are under the control, directly or indirectly, of SOX9.[41,42]

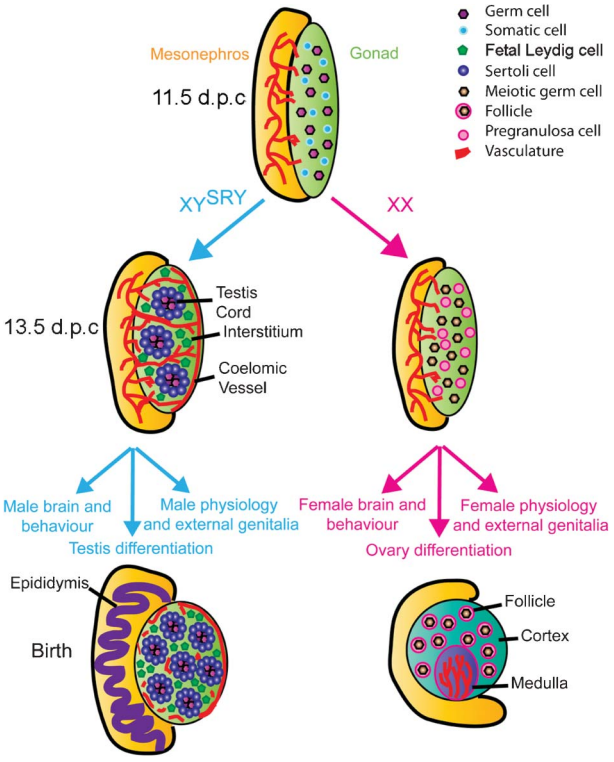

Figure 1 Overview of mouse gonadogenesis. The expression of *Sry* and *Sox9* at 10.5–11.5 d.p.c. in the bipotential gonad initiates testis differentiation. By 13.5 d.p.c., basic testis morphology is established; the formation of testis cords, the coelomic blood vessel, and differentiation and activation of steroidogenesis in Leydig cells has occurred, and androgens are then produced by the testes. In the ovary, further differentiation is delayed. Around 13.5 d.p.c., germ cells have entered meiosis and vascularisation, and remodelling of the ovary to form germ cell cysts occurs. Later, the cortical and medullar domains begin to be established and folliculogenesis takes place. Secondary sexual characteristics include the establishment of the male and female genital tract and duct system, sex-specific brain dimorphisms and behaviours, and external genitalia. The establishment of secondary sexual characteristics involves organ-specific, regulatory gene networks. d.p.c., days post-coitum; FLC, foetal Leydig cell; Sox9, Sry box-containing gene 9; Sry/SRY, sex-determining region Y.

SOX9 AND THE DIFFERENTIATION OF THE SERTOLI CELL

Sox9 is upregulated when a protein complex of SRY and steroidogenic factor 1 ((SF1) nuclear receptor subfamily 5, group A, member 1) binds to a *Sox9* enhancer element known as testis-specific enhancer of *Sox9* core element (TESCO).[40] Like SRY, SOX9 is necessary for testis differentiation: mice lacking *Sox9* undergo complete XY sex reversal,[43,44] while 75% of human patients with a heterozygous mutation in *SOX9* manifest with complete or partial XY sex reversal.[45,46]

The proposed mechanism for XY gonadal transcription of *Sox9* during sex determination consists of three distinct phases, according to Sekido and Lovell-Badge.[40] Firstly, SF1 initiates low-level transcription of *Sox9* in XX and XY genital ridges. Secondly, SF1, in a complex with SRY, activates male-specific transcription of *Sox9* in the male genital ridge *via* TESCO. High levels of SOX9 are then maintained in the XY gonad *via* an autoregulatory feedback loop.[40,47] Indeed, *in vitro* studies using SF1, SRY and SOX9 mutant proteins, modelled on clinical human mutations from 46,XY DSD patients, support this model. These proteins failed to activate the human homologue of TESCO, providing a potential mechanism by which mutations resulting in partially functional proteins can present as DSDs.[48]

It is believed that bipotential supporting cells cell-autonomously differentiate into Sertoli cells under the influence of SRY and SOX9: this conclusion was drawn from XX–XY chimaera studies in which it was found that, when testes formed, almost all Sertoli cells were XY, while other cell types did not exhibit a chromosomal bias.[49,50] However, some Sertoli cells were always found to be XX,[49] indicating the existence of paracrine pathways by which SRY- and SOX9-positive cells can recruit additional cells (such as XX cells in the chimaera experiments, or cells that express unusually low levels of *Sry* in normal XY gonads) to the Sertoli fate.

Two independent mechanisms of Sertoli cell recruitment are known: fibroblast growth factor 9 (FGF9) and prostaglandin D2 (PGD2) recruitment. Kim *et al.*[51] demonstrated using *Fgf9*-null mice, which exhibit XY sex reversal,[52] that FGF9 is required only for the maintenance of SOX9 expression, not its initiation. However, ectopic application of FGF9 to XX gonads induces SOX9 expression.[51,53] Hiramatsu *et al.*[54] showed that *Fgf9* expression occurs in a wave emanating from the central zone of the gonad similar to *Sry* and *Sox9*. Inhibition of FGF signalling repressed the expansion of the *Sox9*-positive domain in the XY gonad. Furthermore, removal of the central segment or isolation of the central domain of the testis before the expansion of *Fgf9* signalling resulted in failure of tubulogenesis in the anterior and posterior segments. Based on these findings, Hiramatsu *et al.*[54] proposed a system where FGF9 was produced in the central domain of the gonad by newly specified Sertoli cells, from which it was secreted and rapidly diffused towards the gonadal poles where it recruited cells to the Sertoli fate by reinforcing the expression of *Sox9*. This mechanism is supported by evidence from *Fgfr2*-null (FGF-receptor 2) mice whose phenotype is similar to *Fgf9*-null mice, displaying male-to-female sex reversal and suggesting FGFR2 is the receptor for FGF9 in the XY gonad. Indeed, conditional deletion of *Fgfr2* in pre-Sertoli cells shows that FGFR2 is required in pre-Sertoli cell differentiation.[55]

Independently, PGD2, an early product of the testis, is also able to induce Sertoli cell differentiation *in vivo* by amplifying SOX9 activity and canalizing the male pathway. Treatment of XX gonads with PGD2 resulted in upregulation in *Sox9* and its direct downstream target *Amh* (the gene encoding anti-Müllerian hormone), masculinizing the XX gonad.[56–58] However, *Pgds* (prostaglandin D2 synthase)-null testes, after a delay in Sertoli cell differentiation, develop normally, indicating that this mechanism is a nonessential backup system for Sertoli cell recruitment.[56] The requirement of theses backup systems and the need to continually reinforce the male programme may stem from the weak but critical role of SRY and the need to actively suppress the underlying female programme. Existence of these recruitment mechanisms ensures that as many cells as required are pulled into the Sertoli fate to allow successful differentiation of the gonad.

THE ROLE OF THE TESTIS VASCULATURE

Vascular patterning in the gonad is a sex-specific process.[59] Testis vasculature is formed by migration of endothelial cells into the developing testes.[60,61] By 12.5 d.p.c., a prominent artery known as the coelomic blood vessel can be seen along the anterior–posterior length of the testis, in addition to extensive microvasculature. Ectopic coelomic vessel-like structures were observed in gonads of XX mice mutant for *Rspo1* (*R-spondin homologue 1*), *Wnt4* (*wingless-related MMTV integration site 4*), *Fst* (*follistatin*) and *Ctnnb1* (*catenin* (*cadherin-associated protein*), *beta 1*).[62–66] *Rspo1* is a regulator of WNT4 signalling which involves *Ctnnb1*, while *Fst* is downstream of WNT4,[67] implicating the WNT signalling pathway in vessel formation and patterning. Additionally, overexpression of *Wnt4* disrupts normal testis vasculature, indicating that WNT4 inhibits formation of gonad vasculature.[68] Notably, where testis vasculature is disrupted, as in the WNT4 overexpressing mice, Sertoli and foetal Leydig cells still differentiate.[65,68]

Recently, it has been discovered that the vascularisation of the testis plays an important instructive role in testis cord formation.[60,61] When endothelial migration was suppressed in testes by blocking vascular endothelial growth factors with VEGF-Trap or by using an antibody against vascular endothelial cadherin, testis cord morphogenesis was impaired.[60,69] Antagonizing vessel maturation also reduced proliferation of interstitial mesenchymal cells that appear to segregate the precursor territories for testis cords; this proliferation could be rescued by the addition of platelet derived growth factor isoform BB (PDGF-BB).[61,69,70] However, the mechanisms governing testis vascularisation and cord segregation are still unclear.

LEYDIG CELLS: THE KEY TO PHENOTYPIC MASCULINISATION

Foetal Leydig cells (FLCs) produce steroid hormones that reinforce male-specific differentiation of the testis (for review, see Ref. 71). The FLC populations in humans and mice are similar during foetal life,[72,73] although observation of the induction of steroidogenesis largely limited to steroid level quantification. The origins of FLCs in humans remain unclear. In the mouse, FLCs arise by about 12.5 d.p.c. (for review, see Ref. 74), and recent work involving cell lineage tracing and live imaging suggests that they arise from multiple origins including the coelomic epithelium and the gonad/mesonephros border.[53] Several pathways and molecules have been implicated in their differentiation and maintenance. SF1 marks presteroidogenic and pre-Sertoli cells in the developing genital ridge[75,76] and acts as a key regulator of genes encoding steroid hydroxylases, which later distinguish FLCs.[77] Members of the hedgehog signalling pathway, desert hedgehog (DHH), which is secreted by Sertoli cells, and its receptor patched homologue 1 (PTCH1), which is expressed by the interstitium, have been shown to be positive regulators of FLC differentiation.[78] *Dhh*-null mice have a FLC differentiation defect.[78] Human patients with mutations in DHH present with mixed, partial or pure gonadal dysgenesis through to seemingly unaffected carriers.[79–81] In addition, chemical inhibition of hedgehog signalling at 11.5 d.p.c. completely abolished expression of steroidogenic enzymes, confirming that DHH/PTCH1 signalling is essential for FLC differentiation.[78] *Gli1* (*glioma-associated oncogene family zinc finger 1*) and *Gli2* (*glioma-associated oncogene family zinc finger 2*) are downstream targets of hedgehog signalling and are expressed exclusively in the testis interstitium in a manner similar to PTCH1.[82] However, *Gli1*- and *Gli2*-null mice display normal FLC differentiation, perhaps indicating functional redundancy between the GLI factors in FLCs.[82] Ectopic activation of the hedgehog signalling pathway in SF1-positive ovarian cells is sufficient to differentiate these cells into functional FLCs within an ovarian environment.[83] These ectopic cells upregulated SF1 and were able to partially masculinize the phenotype of the XX embryo.[83] Additionally, *Pdgfr-α* (*platelet-derived growth factor receptor, alpha polypeptide*) and *Arx* (*Aristaless-related homeobox*) have been identified as being critical for FLC differentiation in knockout mouse models.[84,85]

GERM CELLS: THE ORIGIN OF SPERM

Germ cells are the precursors of oocytes and spermatozoa in the foetal gonad. The sexual fate of the germ cell is determined by signalling factors that the germ cells are exposed to upon entry to the gonad,

rather than by their chromosomal constitution.[58,86–89] Much of what is known about the origin and regulation of the germ cells is derived from studies in mice, as discussed below.

In an ovary, germ cells must enter meiosis during foetal life if they are to initiate oogenesis correctly; conversely, meiosis must be avoided in male germ cells in the foetus if they are to embark on the spermatogenic pathway. The interplay between FGF9 and retinoic acid (RA) appears to be key to the correct specification of the germ cells in the mouse: meiosis is induced by RA in the foetal ovary and inhibited by FGF9, which is secreted by Sertoli cells, in the foetal testes.[86–88,90] In the developing testis, meiosis is avoided because RA is degraded by the P450 enzyme CYP26B1 (cytochrome P450, family 26, subfamily b, polypeptide 1).[91] Thus, CYP26B1 acts to suppress meiosis indirectly by the removal of RA, while FGF9 directly suppresses meiosis and acts to maintain pluripotency.[86–88] This mechanism is supported by *in vivo* evidence from *Cyp26B1*-null mice where degradation of RA does not occur in XY gonads, resulting in upregulation of RA-responsive *Stra8* (*stimulated by retinoic acid gene 8*) and germ cell entry into meiosis.[87,91]

Recently, a double-knockout of *Aldh1a2/Aldha1a3* (*aldehyde dehydrogenase family 1, subfamily A2/A3*), genes encoding key synthesizers of RA in the mesonephros, demonstrated that some meiosis still occurred in the foetal ovary.[92] These data indicate that either RA does not drive meiosis or, more likely, that there is an additional source of RA that remains in these mice. More in-depth analysis of this model will be required to clarify this point. Regardless, a strong antagonism exists between meiosis-promoting (female) factors and meiosis-suppressing (male) factors that push the resident germ cells into their respective fates.

Relatively, little is known about whether these mechanisms are used in humans. Culture experiments demonstrate that the RA initiates meiosis in the human ovary and can upregulate *STRA8*.[93,94] However, it appears that the human gonad has the capacity to produce RA, evidenced by the strong expression of *ALDHA1A1* (aldehyde dehydrogenase family 1, subfamily A1) in the ovary around the time of meiosis initiation.[93,94] Most striking is the apparent lack of *CYP26B1* expression in the foetal human testes and the expression of RA receptors, indicating that the testes may be exposed to, and may be able to respond to, RA, unlike the situation in the mouse.[93,95]

Male germ cells are fated to enter G_1/G_0 arrest in the foetal testes.[89] Retinoblastoma 1 is a cell cycle regulator necessary for male germ cells to enter arrest at the appropriate time. In XY *retinoblastoma 1*-null mice, the germ cell population fails to enter G_1/G_0 arrest appropriately.[96] To compensate cell cycle suppressors, cyclin-dependent kinase inhibitors 1b and 2b are upregulated and after a delay can induce arrest.[96]

OVOTESTES: WHAT THEY REVEAL ABOUT MALE–FEMALE ANTAGONISM IN THE EMBRYO

The study of ovotestes in mouse models has provided numerous insights into the antagonism between the male and female pathways during sex determination. When the Y chromosome derived from *Mus poschiavinus*, Y^{POS}, is backcrossed to a C57/BL6 (B6) background, varying degrees of sex reversal are observed in the XY progeny.[97] This phenomenon is thought to be due to defective interaction between *Sry* on Y^{POS} and autosomal sex-determining genes in B6.[98] Detailed expression studies have shown that a delay in the commencement of *Sry* expression, and subsequently, *Sox9* expression is the likely cause of B6-Y^{POS} partial sex reversal.[98–100] Wilhelm *et al.*[30] found that although *Sry* was expressed throughout the genital ridge in B6-Y^{POS} mice, the upregulation of *Sox9* and activation of downstream testis differentiation pathways only took place in the central zone where *Sry* expression was initiated.[25,28,29,31] These findings indicate that expression of *Sry* in the poles, which in ovotestes differentiate into ovarian tissue, does not reach the required expression threshold early enough. This failure to upregulate *Sox9* in pre-Sertoli cells allows the expression of key ovarian differentiation genes and the engagement of the ovarian programme. Therefore, male–female antagonism underlies the successful differentiation of the gonad. When the balance of factors is altered, even slightly, the underlying battle between the testicular and ovarian fate is revealed.

MOLECULAR BALANCING ACTS: EXAMPLES OF ANTAGONISM BETWEEN MALE AND FEMALE PATHWAYS

In order to understand the molecular mechanisms behind male sex determination, we must also understand what is occurring molecularly in the antagonistic female programme at the time of sex determination. It has become clear that the ovarian programme, although it is considered the 'default', is an active genetic programme in its own right.[101] The antagonism between the male and female pathways has been illustrated using genetic approaches (**Figure 2**). In an early study of male–female antagonism, the male pathway was suppressed by knocking out *Fgf9*; as a result, the female pathway was promoted, indicated by the upregulation of WNT4.[51] Conversely, when the female pathway was suppressed by knocking out *Wnt4*, the male pathway was stimulated.[102] This phenomenon correlates to cases in DSD patients where WNT4 loss or mutation results in XX masculinisation and duplication results in XY feminisation.[68,103] This male–female antagonism is further supported by *ex vivo* work. Treatment of XX gonads with ectopic FGF9 suppressed normal WNT4 expression and induced ectopic upregulation of *Sox9*.[51] Thus, readouts of the male

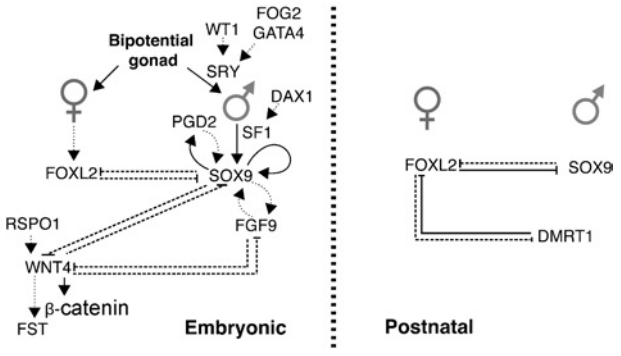

Figure 2 Model of molecular interactions and proposed levels of antagonism in testis and ovary. For details see text. In the embryonic XY gonad, *Sry* is activated *via* a mechanism involving WT1 (indirect regulation illustrated by dotted arrow/line). SRY then directly upregulates *Sox9*, direct regulation illustrated by solid arrow/line) which maintains its own expression; positive feedback loops exists between PGD2/SOX9 and FGF9/SOX9. In the XX gonad, FOXL2 is active as are RSPO1, β-catenin and WNT4, which is required for expression of *Fst*. During embryonic development, antagonism is though to exist between FGF9/WNT4, SOX9/WNT4 and SOX9/FOXL2. Postnatally, antagonism exists between SOX9/FOXL2 and DMRT1/FOXL2. DAX1, Nr0b1, nuclear receptor subfamily 0, group B, member 1; DMRT1, doublesex and mab-3-related transcription factor 1; FGF9, fibroblast growth factor 9; FOG2, 'Friend of Gata1' type 2; FOXL2, forkhead box L2; Fst/FST, follistatin; GATA4, GATA-binding protein 4; PGD2, prostaglandin D2; RSPO1, R-spondin homologue 1; SF1, steroidogenic factor 1; Sox9/SOX9, Sry box-containing gene 9; Sry/SRY, sex-determining region Y; WNT4, wingless-related MMTV integration site 4; WT1, Wilms' tumour 1.

pathway, SOX9 and FGF9 can increase in response to a weakening of the female programme and *vice versa*.

Recent studies have shown that the balance between the antagonistic testicular and ovarian differentiation programmes is also important postnatally. Gonad-specific transcription factors doublesex and mab-3-related transcription factor 1 (DMRT1) and forkhead box L2 (FOXL2) have roles in maintenance of the testes and ovaries respectively.[104] In humans, *DMRT1* hemizygosity may result in hypogonadism, often with streak gonads.[105] *FOXL2/FoxL2* is a key ovarian marker, and its mutation is associated with premature ovarian failure in human patients and knockout mice.[104,106,107] *Dmrt1*-null males were found to have numerous FOXL2-positive cells in the seminiferous tubules 4 months after birth.[108] A Sertoli cell-specific knockout of *Dmrt1* confirmed that loss of DMRT1 in Sertoli cells and not germ cells allows ectopic FOXL2 expression.[108] However, FOXL2 may also be able to repress DMRT1, as shown by strong upregulation of DMRT1, when FOXL2 is ablated postnatally,[109] suggesting the existence of a mutual antagonism necessary for maintaining sex differentiation throughout life.

FOXL2 has also been shown to antagonize SOX9 in the adult ovary and is postulated to also play a role in the embryonic testes. Conditional deletion of *FoxL2* at 8 weeks resulted in transdifferentiation of granulosa cells in the adult ovary to Sertoli-like cells expressing SOX9 even in the presence of oocytes and theca cells, the steroidogenic cells of the ovary, differentiated into Leydig-like cells.[109] In the adult ovary, it was demonstrated using chromatin immunoprecipitation that FOXL2 can repress TESCO activity,[109] providing a possible mechanism for the role of FOXL2 in maintaining ovarian function postnatally. *FoxL2* is also upregulated in XY embryonic gonads of *Sox9*-conditional null mice indicating that a similar mechanism exists during embryonic sex differentiation.[43] However, importantly, expression of male and female factors in the gonad is exclusive, as observed in the ovotestes,[30] such that FOXL2 and SOX9 are never coexpressed in the same cell. Nevertheless, while the factors mentioned in the above section are responsive to each other's loss, direct interaction and antagonism between any of these factors is yet to be demonstrated.

SF1: HIGHLIGHTING THE ROLE OF GENE DOSAGE DIFFERENCES IN THE MOUSE AND HUMAN

SF1 is a striking example of a factor whose effects on gonadal phenotype are sensitive to dosage and genetic background.[75] *Sf1*-null mice undergo early gonadal and adrenal development, but the organs regress by 11.5 d.p.c.[75,110] Transgenic expression of SF1 in *Sf1*-null mice was able to rescue gonad development, but not adrenal development.[111] Additionally, *Sf1*-haploinsufficient mice have disrupted adrenal development but develop testes normally.[112] Together, these results indicate that SF1 is involved in gonad and adrenal organ maintenance and that, in the mouse, the adrenal is more sensitive to *Sf1* dosage than the gonad. However, there is evidence that the reverse is true in humans. Two patients with heterozygous mutations in *SF1* have been shown to exhibit gonadal dysgenesis but normal adrenal function, indicating that, in humans, testis development is more sensitive to *Sf1* dosage than adrenal gland development.[113,114]

DAX1: A QUESTION OF GENE DOSAGE AND GENETIC BACKGROUND

Dax1 (*Nr0b1*, *nuclear receptor subfamily 0*, *group B*, *member 1*) expression in the mouse indicates a role in early sex determination, with *Dax1* being expressed in both sexes initially before being downregulated in the testes.[31,115] Duplications of chromosomal region Xp21.2–21.1, which includes *DAX1*, are sufficient to impair testis differentiation in 46,XY human patients and induce male-to-female sex reversal (dosage-sensitive sex reversal).[116–118] These data imply that DAX1 acts as an antitestis gene, antagonizing the action of *SRY*. Similarly, overexpression of *Dax1* in mice can induce male-to-female sex reversal. However, only mice highly overexpressing *Dax1* and which also have a weakened male sex-determining pathway driven by a Y^{POS} chromosome, show complete male-to-female sex reversal.[31] A common interpretation of these data is that mice and humans may have different sensitivity thresholds for DAX1 dosage.

An alternative explanation is that genetic background and the presence of genetic modifiers can explain whether or not gonad sex reversal occurs. Genetic background is a key determinant in the penetrance of a number of sex reversal phenotypes, with heterozygous mutants often displaying different phenotypes depending on their genetic background. Bouma *et al.*[119] compared sex development in *Gata4* (GATA-binding protein 4)[120,121] and *Fog2* ('Friend of Gata1' type 2; Zfpm2, zinc finger protein, multitype 2)[120,121] heterozygous mutants on B6/Y^{AKR}, B6, D2/Y^{AKR} and D2 backgrounds, which have decreasing sensitivity to sex reversal. They found that ovaries or ovotestes developed in these mutants, but only on the B6/Y^{AKR} background. All other strains developed testes normally. These studies demonstrate the importance of genetic background, and also clearly indicate a role for GATA4 and FOG2 in foetal testis development. A similar background dependance was observed in the generation of sex-reversed *Dax1* mutant mice.[31,122–124] Given that genetic background and the presence of genetic modifiers can explain whether or not gonad sex reversal occurs, it follows that effects attributed to differences in dosage sensitivity between humans and mice might also be explained by genetic background.

Given the expectation that *Dax1* acts as an antitestis gene, deletion of *Dax1* in mice produced a surprising result: ovaries formed normally in *Dax1*-null XX mice, but in XY mice with a deletion of *Dax1*, testis cord formation was abnormal.[123] Moreover, in XY $Dax1^{-/-}$/Y^{POS} mice, complete male-to-female sex reversal was observed.[124] Subsequent studies revealed the cause of the male-to-female sex reversal: *Sox9* is not upregulated in XY *Dax1*-null mice, despite normal expression of *Sry*.[125] Nonetheless, strong overexpression of *Sry* in XY^{POS} *Dax1*-null mice was able to upregulate *Sox9*, correcting testis development and producing fertile males.[125] These results are somewhat in accord with findings in humans, with respect to *DAX1* mutations. 46,XY patients with deletion of, or mutations in, *DAX1*, exhibit the male phenotype, but have hypogonadotrophic hypogonadism and disorganized testis cords, indicating that DAX1 is not essential for the initial stages of human gonad development, but is required for testis development.[117,124,125] As there is evidence that DAX1 can work in both 'antitestis' and 'protestis' capacities, it is possible that correct function in the testis occurs only within a 'window' of activity involving two concentration thresholds. In this scenario, DAX1 activity beyond an upper threshold, for example, in cases of *DAX1* duplication, may act to antagonize testis differentiation, while DAX1 activity below a lower threshold, for example, in cases of mutation, may allow ovarian differentiation to occur.[126]

CONCLUSIONS AND PERSPECTIVES

From the above discussion, it is clear that initial specification of Sertoli cells is a result of SRY expression, with the effects of SRY mediated largely if not entirely by SOX9. A complete understanding of male sex determination and testis morphogenesis, therefore, largely depends on a deeper understanding of the molecular and

cellular roles of SOX9, and therefore, on the discovery and characterisation of all transcriptional targets of SOX9. Further, it remains to be clarified how the Sertoli cell directs events during morphogenesis; that is, what signalling molecules are produced by these cells and how they influence the differentiation of the other testicular cell lineages. How the other cell lineages, once masculinized, then contribute to testis morphogenesis is also a question that requires further investigation. A greater understanding of the molecular interactions involved in the process of testis differentiation will provide new avenues for DSD diagnosis and management.

Commitment to the male fate and then maintenance of that fate is achieved only by overcoming the progress of the female pathway, and antagonistic interplay is seen during foetal life, as well as postnatally. Mutual antagonism is likely to be facilitated by transcription factors such as SOX9 and FOXL2, but assays to determine the molecular interactions that underpin these antagonistic relationships have yet to be completed. Understanding what factors facilitate antagonism between the male and female programmes will lead to a greater understanding of what pushes individuals into or out of the two typical sex phenotypes specified by XX and XY chromosomes.

Additionally, as demonstrated here, sex-determining genes often respond in a dosage-dependent manner that may also be influenced by genetic background. As a result, human DSDs and mouse models may not always phenocopy each other, highlighting the need for a collaborative approach to DSD identification and diagnosis between researchers and clinicians. Human patient cases demonstrate, especially, that gene dosage and genetic background can be important factors in phenotype severity. However, despite this, the investigation of gene dosage effects and the effects of genetic background on sex determining genes in the mouse is a question that few researchers have addressed and that warrants further detailed investigation. Tools, such as inducible knockout and single-copy transgenesis strategies, are now available to study these phenomena in the mouse. Thus, better integration of lessons from both human cases and mouse models must be a priority. Finally, it is clear that integration of clinical findings and mouse models will contribute to a better understanding not only of the causes of human DSDs but also of the basic biology of sex determination in the male.

Abbreviations: DSD, disorder of sex development; DNA, deoxyribonucleic acid; HMG, high-mobility group-box; WT1/*WT1*/*Wt1*, Wilms Tumor 1; K, lysine; T, tyrosine; S, serine; *Sry*, sex determining region of Chr Y; SOX9/*SOX9*/*Sox9*, SRY-box containing gene 9; SF1/*SF1*/*Sf1* (Nr5a1), steroidogenic factor 1 (nuclear receptor subfamily 5, group A, member 1); TESCO, testis-specific enhancer of *Sox9* core element; FGF9/*FGF9*/*Fgf9*, fibroblast growth factor 9; PDG2/*PDG2*/*Pdg2*, prostaglandin D2 synthase; FGF, fibroblast growth factor; FGFR2/*FGFR2*/*Fgfr2*, Fgf-receptor 2; AMH/*AMH*/*Amh*, anti-Mullerian hormone; PGDS/*PGDS*/*Pgds*, prostaglandin D2 synthase; dpc, days post coitum; WNT4/*WNT4*/*Wnt4*, wingless-related MMTV integration site 4; FLC, fetal Leydig cell; DHH/*DHH*/*Dhh*, desert hedgehog; PTCH1/*PTCH1*/*Ptch1*, patched homolog 1; GLI1/2/*GLI1*/*2*/*Gli1*/*2*, glioma-associated oncogene family zinc finger 1/2; PDGFR-α/*PDGFR*-α/PDGFR-α, platelet derived growth factor receptor, alpha polypeptide; ARX/*ARX*/*Arx*, aristaless related homeobox; RA, retinoic acid; STRA8/*STRA8*/*Stra8*, stimulated by retinoic acid gene 8; RB1/*RB1*/*Rb1*, retinoblastoma 1; Cdkn1b/2b/*Cdkn1b*/*2b*/*Cdkn1b*/*2b*, cyclin dependent kinase inhibitors 1b/2b; CYP26B1/*CYP26B1*/*Cyp26b1*, cytochrome P450, family 26, subfamily b, polypeptide 1; Aldh1a1/2/3/*Aldh1a1*/*2*/*3*/*Aldh1a1*/*2*/*3*, aldehyde dehydrogenase family 1, subfamily A1/A2/A3; Y^{POS}, Y chromosome derived from *Mus poschiavinus*; β-catenin/*CTTNB1*/*Ctnnb1*, catenin (cadherin associated protein), beta 1; FOXL2/*FOXL2*/*FoxL2*, forkhead box L2; DMRT1/*DMRT1*/*Dmrt1*, doublesex and mab-3 related transcription factor 1; FOG2/*FOG2*/*Fog2*, *Zfpm2*, zinc finger protein, multitype 2; GATA4/*GATA4*/*Gata4*, GATA binding protein 4; DAX1/*DAX1*/*Dax1*, *Nr0b1*, nuclear receptor subfamily 0, group B, member 1; FST/*FST*/*Fst*, follistatin; RSPO1/*RSPO1*/*Rspo1*, R-spondin homolog; PDGF-BB, platelet derived growth factor isoform BB.

COMPETING FINANCIAL INTERESTS

The authors declare no competing financial interests.

ACKNOWLEDGMENTS

We thank Elanor Wainwright for critical reading of this manuscript. This work was supported by research grants from the Australian Research Council (ARC) and National Health and Medical Research Council of Australia. PK is a Federation Fellow of the ARC.

1 Pasterski V, Prentice P, Hughes IA. Impact of the consensus statement and the new DSD classification system. *Best Pract Res Clin Endocrinol Metab* 2010; **24**: 187–95.
2 Gupta D, Bhardwaj M, Sharma S, Ammini A, Gupta D. Long-term psychosocial adjustments, satisfaction related to gender and the family equations in disorders of sexual differentiation with male sex assignment. *Pediatr Surg Int* 2010; **26**: 955–8.
3 Blackless M, Charuvastra A, Derryck A, Fausto-Sterling A, Lauzanne K *et al*. How sexually dimorphic are we? Review and synthesis. *Am J Hum Biol* 2000; **12**: 151–66.
4 Hughes IA, Houk C, Ahmed SF, Lee PA, LWPES1 Consensus Group *et al*. Consensus statement on management of intersex disorders. *Arch Dis Child* 2006; **91**: 554–63.
5 Looijenga LH, Hersmus R, de Leeuw BH, Stoop H, Cools M *et al*. Gonadal tumours and DSD. *Best Pract Res Clin Endocrinol Metab* 2010; **24**: 291–310.
6 Woodhouse CR. Prospects for fertility in patients born with genitourinary anomalies. *J Urol* 2001; **165**: 2354–60.
7 Koopman P, Gubbay J, Vivian N, Goodfellow P, Lovell-Badge R. Male development of chromosomally female mice transgenic for Sry. *Nature* 1991; **351**: 117–21.
8 Gubbay J, Collignon J, Koopman P, Capel B, Economou A *et al*. A gene mapping to the sex-determining region of the mouse Y chromosome is a member of a novel family of embryonically expressed genes. *Nature* 1990; **346**: 245–50.
9 Lovell-Badge R, Robertson E. XY female mice resulting from a heritable mutation in the primary testis-determining gene, *Tdy*. *Development* 1990; **109**: 635–46.
10 Jager RJ, Anvret M, Hall K, Scherer G. A human XY female with a frame shift mutation in the candidate testis-determining gene *SRY*. *Nature* 1990; **348**: 452–4.
11 Maier EM, Leitner C, Lohrs U, Kuhnle U. True hermaphroditism in an XY individual due to a familial point mutation of the *SRY* gene. *J Pediatr Endocrinol Metab* 2003; **16**: 575–80.
12 Nieto K, Pena R, Palma I, Dorantes LM, Erana L *et al*. 45,X/47,XXX/47,XX, del(Y)(p?)/46,XX mosaicism causing true hermaphroditism. *Am J Med Genet A* 2004; **130A**: 311–4.
13 Margarit E, Coll MD, Oliva R, Gomez D, Soler A *et al*. *SRY* gene transferred to the long arm of the X chromosome in a Y-positive XX true hermaphrodite. *Am J Med Genet* 2000; **90**: 25–8.
14 Sharp A, Kusz K, Jaruzelska J, Tapper W, Szarras-Czapnik M *et al*. Variability of sexual phenotype in 46,XX(*SRY*+) patients: the influence of spreading X inactivation versus position effects. *J Med Genet* 2005; **42**: 420–7.
15 Polanco JC, Koopman P. *Sry* and the hesitant beginnings of male development. *Dev Biol* 2007; **302**: 13–24.
16 Kashimada K, Koopman P. *Sry*: the master switch in mammalian sex determination. *Development* 2010; **137**: 3921–30.
17 Lee SB, Huang K, Palmer R, Truong VB, Herzlinger D *et al*. The Wilms tumor suppressor *WT1* encodes a transcriptional activator of *amphiregulin*. *Cell* 1999; **98**: 663–73.
18 Shimamura R, Fraizer GC, Trapman J, Lau YfC, Saunders GF. The Wilms' tumor gene *WT1* can regulate genes involved in sex determination and differentiation: SRY, Mullerian-inhibiting substance, and the androgen receptor. *Clin Cancer Res* 1997; **3**: 2571–80.
19 Hewitt SM, Fraizer GC, Wu YJ, Rauscher FJ 3rd, Saunders GF. Differential function of Wilms' tumor gene *WT1* splice isoforms in transcriptional regulation. *J Biol Chem* 1996; **271**: 8588–92.
20 Hammes A, Guo JK, Lutsch G, Leheste JR, Landrock D *et al*. Two Splice variants of the Wilms' tumor 1 gene have distinct functions during sex determination and nephron formation. *Cell* 2001; **106**: 319–29.
21 Haber DA, Sohn RL, Buckler AJ, Pelletier J, Call KM *et al*. Alternative splicing and genomic structure of the Wilms tumor gene *WT1*. *Proc Natl Acad Sci USA* 1991; **88**: 9618–22.
22 Hossain A, Saunders GF. The human sex-determining gene *SRY* is a direct target of *WT1*. *J Biol Chem* 2001; **276**: 16817–23.
23 Barbaux S, Niaudet P, Gubler MC, Grunfeld JP, Jaubert F *et al*. Donor splice-site mutations in *WT1* are responsible for Frasier syndrome. *Nat Genet* 1997; **17**: 467–70.

24 Bradford ST, Wilhelm D, Bandiera R, Vidal V, Schedl A *et al*. A cell-autonomous role for *WT1* in regulating *Sry in vivo*. *Hum Mol Genet* 2009; **18**: 3429–38.
25 Hacker A, Capel B, Goodfellow P, Lovell-Badge R. Expression of *Sry*, the mouse sex determining gene. *Development* 1995; **121**: 1603–14.
26 Jeske YW, Bowles J, Greenfield A, Koopman P. Expression of a linear *Sry* transcript in the mouse genital ridge. *Nat Genet* 1995; **10**: 480–2.
27 Koopman P, Munsterberg A, Capel B, Vivian N, Lovell-Badge R. Expression of a candidate sex-determining gene during mouse testis differentiation. *Nature* 1990; **348**: 450–2.
28 Albrecht KH, Eicher EM. Evidence that *Sry* is expressed in pre-Sertoli cells and Sertoli and granulosa cells have a common precursor. *Dev Biol* 2001; **240**: 92–107.
29 Bullejos M, Koopman P. Spatially dynamic expression of *Sry* in mouse genital ridges. *Dev Dyn* 2001; **221**: 201–5.
30 Wilhelm D, Washburn LL, Truong V, Fellous M, Eicher EM *et al*. Antagonism of the testis- and ovary-determining pathways during ovotestis development in mice. *Mech Dev* 2009; **126**: 324–36.
31 Swain A, Narvaez V, Burgoyne P, Camerino G, Lovell-Badge R. *Dax1* antagonizes *Sry* action in mammalian sex determination. *Nature* 1998; **391**: 761–7.
32 Clepet C, Schafer AJ, Sinclair AH, Palmer MS, Lovell-Badge R *et al*. The human *SRY* transcript. *Hum Mol Genet* 1993; **2**: 2007–12.
33 Lahr G, Maxson SC, Mayer A, Just W, Pilgrim C *et al*. Transcription of the Y chromosomal gene, *Sry*, in adult mouse brain. *Brain Res Mol Brain Res* 1995; **33**: 179–82.
34 Mayer A, Lahr G, Swaab DF, Pilgrim C, Reisert I. The Y-chromosomal genes *SRY* and *ZFY* are transcribed in adult human brain. *Neurogenetics* 1998; **1**: 281–8.
35 Dewing P, Chiang CW, Sinchak K, Sim H, Fernagut PO *et al*. Direct regulation of adult brain function by the male-specific factor SRY. *Curr Biol* 2006; **16**: 415–20.
36 Schmahl J, Eicher EM, Washburn LL, Capel B. *Sry* induces cell proliferation in the mouse gonad. *Development* 2000; **127**: 65–73.
37 Karl J, Capel B. Sertoli cells of the mouse testis originate from the coelomic epithelium. *Dev Biol* 1998; **203**: 323–33.
38 Magre S, Jost A. The initial phases of testicular organogenesis in the rat. An electron microscopy study. *Arch Anat Microsc Morphol Exp* 1980; **69**: 297–318.
39 Schmahl J, Capel B. Cell proliferation is necessary for the determination of male fate in the gonad. *Dev Biol* 2003; **258**: 264–76.
40 Sekido R, Lovell-Badge R. Sex determination involves synergistic action of SRY and SF1 on a specific *Sox9* enhancer. *Nature* 2008; **453**: 930–4.
41 Vidal VP, Chaboissier MC, de Rooij DG, Schedl A. *Sox9* induces testis development in XX transgenic mice. *Nat Genet* 2001; **28**: 216–7.
42 Bishop CE, Whitworth DJ, Qin Y, Agoulnik AI, Agoulnik IU *et al*. A transgenic insertion upstream of *Sox9* is associated with dominant XX sex reversal in the mouse. *Nat Genet* 2000; **26**: 490–4.
43 Barrionuevo F, Bagheri-Fam S, Klattig J, Kist R, Taketo MM *et al*. Homozygous inactivation of *Sox9* causes complete XY sex reversal in mice. *Biol Reprod* 2006; **74**: 195–201.
44 Chaboissier MC, Kobayashi A, Vidal VI, Latzkendorf S, van de Kant HJ *et al*. Functional analysis of *Sox8* and *Sox9* during sex determination in the mouse. *Development* 2004; **131**: 1891–901.
45 Foster JW, Dominguez-Steglich MA, Guioli S, Kwok C, Weller PA *et al*. Campomelic dysplasia and autosomal sex reversal caused by mutations in an *SRY*-related gene. *Nature* 1994; **372**: 525–30.
46 Wagner T, Wirth J, Meyer J, Zabel B, Held M *et al*. Autosomal sex reversal and campomelic dysplasia are caused by mutations in and around the *SRY*-related gene *SOX9*. *Cell* 1994; **79**: 1111–20.
47 Sekido R, Lovell-Badge R. Sex determination and SRY: down to a wink and a nudge? *Trends Genet* 2009; **25**: 19–29.
48 Knower KC, Kelly S, Ludbrook LM, Bagheri-Fam S, Sim H *et al*. Failure of SOX9 regulation in 46XY disorders of sex development with SRY, SOX9 and SF1 mutations. *PLoS ONE* 2011; **6**: e17751.
49 Palmer SJ, Burgoyne PS. *In situ* analysis of fetal, prepuberal and adult XX–XY chimaeric mouse testes: sertoli cells are predominantly, but not exclusively, XY. *Development* 1991; **112**: 265–8.
50 Patek CE, Kerr JB, Gosden RG, Jones KW, Hardy K *et al*. Sex chimaerism, fertility and sex determination in the mouse. *Development* 1991; **113**: 311–25.
51 Kim Y, Kobayashi A, Sekido R, DiNapoli L, Brennan J *et al*. *Fgf9* and *Wnt4* act as antagonistic signals to regulate mammalian sex determination. *PLoS Biol* 2006; **4**: e187.
52 Colvin JS, Green RP, Schmahl J, Capel B, Ornitz DM. Male-to-female sex reversal in mice lacking fibroblast growth factor 9. *Cell* 2001; **104**: 875–89.
53 DeFalco T, Takahashi S, Capel B. Two distinct origins for Leydig cell progenitors in the fetal testis. *Dev Biol* 2011; **352**: 14–26.
54 Hiramatsu R, Harikae K, Tsunekawa N, Kurohmaru M, Matsuo I *et al*. FGF signaling directs a center-to-pole expansion of tubulogenesis in mouse testis differentiation. *Development* 2010; **137**: 303–12.
55 Kim Y, Bingham N, Sekido R, Parker KL, Lovell-Badge R *et al*. Fibroblast growth factor receptor 2 regulates proliferation and Sertoli differentiation during male sex determination. *Proc Natl Acad Sci USA* 2007; **104**: 16558–63.
56 Moniot B, Declosmenil F, Barrionuevo F, Scherer G, Aritake K *et al*. The PGD2 pathway, independently of FGF9, amplifies SOX9 activity in Sertoli cells during male sexual differentiation. *Development* 2009; **136**: 1813–21.
57 Wilhelm D, Martinson F, Bradford S, Wilson MJ, Combes AN *et al*. Sertoli cell differentiation is induced both cell-autonomously and through prostaglandin signaling during mammalian sex determination. *Dev Biol* 2005; **287**: 111–24.
58 Adams IR, McLaren A. Sexually dimorphic development of mouse primordial germ cells: switching from oogenesis to spermatogenesis. *Development* 2002; **129**: 1155–64.
59 Brennan J, Karl J, Capel B. Divergent vascular mechanisms downstream of *Sry* establish the arterial system in the XY gonad. *Dev Biol* 2002; **244**: 418–28.
60 Combes AN, Wilhelm D, Davidson T, Dejana E, Harley V *et al*. Endothelial cell migration directs testis cord formation. *Dev Biol* 2009; **326**: 112–20.
61 Cool J, Carmona FD, Szucsik JC, Capel B. Peritubular myoid cells are not the migrating population required for testis cord formation in the XY gonad. *Sex Dev* 2008; **2**: 128–33.
62 Tomizuka K, Horikoshi K, Kitada R, Sugawara Y, Iba Y *et al*. R-spondin1 plays an essential role in ovarian development through positively regulating Wnt-4 signaling. *Hum Mol Genet* 2008; **17**: 1278–91.
63 Chassot AA, Ranc F, Gregoire EP, Roepers-Gajadien HL, Taketo MM *et al*. Activation of beta-catenin signaling by Rspo1 controls differentiation of the mammalian ovary. *Hum Mol Genet* 2008; **17**: 1264–77.
64 Liu CF, Bingham N, Parker K, Yao HH. Sex-specific roles of beta-catenin in mouse gonadal development. *Hum Mol Genet* 2009; **18**: 405–17.
65 Jeays-Ward K, Hoyle C, Brennan J, Dandonneau M, Alldus G *et al*. Endothelial and steroidogenic cell migration are regulated by WNT4 in the developing mammalian gonad. *Development* 2003; **130**: 3663–70.
66 Yao HH, Matzuk MM, Jorgez CJ, Menke DB, Page DC *et al*. *Follistatin* operates downstream of *Wnt4* in mammalian ovary organogenesis. *Dev Dyn* 2004; **230**: 210–5.
67 Tevosian SG, Manuylov NL. To beta or not to beta: canonical beta-catenin signaling pathway and ovarian development. *Dev Dyn* 2008; **237**: 3672–80.
68 Jordan BK, Shen JH, Olaso R, Ingraham HA, Vilain E. *Wnt4* overexpression disrupts normal testicular vasculature and inhibits testosterone synthesis by repressing steroidogenic factor 1/beta-catenin synergy. *Proc Natl Acad Sci USA* 2003; **100**: 10866–71.
69 Cool J, DeFalco TJ, Capel B. Vascular-mesenchymal cross-talk through Vegf and Pdgf drives organ patterning. *Proc Natl Acad Sci USA* 2011; **108**: 167–72.
70 Combes AN, Lesieur E, Harley VR, Sinclair AH, Little MH *et al*. Three-dimensional visualization of testis cord morphogenesis, a novel tubulogenic mechanism in development. *Dev Dyn* 2009; **238**: 1033–41.
71 Wu X, Wan S, Lee MM. Key factors in the regulation of fetal and postnatal Leydig cell development. *J Cell Physiol* 2007; **213**: 429–33.
72 Tapanainen J, Kellokumpu-Lehtinen P, Pelliniemi L, Huhtaniemi I. Age-related changes in endogenous steroids of human fetal testis during early and midpregnancy. *J Clin Endocrinol Metab* 1981; **52**: 98–102.
73 Svechnikov K, Landreh L, Weisser J, Izzo G, Colón E *et al*. Origin, development and regulation of human leydig cells. *Horm Res Paediatr* 2010; **73**: 93–101.
74 Griswold SL, Behringer RR. Fetal leydig cell origin and development. *Sex Dev* 2009; **3**: 1–15.
75 Luo X, Ikeda Y, Parker KL. A cell-specific nuclear receptor is essential for adrenal and gonadal development and sexual differentiation. *Cell* 1994; **77**: 481–90.
76 Hatano O, Takayama K, Imai T, Waterman MR, Takakusu A *et al*. Sex-dependent expression of a transcription factor, Ad4BP, regulating steroidogenic P-450 genes in the gonads during prenatal and postnatal rat development. *Development* 1994; **120**: 2787–97.
77 Ikeda Y, Shen WH, Ingraham HA, Parker KL. Developmental expression of mouse steroidogenic factor-1, an essential regulator of the steroid hydroxylases. *Mol Endocrinol* 1994; **8**: 654–62.
78 Yao HH, Whoriskey W, Capel B. Desert Hedgehog/Patched 1 signaling specifies fetal Leydig cell fate in testis organogenesis. *Genes Dev* 2002; **16**: 1433–40.
79 Umehara F, Tate G, Itoh K, Yamaguchi N, Douchi T *et al*. A novel mutation of desert hedgehog in a patient with 46,XY partial gonadal dysgenesis accompanied by minifascicular neuropathy. *Am J Hum Genet* 2000; **67**: 1302–5.
80 Canto P, Soderlund D, Reyes E, Mendez JP. Mutations in the *desert hedgehog* (*DHH*) gene in patients with 46,XY complete pure gonadal dysgenesis. *J Clin Endocrinol Metab* 2004; **89**: 4480–3.
81 Canto P, Vilchis F, Soderlund D, Reyes E, Mendez JP. A heterozygous mutation in the *desert hedgehog* gene in patients with mixed gonadal dysgenesis. *Mol Hum Reprod* 2005; **11**: 833–6.
82 Barsoum I, Yao HH. Redundant and differential roles of transcription factors *gli1* and *gli2* in the development of mouse fetal Leydig cells. *Biol Reprod* 2011; **84**: 894–9.
83 Barsoum IB, Bingham NC, Parker KL, Jorgensen JS, Yao HH. Activation of the Hedgehog pathway in the mouse fetal ovary leads to ectopic appearance of fetal Leydig cells and female pseudohermaphroditism. *Dev Biol* 2009; **329**: 96–103.
84 Kitamura K, Yanazawa M, Sugiyama N, Miura H, Iizuka-Kogo A *et al*. Mutation of ARX causes abnormal development of forebrain and testes in mice and X-linked lissencephaly with abnormal genitalia in humans. *Nat Genet* 2002; **32**: 359–69.
85 Brennan J, Tilmann C, Capel B. *Pdgfr*-alpha mediates testis cord organization and fetal Leydig cell development in the XY gonad. *Genes Dev* 2003; **17**: 800–10.
86 Bowles J, Feng CW, Spiller C, Davidson TL, Jackson A *et al*. FGF9 suppresses meiosis and promotes male germ cell fate in mice. *Dev Cell* 2010; **19**: 440–9.
87 Bowles J, Knight D, Smith C, Wilhelm D, Richman J *et al*. Retinoid signaling determines germ cell fate in mice. *Science* 2006; **312**: 596–600.
88 Koubova J, Menke DB, Zhou Q, Capel B, Griswold MD *et al*. Retinoic acid regulates sex-specific timing of meiotic initiation in mice. *Proc Natl Acad Sci USA* 2006; **103**: 2474–9.
89 McLaren A, Southee D. Entry of mouse embryonic germ cells into meiosis. *Dev Biol* 1997; **187**: 107–13.

90 Colvin JS, Feldman B, Nadeau JH, Goldfarb M, Ornitz DM. Genomic organization and embryonic expression of the mouse *fibroblast growth factor 9* gene. *Dev Dyn* 1999; **216**: 72–88.
91 MacLean G, Li H, Metzger D, Chambon P, Petkovich M. Apoptotic extinction of germ cells in testes of *Cyp26b1* knockout mice. *Endocrinology* 2007; **148**: 4560–7.
92 Kumar S, Chatzi C, Brade T, Cunningham TJ, Zhao X *et al*. Sex-specific timing of meiotic initiation is regulated by *Cyp26b1* independent of retinoic acid signalling. *Nat Commun* 2011; **2**: 151.
93 Childs AJ, Cowan G, Kinnell HL, Anderson RA, Saunders PT. Retinoic acid signalling and the control of meiotic entry in the human fetal gonad. *PLoS ONE* 2011; **6**: e20249.
94 le Bouffant R, Guerquin MJ, Duquenne C, Frydman N, Coffigny H *et al*. Meiosis initiation in the human ovary requires intrinsic retinoic acid synthesis. *Hum Reprod* 2010; **25**: 2579–90.
95 Cupp AS, Dufour JM, Kim G, Skinner MK, Kim KH. Action of retinoids on embryonic and early postnatal testis development. *Endocrinology* 1999; **140**: 2343–52.
96 Spiller CM, Wilhelm D, Koopman P. Retinoblastoma 1 protein modulates XY germ cell entry into G_1/G_0 arrest during fetal development in mice. *Biol Reprod* 2010; **82**: 433–43.
97 Eicher EM, Washburn LL, Whitney JB, Morrow KE. Mus poschiavinus Y chromosome in the C57BL/6J murine genome causes sex reversal. *Science* 1982; **217**: 535–7.
98 Albrecht KH, Young M, Washburn LL, Eicher EM. *Sry* expression level and protein isoform differences play a role in abnormal testis development in C57BL/6J mice carrying certain sry alleles. *Genetics* 2003; **164**: 277–88.
99 Bullejos M, Koopman P. Delayed *Sry* and *Sox9* expression in developing mouse gonads underlies B6-Y^{DOM} sex reversal. *Dev Biol* 2005; **278**: 473–81.
100 Nagamine CM, Morohashi KI, Carlisle C, Chang DK. Sex reversal caused by Mus musculus domesticus Y chromosomes linked to variant expression of the testis-determining gene *Sry*. *Dev Biol* 1999; **216**: 182–94.
101 Nef S, Schaad O, Stallings NR, Cederroth CR, Pitetti JL *et al*. Gene expression during sex determination reveals a robust female genetic program at the onset of ovarian development. *Dev Biol* 2005; **287**: 361–77.
102 Vainio S, Heikkila M, Kispert A, Chin N, McMahon AP. Female development in mammals is regulated by Wnt-4 signalling. *Nature* 1999; **397**: 405–9.
103 Biason-Lauber A, Konrad D, Navratil F, Schoenle EJ. A *WNT4* mutation associated with Müllerian-duct regression and virilization in a 46,XX woman. *N Engl J Med* 2004; **351**: 792–8.
104 Schmidt D, Ovitt CE, Anlag K, Fehsenfeld S, Gredsted L *et al*. The murine winged-helix transcription factor Foxl2 is required for granulosa cell differentiation and ovary maintenance. *Development* 2004; **131**: 933–42.
105 Muroya K, Okuyama T, Goishi K, Ogiso Y, Fukuda S *et al*. Sex-determining gene(s) on distal 9p: clinical and molecular studies in six cases. *J Clin Endocrinol Metab* 2000; **85**: 3094–100.
106 Crisponi L, Deiana M, Loi A, Chiappe F, Uda M *et al*. The putative forkhead transcription factor *FOXL2* is mutated in blepharophimosis/ptosis/epicanthus inversus syndrome. *Nat Genet* 2001; **27**: 159–66.
107 Uda M, Ottolenghi C, Crisponi L, Garcia JE, Deiana M *et al*. *Foxl2* disruption causes mouse ovarian failure by pervasive blockage of follicle development. *Hum Mol Genet* 2004; **13**: 1171–81.
108 Matson CK, Murphy MW, Sarver AL, Griswold MD, Bardwell VJ *et al*. DMRT1 prevents female reprogramming in the postnatal mammalian testis. *Nature* 2011; **476**: 101–4.
109 Uhlenhaut NH, Jakob S, Anlag K, Eisenberger T, Sekido R *et al*. Somatic sex reprogramming of adult ovaries to testes by *FOXL2* ablation. *Cell* 2009; **139**: 1130–42.
110 Sadovsky Y, Crawford PA, Woodson KG, Polish JA, Clements MA *et al*. Mice deficient in the orphan receptor steroidogenic factor 1 lack adrenal glands and gonads but express P450 side-chain-cleavage enzyme in the placenta and have normal embryonic serum levels of corticosteroids. *Proc Natl Acad Sci USA* 1995; **92**: 10939–43.
111 Fatchiyah, Zubair M, Shima Y, Oka S, Ishihara S *et al*. Differential gene dosage effects of Ad4BP/SF-1 on target tissue development. *Biochem Biophys Res Commun* 2006; **341**: 1036–45.
112 Bland ML, Fowkes RC, Ingraham HA. Differential requirement for steroidogenic factor-1 gene dosage in adrenal development versus endocrine function. *Mol Endocrinol* 2004; **18**: 941–52.
113 Hasegawa T, Fukami M, Sato N, Katsumata N, Sasaki G *et al*. Testicular dysgenesis without adrenal insufficiency in a 46,XY patient with a heterozygous inactive mutation of steroidogenic factor-1. *J Clin Endocrinol Metab* 2004; **89**: 5930–5.
114 Mallet D, Bretones P, Michel-Calemard L, Dijoud F, David M *et al*. Gonadal dysgenesis without adrenal insufficiency in a 46,XY patient heterozygous for the nonsense C16X mutation: a case of SF1 haploinsufficiency. *J Clin Endocrinol Metab* 2004; **89**: 4829–32.
115 Swain A, Zanaria E, Hacker A, Lovell-Badge R, Camerino G. Mouse *Dax1* expression is consistent with a role in sex determination as well as in adrenal and hypothalamus function. *Nat Genet* 1996; **12**: 404–9.
116 Bardoni B, Zanaria E, Guioli S, Floridia G, Worley KC *et al*. A dosage sensitive locus at chromosome Xp21 is involved in male to female sex reversal. *Nat Genet* 1994; **7**: 497–501.
117 Muscatelli F, Strom TM, Walker AP, Zanaria E, Recan D *et al*. Mutations in the *DAX-1* gene give rise to both X-linked adrenal hypoplasia congenita and hypogonadotropic hypogonadism. *Nature* 1994; **372**: 672–6.
118 Zanaria E, Muscatelli F, Bardoni B, Strom TM, Guioli S *et al*. An unusual member of the nuclear hormone receptor superfamily responsible for X-linked adrenal hypoplasia congenita. *Nature* 1994; **372**: 635–41.
119 Bouma GJ, Washburn LL, Albrecht KH, Eicher EM. Correct dosage of *Fog2* and *Gata4* transcription factors is critical for fetal testis development in mice. *Proc Natl Acad Sci USA* 2007; **104**: 14994–9.
120 Tevosian SG, Albrecht KH, Crispino JD, Fujiwara Y, Eicher EM *et al*. Gonadal differentiation, sex determination and normal *Sry* expression in mice require direct interaction between transcription partners GATA4 and FOG2. *Development* 2002; **129**: 4627–34.
121 Tevosian SG, Deconinck AE, Cantor AB, Rieff HI, Fujiwara Y *et al*. FOG-2: A novel GATA-family cofactor related to multitype zinc-finger proteins Friend of GATA-1 and U-shaped. *Proc Natl Acad Sci USA* 1999; **96**: 950–5.
122 Park SY, Lee EJ, Emge D, Jahn CL, Jameson JL. A phenotypic spectrum of sexual development in *Dax1* (*Nr0b1*)-deficient mice: consequence of the C57BL/6J strain on sex determination. *Biol Reprod* 2008; **79**: 1038–45.
123 Meeks JJ, Crawford SE, Russell TA, Morohashi K, Weiss J *et al*. Dax1 regulates testis cord organization during gonadal differentiation. *Development* 2003; **130**: 1029–36.
124 Meeks JJ, Weiss J, Jameson JL. Dax1 is required for testis determination. *Nat Genet* 2003; **34**: 32–3.
125 Bouma GJ, Albrecht KH, Washburn LL, Recknagel AK, Churchill GA *et al*. Gonadal sex reversal in mutant *Dax1 XY* mice: a failure to upregulate *Sox9* in pre-Sertoli cells. *Development* 2005; **132**: 3045–54.
126 Ludbrook LM, Harley VR. Sex determination: a 'window' of DAX1 activity. *Trends Endocrinol Metab* 2004; **15**: 116–21.

BIOLOGY OF REPRODUCTION (2013) **89**(2):34, 1–12
Published online before print 10 July 2013.
DOI 10.1095/biolreprod.113.110155

SOX9 Regulates MicroRNA *miR-202-5p/3p* Expression During Mouse Testis Differentiation[1]

Elanor N. Wainwright,[5] Joan S. Jorgensen,[6] Youngha Kim,[6] Vy Truong,[5] Stefan Bagheri-Fam,[7] Tara Davidson,[5] Terje Svingen,[3,5] Selene L. Fernandez-Valverde,[4,8] Kathryn S. McClelland,[5] Ryan J. Taft,[8] Vincent R. Harley,[7] Peter Koopman,[5] and Dagmar Wilhelm[2,5]

[5]*Division of Molecular Genetics and Development, Institute for Molecular Bioscience, The University of Queensland, Brisbane, Queensland, Australia*
[6]*Department of Comparative Biosciences, University of Wisconsin, Madison, Wisconsin*
[7]*Molecular Genetics and Development Division, Prince Henry's Institute of Medical Research, Clayton, Melbourne, Victoria, Australia*
[8]*Division of Genomics and Computational Biology, Institute for Molecular Bioscience, The University of Queensland, Brisbane, Queensland, Australia*

ABSTRACT

MicroRNAs are important regulators of developmental gene expression, but their contribution to fetal gonad development is not well understood. We have identified the evolutionarily conserved gonadal microRNAs *miR-202-5p* and *miR-202-3p* as having a potential role in regulating mouse embryonic gonad differentiation. These microRNAs are expressed in a sexually dimorphic pattern as the primordial XY gonad differentiates into a testis, with strong expression in Sertoli cells. In vivo, ectopic expression of *pri-miR-202* in XX gonads did not result in molecular changes to the ovarian determination pathway. Expression of the primary transcript of *miR-202-5p/3p* remained low in XY gonads in a conditional *Sox9*-null mouse model, suggesting that *pri-miR-202* transcription is downstream of SOX9, a transcription factor that is both necessary and sufficient for male sex determination. We identified the *pri-miR-202* promoter that is sufficient to drive expression in XY but not XX fetal gonads ex vivo. Mutation of SOX9 and SF1 binding sites reduced ex vivo transactivation of the *pri-miR-202* promoter, demonstrating that *pri-miR-202* may be a direct transcriptional target of SOX9/SF1 during testis differentiation. Our findings indicate that expression of the conserved gonad microRNA, *miR-202-5p/3p,* is downstream of the testis-determining factor SOX9, suggesting an early role in testis development.

microRNAs, mouse gonad development, testis differentiation, transcriptional regulation, transgenic mice

INTRODUCTION

Differentiation of the gonads during mammalian embryogenesis is a critical developmental process because it determines the phenotypic sex of the fetus. Gonads develop from the indifferent or bipotential genital ridges, which can differentiate into two morphologically and functionally distinct organs, testes, or ovaries. This decision depends on whether or not the Y chromosomal, male-determining *Sry* gene is expressed. The expression of *Sry* initiates a cascade of gene expression and regulation resulting in the formation of a testis [1]. Subsequently, hormones produced by the testis orchestrate the differentiation of the rest of the body to a male phenotype. The critical transcriptional target of SRY is *Sox9*, which is both necessary and sufficient for male sex determination and development. In humans, loss of a fully functional SOX9 results in the disorder campomelic dysplasia, which is frequently characterized by sex reversal in XY individuals [2, 3].

In the absence of a completely functional *Sry*, the female program of gene expression marked by *Wnt4*, *Rspo1*, and *Foxl2* is initiated, and an ovary will develop, which in turn results in a female phenotype. There is a fine balance between the testicular- and ovarian-specific network of gene expression, and disturbance can result in a tipping of the balance in one direction or the other [4].

MicroRNAs are a class of single-stranded noncoding RNAs of approximately 22 nucleotides (nt) in length that post-transcriptionally regulate mRNAs. Most microRNAs (miRNAs) are transcribed by RNA polymerase II as the long primary transcript termed pri-miRNA. In the nucleus, the microprocessor complex consisting of the RNase-III enzyme Drosha and its RNA-binding partner DGCR8 processes the pri-miRNA into a precursor miRNA of ~70 nt, the pre-miRNA hairpin [5, 6]. The pre-miRNA is then processed in the cytoplasm to a ~22-nt double-stranded RNA by the RNAase III enzyme Dicer [6]. One of the strands or both strands (3p and 5p) are incorporated into the RNA-induced silencing complex RISC. The miRNA-loaded RISC then regulates its target mRNA by affecting mRNA translation and/or stability usually by binding to 3′ untranslated regions (3′UTR) (reviewed in [7]). MicroRNAs are important regulators of developmental gene expression, but their role in fetal gonad development is poorly understood.

Several studies have indicated that miRNAs are likely to regulate the mammalian reproductive system. Microarray and

[1]Supported by Australian Research Council (ARC) grant DP0879913 and National Health and Medical Research Council of Australia grant 631460. D.W. is a Future Fellow of the ARC (FT110100327).
[2]Correspondence and Current address: Dagmar Wilhelm, Department of Anatomy and Developmental Biology, Monash University, Clayton, VIC 3800, Australia. E-mail: dagmar.wilhelm@monash.edu
[3]Current address: Department of Growth and Reproduction, Copenhagen University Hospital, Copenhagen, Denmark
[4]Current address: School of Biological Sciences, The University of Queensland, Brisbane, QLD 4072, Australia

Received: 17 April 2013.
First decision: 17 May 2013.
Accepted: 1 July 2013.

eISSN: 1529-7268 http://www.biolreprod.org
ISSN: 0006-3363

cloning approaches have identified known and novel miRNAs in the fetal and postnatal testis and ovary in a variety of species [8–12]. The contribution of miRNAs in general has been studied using *Dicer1*-null mice, in which the processing of canonical miRNAs is abolished. While mutant embryos generated from *Dicer1*-null oocytes failed to proceed to a two-cell embryo, mice homozygous for a hypomorphic allele developed normally except for female infertility associated with corpus luteum insufficiency [13]. Furthermore, mice with *Dicer1* deleted specifically in germ cells showed arrest of spermatogenesis [14–18].

Deletion of *Dicer1* in the Sertoli cell lineage at 13.5 days post coitum (dpc), using *Dicer1*$^{fl/fl}$:*Amh*^{cre} mice, resulted in progressive postnatal testis degeneration and infertility from a failure of Sertoli cell maturation [19, 20]. In addition, genetic ablation of *Dicer1* alleles in SF1-positive gonadal somatic cells from 10 dpc resulted in postnatal testis degeneration [21]. While these studies demonstrate that miRNAs have a significant role in postnatal testicular somatic cell function, the mouse models do not address the role of miRNAs in fetal Sertoli cells, because it is unclear at what stage Dicer1 protein is lost. Moreover, when *Dicer1* alleles were excised at 13.5 dpc, a significant decrease in the expression of miRNAs was evident only at postnatal day 5 [19].

We previously screened the small RNA population of differentiating XY and XX gonads, using high-throughput sequencing to identify microRNAs that may regulate mouse embryonic gonad development [22]. We detected the microRNAs *miR-140-5p*/*miR-140-3p* being expressed in differentiating testes. Investigation of *pre-miR-140* null mice identified the fact that Leydig cell development was perturbed with an increase in Leydig cell number, supporting a role for microRNAs in early gonad development [22]. To further characterize the role of microRNAs in regulating developmental events during sex determination and gonadal development, we investigated the expression and regulation of the conserved gonadal microRNAs *miR-202-5p* and *miR-202-3p* and found them to be expressed in a testis-enriched pattern, with strong expression in Sertoli cells, the organizing cells of the XY gonad. We showed that *pri-miR-202* is likely to be a direct transcriptional target of SOX9, suggesting an early role in testis-specific organogenesis.

MATERIALS AND METHODS

Mouse Strains

Embryos were collected from timed matings of outbred CD1 mice, with noon of the day on which the mating plug was observed designated 0.5 dpc. For more accurate staging, the tail somite (ts) stage of the embryo was determined by counting the number of somites posterior to the hind limb [23]. Using this method, 10.5 dpc corresponds to approximately 8 ts, 11.5 dpc to 18 ts, and 12.5 dpc to 30 ts. *Zfy* PCR was used to determine the sex of the embryos before morphological gonad differentiation [24]. Generation of cytokeratin 19 *Ck19;Sox9*-null mice have been described previously [25]. Generation of *Cited2*-null mice on a C57BL/6 background has been described previously [26]. *Cited2*-null mouse samples were between 24 and 27 ts. The bacterial artificial chromosome (BAC) transgenic mouse vector used to drive *pri-miR-202* under the control of the regulatory regions of *Wt1*, and the BAC *Wt1:202-IRESeGFP* transgenic lines were generated as described previously [27]. Seven positive transgenic mice were generated that stably transmitted the *Wt1:202-IRES-eGFP* transgene (Tg) through the germ line. However, analysis detected expression only of the Tg in one mouse line. This line was subsequently characterized further. Tg mice were analyzed on a mixed Agouti and C57BL/6 background. Genotyping primers used are provided in Supplemental Table S1 (all Supplemental Data are available online at www.biolreprod.org). Protocols and use of animals were approved by the Animal Welfare Unit of the University of Queensland, which is registered as an institution that uses animals for scientific purposes under the Queensland Animal Care and Protection Act (2001).

In Situ Hybridization

Probes used were *pri-miR-202* (entire *AK144366* transcript), *miR-202-3p* (miRCURY locked nucleic acid [LNA] detection probe, 39487-01; Exiqon), *miR-202-5p* (miRCURY LNA detection probe, 39486-01; Exiqon), Scrambled (miRCURY LNA detection probe, 99004-01; Exiqon). Section in situ hybridization (sISH) for *pri-miR-202* was performed as previously described [28] with hybridization of the probe at 65°C. The color reaction was performed for equal amounts of time on XY and XX sections at the same time point. For microRNA section in situ hybridization with digoxigenin (DIG)-labeled LNA probes, whole embryos were fixed in 4% (w/v) paraformaldehyde (PFA) at 4°C overnight, then washed with 1× PBS, incubated in 30% sucrose solution for 6 h and then snap frozen in OCT (Tissue Tek). LNA sISH was performed with 10-μm sagittal sections as described previously [28, 29], unless otherwise stated. After proteinase K digestion and 4% PFA fixation, slides were incubated in imidazole (Sigma-Aldrich) buffer (1.6 ml imidazole, 148.35 ml of water, 450 μl of HCl [32%] and 9.6 ml of 5M NaCl). A 2-h fixation with 1-ethyl-3-(3-dimethylaminopropyl) carbodiimide (Sigma-Aldrich) solution diluted in imidazole buffer, at a final concentration of 0.16 M, pH8 [29]. Hybridization of the probes was performed at 20°C below the probe melting temperature, as recommended by the manufacturer (Exiqon); 56°C for *miR-202-3p*, 47°C for *miR-202-5p*, and 47°C for Scrambled. RNA probe was detected by incubation with BM Purple, alkaline phosphatase substrate (Roche). Slides were mounted in 70% glycerol and imaged with a BX-51 microscope (Olympus). Section ISH followed by immunohistochemistry was performed as described previously [30].

For fluorescence sISH, embryos were dissected at 13.5 dpc and fixed in 4% (w/v) PFA at 4°C overnight and washed with 1× PBS and embedded in paraffin. Paraffin sections (7 μm) were mounted on Superfrost Plus slides (Menzel-Glaser) and processed as previously described [28]. Fluorescence detection of the DIG-labeled probe was achieved by incubation in detection buffer (100 mM Tris HCl, pH8, 100 mM NaCl, 10 mM $MgCl_2$) twice for 20 min each and then incubation in 10 μl of 2-hydroxy-3-naphtoic acid-2′-phenylanilide phosphate (HNPP; Roche) and 10 μl of Fast Red TR (Roche) solution per milliliter of detection buffer for 2 h at room temperature.

For whole-mount ISH, dissected gonads/mesonephroi were fixed in 4% PFA in PBTX (PBS containing 0.1% Triton X-100) for several hours at 4°C. Whole-mount ISH with DIG-labeled RNA probes was carried out as described elsewhere [31].

Immunofluorescence

Paraffin sections (7 μm) of mouse embryos were processed as described previously [27]. The primary antibodies against endogenous mouse antigens used for this study were goat anti-green fluorescent protein (GFP; code AB5450; Abcam) at 1:200 dilution; rabbit anti-mouse vasa homologue (MVH; code 13840; Abcam) at 1:400 dilution; rabbit anti-FOXL2 [27] at 1:600 dilution; goat anti-Mullerian hormone (AMH; code SC-5279; Santa Cruz Biotechnology) at 1:400 dilution; rabbit anti-SOX9 at 1:200 dilution [32]; rabbit anti-SCC [33] and anti-isolectin B4 (code L2140; Sigma Aldrich) at 1:200 dilution. The secondary antibodies used were donkey anti-goat Alexa 488 (code A11055; Invitrogen) at 1:200 dilution; donkey anti-goat horseradish peroxidase (code 705-035-003; Abacus ALS); goat anti-rabbit Alexa 594 (code A11034; Invitrogen) at 1:200 dilution; donkey anti-rabbit Alexa 568 (code A10042; Invitrogen) at 1:200 dilution; biotinylated anti-rabbit (Amersham); and 4′,6-diamidino-2-phenylindole (DAPI; 2 ng/μl in PBS; Molecular Probes) at 1:1000 dilution to visualize nuclear DNA in immunofluorescence, using a confocal microscope (LSM 510 Meta; Zeiss).

Quantitative RT-PCR

Quantitative RT-PCR (qRT-PCR) using SYBR green (Invitrogen) was performed as described previously [34]. Quantitative RT-PCR at all time points was performed with gonad-only samples, with mesonephroi removed. *Sox9*-null samples were normalized to the endogenous housekeeping genes *Rn18s* [34]. *Cited2*-null samples were normalized to *Sdha*, n = 3 [34]. *WT1-202* Tg samples were normalized to *Tbp,* n = 3–4 [34]. TaqMan miRNA qRT-PCR reactions were performed according to the manufacturer (Applied Biosystems) instructions for *miR-202-5p* (no. 4395709), *miR-202-3p* (no. 4373311), and *sno202* (no. 4380914*)*. Reverse transcriptase reactions were set up with 50 ng of RNA per sample. Quantitative PCR reactions were normalized to the small nucleolar RNA *sno202* [35] and used to calculate the relative fold change in accordance with the delta-delta CT method [36]. Where appropriate, comparisons of gene expression levels were analyzed using unpaired two-tailed Student *t*-tests (PRISM version 5.0 software; GraphPad). The SYBR green primers used are provided in Supplemental Table S1.

Cell Sorting

Two 13.5 dpc Sf1-eGFP [37] litters were dissected in cold PBS, and the sex was determined by the presence or absence of testis cords before the gonad was separated from the mesonephros. Gonads were enzymatically dissociated into a single cell suspension in 0.25% Trypsin-EDTA (Gibco) with 5 U/ml DNase1 (Sigma) for 20 min at 37°C while rocking. Cells were further dissociated using an 18-gauge and then 23-gauge syringe. Cells were pelleted by centrifugation at 3000 rpm at 4°C. The dissociation solution was removed, and cells were resuspended in 400 µl of ice-cold PBS and stored on ice. Cells were incubated with 2 µl of SSEA1-PE antibody (BD Biosciences) for 20 min to tag germ cells, and germ and eGFP-positive cells were sorted using a BD FACSAria cell sorter at the Queensland Brain Institute of the University of Queensland, Brisbane, Australia. Collected cell populations were kept on ice before RNA extraction. Cells from two independent sorting experiments were pooled for analysis.

Electrophoretic Mobility Shift Assay

Electrophoretic mobility shift assay was performed as described previously [28] using recombinant, bacterially expressed glutathione S-transferase (GST) fusion proteins of the full-length mouse SOX9 and FGFR2. The oligonucleotides harboring the SOX site are provided in Supplemental Table S1.

Gonad Explant Culture and Transient Transfection Analysis

Promoter fragments were cloned into the pGL2 vector. Primers used to amplify promoters and to perform site-directed mutagenesis are listed in Supplemental Table S1. Transient transfection assays in gonad explant cultures were performed using previously described methods [38]. Briefly, gonads were harvested from 13.5- to 14.5-dpc embryos of CD1 mice. Transfections were performed by injecting a DNA cocktail containing 4 µg/µl pGL2 construct plus 2 µg/µl SV40-*Renilla* plasmid DNA. Less than 1 µl of DNA was injected, spread over three sites within the gonad. Following injection, 20 µl of sterile PBS was placed on the gonad for electroporation. Immediately thereafter, 5 square electrical pulses of 65 volts, 50 ms each at 100-ms intervals, were delivered through platinum electrodes from an electroporator. After electroporation, gonads were placed back into culture for 24 h. Explant cultures were maintained at 37°C with 5% CO_2/95% air in a 50-µl droplet of Dulbecco minimal Eagle medium supplemented with 10% fetal calf serum and 50 mg/ml ampicillin [39]. Upon harvest, transfected gonad explants were washed three times with PBS and then placed in 40–100 µl of passive lysis buffer (Promega) and manually disrupted with a pipet tip and subjected to three freeze/thaw cycles to optimize cell lysis. Reporter activity was measured using 20 µl of cell lysate, using the dual reporter detection system according to manufacturer's recommendations (Promega). Each construct was injected in at least three gonads of each sex, and each experiment was repeated at least four times. Data were subjected to one-way ANOVA and a Dunnett multiple comparisons post hoc test, where all the columns were tested relative to the control promoter.

MicroRNA Target Prediction

Messenger RNA targeted by the most prevalent strands of *miR-140-3p* (*miR-140**) and *miR-202-5p* were predicted using TargetScan 5.2 Custom [40], MirWalk [41] and RNA22 [42]. For TargetScan only genes with an exact match to positions 2–8 of the mature miRNA were considered as truly targeted (8 mer and 7 mer-m8 site types). Genes predicted to be targeted by at least two of these programs were considered as a conservative set of *miR-202-5p* targets. Genes predicted to be targeted by both *miR-140-3p* and *miR-202-5p* by any of these programs were considered shared targets of these miRNAs.

RESULTS

miR-202 *Is a Conserved microRNA Expressed in Mouse Embryonic Gonads*

We have previously screened the small RNA population of differentiating XY and XX gonads by using high-throughput sequencing to identify microRNAs that may regulate embryonic gonad development [22]. This strategy was used to identify the microRNA *miR-140-3p/5p*, which modulates Leydig cell differentiation in the fetal XY gonad, validating the fact that the screen identified functionally important microRNAs. This approach also revealed *miR-202-5p/3p* as potential candidates to regulate fetal testis differentiation [22]. Furthermore, we found the primary transcript *pri-miR-202* to be testis-enriched expressed during mouse gonad development in a microarray designed to detect long noncoding RNAs [43]. While some pre-miRNAs are processed from introns of protein-encoding genes, *pri-miR-202* is transcribed as the independent noncoding transcript *AK144366*. The sequence of the microRNA *miR-202* is conserved in vertebrates (Fig. 1A) and was previously shown to be expressed in adult testes of human, mouse, *Xenopus*, Atlantic halibut [10, 11, 44, 45], and fetal testes of chicken [9]. In order to determine whether *miR-202* is expressed in mouse embryonic gonads, we performed section ISH for the primary transcript of *miR-202*, *pri-miR-202* (Fig. 1B). *Pri-miR-202* was detected in both XY and XX gonads at 11.5 dpc. As the gonads differentiate, strong expression of *pri-miR-202* was evident in the testis around the edge of the cords. Testis cords are composed of clusters of germ cells surrounded by Sertoli cells, suggesting that *pri-miR-202* is expressed in Sertoli cells. Detection of weak *pri-miR-202* expression in the ovary at 12.5 and 13.5 dpc demonstrated that it is dimorphically expressed as the gonads differentiate. Fluorescent ISH with XY gonads at 13.5 dpc detected *pri-miR-202* in nuclear subdomains (Fig. 1C), as would be expected for a primary miRNA transcript. Section ISH, combined with immunohistochemistry staining for the cytoplasmic Sertoli cell marker AMH showed that *pri-miR-202* and AMH colocalize within the same cells (Fig. 1D). Therefore, *pri-miR-202* is expressed within the nuclei of Sertoli cells. Expression of *pri-miR-202* was not detected at earlier stages of embryonic development (Supplemental Fig. S1).

Expression of miR-202-5p *and* miR-202-3p *Is Sexually Dimorphic*

Having detected embryonic expression of *pri-miR-202* in fetal gonads, we next investigated whether *pri-miR-202* is processed to mature miRNAs, and quantified the relative expression levels between XY and XX gonads. Quantitative RT-PCR with gonad-only tissue detected expression of both *miR-202-3p* and *miR-202-5p* in embryonic gonads, with increasing levels of expression as the gonads differentiated (Fig. 2A). By 13.5 dpc, the expression of both strands was significantly higher in testes than in ovaries. This expression pattern was congruent with that observed in our high-throughput sequencing approach using RNA from mouse embryonic gonads from 11.5 to 13.5 dpc (Supplemental Fig. S2, [22]), which also indicated that in the embryonic gonad, *miR-202-5p* is the predominantly expressed miRNA strand from the *pre-mir-202* hairpin.

LNA section ISH was then used to confirm that *miR-202-3p* is processed within the same cell type as the primary transcript (Fig. 2B). In the XY gonad, *miR-202-3p* was detected in the cytoplasm of cells toward the edge of the testis cords, a pattern consistent with expression in Sertoli cells. The opposing hairpin strand, *miR-202-5p*, was also detected by LNA ISH in Sertoli cells; however, signal was also detected at other sites in the embryo that we were unable to validate by high-throughput sequencing (data not shown), suggesting that the *miR-202-5p* probe may not be specific. To further confirm the expression of *miR-202-5p* in somatic but not germ cells, we performed qRT-PCR with sorted gonadal cells from 13.5-dpc Sf1-eGFP embryos [37]. Germ cells were isolated using an anti-SSEAI antibody and pooled Sertoli and Leydig cells based on the expression of eGFP driven by the *Sf1* promoter [37]. Quantitative RT-PCR with the Sertoli cell marker *Sox9* and the germ cell marker *Mvh* showed that while some germ cells were present in the eGFP-positive cell population, the germ cell

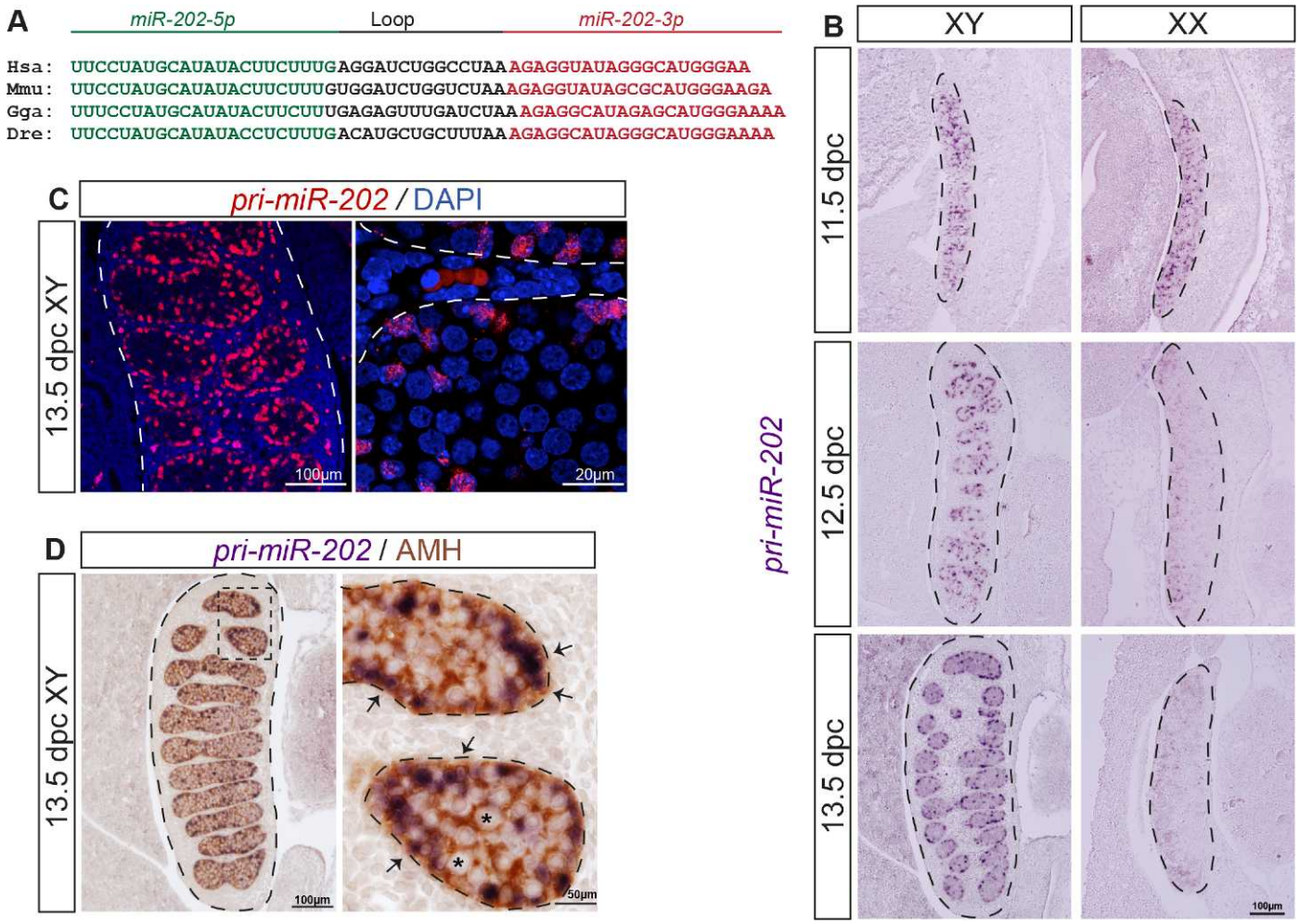

FIG. 1. *pri-miR-202* is expressed in the nuclei of Sertoli cells in the embryonic XY gonad. **A**) The sequences of *miR-202-5p* (green) and *miR-202-3p* (red) are conserved in vertebrates: Hsa, human; Mmu, mouse; Gga, chicken; Dre, zebrafish. **B**) Section ISH in XY and XX gonads for *pri-miR-202* at 11.5, 12.5, and 13.5 dpc demonstrated expression in testis cords. Bar = 100 μm. **C**) Section fluorescent ISH of 13.5-dpc testes for *pri-miR-202* (red) and DAPI marking the nuclei (blue). Arrow indicates *pri-miR-202* in nuclear subdomains within the testis cords. At low magnification, dotted line marks gonad, and at high magnification, dotted line marks testis cords. Bars = 100 μm (left panel) and 50 μm (right panel). **D**) Section ISH of XY gonads at 13.5 dpc for *pri-miR-202* (purple) with immunohistochemistry for AMH (brown). Arrows indicate nuclear *pri-miR-202* and cytoplasmic AMH within the same cell. Asterisks mark germ cells with no AMH or *pri-miR-202* expression. At low magnification, dotted line marks gonad, and at high magnification (region marked by rectangle in left panel), dotted line marks testis cords. Bars = 100 μm (left panel) and 50 μm (right panel).

population was free of Sertoli and Leydig cells (Fig. 2C, left and middle panels). Quantitative RT-PCR for *miR-202-5p* demonstrated that this miRNA was highly enriched (500-fold higher) in the eGFP-positive cell fraction compared to that in isolated germ cells (Fig. 2C, right panel), further corroborating our ISH results. Therefore, *miR-202-5p*/*miR-202-3p* are expressed in a sexually dimorphic pattern during embryonic gonad development and localize to Sertoli cells in the testis.

In Vivo Overexpression of pri-miR-202 *in XX Gonads*

To investigate the function of *pri-miR-202* in vivo, we generated a mouse model in which *pri-miR-202* was overexpressed in embryonic gonadal somatic cells. This mouse model was used to determine whether overexpression of *pri-miR-202* disturbs the ovarian pathways of gene expression. We overexpressed *pri-miR-202* together with eGFP driven by an internal ribosome entry site (IRES) under the control of the regulatory region of the Wilms tumor suppressor gene *Wt1*. We chose the regulatory region of *Wt1* because this gene is expressed in the somatic cells of XX and XY genital ridges from approximately 10.5 dpc [46]. This strategy was used previously to show that ectopic expression of *Sox10* in an XX gonad was able to direct testicular development [27]. All transgenic XX and XY mice were fertile and survived to adulthood.

Investigation of transgenic testes by immunofluorescence showed that eGFP is expressed in Sertoli cells at 13.5 dpc as expected (Supplemental Fig. S3A). However, surprisingly, although the primary transcript *pri-miR-202* was increased approximately 2-fold (Supplemental Fig. S3B, left panel), the level of the processed, mature microRNA *miR-202-5p* was not significantly changed (Supplemental Fig. S3B, right panel). Accordingly, we did not observe any phenotypic changes in developing transgenic testes at 13.5 dpc as determined by immunofluorescence for the Sertoli cell marker AMH, the germ cell marker MVH, the Leydig cell marker SCC, and the endothelial cell marker isolectin B4 (Supplemental Fig. S3C).

Analysis of transgene expression by immunofluorescence-detected eGFP in the XX gonad at 11.5, 13.5, and 15.5 dpc in heterozygous transgenic mice (Fig. 3A), demonstrating that the transgene is also expressed during XX embryonic gonad

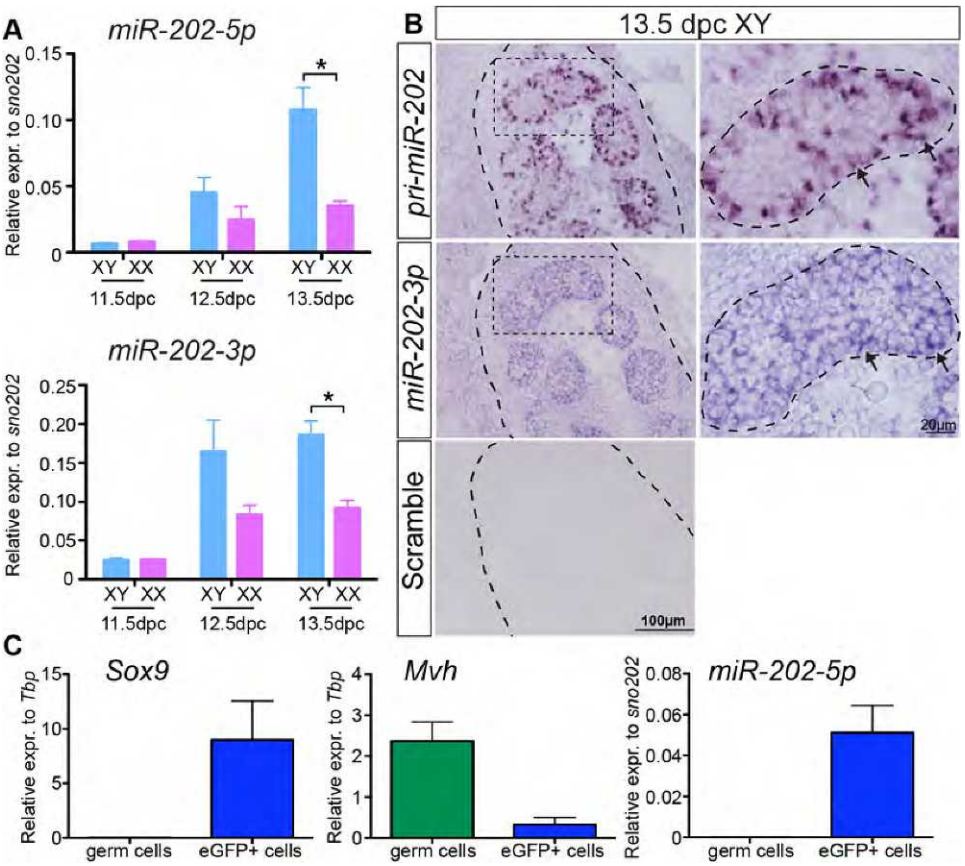

FIG. 2. The miRNAs *miR-202-5p/3p* are expressed in a dimorphic manner, as gonads differentiate. **A**) TaqMan qRT-PCR detected expression of *miR-202-3p* and *miR-202-5p* in XY (blue) and XX (pink) gonads at 11.5, 12.5, and 13.5 dpc. n = 3; error bars represent SEM. *$P < 0.05$ by unpaired Student *t*-test. **B**) Section ISH for *pri-miR-202*, *miR-202-3p* (LNA modified probe), and scrambled (LNA modified probe) in XY gonads at 13.5 dpc. Arrows indicate colocalization on adjacent sagittal sections between *pri-miR-202* nuclear staining and *miR-202-3p* cytoplasmic staining. At low magnification, dotted line marks gonad tissue, and at high magnification, dotted line marks testis cords. Bars = 100 µm (left panels) and 20 µm (right panels). **C**) Quantitative RT-PCR for the Sertoli cell marker *Sox9* (left panel), the germ cell marker *Mvh* (middle panel), and *miR-202-5p* (right panel) relative to *Tbp* and *sno202*, respectively, of isolated germ cells and eGFP-positive cells from 13.5 dpc Sf1-eGFP testes. Error bars represent technical SEM.

development. Colocalization of eGFP with markers of XX somatic cells (FOXL2) and germ cells (MVH) at 13.5 dpc demonstrated that this expression was restricted to the somatic cell lineage in the XX gonad, as expected (Fig. 3B). Quantitative RT-PCR at 13.5 dpc detected significantly increased expression of *pri-miR-202* and *miR-202-5p* in the heterozygous (*Tg*/*Wt*) and homozygous (*Tg*/*Tg*) transgenic XX gonads compared to that in wild-type XX gonads (*Wt*/*Wt*). The expression of *pri-miR-202* in XX *Tg*/*Wt* gonads and the expression of the predominant mature microRNA *miR-202-5p* in XX *Tg*/*Tg* gonads were comparable to the level in wild-type testes (Fig. 3C).

To determine whether ovarian development was perturbed in *Tg*/*Tg* XX mice, we examined several markers of XX and XY gonad development. FOXL2, a marker of ovarian somatic cells, was expressed at wild-type levels in *Tg*/*Wt*, *Tg*/*Tg* XX gonads at 11.5, 13.5, and 15.5 dpc (Fig. 4A). Furthermore, the ovarian somatic cell genes *Wnt4* and *Rspo1* showed no significant change in expression in XX *Tg*/*Wt*, *Tg*/*Tg* gonads compared to XX *Wt*/*Wt* at 13.5 dpc (Fig. 4B), suggesting that ovarian somatic cell determination proceeds normally. In addition, the expression of Sertoli cell genes *Sox9* and *Amh*, and the Leydig cell gene *Hsd3*β, were unchanged in *Tg*/*Wt*, *Tg*/*Tg* XX gonads compared to wild-type at 13.5 dpc (Fig. 4B), showing that the cells did not differentiate into testicular somatic cells. Furthermore, there was no change in the expression of the germ cell marker *Mvh*, suggesting that germ cells are present at wild-type numbers. Taken together, no changes to molecular sex determination pathways and gonad development were detected in transgenic gonads.

To further assess *miR-202-5p* function, we queried for potential target genes using TargetScan, miRWalk, and RNA22 [40–42]. This analysis identified a total of 36 genes that were predicted to be targeted by at least two algorithms (Supplemental Table S2). Interestingly, 11 of the 36 target genes were also putative target genes of *miR-140-3p* (Supplemental Table S2, right column), a microRNA we previously showed to be expressed in Sertoli cells of the developing testis [22].

Expression of pri-miR-202 *Is Perturbed in the Absence of SOX9 and SF1*

Expression of *pri-miR-202* in Sertoli cells during XY gonad differentiation suggested that regulation of *pri-miR-202* transcription might be downstream of the transcription factor SOX9. To test this hypothesis, *pri-miR-202* expression was investigated in a mouse model where SOX9 expression is absent. The expression of *pri-miR-202* was examined in testes of mouse embryos in which *Sox9* was conditionally inactivated from 10.5 dpc; these embryos were generated by mating $Sox9^{flox/flox}$ mice with mice expressing Cre recombinase under the control of the cytokeratin 19 promoter [25]. Expression of

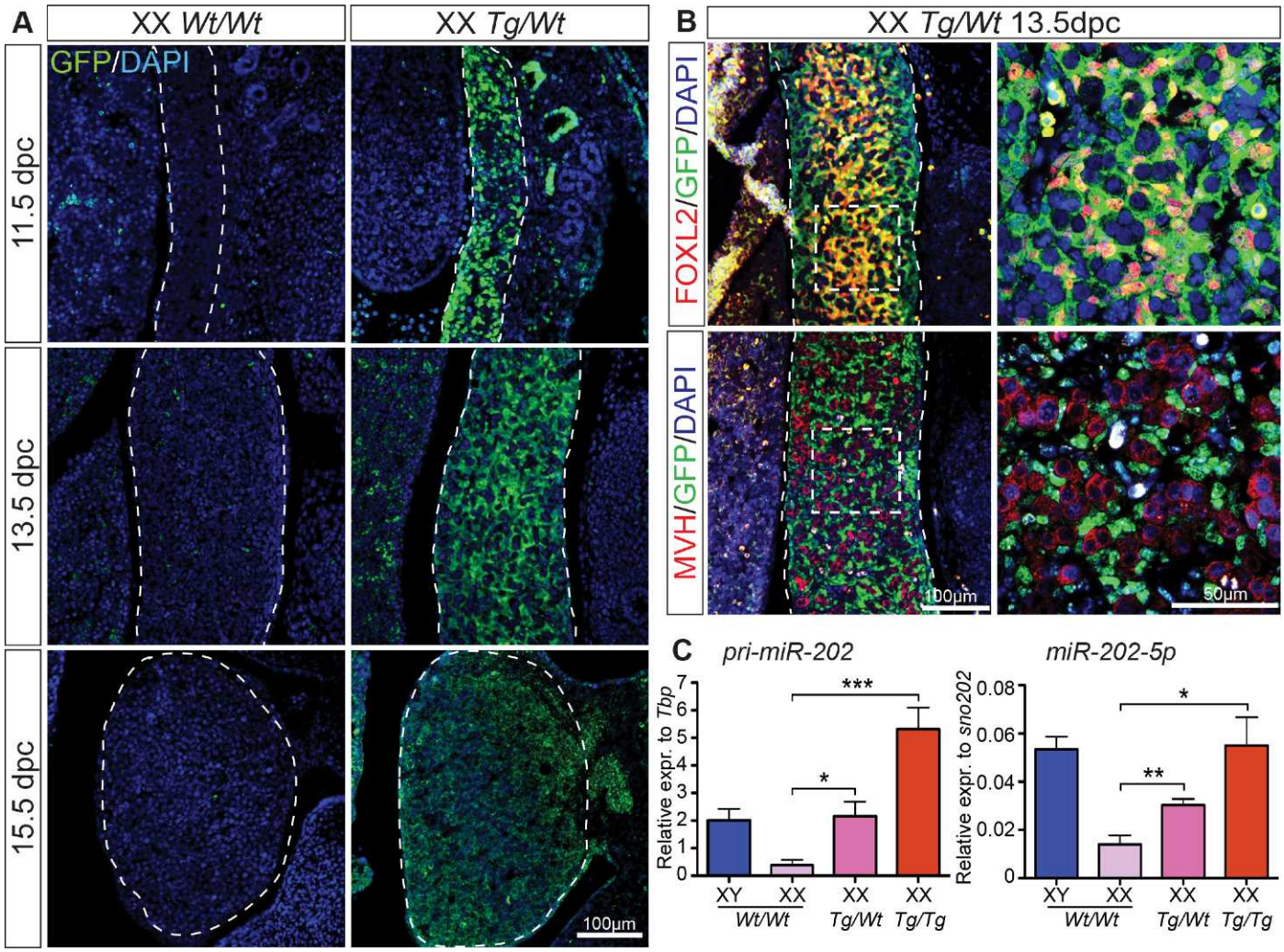

FIG. 3. *Wt1:202-IRES-eGFP* transgenic mice express *pri-miR-202* in ovarian somatic cells. **A**) Immunofluorescence on paraffin sections for eGFP (green) detected transgene expression in transgenic mice from 11.5 to 15.5 dpc. Bar = 100 μm. **B**) In the XX gonad at 13.5 dpc, eGFP (green) colocalizes with FOXL2 (red) in a subset of somatic cells (upper panels) but not MVH (red) in germ cells (bottom panels). White dashed lines indicate gonad tissue and cell nuclei are visualized with DAPI (blue). Bars = 100 μm (left panels) and 50 μm (right panels). **C**) Quantitative RT-PCR detected expression of *pri-miR-202* and *miR-202-5p* at 13.5 dpc, with increasing expression in XX heterozygous *Tg/Wt* and XX homozygous *Tg/Tg* gonads compared to XX wild-type (WT). Expression of *pri-miR-202* was normalized to that of *Tbp*, and expression of *miR-202-5p* was normalized to that of the small nucleolar RNA *sno202*. n = 3–6. Error bars represent SEM. $^{*}P < 0.05$; $^{**}P < 0.01$.

pri-miR-202 was examined in testes between 15 ts (approximately 11.2 dpc) and 27 ts (approximately 12.5 dpc). At all stages tested, the expression of *pri-miR-202* in *Sox9*-null XY gonads was weaker than that seen in wild-type XY gonads (Fig. 5A). These mice display complete sex reversal, with occasional ovotestis formation [25]. Importantly, the expression of *pri-miR-202* was reduced in those samples prior to morphological sex reversal (15, 16, and 18 ts). Therefore, these data suggest that *pri-miR-202* transcription is downstream of SOX9.

Because SOX9 directly up-regulates a number of genes in testes in conjunction with SF1 [47, 48], we investigated the expression of *pri-miR-202* in *Cited2* (Glu/Asp-rich carboxyl-terminal domain 2) null mice. *Sf1*-null mice display complete gonad agenesis with gonads regressing after sex determination [49], thus prohibiting investigation of downstream targets of SF1 in this mouse model. CITED2 interacts with the transcription factor WT1 and together they function to ensure elevated *Sf1* levels. *Cited2*-null mice exhibit a delay in the testis determination program that results from the failure of enhanced *Sf1* expression and not as a direct consequence of loss of *Cited2* [50]. *Sf1* expression levels recover by 12.5 dpc (30 ts) in *Cited2*-null gonads [51], so we examined the expression of *pri-miR-202* at 24–27 ts in XY gonads. Relative to the wild-type, the expression of *pri-miR-202* was significantly reduced in *Cited2*-null testes, suggesting that *pri-miR-202* transcription is downstream of SF1 (Fig. 5B).

SOX9 and SF1 Regulate pri-miR-202 *Expression via a 4-kb Promoter*

Because *pri-miR-202* transcription is evidently downstream of SOX9, we reasoned that SOX9 might directly transactivate the *pri-miR-202* promoter. A ~4-kb region proximal to the *pri-miR-202* transcription start site (Fig. 6A), WT promoter 1 (WT prom 1), was cloned into a luciferase reporter plasmid to study the putative promoter activity. This vector was electroporated into fetal gonad explants and ex vivo luciferase assays were performed. The ~4-kb promoter region showed 5- to 6-fold transactivation in 13.5 dpc XY gonads compared to 13.5 dpc

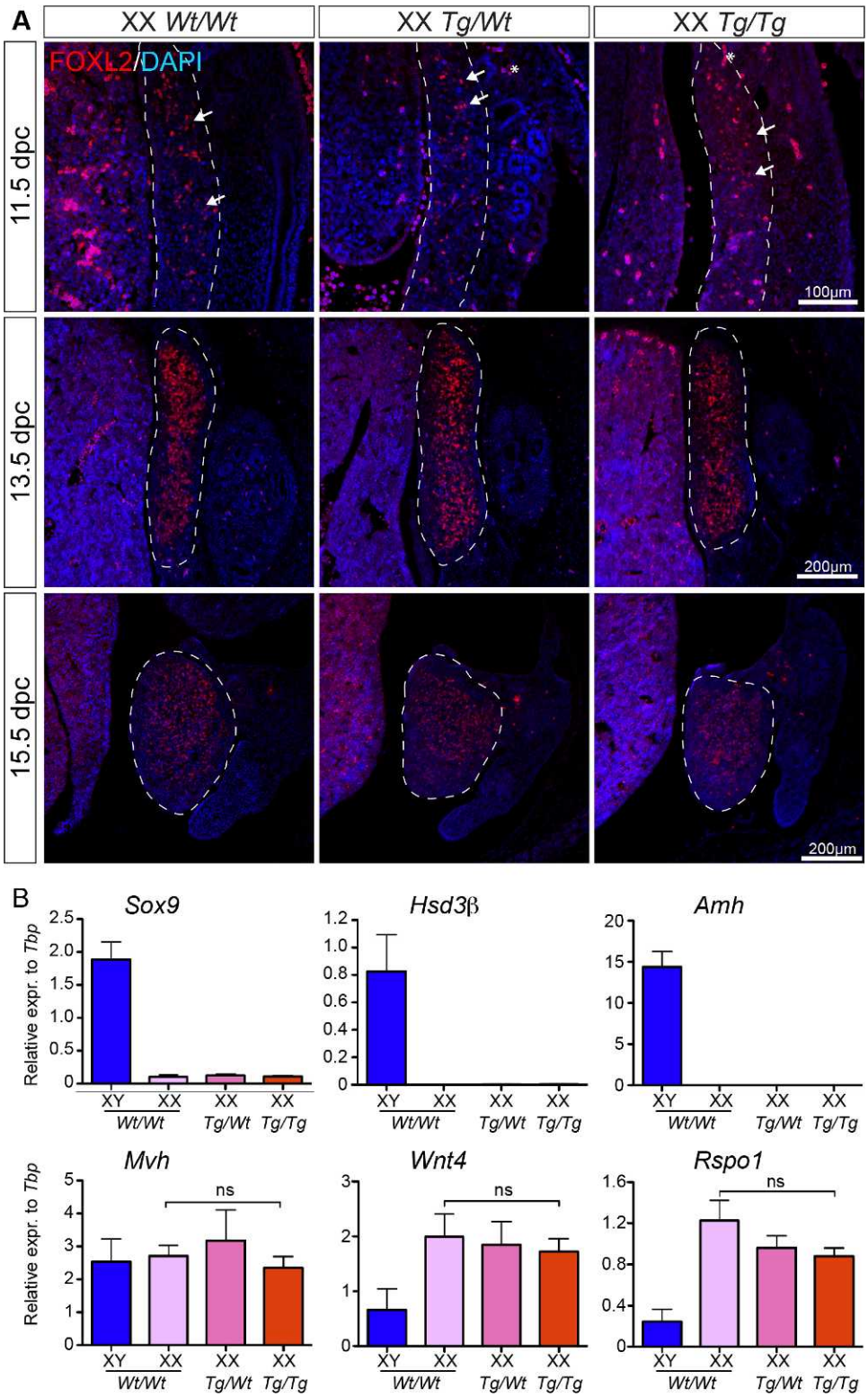

FIG. 4. Sexual development of the gonad is normal in XX *Wt1:202-IRES-eGFP* mice. **A**) Immunofluorescence on paraffin sections for FOXL2 detected somatic cells at 11.5, 13.5, and 15.5 dpc XX *Wt1:202-IRES-eGFP* mice. Arrows indicate FOXL2 positive cells and asterisks indicate nonspecific fluorescence of blood cells. Bars = 100 μm for 11.5 dpc (top panel) and 200 μm for 12.5 and 13.5 dpc (middle and bottom panel). **B**) Quantitative RT-PCR did not detect any change in expression of male somatic cell marker *Sox9*, fetal Leydig cell marker *Hsd3*β and germ cell marker *Mvh* or female somatic cell markers *Wnt4* and *Rspo1*. Error bars represent SEM, n = 3–4. ns, not significant.

XX gonads (Fig. 6B), suggesting that this region contains at least some of the regulatory elements required for *pri-miR-202* transactivation. For the majority of assays, transactivation of WT promoter 1 in XX gonads was too low to be detected.

Bioinformatics analysis of the 4-kb proximal promoter identified several SOX and SF1 consensus binding sites (Fig. 6A), (A/T)(A/T)CAA (A/T)G and GTCAAGGTCA respectively [47, 48]. Based on mammalian conservation and

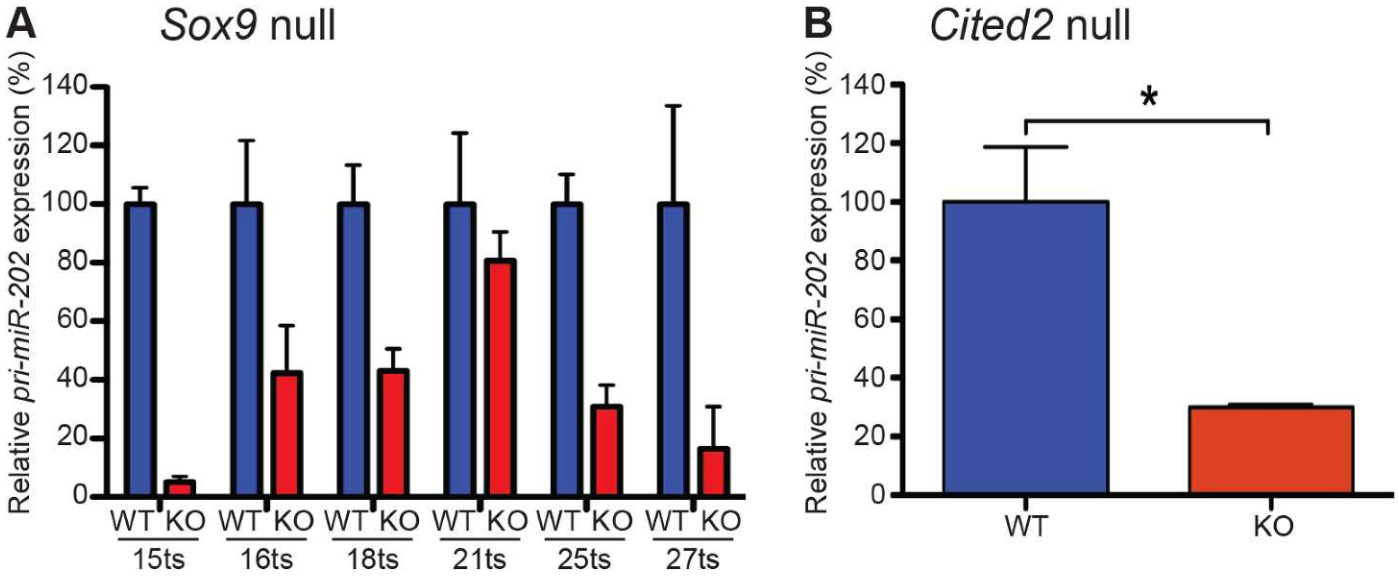

FIG. 5. *pri-miR-202* expression is reduced in *Sox9*-null and *Cited2*-null XY gonads. **A**) *pri-miR-202* expression in cytokeratin 19;*Sox9*-null mice. Each datum point is representative of n = 1 and is shown relative to a tail somite-matched wild-type sample. Expression is normalized to that of 18S. Error bars represent technical error. **B**) *pri-miR-202* expression in XY *Cited2*-null mice at 12.25 dpc. n = 3; expression is normalized to *Sdha* and is represented relative to wild-type expression. $*P < 0.05$, by unpaired students *t*-test. Error bars represent SEM.

proximity to putative SF1 binding sites, several putative SOX sites were selected for analysis of in vitro SOX9 binding, including a SOX site 0.1 kb proximal to the transcription start site SOX-0.1 (Fig. 6, A and C).

Electrophoretic mobility shift assays were performed to identify whether SOX9 could bind directly to these elements (only SOX-0.1 is shown). Nondenaturing polyacrylamide gel electrophoresis identified a shift in the migration of wild-type (WT) SOX-0.1 DNA fragment with GST-tagged SOX9 that was not evident with GST-tagged fibroblast growth factor receptor 2 (FGFR2) protein, suggesting that GST-SOX9 bound to the SOX-0.1 element (Fig. 6D). Mutation of the SOX consensus site (MUT SOX-0.1) prevented this binding, suggesting that it was a sequence-specific interaction (Fig. 6D). Therefore, these data show that SOX9 binds to SOX-0.1 in vitro.

Site-directed mutagenesis was then used to introduce the mutated SOX-0.1 into the 4-kb putative *pri-miR-202* promoter luciferase reporter vector that was previously used for the ex vivo gonad luciferase assays. In addition, three other promoter reporters were generated: the full-length 4-kb promoter with a mutated SF1-0.1 site and two truncated regions of the 4-kb wild-type promoter (WT promoter 2 and 3), 3.5 kb and 0.5 kb (Fig. 6A). Subsequently, ex vivo gonad luciferase assays of XY gonads were performed using these modified promoter regions. Truncation of the 4-kb wild-type promoter region resulted in a loss of promoter activity, suggesting that critical regulatory elements were contained within the full-length 4-kb region. Furthermore, mutation of the SOX-0.1 site or the SF1-0.1 site abolished transactivation of the wild-type promoter, suggesting that SOX9 and SF1 directly regulates the *pri-miR-202* promoter via these regulatory elements (Fig. 6E).

DISCUSSION

Mammalian sex is determined by a balance of male- and female-inducing factors, most notably SRY, SOX9, and FGF9, promoting testicular differentiation, and WNT4, RSPO1 and FOXL2, promoting ovarian differentiation. Because microRNAs are known to function in fine-tuning of gene expression and enforcing developmental decisions, we investigated whether microRNA gene regulation plays a role in sex determination in the mouse model system. Here, we examined the expression, regulation, and function of the microRNAs *miR-202-5p* and *miR-202-3p* in mouse embryonic gonads, identifying these miRNAs as candidates that regulate embryonic testis development. In addition, we showed that the expression of these miRNAs are likely to be regulated directly by the testis-determining factor SOX9, demonstrating that SOX9 function is not only important for the regulation of protein-encoding genes but also nonencoding RNAs.

Conserved Testicular Expression of miR-202-5p/3p

The miRNA *miR-202-5p/3p* is a member of the *let-7* family. The *let-7* family members are highly conserved across species both in sequence and function, with an increase of *let-7* expression generally associated with cell differentiation (for review see [52]). We found that *miR-202-5p/3p* is upregulated in Sertoli cells during mouse testis differentiation. Interestingly, previous studies have suggested that *miR-202* is expressed in both somatic and germ cells postnatally [10], suggesting that its expression is upregulated in germ cells at later stages during development. The testis-enriched expression during gonad differentiation is conserved in birds, with chicken showing high *miR-202-5p/3p* expression in developing testes compared to ovaries [9]. Furthermore, the association of *pri-miR-202* with the male gonad differentiation program was investigated in an avian model of sex reversal where estrogen synthesis was manipulated in ovo. In this sex reversal system, the expression of *miR-202-5p* decreased in feminized ZZ gonads and increased in masculinized ZW gonads, demonstrating that *miR-202-5p* expression is associated with male gonad development.

In addition, the expression of *miR-202-5p/3p* has been detected in immature and mature gonads in a number of vertebrate species, including Atlantic halibut, pig, human, mouse, and *Xenopus* [10, 11, 13, 45, 53]. Thus, the evolutionarily conserved expression pattern of *miR-202-5p/3p*

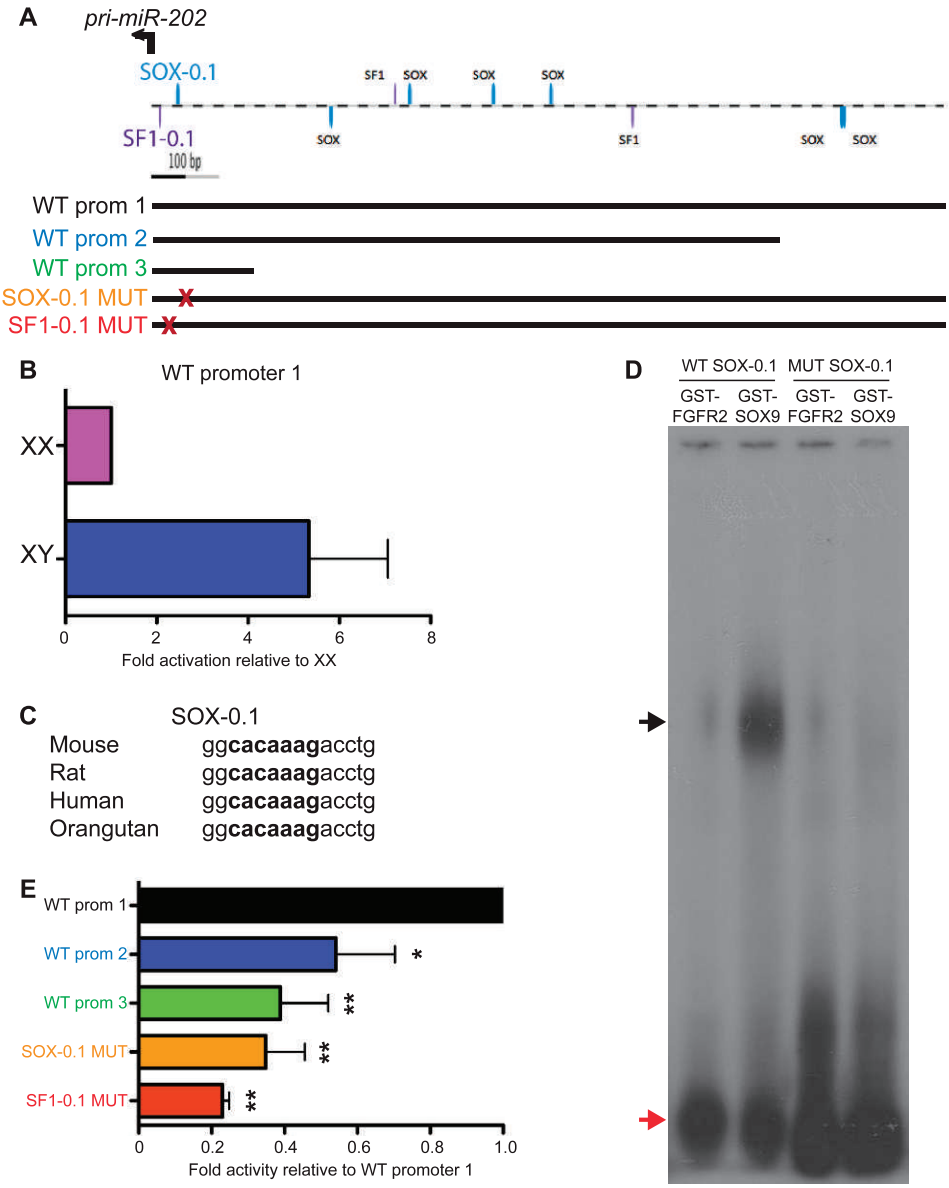

FIG. 6. *pri-miR-202* promoter activity requires SOX9 binding element. **A**) In silico analysis of the putative *pri-miR-202* promoter shows several potential SOX binding sites (blue) and SF1 binding sites (purple) with emphasis on SOX-0.1 and SF1-0.1 sites. Regions included in promoter constructs used in **B** and **E** (WT prom 1 2 and 3, SOX-0.1 MUT and SF1-0.1 MUT) are indicated. **B**) *Ex vivo* gonad luciferase assays with 4 kb wild-type promoter in XY and XX 13.5 dpc gonads. In most assays, transactivation was not detected in XX gonads, and XX transactivation reflects the few assays that detected activity above baseline. **C**) Conservation of the DNA sequence in mammals of the SOX-0.1 element. **D**) Electrophoretic mobility shift assay with wild-type (WT) or mutated (MUT) SOX-0.1 element from the *pri-miR-202* promoter. Radioactively labeled DNA was incubated with either GST-SOX9 or GST-FGFR2 as control. Black arrow indicates bound probe, red arrow indicates free probe. **E**) Ex vivo gonad luciferase assays in XY 13.5 dpc gonads with 4-kb wild-type promoter (WT prom 1), 3.5-kb wild-type promoter (WT prom 2), 0.5-kb wild-type promoter (WT prom 3), SOX-0.1 mutant promoter, and SF1-0.1 mutant promoter. Dual luciferase activity of each promoter was normalized to testes electroporated with pGL2-basic control vector. Following normalization, the fold change of each promoter construct was calculated relative to the WT promoter 1 activity. None of the promoter constructs expressed measurable luciferase activity in XX gonads (data not shown). Error bars represent SEM. Data was subjected to a one-way ANOVA and a Dunnett multiple comparison post hoc test relative to the control WT promoter 1. $*P < 0.05$; $**P < 0.01$, $n = 4$.

suggests that it plays a role during fetal testis differentiation and possibly has a function in postnatal testis and ovary.

Transcriptional Regulation of pri-miR-202 *Expression*

The transcription of microRNAs as long primary transcripts by RNA polymerase II is regulated by transcription factors. SOX9 is a master regulator of Sertoli cell differentiation in mouse and humans, being both necessary and sufficient for testis determination [3, 54, 55]. A number of direct target genes for SOX9 have been identified and shown to have important functions in Sertoli cell differentiation, maintenance, and male sex determination, such as anti-Müllerian hormone, which promotes regression of the Müllerian duct [47, 56], and prostaglandin D synthase, which functions in a positive feedback loop to ensure *Sox9* expression and therefore Sertoli cell differentiation [28, 32]. SOX9 has previously been shown to regulate the expression of another miRNA, *pri-miR-140*, which is contained within an intron of the *Wwp2* gene [57, 58]. Therefore, direct transcriptional regulation of microRNA gene expression may be an important contribution to the function of SOX9 protein.

Investigation of *pri-miR-202* expression in the *Ck19;Sox9*-null mouse model demonstrated that *pri-mR-202* expression was dependent on SOX9. There were several limitations to using this mouse model. The number of samples available was limited, with only 1 in 64 embryos generated carrying the correct *Sox9*-null XY genotype [25]. Furthermore, the dynamic increase in expression of *Sox9* [59] and *pri-miR-202* from 11.5 to 12.5 dpc prohibited similarly staged samples such as 15, 16, and 18 ts from being pooled as previously published [60]. However, at all time points there was a clear trend showing that *pri-miR-202* expression was reduced, and notably, expression was reduced in samples prior to morphological sex reversal.

Characterization of the putative *pri-miR-202* promoter ex vivo suggested that SOX9 and SF1 transactivate *pri-miR-202* through this genomic region, with mutation of a specific SOX and SF1 binding site ameliorating this transactivation. These results were further supported in vivo in the *Cited2*-null mouse model. These mice have been previously shown to have reduced *Sf1* expression [50, 51], which was associated with reduced *pri-miR-202* expression. However, a truncation of the wild-type promoter region, which still contained the identified SOX and SF1 binding sites, also reduced transactivation, demonstrating that additional regulatory elements are required for full promoter activity. Bioinformatics analysis identified, in addition to the SOX and SF1 binding sites, GATA4, FOXL2, SMAD, and KRAB binding sites, all factors that have been shown to play a role in mammalian gonad development [61–63]. Given that *pri-miR-202* is expressed in the developing ovary at 11.5 dpc but is downregulated thereafter, it is possible that the putative FOXL2 binding sites are important for the repression of this noncoding RNA in ovarian somatic cells. In addition, we identified a putative paired-SOX binding site within this deleted region. Paired-SOX sites have been shown to be important for full activation by SOX9 [64]. However, electrophoretic mobility shift assays did not confirm SOX9 binding to this DNA sequence in vitro (data not shown), suggesting that SOX9 binding to this paired-SOX site does not play a role in the transcriptional activation of *pri-miR-202*. In summary, our data from the expression analysis of *Sox9* and *Sf1* loss-of-function mouse models and mutation of the *pri-miR-202* promoter support the conclusion that SOX9/SF1 positively regulates *pri-miR-202* expression during testicular development.

Function of miR-202-5p/3p

Previous studies have addressed the global function of microRNAs by deletion of *Dicer1* in the Sertoli cell lineage at 13.5 dpc, using the *Amh-Cre,* or at 10 dpc by using the *Sf1-Cre* [19, 20, 65, 66]. In both mouse models, a phenotype was evident only in the postnatal testis [19, 20, 65, 66]. Interestingly, the expression of Sertoli cell-specific miRNAs in *Dicer1;Amh-Cre* testes were significantly reduced only at P5, despite ablation of *Dicer1* 12 days earlier [19], suggesting that miRNAs are inherently stable in Sertoli cells and/or DICER1 protein itself has a long half-life in Sertoli cells, making it difficult to study the function of miRNAs in fetal sex determination and early gonad development. Therefore, the function of microRNAs in somatic gonad development should be addressed by a candidate-based approach.

To date, no direct physiological function for *miR-202-5p/3p* has been identified. Our present data suggest that ectopic expression of *pri-miR-202* in XX transgenic mice does not overtly influence sex determination, although it may prove to have an important role in testis differentiation and function. A possible explanation for the lack of observable effect is that the endogenous targets of *miR-202-5p/3p* may not be present in ovarian somatic cells and thus, rather than inhibiting ovary-determining pathways, *miR-202-5p/3p* may regulate testis-specific gene networks. Bioinformatics analysis, using the stringent criterion that a gene must be identified as a potential target by at least two algorithms, revealed 36 genes as target genes of *miR-202-5p* (Supplemental Table S2). Eleven of the 36 *miR-202-5p* target genes were also predicted to be targeted by *miR-140-3p* (Supplemental Table S2), which is coexpressed with *miR-202-5p* in Sertoli cells in the early XY gonad [22]. However, none of these targets has a known role in sex determination and early gonad development. In the gain-of-function experiment we have tested whether *pri-miR-202* can act as a dominant testis-determining factor, which precludes analysis of a possible function in enforcing the male determination program or in supporting decisions of testis differentiation. Therefore, the generation of *pri-miR-202*-null mice is required before the function of *miR-202-5p/3p* can be defined in XY gonadal somatic cells.

Our transgenic mouse model resulted in the overexpression of *pri-miR-202* not only in somatic cells of the ovary but also in Sertoli cells within the developing testis. Intriguingly, while we detected an increase in the level of the primary transcript in transgenic testes, this did not result in an increase in the processed, mature miRNA, suggesting a testis-specific negative feed-forward loop. This regulation could be at the Drosha level, as has been described for a number of proteins and signaling pathways such as the DE-AD-box RNA helicases p68 and p72 [67], BMP signaling [68], and LIN28 (for review see [69]), at the level of miRNA export by exportin-5, similar to what has been described for *miR-105*, *miR-128*, and *miR-31* [70], or through the control of cleavage by Dicer. The exact mechanism of the here-identified testis-specific processing is currently not known and needs further, more detailed investigation, including its specificity for processing of *miR-202*.

In the emerging paradigm of miRNA regulation of gene expression, it appears that microRNAs can be grouped into three categories. First, miRNAs may act as a switch to regulate a sharp developmental decision, usually through one main target gene. Second, miRNAs may regulate networks of genes to enforce stochastic developmental decisions. Third, miRNAs may regulate gene networks that buffer perturbation of normal physiological processes (reviewed in [71, 72]). To that end, it would be interesting to cross *pri-miR-202*-overexpressing transgenic mice onto a partial XX sex reversed genetic background, such as *Wnt4*-null mice, to determine whether *pri-miR-202* can enforce testicular differentiation in the context of a weaker ovarian program.

Alternatively to its physiological role, *miR-202-5p/3p* expression has been shown to be associated with pathological conditions, suggesting a function in a disease setting. Human *miR-202-5p* was one of 10 microRNAs upregulated in ovarian endometriomas compared with normal endometrium [73]. In addition, *miR-202-3p* was found to directly repress the expression of the proto-oncogene myelocytomatosis virus-related oncogene, neuroblastoma-derived (avian) *Mycn*, suggesting a function for *miR-202-5p/3p* as a tumor suppressor [74]. Should *miR-202-5p/3p* function to provide robustness to gene networks by attenuating aberrant transcripts; perhaps investigation of *miR-202-5p/3p* in mouse models of ovarian and testicular cancer will clarify its biological function.

In summary, we have determined that *pri-miR-202* and *miR-202-5p*/*miR-202-3p* are upregulated during fetal testis differentiation with strong expression in Sertoli cells. In vivo, expression of *pri-miR-202* in XX gonads does not disrupt XX embryonic sex determination and differentiation. Furthermore,

we have demonstrated that a 4-kb putative promoter region of *pri-miR-202* is sufficient to drive dimorphic expression between XY and XX gonads ex vivo and that *pri-miR-202* may be a direct transcriptional target of SOX9/SF1. From the reported data, we conclude that upregulation of *miR-202-5p/miR-202-3p* marks XY gonad differentiation and functions downstream of the testis-determining factors SOX9 and SF1. However, definition of the function of *pri-miR-202* in the XY gonad requires the generation of *pri-miR-202*-null mice.

ACKNOWLEDGMENT

We thank Dr. Pascal Bernard (Monash University, Melbourne, Australia) for help with bioinformatics analysis of transcription factor binding sites in the *miR-202* promoter. Confocal microscopy was performed at the Australian Cancer Research Foundation Dynamic Imaging Centre for Cancer Biology.

REFERENCES

1. Koopman P, Gubbay J, Vivian N, Goodfellow P, Lovell-Badge R. Male development of chromosomally female mice transgenic for *Sry*. Nature 1991; 351:117–121.
2. Foster JW, Dominguez-Steglich MA, Guioli S, Kwok C, Weller PA, Weissenbach J, Mansour S, Young ID, Goodfellow PN, Brook JD, Schafer AJ. Campomelic dysplasia and autosomal sex reversal caused by mutations in an *SRY*-related gene. Nature 1994; 372:525–530.
3. Wagner T, Wirth J, Meyer J, Zabel B, Held M, Zimmer J, Pasantes J, Bricarelli FD, Keutel J, Hustert E, Wolf U, Tommerup N, et al. Autosomal sex reversal and campomelic dysplasia are caused by mutations in and around the *SRY*-related gene *SOX9*. Cell 1994; 79:1111–1120.
4. Kim Y, Kobayashi A, Sekido R, DiNapoli L, Brennan J, Chaboissier MC, Poulat F, Behringer RR, Lovell-Badge R, Capel B. Fgf9 and Wnt4 act as antagonistic signals to regulate mammalian sex determination. PLoS Biol 2006; 4:e187.
5. Lee Y, Ahn C, Han J, Choi H, Kim J, Yim J, Lee J, Provost P, Radmark O, Kim S, Kim VN. The nuclear RNase III Drosha initiates microRNA processing. Nature 2003; 425:415–419.
6. Hutvagner G, McLachlan J, Pasquinelli AE, Balint E, Tuschl T, Zamore PD. A cellular function for the RNA-interference enzyme Dicer in the maturation of the let-7 small temporal RNA. Science 2001; 293:834–838.
7. Bartel DP. MicroRNAs: genomics, biogenesis, mechanism, and function. Cell 2004; 116:281–297.
8. Ro S, Song R, Park C, Zheng H, Sanders KM, Yan W. Cloning and expression profiling of small RNAs expressed in the mouse ovary. RNA 2007; 13:2366–2380.
9. Bannister SC, Tizard ML, Doran TJ, Sinclair AH, Smith CA. Sexually dimorphic microRNA expression during chicken embryonic gonadal development. Biol Reprod 2009; 81:165–176.
10. Ro S, Park C, Sanders KM, McCarrey JR, Yan W. Cloning and expression profiling of testis-expressed microRNAs. Dev Biol 2007; 311:592–602.
11. Michalak P, Malone JH. Testis-derived microRNA profiles of African clawed frogs (Xenopus) and their sterile hybrids. Genomics 2008; 91: 158–164.
12. Mishima T, Takizawa T, Luo SS, Ishibashi O, Kawahigashi Y, Mizuguchi Y, Ishikawa T, Mori M, Kanda T, Goto T, Takizawa T. MicroRNA (miRNA) cloning analysis reveals sex differences in miRNA expression profiles between adult mouse testis and ovary. Reproduction 2008; 136: 811–822.
13. Otsuka M, Zheng M, Hayashi M, Lee JD, Yoshino O, Lin S, Han J. Impaired microRNA processing causes corpus luteum insufficiency and infertility in mice. J Clin Invest 2008; 118:1944–1954.
14. Hayashi K, Chuva de Sousa Lopes SM, Kaneda M, Tang F, Hajkova P, Lao K, O'Carroll D, Das PP, Tarakhovsky A, Miska EA, Surani MA. MicroRNA biogenesis is required for mouse primordial germ cell development and spermatogenesis. PLoS One 2008; 3:e1738.
15. Korhonen HM, Meikar O, Yadav RP, Papaioannou MD, Romero Y, Da Ros M, Herrera PL, Toppari J, Nef S, Kotaja N. Dicer is required for haploid male germ cell differentiation in mice. PLoS One 2011; 6:e24821.
16. Liu D, Li L, Fu H, Li S, Li J. Inactivation of Dicer1 has a severe cumulative impact on the formation of mature germ cells in mouse testes. Biochem Biophys Res Commun 2012; 422:114–120.
17. Romero Y, Meikar O, Papaioannou MD, Conne B, Grey C, Weier M, Pralong F, De Massy B, Kaessmann H, Vassalli JD, Kotaja N, Nef S. Dicer1 depletion in male germ cells leads to infertility due to cumulative meiotic and spermiogenic defects. PLoS One 2011; 6:e25241.
18. Wu Q, Song R, Ortogero N, Zheng H, Evanoff R, Small CL, Griswold MD, Namekawa SH, Royo H, Turner JM, Yan W. The RNase III enzyme DROSHA is essential for microRNA production and spermatogenesis. J Biol Chem 2012; 287:25173–25190.
19. Papaioannou MD, Pitetti JL, Ro S, Park C, Aubry F, Schaad O, Vejnar CE, Kuhne F, Descombes P, Zdobnov EM, McManus MT, Guillou F, et al. Sertoli cell Dicer is essential for spermatogenesis in mice. Dev Biol 2009; 326:250–259.
20. Kim GJ, Georg I, Scherthan H, Merkenschlager M, Guillou F, Scherer G, Barrionuevo F. Dicer is required for Sertoli cell function and survival. Int J Dev Biol 2010; 54:867–875.
21. Huang CC, Yao HH. Inactivation of Dicer1 in steroidogenic factor 1-positive cells reveals tissue-specific requirement for Dicer1 in adrenal, testis, and ovary. BMC Dev Biol 2010; 10:66.
22. Rakoczy J, Fernandez-Valverde SL, Glazov EA, Wainwright EN, Sato T, Takada S, Combes AN, Korbie DJ, Miller D, Grimmond SM, Little MH, Asahara H, et al. MicroRNAs-140-5p/140-3p modulate Leydig cell numbers in the developing mouse testis. Biol Reprod 2013; 88:143.
23. Hacker A, Capel B, Goodfellow P, Lovell-Badge R. Expression of *Sry*, the mouse sex determining gene. Development 1995; 121:1603–1614.
24. Svingen T, Beverdam A, Verma P, Wilhelm D, Koopman P. Aard is specifically up-regulated in Sertoli cells during mouse testis differentiation. Int J Dev Biol 2007; 51:255–258.
25. Barrionuevo F, Bagheri-Fam S, Klattig J, Kist R, Taketo MM, Englert C, Scherer G. Homozygous Inactivation of Sox9 causes complete XY sex reversal in mice. Biol Reprod 2006; 74:195–201.
26. Barbera JP, Rodriguez TA, Greene ND, Weninger WJ, Simeone A, Copp AJ, Beddington RS, Dunwoodie S. Folic acid prevents exencephaly in Cited2 deficient mice. Hum Mol Genet 2002; 11:283–293.
27. Polanco JC, Wilhelm D, Davidson TL, Knight D, Koopman P. Sox10 gain-of-function causes XX sex reversal in mice: implications for human 22q-linked disorders of sex development. Hum Mol Genet 2010; 19: 506–516.
28. Wilhelm D, Hiramatsu R, Mizusaki H, Widjaja L, Combes AN, Kanai Y, Koopman P. SOX9 regulates prostaglandin D synthase gene transcription in vivo to ensure testis development. J Biol Chem 2007; 282: 10553–10560.
29. Pena JT, Sohn-Lee C, Rouhanifard SH, Ludwig J, Hafner M, Mihailovic A, Lim C, Holoch D, Berninger P, Zavolan M, Tuschl T. miRNA in situ hybridization in formaldehyde and EDC-fixed tissues. Nat Methods 2009; 6:139–141.
30. Kashimada K, Pelosi E, Chen H, Schlessinger D, Wilhelm D, Koopman P. FOXL2 and BMP2 act cooperatively to regulate follistatin gene expression during ovarian development. Endocrinol 2011; 152:272–280.
31. Hargrave M, Koopman P. *In situ* hybridization of whole mount embryos In: Darby I (ed.), In Situ Hybridization Protocols, vol. 123, 2nd ed. Totowa: Humana Press; 1999; 279–289.
32. Wilhelm D, Martinson F, Bradford S, Wilson MJ, Combes AN, Beverdam A, Bowles J, Mizusaki H, Koopman P. Sertoli cell differentiation is induced both cell-autonomously and through prostaglandin signaling during mammalian sex determination. Dev Biol 2005; 287:111–124.
33. Svingen T, Francois M, Wilhelm D, Koopman P. Three-dimensional imaging of Prox1-EGFP transgenic mouse gonads reveals divergent modes of lymphangiogenesis in the testis and ovary. PLoS One 2012; 7: e52620.
34. Svingen T, Spiller CM, Kashimada K, Harley VR, Koopman P. Identification of suitable normalizing genes for quantitative real-time RT-PCR analysis of gene expression in fetal mouse gonads. Sex Dev 2009; 3:194–204.
35. Bjork JK, Sandqvist A, Elsing AN, Kotaja N, Sistonen L. miR-18, a member of Oncomir-1, targets heat shock transcription factor 2 in spermatogenesis. Development 2010; 137:3177–3184.
36. Livak KJ, Schmittgen TD. Analysis of relative gene expression data using real-time quantitative PCR and the 2(-Delta Delta C(T)) Method. Methods 2001; 25:402–408.
37. Beverdam A, Koopman P. Expression profiling of purified mouse gonadal somatic cells during the critical time window of sex determination reveals novel candidate genes for human sexual dysgenesis syndromes. Hum Mol Genet 2006; 15:417–431.
38. Gao L, Kim Y, Kim B, Lofgren SM, Schultz-Norton JR, Nardulli AM, Heckert LL, Jorgensen JS. Two regions within the proximal steroidogenic factor 1 promoter drive somatic cell-specific activity in developing gonads of the female mouse. Biol Reprod 2011; 84:422–434.
39. Yao H, Capel B. Disruption of testis cords by cyclopamine or forskolin

reveals independent cellular pathways in testis organogenesis. Dev Biol 2002; 246:356–365.
40. Lewis BP, Burge CB, Bartel DP. Conserved seed pairing, often flanked by adenosines, indicates that thousands of human genes are microRNA targets. Cell 2005; 120:15–20.
41. Dweep H, Sticht C, Pandey P, Gretz N. miRWalk–database: prediction of possible miRNA binding sites by ''walking'' the genes of three genomes. J Biomed Inform 2011; 44:839–847.
42. Miranda KC, Huynh T, Tay Y, Ang YS, Tam WL, Thomson AM, Lim B, Rigoutsos I. A pattern-based method for the identification of MicroRNA binding sites and their corresponding heteroduplexes. Cell 2006; 126: 1203–1217.
43. Chen H, Palmer JS, Thiagarajan RD, Dinger ME, Lesieur E, Chiu H, Schulz A, Spiller C, Grimmond SM, Little MH, Koopman P, Wilhelm D. Identification of novel markers of mouse fetal ovary development. PLoS One 2012; 7:e41683.
44. Novotny GW, Nielsen JE, Sonne SB, Skakkebaek NE, Rajpert-De Meyts E, Leffers H. Analysis of gene expression in normal and neoplastic human testis: new roles of RNA. Int J Androl 2007; 30:316–326.
45. Bizuayehu TT, Babiak J, Norberg B, Fernandes JM, Johansen SD, Babiak I. Sex-biased miRNA expression in Atlantic halibut (*Hippoglossus hippoglossus*) brain and gonads. Sex Dev 2012; 6:257–266.
46. Armstrong JF, Pritchard-Jones K, Bickmore WA, Hastie ND, Bard JB. The expression of the Wilms' tumour gene, WT1, in the developing mammalian embryo. Mech Dev 1993; 40:85–97.
47. de Santa Barbara P, Bonneaud N, Boizet B, Desclozeaux M, Moniot B, Südbeck P, Scherer G, Poulat F, Berta P. Direct interaction of SRY-related protein SOX9 and steroidogenic factor 1 regulates transcription of the human anti-Müllerian hormone gene. Mol Cell Biol 1998; 18:6653–6665.
48. Sekido R, Lovell-Badge R. Sex determination involves synergistic action of SRY and SF1 on a specific Sox9 enhancer. Nature 2008; 453:930–934.
49. Luo X, Ikeda Y, Parker KL. A cell-specific nuclear receptor is essential for adrenal and gonadal development and sexual differentiation. Cell 1994; 77:481–490.
50. Buaas FW, Val P, Swain A. The transcription co-factor CITED2 functions during sex determination and early gonad development. Hum Mol Genet 2009; 18(16):2989–3001.
51. Combes AN, Spiller CM, Harley VR, Sinclair AH, Dunwoodie SL, Wilhelm D, Koopman P. Gonadal defects in Cited2-mutant mice indicate a role for SF1 in both testis and ovary differentiation. Int J Dev Biol 2010; 54(4):683–689.
52. Roush S, Slack FJ. The let-7 family of microRNAs. Trends Cell Biol 2008; 18:505–516.
53. Li M, Liu Y, Wang T, Guan J, Luo Z, Chen H, Wang X, Chen L, Ma J, Mu Z, Jiang AA, Zhu L, et al. Repertoire of porcine microRNAs in adult ovary and testis by deep sequencing. Int J Biol Sci 2011; 7:1045–1055.
54. Chaboissier MC, Kobayashi A, Vidal VI, Lutzkendorf S, van de Kant HJ, Wegner M, de Rooij DG, Behringer RR, Schedl A. Functional analysis of Sox8 and Sox9 during sex determination in the mouse. Development 2004; 131:1891–1901.
55. Vidal V, Chaboissier M, de Rooij D, Schedl A. *Sox9* induces testis development in XX transgenic mice. Nat Genet 2001; 28:216–217.
56. Arango N, Lovell-Badge R, Behringer R. Targeted mutagenesis of the endogenous mouse *Mis* gene promoter: In vivo definition of genetic pathways of vertebrate sexual development. Cell 1999; 99:409–419.
57. Nakamura Y, Yamamoto K, He X, Otsuki B, Kim Y, Murao H, Soeda T, Tsumaki N, Deng JM, Zhang Z, Behringer RR, Crombrugghe B, et al. Wwp2 is essential for palatogenesis mediated by the interaction between Sox9 and mediator subunit 25. Nat Commun 2011; 2:251.
58. Yamashita S, Miyaki S, Kato Y, Yokoyama S, Sato T, Barrionuevo F, Akiyama H, Scherer G, Takada S, Asahara H. L-Sox5 and Sox6 proteins enhance chondrogenic miR-140 microRNA expression by strengthening dimeric Sox9 activity. J Biol Chem 2012; 287:22206–22215.
59. Bullejos M, Koopman P. Delayed Sry and Sox9 expression in developing mouse gonads underlies B6-Y(DOM) sex reversal. Dev Biol 2005; 278: 473–481.
60. Bowles J, Feng CW, Knight D, Smith CA, Roeszler KN, Bagheri-Fam S, Harley VR, Sinclair AH, Koopman P. Male-specific expression of Aldh1a1 in mouse and chicken fetal testes: implications for retinoid balance in gonad development. Dev Dyn 2009; 238:2073–2080.
61. Ottolenghi C, Omari S, Garcia-Ortiz JE, Uda M, Crisponi L, Forabosco A, Pilia G, Schlessinger D. Foxl2 is required for commitment to ovary differentiation. Hum Mol Genet 2005; 14:2053–2062.
62. Polanco JC, Wilhelm D, Mizusaki H, Jackson A, Browne C, Davidson T, Harley V, Sinclair A, Koopman P. Functional analysis of the SRY-KRAB interaction in mouse sex determination. Biol Cell 2009; 101:55–67.
63. Tevosian SG, Albrecht KH, Crispino JD, Fujiwara Y, Eicher EM, Orkin SH. Gonadal differentiation, sex determination and normal Sry expression in mice require direct interaction between transcription partners GATA4 and FOG2. Development 2002; 129:4627–4634.
64. Bridgewater LC, Walker MD, Miller GC, Ellison TA, Holsinger LD, Potter JL, Jackson TL, Chen RK, Winkel VL, Zhang Z, McKinney S, de Crombrugghe B. Adjacent DNA sequences modulate Sox9 transcriptional activation at paired Sox sites in three chondrocyte-specific enhancer elements. Nucleic Acids Res 2003; 31:1541–1553.
65. Gonzalez G, Behringer RR. Dicer is required for female reproductive tract development and fertility in the mouse. Mol Reprod Dev 2009; 76: 678–688.
66. Nagaraja AK, Andreu-Vieyra C, Franco HL, Ma L, Chen R, Han DY, Zhu H, Agno JE, Gunaratne PH, DeMayo FJ, Matzuk MM. Deletion of Dicer in somatic cells of the female reproductive tract causes sterility. Mol Endocrinol 2008; 22:2336–2352.
67. Fukuda T, Yamagata K, Fujiyama S, Matsumoto T, Koshida I, Yoshimura K, Mihara M, Naitou M, Endoh H, Nakamura T, Akimoto C, Yamamoto Y, et al. DEAD-box RNA helicase subunits of the Drosha complex are required for processing of rRNA and a subset of microRNAs. Nat Cell Biol 2007; 9:604–611.
68. Davis BN, Hilyard AC, Lagna G, Hata A. SMAD proteins control DROSHA-mediated microRNA maturation. Nature 2008; 454:56–61.
69. Viswanathan SR, Daley GQ. Lin28: A microRNA regulator with a macro role. Cell 2010; 140:445–449.
70. Lee EJ, Baek M, Gusev Y, Brackett DJ, Nuovo GJ, Schmittgen TD. Systematic evaluation of microRNA processing patterns in tissues, cell lines, and tumors. RNA 2008; 14:35–42.
71. Ebert MS, Sharp PA. Roles for microRNAs in conferring robustness to biological processes. Cell 2012; 149:515–524.
72. Herranz H, Cohen SM. MicroRNAs and gene regulatory networks: managing the impact of noise in biological systems. Genes Dev 2010; 24: 1339–1344.
73. Hawkins SM, Creighton CJ, Han DY, Zariff A, Anderson ML, Gunaratne PH, Matzuk MM. Functional microRNA involved in endometriosis. Mol Endocrinol 2011; 25:821–832.
74. Buechner J, Tomte E, Haug BH, Henriksen JR, Lokke C, Flaegstad T, Einvik C. Tumour-suppressor microRNAs let-7 and mir-101 target the proto-oncogene MYCN and inhibit cell proliferation in MYCN-amplified neuroblastoma. Br J Cancer 2011; 105:296–303.